Design, Preparation and Characterization of Novel Pseudorotaxanes, Semirotaxanes, Rotaxanes, Non-Covalent Supramolecular Polymers and Polycatenanes

Zhenbin Niu

Dissertation submitted to the faculty of the Virginia Polytechnic Institute and State University in partial fulfillment of the requirements for the degree of

Doctor of Philosophy
In
Chemistry

Harry W. Gibson, Chair

Harry C. Dorn

Richard D. Gandour

S. Richard Turner

September 6th, 2011
Blacksburg, VA

Keywords: Crown Ether, Cryptand, Paraquat, Bisparaquat, Diquat, Pseudorotaxane, Pseudocryptand, Acid-Base Adjustable, Association Constant, Supramolecular Polymer, Polycatenane, Self-Assembly, X-ray Crystallography.

Design, Preparation and Characterization of Novel Pseudorotaxanes, Semirotaxanes, Rotaxanes, Non-Covalent Supramolecular Polymers and Polycatenanes

Zhenbin Niu

ABSTRACT

Design and preparation of novel host/guest systems, such as pseudorotaxanes, semirotaxanes, rotaxanes and catenanes, with high association constants, enhanced yields and the abilities to respond to external stimuli are of great importance and significance due to their topological novelty and potential application. The convergence of supramolecular chemistry with polymer science provides an important way to extend the scope of polymer and material sciences by incorporating designed host/guest systems into polymers, and the resulting non-covalently linked supramolecular polymers are expected to have unusual properties due to their unique architectures compared with traditional polymers.

After discovery of bis(*meta*-phenylene)-32-crown-10 (BMP32C10) derivative/paraquat complexes, for about a quarter century only “taco”-shaped complexes were observed by X-ray crystallography. Here, by the self-assembly of a BMP32C10 bearing two electron-donating groups (carbazoles) with electron-accepting paraquat derivatives, the first [2]pseudorotaxane and the first pseudocryptand-type poly[2]pseudorotaxane based on BMP32C10 were isolated as crystalline solids as shown by X-ray analyses.

The first dual component pseudocryptand-type [2]pseudorotaxanes were designed and prepared via the self-assembly of synthetically easily accessible BMP32C10 pyridyl, quinolyl and naphthyridyl derivatives with paraquat. The formation of the pseudocryptand structures in the complexes remarkably improved the association constants by forming the third pseudo-bridge via H-bonding with the guest and π–stacking of the heterocyclic units.

A pseudocryptand-type [2]pseudorotaxane was formed via the self-assembly of a dipyridyl BMP32C10 derivative and a paraquat derivative. Due to the basicity of the

pyridyl group, which forms the third pseudo-bridge of the pseudocryptand, this pseudorotaxane represents the first system with acid-base adjustable association constants, i. e., finite both under acidic and neutral conditions.

The first pseudocryptand-type supramolecular [3]pseudorotaxane was designed and prepared via the self-assembly of a bispicolinate BMP32C10 derivative and a bisparaquat. The complexation behavior was cooperative. In addition, the complex comprised of the BMP32C10 derivative and a cyclic bisparaquat demonstrated strong binding; interestingly, a poly[2]pseudocatenane structure was formed in the solid state for the first time.

Two novel BMP32C10 cryptands, bearing covalent and metal complex linkages, were designed and prepared. By employing the self-assembly of these biscryptands, which can be viewed as AA monomers, and a bisparaquat, which can be viewed as a BB monomer, the first AA/BB-type linear supramolecular polymers with relatively high molecular weights were successfully prepared.

Via the self-assembly of two BMP32C10-based cryptands, bearing covalent and metal complex (ferrocene) linkages, with dimethyl paraquat, novel [3]pseudorotaxanes were formed statistically and anticooperatively, respectively.

From a hydroxyl-functionalized secondary ammonium salt a [2]semirotaxane and a [2]rotaxane were prepared successfully with dibenzo-24-crown-8 (DB24C8). X-ray analysis of a single crystal of the [2]semirotaxane confirmed its semirotaxane nature. In addition, the formation of the [2]semirotaxane can be reversibly controlled by adding KPF_6 and 18C6 sequentially. This system affords a way to prepare novel supramolecular polymers.

Dibenzo-30-crown-10 (DB30C10) derivatives and pyridine-based DB30C10 cryptands were prepared by employing the templating method established by our group. A [2]pseudorotaxane was prepared based on DB30C10 diol and paraquat diol. The [3]pseudorotaxane formed via the self-assembly between DB30C10 cryptand and bisparaquat diol occurred in a cooperative manner. In addition, a bromo-functionalized DB30C10 cryptand was successfully designed and prepared. An alkyne-functionalized DB30C10 cryptand was designed and is under preparation; its precursors have been prepared successfully. In the future, based on these functionalized cryptands and paraquat

salts, AA and AB type monomers will be prepared. Via the self-assembly between these monomers, non-covalent supramolecular polymers with high molecular weight will be afforded.

A novel DB30C10 cryptand bearing an organometallic bridge, ferrocene, was prepared via 1-(3'-dimethylaminopropyl)-3-ethylcarbodiimide hydrochloride (EDCI) coupling of the crown ether diol with ferrocene dicarboxylic acid. The cryptand is dimerized in the solid state via π, π-stacking and hydrogen bonds. The ferrocene-based cryptand formed novel [2]pseudorotaxanes with paraquat and diquat PF_6 salts with association constants (K_a) of 1.7 ± 0.1 x 10^3 and 4.2 ± 0.3 x 10^4 M^{-1} in acetone-d_6, respectively.

In order to prepare linear polycatenanes, the preparation of which represent a real synthetic challenge, a series phenanthroline derivatives were designed and prepared. A "U" shaped monomer was successfully prepared in relative high yield with good solubility. In the future, real linear polycatenanes will be prepared. In addition, a novel diphenanthroline-based BMP32C10 derivative was prepared in high yield and the complexation behavior between it and dimethyl paraquat was studied.

Dedication

Dedicated to my wife, Li Xu,

my parents, Yaomin Niu and Xiuyun Guo,

my sister, Xiaoyan Niu

and my lovely angels Jenny Niu and Erric Niu

for their endless support and love

衷心感谢我的妻子许丽

我的父母牛耀民，郭秀云

我的姐姐牛晓燕

和我最爱的天使们-Jenny Niu 和 Erric Niu

无尽的支持和无尽的爱

Acknowledgements

Most of all, I would like to show my gratitude to my advisor, Professor Harry W. Gibson, for his inspiration, encouragement, patience, supports and guidance throughout this achievement, and for giving me the opportunity to work in his wonderful group. His profound knowledge, enthusiasm and keen insight in organic and polymer chemistry gave me a big impression during the whole of my graduate life and inspired me to become an outstanding chemist like him in the future.

I would like to thank my committee members, Professors Harry C. Dorn, Richard D. Gandour, S. Richard. Turner and Alan R. Esker for their suggestions, constant support and comments on my research and dissertation.

I want to give special thanks to Dr. Carla Slebodnick for her valuable and professional assistance in X-ray crystallography; Dr. Hugo Azurmendi for all his help with NMR spectroscopy; Mr. Stephen McCartney for his help with SEM analysis; Mr. William Bebout, Mr. Kim Harich and Dr. Mehdi Ashraf-Khorassani for all their help with mass spectroscopy.

I also grateful to the following colleagues and mentors for their kind help and support during my graduate career at Virginia Tech: Dr. Lee Minjae (Samsung, Korea), Prof. Feihe Huang (Zhejiang Univ., China), Dan Schoonover, Dr. Manav Gupta (Cytec Industries, CT), Dr. Bin Li, Dr. Anuj Mittal, Terry Price, Dr. Adam Pederson, Mason Rouser, Jeffrey Bowers and Hanlie R. Wessels.

Table of Contents

Table of Figures

Chapter 1: Supramolecular Chemistry based on Crown Ethers

Chapter 2: Polycatenanes

Chapter 5. Pseudocryptand-type [2]Pseudorotaxanes Based on Bis(metaphenylene)-32-Crown-10 Derivatives and Paraquats with Remarkably Improved Association Constants

Chapter 6. An Acid-Base Adjustable Pseudocryptand-type [2]Pseudorotaxane Based on a Bis(*meta*-phenylene)-32-Crown-10 Derivative and Paraquat

Chapter 9. Contrasting Biscryptand/Dimethyl Paraquat [3]Pseudorotaxanes: Statistical vs. Anticooperative Complexation Behavior

Chapter 10. [2]Semi-rotaxane and [2]rotaxane based on Dibenzo-24-crown-8 (DB24C8) and Secondary Ammonium Salts

Chapter 12. Novel [2]Pseudorotaxanes Formed via the Self-Assembly of a Ferrocene-Based *cis*(*4,4'*)-Dibenzo-30-crown-10 Cryptand with Praquat and Diquat

Chapter 13. Attempts to Prepare Real Linear Polycatenanes and Preparation and Characterization of [2]Pseudorotaxane based on Bis(*meta*-phenylene)-32-crown-10 (BMP32C10) and Bisphenanthroline

Table of Schemes

Chapter 11. [2] and [3]Pseudorotaxane based on *cis*(*4,4'*)-Dibenzo-30-crown-10 (DB30C10) Crown Ether/Cryptand and Preparation of Functionalized DB30C10 Cryptands

Chapter 13. Attempts to Prepare Real Linear Polycatenanes and Preparation and Characterization of [2]Pseudorotaxane based on Bis(*meta*-phenylene)-32-crown-10 (BMP32C10) and Bisphenanthroline

Chapter 14. Conclusions and Future Work

Table of Tables

All the publications based on this dissertation are listed below:

(1) **Niu, Z**.; Gibson, H. W. Chapter of "Polycatenanes" for the book of "Synthesis of Polymers" edited by Prof. A. Dieter Schlüter. (ASAP). – Chapter 2.

(2) **Niu, Z**.; Slebodnick, C.; Bonrad, K.; Huang, F.; Gibson, H. W.; The First [2]Pseudorotaxane and the First Pseudocryptand-Type Poly[3]pseudorotaxane based on Bis*(meta*-phenylene)-32-Crown-10 and Paraquat derivatives. *Organic Letter,* **2011**, *13*, 2872–2875. – Chapter 4.

(3) **Niu, Z**.; Slebodnick, C.; Schoonover, D.; Azurmendi, H.; Harich, K.; Gibson, H. W.; Pseudocryptand-type [2]Pseudorotaxanes Based on Bis(meta-phenylene)-32-Crown-10 Derivatives and Paraquats with Remarkbly Improved Association Constants. *Organic Letter.* **2011**, *13*, 3992-3995. – Chapter 5.

(4) **Niu, Z**.; Slebodnick, C.; Huang, F.; Azurmendi, H.; Gibson, H. W.; An Acid-Base Adjustable Pseudocryptand-type [2]Pseudorotaxane Based on a Bis(*meta* phenylene)-32-Crown-10 Derivative and Paraquat. *Tetrahedron Letter*, (ASAP). – Chapter 6.

(5) **Niu, Z**.; Slebodnick, C.; Gibson, H. W.; Pseudocryptand-type [3]Pseudorotaxane and "Hook-Ring" Polypseudo[2]catenane. *Organic Letter*, **2011**, *13*, 4616–4619. – Chapter 7.

(6) **Niu, Z**.; Huang, F.; Gibson, H. W.; Supramolecular AA BB Type Linear Polymers with Relatively High Molecular Weights via the Self-Organization of Bis(*meta*-phenylene)-32-Crown-10 Cryptands and a Bisparaquat Derivative. *Journal of the American Chemical Society*, **2011**, *133*, 2836-2839. (**Featured in *Science,* February 2011, *331,* 998 in Editors' Choice: Highlights of the recent literature**.) - Chapter 8.

(7) **Niu, Z**.; Gibson, H. W.; Novel Biscryptand/Dimethyl Paraquat [3]Pseudorotaxanes by Statistical and Anticooperative Complexation. *Organic and Biomolecular Chemistry*, **2011**, (ASAP). – Chapter 9.

(8) **Niu, Z**.; Slebodnick, C.; Gibson, H. W.; Novel [2]Pseudorotaxanes Formed via the Self-Assembly Between Ferrocene-Based *cis*(*4,4′*)-Dibenzyl-30-crown 10 Cryptand and Praquat and Diquat. (Manuscript in preparation).

Chapter 1

Supramolecular Chemistry based on Crown Ethers

1.1 Introduction

Supramolecular chemistry is chemistry based on non-covalent interactions between molecules. Compared with traditional chemistry, which is mainly concerned with the making and breaking of covalent bonds to form the new molecules, supramolecular chemistry utilizes weaker and reversible noncovalent interactions, such as hydrogen bonds, metal coordination, π-π stacking interactions, and hydrophobic effects.[1-12] The energy of most covalent interactions always is higher than 200 kJ/mol and the energy of most noncovalent interactions is within the range of 0-40 kJ/mol. Although the noncovalent interactions are weaker than the covalent interactions, stable compounds can be formed if large numbers of noncovalent interactions work together.

The origination of supramolecular chemistry can be tracked back to the Pederson's pioneering discovery that crown ethers can complex with metal ions, e.g., dibenzo-18-crown-6 complexed with a potassium ion.[13,14] After that, Lehn *et al.* reported the syntheses and binding abilities of cryptands which are the cage-like bicyclic molecules.[15] Cram *et al.* optimized the synthetic methods for cryptands, reported a series of photoactive cryptands[16] and proposed the concept of host and guest chemistry. Based on that, Lehn presented the concept of supramolecular chemistry.[17] Pedersen, Lehn and Cram's pioneering work stimulated a new line of research and was recognized with the award of the 1987 Nobel Prize for Chemistry. In the following years, supramolecular chemistry has attracted great interest among scientists all over the world and developed quickly.

Commonly, supramolecules are composed of "hosts" and "guests". The role of "hosts" is usually played by cyclic molecules which are the natural products or can be artificially synthesized, such as crown ethers, cryptands, cyclodextrins, and calixarenes. The "guests" are

ions or molecules that bind with a host by noncovalent bonds. Guests can be a diverse group of molecules from small particles (inert gas atoms, metal ions, etc.) to larger molecules (ammonium salts, paraquats, fullerenes, etc.).[18] From the beginning of supramolecular chemistry, crown ethers have been intensely studied with respect to their ability to undergo complexation with metal ions and other species,[13-15, 19-22] in some cases leading to the formation of threaded structures known as pseudorotaxanes, rotaxanes, catenanes, polypseudorotaxanes, polyrotaxanes, and polycatenanes,[23-24] which are attractive to scientists all over the world because of their topological importance and their potential applications.[24-25] A large variety of crown ethers, such as aza- and thia-analogs,[26] bis- and tris- structures,[27-28] caged [29] and acetal crown ethers[30] have been synthesized. Further, cyclodextrins[31-34] and calixarenes[35-37] became the second and third generation of host compounds. Moreover, other new macrocyclic compounds, such as: cryptands,[38] porphyrins,[39-40] phthalocyanines,[41] and so on, are studied extensively.

1.2 Basic concepts in supramolecular chemistry

1.2.1 Molecular recognition

There are two basic concepts in supramolecular chemistry-molecular recognition and molecular self-assembly.[18] Molecular recognition is the ability of a host molecule to distinguish between different guest molecules, to form a complex through noncovalent bonds.[1-12] Molecular recognition includes ionic guest recognition and molecular guest recognition. Complementarity and preorganization are the key points for molecular recognition. Complementarity means the binding sites of the host molecule must have the correct electronic character to match those properties of the guest molecules. For example, hydrogen bond donors are complementary to the acceptors, Lewis acids are complementary to the Lewis bases, etc. In addition, the binding sites of the host molecule must be spaced out on the host in such a way as to make it possible for them to interact with the guest. Therefore, binding ability depends heavily on the complementarity between the hosts and guests during the complexation. On the other hand, if no significant conformational change of the host occurs upon complexation with the guest, the host is called preorganized. Preorganization is a key concept because it yields an enhancement of favorable free energy changes for complexation. If a host is preorganized, the rearrangement energy is small, then the overall energy, which is the difference between the unfavorable reorganization energy and the favorable binding energy, is large, and the complex is stable. Molecular

recognition is the basis for the molecular assembly, which is an important concept in supramolecular chemistry.

1.2.2 Molecular self-assembly

Molecular self-assembly,[18] which is of enormous importance in modern supramolecular chemistry, is the assembly of several molecules by themselves without guidance or control from an outside source. It is a reversible process and leads to the formation of thermodynamically stable structures. There are two types of self-assembly: intramolecular self-assembly[42-43] and intermolecular self-assembly.[44] Molecules used for intramolecular self-assembly are often complex polymers with the ability to assemble from the random coil conformation into a well-defined stable structure (secondary and tertiary structures). Intermolecular self-assembly is the ability of the molecules to form supramolecular assemblies (quarternary structure).

Self-assembly is mainly influenced by three different factors:[18, 39-41]

a. Driving force: Hydrogen bonds are the most common driving force for the self-assembly processes and are responsible for the stability of self-assembled structures, e.g., the DNA double helix (Figure 1). Electrostatic forces and coordination bonds are the other two basic driving forces. The ability to form self-assembled structures and the stabilities of the structures are closely related to the kind and strength of the driving forces.

b. Concentration of the components: The concentrations of the different components play an very important role in the self-assembly. The change of the concentration ratio of the different components in the self-assembling system always lead to a dominant change in the self-assembled structure.

c. Solvent: Solvent can influence the self-assembly process by affecting the effective concentration of the different components and by competing for binding with the host and/or guest species. Different solvents can be used to obtain the optimum conditions for self-assembly.

Self-assembled structures are formed in nature. A good example is naturally occurring DNA, which is the most famous self-assembling structure in biological systems. DNA exists in a double helical form (Figure 1-1-a).[45-46] The two single strands are held together by a number of hydrogen bonds, involving acidic hydrogen atoms (hydrogen bonding donor), oxygen (hydrogen bonding acceptor), and nitrogen atoms (hydrogen bonding acceptor) of the purine and pyrimidine

bases in order to maintain the helical structure. In this double helix, guanine (G) forms triple hydrogen bonds with cytosine (C), and adenine (A) forms double hydrogen bonds with thymine (Figure 1-1-b). Guanine selectively interacts with cytosine because the G-C complex is much more stable than the G-T complex which would form only one hydrogen bond. Similarly, adenine exclusively complexes with thymine because adenine would form no hydrogen bonds with cytosine. Indeed, in the living world, both structural and functional features of biological assemblies are mainly generated through self-assembly processes. Thus, self-assembly is a very powerful strategy for the generation of structural and functional complexity.

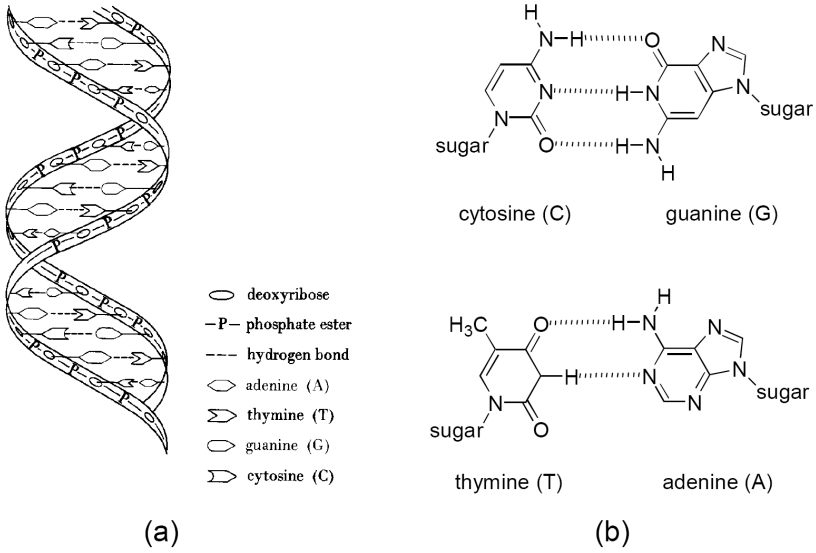

Figure 1-1. a) Representative cartoon of DNA helical structure and b) Base pairing in DNA (guanine and cytosine form triple hydrogen bonds; adenine and thymine form double hydrogen bonds).[46]

1.3 Pseudorotaxanes

A very important construct in supramolecular chemistry is the pseudorotaxane[23] (Figure 1-2). A pseudorotaxane is a supramolecular species consisting of a linear molecular component (guest) encircled by a macrocyclic component (host). Since the linear guest molecules can dethread and rethread, the pseudorotaxane is always in equilibrium with its two components-the host and the guest. If a bulky stopper, whose size is much bigger than the central cavity size of the host, is

attached to one end of the linear guest, a semi-rotaxane will be afforded. If two bulky stopper are attached to both ends of the linear guest in the pseudorotaxane, a rotaxane will be obtained. Since bulky stoppers can prevent the dethreading and rethreading, a rotaxane is viewed as a compound comprised of two mechanically linked single molecules. If a ring closure reaction is applied on a pseudorotaxane, a catenane will be formed. In addition, the introduction of pseudorotaxanes, rotaxanes and catenanes into polymers leads to formation of polypseudorotaxanes, polyrotaxanes and polycatenanes. Thus, pseudorotaxanes are fundamental precursors for advanced supramolecular species. In addition, pseudorotaxanes have been widely employed as molecular machines which can be controlled by external stimuli, such as: electrochemical control,[47] pH-changes[48-49] and other stimuli.[50-51] Therefore, the design and preparation of novel pseudorotaxanes are very important and attractive.

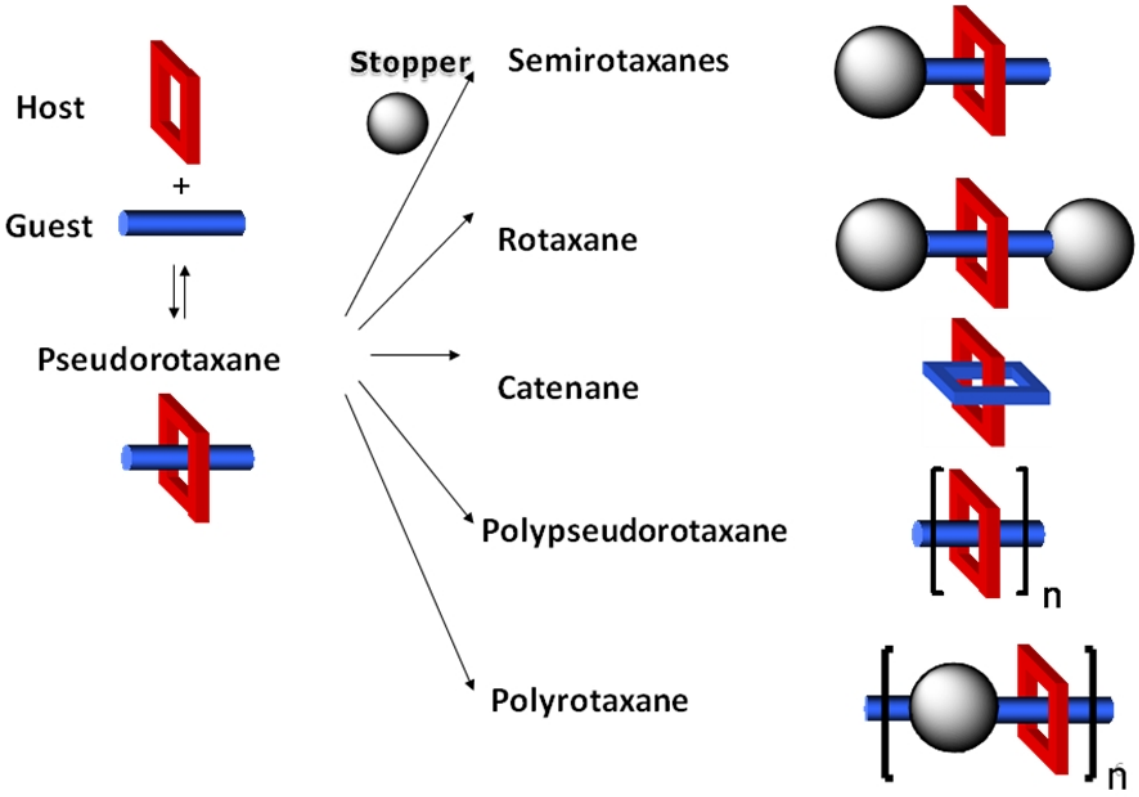

Figure 1-2. Representative cartoons of the structures of pseudorotaxanes, rotaxanes, catenanes, polypseudorotaxanes and polyrotaxanes.

1.3.1 Determination of Association Constants (K_a)

Because a pseudorotaxane always is in equilibrium with the host and guest molecules, association constants (K_a) (equation 1-a in Scheme 1, "f" represent the uncomplexed or free species in the systems.) are calculated to evaluate the equilibrium and the stability of the complex. A high association constant means strong complexation and high stability of the corresponding pseudorotaxane structure. Thus, the association constant (K_a) is an important parameter to measure the thermal stability of pseudorotaxane and it can be determined by nuclear magnetic resonance (NMR), isothermal titration calorimetry (ITC) and ultraviolet–visible spectroscopy (UV-vis).[52-55] Since the NMR method is the major tool I used to determine K_a values in this dissertation, I will mainly talk about it.

$$\mathbf{Host_f + Guest_f} \overset{K_a}{\rightleftharpoons} \mathbf{Pseudorotaxane}$$

$$K_a = \frac{[Pseudorotaxane]}{[host]_{free}[guest]_{free}} \qquad (1\text{-a})$$

When the NMR method is employed to determine the K_a values of pseudorotaxanes, there are two cases: slow exchange and fast exchange (Figure 1-3). In the case of slow exchange, the host/guest equilibrium has a very slow exchange rate compared with NMR time scale and thus two sets of peaks show up. One set of peaks represent the complexed species in the complex and the other one represent the uncomplexed/free species. Both sets of peaks can be integrated independently. In this case, single point method can be used to determine K_a. The integration ratio (b) between complexed and uncomplexed/free species equal to the concentration ratio between the complexed species and uncomplexed/free species (equation 1-b). If the initial concentration of host ($[Host]_0$) and guest ($[Guest]_0$) are known, K_a can be determined by using equation 1-c. In the case of fast exchange, the host/guest equilibrium has a faster exchange rate compared with NMR time scale and thus only one set of time-averaged peaks can be observed (Figure 1-3). As a result, the single point method can not be used. Continuous titration methods must be employed to determine K_a. First, the initial concentration of host or guest is kept constant. For example, If the initial concentration of host ($[Host]_0$) is fixed, ^{1}H-NMR characterizations were done on mixture solutions with constant $[Host]_0$ and varied $[Guest]_0$. Based on these NMR data, the variation of chemical shift (Δ) can be determined as $\delta_u - \delta_c$, where

δ_u is the chemical shift of peaks corresponding to the uncomplexed/free host and δ_c is chemical shifts of time-averaged partially complexed peaks. Then, Δ_0, the difference in δ values for protons of host in the uncomplexed and fully complexed species, was determined as the y-intercept of a plot of $\Delta = \delta - \delta_u$ *vs.* $1/[Guest]_0$ in the high initial concentration range of the guest. Then, *p*, the percentage of complexed species, can be calculated as $p = \Delta/\Delta_0$ (1-d). Based on *p*, K_a can be calculated by employing equation 1-e. Commonly, the NMR method can be used to determine K_a up to 5×10^4 M^{-1}. However, this method is more accurate in the low range of K_a ($< 10^4$ M^{-1}). [52-55]

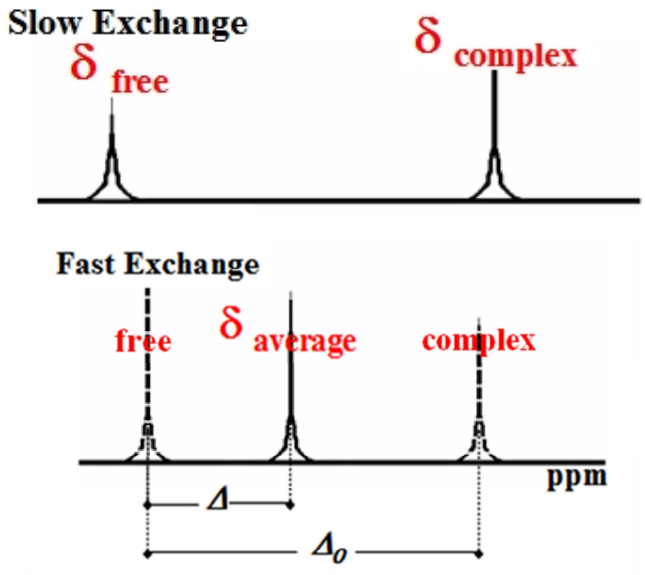

Figure 1-3. A cartoon depiction of ^{1}H-NMR spectra for: slow exchange and fast exchange.

$$b = \frac{\text{Int}_{\text{complex}}}{\text{Int}_{\text{free}}} = \frac{[\text{Host}]_c}{[\text{Host}]_f} \qquad (1\text{-b})$$

$$\therefore \quad K_a = \frac{\text{Int}_{\text{complex}}}{[\text{Guest}] * \text{Int}_{\text{free}}} = \frac{b}{\{[\text{Guest}]_0 - b * [\text{Host}]_0\}} \qquad (1\text{-c})$$

$$p = \text{percent complexed} = \frac{\Delta}{\Delta_0} \qquad (1\text{-d})$$

$$K_a = \frac{p}{\{(1-p)\} * \{[Guest]_0 - p * [Host]_0\}} \qquad (1\text{-e})$$

Isothermal titration calorimetry (ITC)[56-58] is an efficient and low cost method to

determine K_a compared with the NMR method. In addition, it has a widely applicable window (can determine K_a in the range of 10^2 to 10^9 M^{-1}). The isothermal titration calorimeter consists of two separate identical cells-a sample cell and a reference cell, which are made of highly-efficient thermally conductive materials, in the same a adiabatic chamber. Highly sensitive thermopile circuits are equipped to measure the temperature differences between two cells. During the experiment, first, a constant power is put on the reference cell, directing a feedback circuit and activating a heating circuit around the sample cell. Then, a host (or guest) solution in a stirring syringe is titrated into the guest (or host) solution in sample cell in precisely known volume and the complexation behavior between host and guest causes heat to be either released or absorbed. The time-dependent input power to maintain equal temperatures between the two cells is monitored. Following the continuous injection of host (or guest), the amount of free/uncomplexed macromolecule in sample cell decreases accordingly and the amount of heat released or absorbed become small gradually. The association constant K_a can be determined by non-linear least squares curve-fitting using a suitable model.[59-60] For example 1:1 binding:

$$\frac{\Delta Q}{\Delta [G]_t} = \frac{\Delta H^0 V_0}{2} \{1 + \frac{1 - [G]_t/[H]_t - n/K_a[H]_t}{\sqrt{1 + [G]_t/[H]_t + n/K_a([H]_t)^2 - 4[G]_t/[H]_t}}\} \qquad \text{(1-f)}$$

Where, [G]t and [H]t are the total guest and host concentrations, respectively, V_0 is the effective volume of the sample cell, and ΔQ is the heat change for each injection during the titration.

The ultraviolet–visible spectroscopic (UV-vis) method, which employs the same mathematical treatments as NMR method, is another effective method for association determination. It requires independent signals for the free and complexed species. UV-vis is more sensitive than the NMR method and thus can determine K_a at very low concentrations compared with NMR method. However, the UV-vis can not be used for light-sensitive complex systems.

1.4 Rotaxanes

The word “Rotaxane” is derived from the Latin words “rota” and “axis” meaning wheel and axle, respectively. The three most common methods of rotaxane self-assembly are clipping, slipping and threading, as shown in Figure 1-4. The threading approach is a two-step process

beginning with pseudorotaxane formation and subsequent attachment of two bulky stopper groups to the ends of the linear guest species. As for the slipping approach, heating of the system is required to allow slippage of the cyclic species over the bulky end groups of the linear species to form the rotaxane. This reversible slippage process depends heavily on the selection of host/guest/bulky end group, reaction medium and temperature. The clipping approach uses the linear guest species to partially complex with part of the cyclic host species. The ends of the templated precursor species then react with another molecule to form the full cyclic species, now threading completely to form the rotaxanes. Generally speaking, the threading approach is the most commonly used method due to its relatively high synthetic efficiency. The first rotaxane was prepared by Harrison via the threading approach.[61] Catenanes are another type of very interesting supramolecular species, which will be discussed in chapter 2.

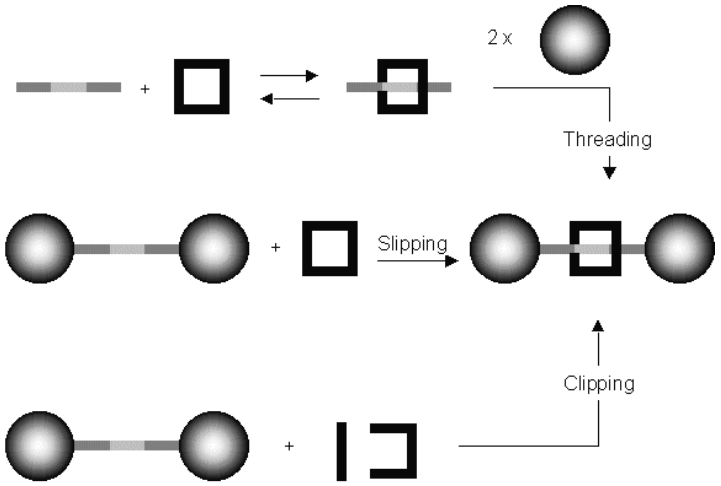

Figure 1-4. Synthetic strategies to prepare rotaxanes: clipping, slipping and threading.

1.5 Polypseudorotaxanes and polyrotaxanes

Based on the pseudorotaxanes and rotaxanes, polypseudorotaxanes and polyrotaxanes are formed simply by incorporating pseudorotaxane and rotaxane moieties into polymers.[24a] Because the main chains or side chains in the polypseudorotaxanes and polyrotaxanes are connected by non-covalent linkages, the architectures of the polypseudorotaxane and polyrotaxane molecules are different from traditional polymers that only bear covalent linkages. As a result,

polypseudorotaxanes and polyrotaxanes are expected to have some unique properties compared with traditional polymers.[24-25]

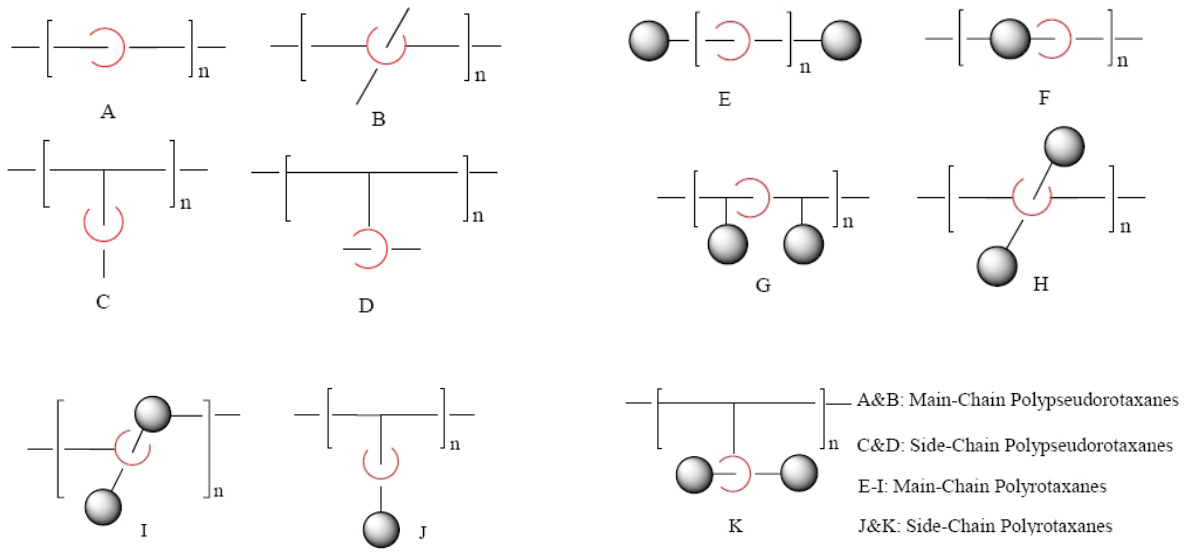

Figure 1-5. Various types of polypseudorotaxanes and polyrotaxanes. (Reprinted with permission from ref. 24a © Elsevier).

According to the location of the pseudorotaxane and rotaxane units, the polypseudorotaxanes and polyrotaxanes can be simply divided into two major types: main-chain polypseudorotaxanes/polyrotaxanes and side-chain polypseudorotaxanes /polyrotaxanes (Figure 1-5). In the main-chain polypseudorotaxanes/polyrotaxanes, the pseudorotaxane/rotaxane repeating units are incorporated in the main chains of the polymer. In the side-chain polypseudorotaxanes /polyrotaxanes, the pseudorotaxanes and rotaxanes repeating units are located in the side chains of the polymer.

2.4.1 Main-chain polypseudorotaxanes and polyrotaxanes

For the main-chain polypseudorotaxane and polyrotaxanes, there are several different ways[24a] to make them. As shown in Scheme 1-1, Route Ⅰ involves the polymerization of pseudorotaxanes. Route Ⅱ involves threading of a macrocyclic host onto existing polymer main chains. Route Ⅲ is performed by the polymerization of existing rotaxanes. Route Ⅳ involves the polymerization of chain molecules, bulky stoppers and macrocycles. Route Ⅴ involves the

polymerization of host macrocycles of existing pseudorotaxanes. In route Ⅵ, the molecules of the guest thread into the macrocycles of the polymer main chains and then bulky stoppers are introduced to produce polyrotaxanes. In route Ⅶ, polymerization of macrocycles in the rotaxane monomers are used to form polypseudorotaxanes. Route Ⅷ involves polymerization of pseudorotaxane monomers with functional groups in the macrocycles and bulky stoppers. The syntheses of main-chain polypseudorotaxanes/polyrotaxanes are mainly based on crown ethers,[62-64] cyclodextrins,[65-68] cyclobisparquets,[69] and calixarenes.[70]

2.4.2 Side-chain polypseudorotaxanes and polyrotaxanes

As for the side-chain polypseudorotaxanes and polyrotaxanes, the pseudorotaxane and rotaxane repeating units are located in the side chains of the polymer. Several routes[24a] (see Scheme 1-2) have been employed to synthesize the side-chain polypseudorotaxanes and polyrotaxanes: In route i, side chains of the existing polymer main chain are threaded into the macrocyclic monomers to form the polypseudorotaxanes and further produce the polyrotaxane by introducing bulky groups to the ends of the side chains. Route ii involves reactions between an existing polymer with functional side groups and semi-rotaxanes with functional groups at the opposite end of the bulky end. In route iii, linear molecules (guests) thread into the macrocycles on the side chains of an existing polymer to produce polypseudorotaxanes and further polyrotaxanes are formed by introducing bulky groups at the end of the linear molecules. Route iv involves reactions between an existing polymer with functional side groups and rotaxanes with functional groups on the macrocycles. From v to viii, polypseudorotaxanes or polyrotaxanes are formed by the homopolymerization of the pseudorotaxane or rotaxane monomers. Up till now, side-chain polypseudorotaxanes and polyrotaxanes are synthesized mainly based on crown ethers[71-73] and cyclodextrins.[74-76]

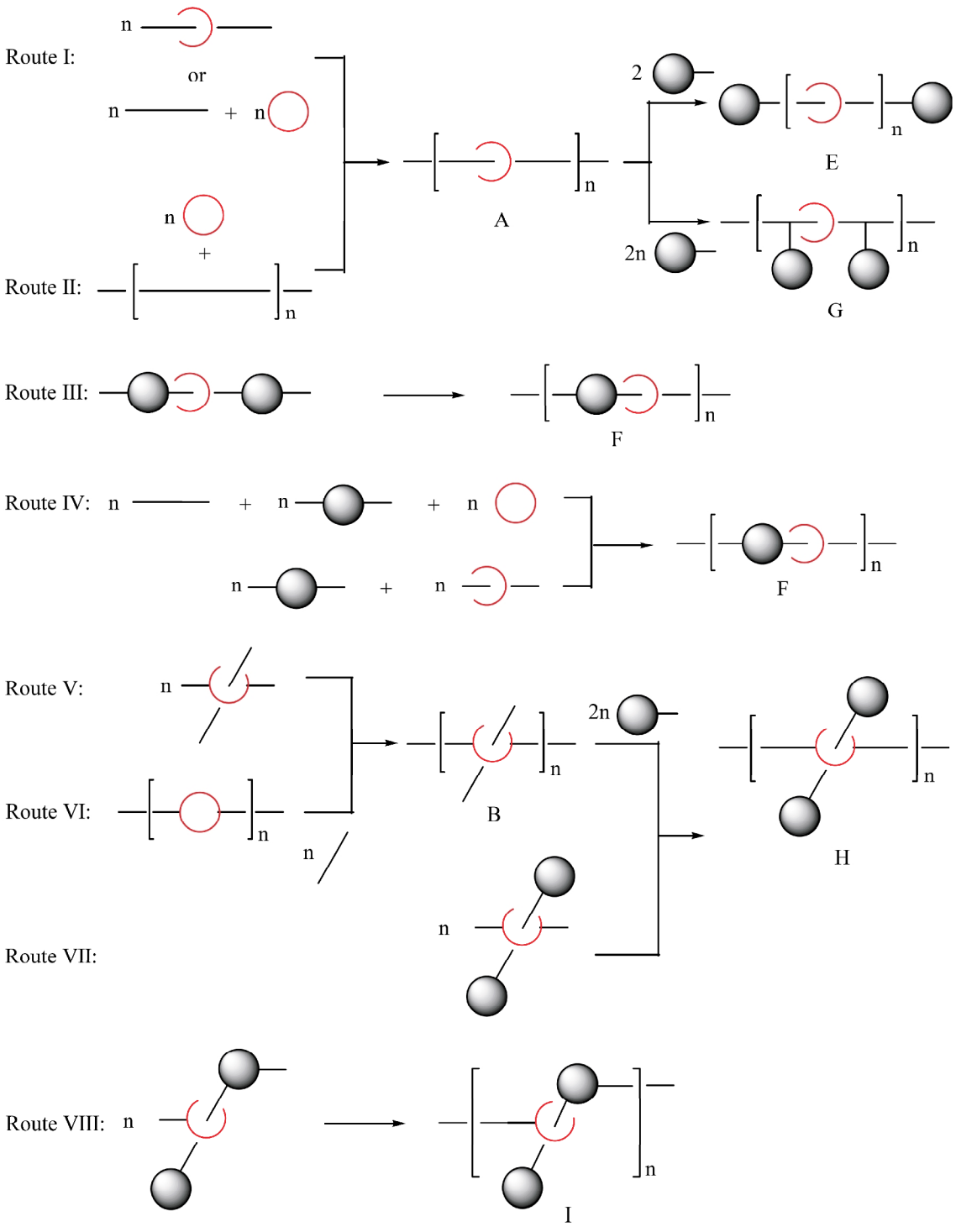

Scheme 1-1. Synthetic routes for main-chain polypseudorotaxanes and polyrotaxanes. (Reprinted with permission from ref. 24a© Elsevier).

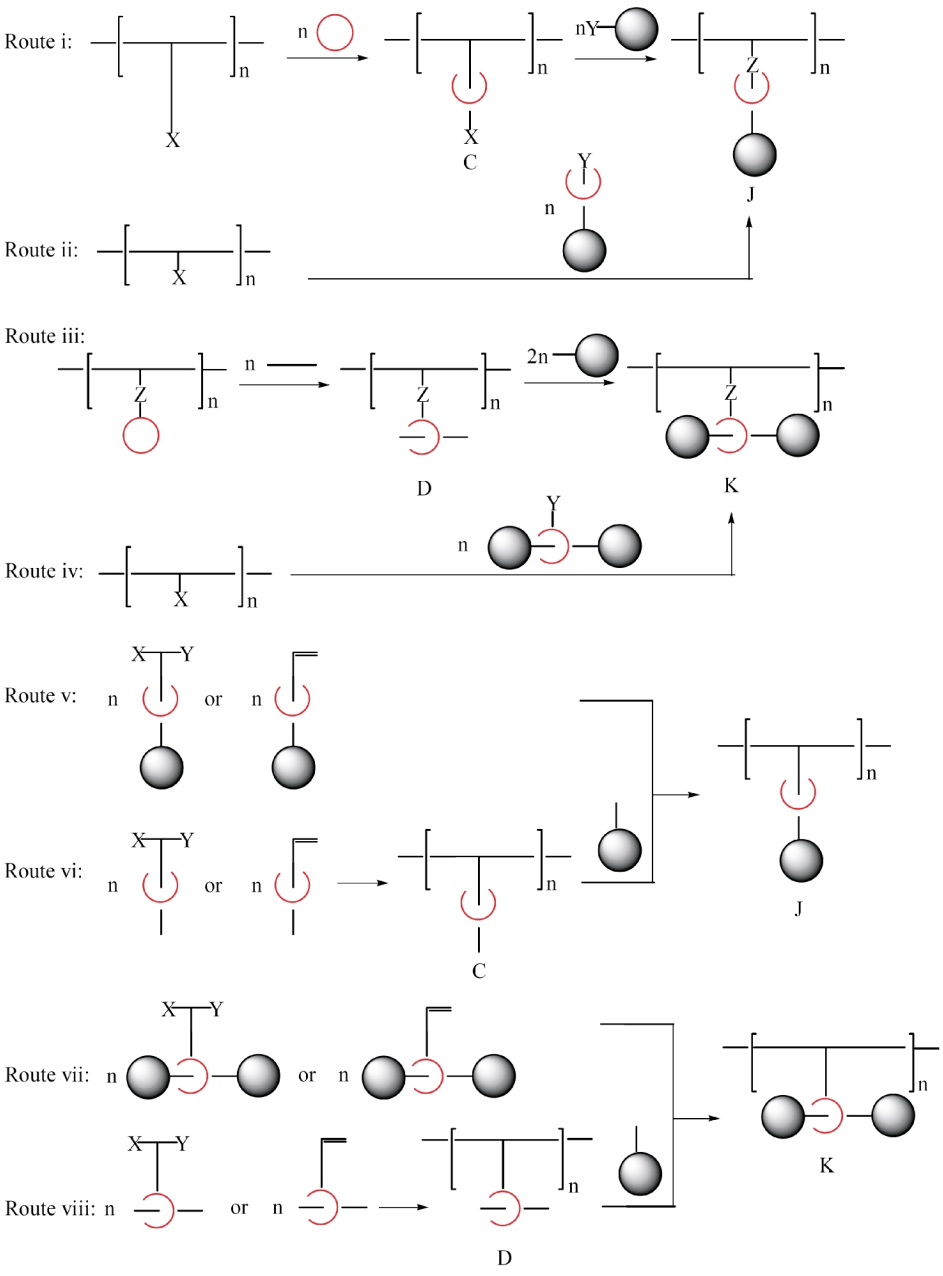

Scheme 1-2. Synthetic routes for side-chain polypseudorotaxanes and polyrotaxanes. (Reprinted with permission from ref. 24a© Elsevier).

1.5.3 Properties and potential applications

Compared with common polymers or molecules that only have covalent linkages, polypseudorotaxanes and polyrotaxanes have two types of linkages-covalent and noncovalent in the same polymer chains. As a result, there are tremendous differences in properties:

a. Solubility: The solubility of polypseudorotaxanes and polyrotaxanes always are very different from their components. The best examples are systems based on cyclodextrins. Not similar to their parent polymers which always are hydrophobic and insoluble in the polar solvents, the cyclodextrin-based polypseudorotaxanes and polyrotaxanes can be dissolved in polar solvents because of the high polarity of the exterior of the cyclodextrins.[77-79] Also, because hydrogen bonds can be formed between crown ethers and polar solvents, the solubility of crown ether-based polypseudorotaxanes and polyrotaxanes improve to some extent.[63,80] These properties can be used to make biodegradable materials.[78-79]

b. Stability: Noncovalent bonds in the main chains or the side chains make polypseudorotaxanes and polyrotaxanes more stable thermodynamically than the parent compounds which lack noncovalent bonds. Yui's[81-82] and Kim's[83] works provide strong evidence for this conclusion.

c. Viscosity: The viscosity of polypseudorotaxanes and polyrotaxanes mainly depend on the properties of macrocyclic components and polymer backbone, degree of threading and the types of solvent. Gibson and co-workers[84] found that a high degree of threading leads to high intrinsic viscosity. They believed several factors contributed to this phenomenon. Threading will lead to high solvated volume, chain extension as a result of ionic repulsion, and a high repulsive force results from as increase of threading. They also found that poly(ester rotaxane)s have higher intrinsic viscosities than their parent polymers because of the increase of hydrodynamic volume arising from the presence of the cyclic components.[63] Due to the differential solvation of the linear and cyclic components, the types of solvents can also affect the viscosity of polyrotaxanes.[63] Unlike the solution viscosity results, Gibson's group found that the melt viscosity of poly(ester rotaxane)s was lower than that of the corresponding polymer due to the decrease of polymer chain entanglements caused by the cyclic components.

d. Phase behavior - glass transition temperatures (T_g) and melting points (T_m): The glass transition temperature and melting point are two important parameters in polymer science. The T_g change resulting from threading depends on the miscibility of the cyclic species and the polymer backbone. If they are compatible, only one phase will be present and only one T_g value will be observed. If they are immiscible, two phases will be present and two T_gs will be observed. One T_g will correspond to the polymer backbone and the other T_g will be related to the cyclic component. Similar to T_g, T_m also depends on the miscibility of the cyclic species and the polymer backbone. The cyclic component can aggregate along the polymer backbone. If the cyclic component and polymer backbone are immiscible, two T_ms will be observed.[63,80,85]

e. Photoelectronic properties: Photo- and electronically-active elements can be introduced into polypseudorotaxanes and polyrotaxanes and further photoelectronic properties can be studied. Sauvage's group made some conducting polyrotaxanes and found that Cu(1) binding was reversible only if lithium was present during copper removal.[86] Ueno *et al.* synthesized a series of polyrotaxanes as a light-harvesting antenna model. They found that the antenna effect becomes more marked with increasing number of naphthalene-appended α-CD units in the polyrotaxanes, but energy transfer efficiency decreases.[87-89]

1.6 Crown ethers and crown ether-based cryptands

1.6.1 Crown ethers

Crown ethers are cyclic compounds containing several ethyleneoxy linkages around a central cavity. Because the ethyleneoxy linkages are relatively chemically inert and the central cavity is electronegative, crown ethers can bind the guest without reacting with it. The first crown ether-dibenzo-18-crown-6 was discovered by Charles Pederson in 1967 (Scheme 1-3)[13,14] and he won Nobel prize for chemistry in 1987 due to his pioneering work in crown ether/metal ion complexes. Crown ethers are name as x-crown-y: x is the total number of atoms in the ring and y is the total number of the oxygen atoms in the ring. For example, dibenzo-18-crown-6 (Scheme 1). Crown ethers have the following advantages: (a) Crown ethers can be designed. (b) Various functional groups can be introduced into crown ethers to prepare functionalized crown

ethers. (c) Crown ethers are compatible with organic solvents and thus have good solubility in most organic solvents.

The initial synthesis of crown ether dibenzo-18-crown-6 was by accident. Pederson attempted to prepare diphenol **5** via the reaction between tetrahydopyran ring protected catechol derivative **1** and dichloride **3**. However, the starting material was contaminated by pyrocatechol **2**. After reaction, Pederson noticed that small amount of dibenzo-18-crown-6 (**4**) (0.4% yield) coexisted with major product **5**. Obviously, the discovery of the first crown ether owes to Pederson's academic rigor.

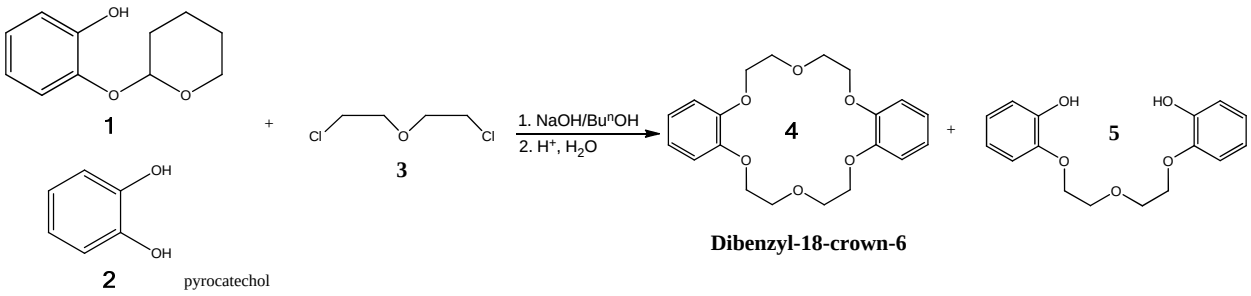

Scheme 1-3. Synthesis of dibenzo-18-crown-6 (**4**).

Commonly, crown ethers are synthesized via routes a-e, as shown in Figure 1-7. Route-a is a typical so-called "one-step" method. First two kinds of half-cycle precursors bearing different type of functional end groups are prepared. Then, the crown ether is afforded via the coupling reaction between the two kinds of half-cycle precursors. Route-b is another typical "one-step" method. Two half-cycle difunctionalized precursors are linked by a linear difunctionalized molecule and the crown ether is obtained accordingly. In route-c, a half-cycle precursor with one functional end group and one protected functional group is prepared. Then the half-cycle precursor reacts with difunctional linear molecule and a double-size half-cycle precursor with two protected functional end groups is afforded. After a deprotection reaction, the double-size half cycle molecules bearing two functional end group react with another linear difunctional linear molecule and the crown ether is obtained. Route-d is similar to

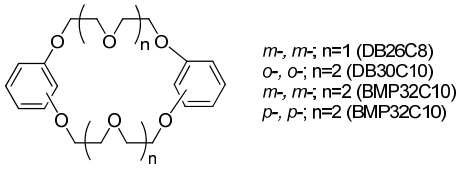

Figure 1-6. Chemical structures of representative dibenzo-crown ethers.

router-a. A half-cycle precursor bearing two different type of functional end groups is prepared first. Then, the coupling reaction between two precursors gives crown ether. In route-e, the two functional end groups of the same half-cycle precursor react with each other and crown ether is formed accordingly. Among them, route-b and route-c are the most commonly used methods to prepare crown ethers. It should be noted here that high dilution or pseudo-high dilution (via slow addition with a syringe pump) conditions are almost always required during the synthesis of crown ethers in order to minimize the formation of linear side-products and increase the final yield. After the discovery of DB24C8, some phenylene crown ethers (Figure 1-6) were designed and prepared from resorcinol residues and dibromo-poly(ethylene glycol)s. However, these unfunctionalized simple crown ethers have limited applications. If we want to prepare advanced supramolecular species, such as polycrown ethers and cryptands, difunctional crown ethers are required. The Gibson group worked intensively on preparation of difunctionalized crown ethers during last two decades.

The Gibson group explored the regiospecific synthesis of difunctional dibenzo-24-crown-8 (DB24C8) derivatives and established a highly-efficient templating method (Route-c in Figure 1-7) to prepare *cis*-DB24C8 dimethyl ester (**6**) (Scheme 1-4).[90] **6** was produced in 5 days with 77% overall isolated yield based on methyl 3-hydroxy-4-benzyloxybenzoate. During the reaction, the key synthetic step is the last cyclization step which was templated by potassium ion and did not require the use of high dilution or pseudo-high dilution protocols. *cis*-DB24C8 dimethyl ester (**6**) is converted to *cis*-DB24C8 diol (**7**) in quantitative yield via $LiAlH_4$ reduction. Similarly, *cis*-DB24C8 diacid (**8**) could be made in quantitative yield via the hydrolysis of *cis*-DB24C8 dimethyl ester (**6**).

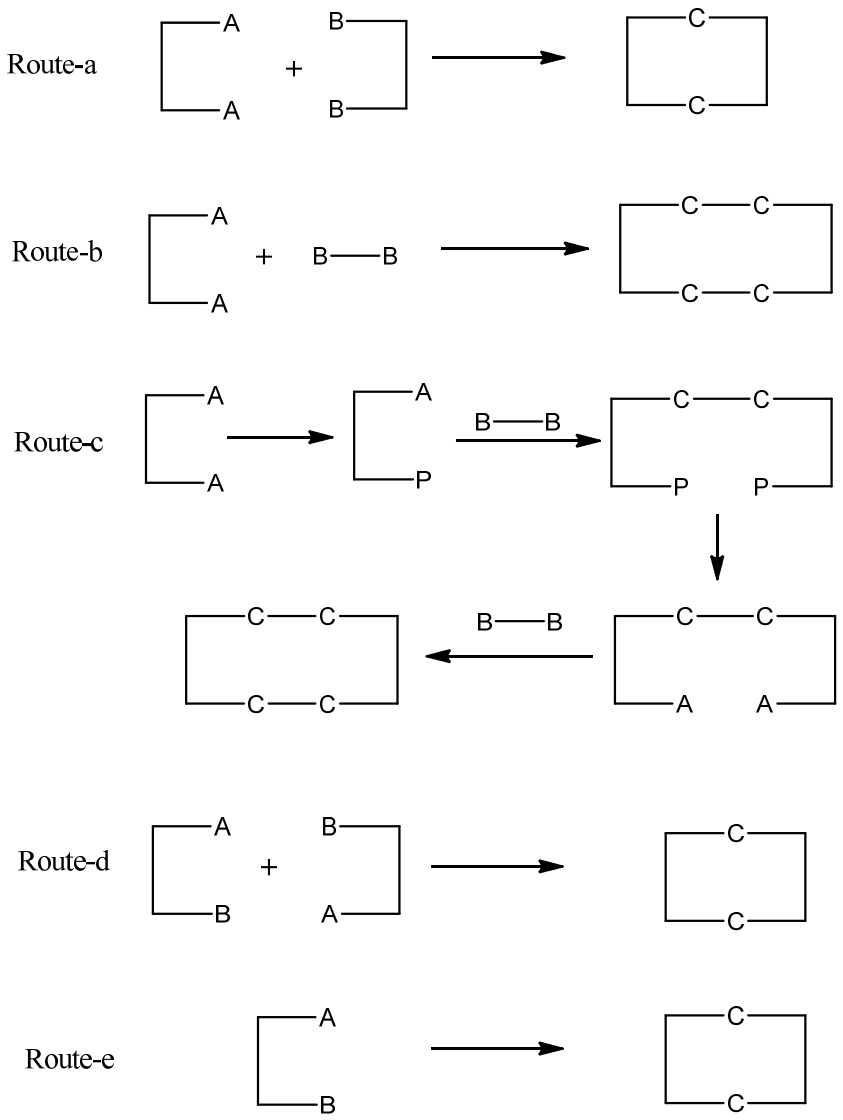

Figure 1-7. Synthetic routes for crown ethers. Functioanl group A reacts with functional group B giving group C. P represents protected functional group.

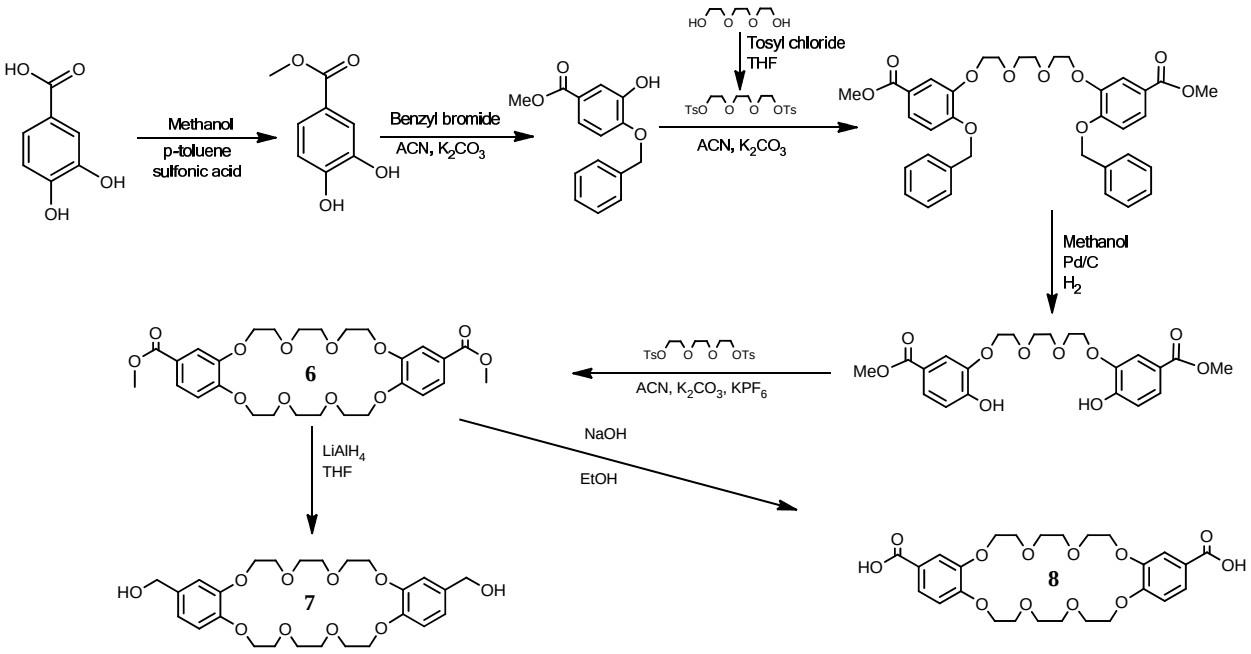

Scheme 1-4. Synthesis of *cis*-DB24C8 derivatives (**6-8**) via templating method.

By employing route-d in Figure 1-7, *trans*-DB24C8 dimethyl ester (**11**) was prepared by Wang *et al.* (Scheme 1-5).[38d, 90] First, the half-cycle precursor **9** bearing a hydroxyl group and a chloride was prepared. Then, the coupling reaction between two **10** molecules gave *trans*-DB24C8 dimethyl ester (**11**). The synthesis took 3 days and produced **11** in 33% overall yield based on methyl 3-hydroxy-4-benzyloxybenzoate. Similarly, **11** could be converted into *trans*-DB24C8 diol (**12**) and *trans*-DB24C8 diacid (**13**) via $LiAlH_4$ reduction and hydrolysis, respectively.

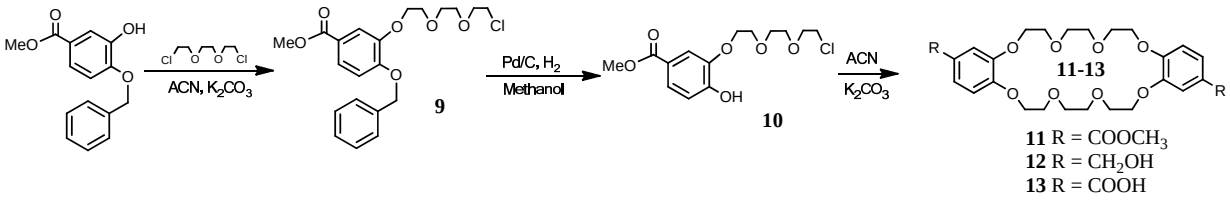

Scheme 1-5. Synthesis of *trans*-DB24C8 derivatives (**11-13**).

One step forward, the Gibson group successfully prepared *cis*-dibenzo-30-crown-10 (*cis*-DB30C10) derivatives in high yield by employing a similar regiospecific synthetic method (Scheme 1-6).[91] Similar to route-c in Figure 1-4, the diprotected half-cycle precursor **14** was prepared first in 80% yield based on methyl 3-hydroxy-4-benzyloxybenzoate. **14** was converted

into **15** bearing two hydroxyl groups after the deprotection reaction. **15** reacted with tetra(ethylene glycol) ditosylate and *cis*-DB30C10 dimethyl ester (**16**) was obtained in 65% overall yield based on 3-hydroxy-4-benzyloxybenzoate. *cis*-DB30C10 diol (**17**) was obtained in quantitative yield by $LiAlH_4$ reduction.

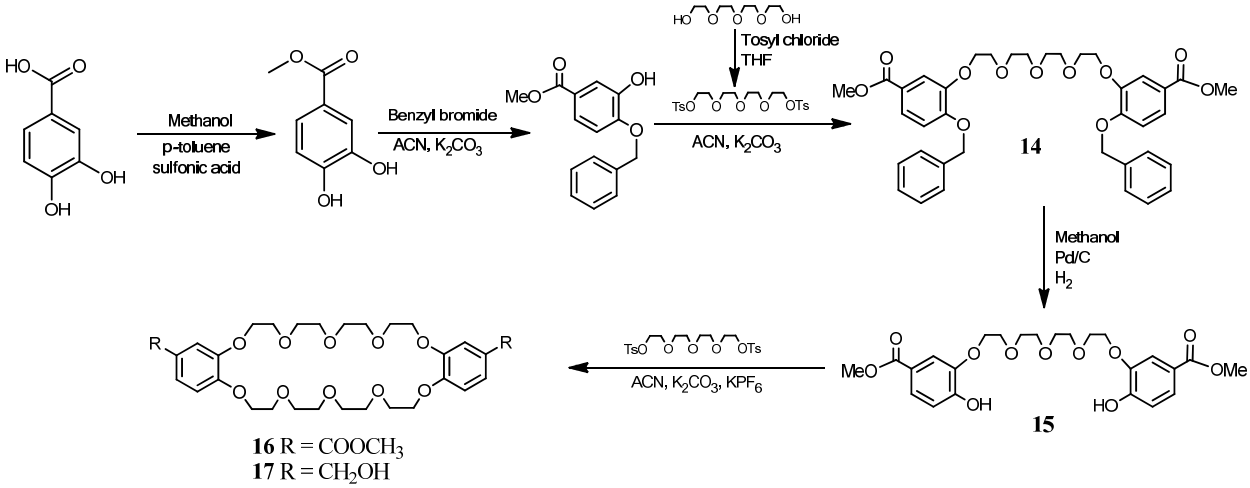

Scheme 1-6. Synthesis of *cis*-DB30C10 derivatives (**16-17**).

Since the first discovery of bis(*meta*-phenylene)-32-crown-10 (BMP32C10) by Stoddart *et al.*, BMP32C10 became an important member of crown ether family and attracted more and more attention during last several decades due to its relative good binding ability for paraquat derivatives. Gibson *et al.* optimized the synthesis of BMP32C10 dimethyl ester.[92] Two methods were explored (Scheme 1-7): the so-called "one step method" (Method I in Scheme) and a mutiple step method (Method II in Scheme). The one step method is the traditional method employed to prepare BMP32C10 (route-b). In the one step method, dimethyl 3,4-dihydroxybenzoate was coupled with tetra(ethylene glycol) dichloride directly and BMP32C10 dimethyl ester (**18**) was obtained in 9% yield based on the 3,4-dihydroxyl benzoate. In method II (route-c), a half-cycle precursor (**21**) was prepared first by the reaction between dimethyl 3,4-dihydroxybenzoate and tetra(ethylene glycol) dichloride. Then the cyclization reaction between **21** and dimethyl 3,4-dihydroxybenzoate afforded **18** in 29% overall yield. Similarly, BMP32C10 diol (**19**) and BMP32C10 diacid (**20**) could be prepared based on BMP32C10 dimethyl ester (**18**). It should be noted here that Gibson *et al.* first found that the complexes between BMP32C10 and paraquats form "taco"-shaped structures,[93a] instead of threaded-through "pseudorotaxane"

structures as determined cy X-ray crystallography (Figure 1-8). Although it was thought the "pseudorotaxane" structures coexisted with the "taco"-complex in the solution, after about a quarter century, only "taco"-shaped complexes had been reported.[93] It is important to clarify this problem in order to prepare advanced supramolecular polymers based on BMP32C10 and paraquats, such as star-shaped polymers and brush-shaped polymers.

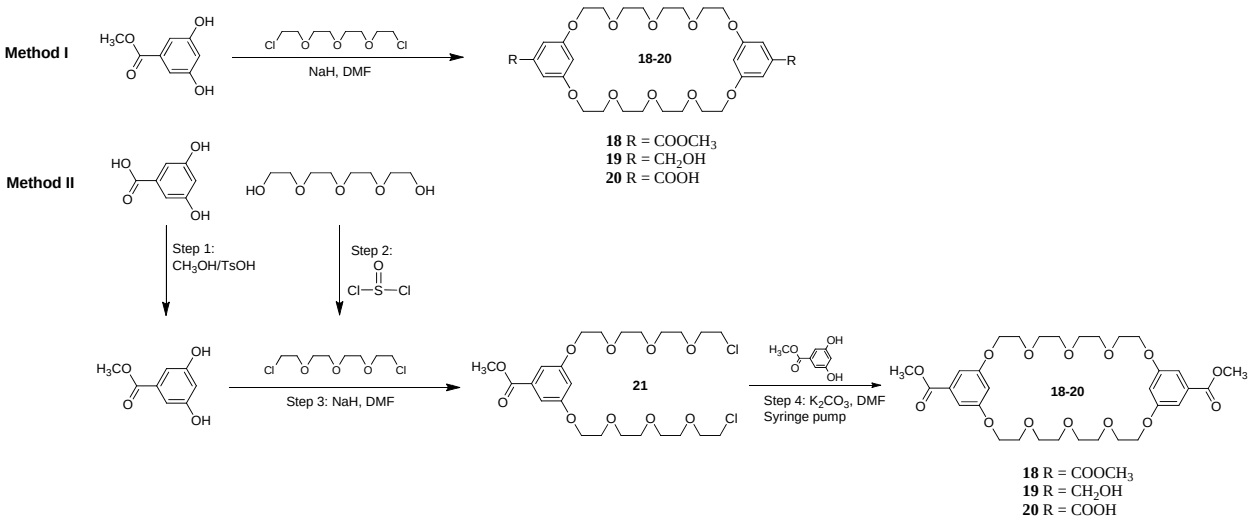

Scheme 1-7. Synthesis of BMP32C10 derivatives (**18-20**).

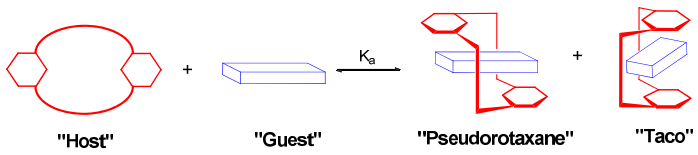

Figure 1-8. Cartoon representations of possible co-conformations of host-guest complexes: "[2]pseudorotaxane" and "taco" geometries.

Stoddart's group designed and prepared another difunctional crown ether - bis-*p*-phenylene-34-crown-10 (BPP34C10) dimethyl ester by employing route-c (Scheme 1-8)..[94] Based on methyl 2,5-dihydroxybenzoate, the half-cycle precursor **22** bearing two protected hydroxyl groups was prepared first. Upon hydrogenolysis, the two hydroxyl groups of **23** were deprotected and half-cycle precursor **24** bearing two hydroxyl groups was obtained. **23** reacted with tetra(ethylene glycol) ditosylate and BPP34C10 dimethyl ester (**24**) was obtained in 40% overall yield based on methyl 2,5-dihydroxybenzoate. One step forward, Stoddart *et al.*

successfully prepared a BPP34C10 tetramethyl ester via route-b (Scheme 1-9). Via the reaction between dimethyl 2,5-dihydroxyterephthalate and tetra(ethylene glycol) ditosylate, BPP34C10 tetramethyl ester (**25**) was prepared in 12% yield.

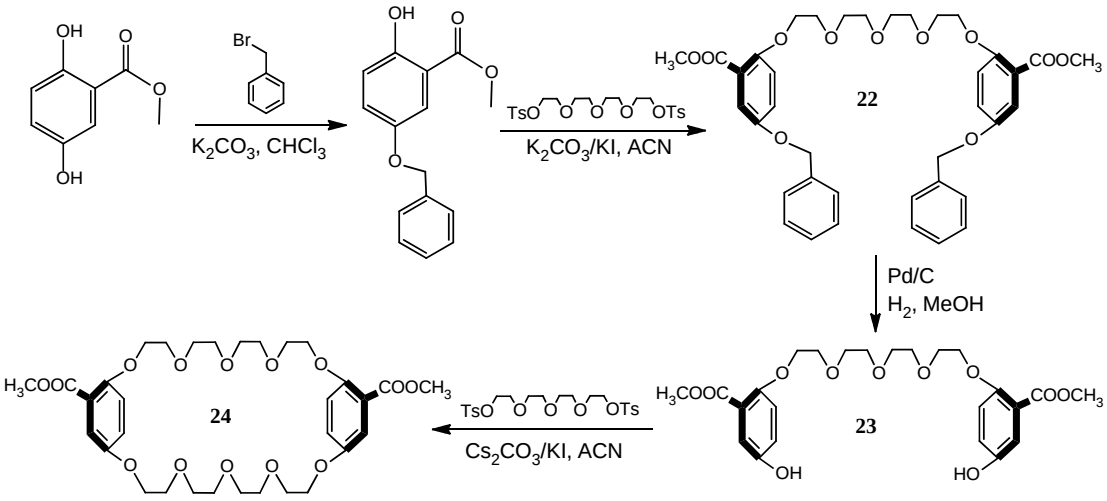

Scheme 1-8. Synthesis of BPP34C10 dimethyl ester (**24**).

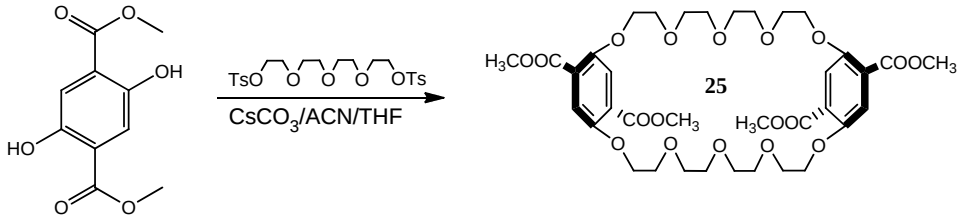

Scheme 1-9. Synthesis of BPP34C10 tetramethyl ester (**25**).

1.6.2 Crown ether-based cryptands

Cryptands are the cyclic compound consisting two or more cycles. Compared with simple crown ethers, the cryptands have been proved to be much better hosts than crown ethers for paraquats.[38,95] As shown in Table 1-1, compared with the association constant (K_a) of BMP32C10 diol (**19**)/dimethyl paraquat (**28**) , the association constant (K_a) of cryptand **26**/**28** is about 100-fold increased and the association constant (K_a) of cryptand **27**/**28** is about 9000-fold

higher. As discussed before, a higher association constant (K_a) means the complexation is stronger and the resulting complex is more stable; **27/28** is 5.4 kcal/mol more stable than **19/28**. In order to prepare large and stable supramolecular species, high association constants (K_a) are always required. Obviously, cryptands give us a way to design and prepare more stable complex systems.

Why do cryptands have higher association constants (K_a) than the corresponding simple crown ethers? There are two reasons. First, cryptands have more or stronger binding sites compared with simple crown ethers. Compared with BMP32C10 diol (**19**), cryptand **26** has the third ethyleneoxy linkage, which provides extra binding sites for the threaded paraquat molecule. Cryptand **27** also has extra binding sites – including the nitrogen atom in the pyridine ring and the oxygen atoms in the ester groups. In addition, the nitrogen is a more effective binding site compared with oxygen atoms. Second, preorganization. For the simple crown ether- BMP32C10 diol (**19**), before complexation it must consume energy to adjust its conformation to bind dimethyl paraquat. However, the cryptands have been preorganized during synthesis and don't need to pay energy to change their confirmation. As a result, the binding abilities of the cryptands are much better than corresponding simple crown ethers and the association constants increase accordingly. Although cryptands have these advantages, the synthetically lower accessibility of cryptands[38,95] (e. g., **26**[38b] and **27**[38c] in 38% and 23% yields, respectively, from **1b**) has limited their further applications. During the synthesis of cryptand, high dilution conditions must be used in order to minimize the formation of linear oligomeric species. In order to save solvent and increase the yield, the pseudo-high dilution technique is always employed. The solutions of the two starting materials are added into a large volume of solvent containing only catalyst via syringe pump at a very low rate (commonly: 0.3-1.0 ml/hour). Each reaction takes at least two weeks and the final yield is still not good (generally: < 45%). Even though the pseudo-high dilution technique is used, the reaction is still solvent-consuming, generally speaking, 2000 mL – 3000 mL solvent is required to synthesize about a half gram of the cryptand. Obviously, the low yield become a bottle-neck for the further application of cryptands.

Table 1-1 Chemical structures of BMP32C10 diol (**19**), cryptand **26** and cryptand **27**. Crystal structure and association constant (K_a) between BMP32C10 diol (**19**), cryptand **26**, cryptand **27** and dimethyl paraquat (**28**) in acetone-d_6. (Crystal structures are reprinted with permission from ref. 95 and 38c © American Chemical Society).[38]

Chemical Structure Of Host	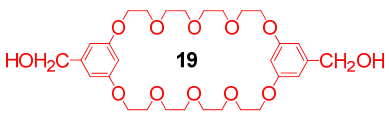	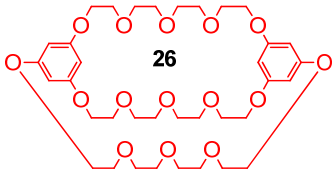	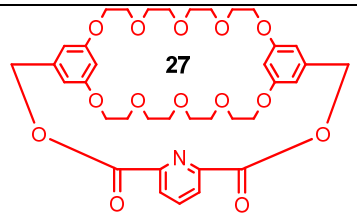
Chemical Structure Of Guest		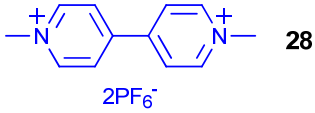	
Crystal structure	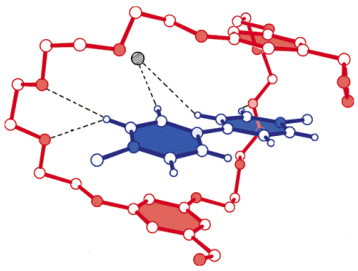	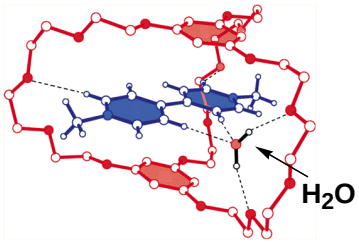	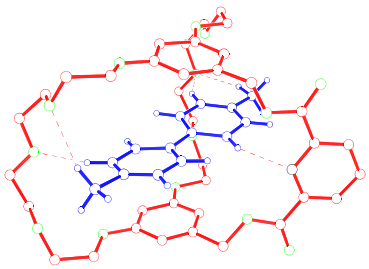
Association Constant (K_a)	5.6×10^2 M^{-1}	6.3×10^3 M^{-1}	5.0×10^6 M^{-1}
ΔG_{298K} (kcal/mol)	3.7	5.2	9.1

Wang *et al.* designed and prepared *cis*-DB24C8 based cryptand **29** and *trans*-DB24C8 based cryptand **30** via the reaction between *cis*-DB24C8 diol **7**/*trans*-DB24C8 diol **12** and pyridine-2,6-dicarbonyl dichloride, respectively.[38d,90] Association constants (K_a) between **29**/**30** and paraquat diol (**38**) were determined to be 1.0 x 10^4 M^{-1}/1.4 x 10^4 M^{-1} by the ^{1}H-NMR method, respectively. The limited cavity space of the cryptands **29**/**30** was thought to be the reason leading to modest K_a.

Pederson *et al.* reported the synthesis of *cis*-DB30C10-based cryptand **31**,[91] *cis*-DB27C9-based cryptand **32** and *cis*-DB27C9-based cryptand **33**.[96] Cryptand **31** demonstrated good

binding ability to dimethyl paraquat (**28**) (K_a = 2.0 × 10^5 M^{-1}) and paraquat diethanol (**38**) (K_a = 1.0 × 10^5 M^{-1}) in acetone. Interestingly, cryptand **31** showed the highest association constant (K_a = 1.9 × 10^6 M^{-1}) with diquat **40**. *cis*-DB27C9-based cryptand **32** exhibited improved complexation with dimethyl paraquat (**28**) (K_a = 2.4 × 10^5 M^{-1}) compared with **31**. However, **32** showed lower K_a values compared with **31** for the other guests - paraquat diethanol (**38**) and diquat **39**. Similarly, compared with **31**, *cis*-DB27C9-based cryptand **33** demonstrated much lower K_a values with all the three guests (Table 1-??).

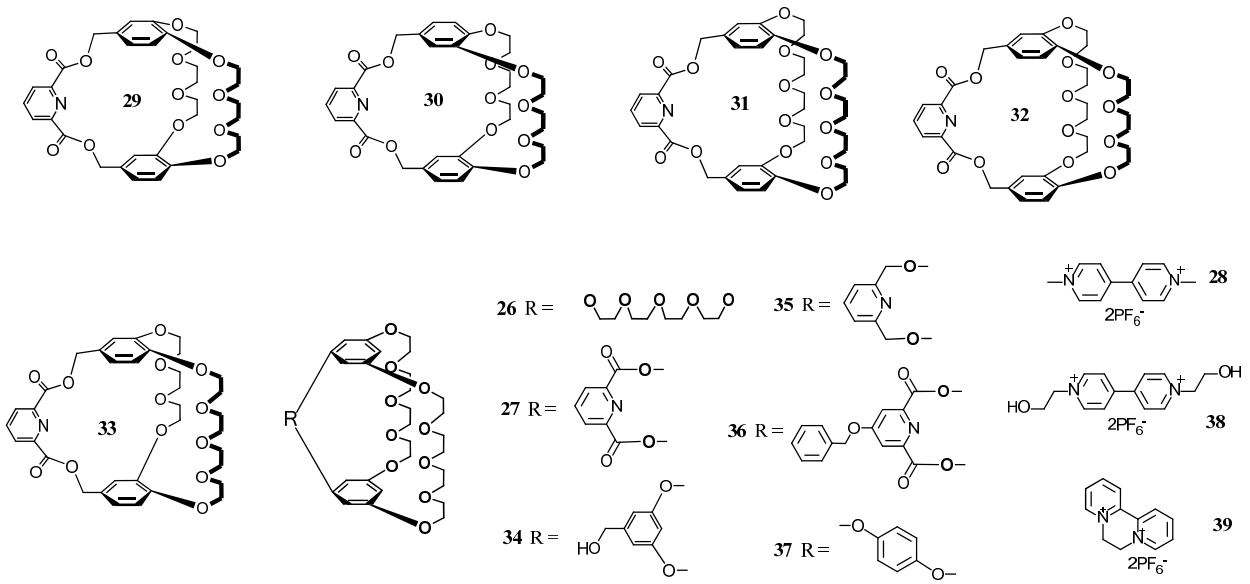

Figure 1-9. Chemical structures of *cis*-DB24C8-based cryptand **29**, *trans*-DB24C8-based cryptand **30**, *cis*-DB30C10-based cryptand **31**, *cis*-DB27C9-based cryptand **32**, *cis*-DB27C9-based cryptand **33**, BMP30C10-based cryptands **33-37**, dimethyl paraquat (**28**), paraquat diethanol (**38**) and diquat (**39**).

The Gibson group designed and prepared a series of BMP32C10-based cryptands **26**, **27**, and **34-38** during last decade (Figure 1-9). As expected, all of them demonstrated improved binding strength to the paraquat derivatives (Table 1-2) relative to simple crown ether analogs.

Table 1-2. Association constants of BMP32C10 based cryptands with dimethyl paraquat (**28**), paraquat diethanol (**38**) and diquat (**39**) determined by the NMR method in acetone-d_6 at room temperature.[38, 90-96]

Cryptand	K_a (M^{-1})		
	Dimethyl paraquat (**28**)	Paraquat diethanol (**38**)	Diquat (**39**)
26	6.0×10^4	6.0×10^4	4.3×10^4
27	5.0×10^{6} *	-	3.3×10^{5} *
34	6.3×10^3	-	-
35	9.4×10^3	-	7.4×10^3
36	9.0×10^{5} *	4.4×10^{6} *	-
37	2.2×10^4	-	9.3×10^2

* K_a was estimated by competitive methods.

1.7 Crown ethers and cryptands-based supramolecular polymers

The increasing use of polymeric materials to supplement or replace traditional materials has stimulated development of more versatile polymeric materials with a wider range of properties. It has been well known that the fundamental properties of polymers depend heavily on chemical composition and architectural aspects of the polymer backbones. Compared with traditional chemistry, which is based on covalent bonds, supramolecular chemistry focuses on non-covalent interactions. Obviously, the combination of supramolecular chemistry and polymer science will lead to the discovery of numerous novel supramolecular polymers, which have unique interlocked structures and are expected to have unique properties. In addition, due to the reversibility of the non-covalent interactions introduced into polymers, supramolecular polymers potentially have the self-healing abilities.[24-25]

As noted above, crown ethers and cryptands are good hosts for guests such as metal ions, paraquats and diquats. Thus, they are good precursors to prepare novel supramolecular polymers, such as polypseudorotaxanes, polyrotaxanes, polycatenanes and pseudorotaxane-type

supramolecular polymers. Pseudorotaxane-type supramolecular polymers, which can be viewed as a special type polypseudorotaxanes, are constructed exclusively by the self-assembly of AA, BB or AB type monomers (Figure 1-10). Except for the potential self-healing properties mentioned above, pseudorotaxane-type supramolecular polymers also can be used as smart materials, which can respond to external stimuli, by introducing external stimuli-responsible pseudorotaxane structures into monomers.[24-25] Moreover, they are inherently recyclable. The polymer structures can be converted to the respective monomers by strong solvent or external stimuli and can be reconstructed under suitable conditions.

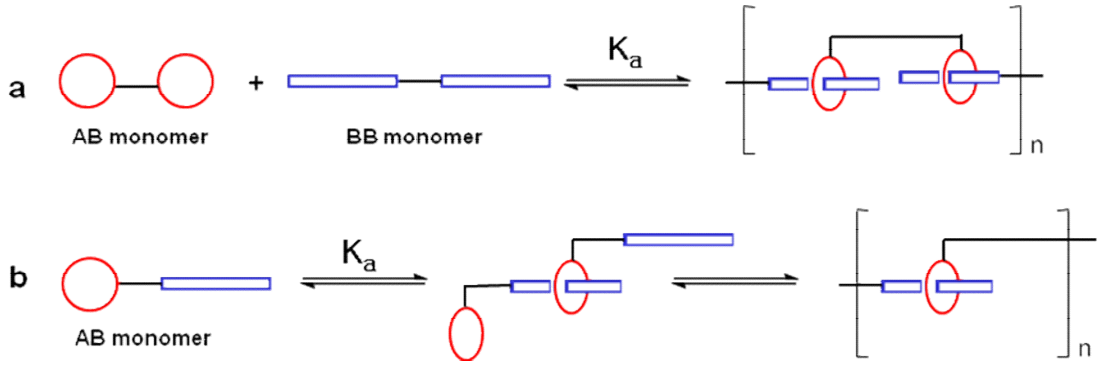

Figure 1-10. Cartoon representations of two kinds of typical pseudorotaxane-type supramolecular polymers: a) A-A B-B pseudorotaxane-type supramolecular polymer system; b) A-B pseudorotaxane-type supramolecular polymer system; The A groups represent cyclic host shown by red circles and the B groups represent linear guests shown by blue bars.

Gibson *et al.* reported AA/BB-type pseudorotaxane-type supramolecular polymers by employing bis-DB24C8 derivatives and a series of bis-dibenzylammonium salt derivatives with different lengths.[97-99] Via the self-assembly between bis-DB24C8 and bis-dibenzylammonium salt, linear supramolecular polymers were formed exclusively in concentrated solutions. However, at low concentrations, the cyclic dimer coexisted with linear oligomers. They found that the amount of cyclic dimer could be reduced by increasing the length of bis-DB24C8 monomer or bis-dibenzylammonium salt monomer due to the increased end-to-end distance effect on cyclization.

Yamaguchi and co-workers designed and prepared an AB type monomer **40** by connecting BMP32C10 and paraquat (Figure 1-11).[100] The rigid heteroditopic AB monomers

self-organized in acetone solution and linear supramolecular polymer **41** formed at high concentration. By employing ^{1}H-NMR data and Carothers equation, the degree of polymerization (n) at different concentrations was estimated. For example: at 2.0 M, n = 50, which corresponds to a polymer with molecular weight (M_n) of 51 kDa; this estimate ignores the formation of cyclic species. Given the relatively low binding constant of BMP32C10 with paraquat it is unlikely that n exceeded a value of 10. Nonetheless, fibers could be pulled from the 2 M solutions, although they were quite brittle because of the rigid nature of the repeat units.

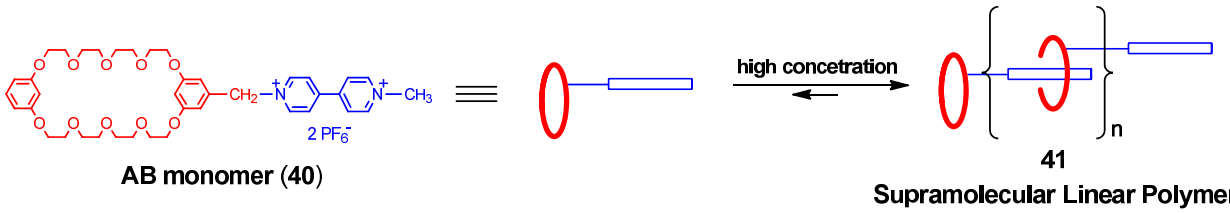

Figure 1-11. Chemical structure of AB monomer **40** and illustration of the formation of linear pseudorotaxane-type supramolecular polymer **41**.

One step forward, Huang *et al.* reported a AA/BB type pseudorotaxane-type supramolecular polymers based on bis-BMP32C10 derivative **42** and bis-paraquat derivative **43** (Figure 1-12).[101] The homoditopic AA monomer **42** bound the BB monomer in solution and linear supramolecular polymer **44** was formed accordingly at high concentration range. For example: at 60.3 mM, n was calculated to be 35.7, M_n = 83.8 kDa, again ignoring the formation of cyclic species.

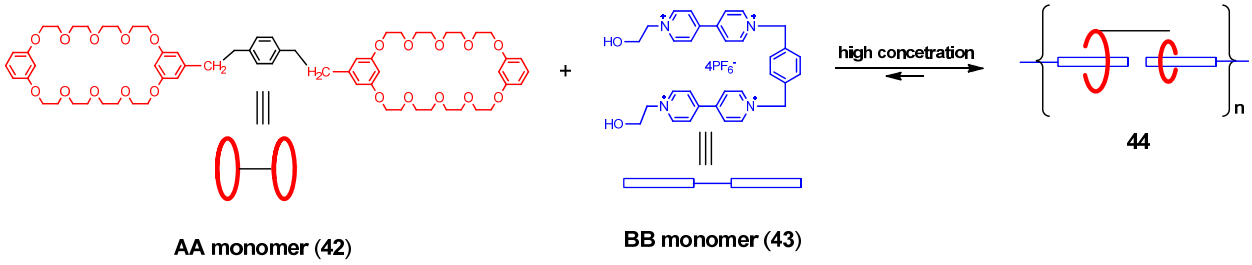

Figure 1-12. Chemical structure of AA monomer **42** and BB monomer **43** and illustration of the formation of linear pseudorotaxane-type supramolecular polymer **44**.

The Gibson group designed and prepared a rigid homoditopic cylindrical bisBMP32C10 **45** and bisparaquat **46** (Figure 1-13).[102] Similarly, at high concentration, a pseudorotaxane-type supramolecular linear polymer was formed in solution. However, due to the rigidity of the bisBMP32C10 **45**, no cyclic oligmer was formed even at low concentration.

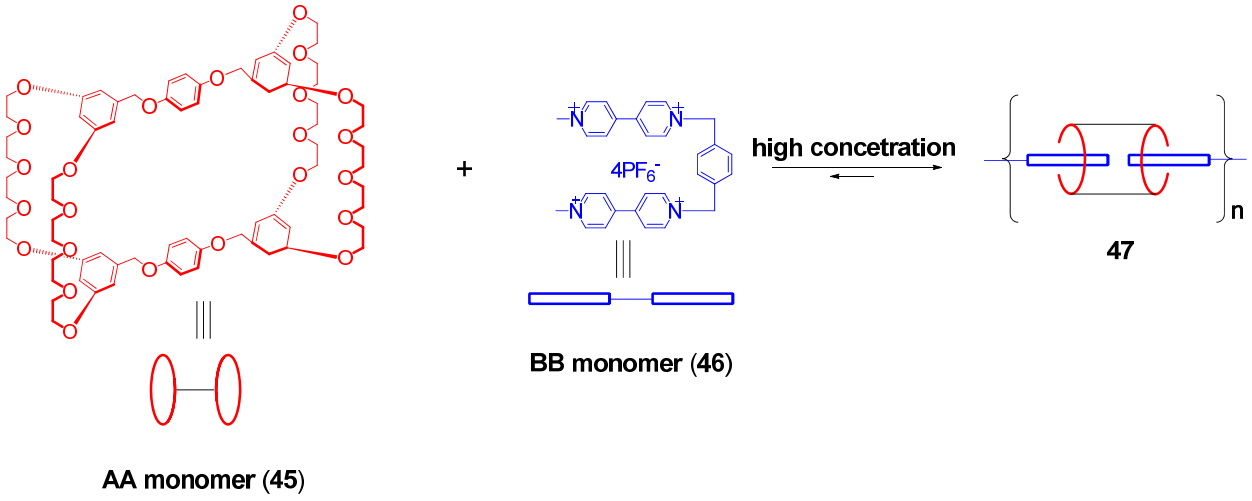

Figure 1-13. Chemical structures of AA monomer **45** and BB monomer **46** and illustration of the formation of linear pseudorotaxane-type supramolecular polymer **47**.

Recently, Huang and co-workers reported a self-sorting pseudorotaxane-type supramolecular polymer (Figure 1-14).[103] First, an AB type monomer **48** bearing DB24C8 end and paraquat salt and a AB type monomer **49** bearing BPP34C10 end and dibenzylammonium salt were designed and prepared. Due to the tremendous difference of the association constants of between the recognition motifs of DB24C8/BPP34C10 and paraquat salt/dibenzylammonium salt, the dibenzylammonium unit of **49** exclusively threaded through the central cavity of **48** and the paraquat unit of **48** exclusively threaded through the central cavity of **49**. As a result, a linear pseudorotaxane-type supramolecular polymer was formed.

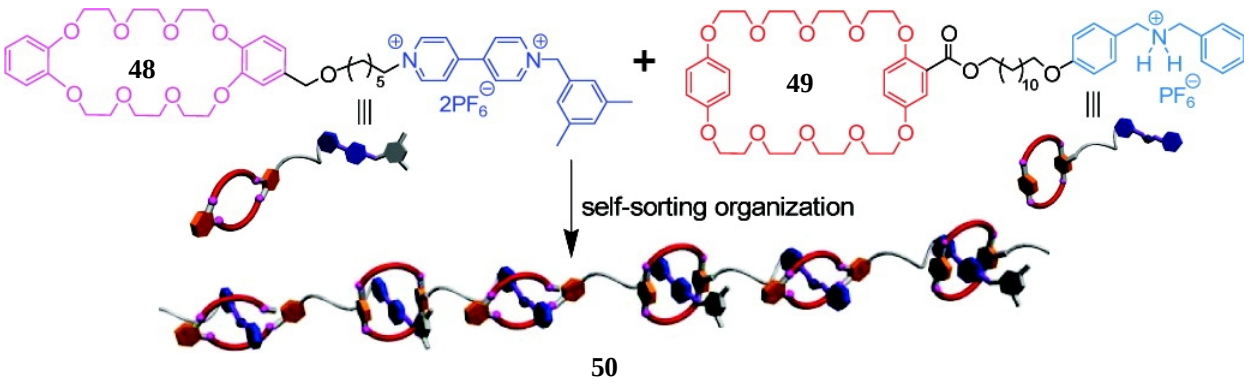

Figure 1-14. Illustration of the formation of linear pseudorotaxane-type supramolecular polymer **50** via the self-assembly between AB monomer **48** and **49**. (Reprinted with permission from ref.103© American Chemical Society)

In addition to the linear pseudorotaxane-type supramolecular polymers, some advanced three dimensionsional supramolecular polymers also have been reported. Huang *et al.* designed and prepared an ABB type monomer **51** by connecting BMP32C10 with two paraquats (Figure 1-15).[104] The monomer **51** self-assembled in acetone and pseudorotaxane-type supramolecular hyperbranched polymer **52** was formed at high concentrations of the monomer. Huang and co-workers also reported a triarm star-shaped supramolecular polymer **55** (Figure 1-16).[105] First, tritopic BMP32C10 host **53** was designed and prepared. Paraquat-ended polystyrene **54** was made via TEMPO-controlled radical polymerization. The interaction between tritopic BMP32C10 host **53** and paraquat-ended polystyrene **54** afforded triarm star-shaped supramolecular polymer **55**.

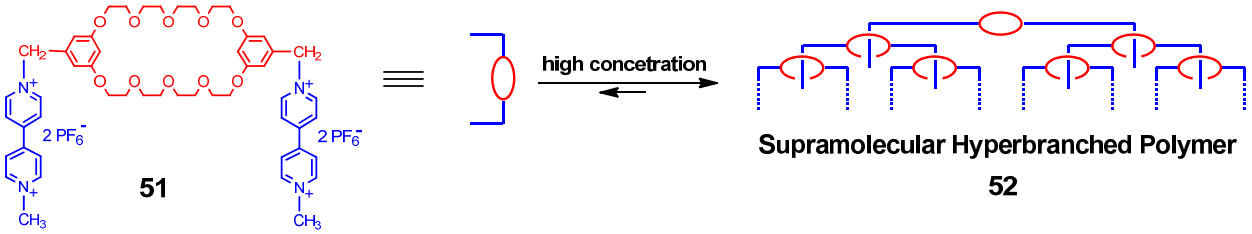

Figure 1-15. Illustration of the formation of hyperbranched pseudorotaxane-type supramolecular polymer **52** via the self-assembly between ABB type monomer **51**.

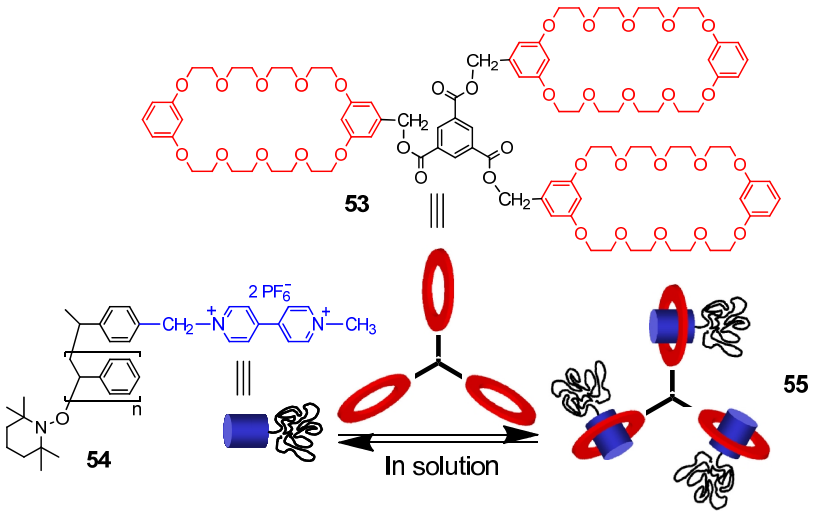

Figure 1-16. Illustration of the formation of triarm star-shaped pseudorotaxane-type supramolecular polymer **55**. (Reprinted with permission from ref.104© American Chemical Society)

Yamaguchi *et al.* reported dendritic supramolecular polymers from cooperative complexation between DB24C8-functionalized dendrons and a complementary homotritopic guest molecule, 1,3,5-tris[*p*-(benzylammoniomethyl)phenyl]benzene tris(hexafluorophosphate).[106]

Based on the Carother's equation, Meijer *et al.* derived the relationship[24c,107] between the degree of polymerization (DP), K_a, and the initial monomer concentration $[H]_0$ to be:

$$DP = \frac{2K_a[H]_o}{\sqrt{(1+2K_a[H]_o)}-1} \qquad (1\text{-g})$$

When $2K_a[H]_0 >> 1$ and $(2K_a[H]_0)^{1/2} >> 1$,

$$DP = \sqrt{2K_a[H]_o} \qquad (1\text{-f})$$

As shown by Equation 1-f, if the initial concentration of monomer is fixed, DP increases with the square root of K_a. In other words, a high K_a value is always required to achieve a high molecular weight at a specific concentration of monomers. For example, in order to reach DP = 100 at 1.0

M, $K \geq 5 \times 10^3 M^{-1}$. Also, in order to prepare large supramolecular polymers, the solubility of the monomer should be good, since the DP is proportional to the square root of the initial monomer concentration. Although crown ethers have been widely employed to construct supramolecular polymers with paraquats or diquats due to their advantages, such as, good solubility in organic solvents and so on, their relative low association constants (400-800 M^{-1}) limit their applications to make supramolecular polymers with relative high molecular weight. There are two ways to solve this problem: a. design and prepare novel crown ether derivatives with stronger binding abilities to paraquats or diquats. b. employ cryptands to replace crown ethers to construct supramolecular polymers. As we have shown, cryptands demonstrated stronger binding abilities to guests compared to corresponding simple crown ethers. Cryptands give us a way to design strong monomers and prepare supramolecular polymers with high molecular weight. However, it should be noted here that the low efficiency and low yield of cryptand syntheses become the bottle-neck to the application of cryptands in preparing supramolecular polymers. New synthetic methods should be established to optimize the syntheses of cryptands in order to prepare them efficiently. Perderson *et al.* attempted to prepare cryptand based supramolecular polymers.[96] However, most attempts didn't succeed.

In summary, since the discovery of crown ethers, they have been an important host family for a variety of electro-positive guests and have been widely studied all over the world. Crown ethers have been employed to construct many supramolecular species, such as pseudorotaxanes, rotaxanes and catenanes. Due to preorganization and more binding sites, cryptands demonstrate much better binding abilities compared with the corresponding simple crown ethers. Thus, cryptands are superior to crown ethers for making advanced supramolecular species. When crown ether-based pseudorotaxanes, rotaxanes, catenanes or other advanced supramolecular species are introduced into polymers, supramolecular polymers are afforded. Unlike traditional polymers that are constructed exclusively by covalent bonds, the supramolecular polymers, which consist of covalent bonds as well as non-covalent bonds, are expected to have unique properties due to their novel architectural aspects and topologies. In order to make large supramolecular polymers, complex systems with high association constants and good solubility are necessary precursors. However, the relative low binding abilities of crown ethers limit their applications in supramolecular polymers. Cryptands are good choices,

but the low time efficiencies and low yields of cryptand syntheses disfavor their usage in supramolecular polymers. As a result, it is very important to design and prepare novel crown ether derivatives with stronger binding abilities to guests. Also, optimizing the syntheses of cryptands and establishing new synthetic methods in order to prepare cryptands efficiently are also important and urgent.

References

(1) Arrighi, V.; Gagliardi, S.; Dagger, A. C.; Semlyen, J. A.; Higgins, J. S.; Shenton, M. J. *Macromolecules* **2004**, *37*, 8057-8065.

(2) Fustin, C. A.; Clarkson, G. J.; Leigh, D. A.; Van, H. F. V.; Jonas, A. M.; Bailly, C. *Macromolecules* **2004**, *37*, 7884-7892.

(3) Steuerman, D. W.; Tseng, H.-R.; Peters, A. J.; Flood, A. H.; Jeppesen, J. O.; Nielsen, K. A.; Stoddart, J. F.; Health, J. R. *Angew. Chem. Int. Ed.* **2004**, *43*, 6486-6491.

(4) Takata, T.; Kihara, N.; Furusho, Y. *Adv. Polym. Sci.* **2004**, *171*, 1-75.

(5) Burchell, T. J.; Eisler, D. J.; Puddephatt, R. J. *Dalton. Trans.* **2005**, 268-272.

(6) Carroll, J. B.; Jordan, B. J.; Xu, H.; Erdogan, B.; Lee, L.; Cheng, L.; Tiernan, C.; Cooke, G.; Rotello, V. M. *Org. Lett.* **2005**, *7*, 2551-2554.

(7) Dirks, A. J.; Van, B. S. S.; Hatzakis, N. S.; Opsteen, J. A.; Van, D. F. L.; Cornelissen, J. J. L. M.; Rowan, A. E.; Van, H. J. C. M.; Rutjes, F. P. J. T.; Nolte, R. J. M. *Chem. Commun.* **2005**, 4172-4174.

(8) Endo, K.; Shiroi, T.; Murata, N. *Polym. J.* **2005**, *37*, 512-516.

(9) Ghosh, S. K.; Bharadwaj, P. K. *Inorg. Chem.* **2005**, *44*, 5553-5555.

(10) Ohga, K.; Takashima, Y.; Takahashi, H.; Kawaguchi, Y.; Yamaguchi, H.; Harada, A. *Macromolecules* **2005**, *38*, 5897-5904.

(11) Vouyiouka, S. N.; Karakatsani, E. K.; Papaspyrides, C. D. *Prog. Polym. Sci.* **2005**, *30*, 10-37.

(12) Zaman, M. B.; Udachin, K.; Ripmeester, J. A.; Smith, M. D.; Zur, L. H.-C. *Inorg. Chem.* **2005**, *44*, 5047-5059.

(13) Pedersen, C. *J. Am. Chem. Soc.* **1967**, *89*, 7017-7036.

(14) Pedersen, C. J. *J. Am. Chem. Soc.* **1967**, *89*, 2495-2496.

(15) Dretrich, B.; Lehn, J. M.; Savage, J.-P. *Tetrahedron. Lett.* **1969**, *10*, 2885-2888.

(16) Helgesen, R. C.; Timko, J. M.; Cram, D. J. *J. Am. Chem. Soc.* **1973**, *95*, 3021-3023.

(17) Lehn, J. M. *Science* **1985**, *227*, 849-856

(18) Steed, J. W.; Atwood, J. L. *Supramolecular Chemistry*; J. Wiley and Sons: New York, 2000.

(19) Izatt, R. M.; Pawlak, K.; Bradshaw, J. S. *Chem. Rev.* **1991**, *91*, 1721-2085.

(20) Izatt, R. M.; Pawlak, K.; Bradshaw, J. S.; Bruening, R. L. *Chem. Rev.* **1995**, *95*, 2529-2586.

(21) Christoph A. Schalley, *Mass Spectr. Rev.* **2001**, 20, 253-309

(22) Gibson, H. W.; Marand, H. *Adv. Mater.* **1993**, *5*, 11-21.

(23) (a) Gibson, H. W. In *Large Ring Molecules*; Semlyen, J. A., Ed.; John Wiley & Sons: New York, 1996; p 191; (b) Raymo, F. M.; Stoddart, J. F. *Chem. Rev.* **1999**, *99*, 1643-1664. (c) Harada, A. *Acc. Chem. Res.* **2001**, 34, 456-464; (d) Hernandez, J. V.; Kay, E. R.; Leigh, D. A. *Science*. **2004**, 306, 1532-1537.

(24) (a) Huang, F.; Gibson, H. W. *Prog. Polym. Sci.* **2005**, *30*, 982-1018. (b) Lehn, J.-M. *Chem. Soc. Rev.* **2007**, *36*, 151-160. (b) Stoddart, J. F. *Chem. Soc. Rev.* **2009**, *38*, 1802-1820. (c) De Greef, T. F. A.; Smulders, M. M. J.; Wolffs, M.; Schenning, A. P. H. J.; Sijbesma, R. P.; Meijer, E. W. *Chem. Rev.* **2009**, *109*, 5687-5754. (d) Harada, A.; Hashidzume, A.; Yamaguchi, H.; Takashima, Y. *Chem. Rev.* **2009**, *109*, 5974-6023. (e) Niu, Z.; Gibson, H. W. *Chem. Rev.* **2009**, *109*, 6024-6046. (i) Fang, L.; Olson, M. A.; Benitez, D.; Tkatchouk, E.; Goddard III, W. A.; Stoddart, J. F. *Chem. Soc. Rev.* **2010**, *39*, 17-29. (i) Durola, F.; Sauvage, J.-P.; Wenger, O. S. *Coord. Chem. Rev.* **2010**, *254*, 1748-1759.

(25) (a) Champin, B.; Mobian, P.; Sauvage, J.-P.; *Chem. Soc. Rev.* **2007**, *36*, 358-366. (b) Hembury, G. A.; Borovkov, V. V.; Inoue, Y. *Chem. Rev.* **2007**, *108*, 1-73. (c) Bonnet, S.; Collin, J.-P. *Chem. Soc. Rev.* **2008**, *37*, 1207-1217. (d) Angelos, S.; Khashab, N. M.; Yang, Y.-W.; Trabolsi, A.; Khatib, H. A.; Stoddart, J. F.; Zink, J. I.; *J. Am. Chem. Soc.* **2009**, *131*, 12912-12914. (e) Leung, K. C.-F.; Chak, C.-P.; Lo, C.-M.; Wong, W.-Y.; Xuan, S.; Cheng, C. H. K.; *Chem. Asian. J.* **2009**, *4*, 364-381.

(26) Takahashi. T.; Uchiyama. A.; Yamada. K.; Lynn, B. C.; Gokel, G.W. *Tetrahedron*

Lett. **1992**, *33*, 3825-3828.

(27) Beer, P.D. *J. Am. Chem. Soc.* **1985**, 1115-1116.

(28) Wang, K.; Han, X.; Gross R. W.; Gokel, G.W. *J. Am. Chem. Soc*, **1995**, 641-642.

(29) Blair, S. M.; Brodbelt, J. S.; Reddy, G. M.; Marchand, A. P. *J. Mass. Spectrom*. **1998**, *33*, 721-728.

(30) Oshima, T.; Matsuda, F.; Fukushima, K.; Tamura, H. *J. Chem. Soc. Perkin. Trans.* **1998**, *2*,145-148.

(31) Hapiot, F.; Tilloy, S.; Monflier, E. *Chem. Rev.* **2006**, *106*, 767-781.

(32) Valle, D.; Martin, E. M. *Process. Biochem.* **2004**, *39*, 1033-1046.

(33) Harada, A. *Acc. Chem. Res*, **2001**, *34*, 456-464.

(34) Harada, A. *J. Poly. Sci, Part A: Polym. Chem.,* **2006**, *44*, 5113-5119.

(35) Gattuso, G.; Liantonio, R.; Metrangolo, P.; Meyer, F.; Pappalardo, A.; Parisi, M. F.; Pilati, T.; Pisagatti, I.; Resnati, G. *Supramol. Chem.* **2006**, *18*, 235-243.

(36) Arduini, A.; Massera, C.; Pochini, A.; Secchi, A.; Ugozzoli, F. *New J. Chem,* **2006**, *30*, 952-958.

(37) Rebek, J. *Chem. Commun,* **2000**, 637-643.

(38) Some recent publications: (a) Huang, F.; Fronczek, F. R.; Gibson, H. W. *J. Am. Chem. Soc.* **2003**, *125*, 9272-9273. (b) Huang, F.; Zhou, L.; Jones, J. W.; Gibson, H. W.; Ashraf-Khorassani, M. *Chem. Commun.* **2004**, 2670-2671. (c) Huang, F.; Switek, K. A.; Zakharov, L. N.; Fronczek, F. R.; Slebodnick, C.; Lam, M.; Golen, J. A.; Bryant, W. S.; Mason, P. E.; Rheingold, A. L.; Ashraf-Khorassani, M.; Gibson, H. W. *J. Org. Chem.* **2005**, *70*, 3231-3241. (d) Gibson, H. W.; Wang, H.; Slebodnick, C.; Merola, J.; Kassel, S.; Rheingold, A. L. *J. Org. Chem.* **2007**, *72*, 3381-3393. (e) Pederson, A. M.-P.; Vetor, R. C.; Rouser, M. A.; Huang, F.; Slebodnick, C.; Schoonover, D. S.; Gibson, H. W.; *J. Org. Chem.* **2008**, *73*, 5570-5573. (f) Li, S.; Zheng, B.; Huang, F.; Zakharov, L.; Slebodnick, C. Rheingold, A.; Gibson, H. W. *Sci. China Chem.* **2010**, *53*, 858-862. (g) Zhang, M.; Zhu, K.; Huang, F. *Chem. Commun.* **2010**, *46*, 8131-8141. (h) Liu M.; Li, S.; Hu, M.; Wang, F.; Huang, F. *Org. Lett.* **2010**, 12, 760-763. (i) Zhang, M.; Zheng, B.; Xia, B.; Zhu, K.; Wu, C.; Huang, F. *Eur. J. Org. Chem.* **2010**, 6804-6809.

(39) Ishore, R. S. K.; Kalsani, V.; Schmittel, M. *Chem. Commun*. **2006**, 3690-3692.

(40) Davidson, G. J .E.; Tong, L. H.; Raithby, P. R.; Sanders, J. K. M. *Chem. Commun.* **2006**, 3087-3089.

(41) Israel G. *Cryst. Eng. Comm*. **2002**, *4*, 109 - 116.

(42) Hayakawa, T.; Yusa, K.; Kouno, M.; Takeda, J.; Horie K. *Gene*. **2006**, *369*, 80-89.

(43) Rotello, V.; Ilhan, F. *Book of Abstracts*, 218th ACS National Meeting, New Orleans, Aug. **1999**, 22-26.

(44) Zeng, F.; Zimmerman, S. C. *Chem. Rev*. **1997**; *97*; 1681-1712.

(45) Stryer, L. *Biochemistry*; Fourth Edition, W. H. Freeman and Company: New York, 1995.

(46) Petrucci, R. H. *General Chemistry: Principles and Modern Applications*; Fifth Edition, Macmillan Publishing Company: New York, 1989.

(47) Sobransingh, D.; Kaifer, A. E. *Org. Lett.*, **2006**, *8*, 3247.

(48) Sindelar, V.; Silvi, S.; Kaifer, A. E. *Chem. Commun*. **2006**, 2185-2187.

(49) Huang, F. H.; Switek, K. A.; Gibson, H.W. *Chem. Commun*. **2005**, 3655-3657**.**

(50) Qu, D. H.; Wang, Q. C.; Ren, J.; Tian, H. *Org. Lett*. **2004**, *6*, 2085-2088.

(51) Murakami, H.; Kawabuchi, A.; Kotoo, K.; Kunitake, M.; Nakashima, N. *J. Am. Chem. Soc*. **1997**, *119*, 7605-7606.

(52) Marshall, A. G. In *Biophysical Chemistry: Principles, Techniques, and Applications*, John Wiley & Sons, New York, NY., 1978, pp 70-77.

(53) Freifelder, D. M. In *Physical Biochemistry*, W. H. Freeman and Co., New York, 1982, pp 659-660.

(54) Perlmutter-Hayman, B. *Acc. Chem. Res.* **1986**, *19*, 90-96.

(55) Connors, K. A. In *Binding Constants*; J. Wiley and Sons, New York, 1987, pp 78-86.

(56) Jelesarov, I.; Bosshard, H. R. *J. Mol. Recognit.* **1999**, *12*, 3-18.

(57) Velazquez-Campoy, A.; Freire, E. *Nat. Protocols* **2006**, *1*, 186-191.

(58) Freyer, M. W.; Lewis, E. A. In *Methods in Cell Biology*; Correia, J. J., Dietrich, H. W., Ed.; Academic Press: 2008; vol. 84, p. 79.

(59) Wiseman, T.; Williston, S.; Brandts, J. F.; Lin, L.-N. *Anal. Biochem.* **1989**, *179*, 131-137.

(60) Indyk, L.; Fisher, H. F. *Method. Enzymol.* **1998**, *295*, 350-364.

(61) Harrison, I. T.; Harrison, S. J. *J. Am. Chem. Soc.* **1967**, *89*, 5723-5724

(62) Gibson, H. W.; Nagvekar, D. S.; Yamaguchi, N.; Bhattacharjee, S.; Wang, H.; Vergne, M. J.; Hercules, D. M. *Macromol.* **2004**, *37*, 7514-29.

(63) Gibson, H. W.; Liu, S.; Gong, C.; Ji, Q.; Joseph, E. *Macromolecules*. **1997**, *30*, 3711-3727.

(64) Gong, C.; Ji, Q.; Subramaniam, C.; Gibson, H. W. *Macromolecules.* **1998**, *31*, 1814-1818.

(65) Wenz, G.; Keller, B. *Angew. Chem. Int. Ed. Engl.* **1992**, 31, 197-199.

(66) Yamaguchi, I.; Osakada, K. *J. Am. Chem. Soc.* **1996**, *118*,1811-1812.

(67) Yui, N.; Ooya, T.; Kumano, T. *Bioconj. Chem.* **1998**, *9*, 118-125.

(68) Huh, K. M.; Tomita, H.; Ooya, T.; Lee, W. K.; Sasaki, S.; Yui, N. *Macromolecules.* **2002**, *35*, 3775-3777.

(69) Werts, M. P. L.; Hadziioannou, G. *Macromolecules*. **2003**, *36*, 7004-7013.

(70) Yamagishi,T. A.; Kawahara, A.; Kita, J.; Hoshima, M.; Umehara, A.; Ishida, S.; *Macromolecules* **2001**, *34*, 6565-6570.

(71) Yamaguchi, I.; Osakada, K.; Yamamoto, T.; *Macromolecules* **2000**, *33*, 2315-2319.

(72) Takata, T.; Kawasaki, H.; Kihara, N.; Furusho, Y.; *Macromolecules* **2001**, *34*, 5449-5456.

(73) Yamaguchi, N.; Gibson, H. W. *Macromol. Chem. Phys.* **2000**, *201*, 815-824.

(74) Born, M.; Ritter, H. *Adv. Mater.* **1996**, *8*, 149-151.

(75) Noll, O.; Ritter, H. *Macromol. Rapid Commun.* **1997**, *18*, 53-58.

(76) Noll, O.; Ritter, H. *Macromol. Chem. Phys.* **1998**, *199*, 791-794.

(77) Huh, K.M.; Ooya, T.; Sasaki, S.; Yui, N. *Macromolecules* **2001**, *34*, 2402–24024.

(78) Yui, N.; Ooya, T.; Kumano, T. *Bioconj. Chem.* **1998**, *9*, 118–125.

(79) Ooya, T.; Yui, N. *Macromol. Chem. Phys*. **1998**. *199*. 2311–2320.

(80) Gibson, H.W.; Liu, S. *Macromol. Symp.* **1996**, *102*, 55–61.

(81) Huh, K. M.; Ooya, T.; Sasaki, S.; Yui, N. *Macromolecules* **2001**, *34*, 2402–2404.

(82) Choi, H. S.; Huh, K. M.; Ooya, T.; Yui, N. *J. Am. Chem. Soc.* **2003**, *125*, 6350–6351.

(83) Choi, S.; Lee, J. W.; Ko, Y. H.; Kim, K. *Macromolecules* **2002**, *35*, 3526–3531.

(84) Gong, C.; Balanda, P. B.; Gibson, H. W. *Macromolecules* **1998**, 31, 5278-5289.

(85) Gibson, H. W.; Liu, S.; Lecavalier, P.; Wu, C.; Shen, Y. X. *J. Am. Chem. Soc*. **1995**, *117*, 852–874.

(86) Divisia, B. B.; Genoud, F.; Borel, C.; Bidan, G.; Kern, J. M. *J. Phys. Chem. B.* **2003**, *107*, 5126–5132.

(87) Tamura, M.; Ueno, A. *Chem. Lett.* **1998**, 369–370.

(88) Tamura, M.; Gao, D.; Ueno, A. *J. Chem. Soc, Perkin. Trans.* **2001**, 2012–2021.

(89) Gao, D.; Ueno, A. *Chem. Eur. J.* **2001**, *7*, 1390–1397.

(90) Gibson, H. W.; Wang, H.; Bonrad, K.; Jones, J. W.; Slebodnick, C.; Zackharov, L. N.; Rheingold, A. L.; Habenicht, B.; Lobue, P.; Ratliff, A. E. *Org. Biomol. Chem.* **2005,** *3*, 2114-2121.

(91) Pederson, A. M. P.; Ward, E. M.; Schoonover, D. V.; Slebodnick, C.; Gibson, H. W. *J. Org. Chem.* **2008**, *73*, 9094-9101.

(92) Gibson, H. W.; Nagvekar, D. S. *Can. J. Chem.* **1997**, *75*, 1375-1384

(93) (a) Bryant, W. S.; Guzei, I.; Rheingold, A. L.; Gibson, H. W. *Org. Lett.* **1999**, *1*, 47-50. (b) Huang, F.; Fronczek, F. R.; Gibson, H. W. *Chem. Commun.* **2003**, 1480−1481. (c) Huang, F.; Zakharov, L. N.; Bryant, W.; Rheingold, A. L.; Gibson, H. W. *Chem. Commun*. **2005**, 3268-3270. (d) Huang, F.; Gantzel, P.; Nagvekar, D. S.; Rheingold, A. L.; Gibson, H. W. *Tetrahedron Lett.* **2006**, *47*, 7841-7844. (e) Li, S.; Liu, M.; Zheng, B.; Zhu, K.; Wang, F.; Li, N.; Zhao, X.-L.; Huang, F. *Org. Lett.* **2009**, *11*, 3350-3353.

(94) Pérez-Alvarez, M.; Raymo, F. M.; Rowan, S. J.; Schiraldi, D.; Stoddart, J. F.; Wang, Z.-H.; White, A. J. P.; Williams, D. J. *Tetrahedron.* **2001**, *57*, 3799-3808.

(95) Bryant, W. S.; Jones, J. W.; Mason, P. E.; Guzei, I.; Rheingold, A. L.; Fronczek, F. R.; Nagvekar, D. S.; Gibson, H. W. *Org. Lett.* **1999**, *1*, 1001-1004.

(96) Pederson, A. M. P.; Ph.D Dissertation. Virginia Tech, 2009.

(97) Yamaguchi, N.; Gibson, H. W. *Angew. Chem. Int. Ed.* **1999**, *38*, 143-147.

(98) Yamaguchi, N.; Gibson, H. W. *Chem. Commun.* **1999**, 789-790.

(99) Gibson, H. W.; Yamaguchi, N.; Jones, J. W. *J. Am. Chem. Soc.* **2003**, *125*, 3522.

(100) Yamaguchi, N.; Nagvekar, D. S.; Gibson, H. W. *Angew. Chem. Int. Ed.* **1998**, *37*, 2361-2364.

(101) Huang, F.; Nagvekar, D. S.; Zhou, X.; Gibson, H. W. *Macromolecules* **2007**, *40*, 3561-3567.

(102) Huang, F.; Gibson, H. W. *Chem. Commun*. **2005**, 1696−1698.

(103) Wang, F.; Han, C.; He, C.; Zhou, Q.; Zhang, J.; Wang, C.; Li, N.; Huang, F. *J. Am. Chem. Soc.* **2008**, *130*, 11254–11255

(104) Huang, F.; Gibson, H. W. *J. Am. Chem. Soc.* **2004**, *126*, 14738-14739.

(105) Huang, F.; Nagvekar, D. S.; Slebodnick, C.; Gibson, H. W. *J. Am. Chem. Soc.* **2005,** *127*, 484-485

(106) Gibson, H. W.; Yamaguchi, N.; Hamilton, L.; Jones, J. W. *J. Am. Chem. Soc.* **2002,** *124*, 4653-4665.

(107) Sijbesma, R. P.; Beijer, F. H.; Brunsveld, L.; Folmer, B. J. B.; Hirschberg, J. H. K. K.; Lange, R. F. M.; Lowe, J. K. L.; Meijer, E. W. *Science* **1997,** *278*, 1601-1604.

TOC Graphic:

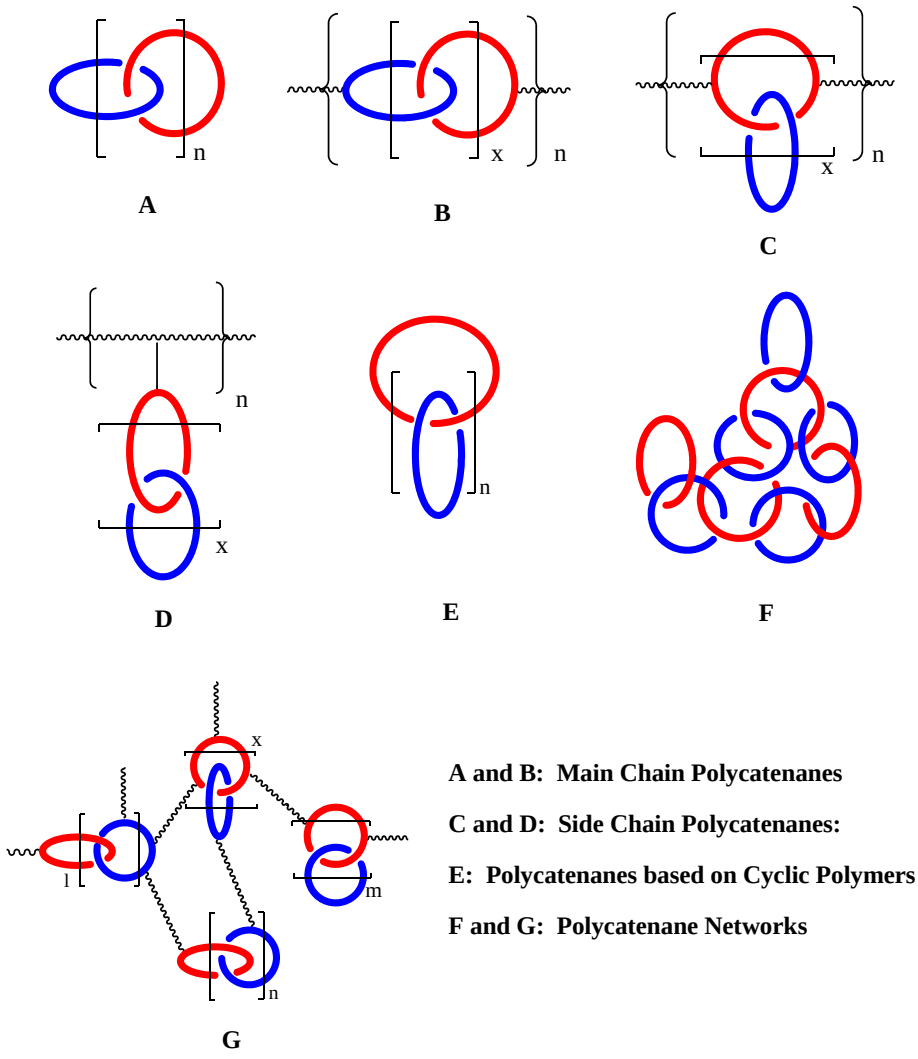

A and B: Main Chain Polycatenanes

C and D: Side Chain Polycatenanes:

E: Polycatenanes based on Cyclic Polymers

F and G: Polycatenane Networks

Chapter 2.

Polycatenanes

2.1 Introduction

2.1.1 Overview

Catenanes are molecular architectures composed of two or more mechanically-interlocked macrocycles. e.g., the [n]catenane (type A in Figure 2-1, the "n" designates the number of cyclic components involved[1]). The name "catenane" is derived from the Latin word "*catena*" meaning "chain". Since catenanes consist of interlocked macrocycles, which can rotate and move within each other, catenane molecules in principle have high degrees of freedom and mobility compared with conventional covalently connected molecules. Also, the interlocked architecture can't be disentangled without breaking at least one of the covalent bonds of the macrocycles. The general precursors to catenanes are pseudorotaxanes (Scheme 2-2-1).[2-9] A pseudorotaxane is a compound that consists of a linear component (generally called a "guest") and a macrocylclic component (generally designated as "host") bound together mechanically in a threaded structure by non-covalent forces. The linear component can dethread and rethread; as a result the pseudorotaxane is always in equilibrium with its two components. A catenane can be prepared via the ring closure reaction of the linear component of a pseudorotaxane.

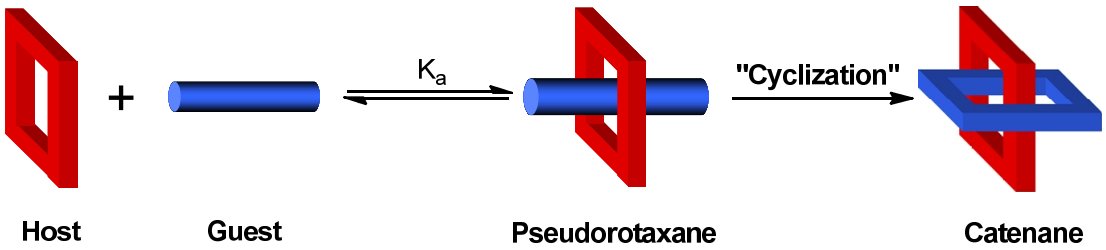

Scheme 2-1. A pseudorotaxane is formed via the threading of a linear guest through the cavity of a cyclic host and the subsequent cyclization of the linear guest yields a [2]catenane.

It has been well known that the fundamental properties of polymers are not only strongly affected by their chemical composition, but also by their architectural aspects, such as conformations and inter-macromolecular interactions. Therefore, catenanes, which possesses high degrees of freedom and mobility, represent an interesting architectural feature can be introduced into polymers and the resulting novel polymers - polycatenanes - contain chain-like mechanically-interlocked components. Compared with conventional polymers which have covalent linkages only, polycatenanes are expected to have more flexibility, different conformations and therefore unique properties, such as, rheological,[11,12] dynamic,[13,14] mechanical[15,16] and thermal properties.[17] As a result, polycatenanes have attracted considerable attention during last decade or so and a lot of progress has been made in this field.[10,18-30] Here, the recent progress from 1995 to 2010 will be discussed.

2. 1.2 Classes of Polycatenanes

The various types of polycatenanes are summarized in Figure 2-1.[10] Polycatenanes of type **A**, which can be viewed as "optimized" [n]catenanes (n is a large number), represent linear polymers constructed only by mechanically-interlocked macrocyclic rings. Since macromolecules of type **A** consist solely of mechanically-interlocked cyclic components, the effects of the topologically-bonded structures on properties will be maximized. Moreover, the structures of type **A** are aesthetically perfect and appealing as far as the concept of polycatenanes is concerned. To the best of our knowledge, polycatenanes of type **A** remain elusive. By incorporating difunctional [x + 1]catenane subunits (x is a small number, e. g., 1 or 2) into linear polymer backbones, polycatenanes of type **B** are obtained. Bifunctional [2] - or bis[2]catenanes can be synthesized efficiently by employing some well-established synthetic methods. Also, poly[2]catenanes (**B**, **C** and **D** in Figure 2-1, when x = 1) possess the basic mechanically-linked structural feature. Therefore, most progress has been made on poly[2]catenane systems. Polycatenanes of type **C** can be viewed as isomers of type **B**. They are constructed by introducing [x + 1]catenane subunits, which bear a difunctional ring, into polymer backbones. When catenane subunits are incorporated into the pendant moieties, polycatenanes of type **D** are afforded. Polycatenanes of type **E** can be viewed as polymeric catenanes or "catenated" polymers. Polycatenanes of type **F** and type **G** illustrate polycatenane networks. The networks of

type **F** are constructed solely by catenane subunits. The networks of type **G**, which represent universal polycatenanes networks, are formed by catenane subunits as well as linear linking units. For simplicity and clarity, the polycatenanes will be discussed in the following four sections: (1) Main-chain polycatenanes; (2) Side-chain polycatenanes; (3) Polymeric catenanes; (4) Catenane structures in the polymer networks.

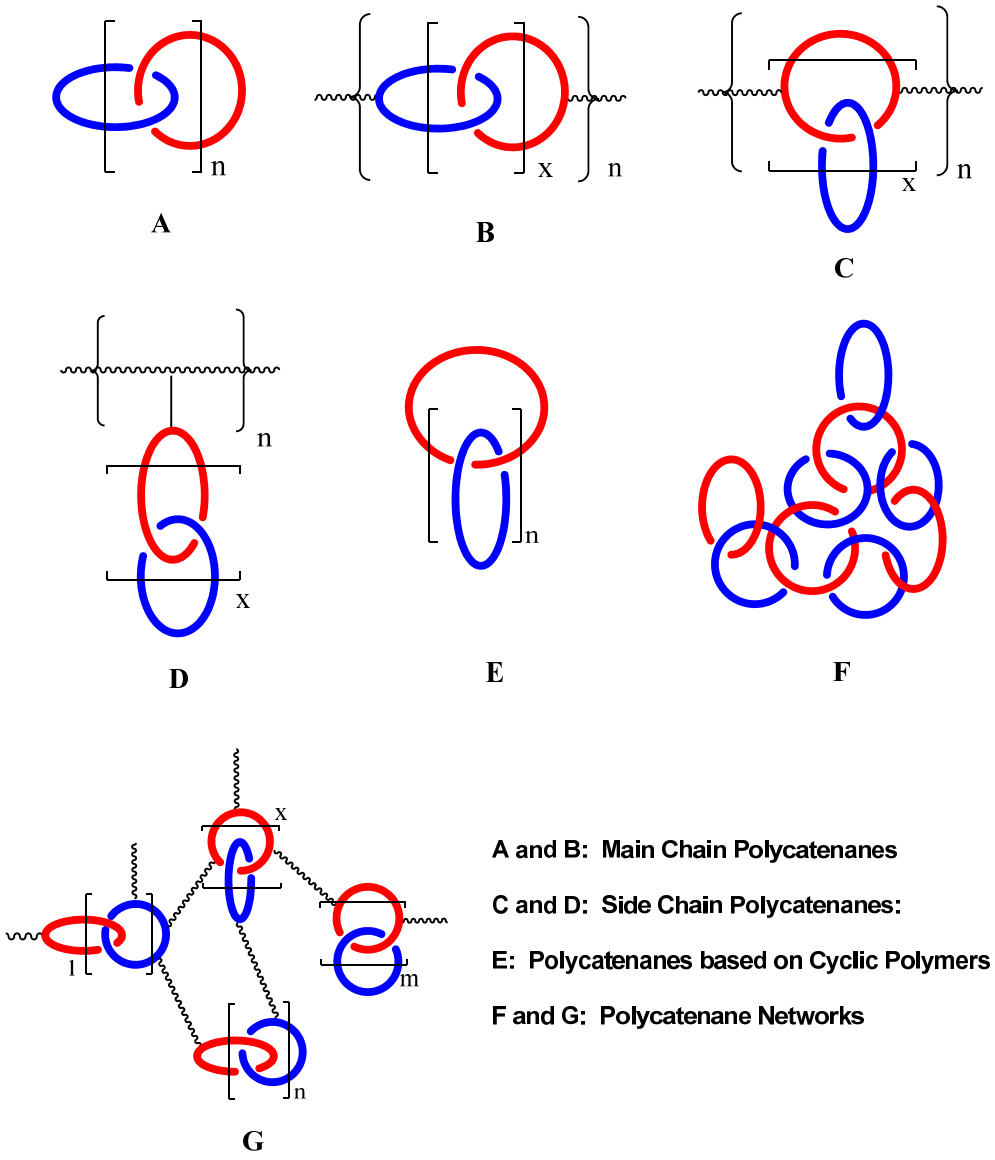

Figure 2-1. Classes of polycatenanes. Blue ring maybe equal to red ring. n, x, m, l ≥ 1. Reprinted with permission from ref.10, Copyright 2010 American Chemical Society.

2.2 Main chain polycatenanes

2.2.1 Linear polycatenanes

As described above, linear polycatenanes (type **A** in Figure 2-1), constructed solely by the mechanically-interlocked repeating cyclic components, are the dream of many researchers. Although several strategies have been proposed and tried, the preparation of linear polycatenanes is still one of the most difficult synthetic goals and is yet to be achieved.

Similar to the synthesis of simple catenanes, preorganization of the macrocyclic precursors is required to favor the cyclization reactions. Template effects, such as hydrogen bonding,[31-35] π-π stacking,[36-38] metal coordination[39-41] and hydrophobic interactions.[35,42-43] are employed to achieve the preorganization. The first proposed strategy (route I in Scheme 2-2) is a one-step polymerization approach.[18,44] Linear polycatenanes are expected to be formed via the polymerization between template-preorganized AA and BB monomers. However, the inevitable branching and cross-linking side reactions during polymerization will lead to an undefined network instead of linear polycatenanes. Shaffer and Tsay[45] proposed another template-directed stepwise polymerization approach (route II in Scheme 2-2). Unlike route I, in this route linear polymers are formed before cyclization reactions and high dilution techniques[46-48] can be used to favor the subsequent cyclization reactions. However, the branching and crosslinking side reactions still can occur during the cyclization step.

Route III shows a template-directed approach employing stepwise threading and cyclization. Theoretically, linear polycatenanes can be prepared in this way. However, it is not suitable to prepare linear polycatenanes with high molecular weight on large scales due to the low yields and tedious separations after each synthetic step. Impressively, Stoddart *et al.*[49-52] successfully prepared linear [5]catenane **1** (Figure 2-2) , which is similar to the symbol of the Olympic movement and was named ‘Olympiadane’, by employing this approach. Moreover, [6]- and [7]-catenanes **2** and **3** were obtained at the same time. As mentioned above, the yield of **1** was pretty low and separation was tedious. Several other approaches taking advantage of interfacial reactions or chemical conversion were proposed,[53-55] but none of them proved successful.

A very smart approach was proposed by Takata *et al.* [27,56] In their approach (Route IV in Scheme 2-2), functionalized [2]catenane monomers were polymerized via Diels-Alder reaction and the following double-bond cleavage by ozonolysis would afford linear polycatenanes.

Takata's group already made some progress by employing this strategy. One ring of a [2]catenane was enlarged successfully via Diels-Alder reaction and ozonolysis.[57] Also, a similar bridged poly[2]catenane was successfully prepared. [58] Since the sbottle-neck steps in previous attempts - threading and cyclization steps - are avoided during polymerization, the approach will possibly lead to a breakthrough for the synthesis of polycatenanes.

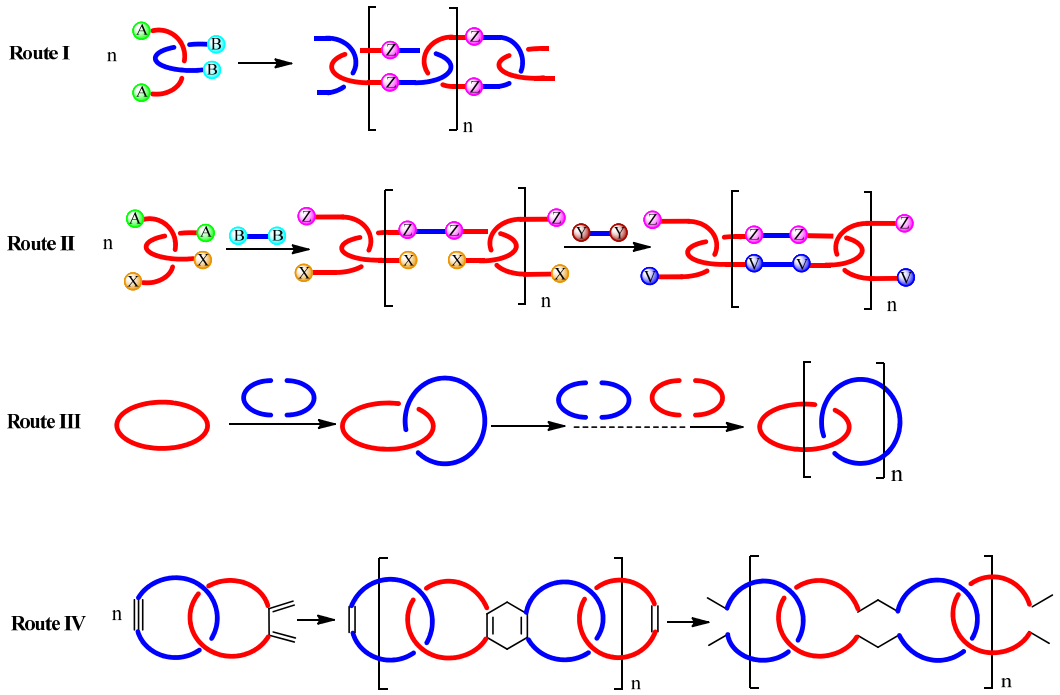

Scheme 2-2. Synthetic approaches towards polycatenanes of type **A**. Functional group A reacts with B to yield Z linkages. Functional group X reacts with group Y to yield V linkages.

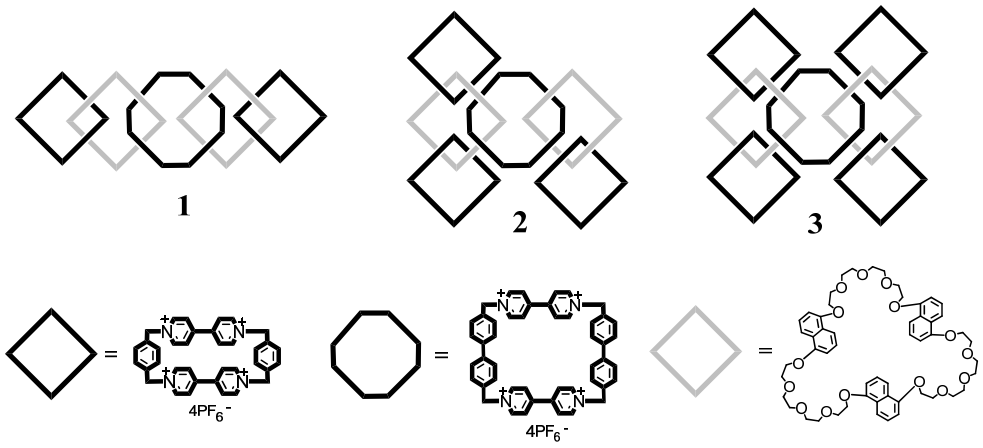

Figure 2-2. [5]Catenane **1** (Olympiadane), [6]catenane **2** and [7]catenane **3**.

2.2.2 Main-Chain Poly[2]catenanes

As noted above, bifunctional [2] - or bis[2]-catenanes can be synthesized efficiently by employing established synthetic methods. Also, poly[2]catenanes possess the basic mechanically-linked structural feature. Thus, most progress has been made on these systems.

The synthetic routes used to prepare main-chain poly[2]catenanes are summarized in Scheme 2-3. Commonly, main-chain poly[2]catenanes are prepared by the polymerization of difunctional [2]catenane monomers. Thus, preparation of difunctional [2]catenane monomers is the key step. In route 1, the cyclization of a preorganized precursor affords the difunctional [2]catenane monomer. In route 2, the difunctional [2]catenane monomer is synthesized directly via the template-directed cyclization reaction of two hemicyclic precursors. In route 3, stepwise threading and cyclization reactions are employed to prepare difunctional [2]catenane monomers. Unlike route 1 to 3, covalent bonds are used as templating units during the second cyclization reactions to prepare difunctional [2]catenane monomers in route 4. Route 5 shows the preparation of difunctional bis[2]catenane monomers. When difunctional [2]catenane or bis[2]catenane monomers are in hand, the main-chain poly[2]catenanes can be prepared via the polymerization of the difunctional catenane monomers.

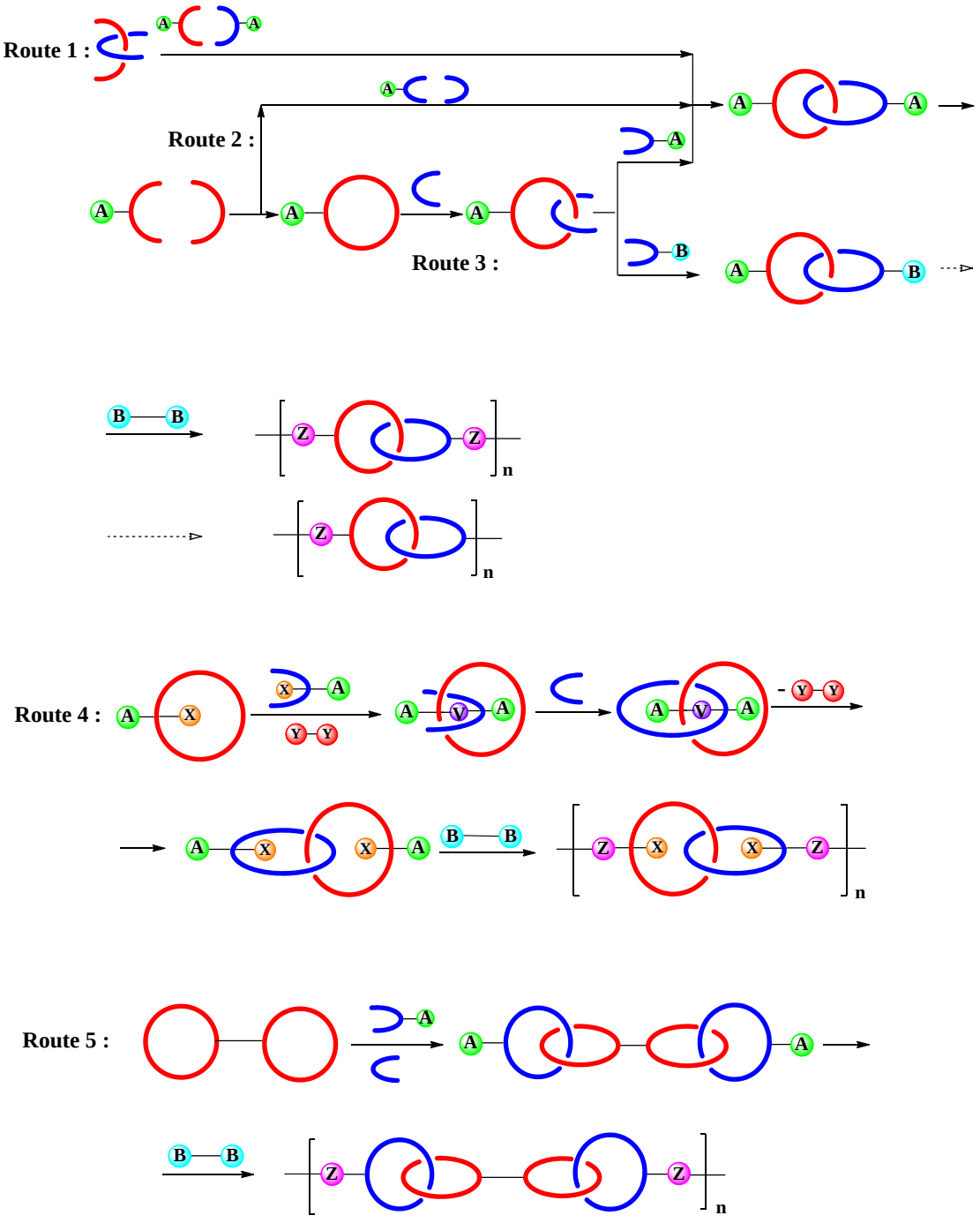

Scheme 2-3. Synthetic routes for linear main chain poly[2]catenanes. Functional group A reacts with group B to produce Z linkages. The functional group X reacts with the spacer with two Y functional groups to produce V linkages.

2.2.2.1 Amide-Based Poly[2]catenanes

Hunter[31,59] and Vögtle[32,60] independently reported the first amide-based [2]catenanes which were synthesized via simple one- or two-step strategies. The easy synthesis and easy functionalization of the amide-based [2]catenane make them attractive.[33,61,62]

By employing route 2 (Scheme 2-3), Geerts *et al*. successfully prepared the first amide-based oligo[2]catenanes in 1995 (Figure 2-3).[63] First, dibromide-functionalized [2]catenane was synthesized via Hunter's two-step strategy. Two isomers - IN-OUT **6a** and OUT-OUT ***6b*** - were obtained in 5% and 9% yield respectively. Due to the intermolecular hydrogen bonding, the isomeric catenanes were conformationally frozen and could not be interconverted even at relatively high temperature.[61-64] Pd^0-catalyzed *coupling* polymerization between **6a** and different rigid comonomers **7a-d** were carried out, but only the reactions between **6a** and **7c, d** afforded oligo[2]catenanes **8a** and **8b** in yields of 84% and 99%. Gel-permeation chromatographic (GPC) analyses gave the number-average molecular weights (M_n) and weight-average molecular weights (M_w): 3.0 kDa, 3.6 kDa for **8a** and 3.3 kDa, 5.0 kDa for **8b**. The degrees of polymerization (DP_n) of **8a** ranged from 1 to 5 based on GPC results. However, fast atom bombardment mass spectrometry (FAB-MS) investigation indicated that higher oligomers (DP_n = 6-8) existed. Although only oligomers were obtained, the glass transition temperature (T_g) for **8b** was 245℃ according to differential scanning calorimetric (DSC) analysis. The conformationally-frozen catenane subunits in the oligomers probably led to the relative high T_g.

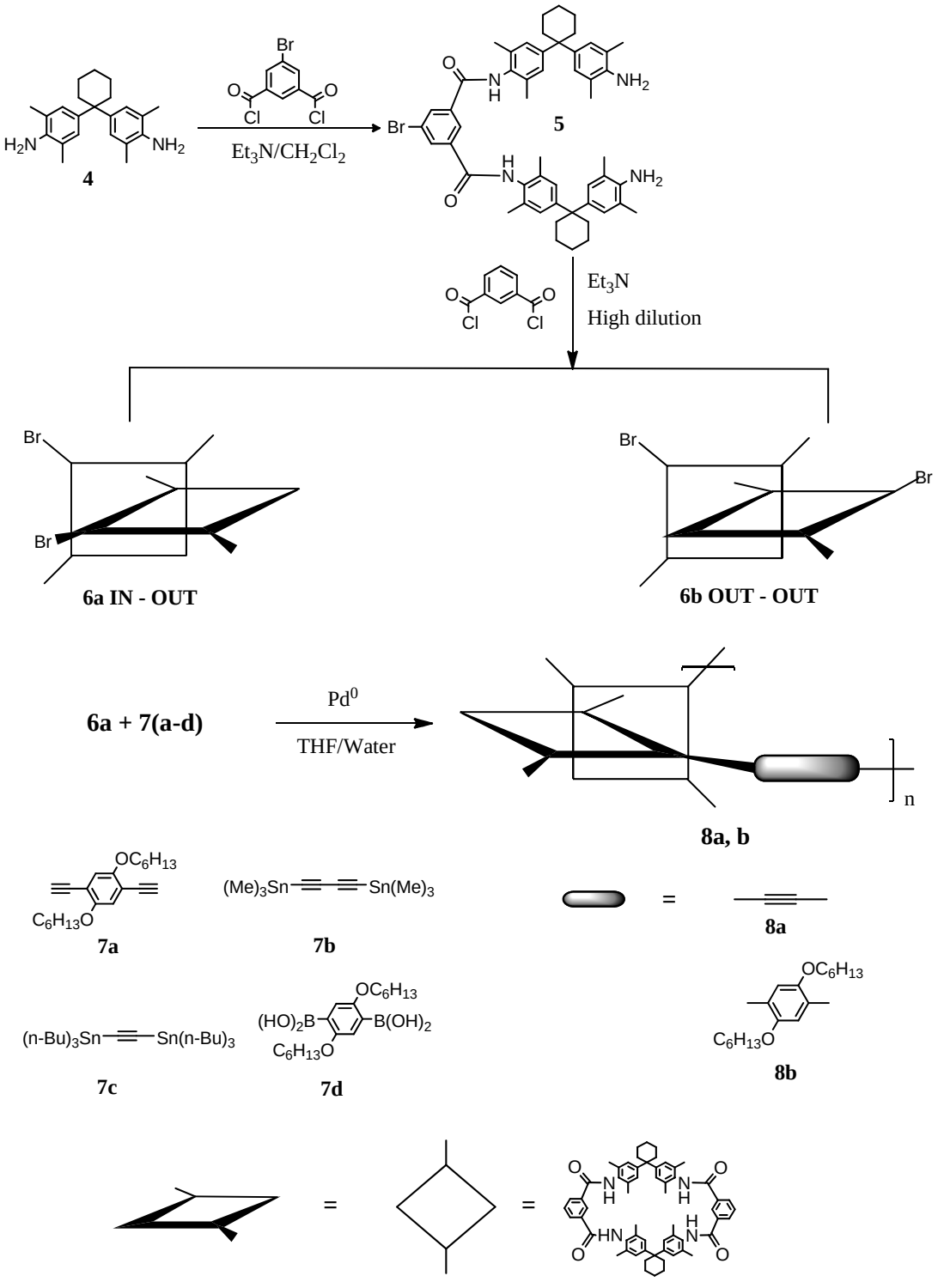

Figure 2-3. Synthesis of amide-based oligo[2]catenanes **8a** and **8b**.

As a further step forward, poly[2]catenanes **12a** and **12b** (Figure 2-4) were successfully prepared by Geerts *et al.* by using more rigid [2]catenane monomers.[65] The poor solubility of Hunter-Vögtle type [2]catenan*es* in common organic solvents, which was caused by their compact structure and intermolecular hydrogen bonding, was considered as the major reason for their inertness towards polymerization. Therefore, the amide functional groups in Hunter-Vögtle type [2]catenan*es* were N-methylated[32] in order to increase the solubility. Dibenzyloxy[2]catenanes isomers, **9a**, IN-OUT and **9b**, OUT-OUT, were prepared via the reaction between the diamine and 5-benzyloxyisophthaloyl chloride. After N-methylation of the amide functional groups and the subsequent hydrolysis of the benzyloxy groups, bisphenolic [2]catenane isomers **10a** (IN-OUT, 7-fold N-methylated [2]catenane) and **10b** (OUT-OUT, 8-fold N-methylated [2]catenane) were obtained in 16% and 8% total yields. As a result of the N-methylation reaction, both were highly soluble in chlorinated solvents. Moreover, proton nuclear magnetic resonance spectroscopic (^{1}H-NMR) investigations on **10a** and **10b** showed that there was no temperature dependence. In other words, the structures of **10a** and **10b** were highly rigid. After the polymerization of **10a** and **10b** with the substituted terephthalic acid **11** under mild conditions,[66] poly[2]catenanes **12a** and **12b** were afforded in yields ranging from 94% to 97%. The molecular weights of **12a** and **12b** were investigated by GPC, viscometry and matrix-assisted laser desorption ionization time of flight mass spectrometry (MALDI-TOF MS). According to these investigations, the molecular weights for **12a** were M_n = 34.0 kDa and M_w = 59.1 kDa and for **12b**: M_n = 46.6 kDa and M_w = 95.6 kDa. DP_n of **12a** and **12b** determined by GPC with MALDI-TOF calibration were 12 and 20, respectively. The solution property studies of **12a** and **12b** were carried out in THF and indicated **12a** forms a more compact coil in solution compared with **12b**. **12a** and **12b** were expected to have good thermal stability due to their polyaromatic amide-ester structures. Thermogravimetric analysis (TGA) confirmed this expectation – no weight loss was observed up to 380℃. Moreover, both poly[2]catenanes had high T_g values: 277℃ for **12a** and 207℃ for **12b** according to DSC analyses. The wide-angle X-ray scattering analyses revealed that both poly[2]catenanes are amorphous.

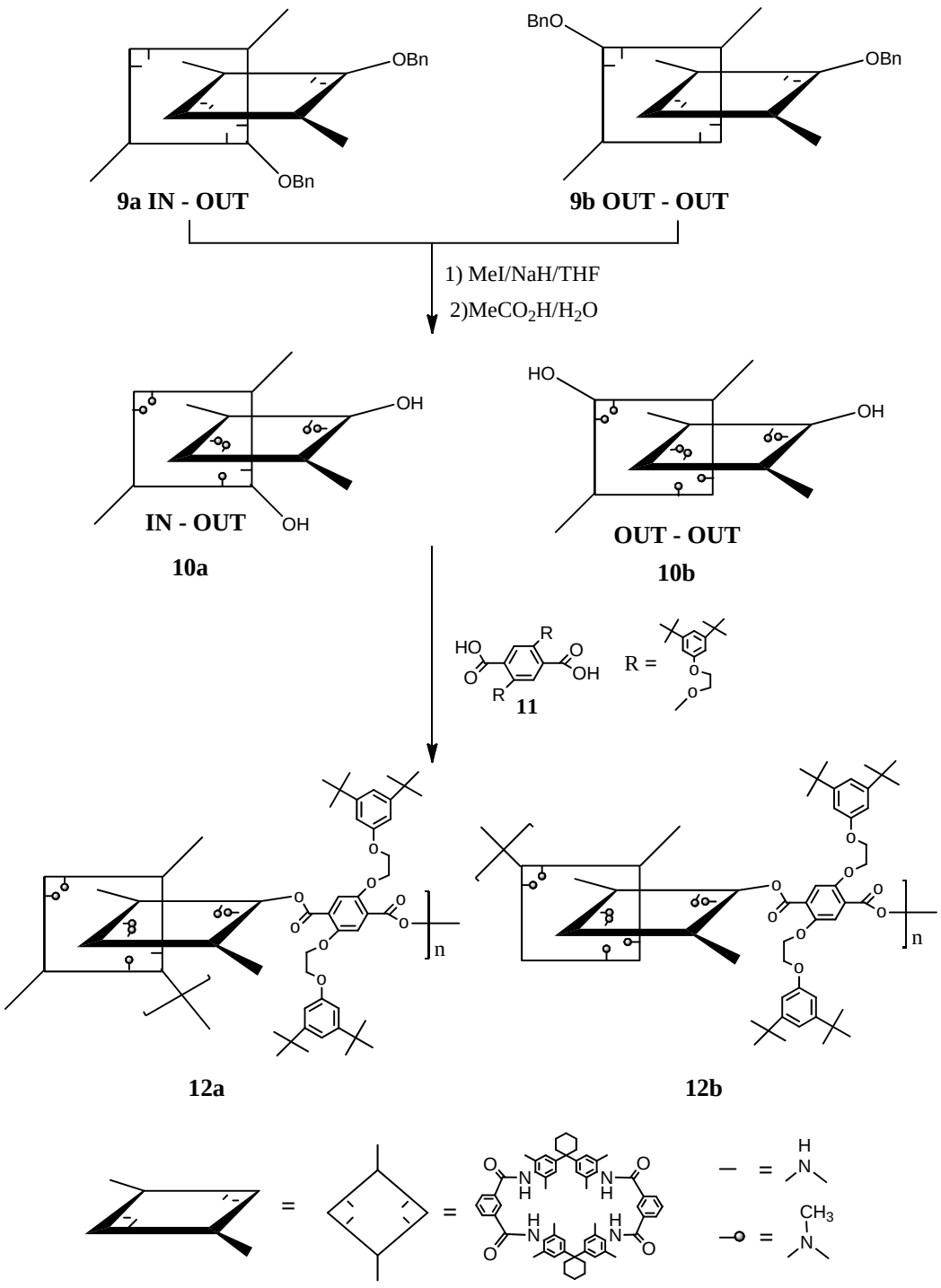

Figure 2-4. Synthesis of amide-based poly[2]catenanes **12a** and **12b.** BnO means benzyloxy group.

Leigh and co-workers reported two other similar amide-based poly[2]catenanes **14a** and **14b**, in which only limited amounts of [2]catenane structures (10-30% w/w) were incorporated into a commercially available polymer - polycarbonate (PC) - by employing solid-state polymerization (SSP) (Figure 2-5).[67-69] It is a smart way to study the effect of the mechanically-interlocked catenane structures on the polymer properties through comparison with the corresponding conventional polymers. By using the two-step strategy, octa-*N*-methylbisphenol [2]catenane **13a** was prepared on a multigram scale without using chromatographic purification. The amide group was methylated in order to increase the mobility of the resulting [2]catenane. Poly[2]catenane **14a** was afforded by the solid-state polymerization[70-72] between different amounts of **13a** and PC prepolymers (M_w = 2.2 kDa, M_n = 1.3 kDa). GPC analysis with a polycarbonate-based universal calibration gave molecular weights for poly[2]catenane **14a**: M_w = 40.1 kDa, M_n = 15.9 kDa, PDI = 2.5 for the copolymer containing 10% (w/w) catenane; M_w = 41.4 kDa, M_n = 9.9 kDa, PDI = 4.2 for the copolymer containing 20% (w/w) catenane; M_w = 38.9 kDa, M_n = 8.1 kDa, PDI = 4.8 for the copolymer containing 30% (w/w) catenane. DSC, ^{1}H-NMR and intrinsic viscosity analyses revealed that the [2]catenane subunits were homogeneously distributed throughout the molecular weight distribution. However, only a small influence of the [2]catenane subunits on the T_g values of the poly[2]catenane **14a** was observed according to DSC and dynamic mechanical analysis (DMA). The high internal mobility of the [2]catenane subunits resulting from the methylation of the amide group in the catenane was considered as the possible reason for the insensitivity. Moreover, the intrinsic viscosity analysis showed that the interaction between the **14a** and the solvent (dichloromethane) was strongly affected by the presence of catenane in copolymer chains. DSC analysis showed that the percentage of catenanes in the copolymers played a small role on the crystallization properties of the copolymers. This observation was ascribed to the fact that the copolymers consisted of both crystallizable (pure bisphenol-A PC) and uncrystallizable segments (composed mainly by catenane subunits) and the catenane subunits accumulated in the uncrystallizable segments upon increasing monomer concentration and thus didn't strongly affect the behavior of the crystallizable segments.[73]

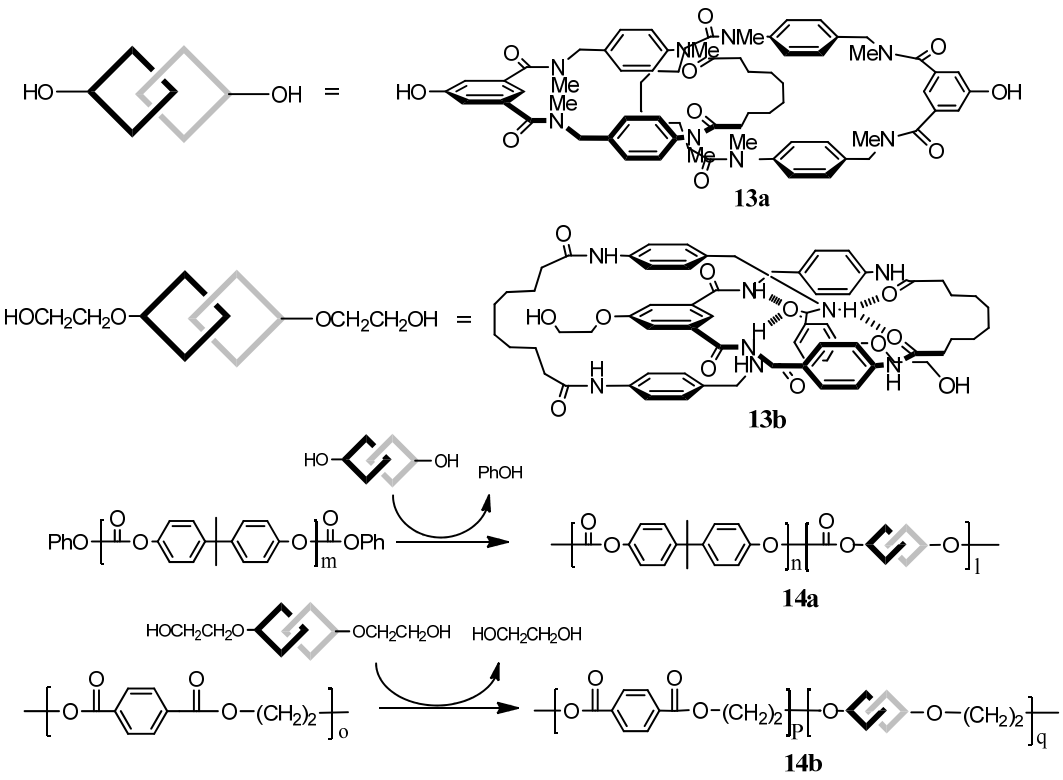

Figure 2-5. Synthesis of amide-based poly[2]catenanes **14a** and **14b**.

Leigh *et al.* further reported another commercially available polymer - poly(ethylene terephthalate) (**PET**) - based poly[2]catenane **14b** (Figure 2-5).[74] In comparison with **PC**, **PET** has good flexibility and a relatively fast crystallization rate.[75,76] Dihydroxy[2]catenane **13b** was prepared via the method used in the synthesis of **13a**. Unlike **13a**, the amide groups on **13b** were kept in order to make a comparative study of the effect of intracatenane macrocyle flexibility on polymer properties. Different amounts of **13b** and PET prepolymers (M_w = 13.0 kDa, M_n = 7.4 kDa) were copolymerized by solid-state copolymerization and poly[2]catenane **14b** was obtained. GPC analysis gave the molecular weight for **14b**: M_w = 67.0 kDa, M_n = 25.0 kDa, PDI = 2.7 for the copolymer containing 5% (w/w) catenane. M_w = 61.0 kDa, M_n = 21.0 kDa, PDI = 2.9 for the copolymer containing 10% (w/w) catenane; M_w = 52.0 kDa, M_n = 17.0 kDa, PDI = 3.0 for the copolymer containing 20% (w/w) catenane. Unlike **14a**, the T_g value of **14b** increased with the catenane percentage in the copolymers, which was attributed to the specific effect of catenane linkage (inter- and intramolecular hydrogen bonding).[77] On the other hand, the T_g value of the

catenane-containing copolymers were lower than the T_g of PET copolymers containing a bulky and rigid comonomer at the same weight content. This observation suggested that the catenane subunits in the copolymer still have some degree of internal mobility. The study of crystallization behavior of **14b** confirmed this deduction. It was found that the catenane percentage had only little effect on the crystallization properties of the copolymers. Like **14a**, the catenane subunits in the copolymer **14b** possessed some degree of internal mobility and thus could accumulate in the amorphous phase.

Yamazaki and coworkers prepared a novel amide-based poly[2]catenane **17** by employing "click' chemistry"[78-81] (Figure 2-6).[82] In their work, the poly[2]catenane **17** was afforded via 1,3-dipolar cycloaddition of diazido[2]catenane **16**, which was prepared via Hunter's two-step method, and 4,4'-diethynylbiphenyl at room temperature. According to GPC analysis, the molecular weight (M_n) of the polymer was 15.0 kDa and the M_n/M_w was 2.0. A side reaction - cyclodimerization - occurred during the polymerization, but it could be inhibited without lowering the molecular weight of the resulting poly[2]catenane by performing the polymerization at lower temperature. For example, polymerization at 0°C gave M_n = 16.0 kDa, M_w/M_n = 2.0.

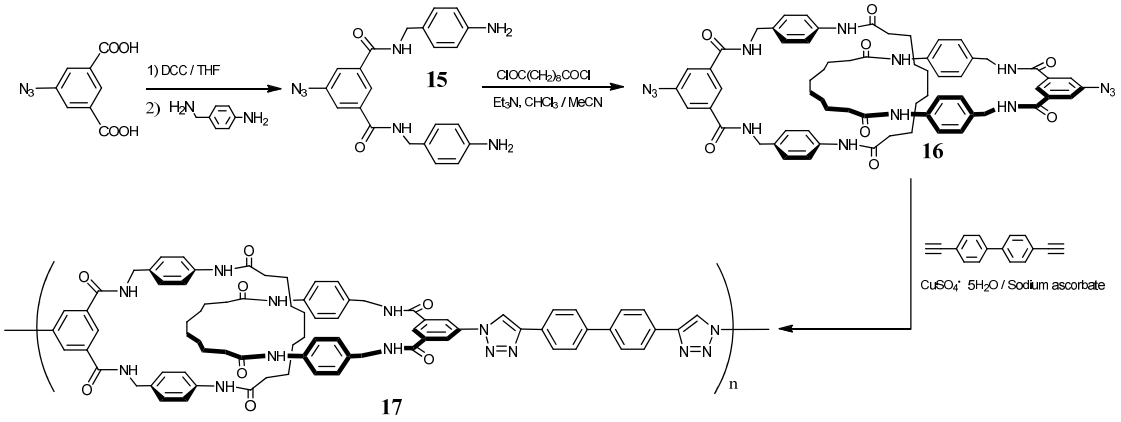

Figure 2-6. Synthesis of amide-based poly[2]catenane **17**. DCC means N,N' dicyclohexylcarbodiimide.

Takata *et al.* reported another very interesting amide-based poly[2]catenane (or oligo[2]catenane) **19** (Figure 2-7).[58] In their work, [2]catenane monomer **18** was synthesized in a high yield by taking advantage of macrocycle-**1** as the template, which was proven to be a good

templating precursor for the synthesis of catenanes.[83,84] Poly[2]catenane **19** was prepared via the Diels-Alder polymerization of **18** at 140 °C without solvent for several hours. According to GPC analysis with PSt standards, for **19**: M_n = 3.1 kDa, PDI = 1.98. As discussed above, this a could be a promising approach to prepare linear polycatenanes, but more efficient polymerization conditions must be developed.

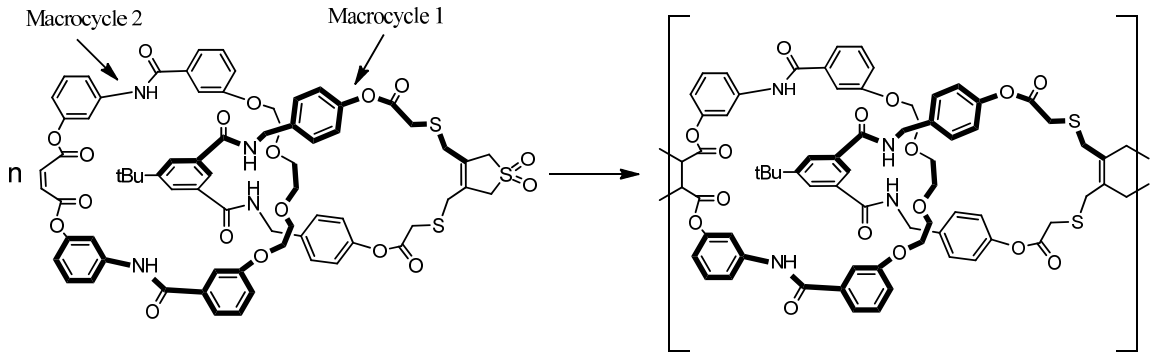

18 **19**

Figure 2-7. Synthesis of bridged poly[2]catenane **19**.

2.2.2.2 Phenanthroline-based Poly[2]catenanes

Sauvage *et al*. prepared the first phenanthroline-based [2]catenanes by taking advantage of the three-dimensional template effect of transition metals (e.g., copper(I) ions) with phenanthroline-type ligands.[40,41,85] The phenanthroline-based [2]catenanes can be synthesized via two possible approaches - route 1 and route 3 in Scheme 2-3. In route 1, the two phenanthroline-type ligands first are entwined around a metal center in a tetrahedral geometry and the subsequent cyclization reaction will afford phenanthroline-based [2]catenane. Route 3 includes stepwise cyclization of hemicyclic phenanthroline ligands. Although route 1 is straightforward, route 3 is the common way to prepare phenanthroline-based [2]catenanes, because it has better yield and possibility of preparing catenanes with two different rings.

Sauvage *et al*. first reported the phenanthroline-type poly[2]catenanes **24a**,**b** via route 3 (Figure 2-8).[86,87] In their work, first the phenanthroline-based macrocyclic precursor **20** entwined with phenanthroline-based hemicyclic precursor **21** via copper(I) ions. The resulting entwined catenane precursor cyclized with diiodide **22** and the following reduction afforded [2]catenane monomer **23a**. Demetallation of **23a** by potassium cyanide (KCN) gave **23b**. Poly[2]catenane

24a was obtained via the polymerization of **23a** with diacid **11**. GPC analysis with polystyrene standards indicated the molecular weight values for **24a** were M_w = 1800 kDa, M_n = 55.0 kDa. However, the presence of copper(I) complex and the PF_6^- counterion in every repeat unit of **24a** led to strong dipolar interactions and thus aggregation occurred. As a result, the molecular weight distribution was overestimated. After demetallation of poly[2]catenane **24a**, **24b** was obtained. Interestingly, the direct polymerization of **23b** with diacid **11** mainly produced cyclic oligo[2]catenanes. The high flexibily of **23b** was considered as the main reason for the formation of cyclic oligo[2]catenanes. According to GPC analysis with universal calibration,[88] the molecular weight ranges for **24b** were: M_w = 42.0 - 47.0 kDa, M_n = 22.0 - 25.0 kDa; DP_n = 8 - 9. TGA analysis indicated reasonable thermal stabilities of **24a** (up to 210 ^oC) and **24b** (up to 300 ^oC). DSC analysis showed that the T_g of **24a** is slightly higher than the T_g of **24b**.

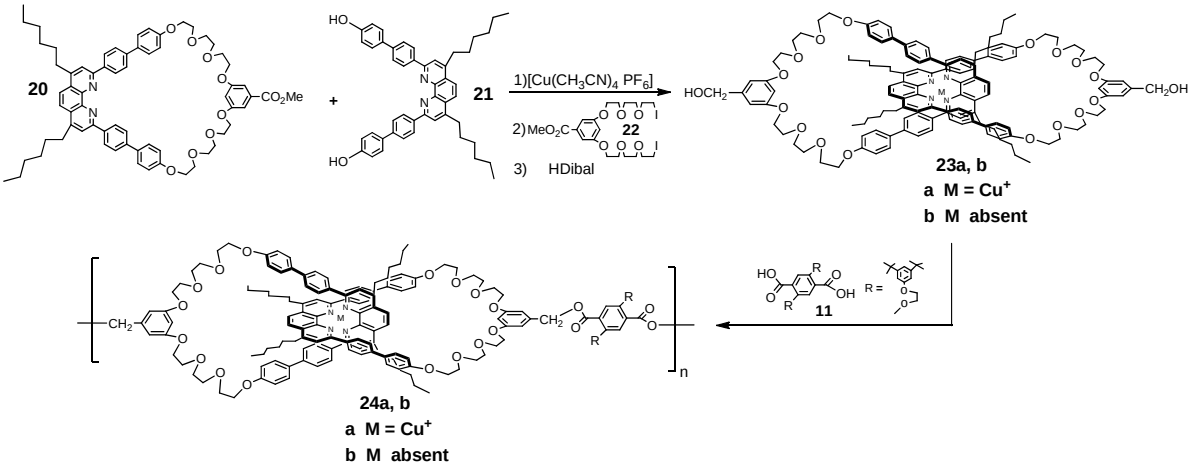

Figure 2-8. Synthesis of phenanthroline-based poly[2]catenanes **24a, b**. HDibal means diisobutylaluminum hydride.

Other high molecular weight phenanthroline-type poly[2]catenanes **26a**,**b** were successfully prepared by Shimada and co-workers (Figure 2-9).[89] By using a similar strategy, [2]catenanes **25a**,**b** were synthesized. Polymerization of **25a** with adipoyl dichloride afforded poly[2]catenane **26a** and the subsequent demetallation afforded **26b**. GPC with polystyrene standard showed that M_w of **26b** was as high as 810 kDa, corresponding to DP_n of 609 and suggesting extensive aggregation. Similar to the polymerization of **23b** and diacid, the direct polymerization of **25b** with adipoyl dichloride only afforded intermolecular cyclization "pretzel"-like products.[90]

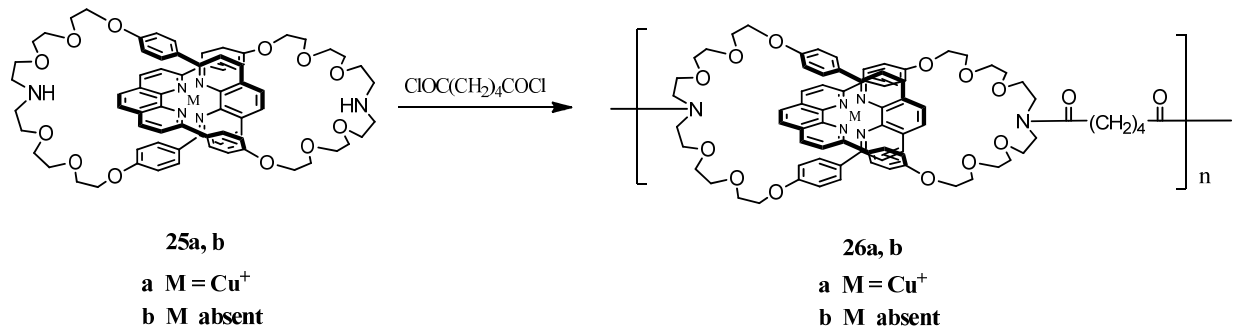

Figure 2-9. Synthesis of phenanthroline-based poly[2]catenanes **26a, b**.

2.2.2.3 Tetracationic Cyclophane – Aromatic Crown Ether based Poly[2]catenanes

Stoddart *et al.* reported the first synthesis of a tetracationic cyclophane (namely $CBPQT^{4+}$)-aromatic crown ether-based [2]catenane by taking advantage of the strong binding affinity between a π-electron-deficient bipyridinium-based cyclophane and a π-electron-rich crown ether ring.[36] The driving forces include π-π stacking, edge-to-face interactions between aromatic rings and hydrogen bonding.

Stoddart's group made many achievements in preparing $CBPQT^{4+}$- aromatic crown ether based [2]catenanes/poly[2]catenanes.[29,91-95] They reported the first $CBPQT^{4+}$- aromatic crown ether based poly[2]catenane **32** (Figure 2-10) by using route 3 in Scheme 2-3.[96,97] In their work, dicationic salt **28** first was threaded through aromatic crown ethers **27** and the resulting preorganized precursors were coupled with dibromide **29** under ultrahigh-pressure.[98] After counterion exchange, difunctionalized [2]catenane monomers **30** and **31** were afforded. Poly[2]catenane **32** was obtained via the polymerization between **30** and bis(4-isocyanatophenyl)methane in acetonitrile. GPC analysis performed on the chloride analog gave a molecular weight M_n of 26.5 kDa for **32**, corresponding to a DP_n of 17. Due to the asymmetry of [2]catenane monomer **30**, the poly[2]catenane **32** possibly was a mixture of different constitutional isomeric types.

The attempted direct polyesterification of AB [2]catenane monomer **31** did not yield any polymer; the failure was ascribed to unfavorable stereoelectronic effects that lower the reactivity of the complementary functional groups. In order to increase the reactivity of the functional groups on the catenane monomer, the CH_2OH groups on **31** were converted into CH_2Br groups and AB [2]catenane monomer **33** was obtained. As a result, the polyesterification of **33** was

successful and the poly[2]catenane **34** was isolated after counterion exchange. According to GPC analysis, the molecular weight (M_n) of **34** was 35.0 kDa, corresponding to a DP_n of 25.

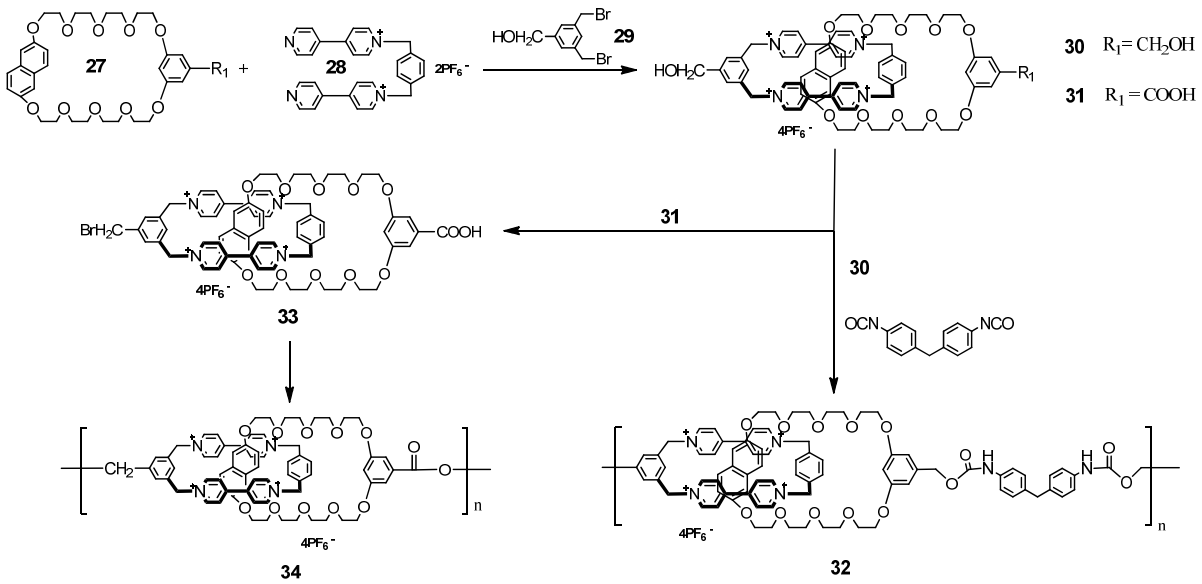

Figure 2-10. Synthesis of tetracationic cyclophane - aromatic crown ether based poly[2]catenanes **32** and **34**.

Moreover, two other novel poly(bis[2]catenane)s **38** and **39** were synthesized by Stoddart and co-workers (Figure 2-11).[99] By employing the same template-directed strategy, dihydroxyl-functionalized [2]catenane monomers **36** and **37** were prepared. The polymerization of **36** and **37** with bis(4-isocyanatophenyl)methane successfully afforded poly(bis[2]catenane)s **38** and **39**. According to GPC results, **38** and **39** had the same molecular weight (M_n): 45.0 kDa (DP_n = 15).

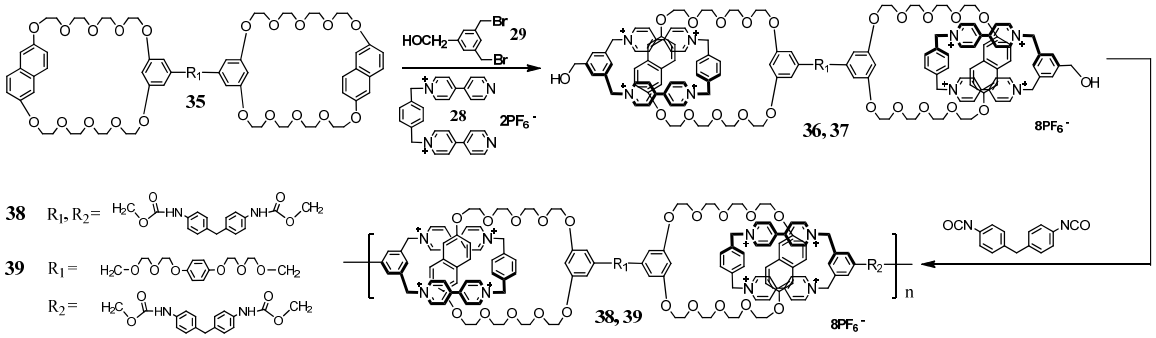

Figure 2-11. Synthesis of tetracationic cyclophane – aromatic crown ether-based poly(bis[2]catenane)s **38** and **39**.

Stoddart *et al.* also reported poly(bis[2]catenane) **41** based on on a transition metal chelation effect (Figure 2-12).[100] Bis[2]catenane monomer **40**, which was prepared by using the same template-directed strategy described above,[101] was mixed with CF_3SO_3Ag in acetonitrile at room temperature and poly(bis[2]catenane) **41** was obtained after counterion exchange. GPC analysis with protein standards indicated the molecular weight (M_n) for **41** was 150 kDa, corresponding to a DP_n of 40.

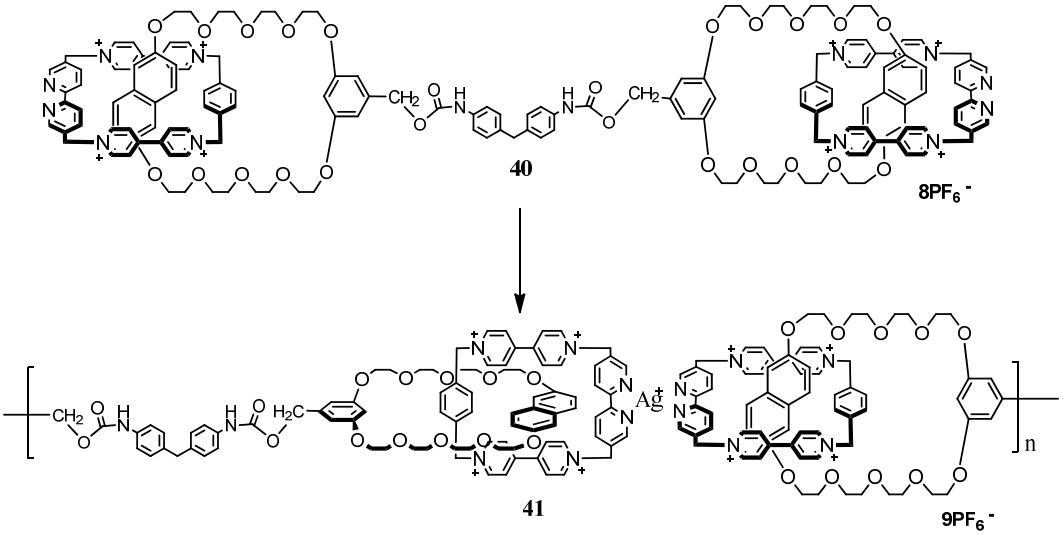

Figure 2-12. Synthesis of tetracationic cyclophane - aromatic crown-ether based poly(bis[2]catenane) **41**.

2.2.2.4 Other kinds of poly[2]catenanes

As shown by route 4 in Scheme 2-3, Godt *et al.* [56,102-104] tried to employ a covalent bond - a carbonate group, instead of the noncovalent interactions used in the above examples, to template the [2]catenane monomer synthesis (Figure 2-13). In their work, first the macrocycle **43** was synthesized via the oxidative cyclodimerization of dialkyne **42**[104] by using the pseudo-high dilution technique. After the phenolic group was converted into a chloroformate group, the sodium salt of **42** was threaded though macrocycle **43** and the following intra-pseudorotaxane carbonate formation afforded **44**. Another cyclization of **44** via oxidative cyclodimerization

reaction yielded **45**. Finally, the carbonate group, which linked the two macrocycles (more than 63-membered), was cleaved and [2]catenanes **46** were obtained. According to electron paramagnetic resonance (EPR) analysis, the macrocycles of the [2]catenanes rotate freely and the [2]catenanes also have a high degree of lateral freedom of movement. Poly[2]catenane **47-m** was obtained via the polyesterification of **46-ma**, bearing two carboxylic groups on each ring, with 1,4-bis(bromomethyl)benzene. The molecular weights determined by GPC analysis for **47-m** were M_w = 95.2 kDa, M_n = 28.9 kDa, and DP_n = 10. Also, a broad mass distribution and intramolecular cyclic pretzel-like product were observed by GPC. Polyesterification of AB monomer **46-mb** afforded poly[2]catenane **48-m**. The average molecular weights given by GPC analysis were: M_w = 56.4 kDa, M_n = 20.9 kDa and DP_n = 7. Like the synthesis of **47-m**, a broad mass distribution and a cyclic product were indicated by GPC. In order to make high molecular weight polymers, the facile acyclic diene metathesis (ADMET)[105-107] polymerization was employed and poly[2]catenane **49-l** was obtained via the polymerization of α,ω–diene **46-lc** with a typical Grubbs catalyst.[108,109] GPC analysis indicated the molecular weights of **49-l** were M_w = 69.3 kDa, M_n = 33.0 kDa, corresponding to DP_n = 12. However, ^{1}H-NMR investigation suggested that the product probably was composed of cyclic oligomers, since no terminal olefinic proton peaks were found. It should be noted here that all the poly[2]catenanes prepared via this approach have relatively low DPs and cyclic side products existed. If the high flexibility of large ring [2]catenanes is considered, this observation is reasonable in light of Shimada's[89] and Sauvage's[86,87] results. This new strategy is meaningful by providing a new methodology for the synthesis of catenane monomers and polycatenanes.

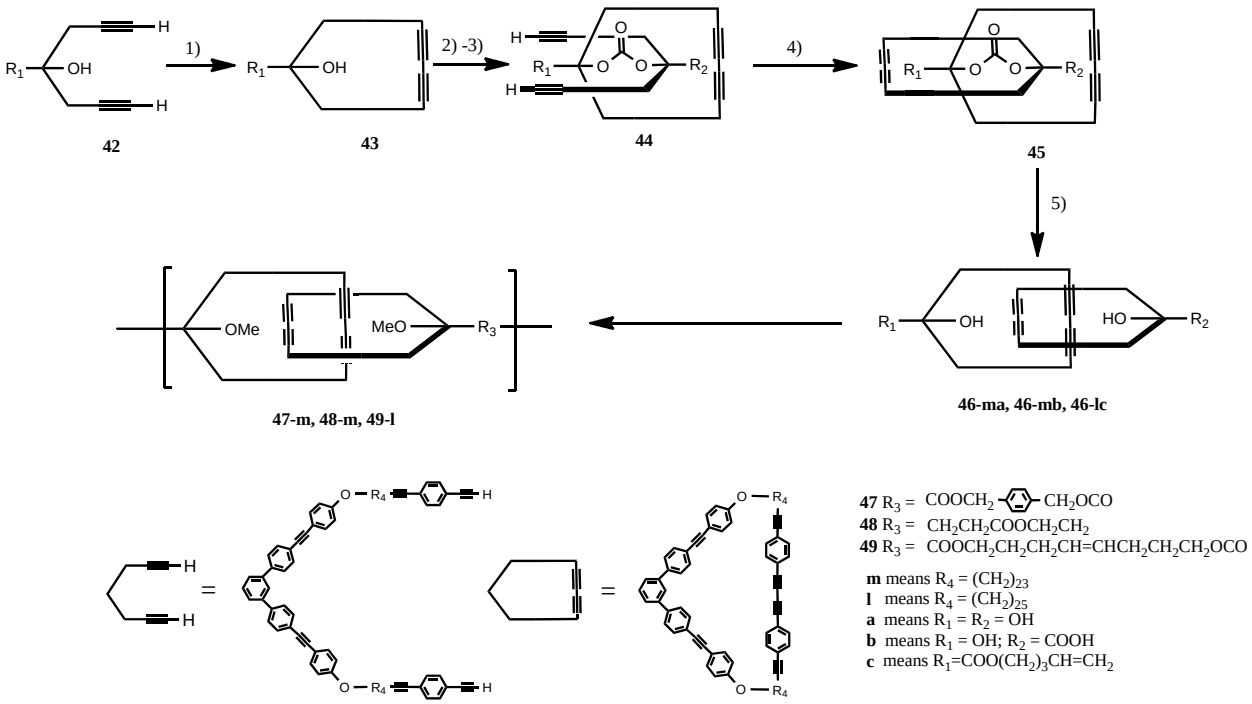

Figure 2-13. Synthesis of poly[2]catenanes **47-m**, **48-m** and **49-l** by utilizing a covalent bond as a "template".

2.3 Side-chain polycatenanes

As shown by **C** and **D** in Figure 2-1, side chain polycatenanes are polymers containing catenane subunits in their pendant groups; they are expected to possess different properties compared with main chain polycatenanes. Due to the same synthetic problem as the preparation of linear poly[n]catenanes, only poly[2]catenane-type side chain polycatenanes have been reported so far.

The typical synthetic approaches to poly[2]catenanes are summarized in Scheme 2-4. In route i, the polymerization of difunctional [2]catenane monomers bearing both functional groups on the same macrocycle afford side-chain poly[2]catenanes. In route ii, polymers containing macrocycles in their backbones are prepared first and the following cyclization reactions of the other macrocycle's precursors through the macrocycles in the polymer backbones produce side-chain poly[2]catenanes. In route iii, side-chain poly[2]catenanes are obtained by grafting monofunctionalized [2]catenanes onto polymer side chains. Route iv is similar to route ii; polymers containing macrocycles as pendants are synthesized first and the subsequent

cyclization reactions of the other macrocycle's precursors through the pendant macrocycles afford side-chain poly[2]catenanes. As far as the synthetic feasibility and the integrity of the resulting polymers are concerned, route i is the best approach to prepare side-chain poly[2]catenanes and thus is the most commonly used synthetic method so far.

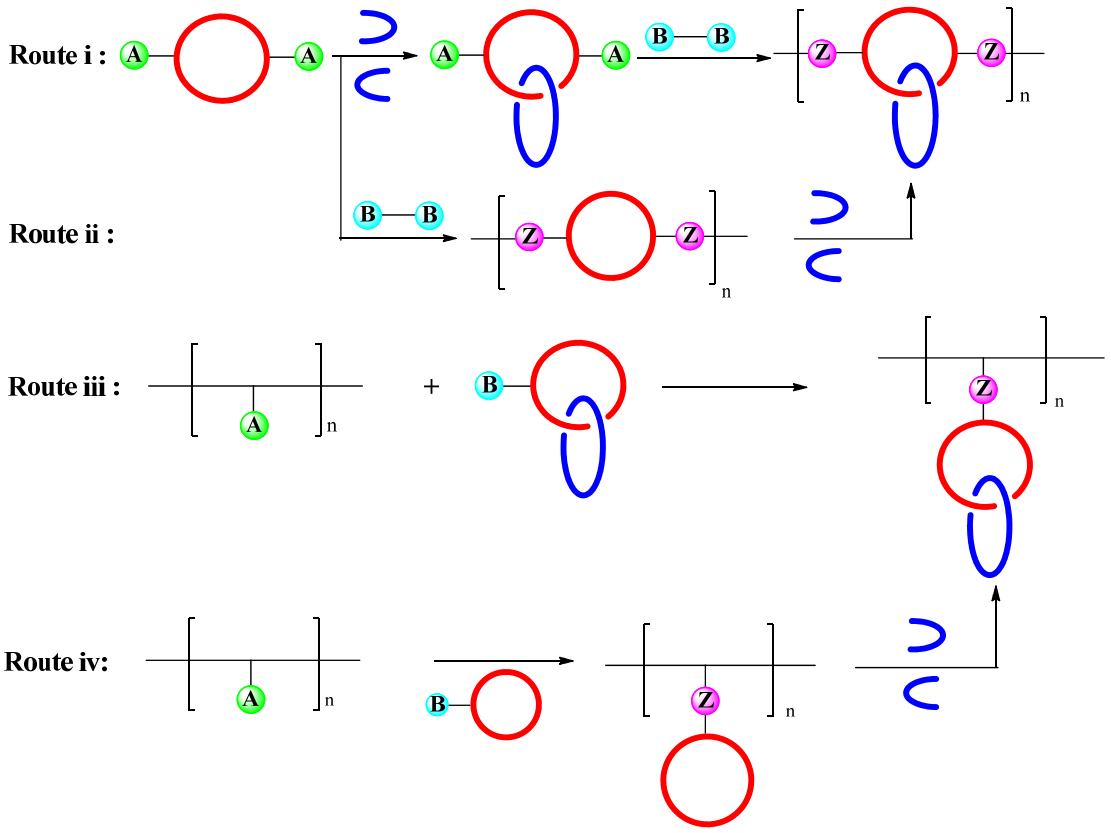

Scheme 2-4. Synthetic routes for side chain poly[2]catenanes. Functional group A reacts with group B to produce group Z.

Stoddart *et al.* reported the first tetracationic cyclophane - aromatic crown ether type side chain poly[2]catenanes **51**[99,110] via route i (Figure 2-14). In their work, the dihydroxyl functionalized [2]catenane monomer **50** was prepared first by employing a template method similar to that discussed before. Side-chain poly[2]catenane **51** was prepared by the polymerization between **50** and bis(4-isocyanatophenyl)methane. According to GPC analysis the molecular weight (M_n) of **51** was 27.0 kDa, corresponding to a DP_n of 20.

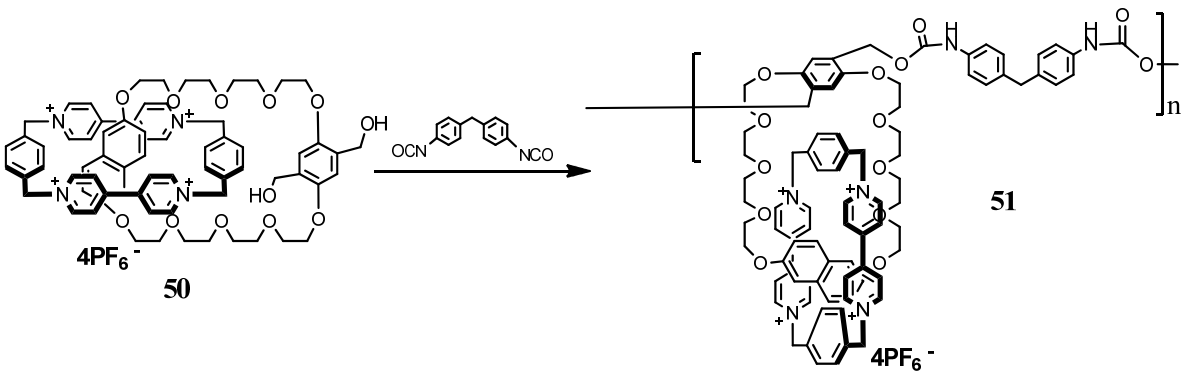

Figure 2-14. Synthesis of side-chain poly[2]catenane **51**.

Another tetracationic cyclophane–aromatic crown ether type side chain poly[2]catenane **53** was prepared by Simone *et al.* via route i (Figure 2-15).[111] Bis-3,4-(ethylenendioxy)thiophene functionalized [2]catenane monomer **52** was prepared first and then electrochemical polymerization of the thiophene units of **52** led to side-chain poly[2]catenane **53**, which was proven by cyclic voltammetry.[112]

Bria *et al.* synthesized a tetracationic cyclophane–aromatic crown ether type side-chain poly[2]catenane **59** by employing "click chemistry" via route iii (Figure 2-16).[113] First, the template-directed coupling reaction between bis(bipyridinium) salt **28** and the alkyne-substituted *p*-xylylene dibromide **55** in the presence of dinaphtho crown ether **54** afforded an alkyne functionalized [2]catenane **56**.[114] The substitution of the chloro group on styrene-vinylbenzyl chloride copolymer **57** (M_n = 3.7 kDa, M_w = 6.3 kDa) with sodium azide gave azide-functionalized polymer **58**.[85,115-117] By employing $CuSO_4$/ascorbic acid as catalyst,[118-122] "click chemistry" between azide-functionalized polymer **58** and alkyne functionalized [2]catenane **56** afforded side-chain poly[2]catenane **59**. The successful formation of **59** was proven by FTIR and ^{1}H-NMR analyses. However, ^{1}H-NMR and FTIR investigations revealed that the reaction of the azide groups wasn't complete and the observation was ascribed to Coulombic repulsion of the cyclophane units and steric hindrance caused by the bulky catenane units.[123]

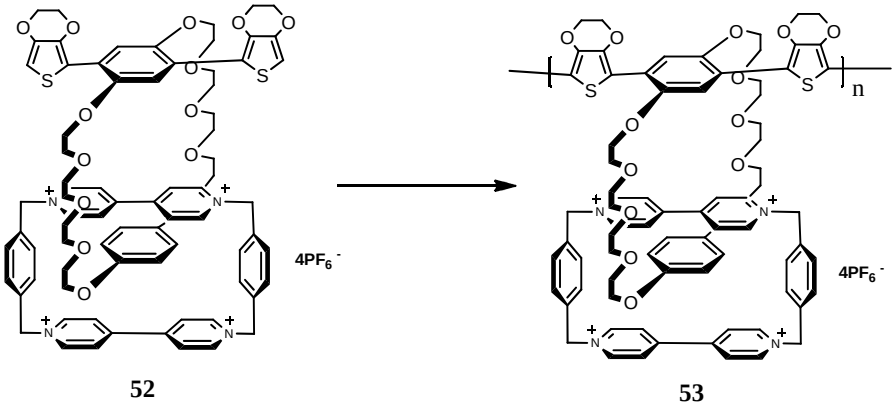

Figure 2-15. Synthesis of side-chain poly[2]catenane **53**.

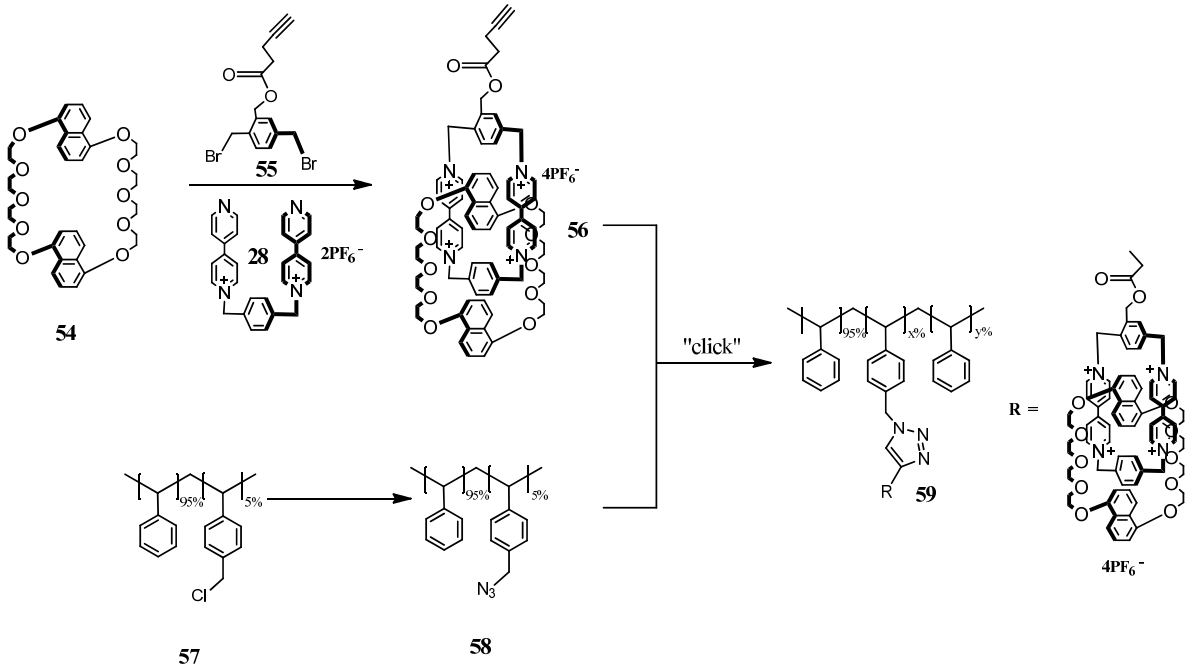

Figure 2-16. Synthesis of side-chain poly[2]catenane **59.**

Another similar bistable side-chain poly[2]catenane **64** was reported by Stoddart and co-workers (Figure 2-17) by employing a method similar to the preparation of **59**.[124] [2]Catenane monomer **60** bearing an alkyne group was prepared first as described above. As shown in Figure 2-17, monomer **60** was bistable and was composed of two switchable isomers - a ground-state co-conformation (GSCC) and the metastable-state co-conformation (MSCC) corresponding to different locations of the tetrathiafulvalene (TTF) and dioxynaphthalene (DNP) units in

$CBPQT^{4+}$ ring within the polyether ring. The ratio between the GSCC isomer and the MSCC isomer is about 9:1 at 298 K.[125] On the other hand, the reaction between 2-(2'-(2"-azidoethoxy)ethoxy)ethanol **61** and methacryloyl chloride gave azide-functionalized monomer **62** and the subsequent atom transfer radical polymerization (ATRP) of **62** afforded side-chain azide-functionalized polymer **63** (M_w = 55.0 kDa, M_n = 39.0 kDa, PDI = 1.4). Finally, "click chemistry" between azide-functionalized polymer **63** and alkyne-functionalized [2]catenane monomer **60** produced side-chain poly[2]catenane **64**. According to ^{1}H-NMR analysis, the molecular weight (M_n) of **64** was 128.0 kDa. However, size exclusion chromatography performed with multi-angle light scattering (SEC-MALS) demonstrated that M_n = 870.0 ± 61.0 kDa, M_w = 1300.0 ± 70.0 kDa and PDI = 1.5 ± 0.1 and the observation suggested aggregation. Interestingly, the poly[2]catenane **64** formed a supramolecular architecture consisting of hollow spherical nanoparticles by self-assembly in solution according to SEC-MALS, dynamic light scattering (DLS) and scanning electron microscopic (SEM) analyses. Moreover, the reversible two electron oxidation process of TTF ($TTF/TTF^{\cdot +}/TTF^{2+}$), which could be achieved chemically or electrochemically, was able to trigger switching of the $CBPQT^{4+}$ ring within the polyether ring. These observation demonstrated that the bistable poly[2]catenane **64** worked as a molecular switch under chemical or electrochemical control even in the supramolecular assemblies.

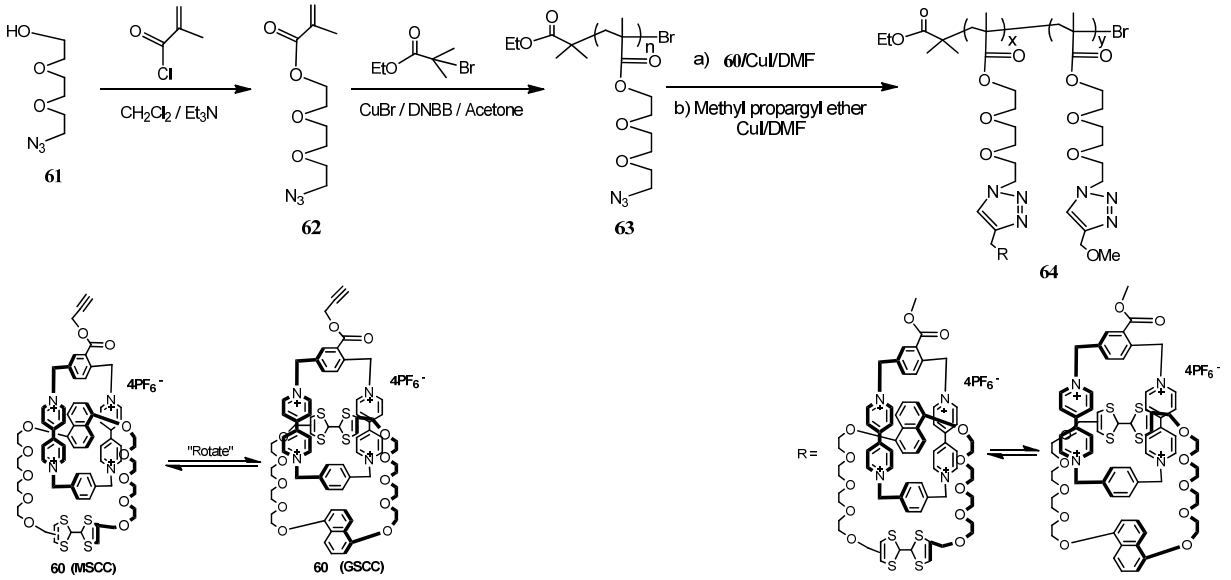

Figure 2-17. Synthesis of bistable side-chain poly[2]catenane **64**.

2.4 Polymeric Catenanes

A polymeric catenane, as shown by type **E** in Figure 2-1, consists of at least one cyclic polymer threading through other cyclic polymers or small rings. These catenanes haves been well known for a long time as the side products formed during the preparation of cyclic polymers.[23,126-127] The synthetic methods proposed or used toward polymer catenanes commonly include threading and cyclization steps - a linear polymer threads through cyclic polymer rings/small rings and then cyclization carried out on the resulting pseudorotaxane produces the polymeric catenane.[128-130] In order to favor the cyclization process and suppress linear chain extension, the cyclization step is always performed under high-dilution or pseudo-high dilution conditions. The purification of polymeric catenanes is always difficult due to the complexity of the crude product, possibly containing desired catenated, cyclic and linear polymers.[131]

Hogen-Esch *et al.* reported a polystyrene-"catenated"-poly(2-vinylpyridine) (**PS-P2VP) 67**[132,133] (Figure 2-18). First, Polymerization of 2-vinylpyridine initiated by lithium naphthalenide gave linear **P2VP** dianion **65**, which was mixed with a relatively high concentration of cyclic polystyrene **66**[134] (apparent peak molecular weight: M_P = 4.5 kDa) in order to favor the formation of the intermediate pseudorotaxane. The resulting pseudorotaxane was coupled with 1,4-bis(bromomethyl)benzene and polystyrene-"catenated"-poly(2-vinylpyridine) (**PS-P2VP) 67** was formed. Orthogonal solubility[135] between the "catenated" cyclic polymer and other side products was taken advantage of to efficiently separate **67** from the crude product. The crude product was washed with methanol, which is a good solvent for **P2VP** but a poor solvent for **PS** and polymeric catenane **67,** and cyclohexane, which is a good solvent for cyclic **PS** but a poor solvent for **P2VP** and polymeric catenane **67**. After washing, pure **67** was obtained. GPC analysis indicated the molecular weight (M_P) of **67** was about 10.3 kDa, corresponding to the mass sum of the "catenated" **PS** and **P2VP** rings. Fluorescence investigation demonstrated the unusual topology of **67** and further confirmed its formation.

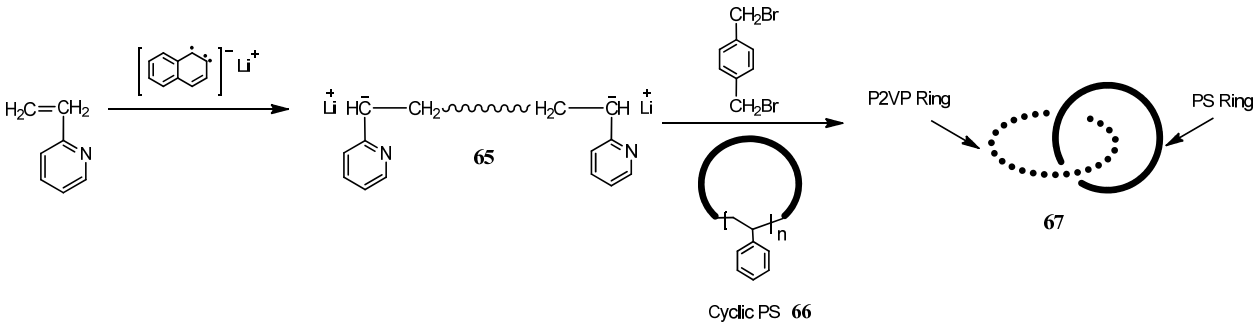

Figure 2-18. Synthesis of polystyrene-poly(2-vinylpyridine) (**PS-P2VP)** based polymer catenane **67**.

A high molecular weight poly(isopropenylnaphthalene-*b*-styrene-*b*-isopro- -penylnaphthalene)-"catenated"-polyisoprene (**PI**) **71** was reported by Takano *et al.* (Figure 2-19).[136] In their work, cyclodimerization of the poly(isopropenylnaphthalene-*b*-styrene-*b*-isopropenylnaphthalene) **68**,[137-138] which was prepared via anionic polymerization followed by modification of the chain ends, initiated by potassium naphthalenide under high dilution conditions, afforded cyclic polymer **69** (M_P = 11.3 kDa). By employing a similar method, polyisoprene (**PI**) **70** was obtained and cyclodimerized by electron transfer in a solution of cyclic triblock polymer **68** and potassium metal under high dilution conditions to produce polymeric catenane **71 (**M_n = 36.8 kDa), as confirmed by GPC, NMR and ozonolysis. Interestingly, **71** exhibited a nanophase-separated structure in the bulk according to transmission electron microscopic (TEM) analysis.

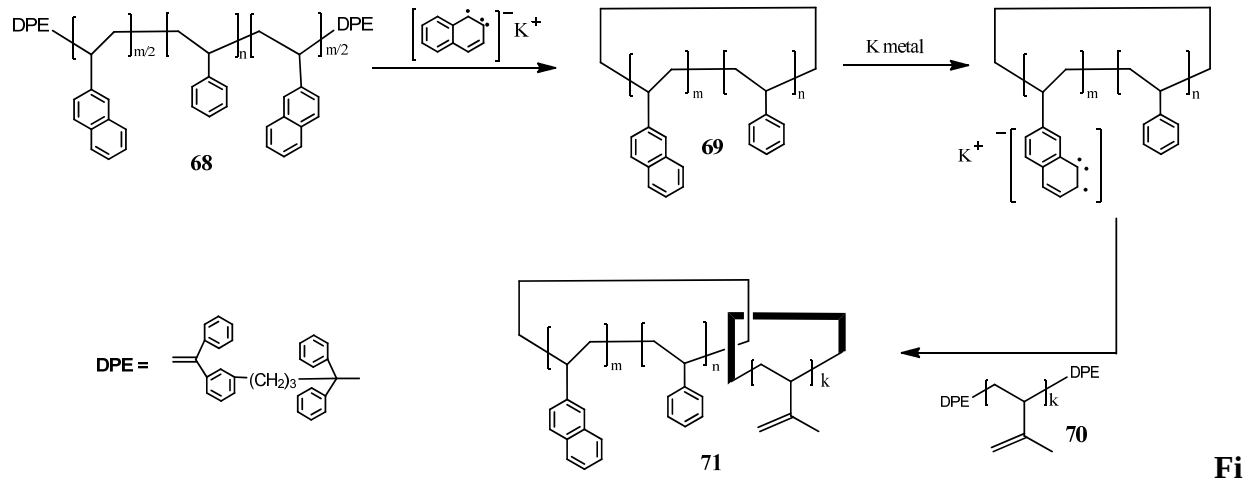

Figure 2-19. Synthesis of polystyrene (**PS**) – polyisoprene (**PI**) based polymer catenane **71**.

Harada *et al.* reported a polymeric catenane **75** based on cyclodextrins[139] (Figure 2-20). Unlike the polymeric catenanes discussed above which consisted of two cyclic polymers, **75** was constructed from a cyclic polymer and relatively small rings. Cyclodextrins (CDs),[140-146] which consist of six or more 1,4-linked D-glucopyranoside units, have hydrophilic external faces and hydrophobic interior faces and thus linear molecules having a hydrophobic middle part with suitable sizes will efficiently thread through the cavities of CDs in polar solvents. Therefore, cyclodextrins (CDs) are good and important hosts in supramolecular chemistry. α-, β- and γ-Cyclodextrins (CDs) (Figure 2-22), corresponding to molecules containing 6, 7 and 8 glucopyranoside units, are commonly used. In their work, α-CD was selected as a cyclic component and **PEG** was selected as the axle to make a "catenated" cyclic polymer based on the foundation that α-cyclodextrin (α-CD) forms inclusion complexes with poly(ethylene glycol) (**PEG**).[147,148] **PEG 72** (M_w = 2.0 kDa) with a 9-anthryl group at one end was threaded through α-CDs and semi-polyrotaxane **73** wase obtained. End-capping of the semi-polyrotaxane **73** with a 9-substituted anthracene gave polyrotaxane **74**, containing one CD for every two ethyleneoxy units. Polymeric catenane **75** (DP_n = 2-10) was synthesized via exposure of polyrotaxane **74** to visible light in dilute solution.

Recently, Tezuka *et al.* reported an amide-based polymeric catenane **82** [149] (Figure 2-21) by employing a smart method called "electrostatic self-assembly and covalent fixation process".[150-151] In this process, the linear soft polymer precursors bearing strained cyclic ammonium salt chain ends are preorganized in dilute solution by their electrostatic interaction with multifunctional carboxylate counteranions, in order to favor the cyclization of the soft polymer precursors. The following ring-opening reaction of the cyclic ammonium salt chain ends by the nucleophilic carboxylate counteranions at an elevated temperature affords cyclic polymers (covalent fixation). In their work, first telechelic poly(THF) **76** bearing *N*-phenylpyrrolidinium salt groups with triflate counteranions was prepared via cationic ring-opening polymerization of tetrahydrofuran with trifluoromethanesulfonic anhydride as the initiator and termination with *N*-phenylpyrrolidine. The THF solution of telechelic poly(THF) **76** was added dropwise into an ice-cold aqueous solution containing excess sodium dicarboxylate salt **77** to give telechelic poly(THF) precursor **78** bearing *N*-phenylpyrrolidinium salt end groups with

isophthaloylbenzylic amide-based dicarboxylate counteranions. A heat treatment of a dilute chloroform solution of telechelic poly(THF) precursor **78** induced the so-called "covalent fixation process" and cyclic poly(THF) **79** was obtained. By employing a similar method, amide-based poly(THF) precursor **81** bearing *N*-phenylpyrrolidinium salt groups accompanying biphenyldicarboxylate counteranions was prepared. Amide-based poly(THF) precursor **81** was mixed with poly(THF) precursor **78** and the subsequent "covalent fixation process" afforded polymeric catenane **82**, whose formation was confirmed by MALDI-TOF mass spectra and SEC analysis. This method provides a new and efficient way to prepare cyclic polymers and polymeric catenanes.

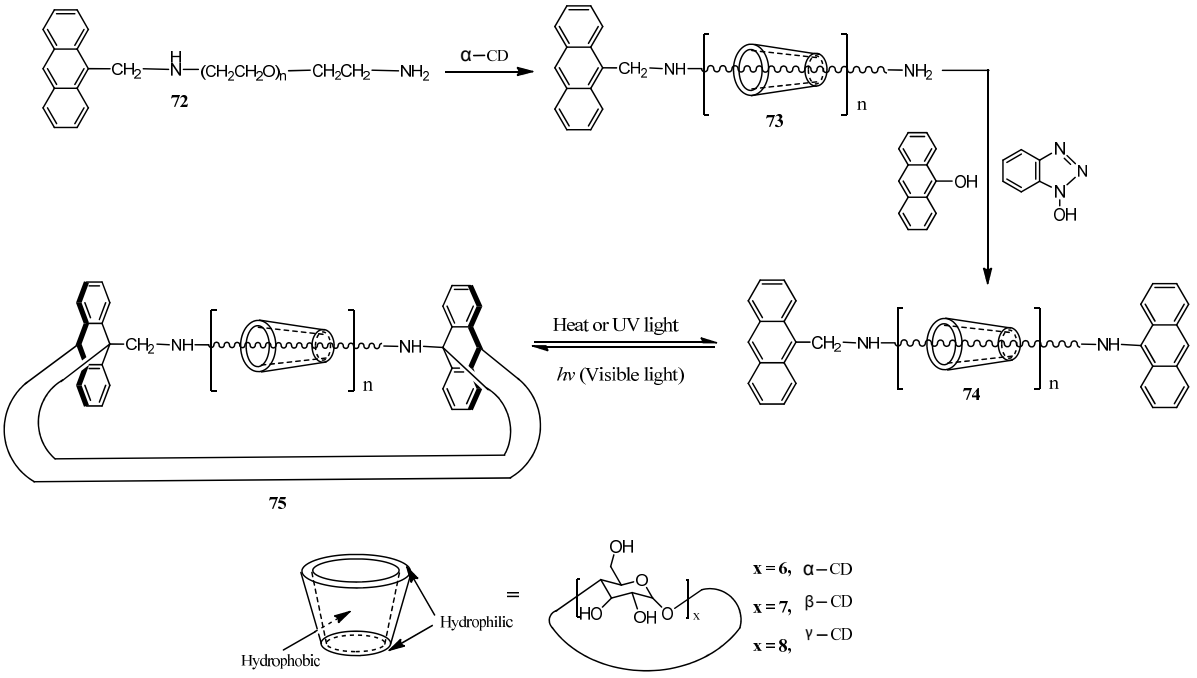

Figure 2-20. Synthesis of polymer catenane **75**.

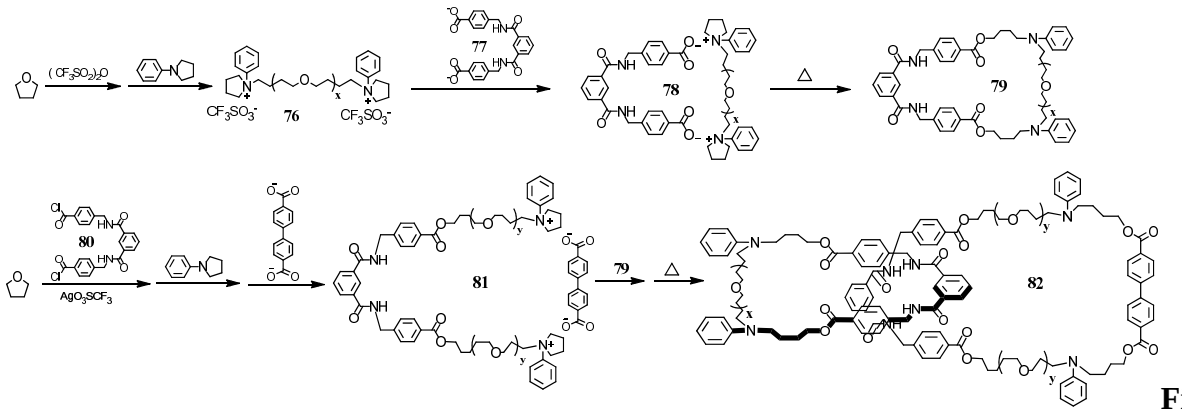

Figure 2-21. Synthesis of polymeric catenane **82**.

2.5 Catenane structures in polymer networks

During the crosslinking process of many polymer networks, catenane structures are possibly formed and exist in the resulting networks. However, recognition and characterization of the catenane structures always are difficult as a result of the complexity of polymer networks and limitation of available analytical techniques. As shown by Figure 2-1, types **G** and **H** represent typical polymer networks containing catenane structures. Type **F** illustrates the ideal polycatenane network, constructed solely from catenane subunits. Compared with type **F**, type **G** represents more general polymer networks containing catenane structures as branches, crosslink points or repeating units. It should be noted here that polycatenane networks (type **F**) were found in nature by investigation of kinetoplast DNA of *Crithidia fasciulata*.[152-153]

Endo *et al.* reported a synthesis of poly(1,2-dithiane) (**PDT**)[154-155] possibly containing polycatenane structures (Figure 2-22). Melt polymerization[156] of 1,2-dithiane **84** without initiators gave polymer **85**. NMR analysis indicated polymer **85** contained large cyclic structures, which were confirmed further by mass spectroscopy and photodegradation analysis. In addition, dynamic viscoelastic measurements showed that the molten state of the polymer **85** has a rubbery plateau and the T_g of **PDT** decreased with increasing molecular weight. These observations, which are different compared with the linear **PDT** analogue, provided other evidence for the formation of polycatenane structures. Making one step further, copolymerization between 1,2-dithiane **83** and lipoic acid (**LPA**) **84** was tried and gave a high molecular weight copolymer **86**,

which was proved to have polycatenane entanglement structures according to NMR and dynamic viscoelasticity measurements.

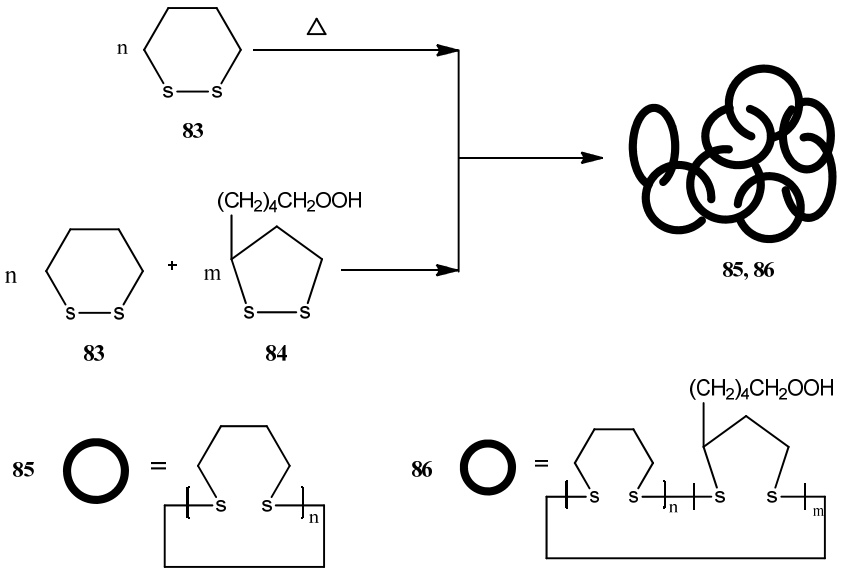

Figure 2-22. Synthesis of poly(1,2-dithiane)s **85** and **86** with polycatenane entanglement structures.

Gibson and co-workers reported poly(amide-crown ether)-based polypseudorotaxanes, which were suggested to have catenane structures (Figure 2-23).[157-158] In their work, poly(amide-crown ether)s **88a-d** and **89a-b** were prepared via the condensation polymerization of bis(5-carboxy-1,3-phenylene)-(3x+2)-crown-x **87a-d** (x = 10, 8, 6 and 4) with 4,4'-oxydianiline (ODA) and bis[4-(*m*-aminophenoxy)phenyl]phenylphosphine, respectively. It was found that the solubility of the resulting polymers depended on the ring size. 32-Membered crown ether-based polymer **88a** and polymer **89a** (n = 3) were totally insoluble in all solvents examined (including H_2SO_4). 26-Membered crown ether-based polymers **88b** and **89b** (n = 2) were soluble in dipolar aprotic solvents (DMSO, DMF and DNP) and 20- and 14-membered crown ether-based polymer **88 c,d** n = 1, 0) were completely soluble. GPC analysis showed that branching decreased with decreasing ring size of the crown ether. ^{1}H-NMR analysis didn't reveal evidence of ring opening. MALDI-TOF mass analysis indicated that cyclic aramides (lactams) were formed in the polymers derived from the 32- and 26-membered crown ether diacids. Thus, it was suggested that branching and network formation took place first by threading of the crown ether moieties, leading to polypseudorotaxane structures. The end-to-end cyclization of the resulting linear

polymers, leading to catenanes and ultimately catenane networks, depending on the cavity size of the crown ether and the propensity for the cyclization of backbone species.

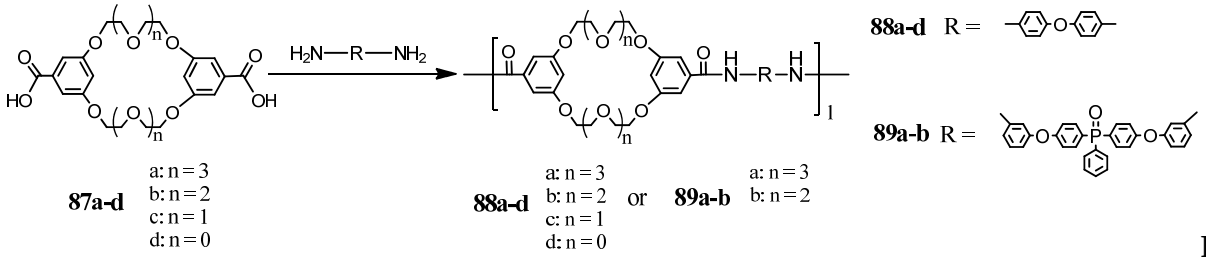

Figure 2-23. Synthesis of polypseudorotaxanes **88a-d** and **89a-d** containing polycatenane structures**.**

Later, gel formation was observed by Garcia *et al.* during the preparation of polyamides containing the benzo-18-crown-6 unit and it was ascribed to the formation of rotaxane/polyrotaxane and catenane/ polycatenane structures.[159] However, as far as the ring size of benzo-18-crown-6 is concerned, it is it is too small to be threaded and thus the gel formation is probably not because of catenane formation via threading of the crown ether moieties

2.6 Conclusions and perspective

There has been great interest in polycatenanes over the last decades, since polycatenanes consisting of mechanically-interlocked structures have novel topologies and are expected to display properties different from commonly-used conventional polymers. Linear polycatenanes (type **A** in Figure 2-1) are aesthetically perfect and expected to possess maximized effects of the topologically bonded structures on properties. However, the synthesis of such linear polycatenanes is still one of the most difficult and unachieved synthetic goals in polymer science. Due to the relatively easy preparation of bifunctionalized [2]catenanes, success in directed synthesis of polycatenanes has been mainly limited to poly[2]catenanes, which contain the essential mechanical linkages. Moreover, some progress has been made towards polymeric catenanes and polycatenane networks.

The salient features of the polycatenanes discussed above are summarized in Table 2-1. A lot of analytical tools, such as NMR spectroscopy, mass spectrometry, GPC and FTIR, have been used to characterize these novel polymers. But the property studies have been limited by the poor yields of the polycatenanes, even with the readily prepared poly[2]catenane systems. Therefore,

development of more efficient synthetic methods or more readily-prepared systems are critical to the polycatenane research and development.

As a result of the current fast pace of study in the field of polycatenanes, many new polycatenanes are expected to be discovered and some unique and interesting properties will no doubt be revealed in the near future.

2.7 Acknowledgements

The authors are grateful to Dr. Dieter Schlüter, Dr. Craig Hawker and Dr. Junji Sakamoto for opportunity to contribute to this interesting book. We also acknowledge generous support from the National Science Foundation through DMR 0704076.

Table 2-1. Properties of Polycatenanes

Polycatenane #		M_n (kDa)	M_w (kDa)	DP_n	PDI	T_g (℃)
1		—	—	5	1.00	—
2				6	1.00	
3		—	—	7	1.00	—
8a		3.0 [a), b)]	3.6 [a), b)]	1-5	1.2	—
8b		3.3 [a), b)]	5.0 [a), b)]	2 [r)]	1.5	245
12a		34.0 [a), c)]	59.1 [a), c)]	12	1.7	277
12b		46.6 [a), c)]	95.6 [a), c)]	20	2.1	207
14a	**10% (w/w)**	15.9 [d)]	40.1 [d)]	11 [r)]	2.5	150
	20% (w/w)	9.9 [d)]	41.4 [d)]	7 [r)]	4.2	150
	30% (w/w)	8.1 [d)]	38.9 [d)]	5 [r)]	4.8	149

14b	**5% (w/w)**	25.0 [b), e)]	67.0 [b), e)]	19 [r)]	2.7	~75
	10% (w/w)	21.0 [b), e)]	61.0 [b), e)]	16 [r)]	2.9	~77
	20% (w/w)	17.0 [b), e)]	52.0 [b), e)]	13 [r)]	3.0	~80
17		15.0 [f)]	30.0 [f)]	11 [r)]	2.0 [f)]	—
		16.0 [g)]	32.0 [g)]	12 [r)]	2.0 [g)]	—
19		3.1 [b), h)]	6.1 [b), h)]	2	1.9	—
24a		55.0 [b), h)]	1800.0 [b), h)]	—	32.7	80
24b		22.0-25.0 [i), j)]	42.0-47.0 [i), j)]	8-9	1.7	75
26a		—	—	—	—	—
26b		810.0 [b), j)]	3321.0 [b), j)]	609	4.1	—
32		26.5 [k), l)]	30.0 [k), l)]	17	1.2	
34		35.0 [k), l)]	—	25	—	—
38		45.0 [k), l)]	—	15	—	—
39		45.0 [k), l)]	—	15	—	—
41		150.0 [k), l)]	—	40 [r)]	—	—
47-m		28.9 [a), b)]	95.2 [a), b)]	10	3.3	—
48-m		20.9 [a), b)]	56.4 [a), b)]	7	2.7	—
49-l		33.0 [a), b)]	69.3 [a), b)]	12	2.1	—
51		27.0 [k), l)]	—	20	—	—
53		—	—	—	—	—
59		—	—	—	—	—
64		870.0 [m)]	1300 [m)]	—	1.5 [m)]	—
67		10.3 [a), b)]	13.39 [a), b)]	—	1.3	—
71		36.8 [a), b)]	37.9 [a), b)]	—	1.0	—

75		—	—	2-10	—	—
82		3.0[a), s)]	—	—	—	—
85		—	813.0 [a), b)]	—	—	—
86		365.0 [a), b), n)]	726.0 [a), b), n)]	—	2.0	-43.3[o)]
88	**a**	—	—	—	—	114
	b	36.0 [i), p)]	189 [i), p)]	51 [r)]	5.2	156
	c	12.9 [i), p)]	55.2 [i), p)]	21 [r)]	4.2	207
	d	53.8 [q), j)]	151 [q), j)]	102 [r)]	2.8	261
89	**a**	—	—	—	—	127
	b	25.6 [i), p)]	235 [i), p)]	26 [r)]	9.1	174

a) In tetrahydrofuran (THF). [b)] Calibration with polystyrene (PSt) standards. [c)] MALDI-TOF calibration. [d)] In dichloromethane. [e)] In chloroform/hexafluoro-2-propanol (HFIP) 98/2. [f)] Polymerization temperature was room temperature. [g)] Polymerization temperature was 0℃. [h)] In $CHCl_3$. [i)] Universal calibration. [j)] In dimethylformamide (DMF). [k)] Chloride salt of the corresponding polycatenanes with water as solvent. [l)] Calibration with protein standards. [m)] Determined by SEC-MALS analysis. [n)] [LPA] in comonomer (mol%): 50. [o)] [LPA] in comonomer (mol%): 58.1. [p)] In N-methylpyrrolidinone (NMP). [q)] Calibration with poly(methyl methacrylate) (PMMA) standards. [r)] Calculated value. DP_n = M_n/Molecular weight of repeating unit. [s)] Peak molecular weight. Tosoh G3000HXL column.

References

(1) Safarowsky, O.; Windisch, B.; Mohry, A.; Vögtle, F. *J. Prakt. Chem.* **2000**, *342*, 437.

(2) Gibson, H. W. In *Large Ring Molecules*; Semlyen, J. A., Ed.; J. Wiley and Sons: New York, 1996; p 191.

(3) Raymo, F. M.; Stoddart, J. F. *Chem. Rev.* **1999**, *99*, 1643.

(4) Gong, C.; Gibson, H. W. In *Molecular Catenanes, Rotaxanes and Knots*; Sauvage, J.-P., Dietrich-Buchecker, C. O., Eds.; Wiley-VCH: Weinheim, 1999; p 277.

(5) Mahan, E.; Gibson, H. W. In *Cyclic Polymers*, 2nd ed.; Semlyen, A. J., Ed.; Kluwer Publishers: Dordrecht, 2000; p 415.

(6) Hubin, T. J.; Busch, D. H. *Coord. Chem. Rev.* **2000**, *200-202*, 5.

(7) Panova, I. G.; Topchieva, I. N. *Russ. Chem. Rev.* **2001**, *70*, 23.

(8) Huang, F.; Gibson, H. W. *Prog. Polym. Sci.* **2005**, *30*, 982.

(9) Wenz, G.; Han, B.-H.; Müller, A. *Chem. Rev.* **2006**, *106*, 782.

(10) Niu. Z.; Gibson, H.W. *Chem. Rev.* **2009,** *109,* 6024.

(11) Plummer, C. J.; Cudré-Mauroux, N., N.; Kausch, H. H. *Polym. Eng. Sci.* **1994**, *34*, 318.

(12) Furukawa, J. *Physical Chemistry of Polymer Rheology*; Kodansha: Tokyo, 2003; p 135.

(13) Shaffer, J. S. *J. Chem. Phys.* **1994**, *105*, 4205.

(14) Gupta, R. K. *Polymer and Composite Rheology*; Marcel Dekker: New York, 2000; p 117.

(15) Wu, S. *J. Polym. Sci., Part B: Polym. Phys.* **1989**, *27*, 723.

(16) Cowie, J. M. G.; Arrighi, V. *Polymers: Chemistry and Physics of Modern Materials*; CRC Press: Boca Raton, FL, 2008; p 274.

(17) Stein, R. S. *Topics in Polymer Physics*; Imperial College Press: London, 2006; p 121.

(18) Gibson, H. W.; Bheda, M. C.; Engen, P. T. *Prog. Polym. Sci.* **1994**, *19*, 843.

(19) Semlyen, J. A.; Wood, B. R.; Hodge, P. *Polym. Adv. Technol.* **1994**, *5*, 473.

(20) Gong, C.; Gibson, H. W. *Curr. Opin. Solid State Mater. Sci.* **1997**, *2*, 647.

(21) Clarkson, G. J.; Leigh, D. A.; Smith, R. A. *Curr. Opin. Solid State Mater. Sci.* **1998**, *3*, 579.

(22) Geerts, Y. In *Molecular Catenanes, Rotaxanes and Knots*; Sauvage, J.-P., Dietrich-Buchecker, C., Eds.; Wiley-VCH Verlag GmbH: Weinheim, 1999; p 247.

(23) Leigh, D. A.; Smith, R. A. In *Cyclic Polymers*, 2nd ed.; Semlyen, A. J., Ed.; Kluwer Academic Publishers: Dordrecht, 2000; p 561.

(24) Brunsveld, L.; Folmer, B. J. B.; Meijer, E. W.; Sijbesma, R. P. *Chem. Rev.* **2001**, *101*, 4071.

(25) Hadjichristidis, N.; Pitsikalis, M.; Pispas, S.; Iatrou, H. *Chem. Rev.* **2001**, *101*, 3747.

(26) Harada, A. *Acc. Chem. Res.* **2001**, *34*, 456.

(27) Carlucci, L.; Ciani, G.; Proserpio, D. M. *Coord. Chem. Rev.* **2003**, *246*, 247.

(28) Takata, T.; Kihara, N.; Furusho, Y. *Adv. Polym. Sci.* **2004**, *171*, 1.

(29) Aricó, F.; Badjic, J. D.; Cantrill, S. J.; Flood, A. H.; Leung, K. C.- F.; Liu, Y.; Stoddart, J. F. *Top. Curr. Chem.* **2005**, *249*, 203.

(30) Beck, J. B.; Rowan, S. J. In *Supramolecular Polymers*; Ciferri, A., Ed.; CRC Press Taylor & Francis Group: Boca Raton, FL, 2005; p 259.

(31) Hunter, C. A. *J. Am. Chem. Soc.* **1992**, *114*, 5303.

(32) Vögtle, F.; Meier, S.; Hoss, R. *Angew. Chem., Int. Ed. Engl.* **1992**, *31*, 1619.

(33) Adams, H.; Fiona, J.; Hunter, C. A. *Chem. Commun.* **1995**, 809.

(34) Kim, K. *Chem. Soc. Rev.* **2002**, *31*, 96.

(35) Busch, D. H. *Top. Curr. Chem.* **2005**, *249*, 1.

(36) Odell, B.; Reddington, M. V.; Slawin, A. M. Z.; Spencer, N.; Stoddart, J. F.; Williams, D. J. *Angew. Chem., Int. Ed. Engl.* **1988**, *27*, 1547.

(37) Stoddart, J. F.; Tseng, H. R. *Proc. Natl. Acad. Sci. U.S.A.* **2002**, *99*, 4797.

(38) Hernandez, R.; Tseng, H. R.; Wong, J. W.; Stoddart, J. F.; Zink, J. I. *J. Am. Chem. Soc.* **2004**, *126*, 3370.

(39) Kern, J.-M.; Sauvage, J.-P.; Bidan, G.; Divisia-Blohorn, B. *J. Polym. Sci., Part A: Polym. Chem.* **2003**, *40*, 3470.

(40) Mobian, P.; Kern, J.-M.; Sauvage, J.-P. *J. Am. Chem. Soc.* **2003**, *125*, 2016.

(41) Mobian, P.; Kern, J.-M.; Sauvage, J.-P. *Inorg. Chem.* **2003**, *42*, 8633.

(42) Brunsveld, L.; Folmer, B. J. B.; Meijer, E. W.; Sijbesma, R. P. *Chem. Rev.* **2001**, *101*, 4071.

(43) Chandler, D. *Nature* **2005**, *437*, 640.

(44) Amabilino, D. B.; Stoddart, J. F. *Chem. Rev.* **1995**, *95*, 2725.

(45) Shaffer, T. D.; Tsay, L.-M. *J. Polym. Sci., Part A: Polym. Chem.* **1991**, *29*, 1213.

(46) Soichi, M. *Farumashia* **1972**, *8*, 557.

(47) Rossa, L.; Vögtle, F. *Top. Curr. Chem.* **1983**, *113*, 1.

(48) Bielawski, C. W.; Benitez, D.; Grubbs, R. H. *Science* **2002**, *297*, 2041.

(49) Amabilino, D. B.; Ashton, P. R.; Reder, A. S.; Spencer, N.; Stoddart, J. F. *Angew. Chem., Int. Ed. Engl.* **1994**, *33*, 1286.

(50) Amabilino, D. B.; Ashton, P. R.; Boyd, S. E.; Lee, J. Y.; Menzer, S.; Stoddart, J. F.; Williams, D. J. *Angew. Chem., Int. Ed. Engl.* **1997**, *36*, 2070.

(51) Amabilino, D. B.; Ashton, P. R.; Balzani, V.; Boyd, S. E.; Credi, A.; Lee, J. Y.; Menzer, S.; Stoddart, J. F.; Venturi, M.; Williams, D. J. *J. Am. Chem. Soc.* **1998**, *120*, 4295.

(52) Ashton, P. R.; Baldoni, V.; Balzani, V.; Claessens, C. G.; Credi, A.; Hoffmann, H. D. A.; Raymo, F. M.; Stoddart, J. F.; Venturi, M.; White, A. J. P.; Williams, D. J. *Eur. J. Org. Chem.* **2000**, 1121.

(53) Karagounis, G.; Kontaraki, E. *Prakt. Akad. Athenon* **1973**, *48*, 197.

(54) Karagounis, G.; Pandi-Agathokli, I.; Kontaraki, E.; Nikolelis, D. *Prakt. Akad. Athenon* **1975**, *49*, 501.

(55) Schober, B. J.; Gordon, B.; Knauss, D. *Polym. Prepr. Am. Chem.Soc. Div. Polym. Chem.* **1989**, *30*, 199.

(56) Godt, A. *Eur. J. Org. Chem.* **2004**, *8*, 1639.

(57) Watanabe, N.; Kihara, N.; Takata, T. *Org. Lett.* **2001**, *3*, 3519.

(58) Watanabe, N.; Ikari, Y.; Kihara, N.; Takata, T. *Macromolecules* **2004**, *37*, 6663.

(59) Hunter, C. A. *Chem. Soc. Rev.* **1994**, *23*, 101.

(60) Hoss, R.; Vögtle, F. *Angew. Chem., Int. Ed. Engl.* **1994**, *33*, 375.

(61) Vögtle, F.; Dunwald, F.; Schmidt, T. *Acc. Chem. Res.* **1996**, *29*, 451.

(62) Jäger, R.; Vögtle, F. *Angew. Chem., Int. Ed. Engl.* **1997**, *36*, 930.

(63) Geerts, Y.; Muscat, D.; Müllen, K. *Macromol. Chem. Phys.* **1995**, *196*, 3425.

(64) Muscat, D.; Geerts, Y.; Witte, A.; Köhler, W.; Müllen, K. *Macromol. Rapid Commun.* **1997**, *18*, 233.

(65) Muscat, D.; Köhler, W.; Räder, H. J.; Martin, K.; Mullins, S.; Müller, B.; Müllen, K.; Geerts, Y. *Macromolecules* **1999**, *32*, 1737.

(66) Moore, J. S.; Stupp, S. I. *Macromolecules* **1990**, *23*, 65.

(67) Fustin, C.-A.; Bailly, C.; Clarkson, G. J.; Groote, P. D.; Galow, T. H.; Leigh, D. A.; Robertson, D.; Slawin, A. M. Z.; Wong, J. K. Y. *J. Am.Chem. Soc.* **2003**, *125*, 2200.

(68) Heim, C.; Udelhofen, D.; Vögtle, F. In *Molecular Catenanes, Rotaxanes and Knots*; Sauvage, J.-P., Dietrich-Buchecker, C. O., Eds.; Wiley-VCH Verlag GmbH: Weinheim, 1999; p 177.

(69) Kidd, T. J.; Leigh, D. A.; Wilson, A. J. *J. Am. Chem. Soc.* **1999**, *121*, 1599.

(70) Duh, B. *J. Appl. Polym. Sci.* **2002**, *83*, 1288.

(71) Vouyiouka, S. N.; Karakatsani, E. K.; Papaspyrides, C. D. *Prog. Polym. Sci.* **2005**, *30*, 10.

(72) Matsumoto, A. *Kobunshi* **2006**, *55*, 270.

(73) Fustin, C.-A.; Bailly, C.; Clarkson, G. J.; Galow, T. H.; Leigh, D. A. *Macromolecules* **2004**, *37*, 66.

(74) Fustin, C.-A.; Clarkson, G. J.; Leigh, D. A.; Hoof, F. V.; Jonas, A. M.; Bailly, C. *Macromolecules* **2004**, *37*, 7884.

(75) Kint, D. P. R.; Munoz-Guerra, S. *Polym. Int.* **2003**, *52*, 321.

(76) Bicerano, J. *J. Macromol. Sci., Rev. Macromol. Chem. Phys.* **1998**, *C38*, 391.

(77) Leigh, D. A.; Moody, K.; Smart, J. P.; Waston, K. J.; Slawin, A. M. Z. *Angew. Chem., Int. Ed. Engl.* **1996**, *35*, 306.

(78) Kolb, H. C.; Finn, M. G.; Sharpless, K. B. *Angew. Chem., Int. Ed.* **2001**, *40*, 2004.

(79) Kolb, H. C.; Sharpless, K. B. *Drug Discovery Today* **2003**, *8*, 1128.

(80) Meldal, M. *Macromol. Rapid Commun.* **2008**, *29*, 1016.

(81) Meldal, M.; Tornøe, C. W. *Chem. Rev.* **2008**, *108*, 2952.

(82) Yamazaki, M.; Suzuki, T.; Hagiwara, T.; Sawaguchi, T.; Yano, S. *Kobunshi Ronbunshu* **2008**, *65*, 496.

(83) Watanabe, N.; Kihara, N.; Takata, T. *Org. Lett.* **2001**, *3*, 3519.

(84) Watanabe, N.; Kihara, N.; Furusho, Y.; Takata, T.; Araki, Y. *Angew. Chem., Int. Ed.* **2003**, *42*, 681.

(85) Dietrich-Buchecker, C. O.; Sauvage, J.-P.; Kintzinger, J.-P. *Tetrahedron. Lett.* **1983**, *46*, 5095.

(86) Weidmann, J.-L.; Kern, Q. J.-M.; Sauvage, J.-P.; Geerts, Y.; Muscat, D.; Müllen, K. *Chem. Commun.* **1996**, 1243.

(87) Weidmann, J.-L.; Kern, J.-M.; Sauvage, J.-P.; Muscat, D.; Mullins, S.; Köhler, W.; Rosenauer, C.; Räder, H. J.; Martin, K.; Geerts, Y. *Chem.-Eur. J.* **1999**, *5*, 1841.

(88) Benoit, H.; Rempp, P.; Grubisic, Z. *J. Polym. Sci.* **1967**, *B5*, 753.

(89) Shimada, S.; Ishikawa, K.; Tamaoki, N. *Acta Chem. Scand.* **1998**, *52*, 374.

(90) Jäger, R.; Schmidt, T.; Karbach, D.; Vögtle, F. *Synlett* **1996**, *8*, 723.

(91) Raymo, F. M.; Stoddart, J. F. *Chem. Rev.* **1999**, 1643.

(92) Miljanic, O. S.; Dichtel, W. R.; Aprahamian, I.; Rohde, R. D.; Agnew, H. D.; Heath, J. R.; Stoddart, J. F. *QSAR Comb. Sci.* **2007**, *26*, 1165.

(93) Saha, S.; Stoddart, J. F. *Chem. Soc. Rev.* **2007**, *36*, 77.

(94) Griffiths, K. E.; Stoddart, J. F. *Pure Appl. Chem.* **2008**, *80*, 485.

(95) Dichtel, W. R.; Miljanić, O. S.; Zhang, W.; Spruell, J. M.; Patel, K.; Aprahamian, I.; Heath, J. R.; Stoddart, J. F. *Acc.Chem. Res.* **2008**, *41*, 1750.

(96) Menzer, S.; White, A. J. P.; Belohradsky, D. J. W.; Hamers, C.; Raymo, F. M.; Shipway, A. N.; Stoddart, J. F. *Macromolecules* **1998**, *31*, 295.

(97) Raymo, F. M.; Stoddart, J. F. *Polym. Mater. Sci. Eng.* **1999**, *80*, 33.

(98) Isaacs, N. S. *Tetrahedron* **1991**, *47*, 8463.

(99) Hamers, C.; Raymo, F. M.; Stoddart, J. F. *Eur. J. Org. Chem.* **1998**, *10*, 2109.

(100) Hamers, C.; Kocian, O.; Raymo, F. M.; Stoddart, J. F. *Adv. Mater.* **1998**, *10*, 1366.

(101) Ashton, P. R.; Balzani, V.; Credi, A.; Kocian, D. O.; Pasini, L. P.; Spencer, N.; Stoddart, J. F.; Tolley, M. S.; Venturi, M.; White, A. J. P.; Williams, D. J. *Chem.- Eur. J.* **1998**, *4*, 590.

(102) Duda, S.; Godt, A. *Eur. J. Org. Chem.* **2003**, *17*, 3412.

(103) Ünsal, Ö.; Godt, A. *Chem.-Eur. J.* **1999**, *5*, 1728.

(104) Godt, A.; Duda, S.; Ünsal, Ö.; Thiel, J.; Härter, A.; Roos, M.; Tschierske, C.; Diele, S. *Chem.-Eur. J.* **2002**, *8*, 5094.

(105) Matloka, P. P.; Wagener, K. B. *J. Mol. Catal. A: Chem.* **2006**, *257*, 89.

(106) Bunz, U. H. F. *Acc. Chem. Res.* **2001**, *34*, 998.

(107) Davidson, T. A.; Wagener, K. B. *Mater. Sci. Technol.* **1999**, *20*, 105.

(108) Tindall, D.; Pawlow, J. H.; Wagener, K. B. *Top. Organomet. Chem.* **1998**, *1*, 183.

(109) Schwendeman, J. E.; Church, A. C.; Wagener, K. B. *Adv. Synth. Catal.* **2002**, *344*, 597.

(110) Asakawa, M.; Ashton, P. R.; Boyd, S. E.; Brown, C. L.; Gillard, R. E.; Kocian, O.; Raymo, F. M.; Stoddart, J. F.; Tolley, M. S.; White, A. J. P.; Williams, D. J. *J. Org. Chem.* **1997**, *62*, 26.

(111) Simone, D. L.; Swager, T. M. *J. Am. Chem. Soc.* **2000**, *122*, 9300.

(112) Yamada, H. *Electrochem.* **2005**, *73*, 518.

(113) Bria, M.; Bigot, J.; Cooke, G.; Lyskawa, J.; Rabani, G.; Rotello, V. M.; Woisel, P. *Tetrahedron* **2009**, *65*, 400.

(114) Hamilton, D. G.; Davies, J. E.; Prodi, L.; Sanders, J. K. M. *Chem.- Eur. J.* **1998**, *4*, 608.

(115) Carroll, J. B.; Jordan, B. J.; Xu, H.; Erdogan, B.; Lee, L.; Cheng, L.; Tiernan, C.; Cooke, G.; Rotello, V. M. *Org. Lett.* **2005**, *7*, 2551.

(116) Dirks, A. J. *Chem. Commun.* **2005**, 4172.

(117) Ladmiral, V.; Mantovani, G.; Clarkson, G. J.; Cauet, S.; Irwin, J. L.; Haddleton, D. M. *J. Am. Chem. Soc.* **2006**, *128*, 4823.

(118) Tornøe, C. W.; Christensen, C.; Meldal, M. *J. Org. Chem.* **2002**, *67*, 3057.

(119) Rostovtsev, V. V.; Green, L. G.; Fokin, V. V.; Sharpless, K. B. *Angew. Chem., Int. Ed.* **2002**, *41*, 2596.

(120) Bock, V. D.; Hiemstra, H.; van Maarseveen, J. H. E. *Eur. J. Org. Chem.* **2006**, 51.

(121) Wu, P.; Fokin, V. V. *Aldrichim. Acta* **2007**, *40*, 7.

(122) Becer, C. R.; Hoogenboom, R.; Schubert, Ulrich S. *Angew. Chem. Int. Ed.* **2009**, *48*, 4900.

(123) Gao, H.; Matyjaszewski, K. *J. Am. Chem. Soc.* **2007**, *129*, 6633.

(124) Olson, M. A.; Braunschweig, A. B.; Fang, L.; Ikeda, T.; Klajn, R.; Trabolsi, A.; Wesson, P. J.; Bentez, D.; Mirkin, C. A.; Grzybowski, B. A.; Stoddart, J. F. *Angew. Chem., Int. Ed.* **2009**, *48*, 1792.

(125) Steuerman, D. W.; Tseng, H.-R.; Peters, A. J.; Flood, A. H.; Jeppesen, J. O.; Nielsen, K. A.; Stoddart, J. F.; Heath, J. R. *Angew. Chem., Int. Ed.* **2004**, *43*, 6486–6491.

(126) Roovers, J. R.; Toporowski, P. M. *Macromolecules* **1983**, *16*, 643.

(127) Yin, R.; Hogen-Esch, T. *Macromolecules* **1993**, *26*, 6952.

(128) Schober, B. J.; Gordon, B.; Knauss, D. *Polym. Prepr. (Am. Chem. Soc. Div. Polym. Chem.)* **1989**, *30*, 199.

(129) Coqueret, X.; Wegner, G. *Makromol. Chem.* **1992**, *193*, 2929.

(130) Wood, B. R.; Semlyen, J. A.; Hodge, P. *Polymer* **1994**, *35*, 1542.

(131) Seeman, N. C. *Acc. Chem. Res.* **1997**, *30*, 35.

(132) Gan, Y.; Dong, D.; Hogen-Esch, T. E. *Polym. Prepr. (Am. Chem. Soc., Div. Polym. Chem.)* **1995**, *36*, 408.

(133) Gan, Y.; Dong, D.; Hogen-Esch, T. E. *Macromolecules* **2002**, *35*, 6799.

(134) Gan, Y.; Dong, D.; Hogen-Esch, T. E. *Macromolecules* **1995**, *28*, 383.

(135) Agam, G.; Gravier, D.; Zilkha, A. *J. Am. Chem. Soc.* **1976**, *98*, 5260.

(136) Ohta, Y.; Kushida, Y.; Kawaguchi, D.; Matsushita, Y.; Takano, A. *Macromolecules* **2008**, *41*, 3957.

(137) Matsushita, Y.; Mori, K.; Saguchi, R.; Nakao, Y.; Noda, I.; Nagasawa, M. *Macromolecules* **1990**, *23*, 4313.

(138) Zhu, Y.; Gido, S. P.; Iatrou, H.; Hadjichristidis, N.; Mays, J. W. *Macromolecules* **2003**, *36*, 148.

(139) Okada, M.; Harada, A. *Macromolecules* **2003**, *36*, 9701.

(140) Choi, H. S.; Yui, N. *Prog. Polym. Sci.* **2006**, *31*, 121.

(141) Hapiot, F.; Tilloy, S.; Monflier, E. *Chem. Rev.* **2006**, *106*, 767.

(142) Harada, A. *J. Polym. Sci., Part A: Polym. Chem.* **2006**, *44*, 5113.

(143) Harada, A.; Hashidzume, A.; Takashima, Y. *Adv. Polym. Sci.* **2006**, *201*, 1.

(144) Roux, M.; Perly, B.; Djedaini-Pilard, F. *Eur. Biochem. J.* **2007**, *36*, 861.

(145) Funasaki, N.; Ishikawa, S.; Neya, S. *Pure Appl. Chem.* **2008**, *80*, 1511.

(146) Ogoshi, T.; Harada, A. *Sensors* **2008**, *8*, 4961.

(147) Harada, A.; Kamachi, M. *Macromolecules* **1990**, *23*, 2821.

(148) Harada, A.; Li, J.; Nakamitsu, T.; Kamachi, M. *J. Org. Chem.* **1993**,*58*, 7524.

(149) Ishikawa, K.; Yamamoto, T.; Asakawa, M.; Tezuka, Y. *Macromolecules*. **2010**, *43*, 168.

(150) Tezuka, Y.; Oike, H. *Prog. Polym. Sci.* **2002**, *27*, 1069

(151) Tezuka, Y. *J. Polym. Sci., Part A: Polym. Chem.* **2003**, *41*, 2905.

(152) Adams, D. E.; Shekhtman, E. M.; Zechiedrich, E. L.; Schmid, M. B.; Cozzarelli, N. R. *Cell* **1992**, *71*, 277.

(153) Chen, J.; Rauch, C. A.; White, J. H.; Englund, P. T.; Cozzarelli, N. R. *Cell* **1995**, *80*, 61.

(154) Endo, K.; Shiroi, T.; Murata, N.; Kojima, G.; Yamanaka, T. *Macromolecules* **2004**, *37*, 3143.

(155) Endo, K.; Shiroi, T.; Murata, N. *Polym. J.* **2005**, *37*, 512.

(156) Endo, K.; Yamanaka, T. *Macromolecules* **2006**, *39*, 4038.

(157) Delaviz, Y.; Gibson, H. W. *Macromolecules* **1992**, *25*, 4859.

(158) Gibson, H. W.; Nagvekar, D. S.; Yamaguchi, N.; Bhattacharjee, S.; Wang, H.; Vergne, M. J.; Hercules, D. M. *Macromolecules* **2004**, *37*, 7514.

(159) Calderón, V.; Schwarz, G.; García, F.; Tapia, M. J.; Valente, A. J. M.; Burrows, H. D.; García, J. M. *J. Polym. Sci., Part A: Polym. Chem.***2006**, *44*, 6252.

Chapter 3.

Dissertation Statement

Since the first discovery of crown ethers by Charles Pedersen in 1967,[1-2] crown ether-based supramolecular chemistry has been a topic of interest and widely studied all over the world. The Gibson group has made remarkable achievements in the field of crown ether-based supramolecular chemistry. A lot of novel crown ethers, cryptands, pseudorotaxanes, rotaxanes, polypseudorotaxanes, polycatenanes and other advanced supramolecular species have been designed and successfully prepared by the Gibson group.[3] Today the Gibson group works intensively to achieve the following objectives: a. improving hosts, such as crown ethers and cryptands and guests, such as paraquats and diquats. b. Design and preparation of novel host/guest complex systems with high association constants or with novel topologies; c. design and preparation of novel host/guest complex systems which can response to the external stimuli. d. study and clarification of the conformations of complex systems in solution and solid state by X-ray analysis, NMR or other analytical methods. e. design and synthesis of novel supramolecular polymers, such as, polypseudorotaxanes, polyrotaxanes and polycatenanes, by incorporating these novel complex systems into polymers.

In this dissertation, Chapter 4 describes the first [2]pseudorotaxane and the first pseudocryptand-type poly[2]pseudorotaxane based on BMP32C10 and paraquat derivatives. This chapter solves a long-standing question: does the “threaded-through” pseudorotaxane conformation coexist with the “taco” complex for the BMP32C10/paraquat complex systems. In Chapter 5, a series of novel BMP32C10 derivatives are designed and prepared. They demonstrated remarkably improved association constants to paraquats by forming pseudocryptand-type pseudorotaxane structures for the first time in solution and solid state. Chapter 6 demonstrates the first supramolecular pseudorotaxane with an acid-base adjustable association constant. In Chapter 7, the first supramolecular [3]pseudorotaxane and a “hook-ring” type poly[2]catenane are designed and prepared. Chapter 8 describes the preparation and characterization of the first kind of AA/BB type pseudorotaxane-type supramolecular polymers

based on BMP32C10 cryptands with relative high molecular weight. In Chapter 9, novel [3]pseudorotaxanes are prepared. They exhibit contrasting statistical vs. anticooperative complexation behavior. In Chapter 10, the preparation of a semi-rotaxane and a rotaxane based on DB24C8 and a dibenzylammonium salt are reported. Chapter 11 mainly discusses the attempts to prepare functionalized pyridine-based DB30C10 cryptands, which will be used to construct high molecular weight supramolecular polymers. In Chapter 12, a novel DB30C10 cryptand with an organometallic third bridge is prepared and its complexation behavior with paraquat and diquat is studied. Chapter 13 mainly discusses attempts to prepare real linear polycatenanes.

References

(1) Pedersen, C. J. *J. Am. Chem. Soc.* **1967,** *89*, 7017-7036.

(2) Pedersen, C. J. *J. Am. Chem. Soc.* **1967**, *89*, 2495-2496.

(3) Some recent publications: (a) Huang, F.; Fronczek, F. R.; Gibson, H. W. *J. Am. Chem. Soc.* **2003**, *125*, 9272-9273. (b) Huang, F.; Zhou, L.; Jones, J. W.; Gibson, H. W.; Ashraf-Khorassani, M. *Chem. Commun.* **2004**, 2670-2671. (c) Huang, F.; Switek, K. A.; Zakharov, L. N.; Fronczek, F. R.; Slebodnick, C.; Lam, M.; Golen, J. A.; Bryant, W. S.; Mason, P. E.; Rheingold, A. L.; Ashraf-Khorassani, M.; Gibson, H. W. *J. Org. Chem.* **2005**, *70*, 3231-3241. (d) Gibson, H. W.; Wang, H.; Slebodnick, C.; Merola, J.; Kassel, S.; Rheingold, A. L. *J. Org. Chem.* **2007**, *72*, 3381-3393. (e) Pederson, A. M.-P.; Vetor, R. C.; Rouser, M. A.; Huang, F.; Slebodnick, C.; Schoonover, D. S.; Gibson, H. W. *J. Org. Chem.* **2008**, *73*, 5570-5573. (f) Lee, M.; Niu, Z.; Schoonover, D. V.; Slebodnick, C.; Gibson, H. W. *Tetrahedron*, **2010**, *66*, 7077-7082. (g) Lee, M.; Niu, Z.; Slebodnick, C.; Gibson, H. W. *J. Phy. Chem. B*, **2010,** *114*, 7312-7319. (h) Gibson, H. W.; Yamaguchi, N.; Niu, Z.; Jones, J. W.; Slebodnick, C.; Rheingold, A. L.; Zakharov, L. N., *J. Poly. Sci. Part A: Poly. Chem.* **2010**, *48*, 975-985. (i) Niu, Z.; Slebodnick, C.; Schoonover, D.; Azurmendi, H.; Harich, K.; Gibson, H. W.; *Org. Lett.* **2011**, *13*, 3992-3995. (j) Gibson, H. W.; Rasco, M. L.; Niu, Z.; *J. Poly. Sci. Part A: Poly. Chem.* **2011**, *49*, 3842-3851. (k) Niu, Z.; Slebodnick, C.; Bonrad, K.; Huang, F.; Gibson, H. W.; *Org. Lett.* **2011**, *13*, 2872–2875. (l) Niu, Z.; Huang, F.; Gibson, H. W.;

J. Am. Chem. Soc. **2011**, *133*, 2836-2839. (m) Niu, Z.; Slebodnick, C.; Gibson, H. W. *Org. Lett*. **2011**, *13,* ASAP August 3. (n) Niu, Z.; Slebodnick, C.; Azurmendi, H.; Huang, F.; Gibson, H. W. *Org. Biomol. Chem.* DOI: 10.1039/c1ob06299a.

TOC Graphic:

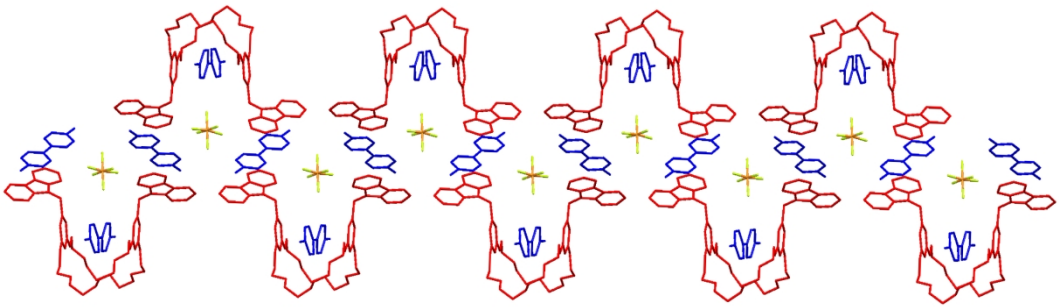

Abstract:

By the self-assembly of a bis(meta-phenylene)-32-crown-10 bearing two electron-donating groups (carbazoles) with electron-accepting paraquat derivatives, the first [2]pseudorotaxane and the first pseudocryptand-type poly[2]pseudorotaxane based on bis(meta-phenylene)-32-crown-10 were isolated as crystalline solids as shown by X-ray analyses.

Chapter 4.

The First [2]Pseudorotaxane and the First Pseudocryptand-Type Poly[2]pseudorotaxane based on Bis(meta-phenylene)-32-Crown-10 and Paraquat derivatives

4.1 Introduction

Pseudorotaxanes, which consist of a linear molecular component ("guest") encircled by a macrocyclic component ("host"), have been a topic of great interest and widely studied all over the world,[1] since pseudorotaxanes are the fundamental building blocks for preparation of advanced supramolecular species, such as rotaxanes, catenanes, polyrotaxanes, polypseudorotaxanes, and polycatenanes [2] with unique properties and potential applications.[1-2] Paraquat (*N,N'*-dialkyl-4,4'-bipyridinium) derivatives and crown ethers have been widely employed in the construction of pseudorotaxanes.[3] Our group first demonstrated that the complexes between bis(*meta*-phenylene)-32-crown-10 (BMP32C10) (**1a**) and its diol (**1b**) and paraquat derivatives, instead of forming pseudorotaxanes, were folded into "taco" shapes (Scheme 4-1), as proven by their X-ray crystal structures.[4] Although it was thought that the pseudorotaxane conformation probably coexisted in solution and indirect evidence was reported,[5] nearly a quarter of a century after the first report of a BMP32C10-paraquat complex,[6] only "taco"-shaped solid state complexes have been reported.[3a,4,5,7] Here, we report the first [2]pseudorotaxane based on a BMP32C10 derivative and a paraquat derivative. Interestingly, the first pseudocryptand-type poly[2]pseudorotaxane supramolecular polymer also formed in the solid state.

4.2 Results and discussion

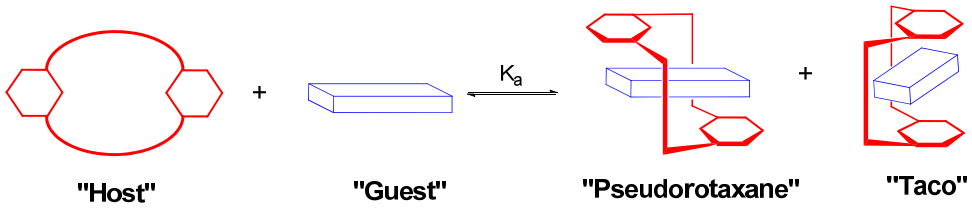

Scheme 4-1. Cartoon representations of possible co-conformations of host-guest complexes: "[2]pseudorotaxane" and "taco" geometries.

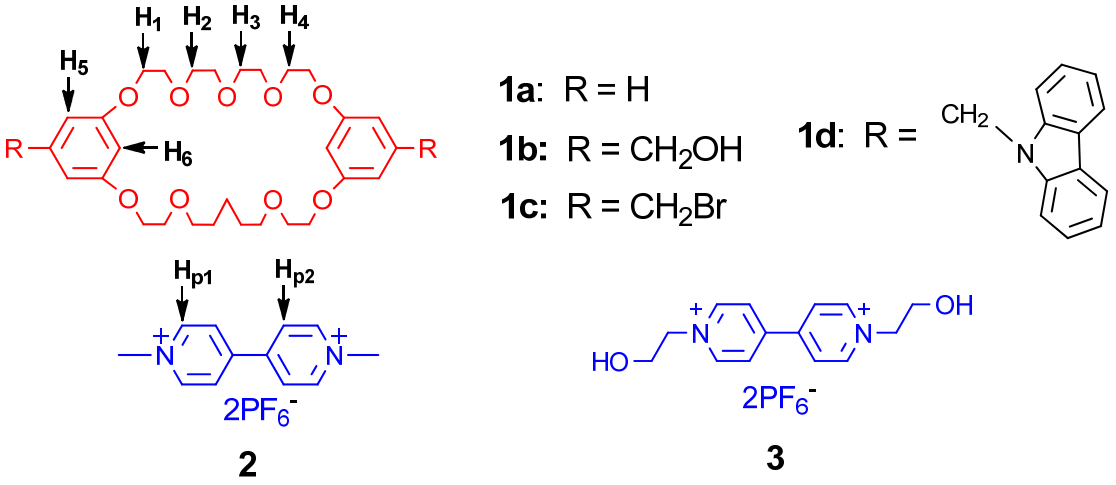

Figure 4-1. . Structures of BMP32C10 derivatives **1a-d** and paraquat derivatives **2** and **3**.

Bis[5-(N-carbazylmethyl)-1,3-phenylene]-32-crown-10 (**1d**) (Figure 4-1) was prepared via the reaction between BMP32C10 dibromide (**1c**)[8] and the anion of carbazole. Solutions of **1d** and **2** in $CDCl_3/CD_3CN$ = 1/1 <v/v> were yellow due to the charge-transfer interaction between the electron-rich aromatic rings of **1d** and the electron-poor pyridinium rings of bisparaquat **2**, evidence for complexation. ^{1}H-NMR spectra of equimolar solutions of host **1d** and guest **2** displayed only one set of peaks, indicating fast exchange (Figure 4-2). After complexation, peaks corresponding to H_1, H_5 and H_6 of **1d** and H_{p1}, H_{p2} of **2** moved upfield, while H_2 and H_3 of **1d** moved downfield. A Job plot[9] (Figure 4-8) based on proton NMR data demonstrated that the stoichiometry between **1d** and **2** in $CDCl_3/CD_3CN$ = 1/1 <v/v> was 1:1, which was confirmed by High-resolution Electrospray Ionization Mass Spectrometry (HRESI-MS): *m/z* 1225.49 [**1d**·**2**-

$PF_6]^+$. The association constants (K_a)[10] between **1d** and **2** and **3**[12] were determined as 440 ± 40 M^{-1} and 214 ± 30 M^{-1}, respectively. The K_a of **1d·2** is higher than the K_a of **1d·3**, as usually observed with these two paraquat derivatives.[13]

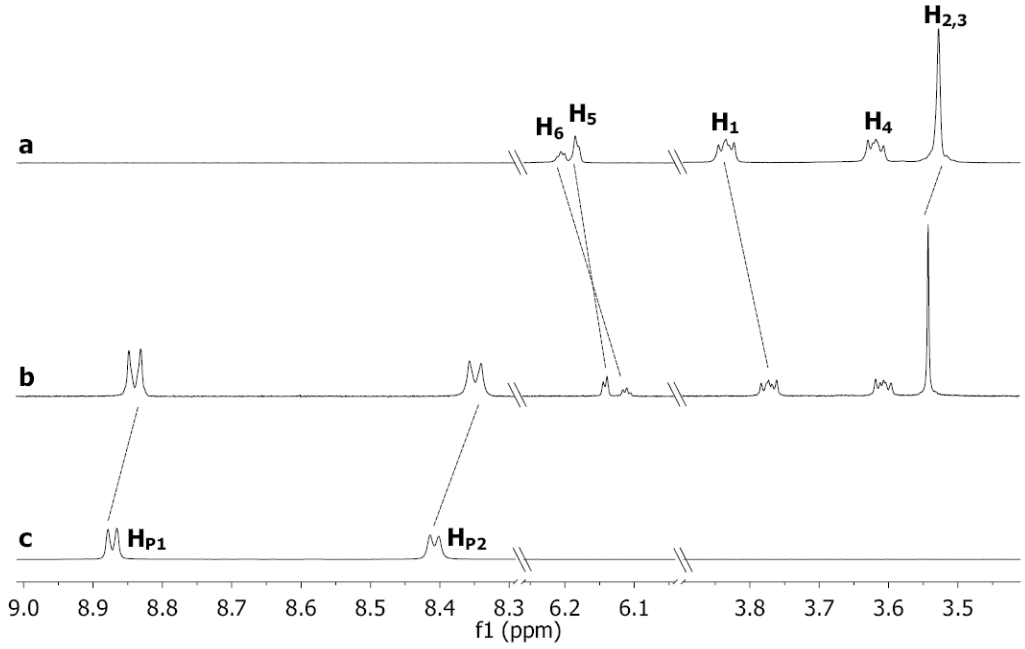

Figure 4-2. Partial proton NMR spectra (400 MHz, $CDCl_3/CD_3CN$ = 1/1 <v/v>, 25 °C) of: (a) 1.00 mM **1d**; (b) **1d** and **2** (1/3, mol/mol, [**1d**] + [**2**] = 1.00 mM); (c) 1.00 mM **2**.

The X-ray analysis of a single crystal, in a form of a colorless plate, which was grown by vapor diffusion of pentane into an acetone solution of **1d,** revealed that this crown ether assumes a deformed two-stair-step structure (Figure 4-3a, 3b). The two phenylene rings and the two carbazole rings are parallel to each other, respectively, but as far apart as possible by extension in opposite directions, while the phenylene and carbazole rings are almost perpendicular to each other (torsion angle = 88.5 degrees).

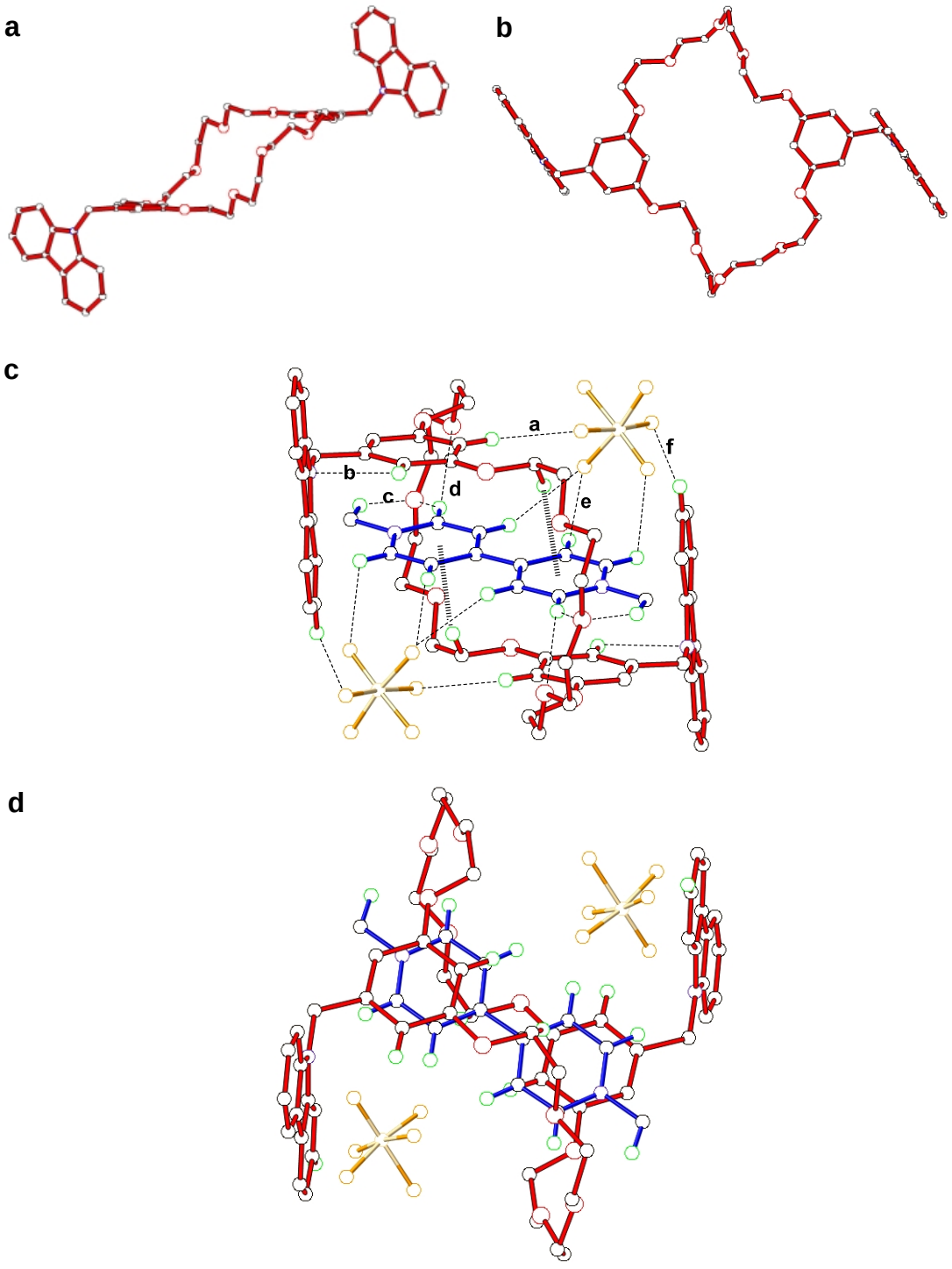

Figure 4-3. (a) and (b): Two views of the X-ray structure of **1d**. **(c)** and **(d)**: Two views of the X-ray structure of **1d·2**. **1d** is red. **2** is blue. Oxygen atoms are red. Carbon atoms are black. Nitrogen atoms are blue. Hydrogen atoms are green. Fluorine atoms

are yellow. Phosphorus atoms are brown. Dashed and hashed lines represent hydrogen bonds and CH_2-π interactions, respectively. The same motif is used in the following crystal structures. Solvent molecules, minor disordered carbon and hydrogen atoms, hydrogen atoms except the ones involved in hydrogen bonding have been omitted for clarity. Hydrogen bonds in (d) were omitted for clarity. Selected hydrogen-bond parameters: H···O(N, F) distances (Å), C···O(N, F) distances (Å), C-H···O(N, F) angles (deg): a 2.631, 3.569, 175.6; b 2.482, 2.828, 101.4; c 2.446, 3.334, 150.6; d 2.389, 3.086, 129.9; e 2.320, 3.110, 140.2; f 2.337, 3.258, 130.8. CH_2-π interaction parameters: H to the centroid distance (Å): 2.799. C-H-centroid angle (deg): 152.7; face-to-face π-stacking parameters: centroid-centroid distances (Å) and dihedral angles (deg): carbazole rings and pyridinium rings: 3.808 and 9.07.

However, two kinds of single crystals were obtained via the vapor diffusion of pentane into an equimolar acetone solution of **1d** and **2**: yellow rods and red rods. When a solution of **1d** and **2** in 2:1 ratio (mol/mol) was used, the yellow rods dominated. In contrast, the red rods dominated from a solution of **1d** and **2** in 1:2 ratio (mol/mol). X-ray analysis of a yellow rod demonstrated that the [2]pseudorotaxane structure indeed formed between **1d** and **2** (Figure 4-3c, 3d). In the complex **1d·2**, crown ether **1d** assumes a "zig-zig" shape. The two carbazole rings and the two phenylene rings are almost parallel to each other, respectively (torsion angle = 1.90 and 0 degrees, respectively), while the carbazole end groups remain almost perpendicular to the phenylene rings (torsion angle = 82.9 degrees) due to hydrogen bonds between the phenylene proton and the nitrogen atoms of the carbazole groups. The paraquat salt **2** is clearly threaded through the central cavity of host **1d** and the resulting [2]pseudorotaxane **1d·2** complex is stabilized by hydrogen bonds, CH_2-π interactions[14] between **1d** and **2** and off-set π-stacking[15] between the electron-rich phenylene rings of host **1d** and the electron-poor pyridinium rings of guest **2**. This represents the first direct observation of a pseudorotaxane structure derived from a BMP32C10 derivative with a paraquat.

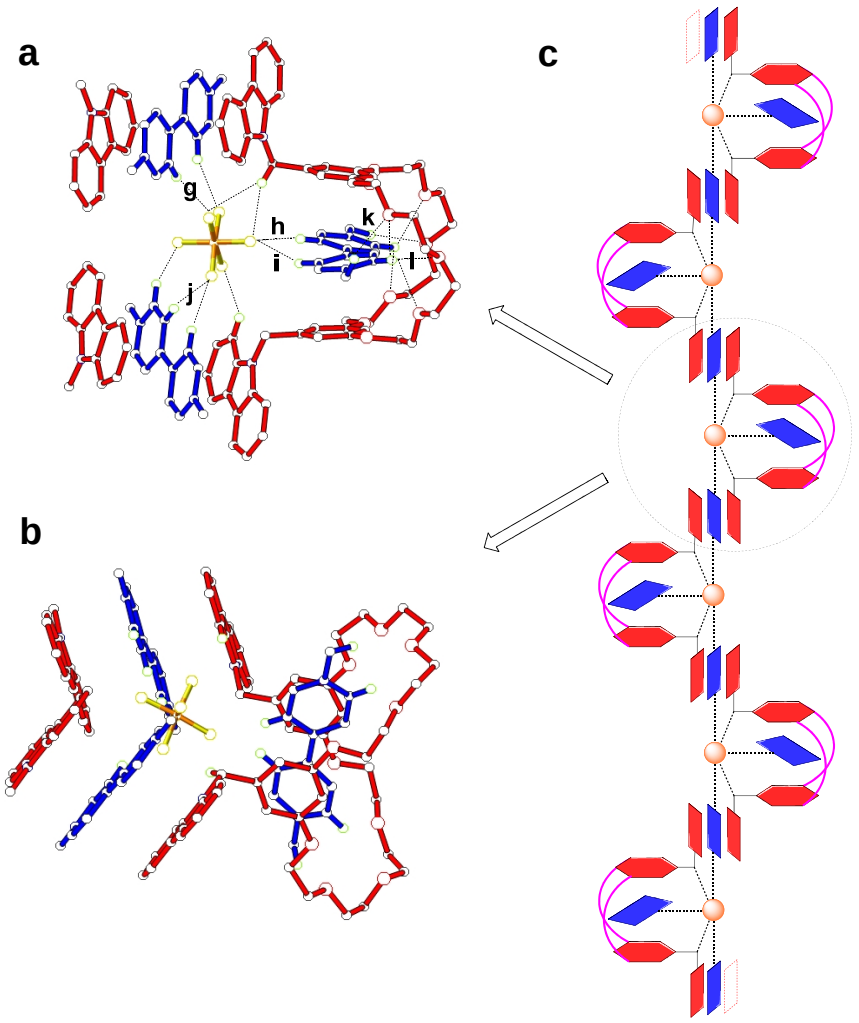

Figure 4-4. **(a)** and **(b)**: Two views of the X-ray structure of poly(**1d**·**2**$_2$). **1d** is red. **2** is blue. Solvent molecules, five PF_6^- ions and hydrogen atoms except the ones involved in hydrogen bonding have been omitted for clarity. The major disordered PF_6^- was chosen to show the hydrogen bonds. Hydrogen bonds in (b) were omitted for clarity. Selected hydrogen-bond parameters: H···O(F) distances (Å), C···O(F) distances (Å), C-H···O(F) angles (deg): g 2.265, 3.083, 143.8; h 2.423, 3.366, 172.5; (c) 2.433, 3.318, 155.0; j 2.409, 3.339, 166.5; k 2.438, 3.282, 144.1; l 2.432, 3.392, 166.76. Off-set face-to-face π-stacking parameters: centroid-centroid distances (Å) and dihedral angles (deg.): carbazole rings and pyridinium rings: 3.427, 3.406 and 1.35, 0.60; aromatic rings of **1d** and pyridinium rings of paraquat **2**: 3.982, 3.902 and 6.54, 7.59. **(c)** Cartoon representation of the supramolecular structure.

Interestingly, X-ray analysis of a red rod showed that one molecule of host **1d** binds two molecules of guest **2**, forming a linear pseudocryptand-type[16,17] poly[2]pseudorotaxane-poly(**1d**·**2**$_2$) in the solid state (Figure 4-4). Similar to the other reported BMP32C10 derivatives,[3a,4,5,7] in the supramolecular polymer **1d** is folded into a "taco"-shaped structure. One paraquat molecule threads through the folded crown ether in "taco" fashion, stabilized by off-set face-to-face π-stacking interactions between the aromatic rings of host **1d** and the pyridinium rings of guest **2** and hydrogen bonds between **1d** and **2**. The central PF_6^- ion acts as a hydrogen bonding bridge, interacting with both host **1d** and guest **2** to close another ring, forming a pseudocryptand.[16,17] Another electron-poor paraquat molecule lies parallel and between the electron-rich carbazole rings in a face-to-face manner,[18] π-stacking (centroid-centroid distances between carbazole rings and pyridinium rings are 3.427 Å and 3.406 Å) and forming a "sandwich" structure which is also stabilized by the hydrogen bonds between the host, guest and the central PF_6^- ion. As a result, a pseudocryptand-type poly[2]pseudorotaxane was formed, in effect because the second paraquat (**2**) acts as glue to hold the carbazole units of adjoining pseudocryptand units together in an extended chain, assisted by interactions with the counterion. To the best of our knowledge, this is the first pseudocryptand-type polypseudorotaxane to be reported.

Similarly, two kinds of crystals-yellow plates and red diamonds-resulted from diffusion of pentane into acetone solutions of host **1d** and paraquat diol (**3**). However, due to the low quality of the red diamonds, only the crystal structure of a yellow plate was obtained (see SI Figure 4-S9); in the complex of **1d**·**3** a "taco"-shaped complex was formed, which is similar to the other reported complexes between BMP32C10 derivatives and paraquat derivatives.[3a,4,5,7] The complex **1d**·**3** is stabilized by off-set face-to-face π-stacking interactions between the aromatic rings of host **1d** and the pyridinium rings of guest **3** and hydrogen bonds between **1d** and **3**. The hydrogen bonds between the ethylene protons of guest **3** and oxygen atoms of host **1d** possibly favor the formation of the "taco"-shaped complex over the pseudorotaxane. Based on the results with **1d**·**2**$_2$, the red diamonds are thought possibly to be the supramolecular polymeric analog **1d**·**3**$_2$.

4.3 Conclusions

In summary, we demonstrated the first [2]pseudorotaxane and the first solid state[19] pseudocryptand-type poly[2]pseudorotaxane based on a BMP32C10 derivative and a paraquat derivative by X-ray analysis. Interestingly, the formation of the [2]pseudorotaxane vs. the poly[2]pseudorotaxane was dependent on the ratio between the dicarbazyl BMP32C10 derivative **1d** and the paraquat. These results represent the first direct confirmation of the existence of pseudorotaxane structures in complexes between BMP32C10 derivatives and paraquat derivatives. Our present efforts are focused on using similar structures to prepare novel supramolecular polymers in solution, for example, complexation with polymers containing backbone paraquat moieties[20] to form 3-dimensional networks. Likewise we expect interesting solid state structures to result from interaction of host **1d** with polymers bearing paraquat end groups.[21]

4.4 Acknowledgements

This work was supported by the National Science Foundation (DMR0097126 and DMR0704076) and the Petroleum Research Fund administered by the American Chemical Society (40223-AC7 and 47644-AC7). We also acknowledge the National Science Foundation for funds to purchase the Agilent 6220 Accurate Mass TOF LC/MS Spectrometer (CHE-0722638).

4.5 Experimental Section

4.5.1 Materials and methods

Carbazole, sodium hydride (NaH) and ammonium hexafluorophosphate were reagent grade and used as received. The bis(*meta*-phenylene)-32-crown-10 BMP32C10 dibromide was prepared according to a literature procedure.[8] Solvents were either used as purchased or dried according to literature procedures. ^{1}H-NMR spectra were obtained on a JEOL ECLIPSE-500 spectrometer with internal standard TMS. ^{13}C-NMR spectra were collected on a JEOL

ECLIPSE-500 spectrometer at 125 MHz. HR-MS were obtained by employing an Agilent LC-ESI-TOF.

4.5.2 Synthesis of BMP32C10 dicarbazole 1d

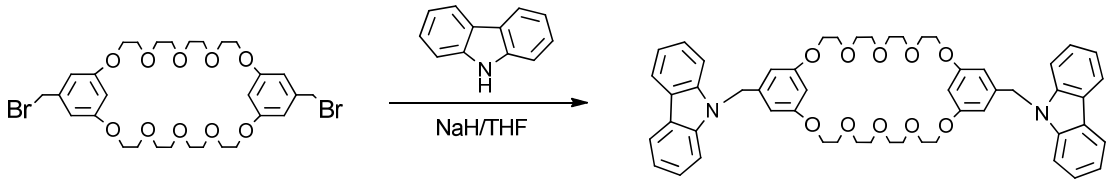

Scheme 4-2. Synthesis of BMP32C10 dicarbazole **1d**.

NaH (56.5 mg, 1.41 mmol) was suspended in THF (40 mL, anhydrous). The suspension was stirred at room temperature for 5 min under N_2. Carbazole (171 mg, 1.02 mmol) was added and the mixture was stirred at room temperature for 30 minutes, then refluxed for another 30 minutes. and cooled to room temperature. BMP32C10 dibromide (170 mg, 0.231 mmol) was added and the mixture was stirred at room temperature for 30 min. and then refluxed for 24 h. DI water (3 mL) was added into the resulting pink suspension to quench the excess NaH. Solvent was removed and a pink solid was obtained. The solid was redissolved in dichloromethane (DCM) and the solution was washed with DI water (x 3). After solvent was removed, a pink solid was again obtained. A silica gel column (gradient elution: dichloromethane, then dichloromethane : methanol = 96 : 4) was employed to purify the crude product. A pale yellow solid was obtained (207 mg, 100%, mp = 185-186 °C). ^{1}H-NMR ($CDCl_3$, 500 MHz) (Figure 4-5): δ: 8.08 (d, ^3J = 8 Hz, 4.0 H), 7.39 (t, ^3J = 8 Hz, 4.1 H), 7.30 (d, ^3J = 8 Hz, 4.1 H), 7.22 (t, ^3J = 8 Hz, 4.0 H), 6.26 (m, 6.2 H,), 5.33 (s, 4.0 H), 5.30 (s, DCM), 3.85 (t, ^3J = 8 Hz, 8.0 H), 3.68 (t, ^3J = 8 Hz, 8.1 H), 3.59 (s, 17 H). ^{13}C-NMR ($CDCl_3$, 126 MHz) (Figure 4-6): δ (ppm): 160.36, 140.75, 139.71, 125.92, 123.06, 120.40, 119.26, 108.97, 105.56, 99.81, 70.84, 70.80, 69.55, 67.45, 46.67. HR-ESIMS (Figure 4-7): calcd for $[M+H]^+$: 895.4164, found *m/z*, 895.4163 $[M + H]^+$, error: -0.11 ppm.

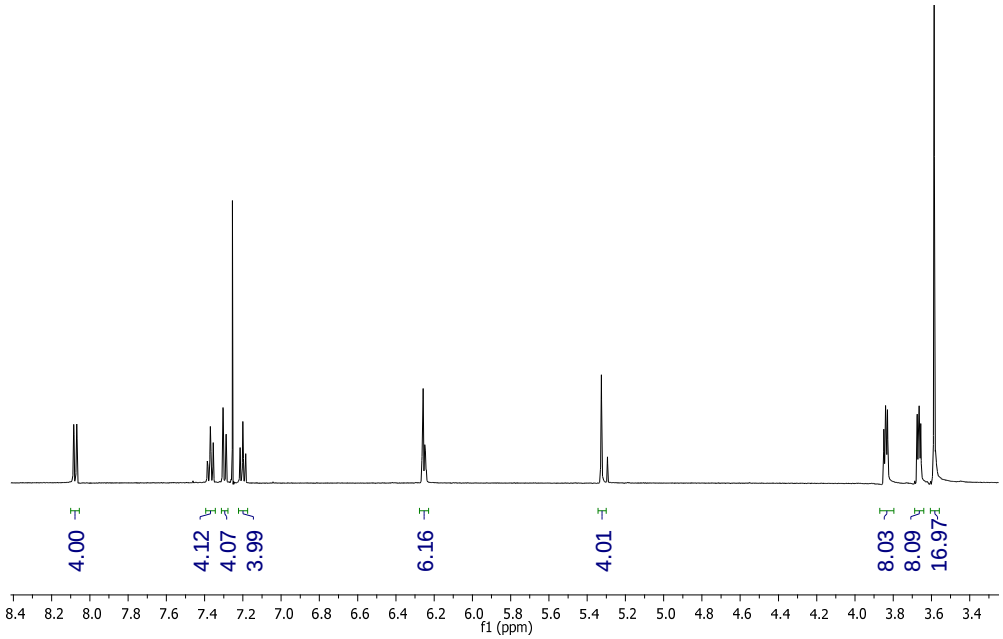

Figure 4-5. ^{1}H-NMR ($CDCl_3$, 500 MHz, room temperature) of BMP32C10 dicarbazole **1d**.

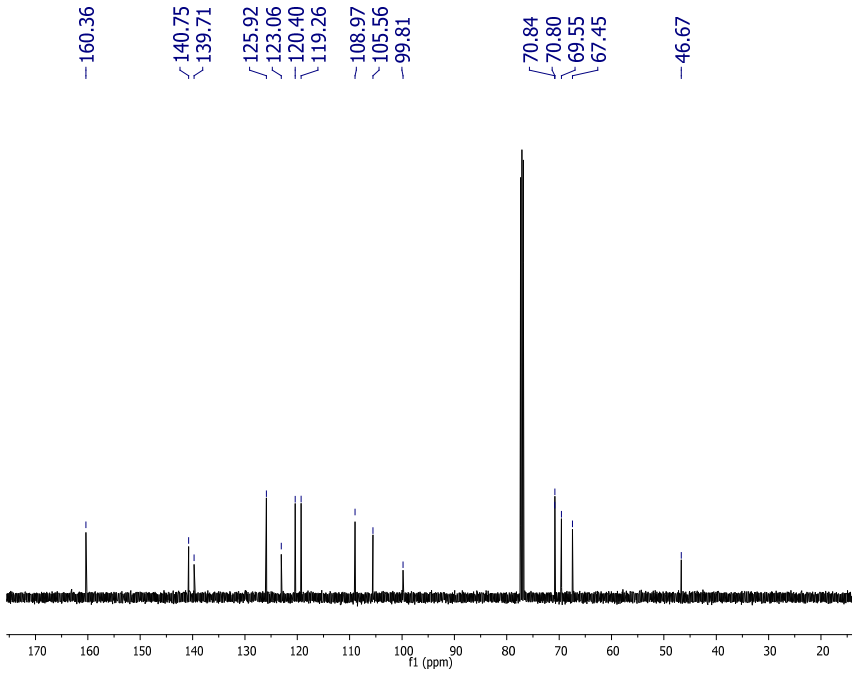

Figure 4-6. ^{13}C-NMR ($CDCl_3$, 125 MHz, room temperature) of BMP32C10 dicarbazole **1d**.

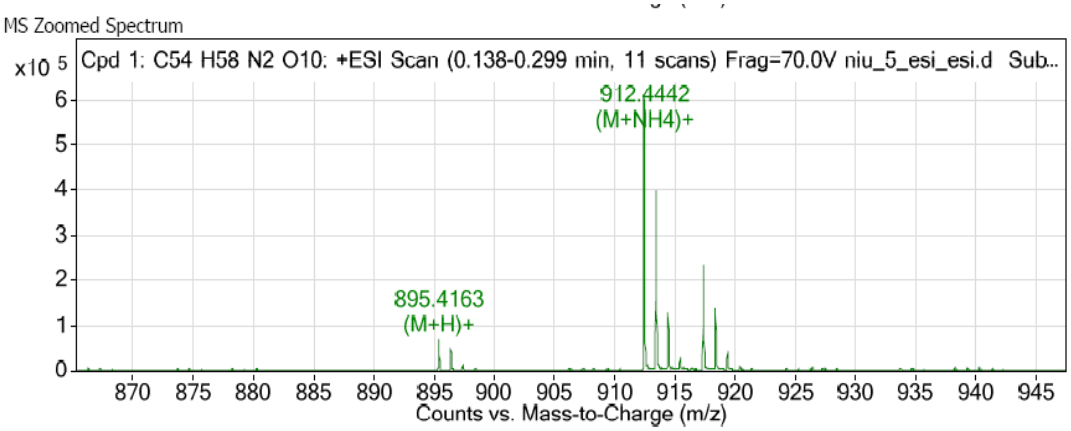

Figure 4-7. Electrospray ionization mass spectrum of BMP32C10 dicarbazole **1d**.

4.5.3 Job plot between 1d and 2

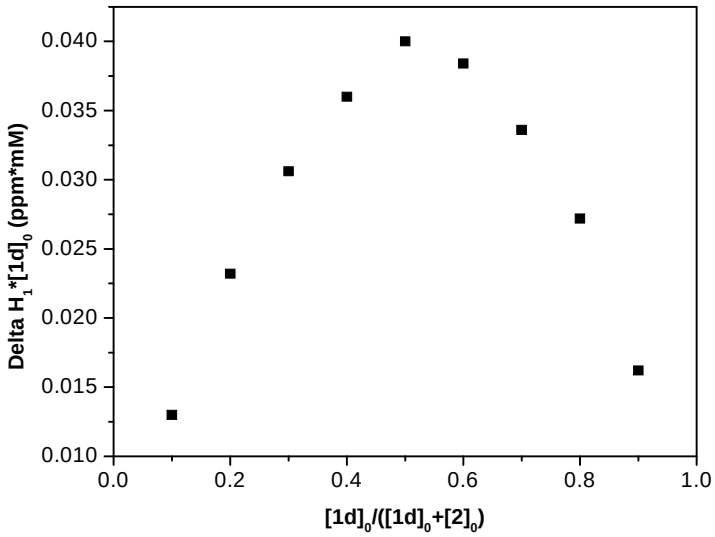

Figure 4-8. Job plot showing the 1:1 stoichiometry of the complex between 1d and 2 in $CDCl_3/CD_3CN$ = 1/1 <v/v>. $[1d]_0 + [2]_0 = 2.00$ mM.

4.5.4 Determination of Δ_0 of 1d·2

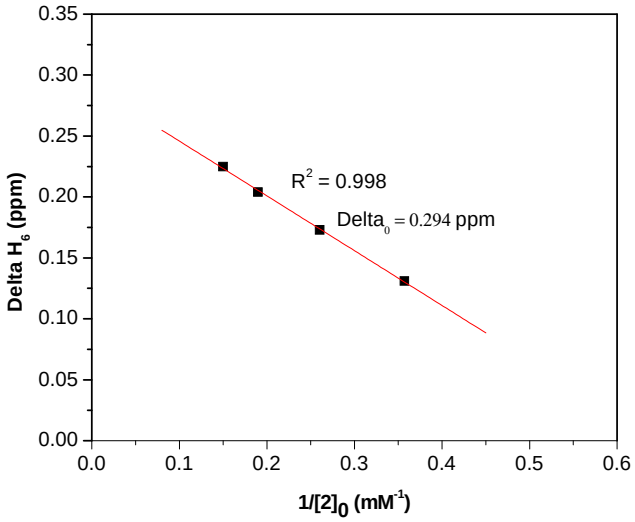

Figure 4-9. Determination of Delta$_0$ of **1d·2** in $CDCl_3/CD_3CN$ = 1/1 <v/v>. [**1d**]$_0$ = 0.176 mM.

4.5.5 Determination of Δ_0 of 1d·3

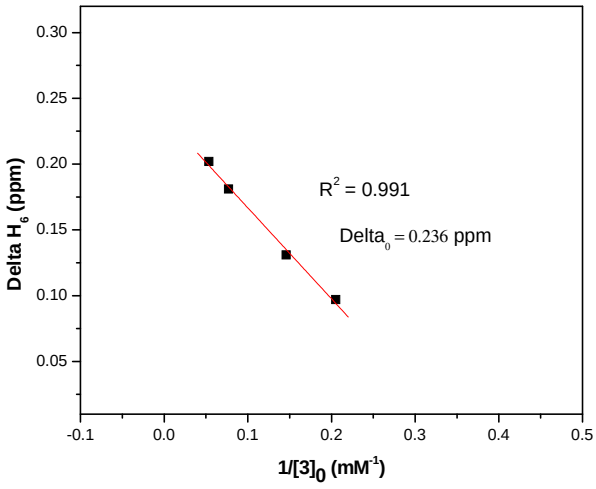

Figure 4-10. Determination of Delta$_0$ of **1d·3** in $CDCl_3/CD_3CN$ = 1/1 <v/v>. [**1d**]$_0$ = 0.416 mM.

4.5.6 Mass spectrum of 1d·2

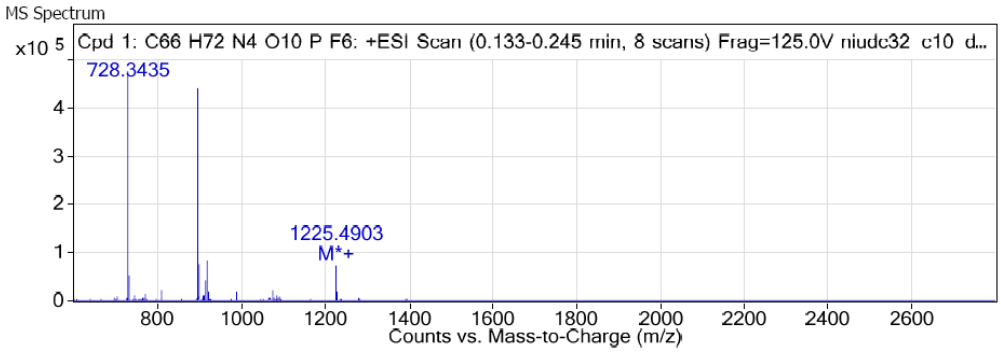

Figure 4-11. Electrospray ionization mass spectrum of **1d·2**.

4.5.7 Mass spectrum of 1d·3

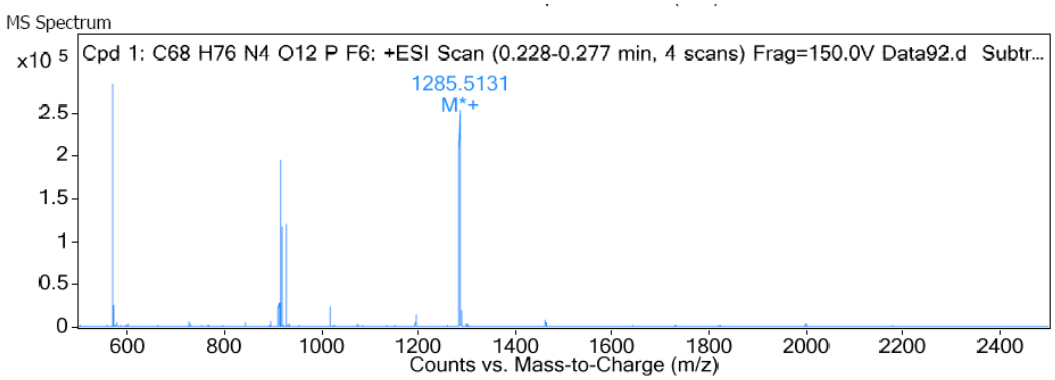

Figure 4-12. Electrospray ionization mass spectrum of **1d·3**. *m/z* 1285.51 [**1d·3**-PF_6]$^+$.

4.5.8 Crystal Structure of 1d·3

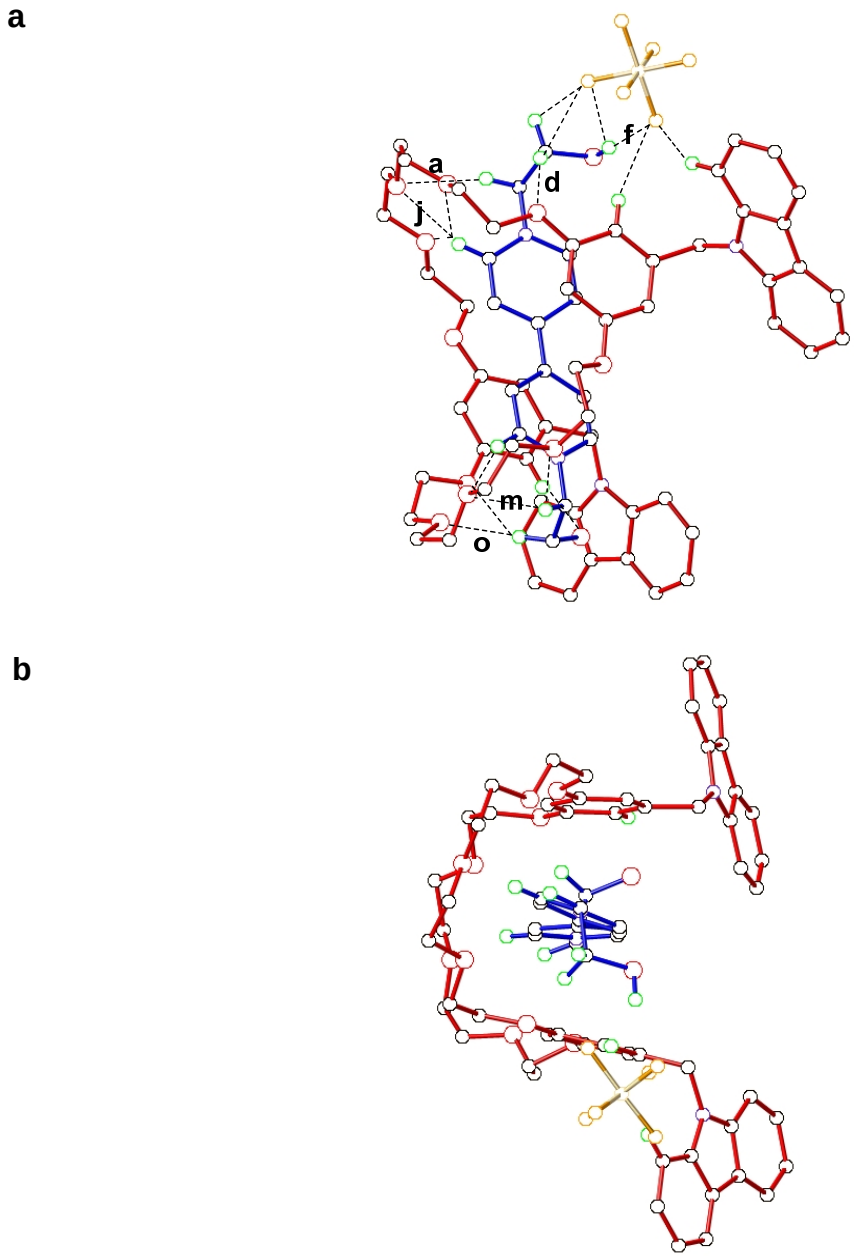

Figure 4-13. **(a)** and **(b)**: Two views of the X-ray structure of **1d·3**. **1d** is red. **3** is blue. Solvent molecules, minor disordered carbon and hydrogen atoms, one PF_6 ion and hydrogen atoms except the ones involved in hydrogen bonding have been omitted for clarity. Hydrogen bonds in (b) were omitted for clarity. Selected hydrogen-bond parameters: H···O(F) distances

(Å), C···O(F) distances (Å), C-H···O(F) angles (deg): o 2.641, 3.582, 159.0; p 2.714, 3.625, 153.32; q 2.109, 2.943, 171.4; r 2.496, 3.406, 160.5; s 2.674, 3.574, 151.4; t 2.479, 3.338, 142.7; Off-set face-to-face π-stacking parameters: centroid-centroid distances (Å) and dihedral angles (deg): aromatic rings of **1d** and pyridinium rings of paraquat **3**: 3.771, 3.828 and 1.58, 7.84.

References

(1) (a) Gibson, H. W. In Large Ring Molecules; Semlyen, J. A., Ed.; John Wiley & Sons: New York, 1996; Chapter 6, pp 191-262. (b) Raymo, F. M.; Stoddart, J. F. *Chem. Rev.* **1999**, *99*, 1643-1664. (c) Harada, A. *Acc. Chem. Res.* **2001**, *34*, 456-464. (d) Herna′ndez, J. V.; Kay, E. R.; Leigh, D. A. *Science*. **2004**, *306*, 1532–1537. (e) Wenz, G.; Han, B. –H.; Müller, A. *Chem. Rev.* **2006**, *106*, 782-817. (f) Lankshear, M. D.; Beer, P. D. *Acc. Chem. Res.* **2007**, *40*, 657-668. (g) Vickers, M. S.; Beer, P. D. *Chem. Soc. Rev.* **2007**, *36*, 211-225. (h) Colquhoun, H. M.; Zhu, Z.; Cardin, C. J.; White, A. J. P.; Drew, M. G. B.; Gan, Y. *Org. Lett.* **2010**, *12*, 3756-3759. (i) Kim, S. K.; Sessler, J. L. *Chem. Soc. Rev.* **2010**, *39*, 3784-3809. (j) Gasa, T. B.; Valente, C.; Stoddart, J. F. *Chem. Soc. Rev.* **2011**, *40*, 57-78.

(2) Reviews: (a) Ciferri, A. *Supramolecular Polymers*; Marcel-Dekker: New York, 2000. (b) Brunsveld, L.; Folmer, B. J. B.; Meijer, E. W.; Sijbesma, R. P. *Chem. Rev.* **2001**, *101*, 4071-4098. (c) Huang, F.; Gibson, H. W. *Prog. Polym. Sci.* **2005**, *30*, 982-1018. (d) Takata, T.; *Polymer J.* **2006**, *38*, 1-20. (e) De Greef, T. F. A.; Smulders, M. M. J.; Wolffs, M.; Schenning, A. P. H. J.; Sijbesma, R. P.; Meijer, E. W. *Chem. Rev.* **2009**, *109*, 5687-5754. (f) Harada, A.; Hashidzume, A.; Yamaguchi, H.; Takashima, Y. *Chem. Rev.* **2009**, *109*, 5974-6023. (g) Niu, Z.; Gibson, H. W. *Chem. Rev.* **2009**, *109*, 6024-6046. (h) Faiz, J. A.; Heitz, V.; Sauvage, J.-P. *Chem. Soc. Rev.* **2009**, *38*, 422-442. (i) Fang, L.; Olson, M. A.; Benitez, D.; Tkatchouk, E.; Goddard III, W. A.; Stoddart, J. F. *Chem. Soc. Rev.* **2010**, *39*, 17-29. (j) Thibeault, D.; Morin, J.-F. *Molecules* **2010**, *15*, 3709-3730. (k) Gavina, P.; Tatay, S. *Curr. Org. Syn.* **2010**, *7*, 24-43.

(3) Some recent publications: (a) Lee, M.; Schoonover, D. V.; Gies, A. P.; Hercules, D. M.; Gibson, H. W. *Macromolecules* **2009**, *42*, 6483-6494. (b) Zhang, M.; Zhu, K.; Huang, F. *Chem. Commun.* **2010**, *46*, 8131-8141. (c) Wang, C.; Olson, M. A.; Fang, L.; Benítez, D.; Tkatchouk, E.; Basu, S.; Basuray, A. N.; Zhang, D.; Zhu, D.; Goddard, W. A.; Stoddart, J. F. *Proc. Nat. Acad. Sci.* **2010**, *107*, 13991-13996. (d) Trabolsi, A.; Fahrenbach, A. C.; Dey, S. K.; Share, A. I.; Friedman, D. C.; Basu, S.; Gasa, T. B.; Khashab, N. M.; Saha, S.; Aprahamian, I.; Khatib, H. A.; Flood, A. H.; Stoddart, J. F. *Chem. Commun.* **2010**, *46*, 871-873. (e) Jiang, Y.; Cao, J.; Zhao, J. –M.; Xiang, J.-F.; Chen, C.-F. *J. Org. Chem.* **2010**, *75*, 1767-1770. (f) Zhang, M.; Luo, Y.; Zheng, B.; Yan, X.; Fronczek, F. R.; Huang, F. *Eur. J. Org. Chem.* **2010**, *35*, 6798-6803. (g) Xu, Z.; Jiang, L.; Feng, Y.; Zhang, S.; Liang, J.; Pan, S.; Yang, Y.; Yang, D.; Cai, Y. *Org. Biomol. Chem.* **2011**, *9*, 1237-1243.

(4) (a) Bryant, W. S.; Guzei, I.; Rheingold, A. L.; Gibson, H. W. *Org. Lett.* **1999**, *1*, 47-50. (b) Huang, F.; Fronczek, F. R.; Gibson, H. W. *Chem. Commun.* **2003**, 1480−1481. (c) Huang, F.; Zakharov, L. N.; Bryant, W.; Rheingold, A. L.; Gibson, H. W. *Chem. Commun*. **2005**, 3268-3270. (d) Huang, F.; Gantzel, P.; Nagvekar, D. S.; Rheingold, A. L.; Gibson, H. W. *Tetrahedron Lett.* **2006**, *47*, 7841-7844. (e) Li, S.; Liu, M.; Zheng, B.; Zhu, K.; Wang, F.; Li, N.; Zhao, X.-L.; Huang, F. *Org. Lett.* **2009**, *11*, 3350-3353.

(5) (a) Huang, F.; Jones, J. W.; Slebodnick, C.; Gibson, H. W. *J. Am. Chem. Soc.* **2003**, *125*, 14458-14464. (b) A rotaxane was prepared in 6% yield based on BMP32C10 and a paraquat derivative. See: Li, S.; Zhu, K.; Zheng, B.; Wen, X.; Li, N.; Huang, F. *Eur. J. Org. Chem.* **2009**, 1053-1057. (c) A [2]catenane was prepared based on cyclobis(paraquat-*p*-phenylene) and BMP32C10 in 17% yield, but strictly speaking, the initial guest (before cyclization) is not a simple paraquat but rather an extended paraquat with a monoquaternized 4,4'-bipyridine moiety. See: Stoddart, J. F.; Williams, D. J.; Amabilino, D. B.; Anelli, P.-L.; Ashton, P. R.; Brown, G. R.; Cordova, E.; Godinez, L. A.; Hayes, W. *J. Am. Chem. Soc.* **1995**, *117*, 11142-11170.

(6) Allwood, B. L.; Shahriari-Zavareh, H.; Stoddart, J. F.; Williams, D. J. *J. Chem. Soc., Chem. Commun.* **1987**, 1058-1061.

(7) (a) Yang, Y.; Hu, H.-Y.; Chen, C.-F. *Tetrahedron Lett.* **2007**, *48*, 3505-3509. (b) Zhu,

K.; Li, S.; Wang, F.; Huang, F. *J. Org. Chem.* **2009**, *74*, 1322-1328. (c) Zhang, M.; Luo, Y.; Zheng, B.; Yan, X.; Fronczek, F. R.; Huang, F. *Eur. J. Org. Chem.* **2010**, *35*, 6798-6803.

(8) Gibson, H. W.; Nagvekar, D. S. *Can. J. Chem.* **1997**, *75*, 1375-1384.

(9) (a) Job, P. *Ann. Chim.* **1928**, *9*, 113-123. (b) Tsukube, H.; Furuta, H.; Odani, A.; Takeda, Y.; Kudo, Y.; Inoue, Y.; Liu, Y.; Sakamoto, H.; Kimura, K. eds. Atwood, J. L.; Davies, J. E. D.; MacNicol, D. D.; Vogtle, F.; Lehn, J.-M. Elsevier Science Ltd., New York, 1996, pp. 425-479. (c) Hirose, K. *J. Inclusion Phenom. Macrocyclic Chem.* **2001**, *39*, 193-209.

(10) ^{1}H-NMR characterizations were done on solutions with constant [**1d**] and varied [**2**] or [**3**]. Based on these NMR data, Δ_0, the difference in δ values for protons of **1d** in the uncomplexed and fully complexed species, was determined as the y-intercept of a plot of $\Delta = \delta - \delta_u$ *vs.* $1/[\mathbf{2}]_0$ or $1/[\mathbf{3}]_0$ in the high initial concentration range of **2** or **3**: Δ_0 = 0.294 ppm for **1d·2** and Δ_0 = 0.236 ppm for **1d·3** based on H_6. K_a was calculated from $K_a = (\Delta/\Delta_0)/[(1-\Delta/\Delta_0)([\mathbf{2}]_0-\Delta/\Delta_0\ [\mathbf{1d}]_0)$ or its analog with [**3**]. It was found that for these systems K_a does not have the concentration dependence we found in two other systems.[5a,11]

(11) (a) Jones, J. W.; Gibson, H. W. *J. Am. Chem. Soc.* **2003**, *125*, 7001-7004. (b) Gibson, H. W.; Jones, J. W.; Zakharov, L. N.; Rheingold, A. L. *Chem. Eur. J.* **2011**, *17*, 3192-3206.

(12) (a) Shen, Y. X.; Engen, P. T.; Berg, M. A. G.; Merola, S. S.; Gibson, H. W. *Macromolecules* **1992**, *25*, 2786-2792. (b) Gong, C.; Gibson, H. W. *Angew. Chem. Int. Ed. Engl.* **1998**, *37*, 310-314.

(13) Huang, F.; Switek, K. A.; Zakharov, L. N.; Fronczek, F. R.; Slebodnick, C.; Lam, M.; Golen, J. A.; Bryant, W. S.; Mason, P. E.; Rheingold, A. L.; Ashraf-Khorassani, M.; Gibson, H. W. *J. Org. Chem.* **2005**, *70*, 3231-3241.

(14) (a) Fujii, A.; Morita, S.; Miyazaki, M.; Ebata, T.; Mikami, N. J. Phys. Chem. A 2004, 108, 2652-2658. (b) Kobayashi, Y.; Saigo, K. J. Am. Chem. Soc. 2005, 127, 15054-15060. (c) Gil, A.; Branchadell, V. Bertran, J.; Oliva, A. J. Phys. Chem. B 2007, 111, 9372-9379. (d) Pederson, A. M.-P.; Vetor, R. C.; Rouser, M. A.; Huang, F.;

Slebodnick, C.; Schoonover, D. V.; Gibson, H. W. J. Org. Chem. 2008, 73, 5570-5573. (e) García-Frutos, E. M.; Hennrich, G.; Gutierrez, E.; Monge, A.; Gómez-Lor, B. J. Org. Chem. 2010, 75, 1070-1076.

(15) (a) Hunter, C. A.; Sanders, J. K. M. J. Am. Chem. Soc. 1990, 112, 5525-5534. (b) Hohenstein, E. G.; Sherrill, C. D. J. Phys. Chem. A 2009, 113, 878-886.

(16) Nabeshima, T. Bull. Chem. Soc. Jpn. 2010, 83, 969-991.

(17) Examples of enhanced complexation of paraquats by crown ethers via pseudocryptand formation: Jones, J. W.; Zakharov, L. N.; Rheingold, A. L.; Gibson, H. W. J. Am. Chem. Soc. 2002, 124, 13378-13379. (b) Huang, F.; Guzei, I. A.; Jones, J. W.; Gibson, H. W. Chem. Commun. 2005, 1693-1695.

(18) Yonemura, H.; Kasahara, M.; Saito, H.; Nakamura, H.; Matsuo, T. J. Phy. Chem. 1992, 96, 5765-5770.

(19) As described previously the modest Ka values of the present systems (and the multi-molecular nature of the poly[2]pseudorotaxanes 1d•22 and 1d•32) greatly limit supramolecular polymer formation even up to multimolar concentrations: (a) Sijbesma, R. P.; Beijer, F. H.; Brunsveld, L.; Folmer, B. J. B.; Hirschberg, J. H. K. K.; Lange, R. F. M.; Lowe, J. K. L.; Meijer, E. W. Science 1997, 278, 1601–1604. (b) Yamaguchi, N.; Nagvekar, D.; Gibson, H. W. Angew. Chem. Int. Ed. Engl. 1998, 38, 2361-2364. (c) Yamaguchi, N.; Gibson, H. W. Angew. Chem. Int. Ed. 1999, 38, 143-147. (d) Hirschberg, J. H. K. K.; Beijer, F. H.; van Aert, H. A.; Magusin, P. C. M. M.; Sijbesma, R. P.; Meijer, E. W. Macromolecules 1999, 32, 2696-2705. (e) Brunsveld, L.; Folmer, B. J. B.; Meijer, E. W.; Sijbesma, R. P. Chem. Rev. 2001, 101, 4071-4097. (f) Gibson, H. W.; Yamaguchi, N.; Jones, J. W. J. Am. Chem. Soc. 2003, 125, 3522-3533. (g) Huang, F.; Nagvekar, D. S.; Gibson, H. W. Macromolecules 2007, 40, 3561-3567. (h) Gibson, H. W.; Yamaguchi, N.; Niu, Z.; Jones, J. W.; Rheingold, A. L.; Zakharov, L. N. J. Polym. Sci., Polym. Chem. Ed. 2010, 48, 975-985. (i) Wang, F.; Zhang, J.; Liu, M.; Zheng, B.; Li, S.; Zhu, K.; Wu, L.; Gibson, H. W.; Huang, F. Angew. Chem. Int. Ed. 2010, 49, 1090-1094. (j) Niu, Z.; Gibson, H. W. J. Am. Chem. Soc. 2011, 133, 2836-2839.

(20) For polymers containing backbone paraquat moieties see: (a) Factor, A.; Heinsohn, G. E. J. Polym. Sci., Polym. Lett. Ed. 1971, 9, 289-295. (b) Rosenblum, M. D.; Lewis, N. S. J. Phys. Chem. 1984, 88, 3103-3107. (c) Shen, Y. X.; Engen, P. T.; Berg, M. A. G.; Merola, J. S.; Gibson, H. W. Macromolecules 1992, 25, 2786-2788. (d) Loveday, D.; Wilkes, G. L.; Bheda, M. C.; Shen, Y. X.; Gibson, H. W. J. Macromol. Sci., A-Chem. 1995, A32, 1-27. (e) Harada, A.; Adachi, H.; Kawaguchi, Y.; Okada, M.; Kamachi, M. Polym. J. 1996, 28, 159-163. (f) Gong, C.; Gibson, H. W. Macromol. Chem. Phys. 1998, 199, 1801-1806. (g) Jain, V.; Yochum, H.; Wang, H.; Montazami, R.; Vidales-Hurtado, M. A.; Mendoza-Galván, A.; Gibson, H. W.; Heflin, J. R. Macromol. Chem. Phys. 2008, 209, 150-157. (h) Bhowmik, P. K.; Cheney, M. A.; Jose, R.; Han, H.; Banerjee, A.; Ma, L.; Hansen, L. D. Polymer 2009, 50, 2393-2401. (i) Ogoshi, T.; Nishida, Y.; Yamagishi, T.; Nakamoto, Y. Macromolecules 2010, 43, 7068-7072.

(21) For polymers with paraquat end groups see: (a) Huang, F.; Nagvekar, D. S.; Slebodnick, C.; Gibson, H. W. J. Am. Chem. Soc. 2005, 127, 484-485. (b) Rauwald, U.; Scherman, O. A. Angew. Chem., Int. Ed. 2008, 47, 3950-3953. (c) Lee, M.; Schoonover, D.; Gies, A.; Hercules, D. M.; Gibson, H. W. Macromolecules 2009, 42, 6483-6494.

TOC Graphic:

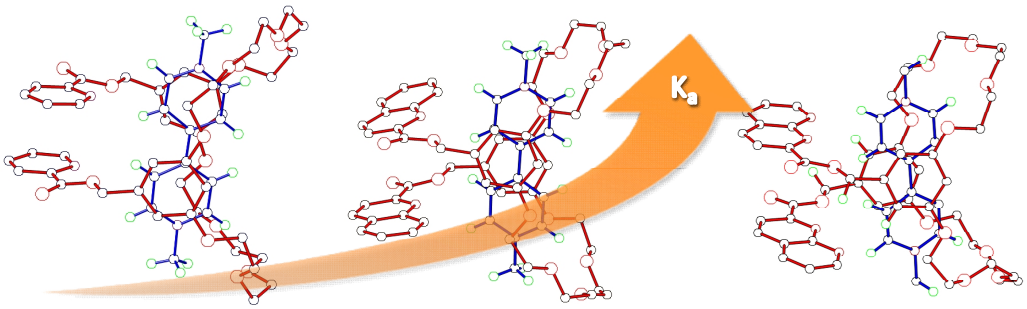

Abstract:

The first dual component pseudocryptand-type [2]pseudorotaxanes were designed and prepared via the self-assembly of synthetically easily accessible bis(meta-phenylene)-32-crown-10 pyridyl, quinolyl and naphthyridyl derivatives with paraquat. The formation of the pseudocryptand structures in the complexes remarkably improved the association constant by forming the third pseudo-bridge via H-bonding with the guest and π–stacking of the heterocyclic units.

Chapter 5.

Pseudocryptand-type [2]Pseudorotaxanes Based on Bis(meta-phenylene)-32-Crown-10 Derivatives and Paraquats with Remarkably Improved Association Constants

5.1 Introduction

Pseudorotaxanes are mechanically interlocked molecular architectures consisting of a linear molecular component ("guest") encircled by a macrocyclic component ("host"). The design and preparation of novel and simple pseudorotaxanes systems[1] with high association constants are of great significance, since stable pseudorotaxanes are the fundamental building blocks for preparation of many novel, more advanced supramolecular species, such as rotaxanes, catenanes, polypseudorotaxanes, polyrotaxanes and polycatenanes,[2] which are expected to have unique properties and potential applications.[2-3] Crown ethers, e. g., **1**, and paraquat (*N,N'*-dialkyl-4,4'-bipyridinium) derivatives have been widely used in the construction of pseudorotaxanes.[4] Moreover, cryptands have proven to be much better hosts for the paraquat derivatives due to preorganization and introduction of more binding sites;[5,6a] however, the synthetically lower accessibility of cryptands[5b-i,6a] (e. g., **4**[5b] and **5**[5c] in 21% and 42% yields, respectively, from **1b**) has limited their further applications. Our group first demonstrated that the complexes between bis(*meta*-phenylene)-32-crown-10 (BMP32C10) derivative (**1b**) and paraquat derivatives instead of being pseudorotaxanes were folded into "taco" shapes[7] in the solid state, as proven by their X-ray crystal structures.[6a,7] Until recently,[6] almost all the complexes of bis(*meta*-phenylene)-32-crown-10 derivatives with paraquat derivatives (such as **2** and **3**[8]) had demonstrated "taco"-shaped structures, which expose one side of the paraquat salts. Inspired by these results, we tried to take advantage of the "taco"-shaped structures, which were tendentiously formed in the complexes of BMP32C10 derivatives with paraquat derivatives to design powerful new hosts with high association constants. Here we first report novel

pseudocryptand-type[9] [2]pseudorotaxanes based on synthetically easily accessible BMP32C10 derivatives with remarkably improved association constants.

5.2 Results and discussion

Crown ether **1c** was prepared via the EDCI/DMAP coupling between BMP32C10 diol (**1b**)[10] and picolinic acid in 94% yield. Equimolar solutions of **1c** and **2** in chloroform/acetonitrile (1/1, v/v) were deep yellow due to the charge-transfer interaction between the electron-rich aromatic rings of **1c** and the electron-poor pyridinium rings of **2**, evidence for complexation.

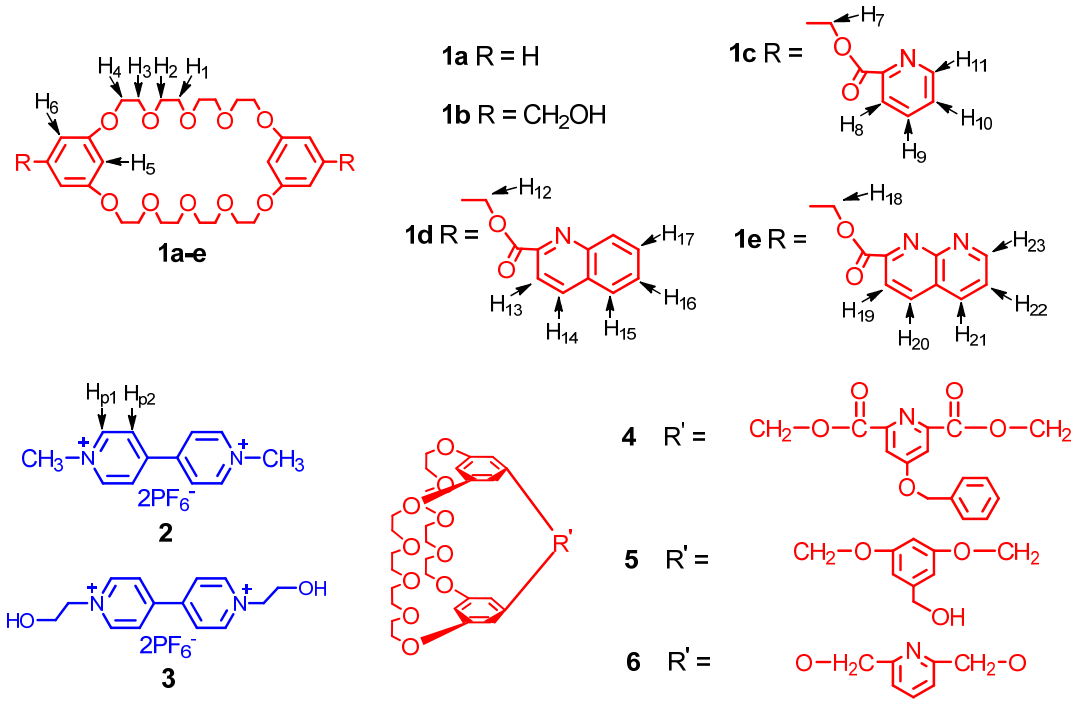

Scheme 5-1. Structures of hosts **1a-e** and **4-6** and paraquat guests **2** and **3**.

^{1}H-NMR spectra of equimolar solutions of **1c** and **2** displayed only one set of peaks, indicating fast exchange.[7] After complexation, peaks corresponding to H_3, H_4, H_5, H_6, H_7, H_8 and H_{11} of **1c** and H_{p2} of **2** moved upfield, while H_1, H_2 and H_{10} of **1c** and H_{p1} of **2** moved downfield. The stoichiometry of the complex between **1c** and **2** was determined to be 1:1 by a Job plot[7,11] and confirmed by an electrospray ionization mass spectrum (ESI-MS): m/z 1137.07 [**1c**·**2**-PF_6]$^+$, 993.13 [**1c**·**2**-2PF_6+H]$^+$, 496.07 [**1c**·**2**-2PF_6+H]$^{2+}$.[7] K_a was determined to be 3.1 ± 0.3 x 10^3 M^{-1} in

$CDCl_3/CD_3CN$ (1/1, v/v) based on the proton NMR data;[12] this value is 8-fold higher than the K_a of the simple BMP32C10 complex **1a·2** (393 ± 30 M^{-1}, in the same solvent).

We reasoned that the association constant increases because the folding of the central part of the crown ether, in order to form the "taco" complex with guest **2**, enables both pyridyl rings to participate in the complexation process by interaction with the α- and -protons of the paraquat, as designed on the basis of the concept underlying lariat ethers.[13] This hypothesis was confirmed by X-ray diffraction analysis of crystals of **1c** and the complex of **1c** with **2** (Figure 5-1). The molecules of host **1c** by themselves assume a stair-step structure[7] common to bis(*m*-phenylene) crown ether derivatives,[14] placing the phenylene rings nearly parallel to each other but as far apart as possible by extension in opposite directions. In contrast, in the complex, **1c** is folded and the two pyridyl rings interact via face-to-face π-stacking,[14b,15] while the two nitrogen atoms are pointed to the central cavity, resulting in a single-molecule pseudocryptand host[9] structure. Paraquat salt **2** is threaded through the central cavity of the pseudocryptand and the complex is stabilized by hydrogen bonds between the oxygen and nitrogen atoms of **1c** with hydrogen atoms on the paraquat salt **2** and off-set face-to-face π-stacking between the phenylene rings of **1c** and the pyridinium rings of **2**. As a result, a pseudocryptand-type [2]pseudorotaxane is formed. It is noteworthy that the ester ether oxygens and the nitrogens of both pyridyl units identically interact with the -protons of the guest. Moreover, the formation of pseudocryptand structure of **1c·2** in solution was confirmed by 1D-NOESY experiments.[7]

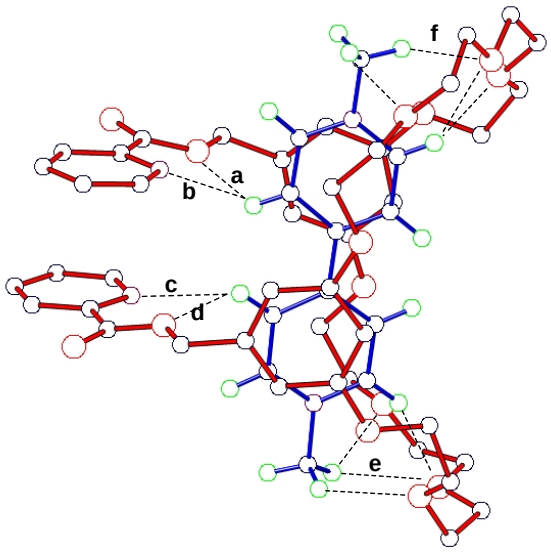

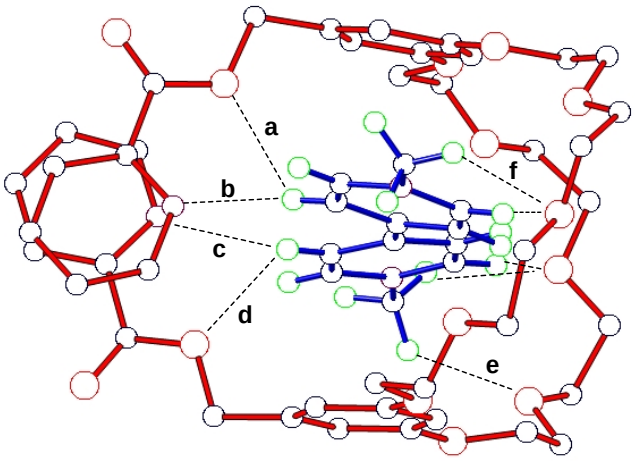

Figure 5-1. Two views of X-ray structure of **1c·2**. Oxygen atoms are red. Carbon atoms are black. Nitrogen atoms are purple. Hydrogen atoms are green. **1c** is red. **2** is green. The same settings are used in the following crystal structures. Solvent molecules, PF_6^- ions, and hydrogens except the ones on **2** and disordered atoms were omitted for clarity. Selected hydrogen-bond parameters: H···O(N) distances (Å), C···O(N) distances (Å), C-H···O(N) angles (deg): a 2.56, 3.14, 120; b 2.41, 3.12, 131; c 2.67, 3.39, 134; d 2.54, 3.17, 124; e 2.53, 3.27, 132; f 2.43, 3.23, 139. In the bottom figure, the overlapped hydrogen bonds are omitted for clarity.

Since the improved K_a of **1c·2** was clearly due to pseudocryptand-type [2]pseudorotaxane structure formation, favored by π-stacking of the pyridyl units, we next chose to incorporate quinoline groups, which afford larger aromatic profiles.[16] The bisquinolyl compound **1d** was prepared via EDCI/DMAP coupling between BMP32C10 diol (**1b**) and quinaldic acid in 98% yield. In ^{1}H-NMR spectroscopy the complexation was a fast-exchange process. A Job plot[7,11] indicated that the stoichiometry between **1d** and **2** was 1:1, as confirmed by matrix-assisted laser desorption/ionisation-time of flight mass spectrometry: m/z 1092 [**1d·2**-2PF_6]$^+$.[7] The K_a was determined to be 12.4 ± 1.3 x 10^3 M^{-1} in $CDCl_3$/CD_3CN (1/1, v/v),[12] which is a 31-fold increase compared with the K_a for simple crown ether **1a** with **2** and a 4-fold increase relative to **1c·2**. Interestingly, this K_a value is even higher than those of some synthetically less accessible cryptand complexes with **2**, such as **5·2** and **6·2**.[17]

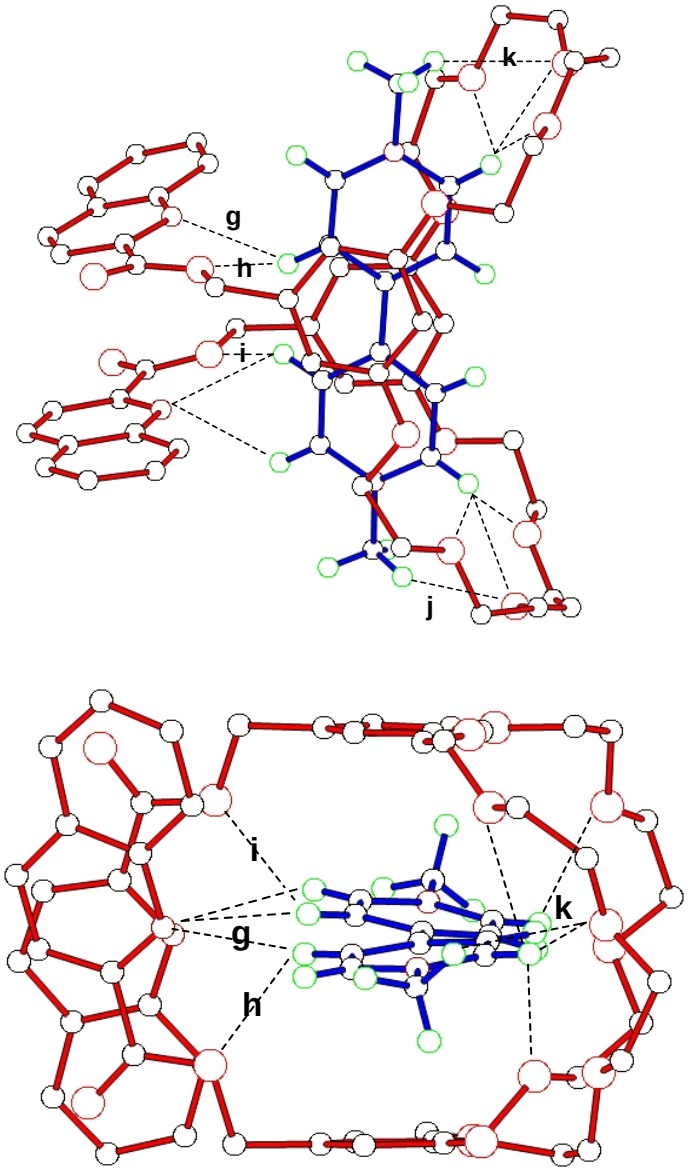

Figure 5-2. The X-ray structure of **1d·2**. Solvent molecules, PF_6^- ions, hydrogens except the ones on **2** and disorder were omitted for clarity. Selected hydrogen-bond parameters: H···O(N) distances (Å), C···O(N) distances (Å), C-H···O(N) angles (deg): g 2.61, 3.34, 134; h 2.57 3.20 125; i 2.59, 3.19, 121; j 2.50, 3.39, 150; k 2.17, 3.05, 150; In the bottom figure, the overlapped hydrogen bonds are omitted for clarity.

Similarly, X-ray analysis of a single crystal of **1d·2** demonstrated the pseudocryptand-type [2]pseudorotaxane structure (Figure 5-2), as expected, revealing off-set face-to-face π-stacking of the quinoline rings and lone-pair-π interactions between carbonyl oxygen atoms and

quinoline rings.[18] Paraquat salt **2** is threaded through the central cavity of the pseudocryptand and the complex is stabilized by hydrogen bonds between the oxygen and nitrogen atoms of **1d** with hydrogen atoms on the paraquat salt **2** and off-set face-to-face π-stacking between the aromatic rings of the host and guest. In contrast to the situation with **1c**·**2** the interactions of the two quinolyl units with the guest are not the same; one interacts with a -proton only via both the ester ether oxygen and the nitrogen atoms, while the other interacts via the nitrogen with both - and -protons and the ether oxygen again interacts with a -proton. Again, the formation of the pseudocryptand-type [2]pseudorotaxane in solution was confirmed by 1D-NOESY experiments.[7]

Based on the crystal structure of pseudocryptand-type [2]pseudorotaxane **1d·2**, we realized that the 8-carbon of the quinoline ring in the complex is pretty close to the α-H (H_{p1}, short distance: 3.63 Å), β-H (H_{p2}, short distance: 3.65) and benzyl proton H_6 of guest **1d** (short distance: 2.84 Å). As a result, if the 8-position carbon is replaced by a hydrogen bond acceptor, it is possible to form extra H-bonds, which can stabilize the pseudocryptand [2]pseudorotaxane structure even more. In addition, the replacement of the 8-carbon by a hydrogen bond acceptor can eliminate the repulsion between the H atom on the 8-carbon and α-H (H_{p1}, short distance: 2.91 Å), β-H (H_{p2}, short distance: 3.09 Å) and the benzyl proton H_6 on **1d** (short distance: 2.28 Å), which disfavor the formation of pseudocryptand-type [2]pseudorotaxane structure. Therefore, the 1,8-naphthyridyl group, which has nitrogen atoms at the 1- and 8-positions, was chosen to be incorporated into BMP32C10.

The bisnaphthyridyl compound **1e** was prepared via EDCI/DMAP coupling between BMP32C10 diol (**1b**) and naphthyridyl acid in 93% yield. ^{1}H-NMR spectroscopy showed that the complexation between **1e** and **2** was fast-exchange. Isothermal titration calorimetry (ITC)[19] indicated the stoichiometry between **1e** and **2** was 1:1, as confirmed by ESI-MS: m/z 1239.43 [**1e·2**-PF_6]$^+$.[7] The K_a was determined to be 2.5 ± 0.2 x 10^5 M^{-1} in $CHCl_3$/CH_3CN (1/1, v/v) by ITC,[7,19] a 625-fold increase compared with the K_a for simple crown ether **1a** with **2** and a 20-fold increase relative to **1d·2**. To the best of our knowledge, this K_a value is the highest reported for BMP32C10 derivatives with **2** and, most important, it is comparable to even the best cryptand hosts, such as **4** (K_a = 9.0 ±1.8 x 10^5 M^{-1} in acetone).[5b]

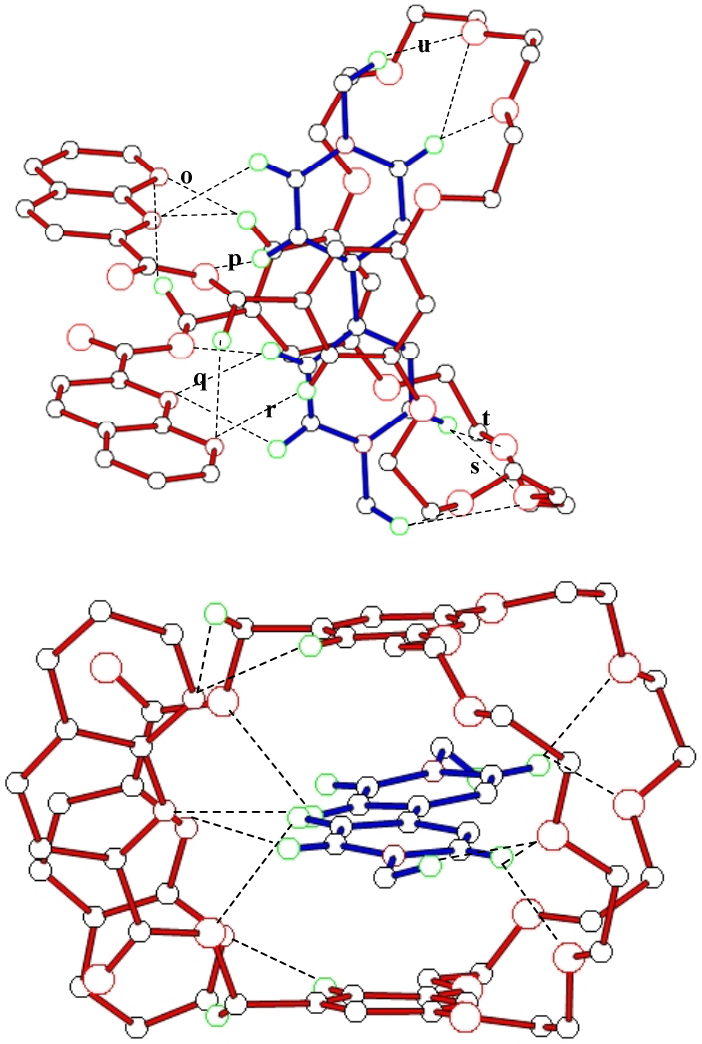

Figure 5-3. The X-ray structure of **1e·2**. Solvent molecules, PF_6^- ions, and hydrogens except the ones involved in hydrogen bonds formation were omitted for clarity. Selected hydrogen-bond parameters: H···O(N) distances (Å), C···O(N) distances (Å), C-H···O(N) angles (deg): o 2.59, 3.47, 155; p 2.73, 3.23, 114; q 2.58, 3.32, 134; r 2.52, 3.31, 153; s 2.41, 3.23, 146; t 2.51, 3.32, 144; u 2.42, 3.38, 164; In the bottom figure, the overlapped hydrogen bonds are omitted for clarity.

As expected, the crystal structure of the complex **1e·2** demonstrated its pseudocryptand-type [2]pseudorotaxane arrangement (Figure 5-3), similar to the complex of **1d·2**. **1e** is folded and the two naphthyridyl rings interact via off-set face to face π-stacking and lone-pair-π

interactions between carbonyl oxygen atoms and naphthyridyl rings, while the four nitrogen atoms are pointed to the central cavity, resulting in a single-molecule pseudocryptand host.[9] Paraquat salt **2** is threaded through the central cavity of the pseudocryptand and the complex is stabilized by hydrogen bonds between oxygen and nitrogen atoms of **1e** with hydrogen atoms on the paraquat salt **2** and off-set face-to-face π-stacking between the aromatic rings of the host and guest. As expected, the nitrogen atoms at the 8-position do interact with α-H (H_{p1}, short distance: 3.33 Å), β-H (H_{p2}, short distance: 3.38 Å). However, these interactions appear to be weak due to the relative long distances. However, the nitrogen atoms at the 8-position formed relatively strong hydrogen bonds with benzyl protons H_6 (short distances: 2.588 and 2.516 Å) and weak hydrogen bonds with CH_2 protons H_{18} (short distances: 3.019 and 2.913 Å). These hydrogen bonds provide extra linkages which stabilize the pseudocryptand-type [2]pseudorotaxane arrangement. In addition, the two naphthyridyl arms of **1e** are much closer to threaded guest **2** compared with **1d·2** system due to the removal of repulsions between the H atom connected with the 8-carbon and α-protons (H_{p1}) and β-protons (H_{p2}) in the latter. As a result, the nitrogen atoms at the 1-position can interact with both α-protons (H_{p1}) and β-protons (H_{p2}) and provide extra hydrogen bonds relative to the **1d·2** system. Clearly, these hydrogen bonds stabilize the pseudocryptand-type [2]pseudorotaxane arrangement. Therefore, the association constant increased remarkably, reflecting G_{298} = -7.4 kcal/mol. Once more, the formation of the pseudocryptand-type [2]pseudorotaxane in solution was confirmed by 1D-NOESY experiments.[7]

5.3 Conclusions

In summary, pyridyl, quinolyl and naphthyridyl based bis(*meta*-phenylene)-32-crown-10 diesters were designed and prepared efficiently in high yield (93-98%) from diol **1b**. Via the self-assembly of a paraquat derivative with these new hosts, the first dual component pseudocryptand-type [2]pseudorotaxanes[20] were prepared. The formation of pseudocryptand structures improves the association constants remarkably (from 393 M^{-1} to 2.5 x 10^5 M^{-1}; doubling G_{298} from -3.5 to -7.4 kcal/mol). The present protocol provides a facile method to prepare pseudorotaxane systems with relatively high association constants. Our current efforts are focused on extending this motif to prepare real cryptand and analogous hosts for construction of supramolecular polymers and polyrotaxanes.

5.4 Acknowledgements

This work was supported by the National Science Foundation (DMR0704076) and the Petroleum Research Fund administered by the American Chemical Society (47644-AC).

5.5 Experimental Section

5.5.1 Materials and methods

Picolinic acid, quinaldic acid, nahthyridine-2-carboxylic acid, 1-(3'-dimethylaminopropyl)-3-ethylcarbodiimide hydrochloride (EDCI) and 4-dimethylaminopyridine (DMAP) were reagent grade and used as received. Bis(*meta*-phenylene)-32-crown-10 (BMP32C10) diol (**1b**)[10a] and dimethyl paraquat PF_6 (**2**)[21] were prepared according to literature procedures. Solvents were either used as purchased or dried according to literature procedures. ^{1}H-NMR spectra were obtained on a JEOL ECLIPSE-500 spectrometer and an INOVA-400 spectrometer with internal standard TMS. ^{13}C-NMR spectra were collected on a JEOL ECLIPSE-500 spectrometer at 125 MHz and an INOVA-400 spectrometer at 101 MHz. HR-MS were obtained by employing an Agilent LC-ESI-TOF and an Applied Biosystems 4800 MALDI TOF/TOF. Isothermal titration calorimetry was performed on a Microcal MCS instrument; raw isotherm data were collected using the Microcal Observer software. Integration and fitting of the isothermal data (K_a and ΔH) were accomplished using Origin software with a one set of sites algorithm.

5.5.2 Synthesis of 1c

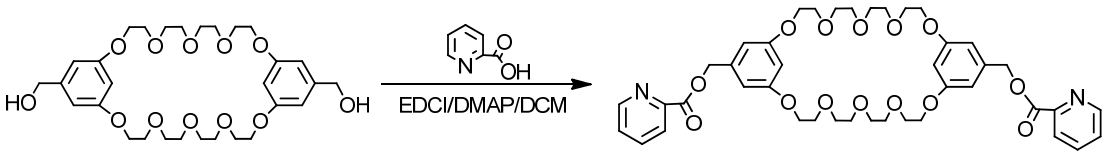

Scheme 5-2. Synthesis of dipicolinate BMP32C10 ester **1c** via EDCI/DMAP coupling.

BMP32C10 diol (410 mg, 0.69 mmol), picolinic acid (340 mg, 2.77 mmol), EDCI (265 mg, 1.38 mmol) and DMAP (169 mg, 1.38 mmol) were dissolved in dichloromethane (DCM, anhydrous, 50 mL). The solution was stirred under N_2 for 2 days at room temperature. The

reaction mixture was washed with DI water (3 times) and a brown oil was obtained, which was dried in a vacuum oven with P_2O_5 overnight. The crude product was purified via a silica gel column by employing gradient elution (DCM to DCM : methanol = 96 : 4) to afford **1c** as a white solid (523 mg, 94%), mp 82.0-83.3 °C. ^{1}H-NMR ($CDCl_3/CD_3CN$ = 1/1 <v/v>, 500 MHz) (Figure 5-4): δ (ppm): 8.71 (ddd, J = 4.7, 1.8, 0.9 Hz, 2H), 8.11-8.05 (dt, J = 7.9, 1.0 Hz, 2H), 7.87 (td, J = 7.7, 1.8 Hz, 2H), 7.53-7.50 (m, 2H), 6.56 (d, J = 2.3 Hz, 4H), 6.39 (t, J = 2.3 Hz, 2H), 5.28 (s, 4H), 4.03-4.01 (m, 8H), 3.77-3.74 (m, 8H), 3.63-3.58 (m, 17H). ^{13}C-NMR ($CDCl_3$, 101 MHz) (Figure 5-5): δ (ppm): 164.86, 160.02, 149.92, 147.89, 137.69, 136.97, 126.93, 125.29, 107.14, 101.32, 70.85, 70.81, 69.59, 67.57, 67.30. HR-ESIMS (Figure 5-6): calcd. for $[M + H]^+$: 807.0855, found: m/z, 807.0876 $[M + H]^+$, error: -2.60 ppm.

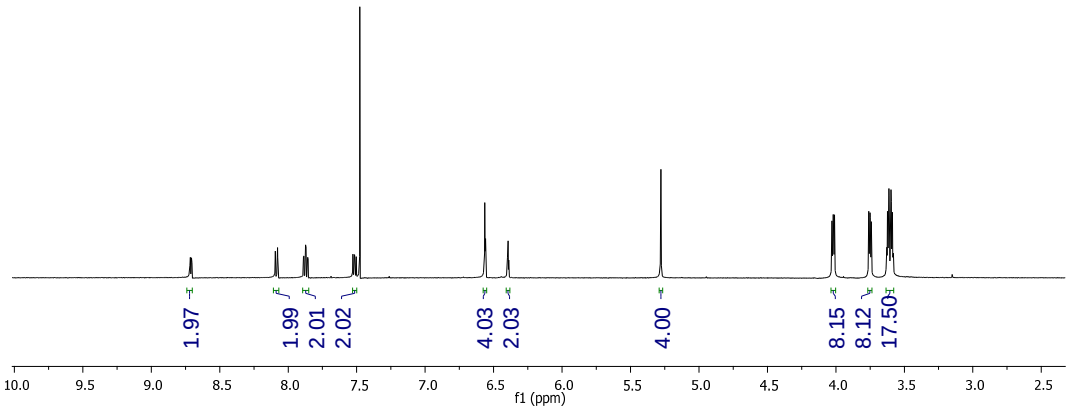

Figure 5-4. ^{1}H-NMR ($CDCl_3/CD_3CN$ = 1/1 <v/v>, 500 MHz, room temperature) of dipicoliniate BMP32C10 ester ***1c***.

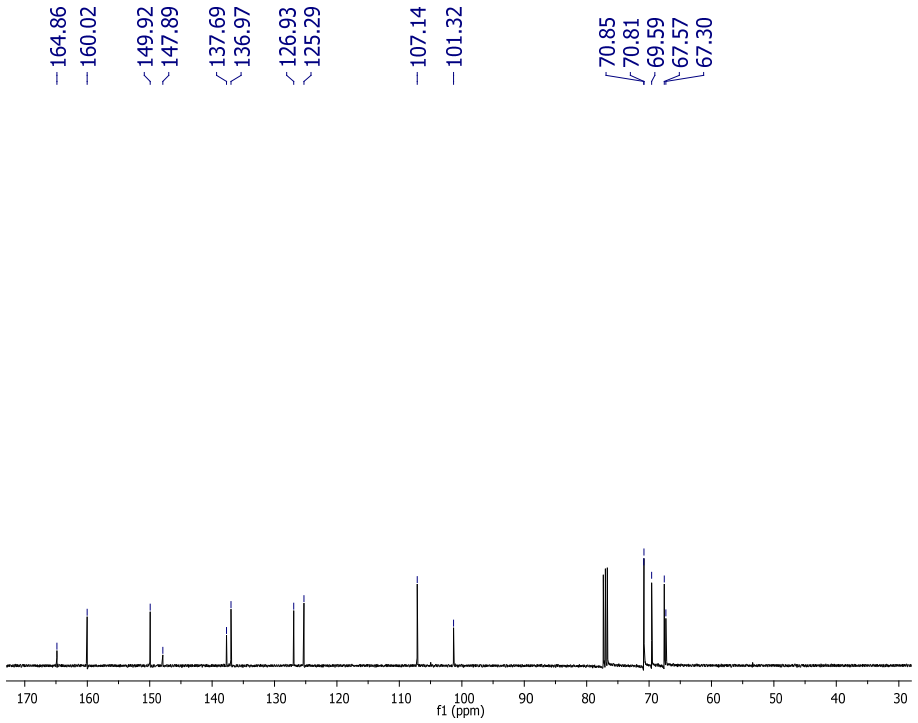

Figure 5-5. ^{13}C-NMR ($CDCl_3$, 101 MHz, room temperature) of dipicolinate BMP32C10 ester **1c**.

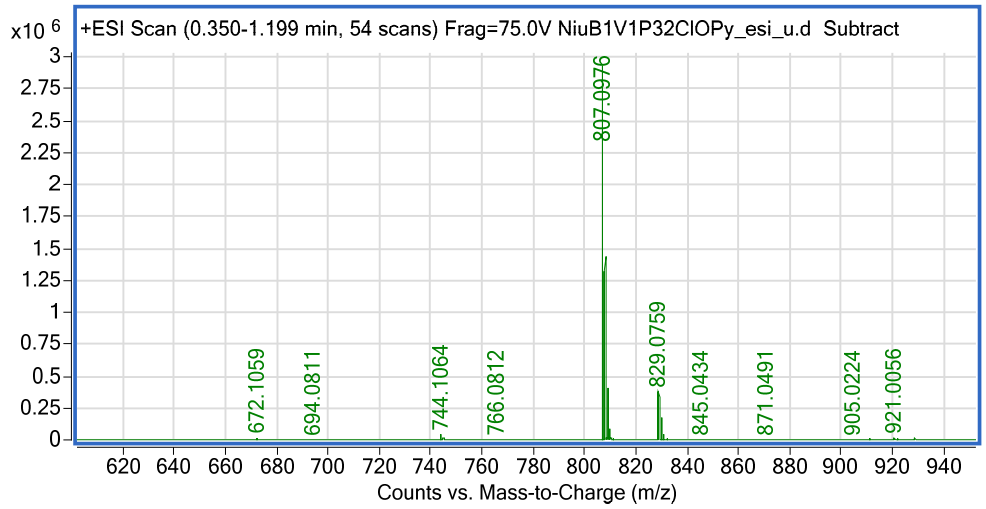

Figure 5-6. Electrospray ionization mass spectrum of dipicolinate BMP32C10 ester **1c**.

5.5.3 Synthesis of 1d

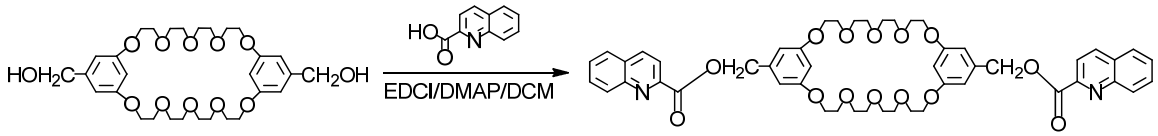

Scheme 5-3. Synthesis of diquinaldate BMP32C10 ester **1d** via EDCI/DMAP coupling.

BMP32C10 diol (216 mg, 0.36 mmol), quinaldic acid (256 mg, 1.45 mmol), EDCI (139 mg, 0.72 mmol) and DMAP (88.7 mg, 0.72 mmol) were dissolved in dichloromethane (DCM, anhydrous, 10 mL). The solution was stirred under N_2 for 2 days at room temperature. The reaction mixture was washed with DI water (3 times) and a dark oil was obtained, which was dried in a vacuum oven with P_2O_5 overnight. The crude product was pre-separated via a short silica gel column (DCM : methanol = 97 : 3). Then further purification was performed on another silica gel column (ethyl acetate first, then DCM to DCM : methanol = 96 : 4) and **1d** was obtained as a colorless oil. The oil was recrystallized in hexane/dichloromethane and a white solid was obtained, 319 mg (98%), mp 110.8 – 112.2℃. ^{1}H-NMR ($CDCl_3$, 500 MHz) (Figure 5-7): δ (ppm): 8.28 (m, 4 H), 8.15 (d, J = 8.5 Hz, 2 H), 7.86 (d, J = 8.2 Hz, 2 H), 7.79-7.75 (m, 2 H), 7.65-7.61 (m, 2 H), 6.64 (d, J = 2.2 Hz, 4 H), 6.44 (t, J = 2.2 Hz, 2 H), 5.40 (s, 4 H), 4.08-4.04 (m, 8 H), 3.83-3.79 (m, 8 H), 3.71-3.64 (m, 17 H). ^{13}C-NMR ($CDCl_3$, 101 MHz) (Figure 5-8): δ (ppm): 165.06, 160.04, 147.86, 147.64, 137.75, 137.22, 130.81, 130.21, 129.29, 128.58, 127.50, 121.12, 107.10, 101.32, 70.86, 70.82, 69.60, 67.58, 67.48. HR-ESIMS (Figure 5-9): calcd. for $[M + H]^+$: 907.3648, found: m/z, 907.3694 $[M + H]^+$, error: 5.15 ppm.

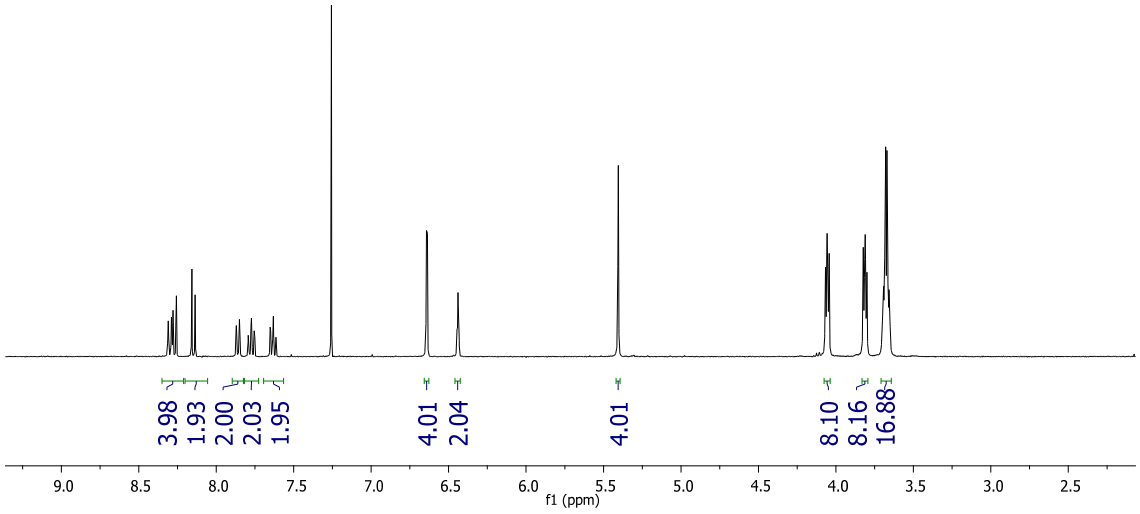

Figure 5-7. ^{1}H-NMR ($CDCl_3$, 500 MHz, room temperature) of diquinaldate BMP32C10 ester **1d**.

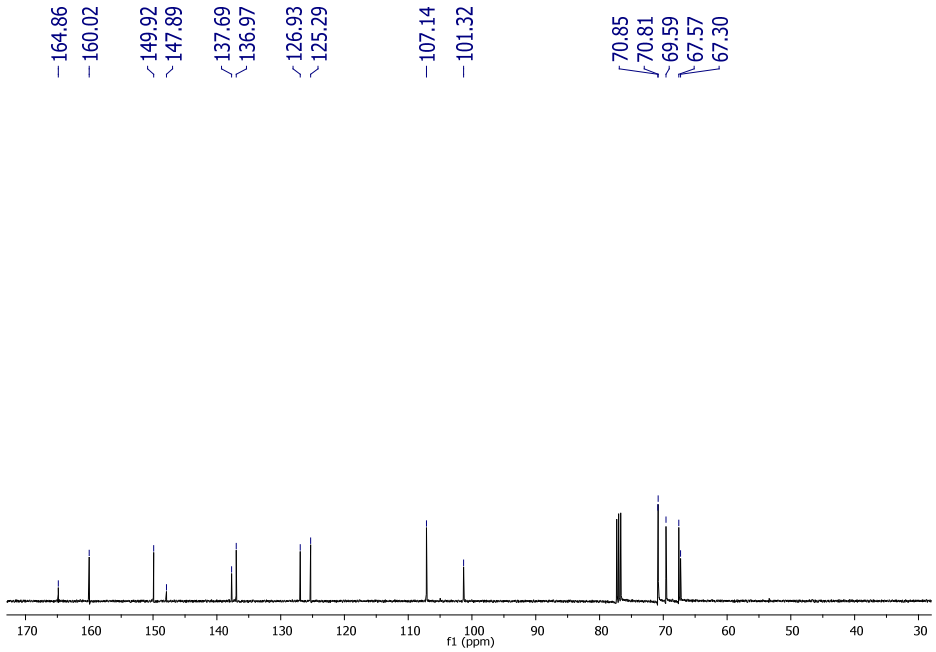

Figure 5-8. ^{13}C-NMR ($CDCl_3$, 101 MHz, room temperature) of diquinaldate BMP32C10 ester **1d**.

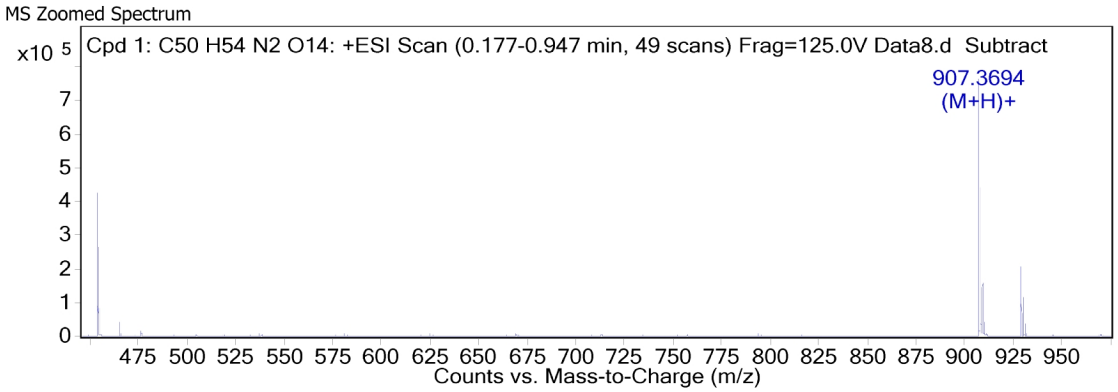

Figure 5-9. Electrospray ionization mass spectrum of diquinaldate BMP32C10 ester **1d**.

5.5.4 Synthesis of 1e

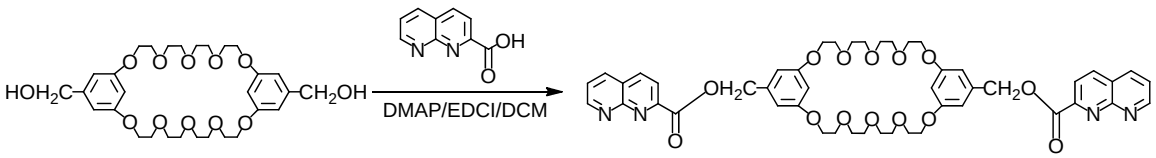

Scheme 5-4. Synthesis of dinaphthyridate BMP32C10 ester **1e**.

BMP32C10 diol (194 mg, 0.33 mmol), naphthyridine-2-carboxylic acid (227 mg, 1.32 mmol), EDCI (504 mg, 2.64 mmol) and DMAP (322 mg, 2.64 mmol) were dissolved in DCM (anhydrous). The reaction mixture was stirred at room temperature under N_2 for 3 days. The organic phase was washed with DI water (5 times) and a brown oil was obtained after solvent was removed. The brown oil was dried in a vacuum oven with P_2O_5 overnight. The crude product was purified by employing a silica gel column (DCM to DCM/MeOH = 95/5) and a pale-yellow solid was obtained (334 mg, 93%), mp 163.6-165.0 °C. ^{1}H-NMR ($CDCl_3$, 500 MHz) (Figure 5-10): δ (ppm): 9.21 (dd, J = 4.2, 2.0 Hz, 2 H), 8.34 (d, J = 8.4 Hz, 2 H), 8.30 – 8.21 (m, 4 H), 7.57 (dd, J = 8.2, 4.2 Hz, 2 H), 6.64 (d, J = 2.2 Hz, 4 H), 6.43 (t, J = 2.2 Hz, 2 H), 5.39 (s, 4 H), 4.07 – 4.03 (m, 8 H), 3.82 – 3.79 (m, 8 H), 3.70 – 3.65 (m, 16 H). ^{13}C-NMR ($CDCl_3$, 101 MHz) (Figure 5-11): δ (ppm): 164.82, 160.02, 155.25, 154.79, 150.92, 138.58, 137.58, 136.78, 124.27, 123.64, 122.15, 107.27, 101.44, 70.86, 70.81, 69.60, 67.68, 67.60. HR-ESIMS (Figure 5-12): calcd. for $[M + H]^+$: 909.3958, found: m/z, 909.3979 $[M + H^+]$, error: -2.3 ppm.

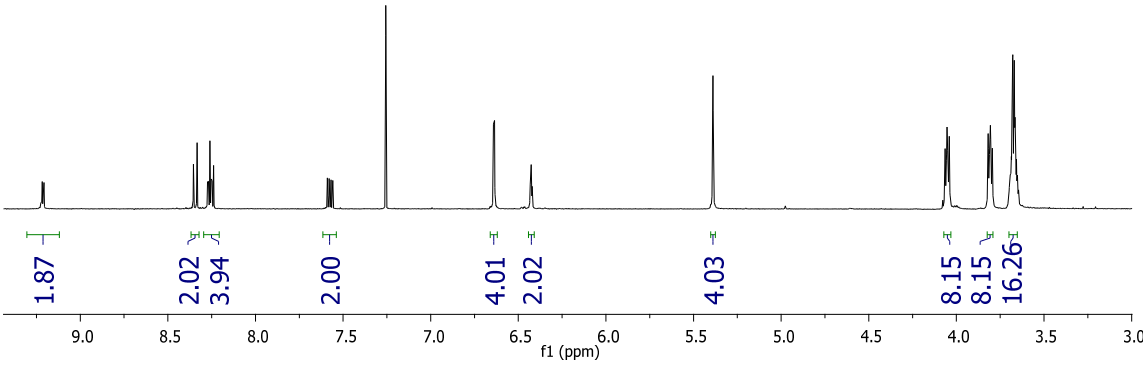

Figure 5-10. ^{1}H-NMR ($CDCl_3$, 500 MHz, room temperature) of dinaphthyridate BMP32C10 ester **1e**.

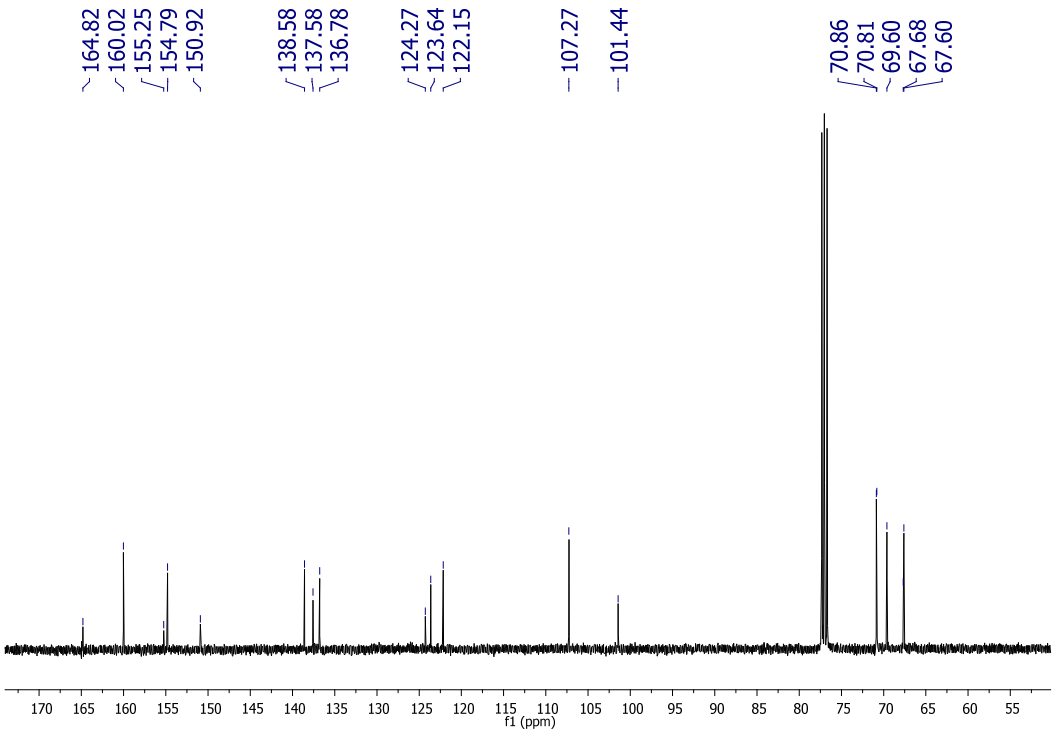

Figure 5-11. ^{13}C-NMR ($CDCl_3$, 101 MHz, room temperature) of dinaphthyridate BMP32C10 ester **1e**.

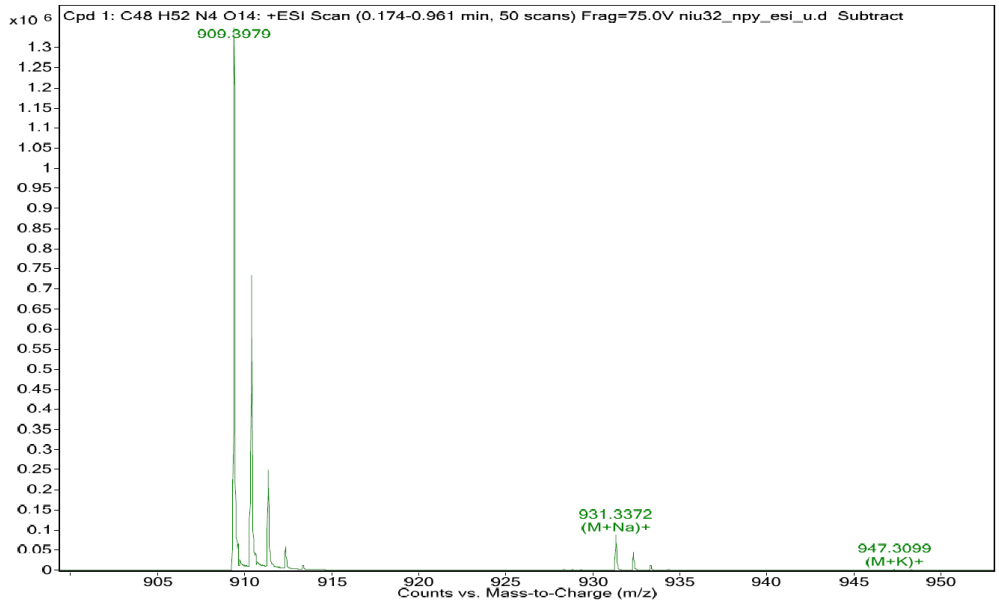

Figure 5-12. Electrospray ionization mass spectrum of dinaphthyridate BMP32C10 ester **1e**.

5.5.5 ^{1}H-NMR spectra for complexation of 1c and 2

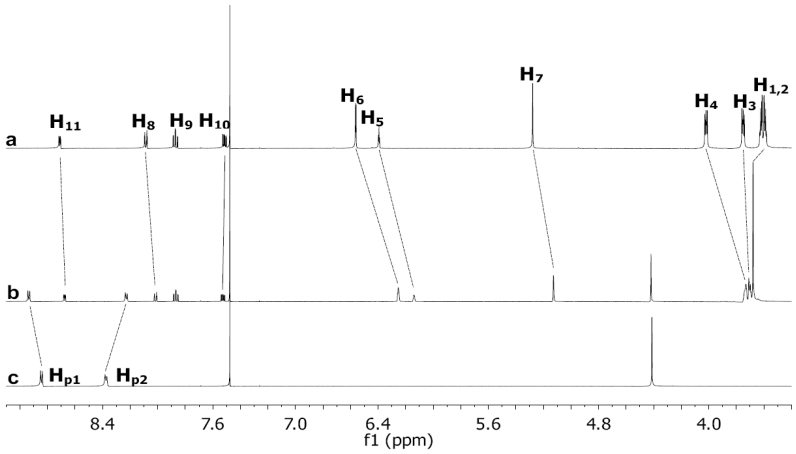

Figure 5-13. Partial proton NMR spectra (500 MHz, $CDCl_3/CD_3CN$ = 1/1 <v/v>, 25°C) of: (a): **1c**; (b): **1c** and **2** ([**1c**] = [**2**] = 1.0 mM); (c): **2**.

5.5.6 Stoichiometry of complexation of 1c and 2

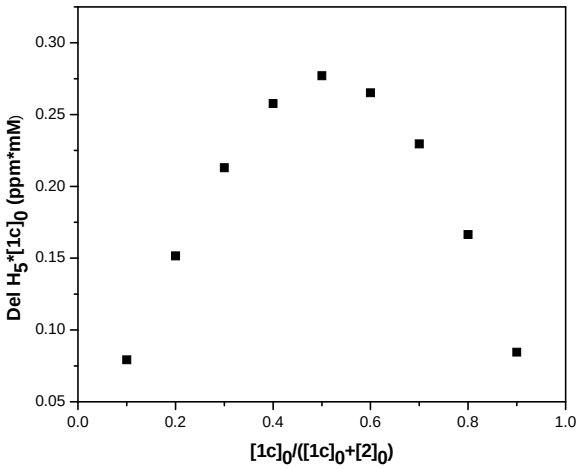

Figure 5-14. Job plot showing the 1:1 stoichiometry of the complex between **1c** and **2** in $CDCl_3/CD_3CN$ = 1/1 <v/v>. $[\mathbf{1c}]_0+[\mathbf{2}]_0$ = 2.00 mM.

5.5.7 Stoichiometry of complexation of 1d and 2

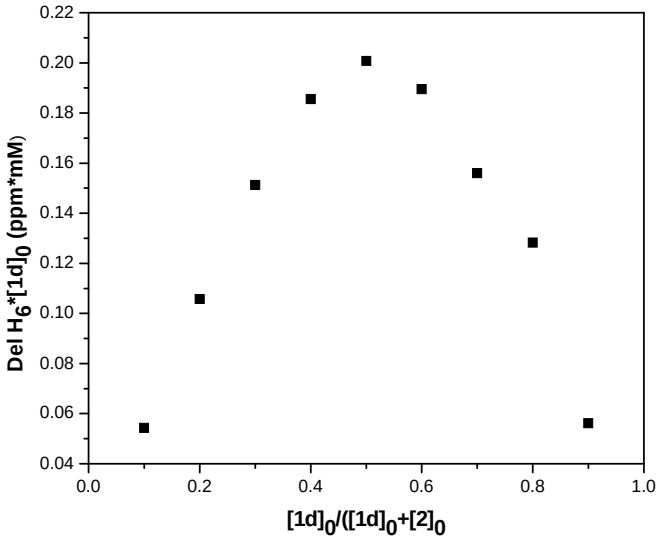

Figure 5-15. Job plot showing the 1:1 stoichiometry of the complex between **1d** and **2** in $CDCl_3/CD_3CN$ = 1/1 <v/v>. $\mathbf{[1d]_0 + [2]}_0$ = 1.22 mM.

5.5.8 Determination of Δ_0 for 1a·2

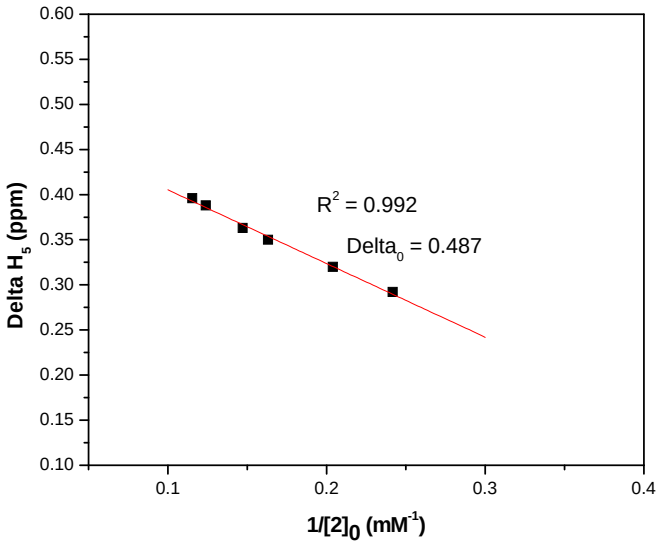

Figure 5-16. Determination of $Delta_0$ of **1a·2** in $CDCl_3/CD_3CN$ = 1/1 <v/v>. $[\mathbf{1a}]_0$ = 0.198 mM.

5.5.9 Determination of Δ_0 for 1c·2

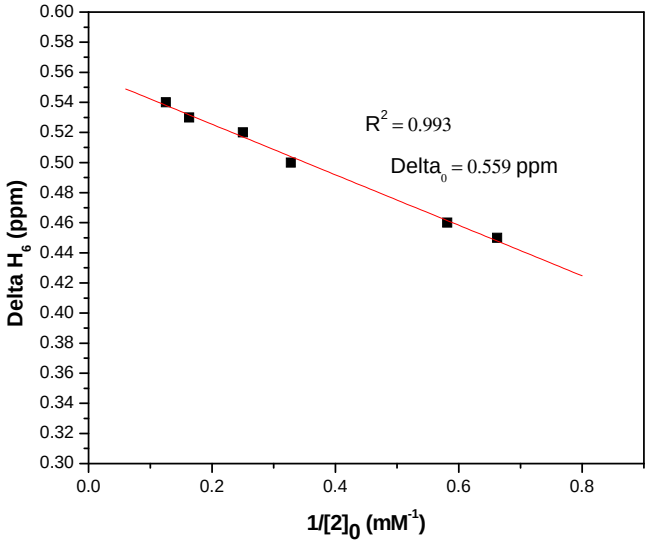

Figure 5-17. Determination of $Delta_0$ of **1c·2** in $CDCl_3/CD_3CN$ = 1/1 <v/v>. $[\mathbf{1c}]_0$ = 0.200 mM.

5.5.10 Determination of Δ_0 for 1d·2

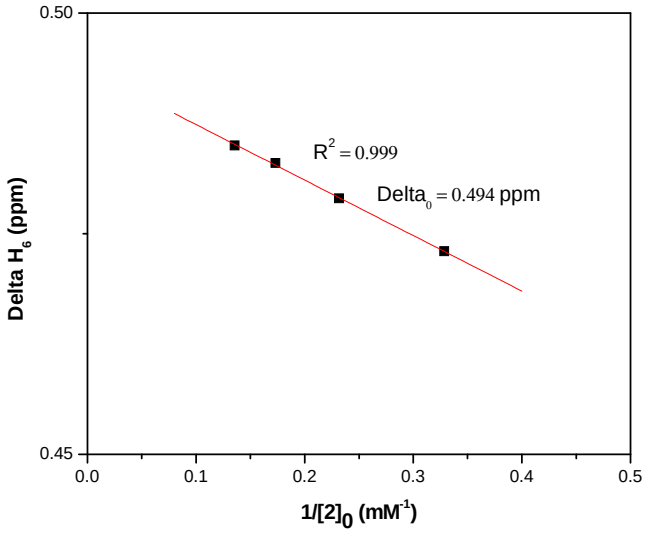

Figure 5-18. Determination of $Delta_0$ of **1d·2** in $CDCl_3/CD_3CN$ = 1/1 <v/v>. $[\mathbf{1d}]_0$ = 0.225 mM.

5.5.11 Isothermal titration calorimetry (ITC) titration curve of 1e·2

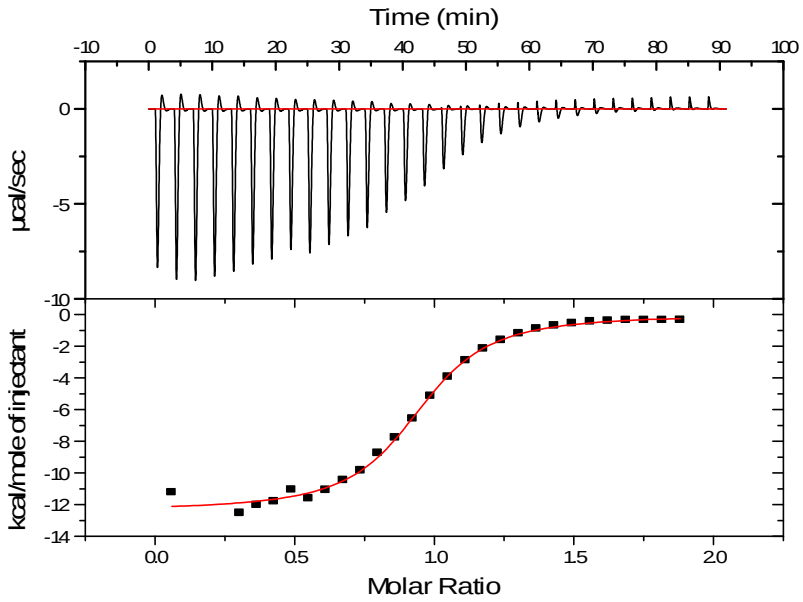

Figure 5-19. ITC curve of **1e·2** in $CHCl_3/CH_3CN$ = 1/1 <v/v>. The host (**1e**) concentration (cell) was 0.211 mM. The guest (**2**) concentration (syringe) was 5.12 mM. The guest solution was titrated into the host solution (cell) at 25°C.

5.5.12 Mass spectrum of 1c·2

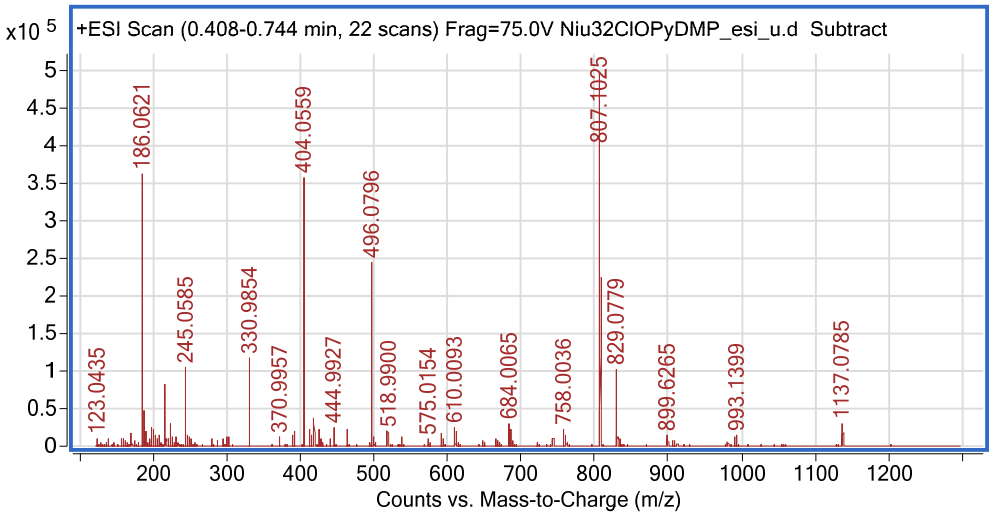

Figure 5-20. Electrospray ionization (ESI) mass spectrum of **1c·2**.

5.5.13 Mass spectrum of 1d·2

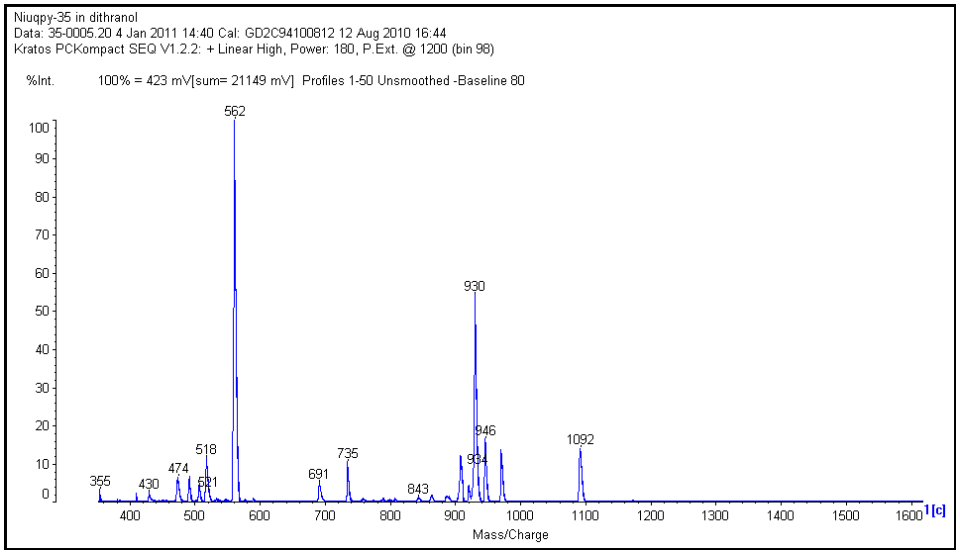

Figure 5-21. Matrix-assisted laser desorption/ionisation-time of flight (MALDI-TOF) mass spectrum of **1d·2**.

5.5.14 Mass spectrum of 1e·2

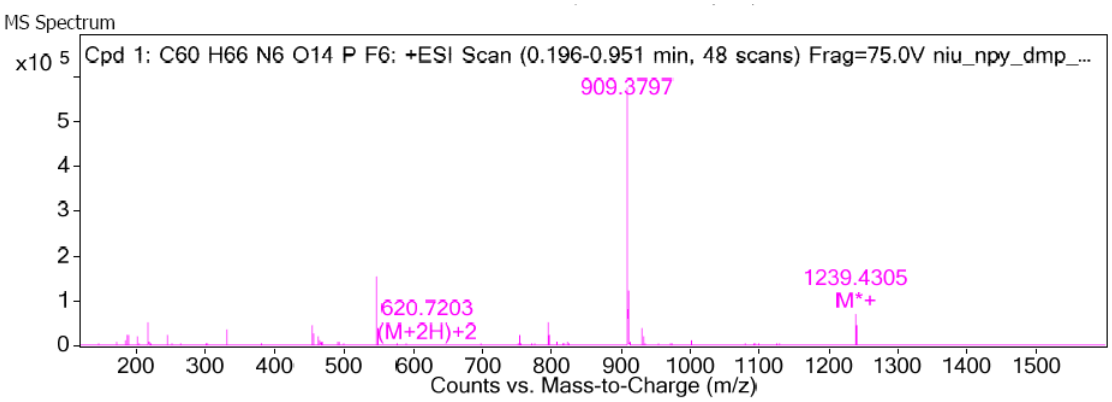

Figure 5-22. Electrospray ionization (ESI) mass spectrum of **1e·2**.

5.5.15 1D-NOESY study of 1c·2, 1d·2 and 1e·2

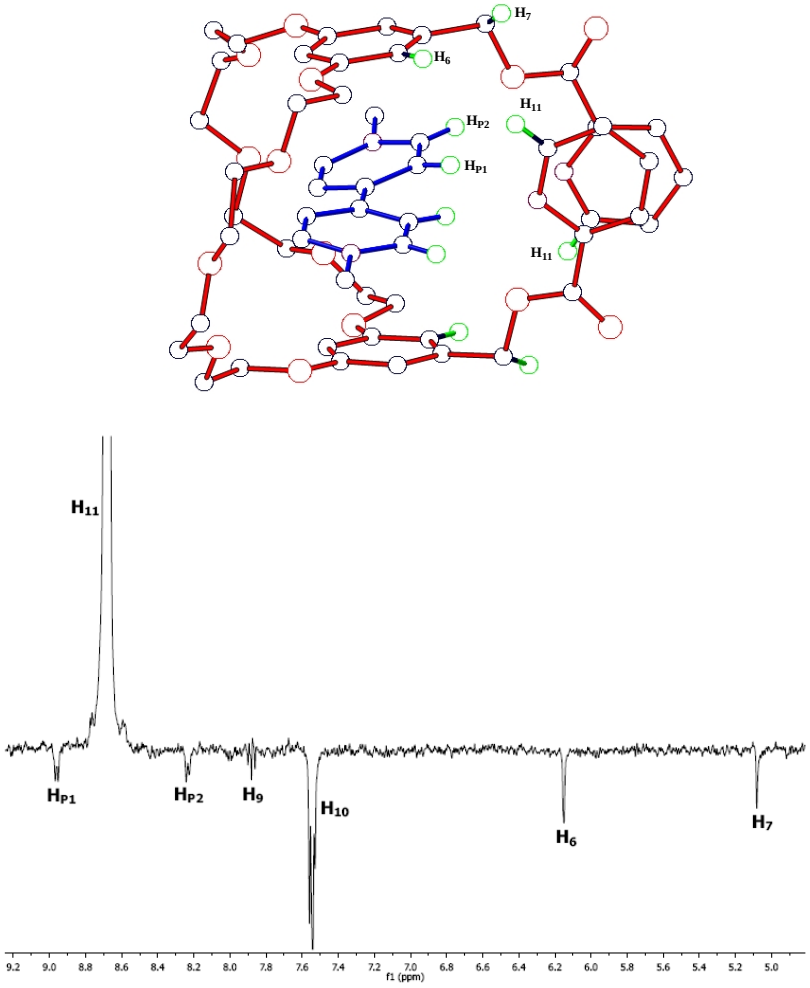

Figure 5-23. 1D-NOESY NMR spectrum (500 MHz, $CDCl_3/CD_3CN$ = 1/1 <v/v>, 25°C) of **1c·2**. Based on the crystal structure of **1c·2** (Figure 5-2), 1D-NOESY experiments were performed by selective irradiation of H_{11} on **1c**. The $H_{11}\cdots H_a$ shortest distances (Å) obtained from crystal structures: a = p1, 3.212; a = p2, 3.507; a = 6, 2.676; a = 7, 3.070. The correlations between H_{11} and H_{P1}, H_{P2}, H_6 and H_7 are clearly observed, which is consistent with results obtained from the crystal structure of **1c·2** and indicate the formation of pseudocryptand-type [2]pseudorotaxane structure in solution.

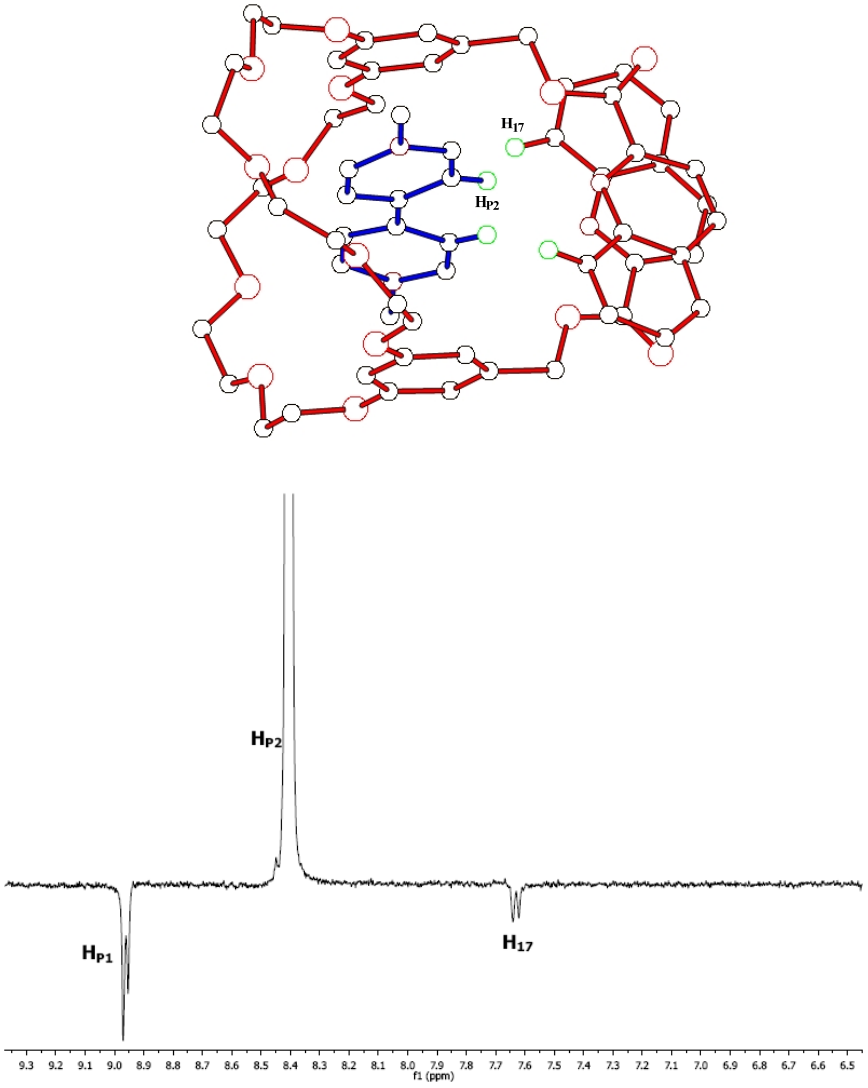

Figure 5-24. 1D-NOESY NMR spectrum (500 MHz, $CDCl_3/CD_3CN$ = 1/1 <v/v>, 25°C) of **1d**·**2**. Based on the crystal structure of **1d**·**2** (Figure 5-2), 1D-NOESY experiments were performed by selective irradiation of H_{p2} on **1c**. The $H_{p2}\cdots H_{17}$ shortest distances (Å) obtained from the crystal structure was 3.093. The correlation between H_{P2} and H_{17} is consistent with the crystal structure.

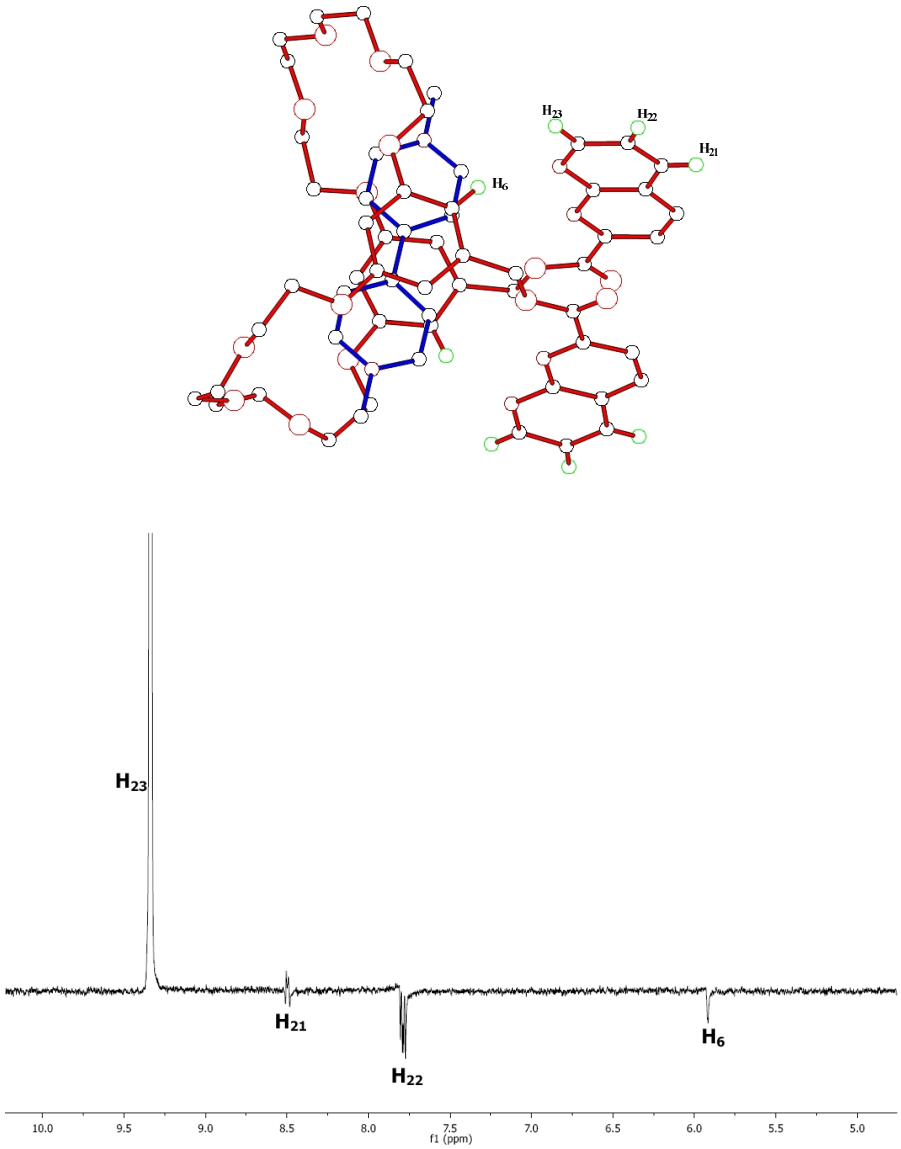

Figure 5-25. 1D-NOESY NMR spectrum (500 MHz, $CDCl_3/CD_3CN$ = 1/1 <v/v>, 25°C) of **1e**·**2**. Based on crystal structure of **1e**·**2** (Figure 5-2), 1D-NOESY experiments were performed by selective irradiation of H_{23} on **1e**. The H_{23}-H_6 shortest distance (Å) obtained from the crystal structure was 2.669. The observed correlation between H_{23} and H_6 is consistent with the crystal structure, while no correlation between H_{23} and H_6 was observed from a solution of **1e** in the same solvent.

5.5.16 Crystal structure of 1c and 1b·2

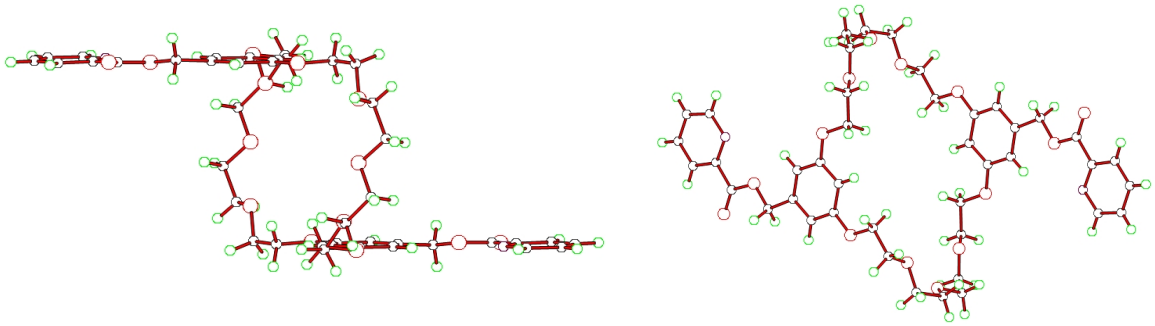

Figure 5-26. Two views of the X-ray structure of **1c**. Oxygen atoms are red. Carbon atoms are black. Nitrogen atoms are purple. Hydrogen atoms are green.

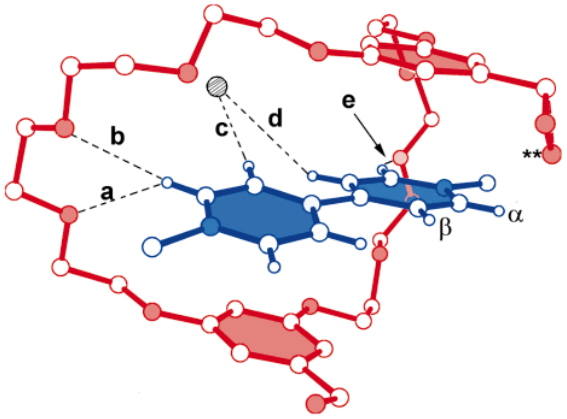

Figure 5-27. X-ray structure of "taco"-shaped **1b·2**. Disordered solvent molecules (water and acetone, which share a site) and counterions omitted for clarity, except for a fluorine atom of one PF6, represented by the gray circle). Both positions of the disordered oxygen atom of the hydroxymethyl group, denoted by **, are shown treated as half populated. H-bond distances in Å: **a**) 2.44, **b**) 2.83, **c**) 2.34, **d**) 2.42, **e**) 2.72. H-bond angles (C-H- -O, C-H- -F, or O-H- -O) in degrees: **a**) 144, **b**) 130, **c**) 168, **d**) 144, **e**) 156. The Figure 5-was reproduced with permission from ref 6a.

References

(1) (a) Gibson, H. W. In *Large Ring Molecules*; Semlyen, J. A., Ed.; John Wiley & Sons: New York, 1996; p 191; (b) Raymo, F. M.; Stoddart, J. F. *Chem. Rev.* **1999**, *99*, 1643-1664. (c) Harada, A. *Acc. Chem. Res.* **2001**, 34, 456-464; (d) Hernandez, J. V.; Kay, E. R.; Leigh, D. A.; *Science*. **2004**, 306, 1532–1537.

(2) (a) Huang, F.; Gibson, H. W. *Prog. Polym. Sci.* **2005**, *30*, 982-1018. (b) Lehn, J.-M. *Chem. Soc. Rev.* **2007**, *36*, 151-160. (b) Stoddart, J. F. *Chem. Soc. Rev.* **2009**, *38*, 1802-1820. (c) De Greef, T. F. A.; Smulders, M. M. J.; Wolffs, M.; Schenning, A. P. H. J.; Sijbesma, R. P.; Meijer, E. W. *Chem. Rev.* **2009**, *109*, 5687-5754. (d) Harada, A.; Hashidzume, A.; Yamaguchi, H.; Takashima, Y. *Chem. Rev.* **2009**, *109*, 5974-6023. (e) Niu, Z.; Gibson, H. W. *Chem. Rev.* **2009**, *109*, 6024-6046. (i) Fang, L.; Olson, M. A.; Benitez, D.; Tkatchouk, E.; Goddard III, W. A.; Stoddart, J. F. *Chem. Soc. Rev.* **2010**, *39*, 17-29. (i) Durola, F.; Sauvage, J.-P.; Wenger, O. S. *Coord. Chem. Rev.* **2010**, *254*, 1748-1759.

(3) (a) Champin, B.; Mobian, P.; Sauvage, J.-P.; *Chem. Soc. Rev.* **2007**, *36*, 358-366. (b) Hembury, G. A.; Borovkov, V. V.; Inoue, Y. *Chem. Rev.* **2007**, *108*, 1-73. (c) Bonnet, S.; Collin, J.-P. *Chem. Soc. Rev.* **2008**, *37*, 1207-1217. (d) Angelos, S.; Khashab, N. M.; Yang, Y.-W.; Trabolsi, A.; Khatib, H. A.; Stoddart, J. F.; Zink, J. I.; *J. Am. Chem. Soc.* **2009**, *131*, 12912-12914. (e) Leung, K. C.-F.; Chak, C.-P.; Lo, C.-M.; Wong, W.-Y.; Xuan, S.; Cheng, C. H. K.; *Chem. Asian. J.* **2009**, *4*, 364-381.

(4) Some recent publications: (a) Zhu, K.; Li, S.; Wang, F.; Huang, F. *J. Org. Chem.* **2009**, 74, 1322-1328. (b) Zhu, K.; He, J.; Li, S.; Liu, M.; Wang, F.; Zhang, M.; Abliz, Z.; Yang, H.; Li, N.; Huang, F. *J. Org. Chem.* **2009**, 74, 3905-3912. (c) Wang, C.; Olson, M. A.; Fang, L.; Benítez, D.; Tkatchouk, E.; Basu, S.; Basuray, A. N.; Zhang, D.; Zhu, D.; Goddard, W. A.; Stoddart, J. F. *Proc. Nat. Acad. Sci.* **2010**, *107*, 13991-13996. (d) Jiang, Y.; Cao, J.; Zhao, J.-M.; Xiang, J.-F.; Chen, C.-F. *J. Org. Chem.* **2010**, *75*, 1767-1770.

(5) Some recent publications: (a) Huang, F.; Fronczek, F. R.; Gibson, H. W. *J. Am. Chem. Soc.* **2003**, *125*, 9272-9273. (b) Huang, F.; Zhou, L.; Jones, J. W.; Gibson, H. W.; Ashraf-Khorassani, M. *Chem. Commun.* **2004**, 2670-2671. (c) Huang, F.; Switek, K. A.; Zakharov, L. N.; Fronczek, F. R.; Slebodnick, C.; Lam, M.; Golen, J. A.; Bryant, W. S.; Mason, P. E.; Rheingold, A. L.; Ashraf-Khorassani, M.; Gibson, H. W. *J. Org. Chem.* **2005**, *70*, 3231-3241. (d) Gibson, H. W.; Wang, H.; Slebodnick, C.; Merola, J.; Kassel, S.; Rheingold, A. L. *J. Org. Chem.* **2007**, *72*, 3381-3393. (e) Pederson, A. M.-P.; Vetor, R. C.; Rouser, M. A.; Huang, F.; Slebodnick, C.; Schoonover, D. S.; Gibson, H. W.; *J. Org. Chem.* **2008**, *73*, 5570-5573. (f) Li, S.; Zheng, B.; Huang, F.; Zakharov, L.; Slebodnick, C. Rheingold, A.; Gibson, H. W. *Sci. China Chem.* **2010**, *53*, 858-862. (g) Zhang, M.; Zhu, K.; Huang, F. *Chem. Commun.* **2010**, *46*, 8131-8141. (h) Liu M.; Li, S.; Hu, M.; Wang, F.; Huang, F. *Org. Lett.* **2010**, 12, 760-763. (i) Zhang, M.; Zheng, B.; Xia, B.; Zhu, K.; Wu, C.; Huang, F. *Eur. J. Org. Chem.* **2010**, 6804-6809.

(6) (a) Bryant, W. S.; Jones, J. W.; Mason, P. E.; Guzei, I.; Rheingold, A. L.; Fronczek, F. R.; Nagvekar, D. S.; Gibson, H. W. *Org. Lett.* **1999**, *1*, 1001-1004. (b) Huang, F.; Fronczek, F. R.; Gibson, H. W. *Chem. Commun.* **2003,** 1480−1481 (c) Li, S.; Liu, M.; Zheng, B.; Zhu, K.; Wang, F.; Li, N.; Zhao, X.-L.; Huang, F. *Org. Lett.* **2009**, *11*, 3350-3353. (d) Zhang, M.; Luo, Y.; Zheng, B.; Yan, X.; Fronczek, F. R.; Huang, F. *Eur. J. Org. Chem.* **2010**, *35*, 6798-6803. (e) Recently, a complex system based on carbazole-BMP30C10 and **2**, which demonstrated the coexistence of [2]pseudorotaxane type structure and [2]taco type structure in the solid state, was reported: Niu, Z.; Slebodnick, C.; Bonrad, K.; Huang, F.; Gibson, H. W. *Org. Lett.* **2011**, *13*, 2872-2875..

(7) See experimental section.

(8) Shen, Y. X.; Engen P. T.; Berg, M. A. G.; Merola, J. S.; Gibson, H. W. *Macromolecules* **1992**, *25*, 2786-2788.

(9) Nabeshima, T. *Bull. Chem. Soc. Jpn.* **2010**, *83*, 969-991.

(10) (a) Gibson, H. W.; Nagvekar, D. S. *Can. J. Chem.* **1997**, *75*, 1375-1384. (b) Gibson,

H. W.; Nagvekar, D. S.; Yamaguchi, N.; Wang, F.; Bryant, W. S.; *J. Org. Chem.* **1997**, *62*, 4798-4803.

(11) (a) Job, P. *Ann. Chim. Appl.* **1928**, 113-203.

(12) ^{1}H-NMR characterizations were done on solutions with constant [**1c**] and varied [**2**]. Based on these NMR data, Δ_o, the difference in δ values for proton H_6 of **1c** in the uncomplexed and fully complexed species, was determined to be 0.559 ppm as the y-intercept of a plot of $\Delta = \delta - \delta_u$ *vs.* $1/[\mathbf{2}]_0$ in the high initial concentration range of **2**. K_a was calculated from $K_a = (\Delta/\Delta_0)/[(1-\Delta/\Delta_0)([\mathbf{2}]_0-\Delta/\Delta_0\ [\mathbf{1c}]_0)$. For **1d·2** the Δ_o value for H_6 was determined to be 0.494 ppm; the K_a value was determined analogously.

(13) (a) Fronczek, F. R.; Gatto, V. J.; Schultz, R. A.; Jungk, S. J.; Colucci, W. J.; Gandour, R. D.; Gokel, G. W. *J. Am. Chem. Soc.* **1983**, *105*, 6717-6718. (b) Arnold, K. A.; Echegoyen, L.; Fronczek, F. R.; Gandour, R. D.; Gatto, V. J.; White, B. D.; Gokel, G. W. *J. Am. Chem. Soc.* **1987**, *109*, 3716-3721. (c) Gokel, G. W.; Leevy, W. M.; Weber, M. E. *Chem. Rev.* **2004**, *104*, 2723–2750.

(14) (a) Delaviz, Y.; Merola, J. S.; Berg, M. A. G.; Gibson, H. W. *J. Org. Chem.* **1995**, *60*, 516-522. (b) Gibson, H. W.; Wang, H.; Chng, C. P.; Glass, C. T. E.; Schoonover, D. S.; Zakharov, L. N.; Rheingold, A. L.; *Heteroatom Chem.* **2008**, *19*, 48-54.

(15) (a) Hunter, C. A.; Sanders, J. K. M.; *J. Am. Chem. Soc.* **1990**, *112*, 5525-5534. (b) Hohenstein, E. G.; Sherrill, C. D.; *J. Phys. Chem. A* **2009**, *113*, 878-886.

(16) (a) Balón, M.; Guardado, P.; Muñoz, M. A.; Carmona, C. *Biospectroscopy* **1998**, *4*, 185-195. (b) Ponnuswamy, M.; Gromiha, M.; Sony, S.; Saraboji, K. In *QSAR and Molecular Modeling Studies in Heterocyclic Drugs I*; S. Gupta, Ed.; Springer Berlin / Heidelberg: 2006; Vol. 3, p 81. (c) Semeniuc, R. F.; Reamer, T. J.; Smith, M. D. *New J. Chem.* **2010**, *34*, 439-452.

(17) The K_a of **4·2** and **5·2** were reported[5d] as $6.3 \pm 0.6 \times 10^3\ M^{-1}$ and $9.4 \pm 0.9 \times 10^3\ M^{-1}$ in $(CD_3)_2CO$, respectively. It should be noted that the solvent affects association constants. However, the association constants in $(CD_3)_2CO$ and $CDCl_3/CD_3CN$ will not differ greatly.

(18) (a) Egli, M.; Sarkhel, S. *Acc. Chem. Res.* **2007**, *40*, 197-205. (b) Gung, B. W.; Zou, Y.; Xu, Z.; Amicangelo, J. C.; Irwin, D. G.; Ma, S.; Zhou, H.-C. *J. Org. Chem.* **2007**, *73*, 689-693. (c) Mooibroek, T. J.; Gamez, P.; Reedijk, J. *CrystEngComm* **2008**, *10*, 1501-1515. (d) Jain, A.; Ramanathan, V.; Sankararamakrishnan, R. *Protein Sci.* **2009**, *18*, 595-605.

(19) Because the ^{1}H-NMR titration method is not suitable for systems with association constants > 10^{4} M^{-1}) such as **1e·2**, ITC was employed. (a) Jelesarov, I.; Bosshard, H. R. *J. Mol. Recognit.* **1999**, *12*, 3-18. (b) Velazquez-Campoy, A.; Freire, E. *Nat. Protocols* **2006**, *1*, 186-191. (c) Freyer, M. W.; Lewis, E. A. In *Methods in Cell Biology*; Correia, J. J., Dietrich, H. W., Ed.; Academic Press: 2008; Vol. 84, p 79.

(20) We previously reported a three component pseudocryptand-based [2]pseudorotaxane complex: Jones, J. W.; Zakharov, L. N.; Rheingold, A. L.; Gibson, H. W. *J. Am. Chem. Soc.* **2002**, *124*, 13378-13379. Later a pseudocryptand dimer formed from three components was reported: Huang, F.; Zakharov, L. N.; Rheingold, A. L.; Jones, J. W.; Gibson, H. W. *Chem. Commun.* **2003**, 2122-2123.

(21) (a) Allwood, B. L.; Shahriari-Zavareh, H.; Stoddart, J. F.; Williams, D. J. Chem. Commun. **1987**, 1058-1061. (b) Asakawa, M.; Ashton, P. R.; Ballardini, R.; Balzani, V.; Bělohradský, M.; Gandolfi, M. T.; Kocian, O.; Prodi, L.; Raymo, F. M.; Stoddart, J. F.; Venturi, M. J. Am. Chem. Soc. **1997**, 119, 302-310.

TOC Graphic:

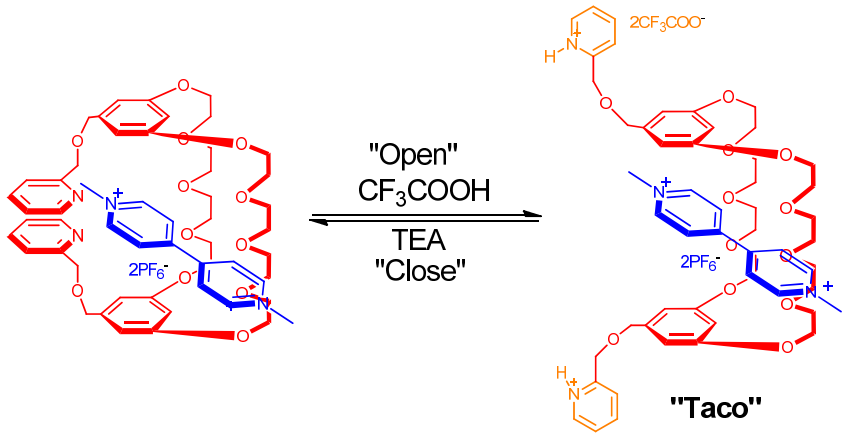

Abstract:

A pseudocryptand-type [2]pseudorotaxane was formed via the self-assembly of a dipyridyl bis(*meta*-phenylene)-32-crown-10 (BMP32C10) derivative and a paraquat derivative. Due to the basicity of the pyridyl group, which forms the third pseudo-bridge of the pseudocryptand, this pseudorotaxane represents the first system with acid-base adjustable association constants, i. e., both finite.

Chapter 6

An Acid-Base Adjustable Pseudocryptand-type [2]Pseudorotaxane Based on a Bis(*meta*-phenylene)-32-Crown-10 Derivative and Paraquat

6.1 Introduction

In the past decade, the design and preparation of new pseudorotaxane systems[1] with abilities to respond to external stimuli have been a topic of great interest and widely studied all over the world, due to their potential for practical applications as fundamental building blocks in the preparation of artificial molecular machines,[2] molecular sensors[3] and drug delivery.[4] The external stimuli that have been employed include chemical, electrochemical and photochemical inputs.[2-4] Among them, acid-base control (a chemical stimulus) has proved to be a convenient and efficient method and therefore has been widely used to manipulate the assembly and disassembly of pseudorotaxanes.[2e-f,5] Although the acid/base controllable systems that cause complexation/decomplexation have been well-studied, to the best of our knowledge, no acid/base adjustable (i. e., non-zero) association constants have been reported. Here, we report a pseudocryptand-type [2]pseudorotaxane based on a bis(*meta*-phenylene)-32-crown-10 (BMP32C10) (**1**) derivative and a paraquat (*N,N'*-diakyl-4,4'-bipyridinium) derivative that exhibits acid-base adjustable association constants for the first time.

6.2 Results and discussion

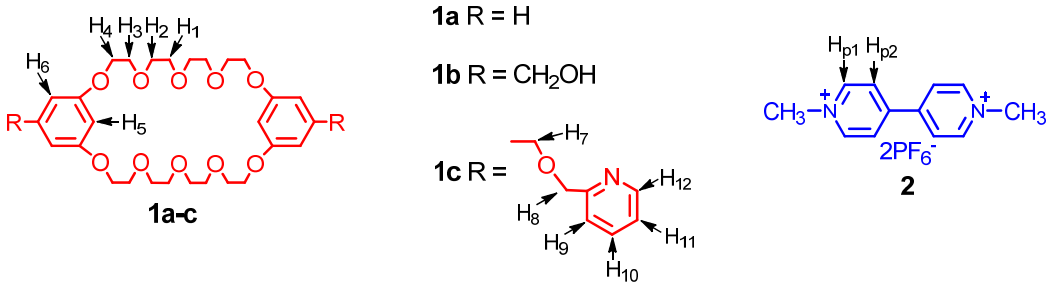

Scheme 6-1. Structure of BMP32C10 derivatives **1a-c** and paraquat derivative **2**.

Crown ether derivatives and paraquat (PQ) derivatives have been widely studied in the construction of pseudorotaxanes.[6] Recently, we reported the first pseudocryptand-type [2]pseudorotaxanes based on synthetically easily-accessible BMP32C10 derivatives and PQ derivatives with remarkably improved association constants.[7b] We realized that the formation of pseudocryptand-type [2]pseudorotaxane complexes affords the possibility to control the "opening" and "closing" of the noncovalent bridges in the pseudocryptands. Therefore, crown ether **1c** was synthesized via the reaction between BMP32C10 diol (**1b**)[8] and 2-bromomethylpyridine hydrobromide in 92% yield. A Job plot[9] (Figure 6-1) showed that the stoichiometry of the complex between **1c** and **2** was 1:1, which was confirmed by eleectrospray ionization mass spectrometry (ESI-MS): m/z 1109.46 [**1c**·**2**-PF_6]$^+$, 482.25 [**1c**·**2**-2PF_6]$^{2+}$.[13] ^{1}H-NMR spectra of equimolar solutions of host **1c** and PQ **2** displayed only one set of peaks, indicating fast exchange (Figure 6-2). The K_a of the complexation process between **1c** and **2** was determined to be 1.1 ± 0.1 x 10^3 M^{-1} in $CDCl_3$/CD_3CN (1/1, v/v) based on the proton NMR data.[10]

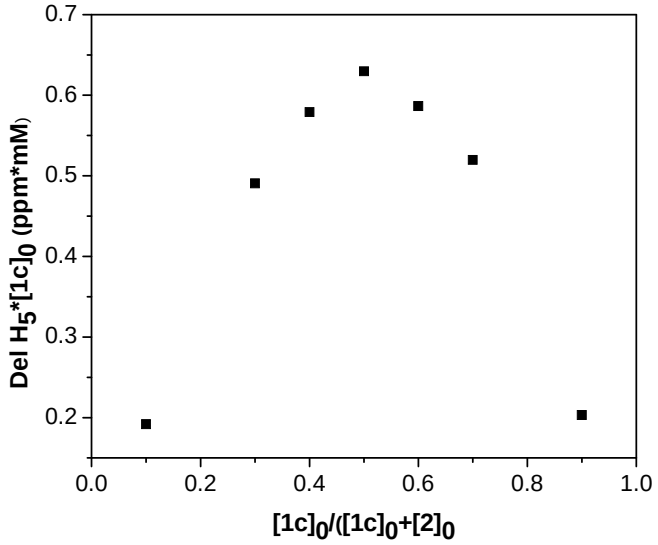

Figure 6-1. Job plot showing the 1:1 stoichiometry of the complex between **1c** and **2** in $CDCl_3/CD_3CN$ = 1/1 <v/v>. $\mathbf{[1c]_0 + [2]_0}$ = 4.74 mM.

Similar to other bis(*m*-phenylene) crown ether derivatives, [11] the molecules of host **1c** assume a stair-step structure in the solid state (Figure 6-3). The phenylene rings in **1c** are nearly parallel to each other but as far apart as possible by extension in opposite directions. However, in the complex, **1c** is folded and the two pyridyl rings interact via off-set face-to-face π-stacking.[12] In order to interact with the threaded paraquat molecule, the two nitrogen atoms of the pyridyl rings are pointed to the central cavity and therefore a single-molecule pseudocryptand host structure was formed. PQ salt **2** is threaded through the central cavity of the pseudocryptand and the complex is stabilized by hydrogen bonds between the oxygen and nitrogen atoms of **1c** with hydrogen atoms on the PQ salt **2** and off-set face-to-face π-stacking between the phenylene rings of **1c** and the pyridinium rings of **2**. Notably, only one of the ether oxygen atoms connected with the pyridyl ring points to the threaded PQ and forms hydrogen bonds with it, although one pyridyl nitrogen atom does interact with a -proton and the other one interacts with both the - and -protons of the PQ guest. In addition, the formation of the pseudocryptand structure of **1c·2** in solution was confirmed by 1D-NOESY experiments.[13]

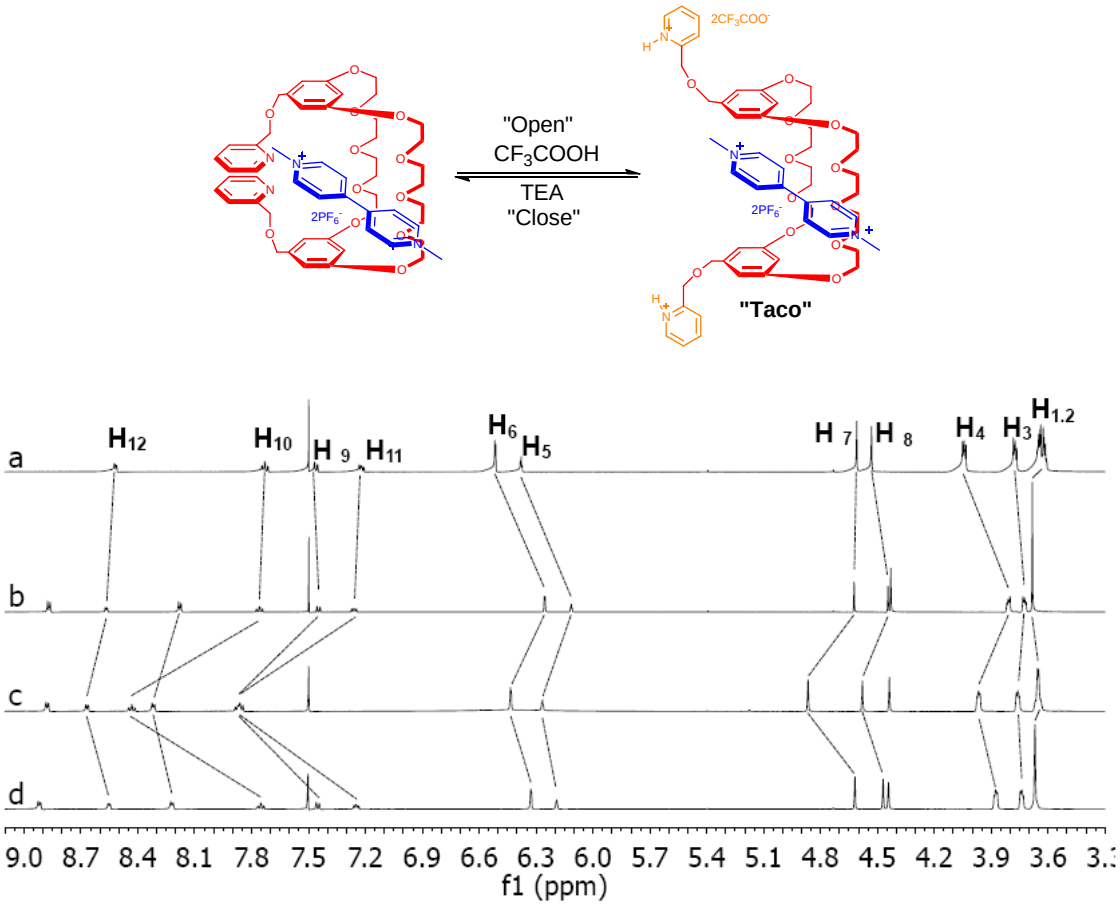

Figure 6-2. Partial proton NMR spectra (500 MHz, $CDCl_3/CD_3CN$ = 1/1 <v/v>, 25°C) of: a) **1c**; b) **1c** and **2** (1/1, mol/mol, $[\mathbf{1c}]_0$ = 2.0 mM,); c) solution **b** after addition of 2.2 equiv. of TFA. d) solution **c** after addition of 2.2 equiv. of TEA.

However, due to the basicity of the pyridine rings, the "opening" and "closing" of the pseudocryptand linkage in **1c·2** can be controlled. As shown by Figure 6-2, large chemical shifts were observed upon complexation between **1c** and **2**: peaks corresponding to H_3, H_4, H_5, H_6, H_8 and H_9 of **1c** moved upfield, while H_1, H_2, H_{12}, H_{10}, $H_{11}$and H_{12} of **1c** moved downfield. When 2.2 equivalents of trifluoroacetic acid (TFA) were added, all the proton peaks shifted toward the uncomplexed state.[14] However, compared with the spectrum of pure host **1c** and guest **2**, the complex **1c·2** did not revert to its components; This was confirmed by ESI-MS: m/z 1077.48, $[\mathbf{1cTFA_2{\cdot}2}\text{-}2PF_6\text{-}CF_3COO\text{-}2H]^+$, 628.22 $[\mathbf{1cTFA_2{\cdot}2}\text{–}2PF_6]^{2+}$, 555.73 $[\mathbf{1cTFA_2{\cdot}2}$ - PF_6 -

$2CF_3COO]^{2+}$.[13] In addition, the color of the solution became light, but still yellow. The structure of the complex **1e**$(TFA)_2$·**2** is thought as the "taco" structure indicated in Figure 6-2.[15]

Moreover, all the protons moved back almost to their original position after 2.2 equivalents of triethyl amine (TEA) were added, indicating that the pseudocryptand-type [2]pseudorotaxane **1c·2** was recovered. This observation confirmed the "opening" and "closing" of the bridge constructed by the pyridyl rings by acid/base control. A 1D-NOESY experiment[13] proved this assumption. The association constant between the bisTFA salt of **1c** and **2** was independently determined to be 375 ± 42 M^{-1}, which is close to the association constant (393 ± 30 M^{-1})[7b] between unsubstituted BMP32C10 (**1a**) and **2**. It is noteworthy in this case that the association constant between **1c** and **2** was adjustable via the acid/base stimuli. Although acid/base controllable systems that cause complexation or complete decomplexation have been reported,[2e-f,5] to the best of our knowledge, this is the first system with an acid/base adjustable (i. e., non-zero) association constant, which can be employed to construct conformationally responsive self-assembled species, either small molecules (e. g., for controlled release) or polymers (e. g., for viscosity or mechanical property manipulation).

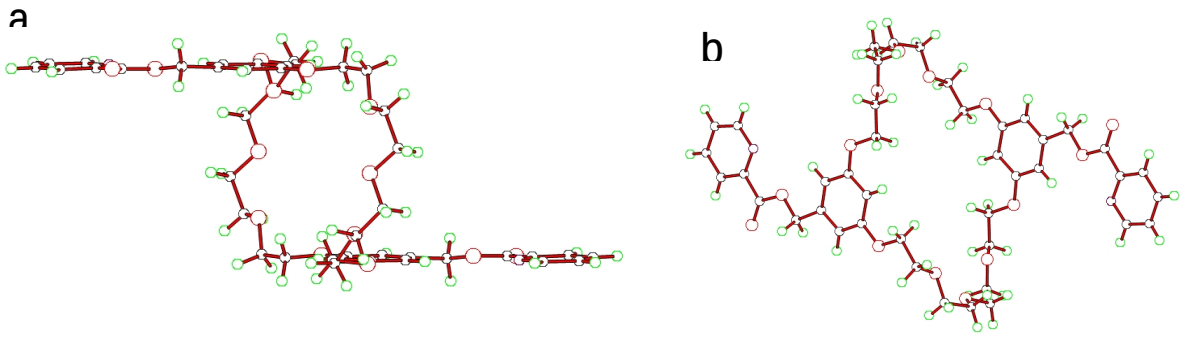

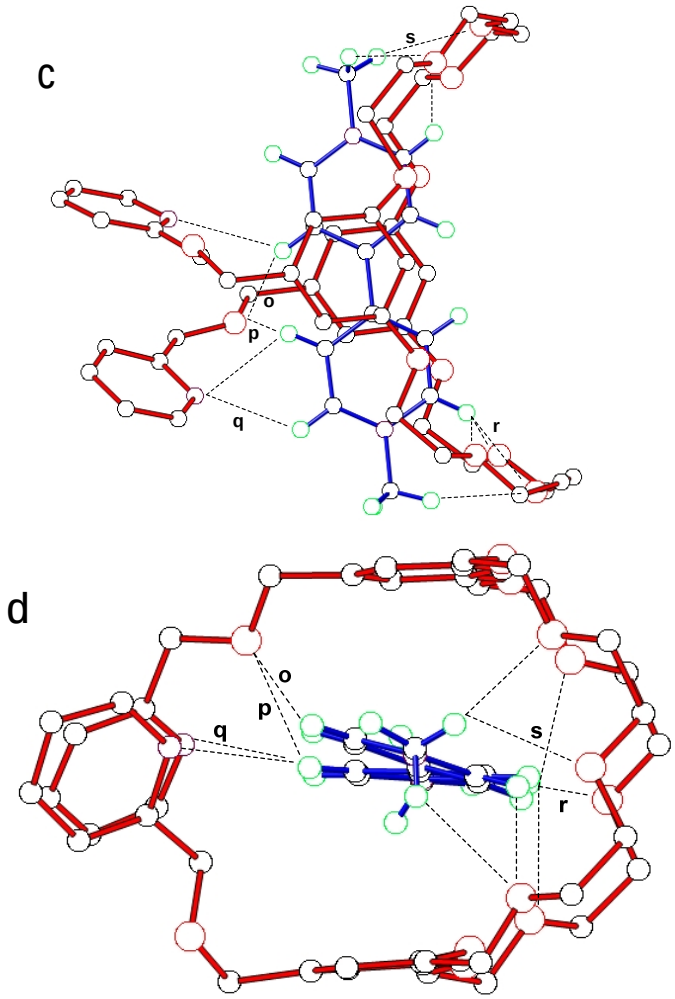

Figure 6-3. (a) and (b): Two views of the X-ray structure of **1c**. (c) and (d): Two views of the X-ray structure of **1c·2**. Oxygen atoms are red. Carbon atoms are black. Nitrogen atoms are purple. Hydrogen atoms are green. **1c** is red. **2** is green. In (c) and (d), Solvent molecules, PF_6^- ions, and hydrogens except the ones on **2** were omitted for clarity. Selected hydrogen-bond parameters: H···O(N) distances (Å), C···O(N) distances (Å), C-H···O(N) angles (deg): o 2.62, 3.47, 148; p 2.64, 3.23, 120; q 2.69, 3.32, 125; r 2.49, 3.37, 156; s 2.71, 3.40, 133; In the bottom figure, overlapping hydrogen bonds are omitted for clarity. Face-to-face π-stacking parameters: centroid-centroid distances (Å): pyridyl rings 4.21 (shortest distance between two planes: 3.31); phenylene rings of **1c** and pyridinium rings of paraquat: 4.33, 4.08, 4.20, 4.39. Ring plane-ring plane inclinations (deg): pyridyl rings 18.7; phenylene rings of **1c** and pyridinium rings of paraquat: 5.58, 19.9, 22.1, 7.14.

6.3 Conclusions

In summary, we demonstrated the formation of a pseudocryptand-type [2]pseudorotaxane by the self-assembly of a pyridyl-based BMP32C10 and a PQ derivative. The formation of the third pseudo-bridge via H-bonding of the heterocyclic units with the PQ guest and π–stacking improved the association constant 2.8-fold. In addition, due to the basicity of the pyridyl group, which formed the third pseudo-bridge, this pseudorotaxane system demonstrated acid-base adjustable association constants for the first time. Our current efforts are focused on extending this motif to incorporate analogous hosts structures into polymer backbones in order to prepare novel pseudocryptand-type polypseudorotaxane, which is acid-base responsive, via the self-assembly between the polymer prepared and paraquat centered polymers.

6.4 Acknowledgements

This work was supported by the National Science Foundation (DMR0704076) and the Petroleum Research Fund administered by the American Chemical Society (47644-AC). We also acknowledge the National Science Foundation for funds to purchase the Innova-400 NMR, JEOL ECLIPSE-500 and Agilent 6220 Accurate Mass TOF LC/MS Spectrometers (CHE-0131124 & CHE-0722638).

6.5 Experimental section

6.5.1 Materials and methods

2-Bromomethylpyridine hydrobromide, *4,4'*-bipyridine, methyl iodide, trifluoroacetic acid (TFA) and triethyl amine (TEA) were reagent grade and used as received. Bis(*meta*-phenylene)-32-crown-10 (BMP32C10) diol (**1b**)[8] and dimethyl paraquat PF_6 (**2**)[16] were prepared according to literature procedures. Solvents were either used as purchased or dried according to literature procedures. ^{1}H-NMR spectra were obtained on a JEOL ECLIPSE-500 spectrometer

and an INOVA-400 spectrometer with internal standard TMS. ^{13}C-NMR spectra were collected on a JEOL ECLIPSE-500 spectrometer at 125 MHz and an INOVA-400 spectrometer at 101 MHz. HR-MS were obtained by employing an Agilent LC-ESI-TOF and Bruker Maxis Q-ToF ESI-MS.

6.5.2 Synthesis of 1c

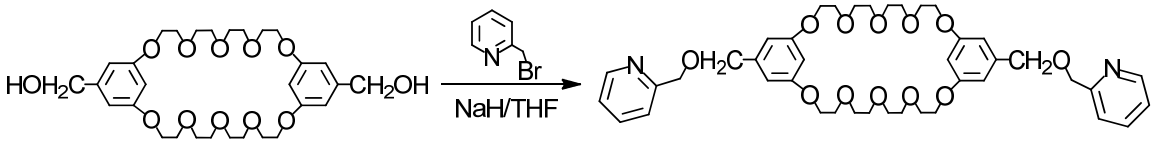

Scheme 6-2. Synthesis of bispyridyl BMP32C10 ether **1c**.

BMP32C10 diol (311 mg, 0.52 mmol), 2-bromomethylpyridine (315 mg, 1.25 mmol) and NaH (334 mg, 8.35 mmol) were suspended in THF (50 mL, anhydrous). The reaction mixture was refluxed under N_2 for 36 hours. Deionized water (DI water) was added dropwise to quench the excess NaH. Solvent was removed. The residue was extracted between DCM and DI water. The organic phase was washed with DI water (5 times) and a dark oil was obtained after the solvent was removed. The dark oil was dried in a vacuum oven with P_2O_5 overnight. The crude product was purified by employing a silica gel column (diethyl ether, then ethyl acetate to ethyl acetate : methanol = 4 : 1) and a white solid was obtained (334 mg, 92%), mp 59.2-60.1 °C. ^{1}H-NMR ($CDCl_3$, 500 MHz) (Figure 6-4): δ (ppm): 8.54 (m, 2 H), 7.68 (m, 2 H), 7.45 (d, *J* = 7.8 Hz, 2 H), 7.23-7.10 (m, 2 H), 6.53 (d, *J* = 2.1 Hz, 4 H), 6.41 (t, *J* = 2.1 Hz, 2 H), 4.64 (s, 4 H), 4.54 (s, 4 H), 4.10-4.03 (m, 8 H), 3.84-3.79 (m, 8 H), 3.72-3.65 (m, 16 H). ^{13}C-NMR ($CDCl_3$, 101 MHz) (Figure 6-5): δ (ppm): 160.11, 158.55, 149.18, 140.35, 136.71, 122.43, 121.49, 106.48, 100.93, 73.15, 72.88, 70.99, 70.94, 69.75, 67.65. HR-ESIMS (Figure 6-6): calcd. for $[M + H]^+$: 779.3750, found: *m/z*, 779.3772 $[M + H^+]$, error: -2.8 ppm.

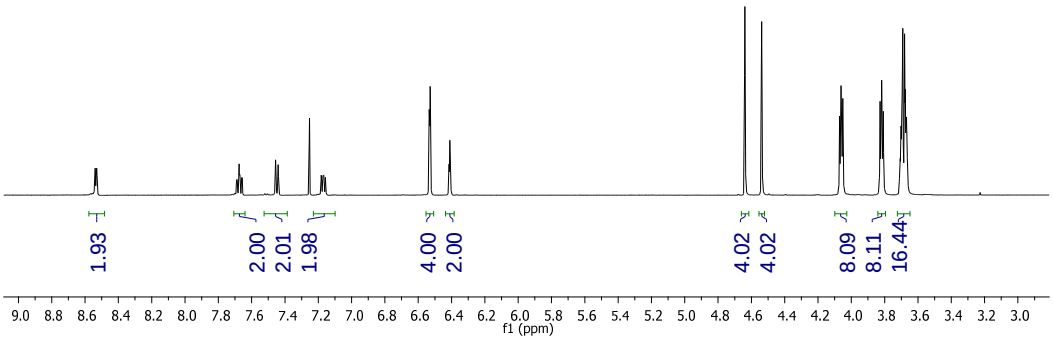

Figure 6-4. ^{1}H-NMR ($CDCl_3$, 500 MHz, room temperature) of bispyridyl BMP32C10 ether **1c**.

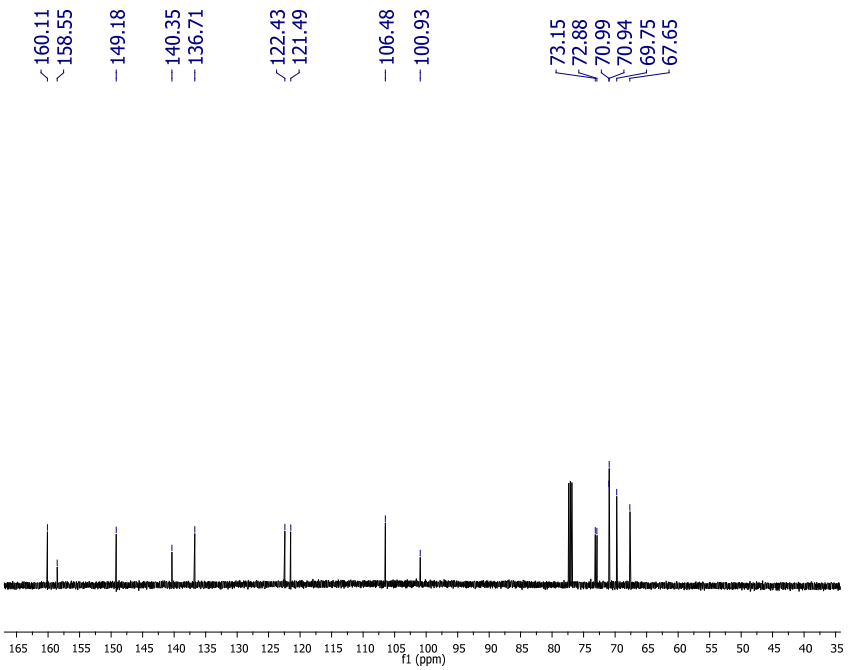

Figure 6-5. ^{13}C-NMR ($CDCl_3$, 101 MHz, room temperature) of bispyridyl BMP32C10 ether **1c**.

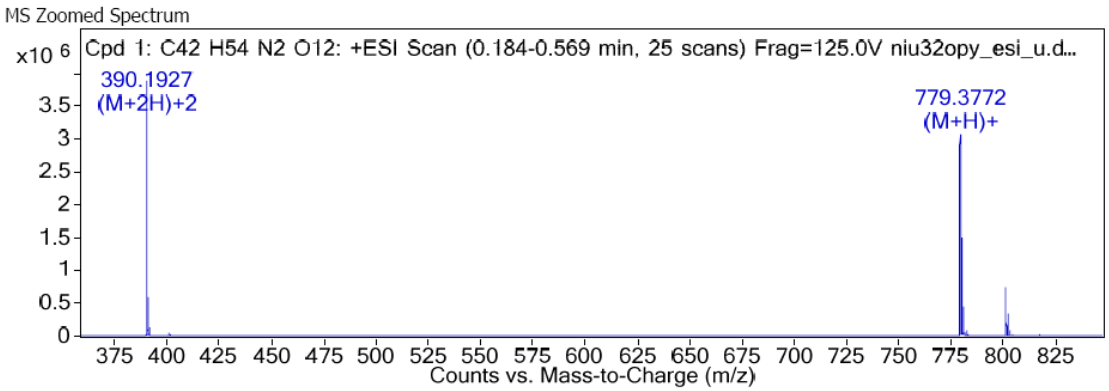

Figure 6-6. Electrospray ionization mass spectrum of bispyridyl BMP32C10 ether **1c**.

6.5.3 Stoichiometry study of 1c(TFA)$_2$·2

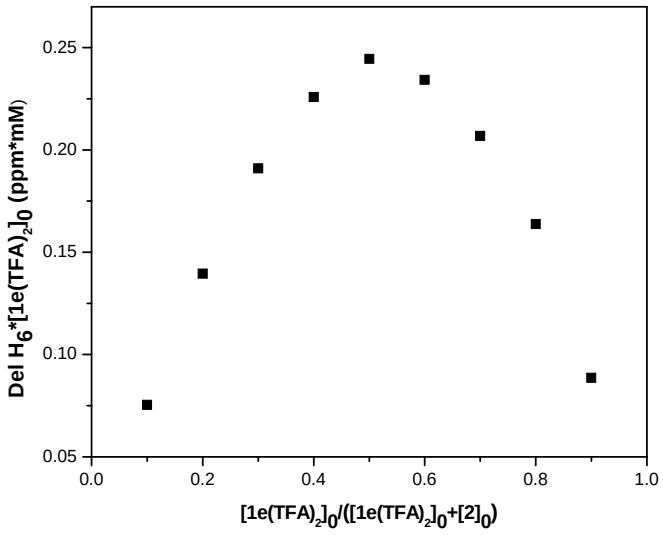

Figure 6-7. Job plot showing the 1:1 stoichiometry of the complex between **1c(TFA)$_2$** and **2** in $CDCl_3/CD_3CN$ = 1/1 <v/v>. **[1c(TFA)$_2$]$_0$ + [2]**$_0$ = 3.79 mM.[17]

6.5.4 Determination of Δ_0 for 1c·2

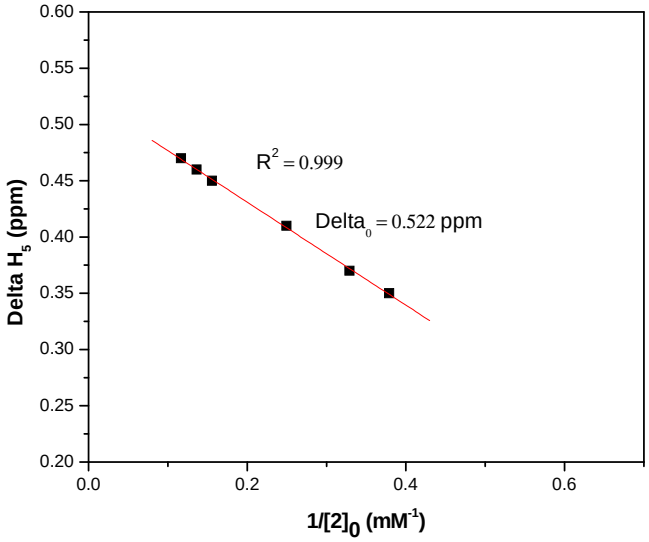

Figure 6-8. Determination of $Delta_0$ for **1c·2** in $CDCl_3/CD_3CN$ = 1/1 <v/v>. $[\mathbf{1c}]_0$ = 0.193 mM.[3]

6.5.5 Determination of Δ_0 for 1c$(TFA)_2$·2

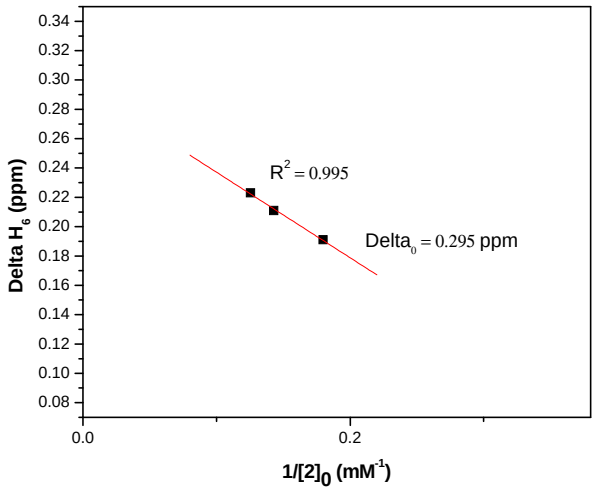

Figure 6-9. Determination of $Delta_0$ for **1c**$(TFA)_2$**·2** in $CDCl_3/CD_3CN$ = 1/1 <v/v>. $[\mathbf{1c}(TFA)_2]_0$ = 0.217 mM.

6.5.6 Mass spectrum of 1c·2

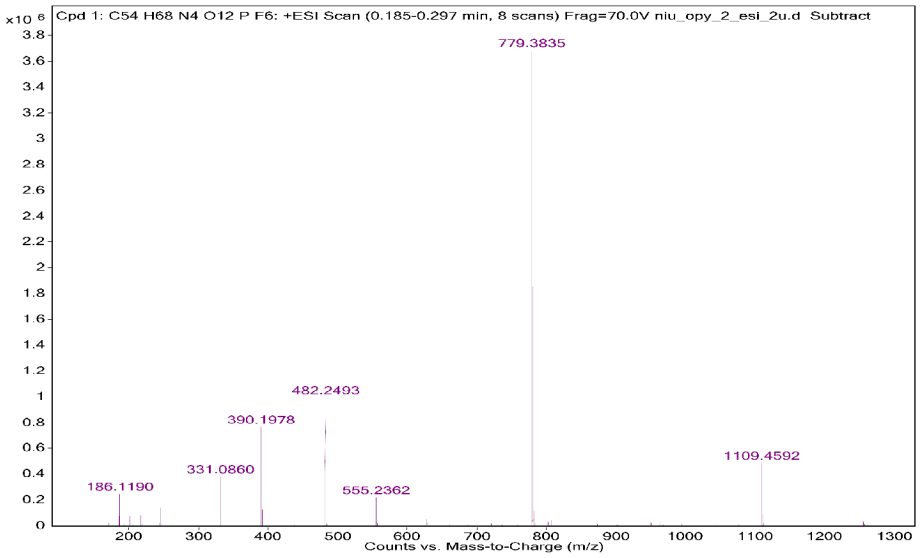

Figure 6-10. Electrospray ionization mass spectrum of **1c·2**.

6.5.7 Mass spectrum of 1c(TFA)$_2$·2

Figure 6-11. Electrospray ionization mass spectrum of **1c**(TFA)$_2$·**2**.[3]

6.5.8 Acid-base control study of 1c

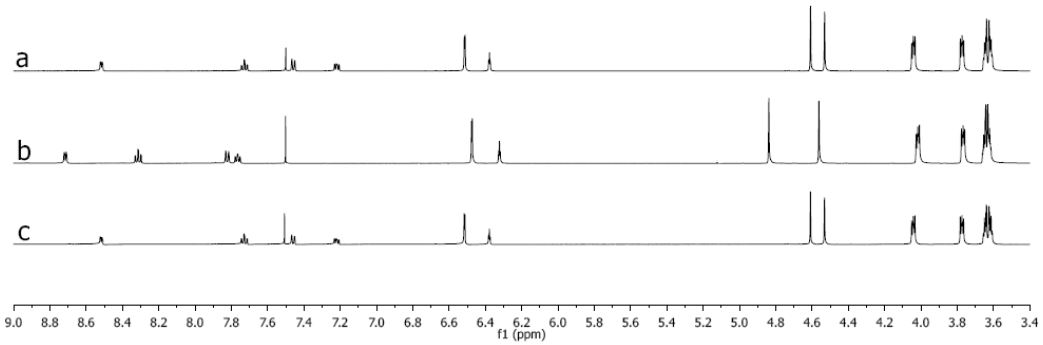

Figure 6-12. Partial proton NMR spectra (500 MHz, $CDCl_3/CD_3CN$ = 1/1 <v/v>, 25°C) of: a) **1c**; b) solution (a) after addition of 2.2 equiv. of TFA. c) solution (b) after addition of 2.2 equiv. of TEA. Upon diprotonation of dipyridyl crown derivative signal shifts are observed, particularly for protons associated with the pyridyl moieties. However, addition of base causes all of the signals to revert to essentially their original positions, demonstrating that the process is reversible and that the presence of tetraethylammonium and trifluoroacetate ions does not significantly affect the chemical shifts of the unprotonated compound.

6.5.9 1D-NOESY study of 1c·2 and 1c(TFA)$_2$·2

a

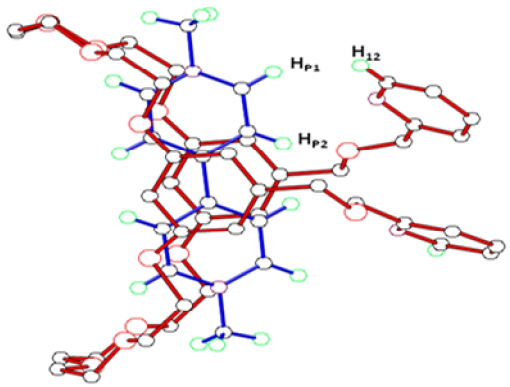

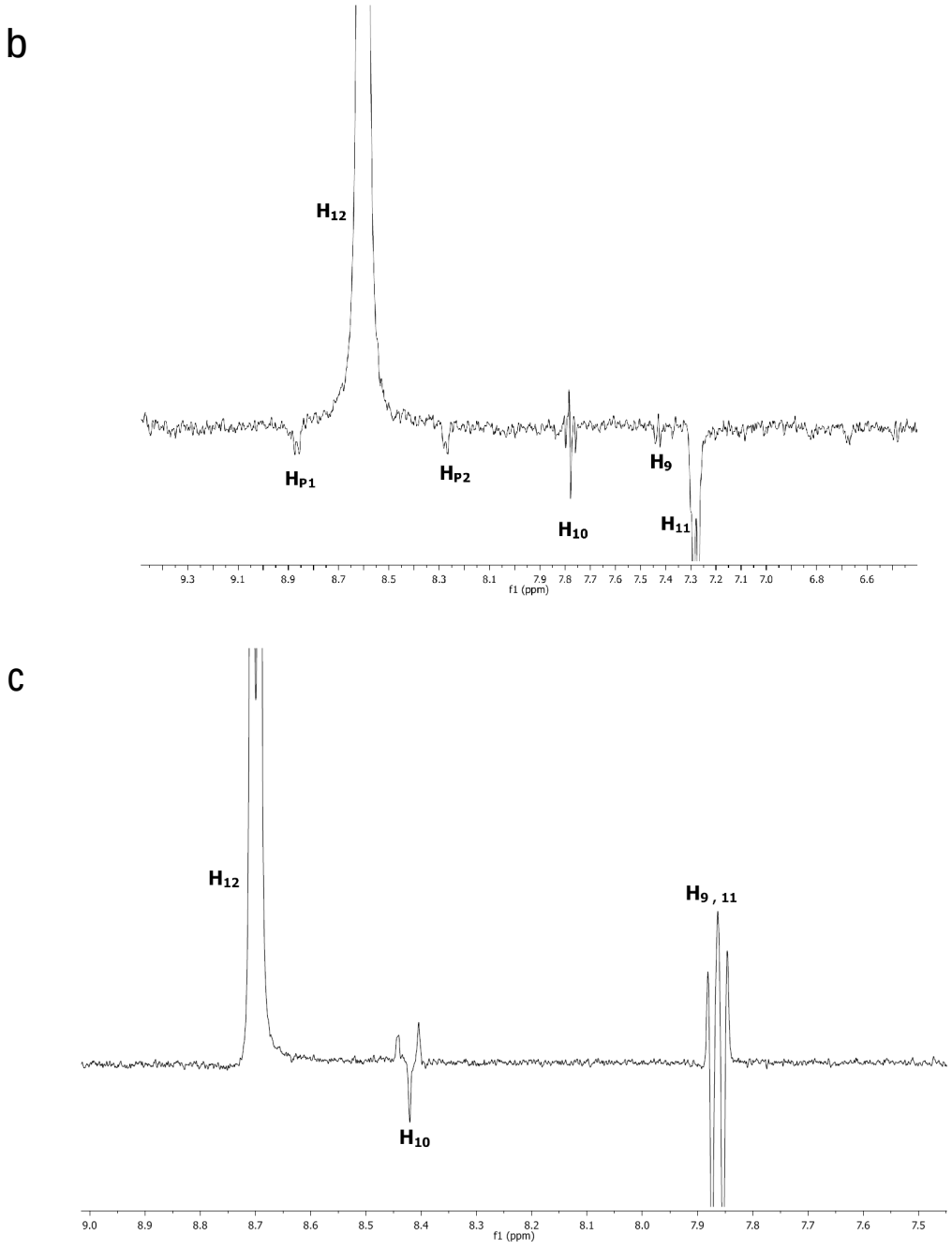

Figure 6-13. (a) Crystal structure of **1c**·**2**; (b) 1D-NOESY NMR spectrum (400 MHz, $CDCl_3/CD_3CN$ = 1/1 <v/v>, 25°C) of **1c**·**2**. Based on the crystal structure of **1c**·**2** (Figure 6-2), 1D-NOESY experiments were performed by selective irradiation of H_{12} on **1c**. The $H_{12}\cdots H_a$ shortest distances (Å) obtained from crystal structures: a =

p1, 2.622; a = p2, 3.539; The correlations between H_{12} and H_{P1} and H_{P2} are clearly observed, which is consistent with results obtained from the crystal structure of **1c**·**2** and indicate the formation of pseudocryptand-type [2]pseudorotaxane structure in solution. (c) 1D-NOESY NMR spectrum (400 MHz, $CDCl_3/CD_3CN$ = 1/1 <v/v>, 25°C) of (b) after addition of 2.2 equiv. TFA. No correlations between H_{12} and H_{P1} and H_{P2} are observed.

References

(1) (a) Gibson, H. W. In Large Ring Molecules; Semlyen, J. A., Ed.; John Wiley & Sons: New York, 1996; Chapter 6, pp 191-262; (b) *Molecular Catenanes, Rotaxanes and Knots,* Sauvage, J.-P.; Dietrich-Buchecker, C. O., Ed., Wiley-VCH, Weinheim, **1999**. (c) Huang F.; Gibson, H. W. *Prog. Poly. Sci*. **2005**, *30*, 982-1018. (d) Wenz, G.; Han, B.-H.; Mueller, A. *Chem. Rev*. **2006**, *106*, 782-817. (e) Griffiths, K.; Stoddart, J. F. *Pure Appl. Chem.* **2008**, *80*, 485-506. (f) Harada, A.; Takashima, Y.; Yamaguchi, H. *Chem. Soc. Rev*. **2009**, *38*, 875-882. (g) Durola, F.; Sauvage, J.-P.; Wenger, O. S. *Coord. Chem. Rev.* **2010**, *254*, 1748-1759. (h) Gassensmith, J. J.; Baumes, J. M.; Smith, B. D. *Chem. Commun.* **2009**, *42*, 6329-6338. (i) Hanni, K. D.; Leigh, D. A. *Chem. Soc. Rev.* **2010**, *39*, 1240-1251.

(2) (a) Balzani, V.; Credi A.; Venturi, M. *Nano Today* **2007**, *2*, 18-25. (b) Champin, B.; Mobian, P.; Sauvage, J.-P. *Chem. Soc. Rev.* **2007**, *36*, 358-366. (c) Hembury, G. A.; Borovkov, V. V.; Inoue, Y. *Chem. Rev.* **2007**, *108*, 1-73. (d) Bonnet S.; Collin, J.-P. *Chem. Soc. Rev.* **2008**, *37*, 1207-1217. (e) Angelos, S.; Khashab, N. M.; Yang, Y.-W.; Trabolsi, A.; Khatib, H. A.; Stoddart, J. F.; Zink, J. I. *J. Am. Chem. Soc.* **2009**, *131*, 12912-12914. (f) Leung, K. C.-F.; Chak, C.-P.; Lo, C.-M.; Wong, W.-Y.; Xuan, S.; Cheng, C. H. K. *Chem. Asian. J.* **2009**, *4*, 364-381.

(3) (a) Montalti, M. *Chem. Commun*., **1998**, 1461-1462. (b) Beer P.; Wong, W. in *Macrocyclic Chemistry*, Ed. K. Gloe, Springer Netherlands, 2005, pp. 105-119. (c) Fernando, I. R.; Bairu, S. G.; Ramakrishna G.; Mezei, G. *New J. Chem.*, **2010**, *34*, 2097-2100.

(4) (a) Higashi, T.; Hirayama, F.; Misumi, S.; Arima H.; Uekama, K. *Biomaterials*, **2008**, *29*, 3866-3871. (b) Bilkova, E.; Sedlak, M.; Dvorak, B.; Ventura, K.; Knotek, P.; Benes, L. *Org.*

Biomol. Chem., **2010**, *8*, 5423-5430. (c) Thomas, C. R.; Ferris, D. P.; Lee, J.-H.; Choi, E.; Cho, M. H.; Kim, E. S.; Stoddart, J. F.; Shin, J.-S.; Cheon, J.; Zink, J. I. *J. Am. Chem. Soc.* **2010**, *132*, 10623-10625. (d) Liu, J.; Du, X.; Zhang, X. *Chem. Eur. J.* **2011**, *17*, 810-815. (e) Hyun H.; Yui, N. *Macromol. Biosci.* **2011**, *11*, 765-771. (f) Li, J. J.; Zhao, F.; Li, J. *Appl. Microbiol. Biotechn.* **2011**, *90*, 427-443.

(5) Some recent publications: (a) Huang, F.; Switek, K. A.; Gibson, H. W. *Chem. Commun.* **2005**, 3655-3657. (b) Leung, K. C. F.; Mendes, P. M.; Magonov, S. N.; Northrop, B. H.; Kim, S.; Patel, K.; Flood, A. H.; Tseng, H.-R.; Stoddart, J. F. *J. Am. Chem. Soc.* **2006**, *128*, 10707-10715. (c) Castillo, D.; Astudillo, P.; Mares, J.; Gonzalez, F. J.; Vela, A.; Tiburcio, J. *Org. Biomol. Chem.* **2007**, *5*, 2252-2256. (d) Casasús, R.; Climent, E.; Marcos, M. D.; Martínez-Máñez, R.; Sancenón, F.; Soto, J.; Amorós, P.; Cano, J.; Ruiz, E. *J. Am. Chem. Soc.* **2008**, *130*, 1903-1917. (e) Wu, J.; Leung, K. C.-F.; Benitez, D.; Han, J.-Y.; Cantrill, S. J.; Fang, L.; Stoddart, J. F. *Angew. Chem., Int. Ed.* **2008**, *47*, 7470-7474. (f) Muraoka, M.; Irie, H.; Nakatsuji, Y. *Org. Biomol. Chem.* **2010**, *8*, 2408-2413.

(6) Some recent publications: (a) Zhang, M.; Zhu, K.; Huang, F. *Chem. Commun.* **2010**, *46*, 8131-8141. (b) Wang, C.; Olson, M. A.; Fang, L.; Benítez, D.; Tkatchouk, E.; Basu, S.; Basuray, A. N.; Zhang, D.; Zhu, D.; Goddard, W. A.; Stoddart, J. F. *Proc. Nat. Acad. Sci.* **2010**, *107*, 13991-13996. (c) Trabolsi, A.; Fahrenbach, A. C.; Dey, S. K.; Share, A. I.; Friedman, D. C.; Basu, S.; Gasa, T. B.; Khashab, N. M.; Saha, S.; Aprahamian, I.; Khatib, H. A.; Flood, A. H.; Stoddart, J. F. *Chem. Commun.* **2010**, *46*, 871-873. (d) Jiang, Y.; Cao, J.; Zhao, J.-M.; Xiang, J.-F.; Chen, C.-F. *J. Org. Chem.* **2010**, *75*, 1767-1770. (e) Xu, Z.; Huang, X.; Liang, J.; Zhang, S.; Zhou, S.; Chen, M.; Tang, M.; Jiang, L. *Eur. J. Org. Chem.* **2010**, *10*, 1904-1911. (f) Wang, F.; Zhang, J.; Liu, M.; Zheng, B.; Li, S.; Zhu, K.; Wu, L.; Gibson, H. W.; Huang, F. *Angew. Chem. Int. Ed.* **2010**, *49*, 940-944. (g) Li, S.; Zheng, B.; Chen, J.; Dong, S.; Ma, Z.; Huang, F.; Gibson, H. W. *J. Polym. Sci. A, Polym. Chem.* **2010**, *48*, 4067-4073.

(7) (a) Niu, Z.; Slebodnick, C.; Bonrad, K.; Huang, F.; Gibson, H. W. *Org. Lett.* **2011**, *13*, 2872-2875. (b) Niu, Z.; Slebodnick, C.; Schoonover, D.; Azurmendi, H.; Harich, K.; Gibson, H. W. *Org. Lett.* DOI 10.1021/ol201502r.

(8) Gibson, H. W.; Nagvekar, D. S. *Can. J. Chem.* **1997**, *75*, 1375-1384.

(9) (a) Job, P. *Ann. Chim. Appl.* **1928**, 113-203. (b) Hirose, K. *J. Incl. Phenom. Macrocyc. Chem.* **2001**, *39*, 193-209. (c) Bruneau, E.; Lavabre, D.; Levy, G.; Micheau, J. C. *J. Chem. Educ.* **1992**, *69*, 833-837.

(10) ^{1}H-NMR characterizations were done on solutions with constant [**1c**] and varied [**2**]. Based on these NMR data, Δ_o, the difference inδvalues for proton H_5 of **1c** in the uncomplexed and fully complexed species, was determined to be 0.522 ppm as the y-intercept of a plot of $\Delta = \delta - \delta_u$ *vs.* 1**c**/[**2**]$_0$ in the high initial concentration range of **2**. K_a was calculated from $K_a = (\Delta/\Delta_0)/[(1-\Delta/\Delta_0)([\mathbf{2}]_0-\Delta/\Delta_0\,[\mathbf{1c}]_0)$.

(11) (a) Delaviz, Y.; Merola, J. S.; Berg, M. A. G.; Gibson, H. W. *J. Org. Chem.* **1995**, *60*, 516-522. (b) Gibson, H. W.; Wang, H.; Chng, C. P.; Glass, C. T. E.; Schoonover, D. S.; Zakharov, L. N.; Rheingold, A. L. *Heteroatom Chem.* **2008**, *19*, 48-54.

(12) (a) Hunter, C. A.; Sanders, J. K. M. *J. Am. Chem. Soc.* **1990**, *112*, 5525-5534. (b) Hohenstein, E. G.; Sherrill, C. D. *J. Phys. Chem. A* **2009**, *113*, 878-886.

(13) See experimental section.

(14) To determine the effect of the added species, 2 equivalents of tetraethylammonium trifluoroacetate were added to a solution of **1c·2** ($CDCl_3/CD_3CN$ = 1/1 <v/v>); no significant chemical shift changes were observed.

(15) It should be noted that until recently, almost all the complexes of bis(*meta*-phenylene)-32-crown-10 derivatives with paraquat derivatives (such as **2**) had demonstrated "taco"-shaped structures, which expose one side of the paraquat salts. Selected publications with "taco" structures: (a) Bryant, W. S.; Jones, J. W.; Mason, P. E.; Guzei, I.; Rheingold, A. L.; Fronczek, F. R.; Nagvekar D. S.; Gibson, H. W. *Org. Lett.* **1999**, *1*, 1001-1004. (b) Huang, F.; Fronczek F. R.; Gibson, H. W. *Chem. Commun.* **2003**, *1480*−1481 (c) Huang, F.; Zakharov, L. N.; Bryant, W. S.; Rheingold, A. L.; Gibson, H. W. *Chem. Commun.* **2005**, 3268-3270. (f) Zhang, M.; Luo, Y.; Zheng, B.; Yan, X.; Fronczek, F. R.; Huang, F. *Eur. J. Org. Chem.* **2010**, *35*, 6798-6803. Recently, however, a complex based on a carbazole-BMP30C10 and **2** demonstrated the coexistence of [2]pseudorotaxane and [2]taco type structures in the solid state: ref. 7a. Possibly, **1e**$(TFA)_2$·**2** formed a true pseudorotaxane structure.

(16) Allwood, B. L.; Shahriari-Zavareh, H.; Stoddart J. F.; Williams, D. J. *Chem. Commun.* **1987**, 1058-1061.

(17) The **1c(TFA)$_2$** salt was made in situ: the desired amount of **1c** was dissolved in a limited amount of solvent in a volumetric flask. Then, 2.05 equiv. of TFA was added and the resulting solution was diluted to the desired volume.

TOC Graphic:

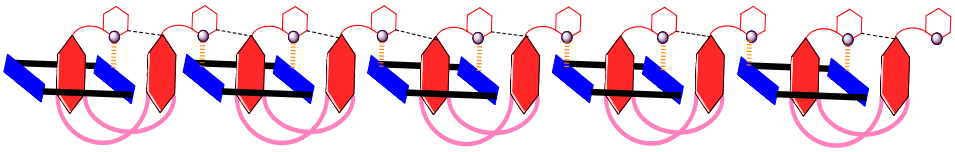

Abstract:

The first pseudocryptand-type supramolecular [3]pseudorotaxane was designed and prepared via the self-assembly of a bispicolinate BMP32C10 derivative and a bisparaquat. The complexation behavior was cooperative. In addition, the complex comprised of the BMP32C10 derivative and a cyclic bisparaquat demonstrated strong binding; interestingly, a poly[2]pseudocatenane structure was formed in the solid state for the first time.

Chapter 7

Pseudocryptand-type [3]Pseudorotaxane and "Hook-Ring" Polypseudo[2]catenane based on a Bis(*meta*-phenylene)-32-crown-10 Derivative and Bisparaquat Derivatives

7.1 Introduction

In supramolecular chemistry, pseudorotaxanes are the supramolecular mechanically-linked species constructed from linear molecular components ("Guests") encircled by macrocyclic components ("Hosts"). Pseudorotaxanes are not only the fundamental precursors for the preparation of novel supramolecular species, such as rotaxanes, catenanes, polyrotaxanes and polycatenanes,[1] but also are applied as functional materials, such as molecular machines, drug delivery devices and so on.[2] Therefore, the design and preparation of pseudorotaxanes, especially with novel topologies, have been topics of current interest.[3] Crown ethers and derivative cryptands, such as **1**, and paraquat derivatives (*N*,*N'*-dialkyl-4,4'-bipyridinium),[4] e. g., linear bisparaquat **2** and cyclobis(paraquat-*p*-phenylene) (CBPQT) **3**, have been widely employed to construct pseudorotaxanes and catenanes.[5] Cryptands, e. g., **1d**, have been proved to be much better hosts for paraquat derivatives compared with the corresponding simple crown ethers, e. g., **1a**.[6] Recently, we reported the first supramolecular cryptand-type [2]pseudorotaxanes based on synthetically easily accessible bis(*meta*-phenylene)-32-crown-10 (BMP32C10) derivatives, including **1c**, and a paraquat derivative with remarkably improved association constants due to the formation of pseudocryptand structures in the complexes.[7] Inspired by these results, here we first report the design and self-assembly of a pseudocryptand-type supramolecular [3]pseudorotaxane via cooperative complexation between BMP32C10 dipicolinate derivative **1c**

and bisparaquat **2**. Moreover, complexation of **1c** and cyclic bisparaquat **3** produced the first "hook-ring" poly[2]pseudocatenane in the solid state.

7.2 Results and discussion

The individual solutions of **1c** and **2** in acetone-d_6 were colorless; however, the mixed solutions of **1c** and **2** in acetone-d_6 were deep yellow due to the charge-transfer interaction between the electron-rich aromatic rings of **1c** and the electron-poor pyridinium rings of **2**, good evidence for complexation. ^{1}H-NMR spectra of the mixed solutions of **1c** and **2** displayed only one set of peaks, indicating the complexation was a fast exchange process. After complexation, peaks corresponding to H_3, H_4, H_5, H_6, H_7, and H_8 of **1c** and H_{p1}, H_{p2}, H_{p3}, H_{p4}, H_{p5}, and H_{p6} of **2** moved upfield, while H_1, H_2 and H_{11} of **1c** and H_{p7} of **2** moved downfield, as normally observed in similar complexes.[5-7]

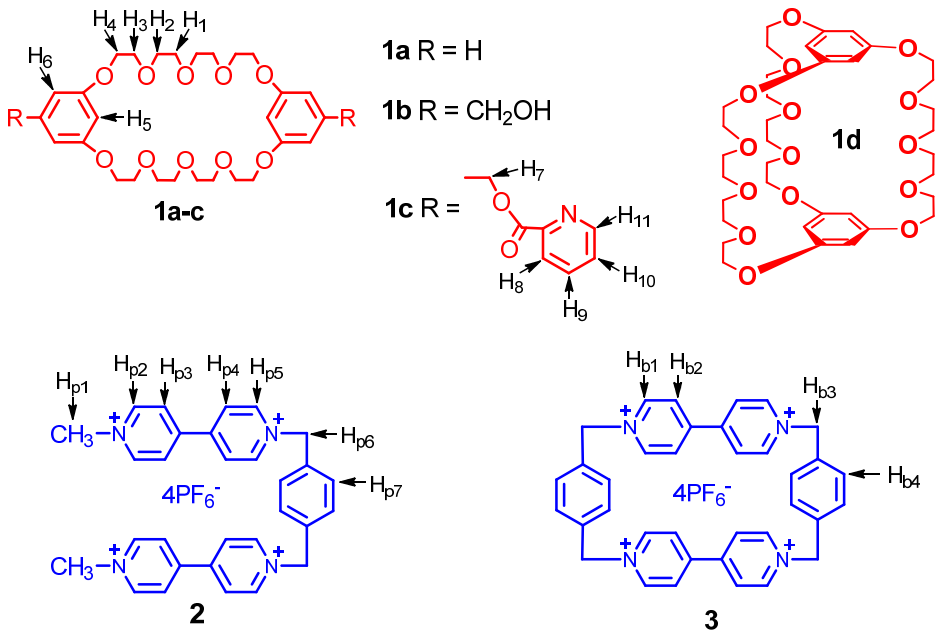

Scheme 7-1. Structures of crown ethers **1a-c**, cryptand **1d** and bisparaquats **2-3**.

The stoichiometry of the complex between dipicolinate host **1c** and linear bisparaquat **2** was determined to be 2:1 by a molar ratio plot (Figure 7-2)[8] and confirmed by an electrospray ionization mass spectrum (ESI-MS): m/z 1174.84 $[\mathbf{1c_2}\cdot\mathbf{2}\text{-}2PF_6+H]^{2+}$, 1101.73 $[\mathbf{1c_2}\cdot\mathbf{2}\text{-}3PF_6]^{2+}$,

734.85 [**1c**$_2$**·2**-3PF_6+H]$^{3+}$, 514.94 [**1c**$_2$**·2**-4PF_6+H]$^{4+}$.[9] It should be noted here that the stoichiometry between the BMP32C10 diol **1b**, which is the precursor of **1c**, and **2** was reported as 1:1, while the stoichiometry between BMP32C10 cryptand **1d** and **2** was reported as 2:1 in the same solvent.[5a] This observation provided an indication of the formation of a cryptand-like structure in the **1c·2** complex.

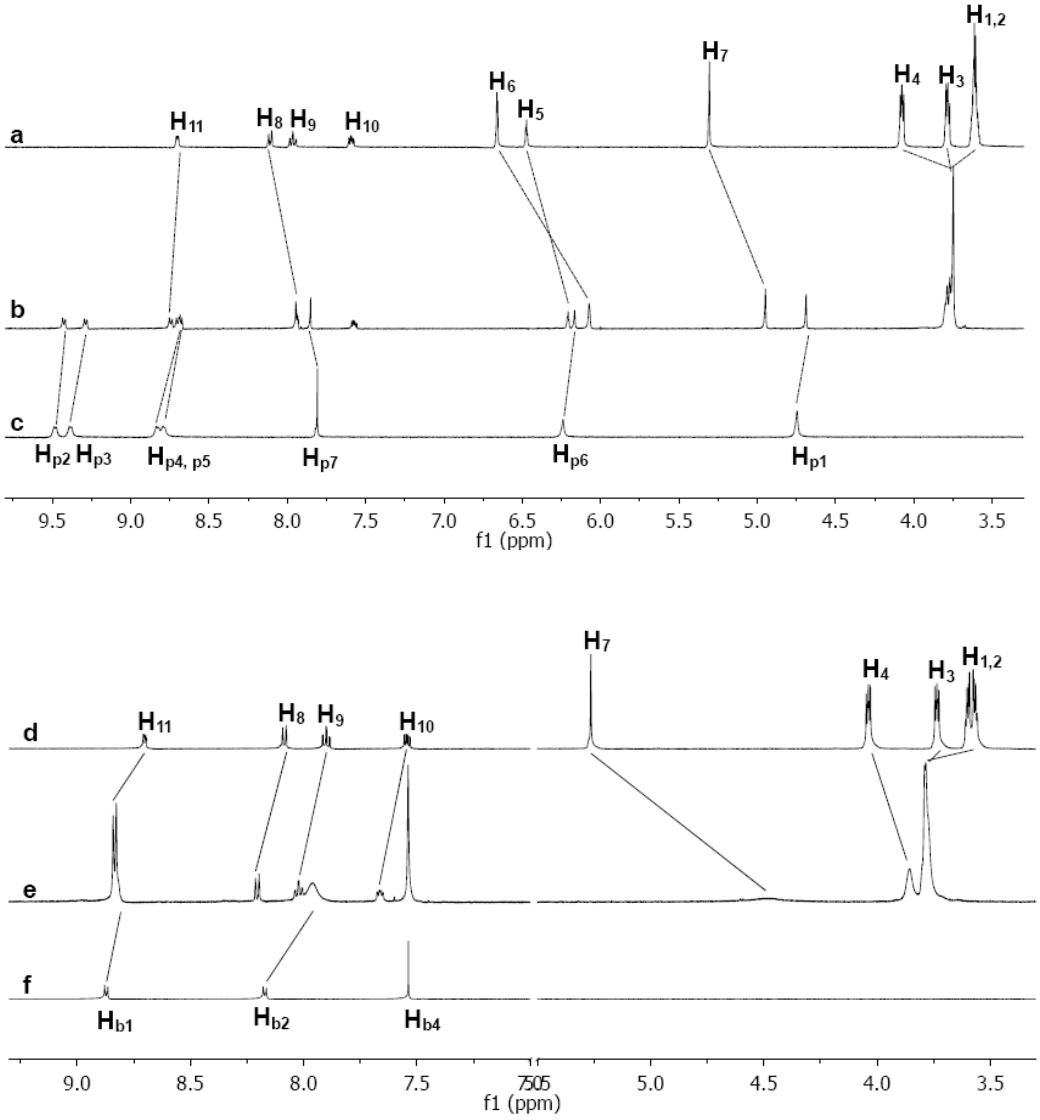

Figure 7-1. Partial proton NMR spectra of: Upper stacked spectra (400 MHz, acetone-d_6, 25 °C): (a) **1c**; (b) **1c** and **2** ([**1c**]$_0$ = 0.95 mM, [**2**]$_0$ = 0.50 mM); (c) **2**. Bottom stacked spectra (500 MHz, acetonitrile-d_3, 25 °C): (d) **1c**; (e) **1c** and **3** ([**1c**]$_0$ = [**3**]$_0$ = 2.18 mM); (f) **3**.

The value of Δ_0, the chemical shift difference for H_{p3} of **2** between the uncomplexed and fully complexed species, was determined to be 0.137 ppm by extrapolation of a plot of Δ, the chemical shift difference for H_{p3} between solutions of the uncomplexed and partially complexed **2**, versus $1/[\mathbf{1c}]_0$ in the high initial concentration range of **1c**.[9] The complexed fraction, *p*, of the bisparaquat **2** can be calculated from $p = \Delta/\Delta_0$. Based on a Scatchard plot, K_1 was estimated to be $6.0 \pm 0.9 \times 10^3$ M^{-1} and K_2 was determined to be $8.1 \pm 0.7 \times 10^3$ M^{-1} in acetone-d_6.[10] The ratio $K_2 / K_1 = 1.35$ is much higher than the value of 0.25 expected for statistical complexation, indicating that the complexation between **1c** and **2** is cooperative.[11] Also, K_2 and K_1 are much higher than the K_a (6.3×10^2 M^{-1}, in acetone-d_6)[5a] between precursor **1b** and **2** due to the formation of a pseudocryptand structure in the complex, as confirmed by the X-ray analysis (see below).

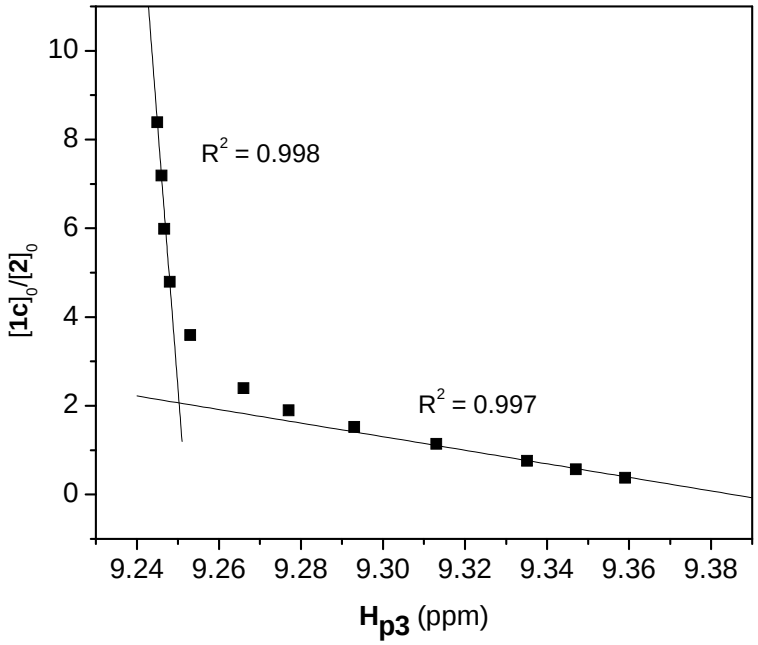

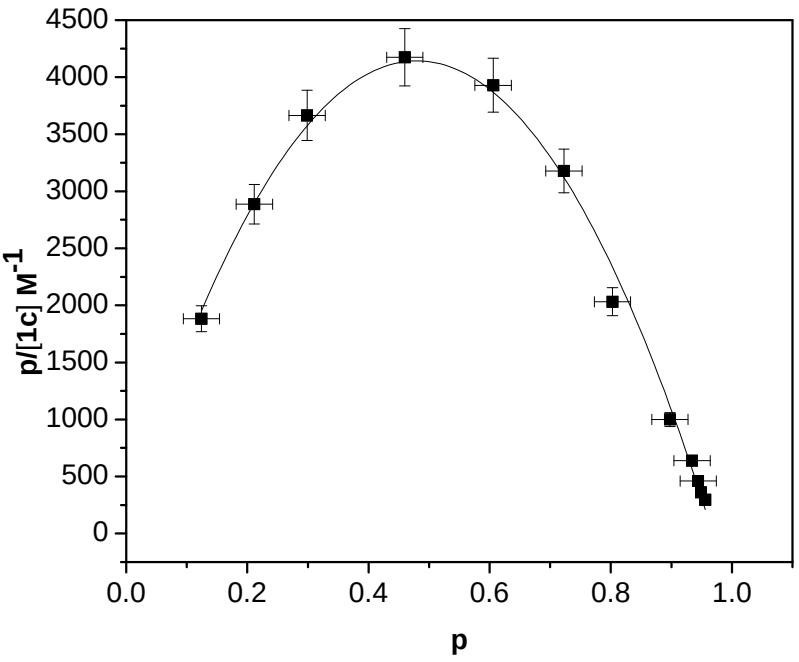

Figure 7-2. Upper plot: Mole ratio plot for **1c** and **2**. Bottom plot: Scatchard plot for complexation of **1c** with **2**. *P* = fraction of bisparaquat **2** units complexed. Error bars in *p*: ± 0.03 absolute. Error bars in *p*/[**1c**]: ± 0.06 relative. The polynomial fit line is simply to guide the reader's eyes. The experiment was performed in acetone-d_6 at 22 °C.

X-ray diffraction analysis of crystals of the complex of **1c** with **2** (Figure 7-3), which was grown via the vapor-diffusion of pentane into an acetone solution, confirmed the stoichiometry between **1c** and **2** and demonstrated the formation of a pseudocryptand-type supramolecular [3]pseudorotaxane structure. In the complex, two molecules of **1c** form a pseudocryptand structure by folding the pyridyl arms; the pyridyl rings interact via off-set face-to-face π-stacking.[12] The bisparaquat molecule **2** is threaded through the central cavity of the pseudocryptand **1c**. The complex is stabilized by hydrogen bonds between pyridyl rings, ether oxygen atoms and the hydrogen atoms of the bisparaquat, off-set π-π stacking between pyridyl rings, aromatic rings of **1c** and pyridinium rings of **2**, and CH-π interactions. It should be noted here that the carbonyl oxgen atoms of one host **1c** form intermolecular hydrogen bonds (bond d in Figure 7-3) with the H_1 of the other threaded **1c** molecule. This favors the threading of the second **1c** molecule and leads to cooperative complexation. Another possible reason for the cooperative complexation is that the threading of the first crown ether **1c** molecule restricts the

conformational freedom of bisparaquat **2** by forming hydrogen bonds (bonds of e and f in Figure 7-3) and CH-π interaction (CH-centroid 2.68 Å) between the first threaded crown ether **1c** and bisparaquat, thereby favoring the threading of the second host molecule.

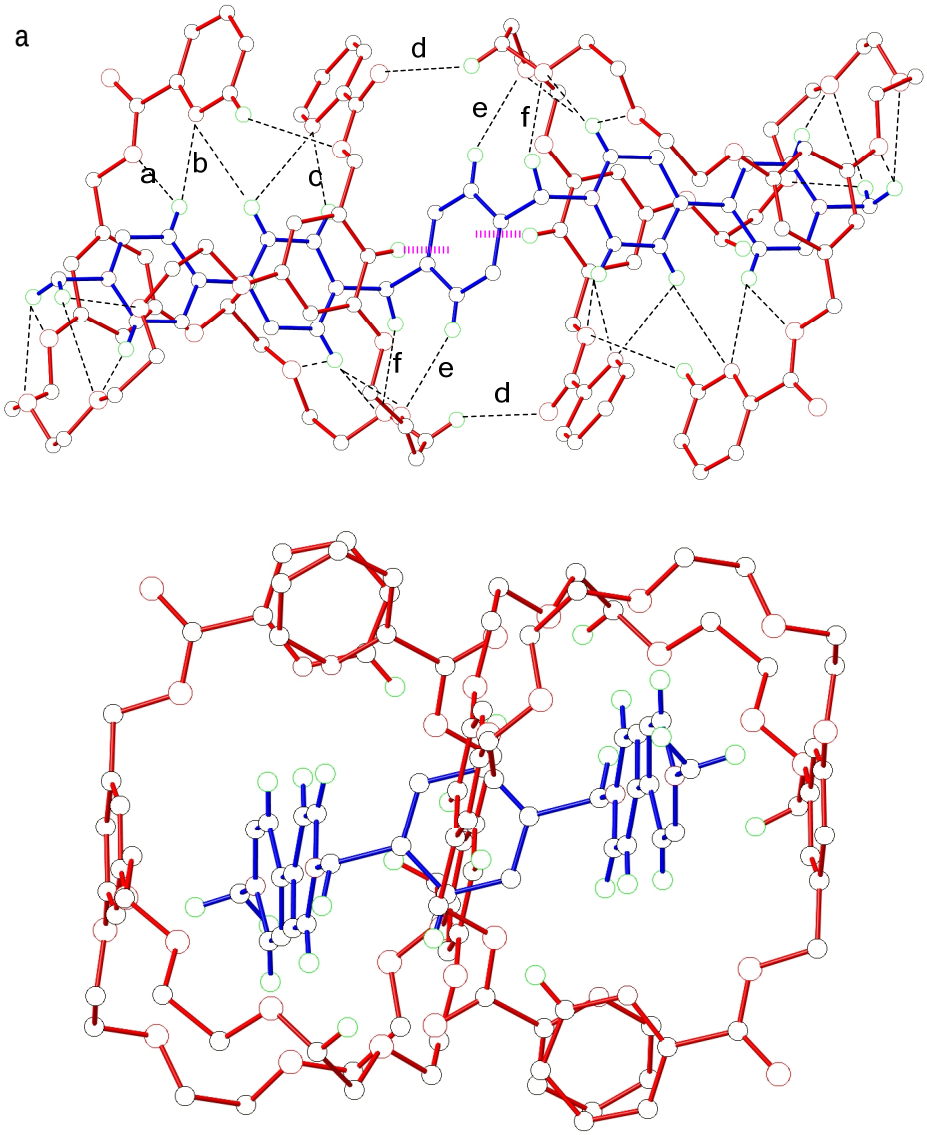

Figure 7-3. Two views of the X-ray structure of **1c**$_2$**·2**. Oxygen atoms are red. Carbon atoms are black. Nitrogen atoms are purple. Hydrogen atoms are green. **1c** is red. **2** is green. The same settings are used in the following crystal structures. Solvent molecules, PF_6^- ions, and hydrogens

except the ones involved in hydrogen bonds were omitted for clarity. Pink dashed lines represent the CH-π interactions. Selected hydrogen-bond parameters: H···O(N) distances (Å), C···O(N) distances (Å), C-H···O(N) angles (deg): a 2.59, 3.29, 130.691; b 2.50, 3.37, 151; c 2.32, 3.10, 138; d 2.46, 3.35, 149; e 2.69, 3.55, 155. F 2.40, 3.34, 159. All the hydrogen bonds are omitted for clarity in the Figure 7-(b).

Similarly, the mixed solutions of dipicolinate **1c** and CBPQT **3** in acetonitrile-d_3 were deep yellow due to the charge-transfer interaction between the electron-rich aromatic rings of **1c** and the electron-poor pyridinium rings of **3**, indicating complexation. ^{1}H-NMR spectra of solutions of **1c** and **3** displayed only one set of signals (Figure 7-1), indicating fast exchange. Upon complexation, signals corresponding to H_7 and H_4 of **1c** and H_{b1} and H_{b2} of **3** moved upfield, while H_1, H_2, H_3, H_9, H_{10}, and H_{11} of **1c** moved downfield as normally observed in similar complexes.[5-7] A Job plot (Figure 7-4)[13] showed that the stoichiometry of the complex between **1c** and **3** was 1:1 and the stoichiometry was confirmed by an electrospray ionization mass spectrum (ESI-MS): m/z 808.44 [**1c·3**-2PF_6]$^{2+}$, 735.79 [**1c·3**-3PF_6]$^{2+}$, 490.66 [**1c·3**-3PF_6]$^{3+}$.[9] K_a was determined to be 1.7 ± 0.2 x 10^4 M^{-1} in acetonitrile-d_3 based on the proton NMR data.[14]

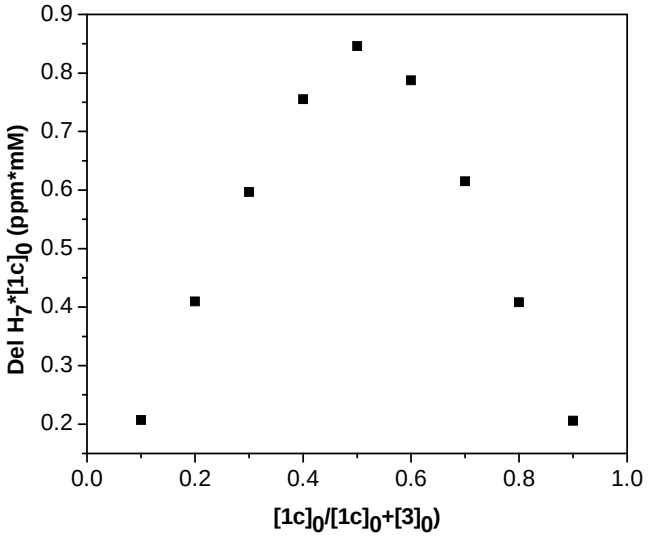

Figure 7-4. Job plot showing 1:1 stoichiometry of the complex between **1c** and **3** in

acetonitrile-d_3. $[\mathbf{1c}]_0 + [\mathbf{3}]_0 = 2.18$ mM

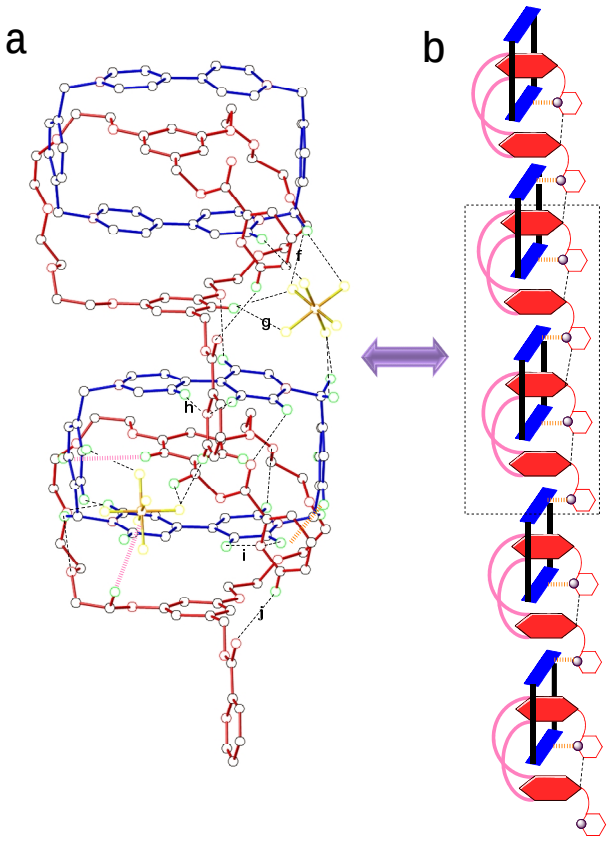

Figure 7-5. (a) X-ray structure of poly(**1c**·**3**). **1c** is red. **3** is blue. Solvent molecules, PF_6^- ions and hydrogen atoms except the ones involved in hydrogen bonding have been omitted for clarity. Selected hydrogen-bond parameters: H···O(F, N) distances (Å), C···O(F, N) distances (Å), C-H···O(F, N) angles (deg): f 2.58, 3.22, 122; g 2.59, 3.44, 155; h 2.41, 3.33, 166; i 2.73, 3.35, 124; j 2.46, 3.35, 134; (b) Cartoon representation of the supramolecular structure.

Interestingly, X-ray analysis of a single crystal of the complex **1c**·**3**, which was grown via the vapor-diffusion of diisopropyl ether into an acetonitrile solution, showed that complex **1c**·**3** forms a "hook-ring" shaped poly[2]pseudocatenane structure in the solid state (Figure 7-5). Different from other crown ether/paraquat complexation systems in which crown ethers always are the hosts, in this system the crown ether **1c** acts as a guest and is threaded through the central cavity of CBPQT **3**, which acts as a host. A **1c**·**3** repeating unit was formed accordingly. One

pyridyl arm of crown ether **1c** interacts with one paraquat side of **3** in the repeating unit and leaves the other paraquat side of **3** open. At the same time, the other pyridyl arm of **1c** acts as a "hook" to interact with the open paraquat side of host **3** ring in an adjacent repeating unit. Also, there is a hydrogen bond between **1c** and a host **3** belonging to an adjacent repeat units. Therefore, **1c·3** units are linked together. In addition, H_{11} of one pyridyl arm of **1c** forms a hydrogen bond with the carbonyl oxygen of the other pyridyl arm on the same **1c**. Two PF_6 counterions act as hydrogen bonding bridges, interacting with both pyridyl arms of **1c** and a paraquat side of host **3**, forming a pseudocatenane structure.[15] As a result, a poly[2]pseudocatenane was formed and stabilized by hydrogen bonds, off-set π-π stacking between aromatic rings of **1c** and pyridinium rings of **3** and CH-π interactions between the H_6 protons of **1c** and aromatic rings of **3** (CH-centroid 2.94 Å). To the best of our knowledge, this is the first poly[2]pseudocatenane to be reported.

7.3 Conclusions

In summary, for the first time, we demonstrated a pseudocryptand-type supramolecular [3]pseudorotaxane based on a BMP32C10 derivative with a linear bisparaquat. The complexation behavior was cooperative. In addition, the complex between the same BMP32C10 derivative and a cyclic bisparaquat derivative exhibits a rather high association constant and leads to the observation of a poly[2]pseudocatenane structure in the solid state for the first time. Currently, we are focusing on introducing similar structures into polymers and preparation of pseudocryptand-based polypseudorotaxanes.

7.4 Acknowledgements

This work was supported by the National Science Foundation (DMR0704076) and the Petroleum Research Fund administered by the American Chemical Society (47644-AC).

7.5 Experimental section

7.5.1 Materials and methods

BMP32C10 derivative **1c**,[7] bisparaquat **2**[5a] and **CBPQT 3**[16] were prepared according to literature procedures. Solvents were either used as purchased or dried according to literature procedures. ^{1}H-NMR spectra were obtained on JEOL ECLIPSE-500 and INOVA-400 spectrometers with internal standard TMS. HR-MS were obtained by employing an Agilent LC-ESI-TOF.

7.5.2 Determination of Δ_0 for $\mathbf{1c_2{\cdot}2}$

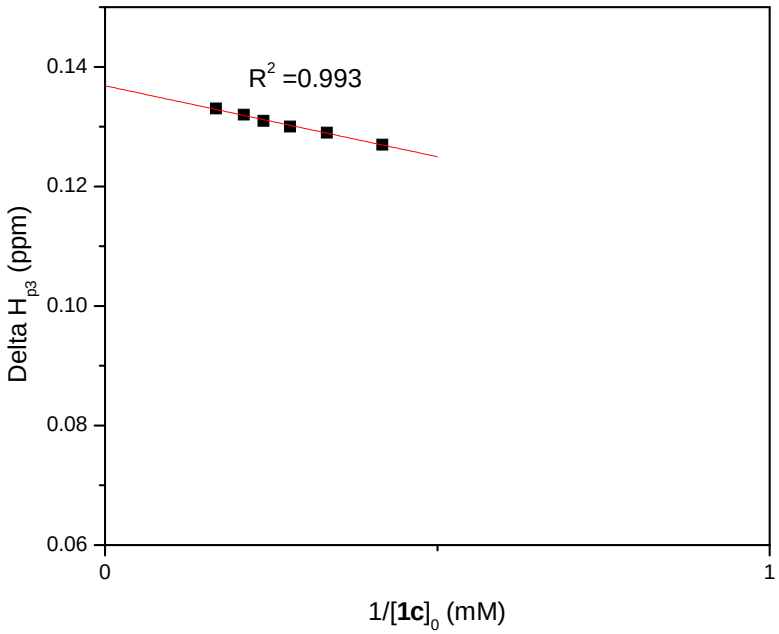

Figure 7-6. Determination of Delta$_0$ of $\mathbf{1c_2{\cdot}2}$ in acetone-d$_6$. [**2**]$_0$ = 0.50 mM. Δ_0 = 0.137 ppm.

7.5.3 Determination of Δ_0 for 1c·3

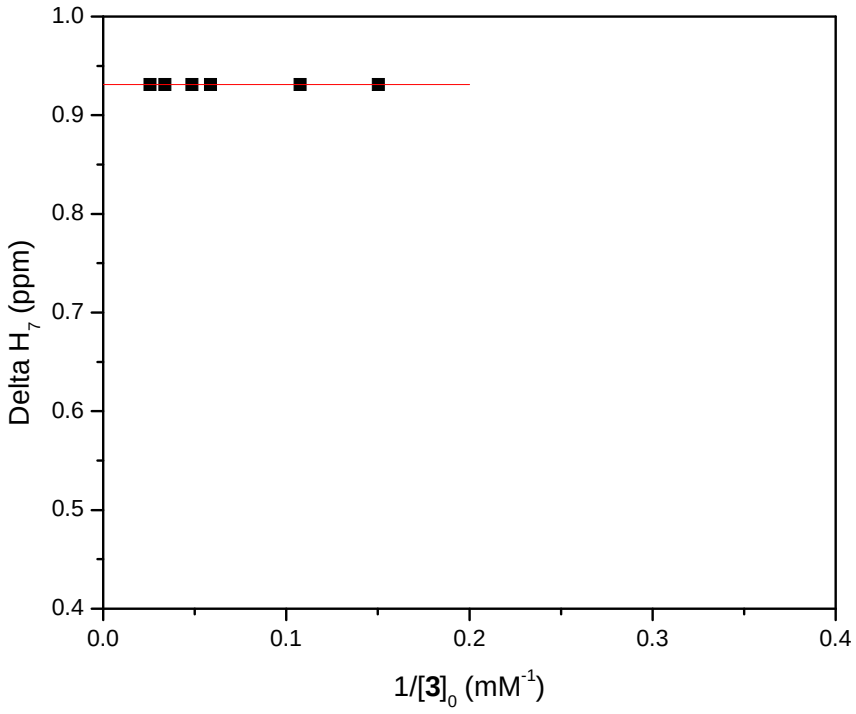

Figure 7-7. Determination of Delta$_0$ of **1c·3** in acetonitrile-d$_3$. [**1c**]$_0$ = 0.85 mM. Δ_0 = 0.930 ppm.

7.5.4 Mass spectrum of $1c_2$·2

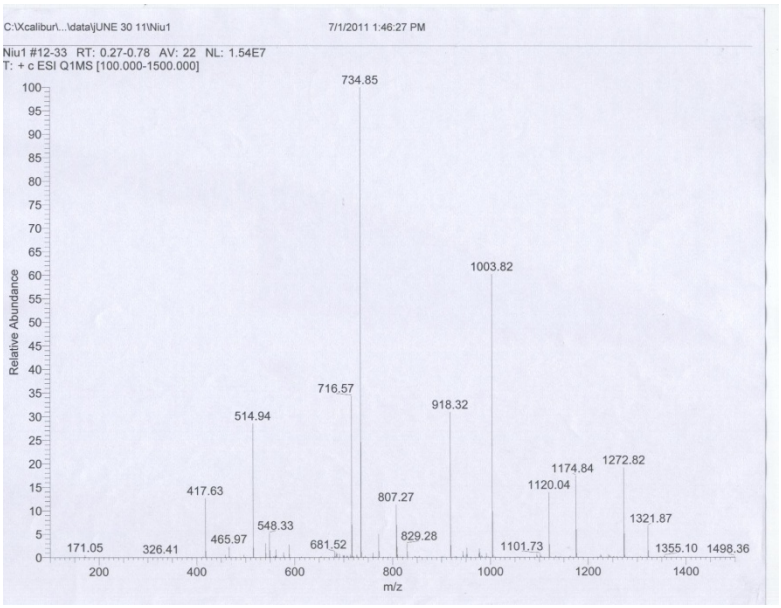

Figure 7-8. Electrospray ionization (ESI) mass spectrum of **$1c_2$·2**.

7.5.5 Mass spectrum of 1c·3

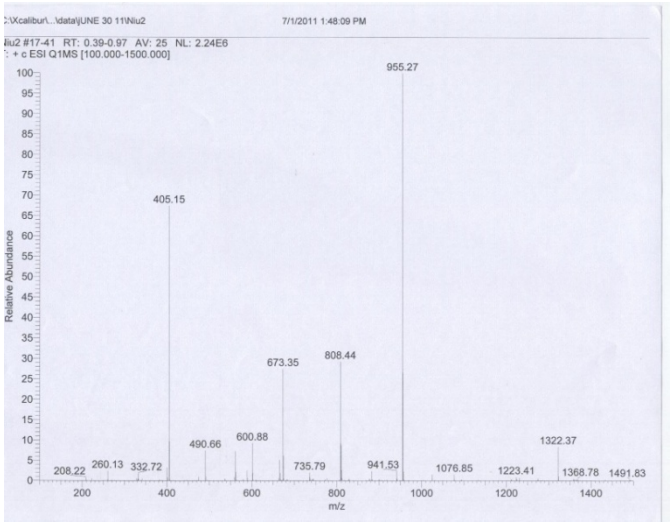

Figure 7-9. Electrospray ionization (ESI) mass spectrum of **1c·3**.

7.5.6 Crystal structure of 1c·3

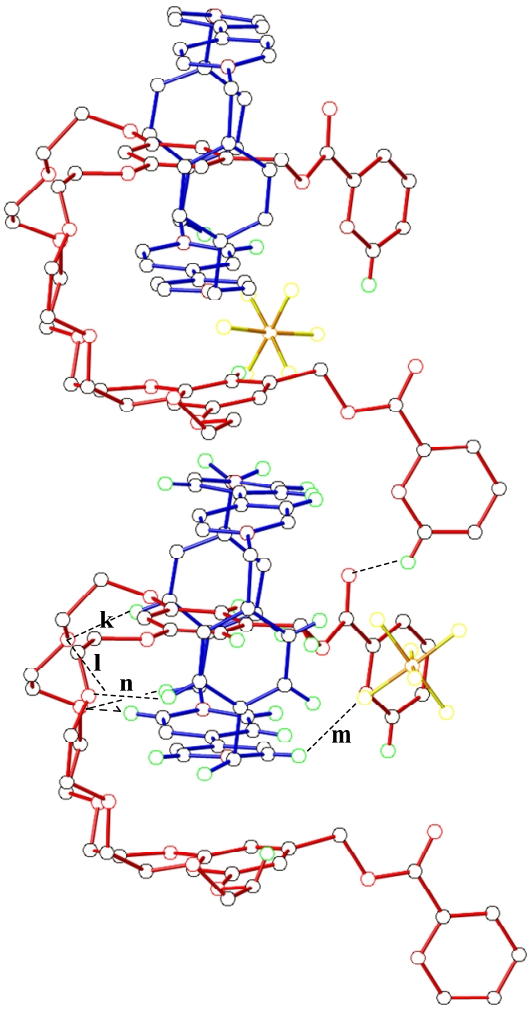

Figure 7-10. Another view of the X-ray structure of poly(**1c·3**). **1c** is red. **3** is blue. Solvent molecules, PF_6^- ions and hydrogen atoms except the ones involved in hydrogen bonding have been omitted for clarity. Hydrogen bonds shown in Figure 7-5 were omitted for clarity. Selected hydrogen-bond parameters: H···O(F, N) distances (Å), C···O(F, N) distances (Å), C-H···O(F, N) angles (deg): k 2.61, 3.35, 135; l 2.66, 3.36, 131; m 2.41, 3.10, 130; n 2.29, 3.13, 146.

References

(1) (a) Huang, F.; Gibson, H. W. *Prog. Polym. Sci.* **2005**, *30*, 982-1018. (b) Lehn, J.-M. *Chem. Soc. Rev.* **2007**, *36*, 151-160. (b) Stoddart, J. F. *Chem. Soc. Rev.* **2009**, *38*, 1802-1820. (c) De Greef, T. F. A.; Smulders, M. M. J.; Wolffs, M.; Schenning, A. P. H. J.; Sijbesma, R. P.; Meijer, E. W. *Chem. Rev.* **2009**, *109*, 5687-5754. (d) Harada, A.; Hashidzume, A.; Yamaguchi, H.; Takashima, Y. *Chem. Rev.* **2009**, *109*, 5974-6023. (e) Niu, Z.; Gibson, H. W. *Chem. Rev.* **2009**, *109*, 6024-6046. (f) Fang, L.; Olson, M. A.; Benitez, D.; Tkatchouk, E.; Goddard III, W. A.; Stoddart, J. F. *Chem. Soc. Rev.* **2010**, *39*, 17-29. (g) Durola, F.; Sauvage, J.-P.; Wenger, O. S. *Coord. Chem. Rev.* **2010**, *254*, 1748-1759.

(2) (a) Champin, B.; Mobian, P.; Sauvage, J.-P. *Chem. Soc. Rev.* **2007**, *36*, 358-366. (b) Hembury, G. A.; Borovkov, V. V.; Inoue, Y. *Chem. Rev.* **2007**, *108*, 1-73. (c) Bonnet, S.; Collin, J.-P. *Chem. Soc. Rev.* **2008**, *37*, 1207-1217. (d) Angelos, S.; Khashab, N. M.; Yang, Y.-W.; Trabolsi, A.; Khatib, H. A.; Stoddart, J. F.; Zink, J. I. *J. Am. Chem. Soc.* **2009**, *131*, 12912-12914. (e) Leung, K. C.-F.; Chak, C.-P.; Lo, C.-M.; Wong, W.-Y.; Xuan, S.; Cheng, C. H. K. *Chem. Asian J.* **2009**, *4*, 364-381. (f) Higashi, T.; Hirayama, F.; Misumi, S.; Arima, H.; Uekama, K. *Biomaterials* **2008**, *29*, 3866-3871. (g) Bilkova, E.; Sedlak, M.; Dvorak, B.; Ventura, K.; Knotek, P.; Benes, L. *Org. Biomol. Chem.* **2010**, *8*, 5423-5430. (h) Thomas, C. R.; Ferris, D. P.; Lee, J.-H.; Choi, E.; Cho, M. H.; Kim, E. S.; Stoddart, J. F.; Shin, J.-S.; Cheon, J.; Zink, J. I. *J. Am. Chem. Soc.* **2010**, *132*, 10623-10625. (i) Liu, J.; Du, X.; Zhang, X. *Chem. Eur. J.* **2011**, *17*, 810-815. (j) Chen, G.; Jiang, M. *Chem. Soc. Rev.* **2011**, *40*, 2254-2266. (k) Li, J.; Zhao, F.; Li, J. *Adv. Biochem. Eng. Biotechn.* **2011**, 1-43.

(3) (a) Gibson, H. W. In *Large Ring Molecules*; Semlyen, J. A., Ed.; John Wiley & Sons: New York, 1996; p 191. (b) Raymo, F. M.; Stoddart, J. F. *Chem. Rev.* **1999**, *99*, 1643-1664. (c) Harada, A. *Acc. Chem. Res.* **2001**, 34, 456-464. (d) Hernandez, J. V.; Kay, E. R.; Leigh, D. A. *Science* **2004**, 306, 1532–1537.

(4) Shen, Y. X.; Engen, P. T.; Berg, M. A. G.; Merola, J. S.; Gibson, H. W. *Macromolecules* **1992**, *25*,2786-2788.

(5) (a) Huang, F.; Fronczek, F. R.; Gibson, H. W. *J. Am. Chem. Soc.* **2003**, *125*, 9272-9273. (b) Huang, F.; Guzei, I. A.; Jones, J. W.; Gibson, H. W. *Chem. Commun.* **2005**, 1693-1695. (c) Bigot, J.; Bria, M.; Caldwell, S. T.; Cazaux, F.; Cooper, A.; Charleux, B.; Cooke, G.; Fitzpatrick, B.; Fournier, D.; Lyskawa, J.; Nutley, M.; Stoffelbach, F.; Woisel, P. *Chem. Commun.* **2009**, 5266-5268. (d) Stephenson, R. M.; Wang, X.; Coskun, A.; Stoddart, J. F.; Zink, J. I. *Phys. Chem. Chem. Phys.* **2010**, *12*, 14135-14143. (e) Hmadeh, M.; Fahrenbach, A. C.; Basu, S.; Trabolsi, A.; Benítez, D.; Li, H.; Albrecht-Gary, A.-M.; Elhabiri, M.; Stoddart, J. F. *Chem. Eur. J.* **2011**, *17*, 6076-6087.

(6) Some recent publications: (a) Huang, F.; Fronczek, F. R.; Gibson, H. W. *J. Am. Chem. Soc.* **2003**, *125*, 9272-9273. (b) Huang, F.; Zhou, L.; Jones, J. W.; Gibson, H. W.; Ashraf-Khorassani, M. *Chem. Commun.* **2004**, 2670-2671. (c) Huang, F.; Switek, K. A.; Zakharov, L. N.; Fronczek, F. R.; Slebodnick, C.; Lam, M.; Golen, J. A.; Bryant, W. S.; Mason, P. E.; Rheingold, A. L.; Ashraf-Khorassani, M.; Gibson, H. W. *J. Org. Chem.* **2005**, *70*, 3231-3241. (d) Gibson, H. W.; Wang, H.; Slebodnick, C.; Merola, J.; Kassel, S.; Rheingold, A. L. *J. Org. Chem.* **2007**, *72*, 3381-3393. (e) Pederson, A. M.-P.; Vetor, R. C.; Rouser, M. A.; Huang, F.; Slebodnick, C.; Schoonover, D. S.; Gibson, H. W.; *J. Org. Chem.* **2008**, *73*, 5570-5573. (f) Li, S.; Zheng, B.; Huang, F.; Zakharov, L.; Slebodnick, C. Rheingold, A.; Gibson, H. W. *Sci. China Chem.* **2010**, *53*, 858-862. (g) Zhang, M.; Zhu, K.; Huang, F. *Chem. Commun.* **2010**, *46*, 8131-8141. (h) Liu M.; Li, S.; Hu, M.; Wang, F.; Huang, F. *Org. Lett.* **2010**, 12, 760-763. (i) Zhang, M.; Zheng, B.; Xia, B.; Zhu, K.; Wu, C.; Huang, F. *Eur. J. Org. Chem.* **2010**, 6804-6809.

(7) Niu, Z.; Slebodnick, C.; Schoonover, D.; Azurmendi, H.; Harich, K.; Gibson, H. W. *Org. Lett. ASAP*.(DOI 10.1021/ol201502r)

(8) (a) Tsukube, H.; Furuta, H.; Odani, A.; Takeda, Y.; Kudo, Y.; Inoue, Y.; Liu, Y.; Sakamoto, H.; Kimura, K. in *Comprehensive Supramolecular Chemistry*, Atwood,

J. L.; Davies, J. E. D.; MacNicol, D. D.; Vogtle, F.; Lehn, J.-M.; Ed.; Elsevier Science Ltd., New York, 1996, pp. 425-479. (b) Hirose, K. *J. Inclusion Phenom. Macrocyclic Chem.* **2001**, *39*, 193-209. (c) Bruneau, E.; Lavabre, D.; Levy, G.; Micheau, J. C. *J. Chem. Educ.* **1992**, *69*, 833-837.

(9) See experimental section.

(10) K_1=[**1c**·**2**]/{[**1c**][**2**]} and K_2 = [**1c**$_2$·**2**]/{[**1c**][**1c**·**2**]}. The intercept of the linear fit straight line based on the first three data points for low *p* (Figure 7-2, lower plot) gave the value of $2K_2$-K_1, while the slope of the last four data points for high *p* (Figure 7-2) gave the value of $-2K_2$.[11c]

(11) (a) Marshall, A. G. In *Biophysical Chemistry: Principles, Techniques, and Applications*, John Wiley & Sons, New York, NY., 1978, pp 70-77. (b) Freifelder, D. M. In *Physical Biochemistry*, W. H. Freeman and Co., New York, 1982, pp 659-660. (c) Perlmutter-Hayman, B. *Acc. Chem. Res.* **1986**, *19*, 90-96. (d) Connors, K. A. In *Binding Constants*; J. Wiley and Sons, New York, 1987, pp 78-86.

(12) (a) Hunter, C. A.; Sanders, J. K. M.; *J. Am. Chem. Soc.* **1990**, *112*, 5525-5534. (b) Hohenstein, E. G.; Sherrill, C. D. *J. Phys. Chem. A* **2009**, *113*, 878-886.

(13) Job, P. *Ann. Chim. Appl.* **1928**, 113-203.

(14) ^{1}H-NMR characterizations were done on solutions with constant [**1c**] and varied [**3**]. Based on these NMR data, Δ_o, the difference in δ values for proton H_7 of **1c** in the uncomplexed and fully complexed species, was determined to be 0.930 ppm as the y-intercept of a plot of $\Delta = \delta - \delta_u$ *vs.* $1/[\mathbf{2}]_0$ in the high initial concentration range of **2**. K_a was calculated from $K_a = (\Delta/\Delta_0)/[(1-\Delta/\Delta_0)([\mathbf{2}]_0-\Delta/\Delta_0\ [\mathbf{1c}]_0)$. Δ/Δ_0 values between 0.2 to 0.8 were used. When the ratio of $[\mathbf{3}]_0/[\mathbf{1c}]_0$ was higher than 7.9/1, no further chemical shift change was observed and **1c** was considered to be fully complexed.

(15) (a) Zhu, X.-Z.; Chen, C.-F. *J. Am. Chem. Soc.* **2005**, *127*, 13158-13159. (b) Zhu, X.-Z.; Chen, C.-F. *Chem. Eur. J.* **2006**, *12*, 5603-5609. (c) Chu, Y.; Hoffman, D. W.; Iverson, B. L. *J. Am. Chem. Soc.* **2009**, *131*, 3499-3508.

(16) Odell, B.; Reddington, M. V.; Slawin, A. M. Z.; Spencer, N.; Stoddart, J. F.;

Williams, D. J. *Angew. Chem. Int. Ed.* **1988**, *27*, 1547-1550.

TOC Graphic:

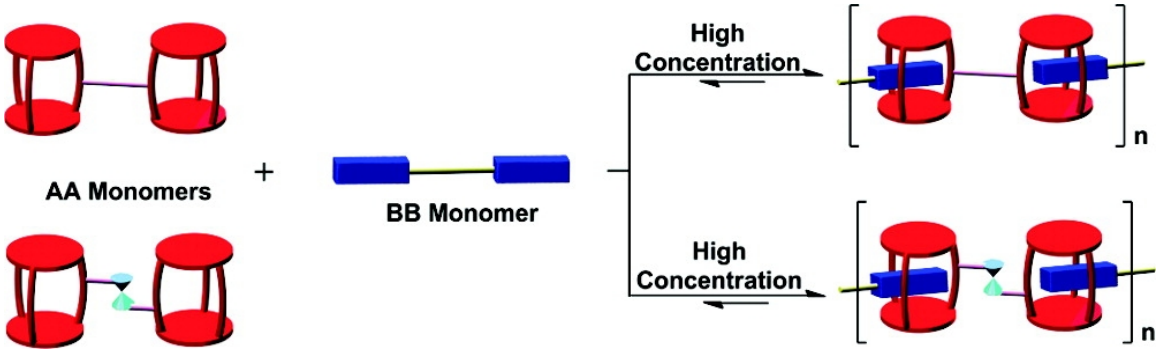

Abstract:

Two novel bis(*meta*-phenylene)-32-crown-10-based cryptands, bearing covalent and metal complex linkages, were designed and prepared. By employing the self-assembly of these biscryptands, which can be viewed as AA monomers, and a bisparaquat, which can be viewed as a BB monomer, the first AA BB-type linear supramolecular polymers with relatively high molecular weights were successfully prepared.

Chapter 8.

Supramolecular AA BB-Type Linear Polymers with Relatively High Molecular Weights via the Self-Assembly of Bis(*meta*-phenylene)-32-Crown-10 Cryptands and a Bisparaquat Derivative

8.1 Introduction

Due to architectural differences from traditional covalent polymers, supramolecular polymers, in which non-covalent mechanically interlocked structures play an important role, are expected to have unique properties and potential applications.[1] In the past decade, supramolecular polymers have been widely studied and a large variety is known.[2-6] Among them, crown-ether-based pseudorotaxane-type supramolecular polymers are very attractive and have been used to prepare different architectures, such as linear,[3] branched,[4] star-shaped[5] and dendronized.[6] However, in order to prepare large supramolecular polymers, monomers with high association constant are required.[3d,3e,7] Cryptands have proved to be much better hosts than corresponding simple crown ethers for paraquat derivatives;[8] for example, the association constant between hydroxyl-functionalized cryptand **6** and dimethyl paraquat (K_a = 6.3 x 10^3 M^{-1} in acetone at 22 °C) is about 13-fold higher than that between bis(*meta*-phenylene)-32-crown-10 (BMP32C10) and dimethyl paraquat.[8d] Morover, unlike the complexes between BMP32C10 and paraquat derivatives with folded or "taco" structures,[9] the complexes between cryptands and paraquat derivatives only demonstrate threaded geometries (pseudorotaxanes) in their X-ray crystal structures.[8] Particularly relevant is the X-ray crystal structure of the pseudorotaxane complex of **6** with dimethyl paraquat.[8d]

Here we report the first two examples of novel AA-BB-type non-covalent supramolecular polymers with relatively high molecular weights based on BMP32C10 cryptands, bearing a covalent linkage (terephthalate) or a metal complex linkage (ferrocene ester), and a bisparaquat.

The resulting supramolecular polymers are expected to have well-defined threaded (pseudorotaxane) structures, making it possible to convert them to rotaxanes by attaching bulky stoppers to the ends of the paraquat moieties.

8.2 Results and discussion

The biscryptands **3** and **4** (AA monomers) were prepared via the 1-(3'-dimethylaminopropyl)-3-ethylcarbodiimide hydrochloride (EDCI) and 4-dimethylaminopyridine (DMAP) promoted coupling reaction of hydroxyl-functionalized cryptand **6**[8d] with terephthalic acid and 1,1'-ferrocenedicarboxylic acid, respectively. The linkers were chosen to assess conformational effects, **4** being much more flexible because of its turnstile-like rotational possibilities vs. **3**, whose rigid linker imposes a rod-like structure. The bisparaquat **5** (BB monomer) was obtained via the reaction between 1-methyl-4,4'-bipyridinium PF_6 and 1,10-dibromodecane followed by counterion exchange; the rather long ten carbon spacer was chosen based on theory[10] and our earlier studies that demonstrated more polymerization and less cyclization the longer the spacer.[3d,11] As a result of the intermolecular complexation between equivalent amounts of AA monomers **3** and **4** with BB monomer **5** in solution, we expected linear supramolecular, non-covalent polymers **1** and **2** to form at high concentrations (Scheme 8-1).

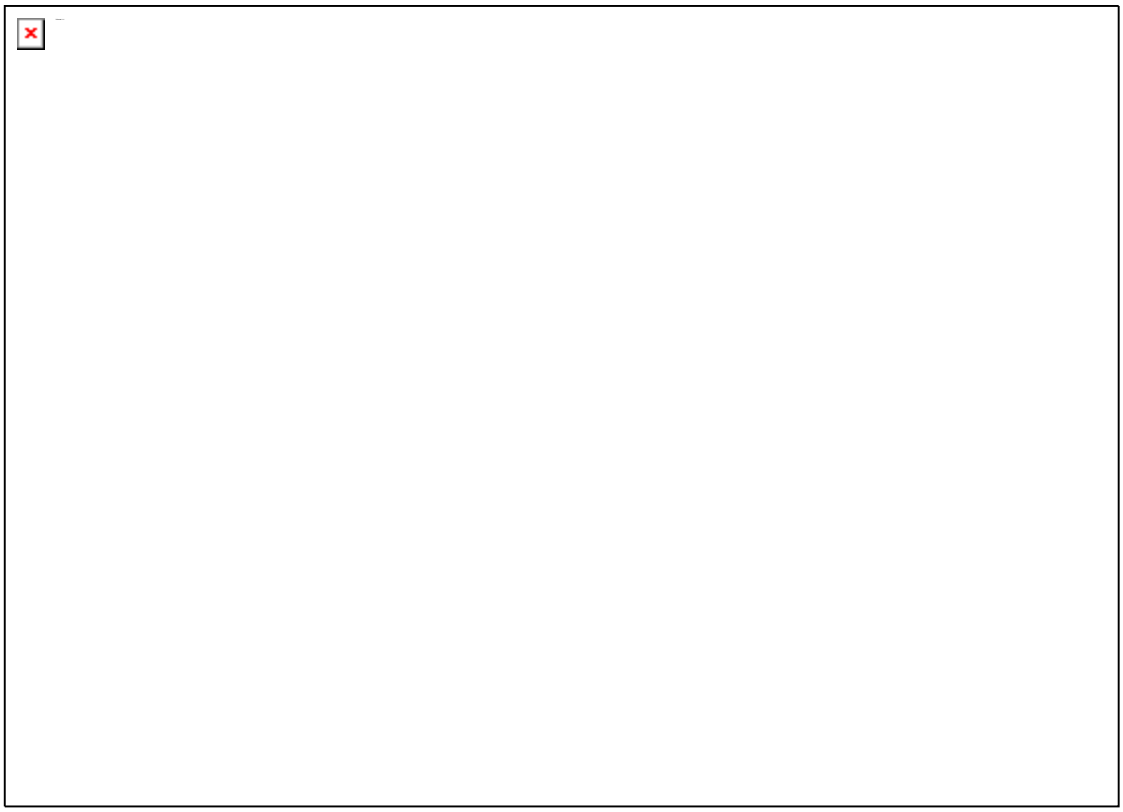

Scheme 8-1. Schematic illustration of the formation of linear supramolecular polymers **1** and **2** by self-assembly of AA monomers **3** and **4** with BB monomer **5**.

Equimolar solutions of **3** and **5** in chloroform:acetonitrile (1:1, v/v) were deep yellow due to the charge-transfer interaction between the electron-rich aromatic rings of biscryptand **3** and the electron-poor pyridinium rings of bisparaquat **5**, which was good evidence for complexation. The ^{1}H-NMR spectra were concentration dependent (Figure 8-1), indicating the involvement of fast-exchanging noncovalent interactions in solution. The large chemical shift change (~0.8 ppm) of H_2 on biscryptand **3** demonstrated that the percentage of complexed species was concentration dependent and the formation of the supramolecular polymer was favored at high concentrations. In addition, all the proton signals became broad at high concentrations, which indicated the formation of high molecular weight polymeric structures. Based on the chemical shift change of H_2 of biscryptand **3**, the fraction *p* of the complexed biscryptand **3**[12a] and degree of polymerization *n* were estimated by employing the Carothers equation (Table 8-1).[12b] With

increasing initial concentrations, the size of the aggregates increased to large values and a supramolecular non-covalent polymer was formed. For example, at 290 mM, the degree of polymerization (*n)* was estimated to be 93 (±47),[12c] which corresponds to polymer **1** with molecular weight (M_n) 241 kDa, which is much higher than the BMP32C10-based systems at similar concentrations.[3a,3e-3g]

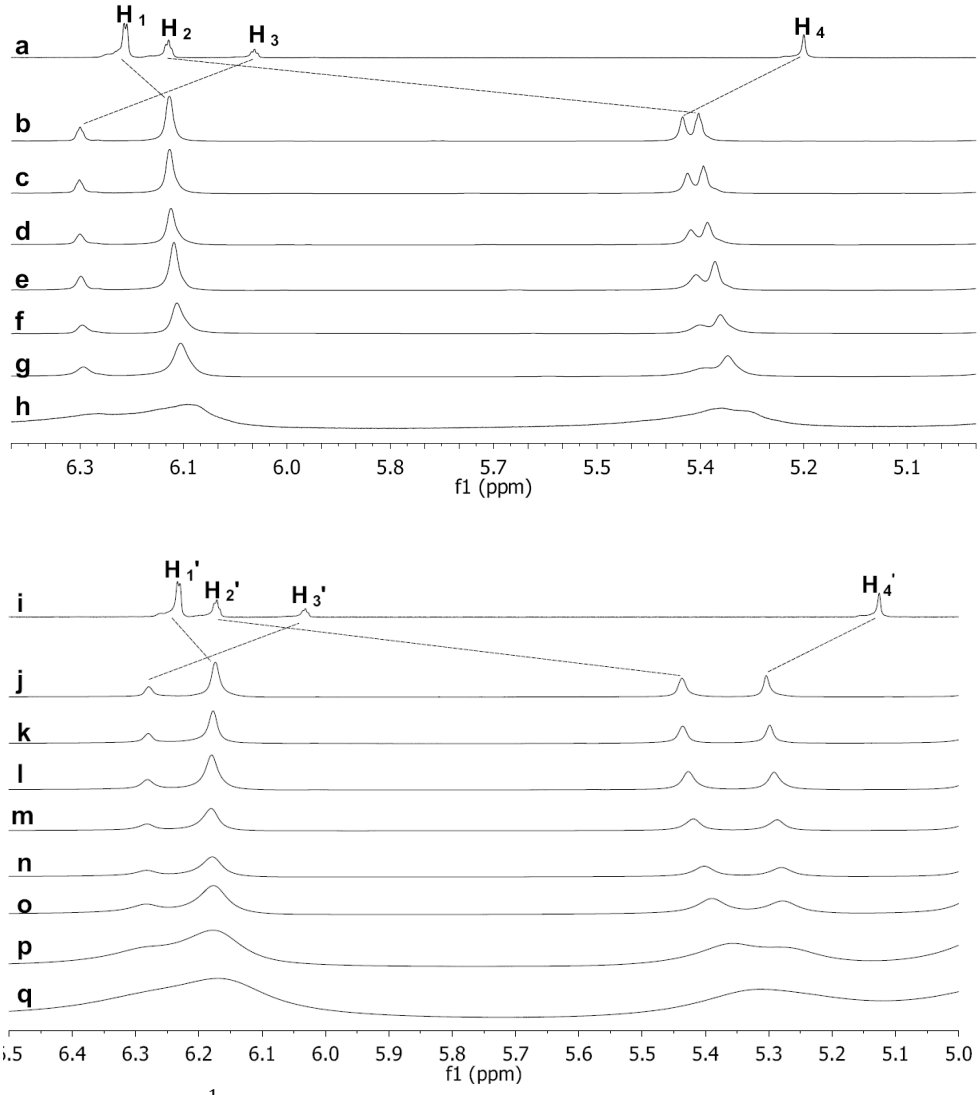

Figure 8-1. Partial ^{1}H-NMR spectra (500 MHz, $CDCl_3/CD_3CN$ = 1/1 <v/v>, 22 ℃). Upper stacked spectra: (a) **3**; equimolar solutions of **3** and **5** at different concentrations: (b) 87, (c) 135, (d) 164, (e) 212, (f) 247, (g) 290, (h) 380 mM. Lower stacked spectra: (i) **4**; equimolar solutions of **4** and **5** at different concentrations: (j) 53, (k) 74, (l) 85, (m) 123, (n) 179, (o) 230, (p) 322, (q) 402 mM.

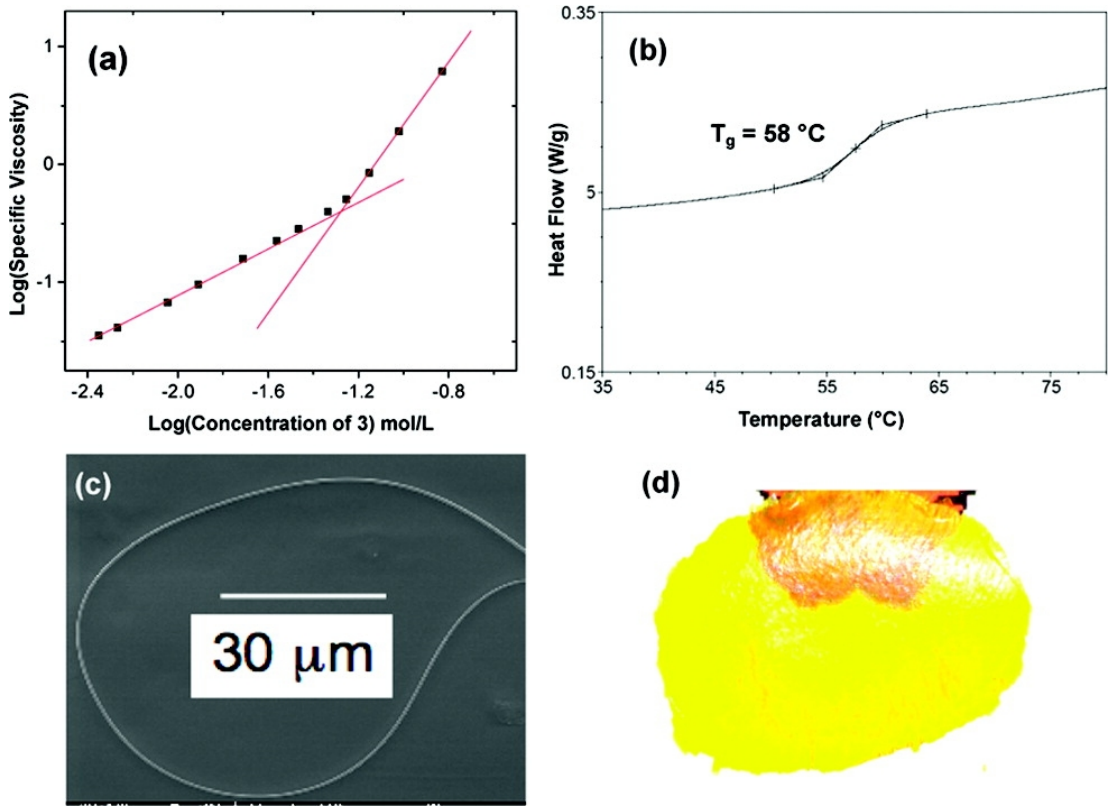

Figure 8-2 (a) Double-logarithmic plot of specific viscosity of equimolar solutions of 3 and 5 in chloroform/acetonitrile (1/1, v/v) versus concentration. (b) DSC curve of supramolecular polymer 1 (second heating); heating rate 10 °C/min. (c) Scanning electron microscopy (SEM) micrograph of (gold coated) fiber drawn from a concentrated solution of equimolar 3 and 5. (d) Yellow film cast from an equimolar solution of 3 and 5.

Alternatively, using the K_a value for the model complexation of **6** with dimethyl paraquat[8d] in the equation[3e,7] $n = (K_a[\text{conc}])^{1/2}$ at 290 mM we calculate n = 43, M_n = 112 kDa for polymer **1**. This equation implicitly assumes that the process is isodesmic and produces no cyclic species and therefore these values are upper bounds.

Further direct physical evidence for the formation of a large supramolecular non-covalent polymer was obtained from a viscosity study. A double-logarithmic plot of specific viscosity versus the initial concentration of equimolar solutions of **3** and **5** in chloroform:acetonitrile (1:1, v/v) yielded a curve with slope 1.02 at low concentrations, indicating the existence of cyclic

species[13] as with other crown ether-based systems.[3] At high concentrations, the curve had a slope of 2.64, indicating the formation of linear supramolecular polymer **1** of increasing size. The critical monomer concentration, $[M]_{crit}$, above which the linear species are formed exclusively, was 53 mM.[14]

As for the interaction between **4** and **5**, similarly, large chemical shift changes of H_2' were observed, dependent on initial concentrations of **4** and **5** (Figure 8-1). All the proton signals were broadened at high concentrations, indicating the formation of large supramolecular species. By determination of p[12a] and employing the Carothers equation,[12b] the degree of polymerization n was estimated (Table 8-2). For example, at 230 mM, the degree of polymerization (*n)* was estimated to be 22 (±2),[12c] which corresponds to polymer **2** with molecular weight (M_n) 59 kDa. In a plot of log(specific viscosity) vs. log(concentration) solutions of **4** and **5** yielded slopes of 1.27 at low concentrations and 2.77 at high concentrations and $[M]_{crit}$ = 71 mM; the higher $[M]_{crit}$ suggested that cyclic species were more abundant in polymer **2** than in polymer **1**, ascribed to the relatively flexible ferrocene linkage, which can rotate in solution, and may favor the formation of cyclic species by reducing the end-to-end distances of linear $(AABB)_n$ species. [10] Since the n values estimated from the NMR results are based on the assumption that there are no cyclic species,[12] these values are erroneously high.

The [M]crit values for **3**/**5** and **4**/**5** are in the range reported for ditopic ureidopyrimidone (UPy) systems: 10-200 mM.[2b,2c] However, the slopes above [M]crit are lower compared to those of the latter systems (slopes of 3-6)[2b,2c] and the theoretically predicted value of 3.5-3.7,[15] consistent with the lower association constant of the present system relative to the UPy systems ($K_a > 10^7$ M^{-1}). Nonetheless, these slopes are among the highest values reported for pseudorotaxane-based supramolecular polymers. Moreover, at the highest measured concentration, 149 mM, the specific viscosity of an equimolar solution of **3** and **5** was 6.3. This is the highest specific viscosity reported for a supramolecular polymer based on pseudorotaxane formation, reflecting the relatively high association constant in this system vs. previously studied crown ether-based systems ($K_a < 10^3$ M^{-1}).

Differential scanning calorimetry (DSC) revealed that the solid from evaporation of solutions of **3** and **5** had a repeatable T_g of 58 °C (Figure 8-2) and the solid from **4** and **5** had a T_g of 47 °C. In contrast, the hosts **3** and **4** and the guest **5** are all crystalline solids (mp 177-8, 75-6

and 276-8 ^{o}C, respectively), but no melting transitions were observed in the solid supramolecular polymers, nor was crystallization observed up to 180 ^{o}C. Thermogravimetric analyses (TGA) revealed that supramolecular polymer **1** underwent 5% weight loss up to 241 °C and supramolecular polymer **2** up to 291 °C.

In addition, flexible, amorphous and transparent films (Figure 8-2d) were cast from concentrated equimolar solutions of **3** and **5**. Such films can generally only be formed by entanglement of linearly connected macro-sized aggregates. Also, although no fibers could be drawn from the individual highly concentrated solutions of monomers **3**, **4** and **5**, long thin fibers could be drawn easily from concentrated equimolar solutions of **3** and **5** (Figure 8-2c), which formed in a manner analogous to dry spinning used for covalently bonded polymers.[16] This provided further direct evidence for the formation of supramolecular polymer **1**. Similarly, a brittle film was cast from a concentrated equimolar solution of **4** and **5** and thin fibers were drawn from the concentrated equimolar solutions of **4** and **5** (see SI). The brittle nature of the films of polymer **2** derived from the flexible monomer **4** was surprising to us; it appears that because of the enhanced possibility of cyclization of **4** with **5**[10] the degree of polymerization of polymer **2** is significantly less than that of polymer **1**, as also indicated by the NMR results.

8.3 Conclusions

In summary, we demonstrated the first formation of AA BB type linear supramolecular polymers based on BMP32C10 cryptands. These supramolecular polymers with well-defined pseudorotaxane structures provide a promising route to irreversibly mechanically linked polymers by attachment of bulky stoppers to the ends of , -difunctional bisparaquat derivatives to form rotaxane units, as demonstrated in several ways with small molecule pseudorotaxanes.[17-20] These extensions will be reported in our future publications.

8.4 Acknowledgements

This work was supported by the National Science Foundation (DMR0704076) and the Petroleum Research Fund administered by the American Chemical Society (47644-AC). We also acknowledge the National Science Foundation for funds to purchase the Agilent 6220 Accurate Mass TOF LC/MS Spectrometer (CHE-0722638). We thank Mr. Stephen McCartney for SEM analysis, Mr. Mason Rouser for providing 1-methyl-4,4'-bipyridinium PF_6 and Dr. Minjae Lee for instruction and assistance in measuring viscosities.

8.5 Experimental section

8.5.1 Materials and methods

Terephthalic acid, 1,1'-ferrocenedicarboxylic acid, 1,10-dibromodecane, ammonium hexafluorophosphate, 1-(3'-dimethylaminopropyl)-3-ethylcarbodiimide hydrochloride (EDCI) and 4-dimethylaminopyridine (DMAP) were reagent grade and used as received. The hydroxyl-functionalized cryptand **6**[8d] and 1-methyl-4,4'-bipyridinium PF_6[21] were prepared according to literature procedures. Solvents were either used as purchased or dried according to literature procedures. ^{1}H-NMR spectra were obtained on a JEOL ECLIPSE-500 spectrometer with internal standard TMS. ^{13}C-NMR spectra were collected on a JEOL ECLIPSE-500 spectrometer at 125 MHz. HR-MS were obtained by employing an Agilent LC-ESI-TOF. Viscosity studies were performed with using Cannon-Ubbelohde semi-micro viscometers at 26.5 °C in chloroform/acetonitrile (1/1, v/v). Differential scanning calorimetry (DSC) investigations were carried out on a DSC 2910 (TA Instruments). Thermogravimetric analyses (TGA) were performed on a TGA Q100 (TA Instruments) under an atmosphere of nitrogen. Scanning electron microscopy investigations were carried out on a QUANTA 600 FEG (FEI Company).

8.5.2 Synthesis of biscryptand 3

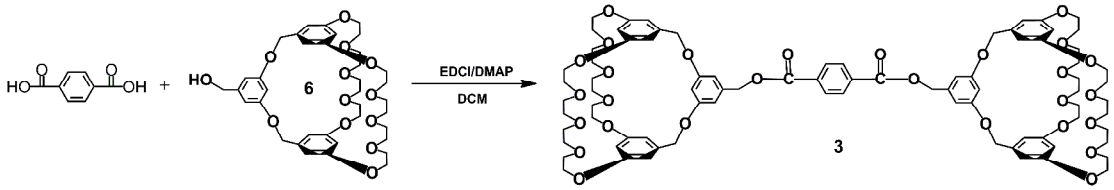

Scheme 8-2. Synthesis of biscryptand **3** via EDCI/DMAP coupling method.

Hydroxyl-functionalized cryptand **6** (300 mg, 0.43 mmol), terephthalic acid (34.0 mg, 0.21 mmol), EDCI (82.0 mg, 0.43 mmol) and DMAP (52.7 mg, 0.43 mmol) were dissolved in dichloromethane (DCM, anhydrous, 50 mL). The solution was stirred under N_2 for 4 days at room temperature. The reaction mixture was washed with DI water (3 times) and a pale yellow solid was obtained after solvent was removed. The solid was dried in a vacuum oven with P_2O_5 overnight. The crude product was purified via a silica gel column by employing gradient elution (DCM to DCM : methanol = 98 : 2) to afford biscryptand **3** as a white powder (295 mg, 92%), mp 177.0-178.2 °C. ^{1}H-NMR ($CDCl_3$, 500 MHz) (Figure 8-3): δ (ppm): 8.20 (s, 4 H), 6.70 (d, ^4J = 2 Hz, 4 H), 6.31 (t, ^4J = 2 Hz, 4 H), 6.26 (d, ^4J = 2 Hz, 8 H), 6.12 (t, ^4J = 2 Hz, 2 H), 5.34 (s, 4 H), 4.99 (s, 8.0 H), 3.80-3.95 (m, 32 H), 3.95 (br, 32 H). ^{13}C-NMR ($CDCl_3$, 125 MHz) (Figure 8-4): δ (ppm): 165.71, 160.14, 160.05, 139.51, 137.98, 134.10, 129.92, 108.91, 104.04, 101.63, 100.66, 71.05, 70.58, 70.21, 69.77, 67.65, 66.80. HR-ESIMS (Figure 8-5): calcd. for $[M + H]^+$: 1531.6317, found: *m/z*, 1531.6363 $[M + H]^+$, error: 2.98 ppm.

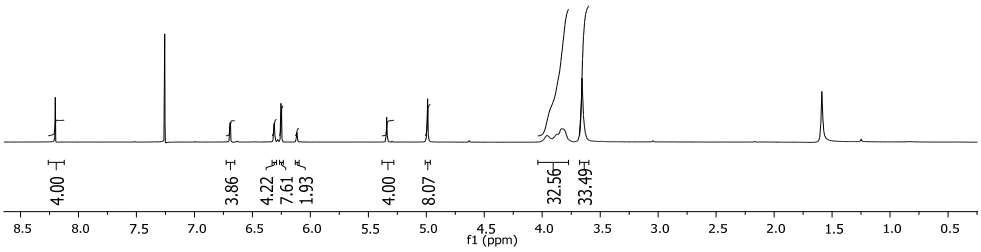

Figure 8-3. ^{1}H-NMR ($CDCl_3$, 500 MHz, room temperature) of biscryptand **3**.

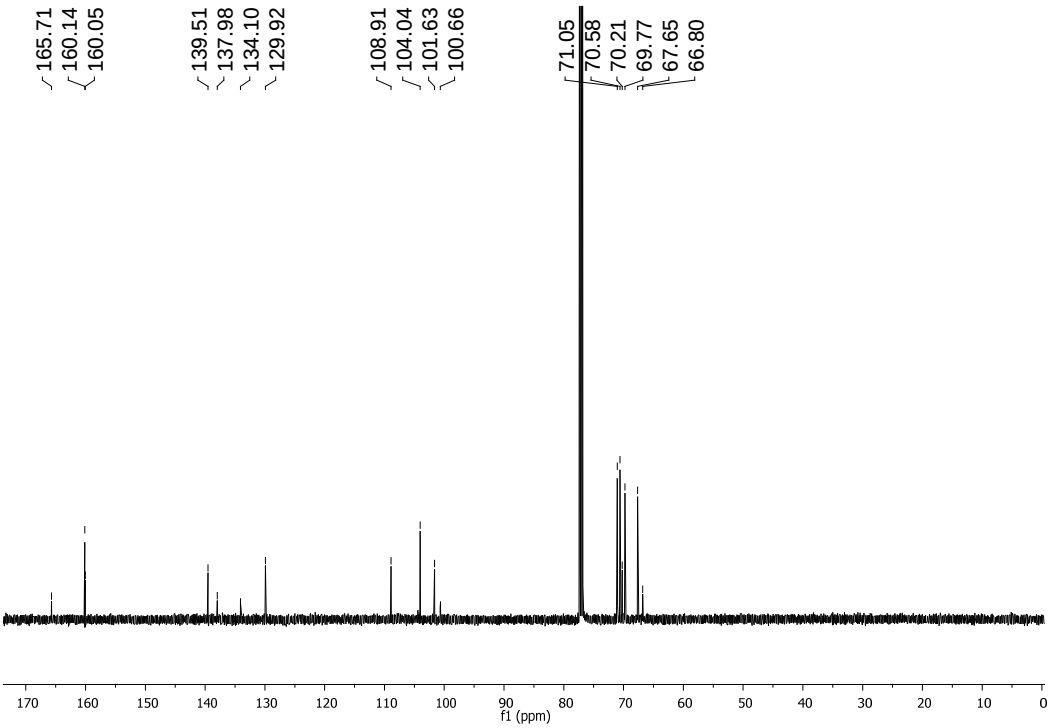

Figure 8-4. ^{13}C-NMR ($CDCl_3$, 125 MHz, room temperature) of biscryptand **3**.

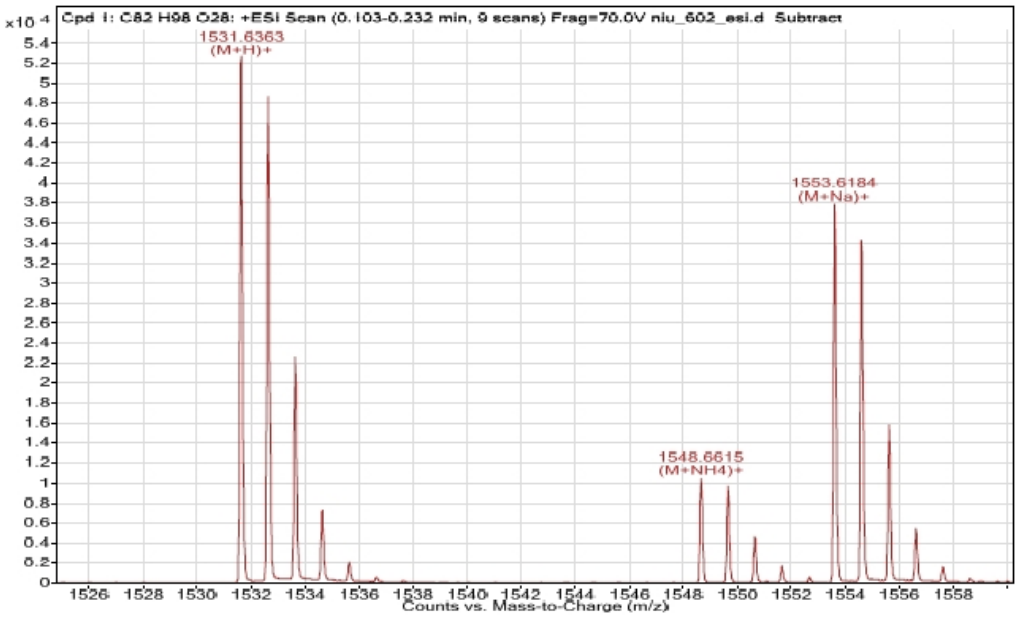

Figure 8-5. Electrospray ionization mass spectrum of biscryptand **3**.

8.5.3 Synthesis of biscryptand 4

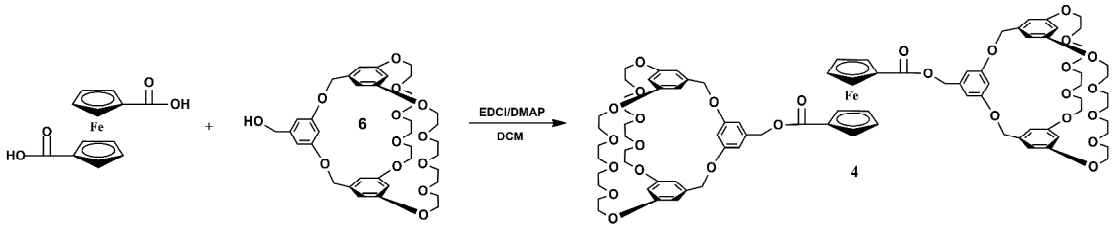

Scheme 8-3. Synthesis of biscryptand **4** via EDCI/DMAP coupling method.

Hydroxyl-functionalized cryptand **6** (315 mg, 0.45 mmol), terephthalic acid (59.1 mg, 0.22 mmol), EDCI (86.3 mg, 0.45 mmol) and DMAP (54.7 mg, 0.45 mmol) were dissolved in DCM (anhydrous, 50 mL)/DMF (anhydrous, 2 mL). The solution was stirred under N_2 for 4 days at room temperature. The reaction mixture was washed with DI water (5 times) and a dark-red oil was obtained after solvent was removed. The oil was dried in a vacuum oven with P_2O_5 overnight. The crude product was purified via a silica gel column (hexane : ethyl acetate = 1 : 10

to DCM : methanol = 96 : 4) to afford biscryptand **4** as a red solid (335 mg, 93%), mp 75.0-76.3 °C. ^{1}H-NMR ($CDCl_3$, 500 MHz) (Figure 8-6): δ: 6.70 (d, ^{4}J = 2 Hz, 4 H), 6.30 (t, ^{4}J = 2 Hz, 4 H), 6.24 (d, ^{4}J = 2 Hz, 8 H), 6.10 (t, ^{4}J = 2 Hz, 2 H), 5.22 (s, 4 H), 4.97 (s, 8 H), 4.92 (t, ^{3}J=2 Hz, 4 H), 4.37 (t, ^{3}J=2 Hz, 4 H), 3.83-3.93 (m, 32 H) 3.65 (br, 32 H). ^{13}C-NMR ($CDCl_3$, 125 MHz) (Figure 8-7): δ (ppm): 170.21, 160.00, 159.94, 139.50, 138.62, 108.81, 103.82, 101.51, 100.31, 73.20, 72.51, 71.66, 70.95, 70.46, 70.15, 69.65, 67.52, 65.61. HR-ESIMS (Figure 8-8): calcd. for $[M + H]^+$: 1639.5980, found: ***m/z***, 1639.6051 $[M + H]^+$, error: 4.33 ppm.

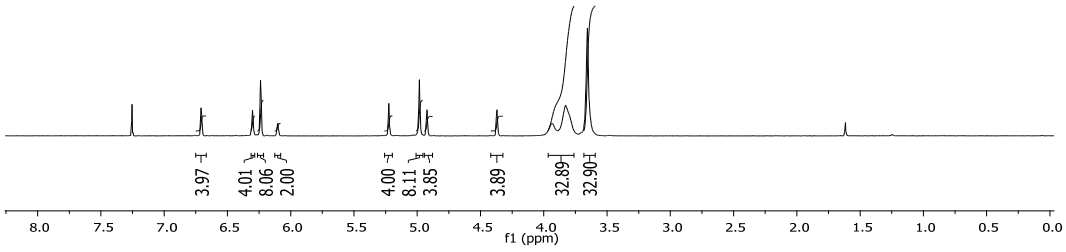

Figure 8-6. ^{1}H-NMR ($CDCl_3$, 500 MHz, room temperature) of biscryptand **4**.

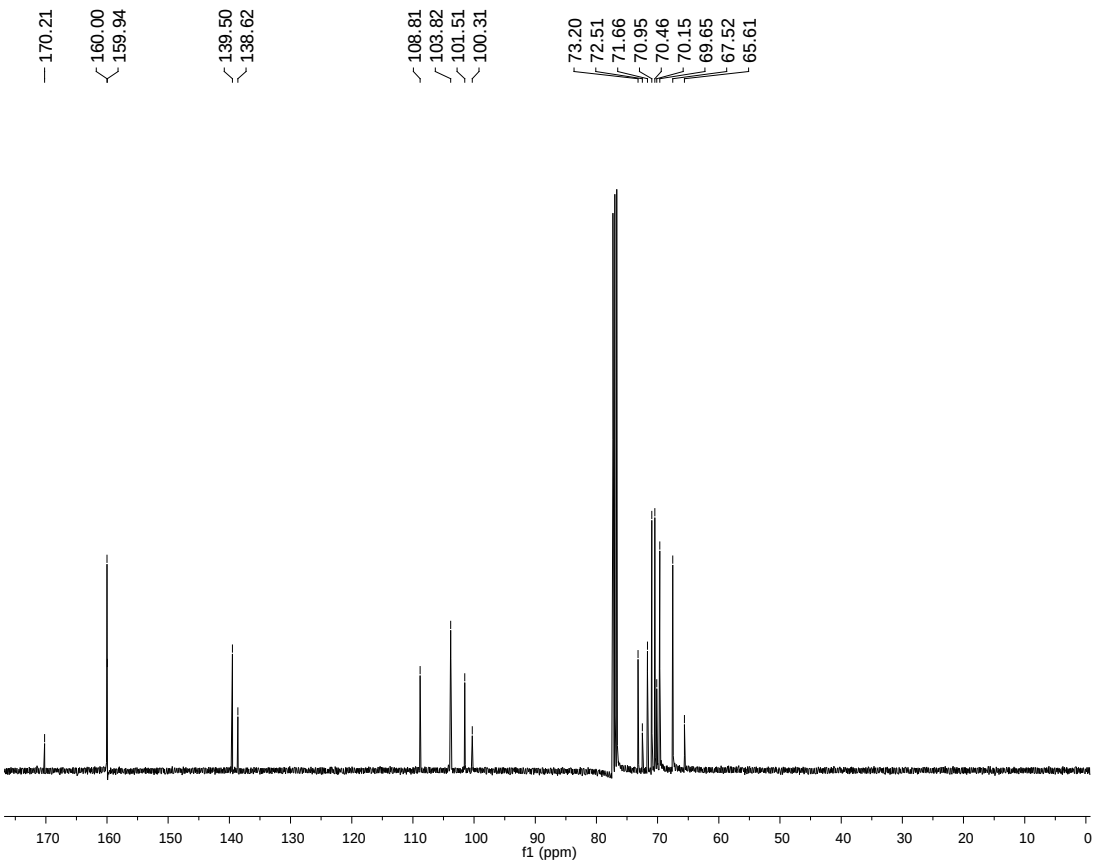

Figure 8-7. ^{13}C-NMR ($CDCl_3$, 125 MHz, room temperature) of biscryptand **4**.

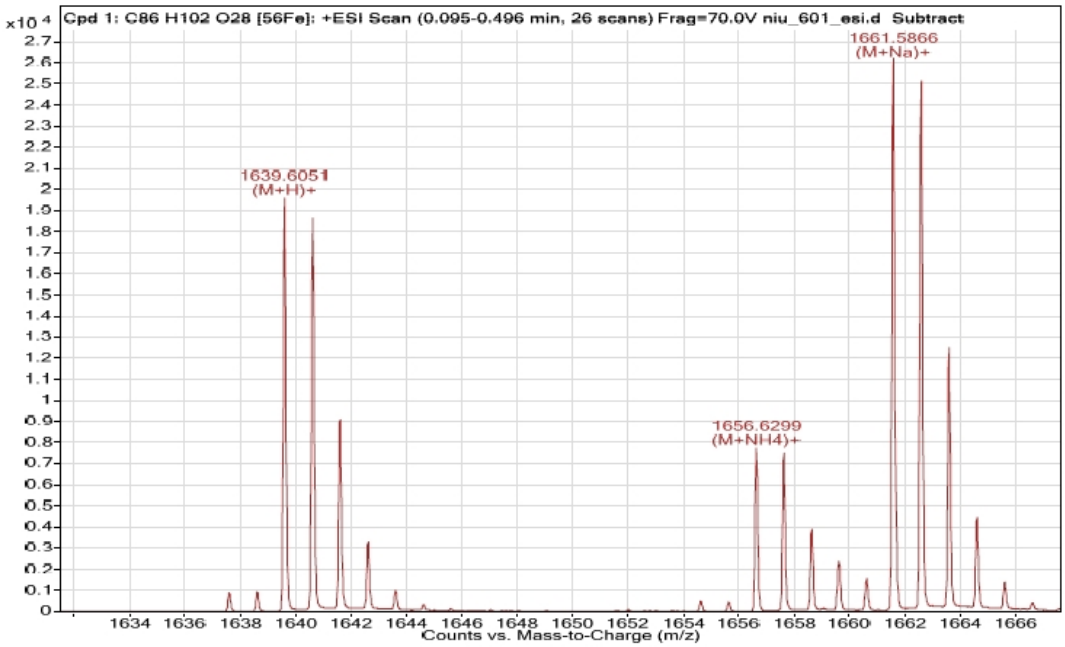

Figure 8-8. Electrospray ionization mass spectrum of biscryptand **4**.

8.5.4 Synthesis of bisparaquat 5

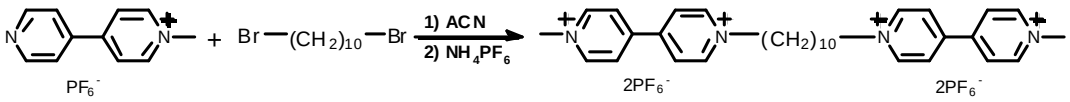

Scheme 8-4. Synthesis of bisparaquat **5**.

1-Methyl-4,4'-bipyridinium PF_6 (700 mg, 1.5 mmol) and dibromodecane (156 mg, 0.51 mmol) were dissolved in anhydrous acetonitrile. The mixture was refluxed for 3 days. The yellow precipitate was collected by filtration and washed with acetonitrile and dichloromethane. The solid obtained was dissolved in a minimum amount of DI water and a saturated aqueous NH_4PF_6 solution was added until no more solid precipitated. After filtration, the white solid was recrystallized in DI water twice, (422 mg, 78%), mp: 276.0-277.5 °C. ^{1}H-NMR ($(CD_3)_2CO$, 500 MHz) (Figure 8-9): δ: 9.38 (dd, ^{3}J = 7 Hz, 8 H), 8.80 (t, ^{3}J = 7 Hz, 8 H), 4.94 (t, ^{3}J = 8 Hz, 4 H), 4.72 (s, 6 H), 2.20 (m, 4 H), 1.31-1.49 (m, 12 H). ^{13}C-NMR (CD_3CN, 125 MHz) (Figure 8-10): δ (ppm): 150.17, 149.94, 146.79, 145.79, 127.46, 127.07, 62.42, 48.89, 31.25, 29.23, 28.89, 25.88.

HR-ESIMS (Figure 8-11); calcd. for $[M\text{-}PF_6]^+$: 917.2329 , found: ***m/z***, 917.2310 $[M + H]^+$, error: -2.12 ppm.

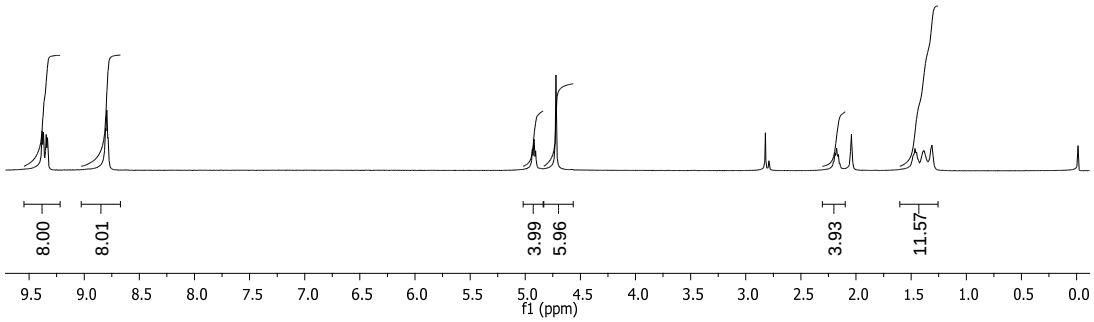

Figure 8-9. ^{1}H-NMR ($(CD_3)_2CO$, 500 MHz, room temperature) of bisparaquat **5**.

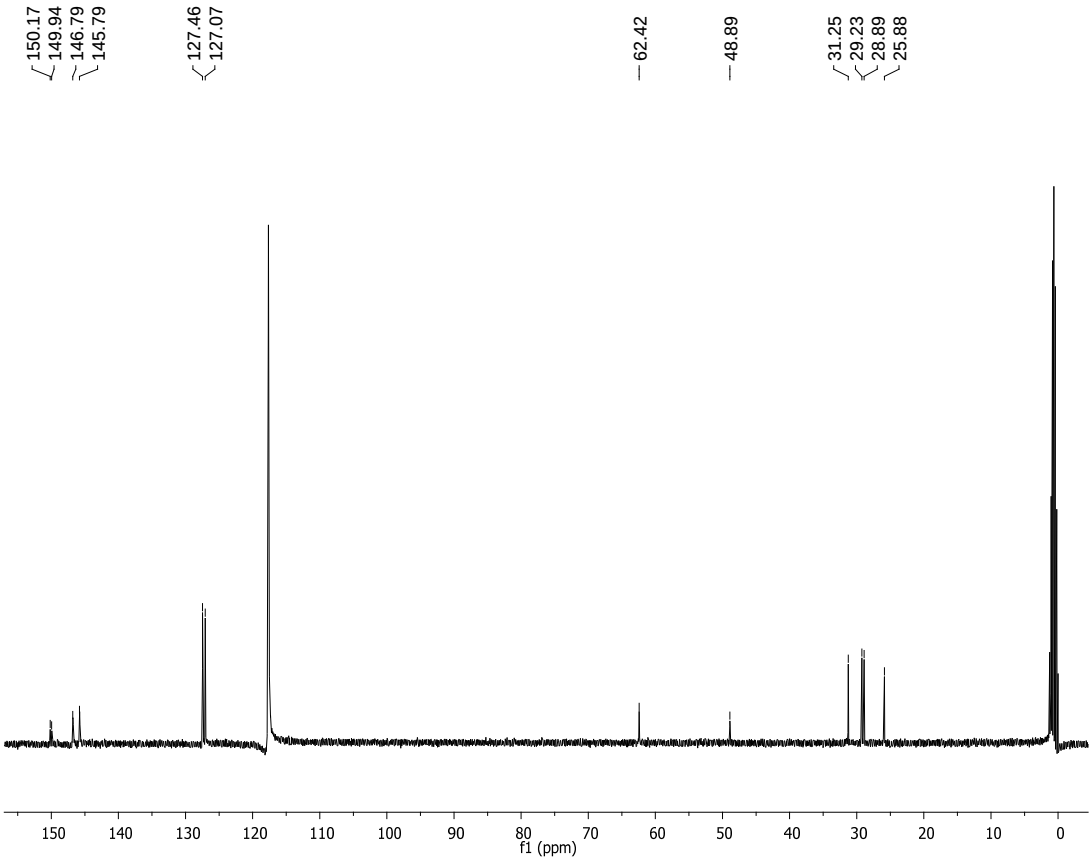

Figure 8-10. ^{13}C-NMR (CD_3CN, 125 MHz, room temperature) of bisparaquat **5**.

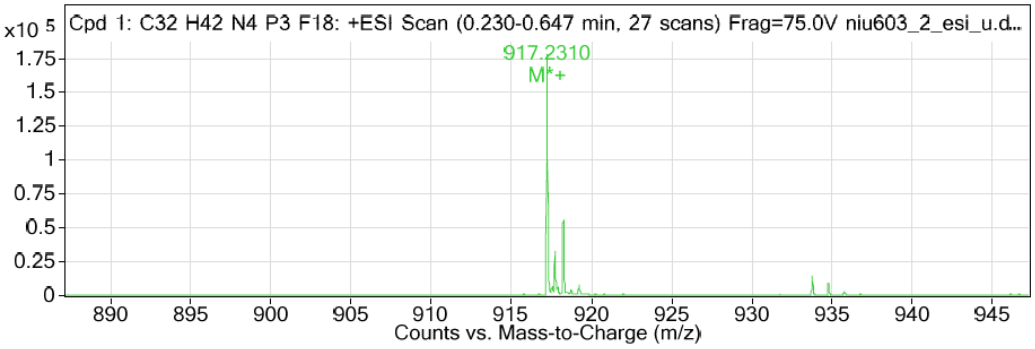

Figure 8-11. Electrospray ionization mass spectrum of bisparaquat **5**.

8.5.5 Determination of Δ_0 of H_2 for biscryptand 3 and bisparaquat 5

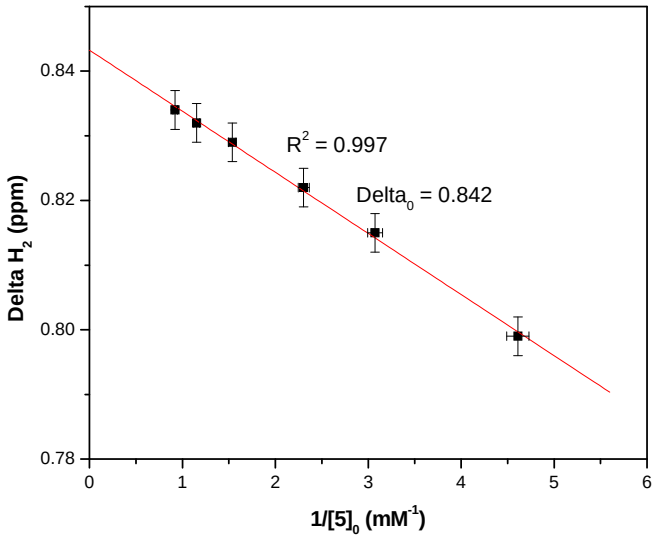

Figure 8-12. Determination of Δ_0 of H_2 for biscryptand **3** and bisparaquat **5** in chloroform-d/acetonitrile-d_3 = 1/1 <v/v>.

8.5.6 Determination of Δ_0 of $H_{2'}$ for biscryptand 4 and bisparaquat 5

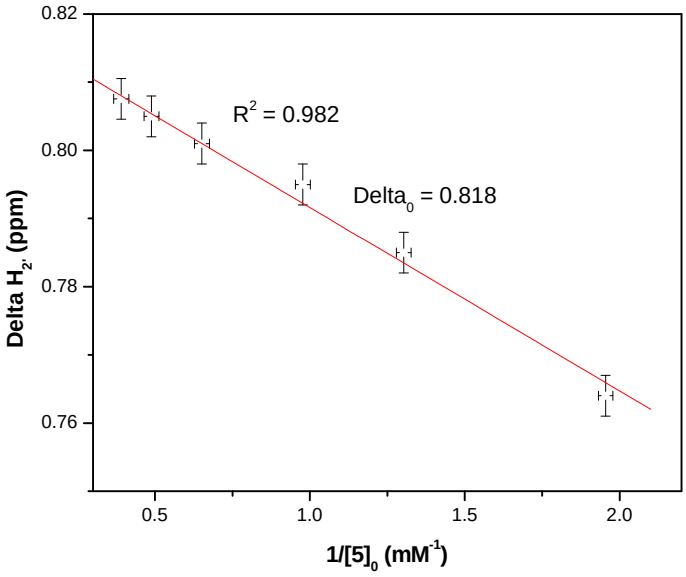

Figure 8-13. Determination of Δ_0 of $H_{2'}$ for biscryptand **4** and bisparaquat **5** in chloroform-d/acetonitrile-d_3 = 1/1 <v/v>.

8.5.7 Calculated values of p and n at different initial concentrations of biscryptand 3 and bisparaquat 5

Table 8-1. Calculated values of *p* and *n* at different initial concentrations of biscryptand **3** (equimolar **3** and **5** in chloroform-*d*/acetonitrile-d_3 = 1/1 <v/v>).

[Biscryptand **3**] (mM)	p^*	$n^\#$
290	0.989	93 ± 47
247	0.980	50 ± 9
212	0.969	32 ± 4
164	0.956	23 ± 2
135	0.949	19 ± 1
87.0	0.938	16 ± 1

* $p = \Delta/\Delta_0$. Δ_0 of H_2 was determined to be 0.842 ppm by extrapolation of a plot of versus 1 / $[\mathbf{5}]_o$ at constant [**3**].

$n = 1/(1-p)$, error bars in *n* are the calculated maximum errors reflecting $p \pm 0.003$ absolute.

8.5.8 Calculated values of p and n at different initial concentrations of biscryptand 4 and bisparaquat 5

Table 8-2. Calculated values of *p* and *n* at different initial concentrations of biscryptand **4** (equimolar **4** and **5** in chloroform-*d*/acetonitrile-d_3 = 1/1 <v/v>).

[Biscryptand **4**] (mM)	p^*	$n^\#$
230	0.955	22 ± 2
179	0.942	17 ± 1
123	0.921	13 ± 1
84.6	0.910	11 ± 1
74.0	0.899	10 ± 1

* $p = \Delta/\Delta_0$. Δ_0 of H_2 was determined to be 0.818 ppm by extrapolation of a plot of versus 1 / $[\mathbf{5}]_o$ at constant [**4**].

$n = 1/(1-p)$, error bars in n are the calculated maximum errors reflecting $p \pm 0.003$ absolute.

8.5.9 Viscosity measurements of equimolar solutions of 4 and 5

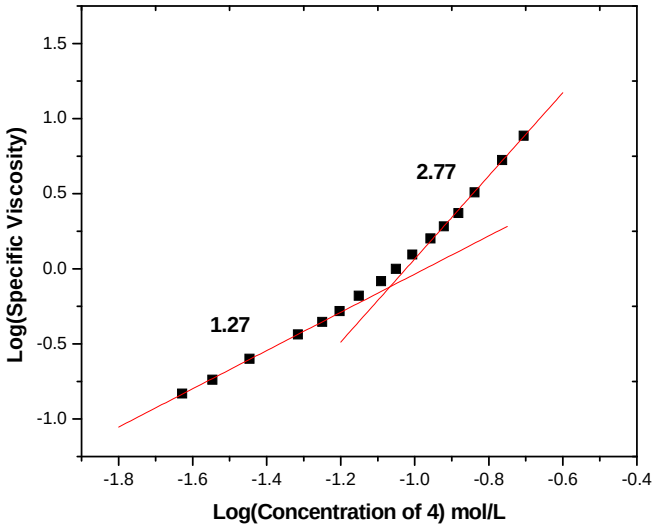

Figure 8-14. Double-logarithmic plot of specific viscosity of equimolar solutions of **4** and **5** in chloroform/acetonitrile (1/1, v/v) versus concentration.

8.5.10 DSC curve of supramolecular polymer 2

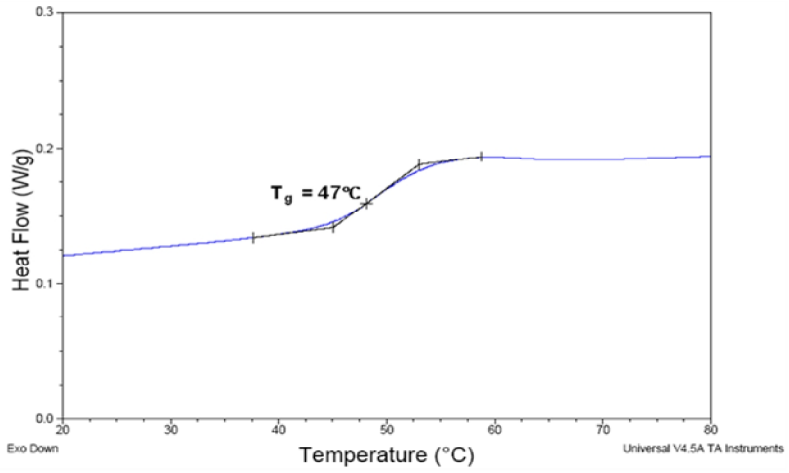

Figure 8-15. DSC curve of supramolecular polymer **2**. Heating rate 10 °C /min; under N_2.

8.5.11 TGA curve of supramolecular polymer 1

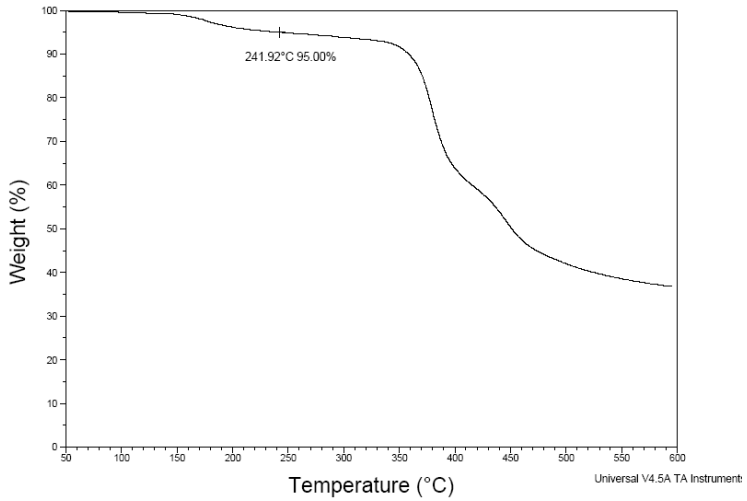

Figure 8-16. TGA curve of supramolecular polymer **1**. Heating rate 10°C/min under N_2.

8.5.12 TGA curve of supramolecular polymer 2

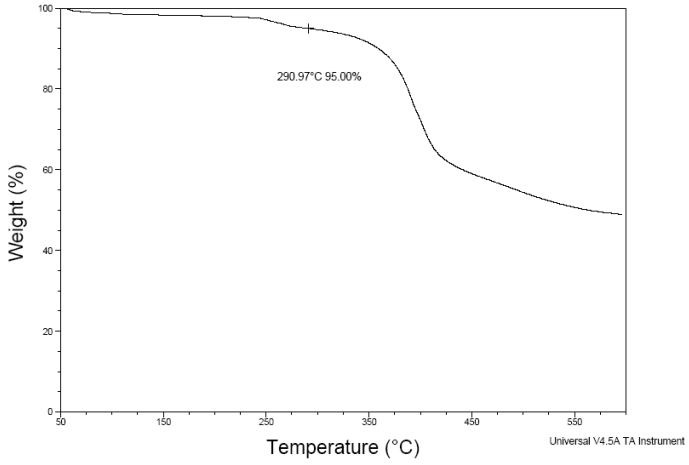

Figure 8-17. TGA curve of supramolecular polymer **2**. Heating rate 10°C/min under N_2

8.5.13 SEM images of supramolecular polymers 1 and 2

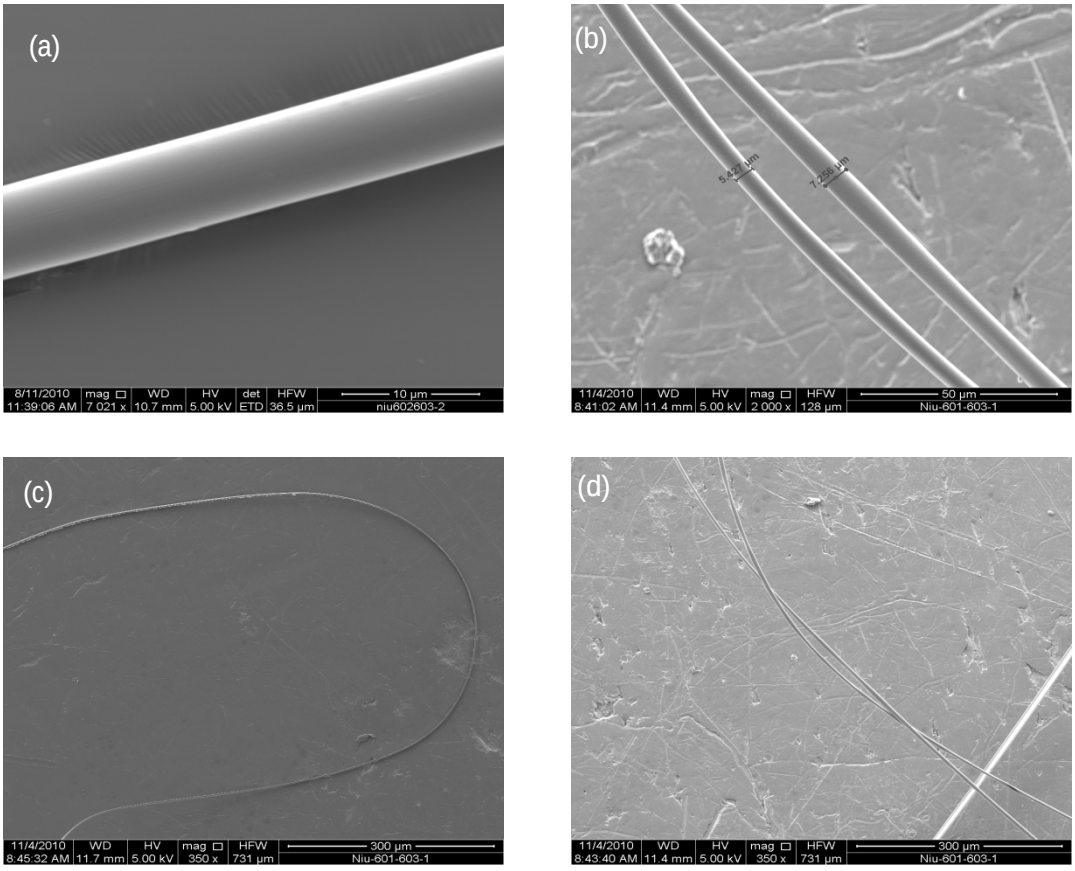

Figure 8-18. Scanning electron micrographs of (gold coated) fibers drawn from concentrated equimolar solutions of: (a) **3** and **5**. (b), (c) and (d) **4** and **5**.

References

(1) Reviews: (a) Ciferri, A. *Supramolecular Polymers*; Marcel-Dekker: New York, 2000. (b) Brunsveld, L.; Folmer, B. J. B.; Meijer, E. W.; Sijbesma, R. P. *Chem. Rev.* **2001**, *101*, 4071-4098. (c) Huang, F.; Gibson, H. W. *Prog. Polym. Sci.* **2005**, *30*, 982-1018. (d) Lehn, J.-M. *Chem. Soc. Rev.* **2007**, *36*, 151-160. (e) Hwang, S.-H.; Moorefield, C. N.; Newkome, G. R. *Chem. Soc. Rev.* **2008**, *37*, 2543-2557. (f) De Greef, T. F. A.; Smulders, M. M. J.; Wolffs, M.; Schenning,

A. P. H. J.; Sijbesma, R. P.; Meijer, E. W. *Chem. Rev.* **2009**, *109*, 5687-5754. (g) Harada, A.; Hashidzume, A.; Yamaguchi, H.; Takashima, Y. *Chem. Rev.* **2009**, *109*, 5974-6023. (h) Niu, Z.; Gibson, H. W. *Chem. Rev.* **2009**, *109*, 6024-6046. (i) Fang, L.; Olson, M. A.; Benitez, D.; Tkatchouk, E.; Goddard III, W. A.; Stoddart, J. F. *Chem. Soc. Rev.* **2010**, *39*, 17-29.

(2) For some recent publications, see: (a) Todd, E. M.; Zimmerman, S. C. *Tetrahedron* **2008**, *64*, 8558-8570. (b) Smulders, M. M. J.; Stals, P. J. M.; Mes, T.; Paffen, T. F. E.; Schenning, A. P. H. J.; Palmans, A. R. A.; Meijer, E. W. *J. Am. Chem. Soc.* **2009**, *132*, 620-626. (c) Burattini, S.; Greenland, B. W.; Merino, D. H.; Weng, W.; Seppala, J.; Colquhoun, H. M.; Hayes, W.; Mackay, M. E.; Hamley, I. W.; Rowan, S. J. *J. Am. Chem. Soc.* **2010**, *132*, 12051-12058. (d) Pensec, S.; Nouvel, N.; Guilleman, A.; Creton, C.; Boué, F. O.; Bouteiller, L. *Macromolecules* **2010**, *43*, 2529-2534. (e) Xu, D.; Hawk, J. L.; Loveless, D. M.; Jeon, S. L.; Craig, S. L. *Macromolecules* **2010**, *43*, 3556-3565. (f) Rancatore, B. J.; Mauldin, C. E.; Tung, S.-H.; Wang, C.; Hexemer, A.; Strzalka, J.; Fréchet, J. M. J.; Xu, T. *ACS Nano* **2010**, *4*, 2721-2729. (g) Tancini, F.; Yebeutchou, R. M.; Pirondini, L.; De Zorzi, R.; Geremia, S.; Scherman, O. A.; Dalcanale, E. *Chem. Eur. J.* **2010**, *16*, 14313-14321. (h) Greuel, J. R.; Andrews, T. E.; Wichman, J. J.; Tessner, J. D.; Wiegel, K. N. *Liquid Cryst.* **2010**, *37*, 1515-1520.

(3) (a) Yamaguchi, N.; Gibson, H. W. *Angew. Chem. Int. Ed.* **1999**, *38*, 143-147. (b) Sohgawa, Y.-H.; Fujimori, H.; Shoji, J.; Furusho, Y.; Kihara, N.; Takata, T. *Chem. Lett.* **2001**, 774-775. (c) Oku, T.; Furusho, Y.; Takata, T. *J. Polym. Sci., Part A: Polym. Chem.* **2003**, *41*, 119-123. (d) Gibson, H. W.; Yamaguchi, N.; Jones, J. W. *J. Am. Chem. Soc.* **2003**, *125*, 3522-3533. (e) Huang, F.; Nagvekar, D. S.; Gibson, H. W. *Macromolecules* **2007**, *40*, 3561-3567. (f) Gibson, H. W.; Yamaguchi, N.; Niu, Z.; Jones, J. W.; Rheingold, A. L.; Zakharov, L. N. *J. Polym. Sci., Polym. Chem.* **2010**, *48*, 975-985. (g) Zhou, Q. Z.; Jiang, H. J.; Ding, L.; Wang, F.; Wu, T. *Sci. China: Chem.* **2010**, 53, 1081-1088.

(4) (a) Huang, F.; Gibson, H. W. *J. Am. Chem. Soc.* **2004**, *126*, 14738-14739. (b) Li, S.; Zheng, B.; Chen, J.; Dong, S.; Ma, Z.; Huang, F.; Gibson, H. W. *J. Polym.*

Sci., Polym. Chem. **2010**, *48,* 4067-4073.

(5) Huang, F.; Nagvekar, D. S.; Slebodnick, C.; Gibson, H. W. *J. Am. Chem. Soc.* **2004**, *127*, 484-485.

(6) (a) Gibson, H. W.; Yamaguchi, N.; Hamilton, L. M.; Jones, J. W. *J. Am. Chem. Soc.* **2002**, *124,* 4653-4665. (b) Jones, J. W.; Bryant, W. S.; Bosman, A. W.; Janssen, R. A. J.; Meijer, E. W.; Gibson, H. W. *J. Org. Chem.* **2003**, *68*, 2385-2389. (c) Leung, K. C. F.; Mendes, P. M.; Magonov, S. N.; Northrop, B. H.; Kim, S.; Patel, K.; Flood, A. H.; Tseng, H.-R.; Stoddart, J. F. *J. Am. Chem. Soc.* **2006**, *128*, 10707-10715.

(7) Sijbesma, R. P.; Beijer, F. H.; Brunsveld, L.; Folmer, B. J. B.; Hirschberg, J. H. K. K.; Lange, R. F. M.; Lowe, J. K. L.; Meijer, E. W. *Science* **1997**, *278*, 1601-1604.

(8) (a) Bryant, W. S.; Jones, J. W.; Mason, P. E.; Guzei, I.; Rheingold, A. L.; Fronczek, F. R.; Nagvekar, D. S.; Gibson, H. W. *Org. Lett.* **1999**, *1*, 1001-1004. (b) Huang, F.; Fronczek, F. R.; Gibson, H. W. *J. Am. Chem. Soc.* **2003**, *125*, 9272-9273. **(**c**)** Huang, F.; Gibson, H. W.; Bryant, W. S.; Nagvekar, D. S.; Fronczek, F. R. *J. Am. Chem. Soc.* **2003**, *125*, 9367-9371. (d) Huang, F.; Switek, K. A.; Zakharov, L. N.; Fronczek, F. R.; Slebodnick, C.; Lam, M.; Golen, J. A.; Bryant, W. S.; Mason, P. E.; Rheingold, A. L.; Ashraf-Khorassani, M.; Gibson, H. W. *J. Org. Chem.* **2005**, *70*, 3231-3241. (e) Huang, F.; Fronczek, F. R.; Ashraf-Khorassani, M.; Gibson, H. W. *Tetrahedron Lett.* **2005**, *46*, 6765-6769. (f) Gibson, H. W.; Wang, H.; Slebodnick, C.; Merola, J.; Kassel, S.; Rheingold, A. L. *J. Org. Chem.* **2007**, *72,* 3381-3393. (g) Pederson, A. M. P.; Vetor, R. C.; Rouser, M. A.; Huang, F.; Slebodnick, C.; Schoonover, D. V.; Gibson, H. W. *J. Org. Chem.* **2008**, *73*, 5570-5573. (h) Pederson, A. M.-P.; Ward, E.; Schoonover, D. S.; Slebodnick, C.; Gibson, H. W. *J. Org. Chem.* **2008**, *73*, 9094-9101. (i) Li, S.; Zheng, B.; Huang, F.; Zakharov, L.; Slebodnick, C.; Rheingold, A.; Gibson, H. W. *Sci. China Chem.* **2010**, *53*, 858-862. (j) Zhang, M.; Zhu, K.; Huang, F. *Chem. Commun.* **2010**, *46*, 8131-8141.

(9) (a) Bryant, W. S.; Guzei, I.; Rheingold, A. L.; Gibson, H. W. *Org. Lett.* **1999**, *1*,

47-50. (b) Huang, F.; Fronczek, F. R.; *Gibson, H. W.* **Chem. Commun**. *2003***,** ***1480***−1481 (c) Huang, F.; Zakharov, L. N.; Bryant, W. S.; Rheingold, A. L.; Gibson, H. W. *Chem. Commun*. **2005**, 3268-3270. (d) Huang, F.; Gantzel, P.; Nagvekar, D. S.; Rheingold, A. L.; Gibson, H. W. *Tetrahedron Lett.* **2006**, *47*, 7841-7844. (e) Li, S.; Liu, M.; Zheng, B.; Zhu, K.; Wang, F.; Li, N.; Zhao, X.-L.; Huang, F. *Org. Lett.* **2009**, *11*, 3350-3353.

(10) (a) Jacobson, H.; Stockmayer, W. H. *J. Chem. Phys.* **1950**, *18*, 1600−1606. (b) Ercolani, G.; Mandolini, L.; Mencarelli, P.; Roelens, S. *J. Am. Chem. Soc.* **1993**, *115*, 3901−3908. (c) Muraoka, T.; Kinbara, K.; Aida, T. *Nature* **2006**, *440*, 512-515.

(11) Yamaguchi, N.; Gibson, H. W. *J. Chem. Soc., Chem. Comm.* **1999,** 789-790.

(12) (a) Connor, K. A. *Binding Constants: The Measurement of Molecular Complex Stability*; J. Wiley and Sons: New York, 1987. (b) Carothers, C. H. *Trans. Faraday Soc.* **1936**, *32*, 39-53. (c) This analysis assumes that all species in solution are linear and thus it overestimates the degree of polymerization. Because of the inverse relationship between *p* and *n* in the Carothers equation, the errors in the latter become large as *p* increases.

(13) De Greef, T. F. A.; Ercolani, G.; Ligthart, G. B. W. L.; Meijer, E. W.; Sijbesma, R. P. *J. Am. Chem. Soc.* **2008**, *130*, 13755-13764.

(14) In the usual manner the data for Figure 8-2a were obtained by sequential dilutions of the initial high concentration solution in the viscometer. The exponential decrease in η with decreasing concentration confirms the reversible nature of the supramolecular polymerization process.

(15) (a) Cates, M. E. *Macromolecules* **1987**, *20,* 2296-2300. (b) Cates, M. E.; Candau, S. J. *J. Phys.: Condens. Matter* **1990**, *2*, 6869-6892.

(16) Allcock, H. R.; Lampe, F. W. *Contemporary Polymer Chemistry*; 2nd ed.; Prentice-Hall: New York, 1990.

(17) Installation of triphenylphosphonium stoppers on . -dihalides: (a) Braunschweig, A. B.; Ronconi, C. M.; Han, J.-Y.; Arico, F.; Cantrill, S. J.;

Stoddart, J. F.; Khan, S. I.; White, A. J. P.; Williams, D. J. *Eur. J. Org. Chem.* **2006**, *8*, 1857-1866. (b) Li, S.; Liu, M.; Zhang, J.; Zheng, B.; Zhang, C.; Wen, X.; Li, N.; Huang, F. *Org. Biomol. Chem.* **2008**, *6*, 2103-2107. (c) Liu, M.; Li, S.; Zhang, M.; Zhou, Q.; Wang, F.; Hu, M.; Fronczek, F. R.; Li, N.; Huang, F. *Org. Biomol. Chem.* **2009**, *7*, 1288-1291. (d) Li, S.; Zhu, K.; Zheng, B.; Wen, X.; Li, N.; Huang, F. *Eur. J. Org. Chem*. **2009**, *7*, 1053-1057.

(18) Installation of stoppers on . -diols with urethane links using isocyanate reagents: (a) Cantrill, S. J.; Fulton, D. A.; Fyfe, M. C. T.; Stoddart, J. F.; White, A. J. P.; Williams, D. J. *Tetrahedron Lett.* **1999**, *40*, 3669-3672. (b) Furusho, Y.; Sasabe, H.; Natsui, D.; Murakawa, K.; Takata, T.; Harada, T. *Bull. Chem. Soc. Japan* **2004**, *77*, 179-185. (c) Sasabe, H.; Inomoto, N.; Kihara, N.; Suzuki, Y.; Ogawa, A.; Takata, T. *J. Polym. Sci., Part A: Polym. Chem.* **2007**, *45*, 4154-4160. (d) Wang, F.; Zhou, Q.; Zhu, K.; Li, S.; Wang, C.; Liu, M.; Li, N.; Fronczek, F. R.; Huang, F. *Tetrahedron* **2009**, *65*, 1488-1494.

(19) Installation of stoppers on α, ω-diols with ester links using anhydride reagents: (a) Kawasaki, H.; Kihara, N.; Takata, T. *Chem. Lett.* **1999**, 1015. (b) Tachibana, Y.; Kawasaki, H.; Kihara, N.; Takata, T. *J. Org. Chem.* **2006**, *71*, 5093-5104. (c) ref. 18d.

(20) Installation of stoppers on α, ω-dienes with isoxazole links using nitrile N-oxide reagents: Matsumura, T.; Ishiwari, F.; Koyama, Y.; Takata, T. *Org. Lett.* **2010**, *12*, 3828-3831.

(21) Harriman, A.; Hissler, M.; Trompette, O.; Ziessel, R. *J. Am. Chem. Soc.* **1999**, *121*, 2516-2525.

TOC Graphic:

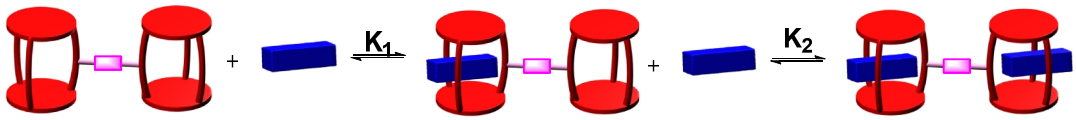

[3]Pseudorotaxane - 3 and 4

Abstract:

Via the self-assembly of two bis(*meta*-phenylene)-32-crown-10-based cryptands, bearing covalent and metal complex (ferrocene) linkages, with dimethyl paraquat, novel [3]pseudorotaxanes were formed statistically and anticooperatively, respectively.

Chapter 9.

Contrasting Biscryptand/Dimethyl Paraquat [3]Pseudorotaxanes: Statistical vs. Anticooperative Complexation Behavior

9.1 Introduction

In supramolecular chemistry, pseudorotaxanes,[1] which consist of a linear molecular component ("Guest") encircled by a macrocyclic component ("Host"), have been topics of great interest due to their topological importance and potential applications as fundamental building blocks for construction of advanced supromolecular species, such as rotaxanes, catenanes, polypseudorotaxanes, polyrotaxanes and polycatenanes.[2] Paraquat (*N*,*N'*-dialkyl-4,4'-bipyridinium) derivatives are commonly used guests with crown ether hosts to prepare pseudorotaxanes.[3] Compared with simple crown ethers, cryptands,[4] multidentate hosts bearing more than two bridges in the molecule, have proved to be much better hosts for paraquat derivatives and cryptand/bispraquat based [3]pseudorotaxanes formed via cooperative complexation have been found.[4b,4f] Here, for the first time, we report two novel biscryptand/dimethyl paraquat (DMP) based [3]pseudorotaxanes, one self-assembled via statistical complexation and the other in an anticooperative fashion.

9.2 Results and discussion

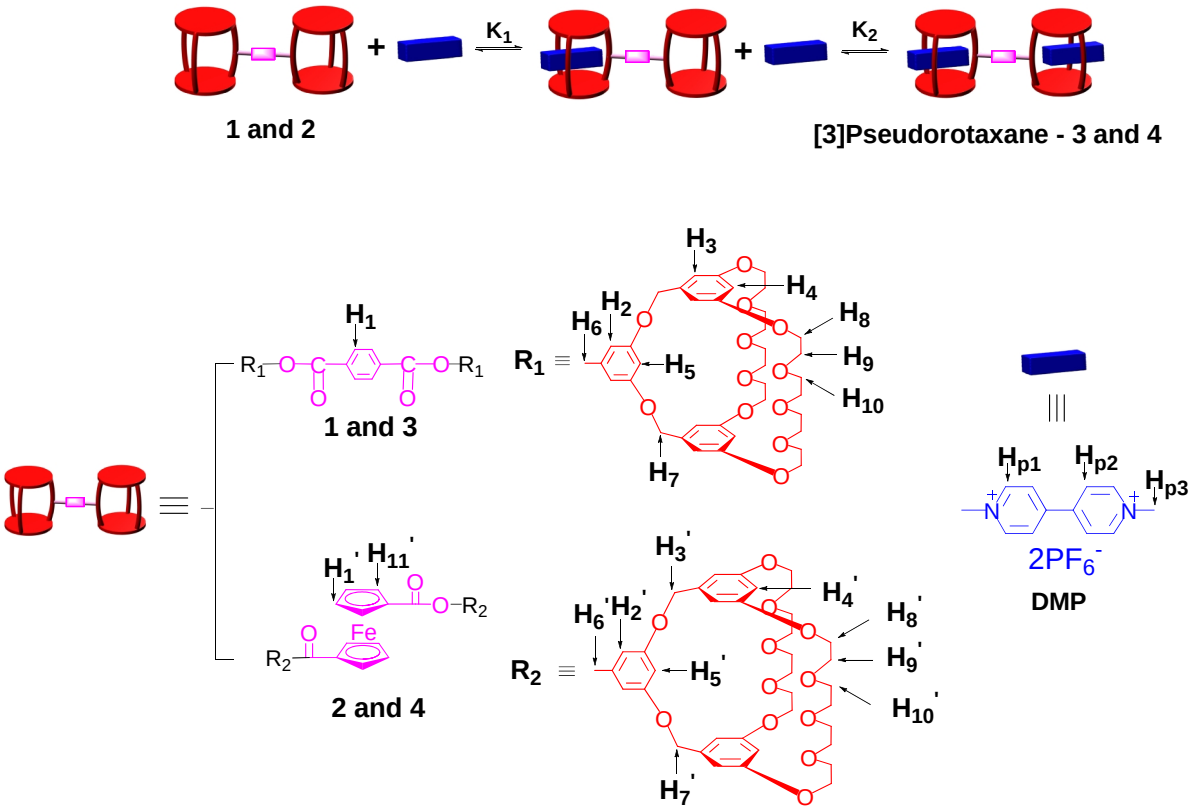

Scheme 9-1. Schematic illustration of the formation [3]pseudorotaxanes **3** and **4** via the self-assembly of bicryptands **1** and **2** with DMP.

The biscryptands **1** and **2** were prepared according to the published procedure.[2j] Although the individual solutions of biscryptand **1** and **DMP** ($CDCl_3/(CD_3)_2CO$ = 1/3 <v/v>) were colorless, a solution of biscryptand **1** and **DMP** was yellow due to the charge-transfer between the electron-rich aromatic rings of the biscryptand and the electron-poor pyridinium rings of the **DMP**. ^{1}H-NMR spectra of solutions of biscryptand **1** and **DMP** displayed only one set of peaks, indicating fast-exchange complexation (Figure 9-1). After complexation, peaks corresponding to pyridine protons (H_{P1}, H_{P2} and H_{P3}) of **DMP** and aromatic proton H_4, ethyleneoxy protons H_8 and H_9 on biscryptand **1** moved upfield. Furthermore, peaks corresponding to H_1, H_2, H_5 and H_6 moved downfield.

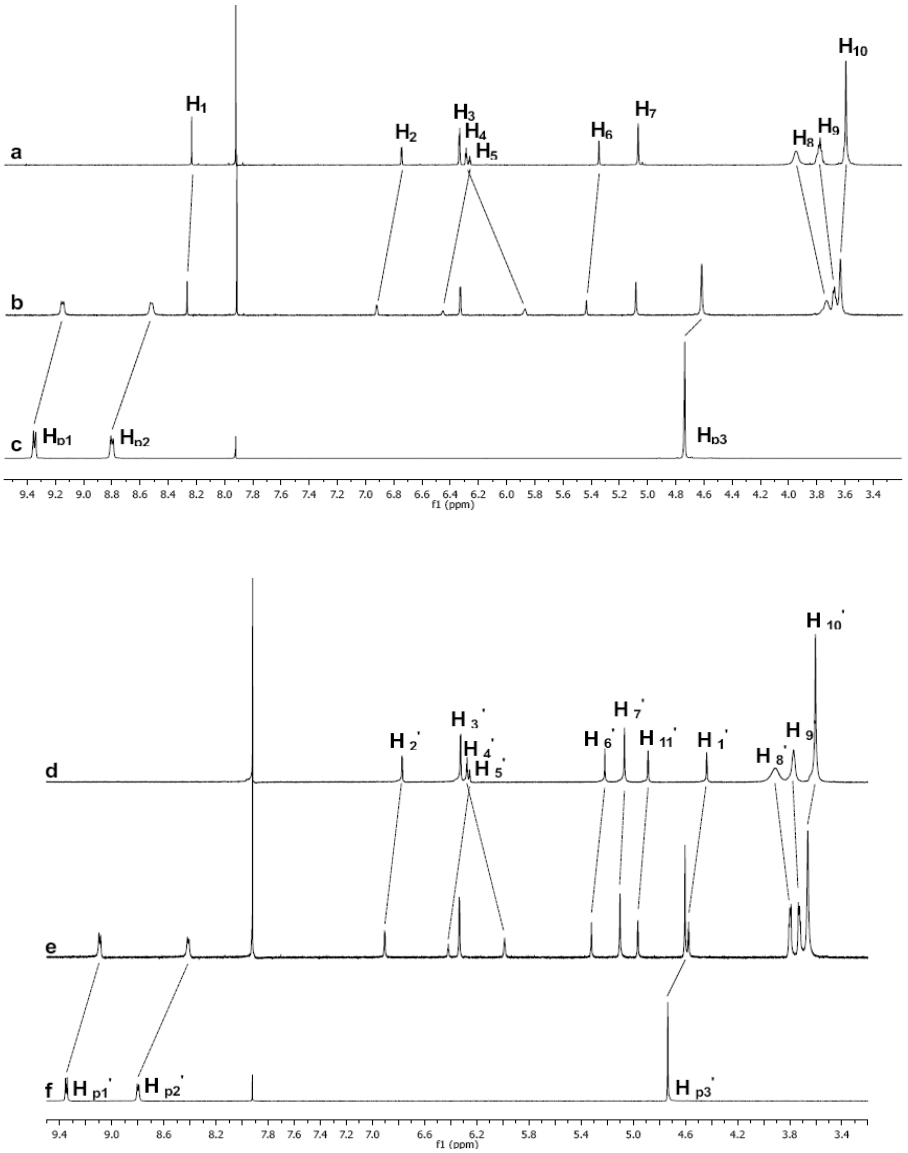

Figure 9-1. Partial ^{1}H-NMR spectra (500 MHz, $CDCl_3/(CD_3)_2CO$ = 1/3 <v/v>, 22°C) of: (a) Pure biscryptand **1**; (b) Mixture of **1** and **DMP** (1/3, mol/mol); (c) Pure **DMP**; (d) Pure biscryptand **2**; (e) Mixture of **2** and **DMP** (1/2, mol/mol); (f) Pure **DMP**;

The stoichiometry of the complex between biscryptand **1** and **DMP** was determined to be 1 : 2 in solution by a mole ratio plot[5] (Figure 9-2). Electrospray Ionization Mass Spectrometry (ESI-MS) confirmed this stoichiometry. Three relevant peaks were found for **1**·**DMP**$_2$: *m/z*

1096.39 [**1**·**DMP**$_2$-2PF$_6$]$^{2+}$, 1031.34 [**1**·**DMP**$_2$-3PF$_6$+OH]$^{2+}$, 475.88 [**1**·**DMP**$_2$-4PF$_6$]$^{4+}$; The value of Δ_0, the chemical shift difference for H_4 between the uncomplexed and fully complexed species, was determined to be 0.631 ppm by extrapolation of a plot of Δ, the chemical shift difference for H_4 between the uncomplexed and complexed species, versus 1/[**DMP**]$_0$ in the high initial concentration range of **DMP**. The complexed fraction, *p*, of the biscryptand **1** can be calculated from $p = \Delta/\Delta_0$ based on data for H_4 on **1**. The linear nature of the Scatchard plot (Figure 9-3) demonstrated that the complexation between biscryptand **1** and **DMP** was statistical,[6] indicating the two cryptand binding sites behave independently. The average association constant was determined to be $K_{av} = 4.3 \pm 0.3 \times 10^3\ M^{-1}$, $K_1 = 6.9 \pm 0.5 \times 10^3\ M^{-1}$ and $K_2 = 1.7 \pm 0.1 \times 10^3\ M^{-1}$.

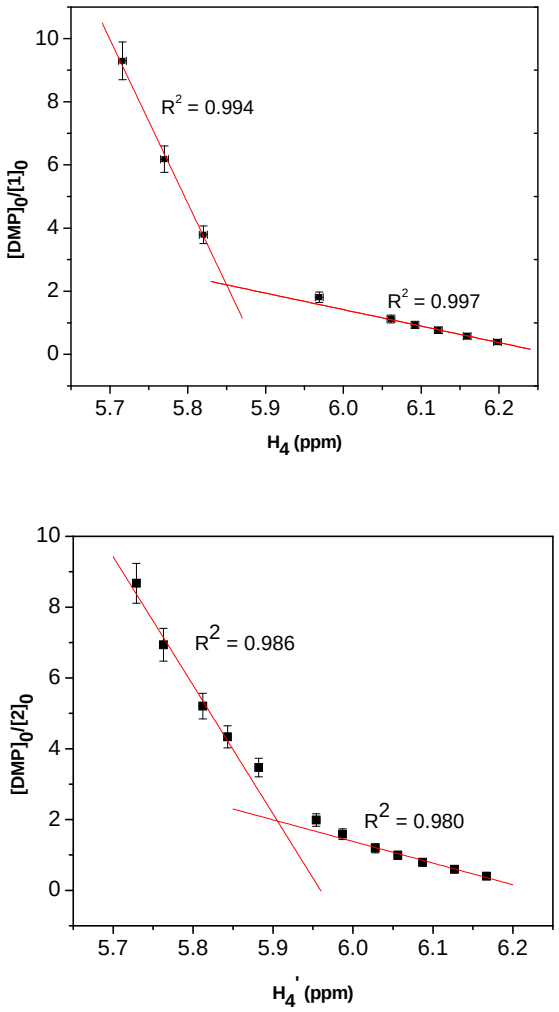

Figure 9-2. Mole ratio plots for **1** and **DMP** (upper) and **2** and **DMP** (lower). The solvent is $CDCl_3/(CD_3)_2CO$ = 1/3 <v/v>.

Solutions of biscryptand **2** and **DMP** were dark red due to the red color of biscryptand **2** and it was hard to see any color change caused by the charge-transfer between the electron-rich aromatic rings of the biscryptand and the electron-poor pyridinium rings of the **DMP**. ^{1}H-NMR spectra of the mixture solution between biscryptand **2** and **DMP** contained only one set of peaks, indicating fast-exchange complexation (Figure 9-1). After complexation, peaks corresponding to pyridine protons (H_{P1}', H_{P2}' and H_{P3}') on **DMP** and aromatic proton H_4', ethyleneoxy protons H_8' and H_9' on biscryptand **1** moved upfield, while peaks corresponding to H_1', H_2', H_5' and H_6' moved downfield. A mole ratio plot showed that the stoichiometry of the complex between biscryptand **2** and **DMP** was 1 : 2 in solution (Figure 9-2). ESI-MS confirmed this stoichiometry. Three relevant peaks were found for **2**·**DMP**$_2$: *m/z* 1138.84 [**2**·**DMP**$_2$-3PF_6-3CH_2+H_2O]$^{2+}$, 1076.64 [**2**·**DMP**$_2$-3PF_6-2H]$^{2+}$. 718.16 [**2**·**DMP**$_2$-3PF_6]$^{3+}$.

The value of Δ_0, the chemical shift difference for H_4' between the uncomplexed and fully complexed species, was determined to be 0.657 ppm by extrapolation of a plot of Δ, the chemical shift difference for H_4' between the uncomplexed and complexed species, versus 1/[**DMP**]$_0$ in the high initial concentration range of **DMP**. The complexed fraction, *p*, of the biscryptand **2** can be calculated from $p = \Delta/\Delta_0$ based on data for H_4 on **2**. The nonlinear nature of the Scatchard plot demonstrated that the complexation between biscryptand **2** and **DMP** was anticooperative,[6,7] indicating the threading of the first **DMP** into biscryptand **2** disfavored the threading of the second **DMP**. Based on the Scatchard plot (Figure 9-3), the K_1 was estimated to be 1.1 ± 0.7 x 10^4 M^{-1}, and K_2 = 0.8 ± 0.1 x 10^3 M^{-1}.[8] The ratio of K_2/K_1 = 0.07 is much lower than the value of 0.25 expected for statistical complexation,[6] confriming that the complexation behavior is anticooperative. The anticooperative behavior is possibly due to the relatively flexible ferrocene linkage,[9] which can rotate in turnstile-fashion in solution. The first threaded paraquat species may interact with both cryptand units, due to this flexibility, thus disfavoring the threading of the second paraquat species.

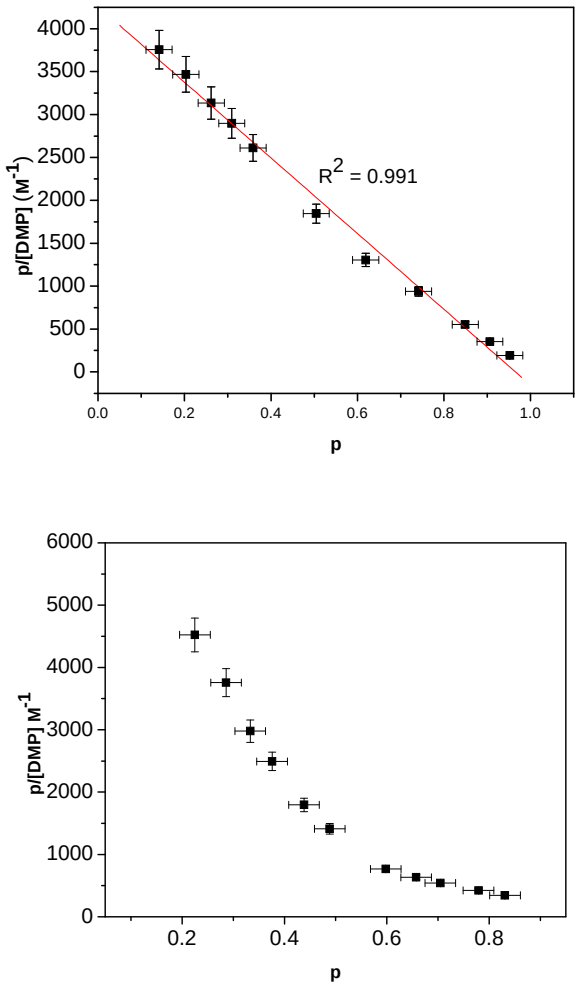

Figure 9-3. Scatchard plots for complexation of **DMP** with: biscryptand **1** (upper) and biscryptand **2** (lower) in $CDCl_3/(CD_3)_2CO$ = 1/3 <v/v> at 22°C. *p* = fraction of biscryptand units complexed. Error bars in *p*: ± 0.03 absolute. Error bars in *p*/[**DMP**]: ± 0.06 relative.

9.3 Conclusions

In summary, two biscryptands were used to prepare novel [3]pseudorotaxanes with a paraquat derivative. In one system the complexation behavior is statistical and the other behaves in an anticooperative manner. This is the first time that anticooperative behavior has been observed in such complexation processes with biscryptands and paraquats. Our future work is focused on preparation of biscryptands for application to polymeric systems.

9.4 Acknowledgements

This work was supported by the National Science Foundation (DMR0704076) and the Petroleum Research Fund administered by the American Chemical Society (47644-AC). We also acknowledge the National Science Foundation for funds to purchase the Innova-400 NMR Agilent 6220 Accurate Mass TOF LC/MS Spectrometers (CHE-0131124 & CHE-0722638, respectively).

9.5 Experimental section

9.5.1 Materials and methods

The bis(*meta*-phenylene)-32-crown-10 (BMP32C10) cryptands **1** and **2**[2j] and guest **DMP**[S2] were prepared according to literature procedures. Solvents were either used as purchased or dried according to literature procedures. ^{1}H-NMR spectra were obtained on a JEOL ECLIPSE-500 spectrometer with internal standard TMS. ^{13}C-NMR spectra were collected on a JEOL ECLIPSE-500 spectrometer at 125 MHz. MS were obtained by employing a Hewlett Packard MSD GCMS.

9.5.2 Determination of Δ_0 for 1·DMP_2

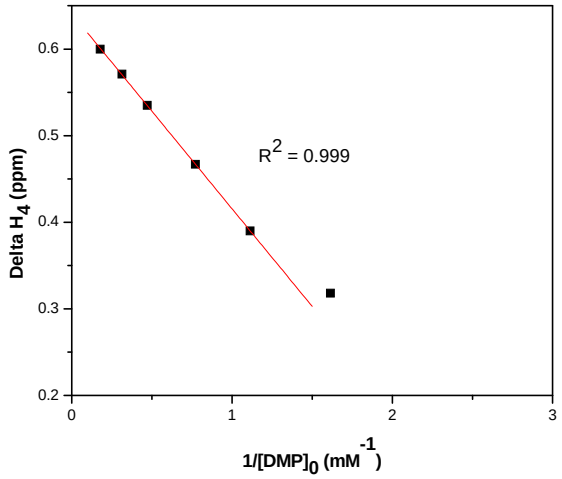

Figure 9-4. Determination of Delta$_0$ of **1·DMP$_2$** in $CDCl_3/(CD_3)_2CO$ = 1/3 <v/v>. [**1**]$_0$ = 0.34 mM. Delta$_0$ = 0.631 ppm.

9.5.3 Determination of Δ_0 orf 2·DMP_2

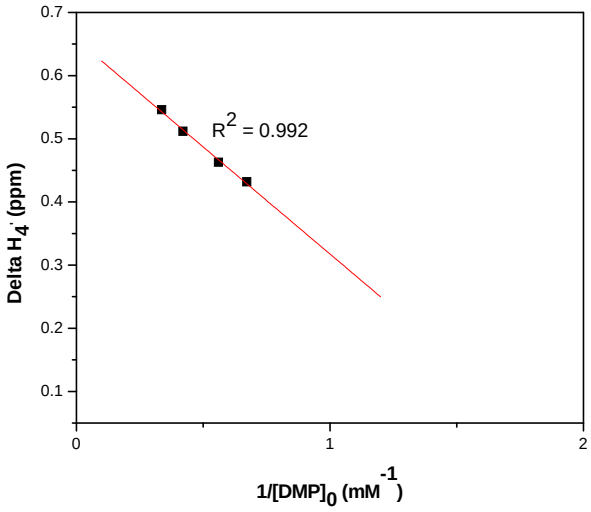

Figure 9-5. Determination of Delta$_0$ of **2·DMP$_2$** in $CDCl_3/(CD_3)_2CO$ = 1/3 <v/v>. [**2**]$_0$ = 0.34 mM. Delta$_0$ = 0.657 ppm.

9.5.4 Mass spectrum of 1·DMP_2

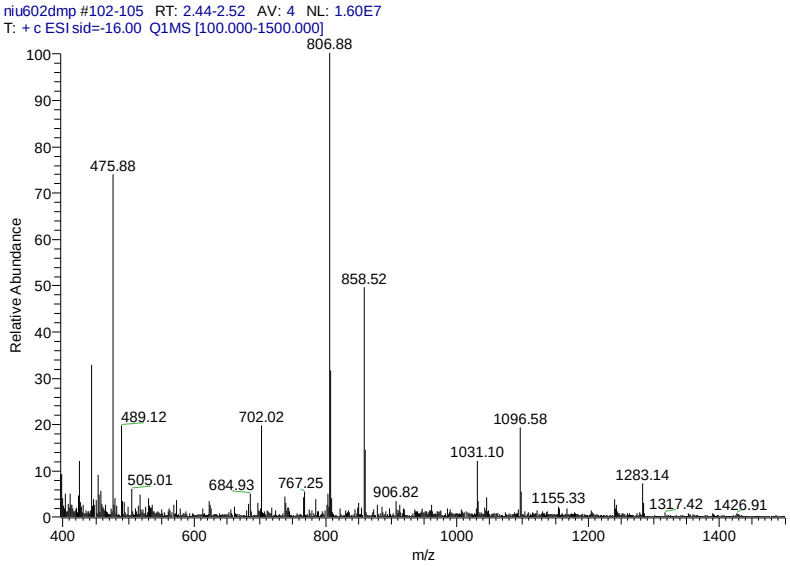

Figure 9-6. Electrospray ionization mass spectrum of **1·DMP_2**.

9.5.5 Mass spectrum of 2·DMP_2

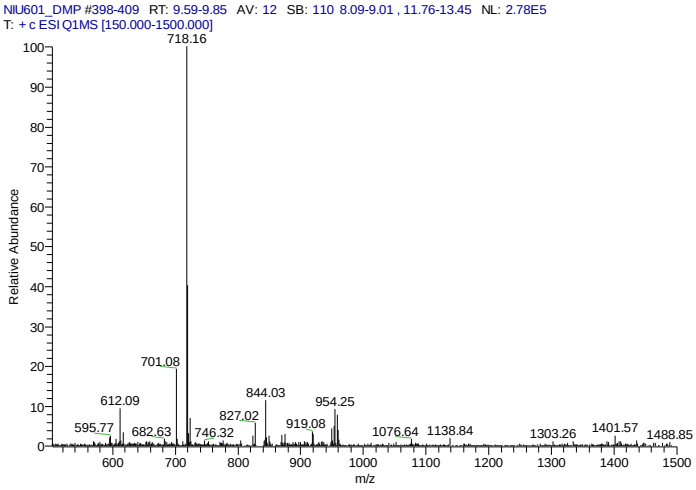

Figure 9-7. Electrospray ionization mass spectrum of **2·DMP_2**.

References

(1) (a) Gibson, H. W. In *Large Ring Molecules*, Semlyen, J. A., Ed.; John Wiley & Sons: New York, 1996; pp 191-262; (b) *Molecular Catenanes, Rotaxanes and Knots,* Sauvage, J.-P.; Dietrich-Buchecker, C. O. eds., Wiley-VCH, Weinheim, 1999. (c) Wenz, G.; Han, B.–H.; Mueller, A. *Chem. Rev*. **2006**, *106*, 782-817. (d) Griffiths, K. Stoddart, J. F. *Pure Appl. Chem.* **2008**, *80*, 485-506. (e) Harada, A.; Takashima, Y.; Yamaguchi, H. *Chem. Soc. Rev*. **2009**, *38*, 875-882. (f) Durola, F.; Sauvage, J.-P.; Wenger, O. S. *Coord. Chem. Rev.* **2010**, *254*, 1748-1759. (g) Gassensmith, J. J.; Baumes, J. M.; Smith, B. D. *Chem. Commun.* **2009**, *42*, 6329-6338. (h) Hanni, K. D.; Leigh, D. A. *Chem. Soc. Rev.* **2010**, *39*, 1240-1251.

(2) (a) Ciferri, A. In *Supramolecular Polymers*; Marcel-Dekker: New York, 2000. (b) Brunsveld, L.; Folmer, B. J. B.; Meijer, E. W.; Sijbesma, R. P. *Chem. Rev.* **2001**, *101*, 4071-4098. (c) Huang, F.; Gibson, H. W. *Prog. Polym. Sci.* **2005**, *30*, 982-1018. (d) Lehn, J.-M. *Chem. Soc. Rev.* **2007**, *36*, 151-160. (e) Hwang, S.-H.; Moorefield, C. N.; Newkome, G. R. *Chem. Soc. Rev.* **2008**, *37*, 2543-2557. (f) De Greef, T. F. A.; Smulders, M. M. J.; Wolffs, M.; Schenning, A. P. H. J.; Sijbesma, R. P.; Meijer, E. W. *Chem. Rev.* **2009**, *109*, 5687-5754. (g) Harada, A.; Hashidzume, A.; Yamaguchi, H.; Takashima, Y. *Chem. Rev.* **2009**, *109*, 5974-6023. (h) Niu, Z.; Gibson, H. W. *Chem. Rev.* **2009**, *109*, 6024-6046. (i) Fang, L.; Olson, M. A.; Benitez, D.; Tkatchouk, E.; Goddard III, W. A.; Stoddart, J. F. *Chem. Soc. Rev.* **2010**, *39*, 17-29. (j) Niu, Z.; Huang F.; Gibson, H. W. *J. Am. Chem. Soc.*, **2011**, *133*, 2836-2839.

(3) Some recent publications: (a) Zhang, M.; Zhu, K.; Huang, F. *Chem. Commun.* **2010**, *46*, 8131-8141. (b) Wang, C.; Olson, M. A.; Fang, L.; Benítez, D.; Tkatchouk, E.; Basu, S.; Basuray, A. N.; Zhang, D.; Zhu, D.; Goddard, W. A.; Stoddart, J. F. P*roc. Nat. Acad. Sci. USA*, **2010**, *107*, 13991-13996. (c) Trabolsi, A.; Fahrenbach, A. C.; Dey, S. K.; Share, A. I.; Friedman, D. C.; Basu, S.; Gasa, T. B.; Khashab, N. M.; Saha, S.; Aprahamian, I.; Khatib, H. A.; Flood, A. H.; Stoddart, J. F. *Chem. Commun.* **2010**, *46*, 871-873. (d) Jiang, Y.; Cao, J.; Zhao, J. -M.; Xiang, J. -F.; Chen, C. -F. *J. Org. Chem.* **2010**, *75*, 1767-1770. (e) Zhu, K.; Li, K.; Wang, S.; Huang, F. *J. Org. Chem.* **2009**, *74*, 1322-1328. (f) Gasa, T. B.; Spruell, J. M.; Dichtel, W. R.; Sørensen, T. J.; Philp, D.; Stoddart, J. F.; Kuzmič, P. C*hem. Eur. J.* **2009**, *15*, 106-116.

(4) (a) Bryant, W. S.; Jones, J. W.; Mason, P. E.; Guzei, I.; Rheingold, A. L.; Fronczek, F. R.; Nagvekar, D. S.; Gibson, H. W. *Org. Lett.* **1999**, *1*, 1001-1004. (b) Huang, F.; Fronczek, F. R.; Gibson, H. W. *J. Am. Chem. Soc.* **2003**, *125*, 9272-9273. (c) Huang, F.; Gibson, H. W.; Bryant, W. S.; Nagvekar, D. S.; Fronczek, F. R. *J. Am. Chem. Soc.* **2003**, *125*, 9367-9371. (d) Huang, F.; Zhou, L.; Jones, J. W.; Gibson, H. W.; Ashraf-Khorassani, M. *Chem. Commun.* **2004**, 2670-2671. (e) Huang, F.; Switek, K. A.; Zakharov, L. N.; Fronczek, F. R.; Slebodnick, C.; Lam, M.; Golen, J. A.; Bryant, W. S.; Mason, P. E.; Rheingold, A. L.; Ashraf-Khorassani,; M. Gibson, H. W. *J. Org. Chem.* **2005**, *70*, 3231-3241. (f) Huang, F.; Guzei, I. A.; Jones, J. W.; Gibson. H. W. *Chem. Commun.* **2005**, 1693-1695. (g) Gibson, H. W.; Wang, H.; Slebodnick, C.; Merola, J.; Kassel, S.; Rheingold, A. L. *J. Org. Chem.* **2007**, *72*, 3381-3393. (h) Pederson, A. M.-P.; Vetor, R. C.; Rouser, M. A.; Huang, F.; Slebodnick, C.; Schoonover, D. S.; Gibson, H. W. *J. Org. Chem.* **2008**, *73*, 5570-5573. (i) Li, S.; Liu, M.; Zhang, J.; Zheng, B.; Zhang, C.; Wen, X.; Li, N.; Huang, F. *Org. Biomol. Chem.* **2008**, *6*, 2103-2107. (j) Li, S.; Liu, M.; Zhang, J.; Zheng, B.; Wen, X.; Li, N.; Huang, F. *Eur. J. Org. Chem.* **2008**, 6128-6133. (k) Wang, F.; Zhou, Q.; Zhu, K.; Li, S.; Wang, C.; Liu, M.; Li, N.; Fronczek, F. R.; Huang, F. Tetrahedron **2009**, *65*, 1488-1494. (l) Liu, M.; Li, S.; Zhang, M.; Zhou, Q.; Wang, F.; Hu, M.; Fronczek, F. R.; Li, N.; Huang, F. *Org. Biomol. Chem.* **2009**, *7*, 1288-1291. (m) Liu, M.; Li, S.; Hu, M.; Wang, F.; Huang, F. Org. Lett. **2010**, *12*, 760-763. (n) Zhu, K.; Wu, L.; Yan, X.; Zheng, B.; Zhang, M.; Huang, F. *Chem. Eur. J.* **2010**, *16*, 6088-6098. (o) Liu, M.; Yan, X.; Hu, M.; Chen, X.; Zhang, M.; Zheng, B.; Hu, X.; Shao, S.; Huang, F. *Org. Lett.* **2010**, *12*, 2558-2661.

(5) (a) Tsukube, H.; Furuta, H.; Odani, A.; Takeda, Y.; Kudo, Y.; Inoue, Y.; Liu, Y.; Sakamoto, H.; Kimura, K. in *Comprehensive Supramolecular Chemistry*, Atwood, J. L.; Davies, J. E. D.; MacNicol, D. D.; Vogtle, F.; Lehn, J.-M. Ed.; Elseiver Science Ltd., New York, 1996, pp. 425-479. (b) Hirose, K. *J. Inclusion Phenom. Macrocyclic Chem.* **2001**, *39*, 193-209. (c) Bruneau, E.; Lavabre, D.; Levy, G.; Micheau, J. C. *J. Chem. Educ.* **1992**, *69*, 833-837.

(6) (a) Marshall, A. G. In *Biophysical Chemistry: Principles, Techniques, and Applications*, John Wiley & Sons, New York, NY., 1978, pp 70-77. (b) Freifelder, D. M. In *Physical Biochemistry*, W. H. Freeman and Co., New York, 1982, pp 659-660. (c) Connors, K. A. In *Binding Constants*; J. Wiley and Sons, New York, 1987, pp 78-86.

(7) Perlmutter-Hayman, B. *Acc. Chem. Res.* **1986**, *19*, 90-96.

(8) K_1=[**DMP**·**2**]/{[**DMP**][**2**]} and K_2 = [**DMP**$_2$·**2**]/{[**DMP**][**DMP**·**2**]}. The intercept of the linear fit straight line based on the first four data points for low *p* (Figure 9-3, lower plot) gave the value of K_1, while the slope of the last five data points for high *p* (Figure 9-3) gave the value of -2K_2.[7] Errors of the two apparent association constants were calculated on the basis of errors of the slopes.

(9) a) Jacobson, H.; Stockmayer, W. H. *J. Chem. Phys.* **1950**, *18*, 1600–1606. b) Ercolani, G.; Mandolini, L.; Mencarelli, P.; Roelens, S. *J. Am. Chem. Soc.* **1993**, *115,* 3901–3908. c) Muraoka, T.; Kinbara, K.; Aida, T. *Nature* **2006**, *440,* 512-515.

(10) Allwood, B. L.; Shahriari-Zavareh, H.; Stoddart, J. F.; Williams, D. J. *Chem. Commun.* **1987**, 1058-1061.

TOC Graphic:

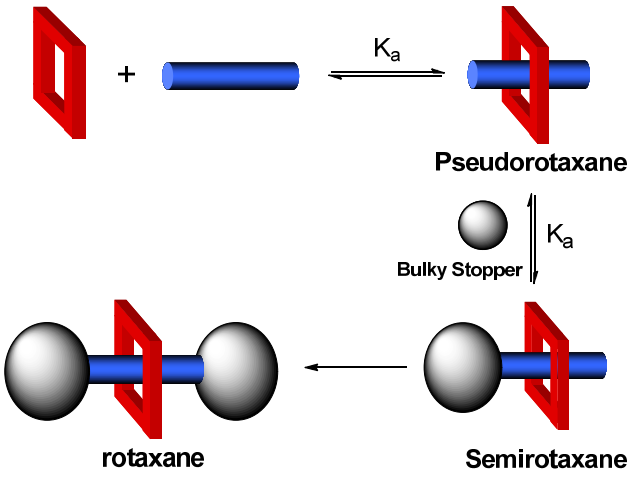

Abstract:

Hydroxyl-functionalized secondary ammonium salts, DB24C8 and secondary ammonium salt-based [2]semirotaxane and [2]rotaxane were prepared successfully. X-ray analysis of a single crystal of the [2]semirotaxane confirmed its semirotaxane nature. In addition, the formation of the [2]semirotaxane can be reversibly controlled by adding KPF_6 and 18C6 sequentially. This system affords a way to prepare novel supramolecular polymers.

Chapter 10.

[2]Semi-rotaxane and [2]rotaxane based on Dibenzo-24-crown-8 (DB24C8) and Secondary Ammonium Salts.

10.1 Introduction

In supramolecular chemistry, pseudorotaxane[1] is an important concept. A pseudorotaxane consists of a linear molecular component ("guest") threaded through a macrocyclic component ("host").[1-2] The linear guest can dethread and rethread, as a result, the pseudorotaxane is always in equilibrium with its two components-host and guest. If a bulky stopper, whose size is much bigger than the central cavity of the cyclic host, is applied to one end of the linear guest, a semi-rotaxane is afforded (Figure 10-1). If two bulky stoppers are applied to the ends of the linear guest, a rotaxane is formed. Similar to pseudorotaxanes, semirotaxanes and rotaxanes are important parts of supramolecular chemistry research. Their interlocked structures have been widely used as molecular machines which can be controlled by external stimuli, such as: electrochemical control,[3] pH-changes [4] and other stimuli.[5]

It has been very known that dibenzo-24-crown-8 (DB24C8) derivatives can form stable pseudorotaxanes with secondary ammonium salts driven by hydrogen bonds and ion-dipole interactions in low-polarity solvents,[6] such as acetone and acetonitrile. Therefore, DB24C8 has been widely empolyed in the preparation of pseudorotaxanes, rotaxanes and catenanes. In this chapter, novel DB24C8 and secondary ammonium salt-based semi-rotaxane and rotaxane are prepared.

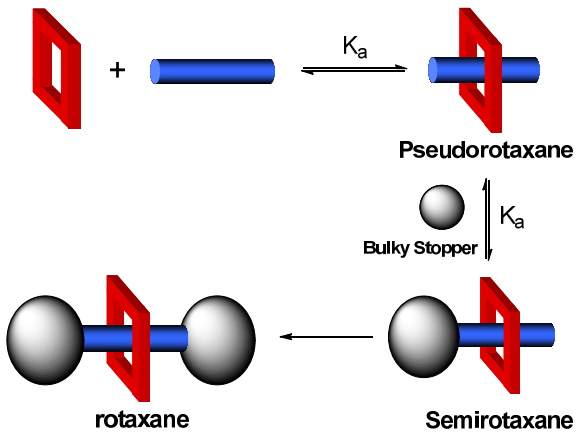

Figure 10-1. Pseudorotaxane, semirotaxane and rotaxane.

10.2 Results and discussion

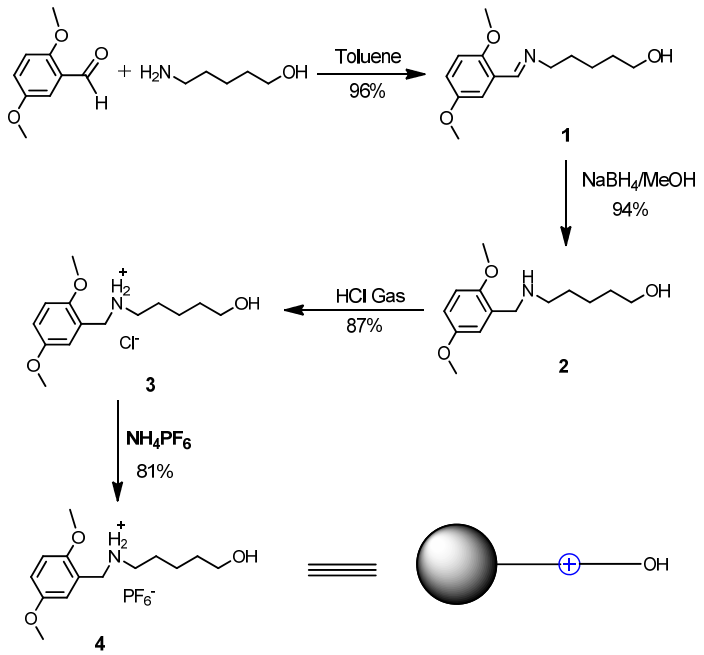

Scheme 10-1. Preparation of hydroxyl-functionalized secondary ammonium salt **4**.

The reaction between 2,5-dimethoxybenzaldehyde and 5-amino-1-pentanol in toluene afforded imine **1** in 96% yield. **1** was reduced by $NaBH_4$ in methanol and amine **2** was obtained in 94% yield. Several attempts were made to prepare secondary ammonium salts **3** and **4**; however, only the method described below worked: N_2 gas was bubbled through a flask containing HCl (37%, aq.) and then bubbled into an ethyl acetate solution of **2**. The

hydrochloride salt **3** precipitated out as a white solid immediately. After filtration, **3** was dissolved in DI H_2O; excess NH_4PF_6 was added and hexafluorophosphate salt **4** was obtained as a white solid precipitate in 81% yield.

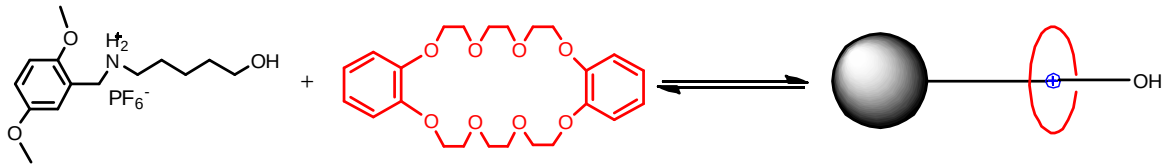

Scheme 10-2. [2]Semirotaxane based on DB24C8 and secondary ammonium salt **4.**

The complexation behavior between DB24C8 and secondary ammonium salt **4** was studied by ^{1}H-NMR. Upon mixing **4** and DB24C8 in acetone-d_6, the peak corresponding to proton H_γ shifted upfield, whereas peaks of H_1, H_α and H_β shifted downfield (Figure 10-2). These observations suggested that a stable complex between **4** and DB24C8 was formed. The ESI-MS[7] confirmed the formation of the [2]semirotaxane. A peak corresponding to $[M\text{-}PF_6^-]^+$ was found at 702.3874 (calcd.: 702.3853, error: 2.97 ppm). No other related peaks were observed.

Similar to the other reported DB24C8/secondary ammonium salt-based pseudorotaxanes,[8] the complexation could be controlled by adding KPF_6 and 18-crown-6 (18C6) into the solution. As shown by Figure 10-3, when excess KPF_6 was added into a solution of **4** and DB24C8, the [2]semirotaxane between **4** and DB24C8 was destroyed. H_1 shifted upfield to the same position corresponding to the H_1 of free **4** and H_α, H_β and H_γ shifted to the positions corresponding to the H_α, H_β and H_γ of pseudorotaxane between KPF_6 and DB24C8. When 18C6 was then added, the [2]semirotaxane based on **4** and DB24C8 was regenerated and all the peaks shifted back to their original positions. This is due to the facts that DB24C8 binds KPF_6 much more strongly than ammonium salt **4**, but 18C6 in turn binds KPF_6 very strongly, but does not interact strongly with ammonium salt **4**.

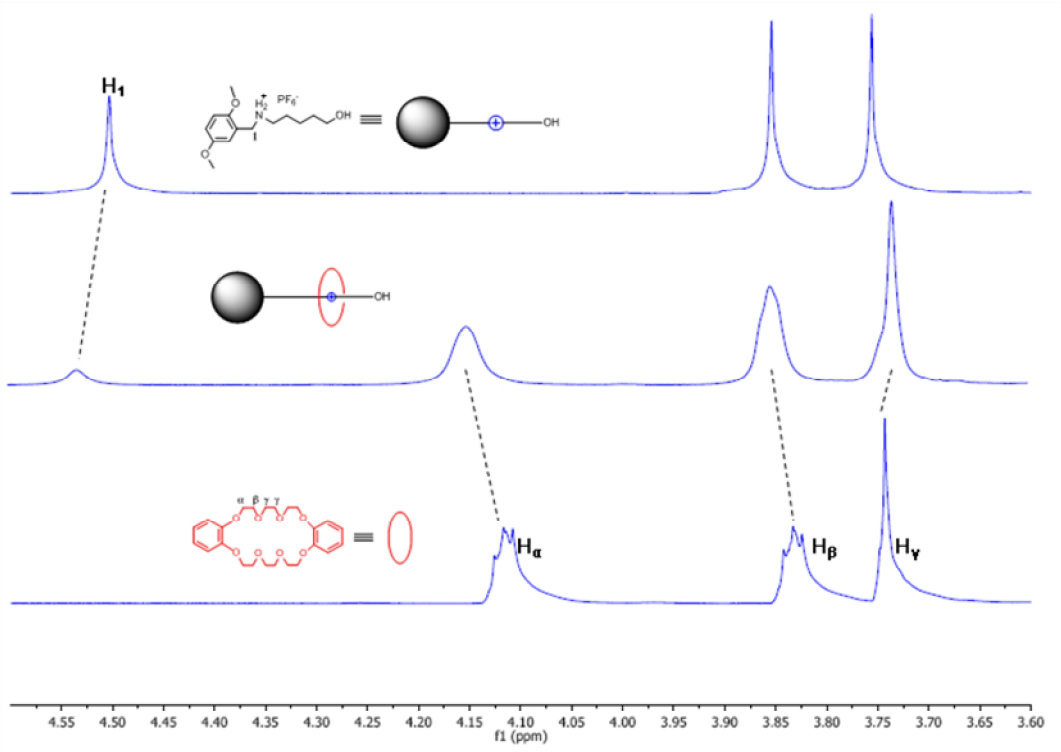

Figure 10-2. Partial ^{1}H-NMR spectra (400 MHz, Acetone-d_6, 298K) of free DB24C8 (Bottom spectrum). Mixture of DB24C8 and ammonium salt **4** (1:1 equiv, middle line). Free **4** (upper spectrum).

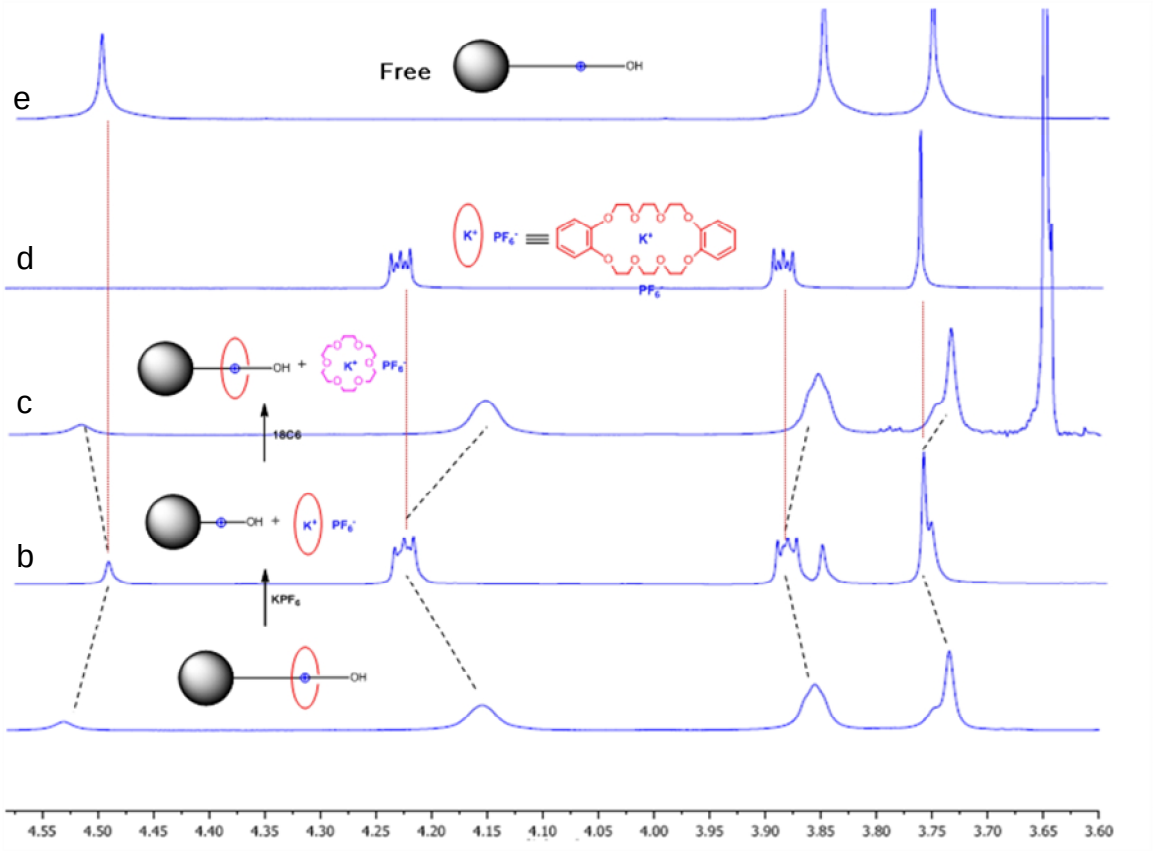

Figure 10-3. Partial ^{1}H-NMR spectra (400 MHz, acetone-d_6, 298K) of **a**. DB24C8 and ammonium salt **4** (1:1 <mol/mol>, 1.0 mM). **b**. The mixture obtained after adding KPF_6 (1.2 equiv) into solution a. **c**. The mixture obtained after adding 18C6 (1.2 equiv) into solution b. **d**. DB24C8 and KPF_6 (1:1 <mol/mol>). **e**. Free **4**.

X-ray analysis of a single crystal of DB24C8, which was obtained via the vapor difussion of pentane into an acetone solution, indicated that DB24C8 assumes "zig-zag" shape. As expected, X-ray analysis of a single crystal of the complex DB24C8·**4** indicated the formation of a semi-rotaxane. The complex is stabilized by hydrogen bonds between the host DB24C8 and guest **4**. As expected, the bulky end is much bigger than the cavity size of DB24C8. Therefore, if another bulky stopper is applied to the other end of the linear guest in the semi-rotaxane, obviously, a [2]rotaxane will be afforded.

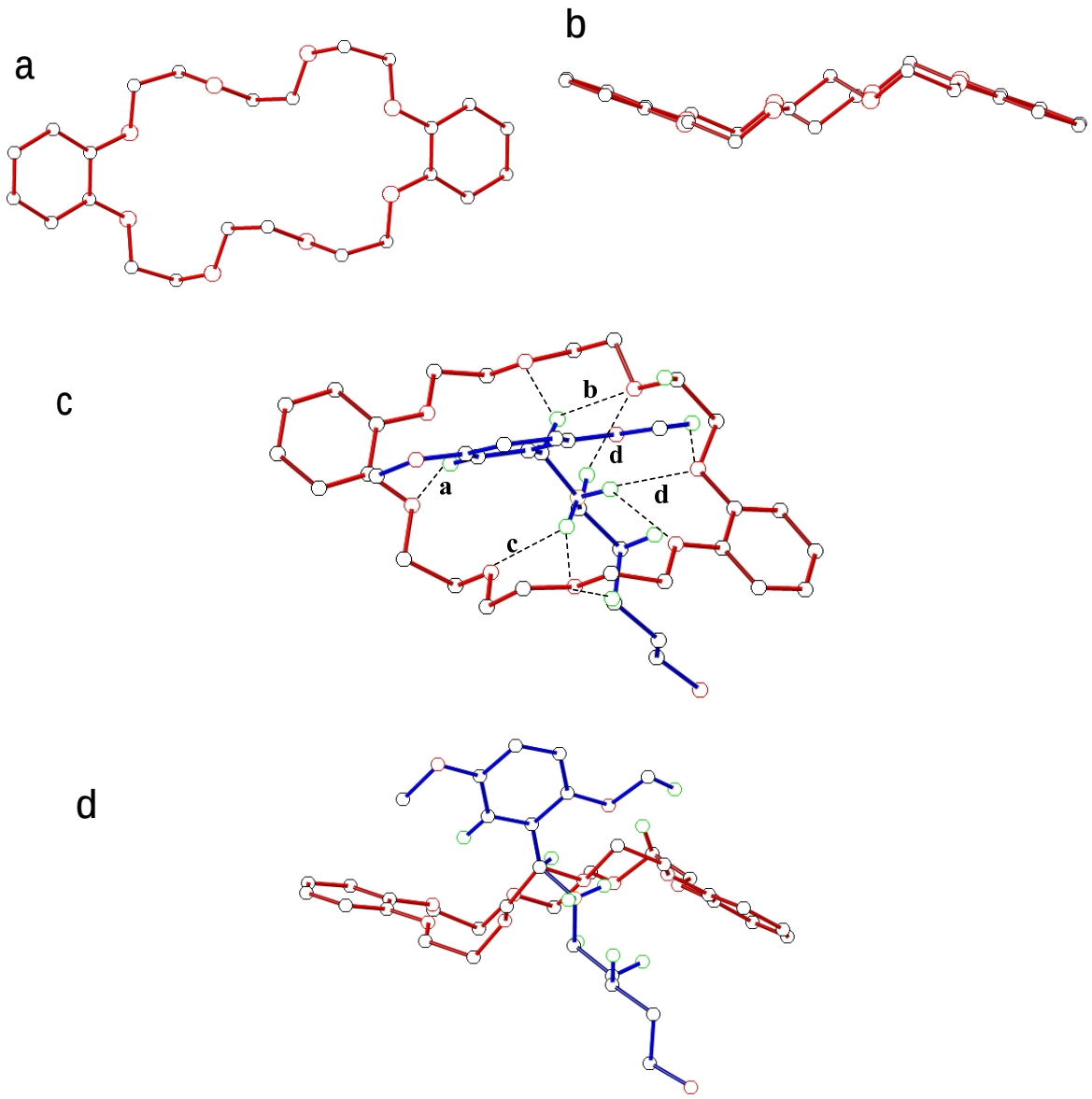

Figure 10-4. (a) and (b) Two views of the X-ray structure of DB24C10 polymorphism. (c) and (d): Two views of the X-ray structure of **DB24C8·4**. DB24C8 is red. **4** is blue. Oxygen atoms are red. Carbon atoms are black. Nitrogen atoms are blue. Hydrogen atoms are green. Solvent molecules, minor disordered carbon and hydrogen atoms, hydrogen atoms except the ones involved in hydrogen bonding have been omitted for clarity. Hydrogen bonds in (d) were omitted for clarity. Selected hydrogen-bond parameters: H···O(N) distances (Å), C···O(N) distances (Å), C-H···O(N) angles (deg): a 2.705, 3.586, 154.5; b 2.569, 3.374, 138.4; c 2.264, 2.980, 134.3; d 2.328, 3.177, 153.2;

A solid mixture **4** and DB24C8 was dried in a drying pistol with P_2O_5 at 65 °C overnight. The solid mixture was dissolved in DCM. 3,5-Dimehoxyphenyl isocyanate and di(n-butyl)tin dilaurate (DBTDL) were added to the solution. The solution was stirred at RT for 2 days. After purification, [2]rotaxane **5** was obtained in 76% yield.

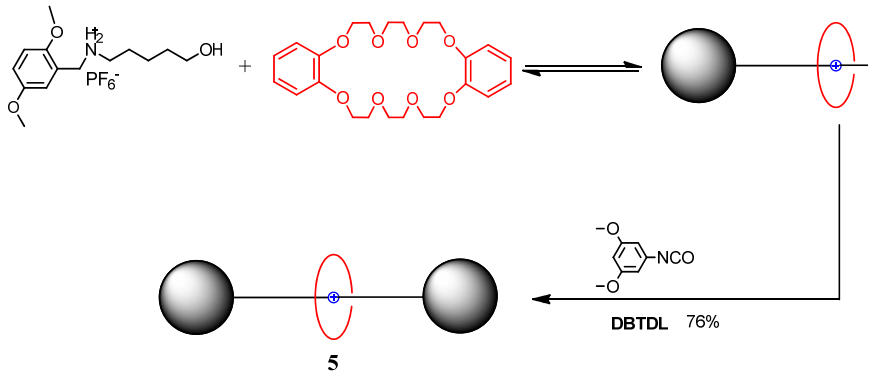

Scheme 10-3. Preparation of [2]rotaxane **5**.

10.3 Conclusions

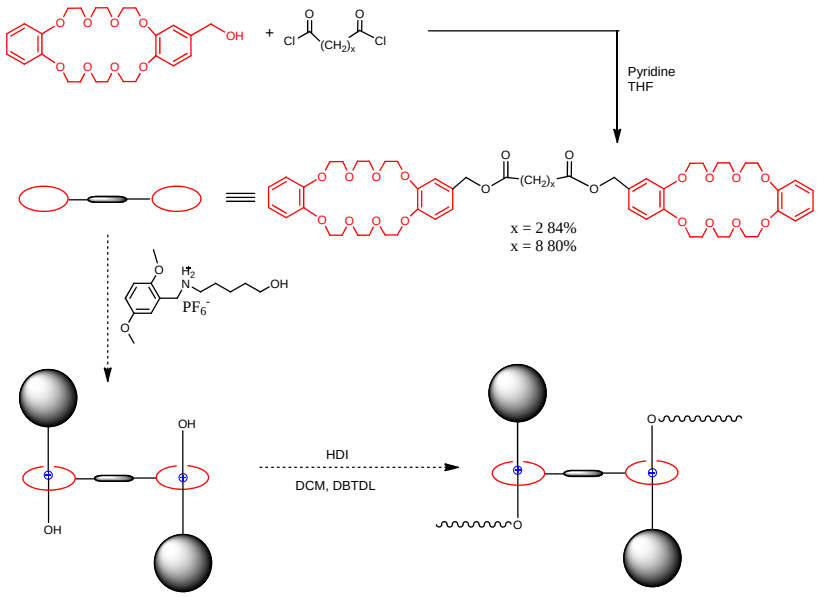

Scheme 10-4. Preparation of novel supramolecular polymer based on bisDB24C8 and hydroxyl-functionalized secondary ammonium salts.

In summary, a hydroxyl-functionalized secondary ammonium salt with DB24C8 produced a [2]semirotaxane and the corresponding rotaxane was prepared successfully by attaching a second terminal blocking group or stopper. X-ray analysis of the single crystal of the

[2]semirotaxane confirmed the formation of semirotaxane structures. In addition, the formation of [2]semirotaxane can be controlled by adding KPF_6 and 18C6. This system affords a way to prepare novel supramolecular polymers as shown by Scheme 10-4.

10.4 Acknowledgements

This work was supported by the National Science Foundation (DMR0704076) and the Petroleum Research Fund administered by the American Chemical Society (47644-AC). We also acknowledge the National Science Foundation for funds to purchase the Innova-400 MHz NMR and the Agilent 6220 Accurate Mass TOF LC/MS Spectrometers (CHE-0131124 & CHE-0722638, respectively).

10.5 Experimental section

10.5.1 Synthesis of 1

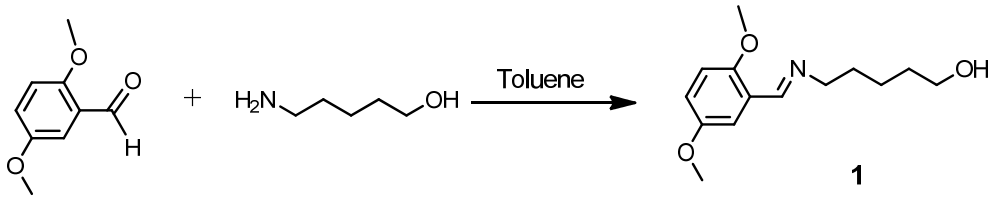

Scheme 10-5. Preparation of **1**.

2,5-Dimethoxybenzaldehyde (2.0 g, 12 mmol) was dissolved in toluene (20 mL) and the solution was put into 500 mL flask equipped with Dean-Stark trap. 5-Amino-1-pentanol (1.2 g, 12 mol) in toluene (5 mL) was added to the flask dropwise. The solution was refluxed for 2 days. The solvent was removed and a brown oil was obtained. A short silica gel column was used to purify the crude product. After the column, a yellow oil was obtained (2.90 g, 96%). ^{1}H-NMR ($CDCl_3$, 500MHz, Figure 10-5): δ: 8.64 (s, 1.0 H, H_1), 7.46 (d, ^4J = 3 Hz, 1.0 H, H_4), 6.93 (m, 1.0 H, H_2), 6.83 (d, ^3J = 8 Hz, 1.0 H, H_3), 3.80 (s, 2.7 H, OCH_3), 3.78 (s, 3.0H, OCH_3), 3.62 (m, 4.2 H, H_5 and H_9), 2.31(s, 1.1H, -OH), 1.72 (m, 2.1 H, H_6), 1.59 (m, 2.1 H, H_8), 1.72 (m, 2.1 H, H_7). 7.31, 7.12 and 7.10 (toluene peaks). ESI-MS (Figure 10-6); calcd. for **1**: *m/z* 251.1527, found: 251.1521, error: 2.17 ppm.

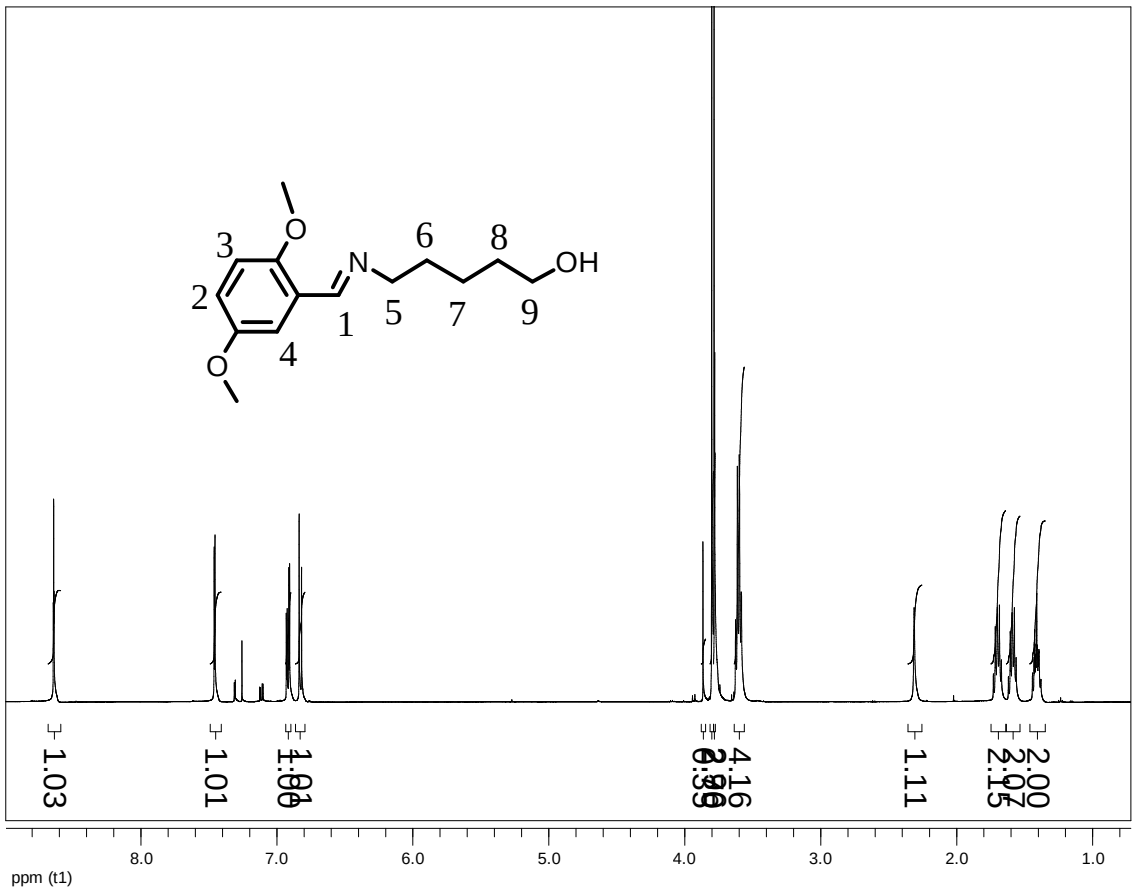

Figure 10-5. 500 MHz ^{1}H-NMR spectrum ($CDCl_3$, room temperature) of **1**.

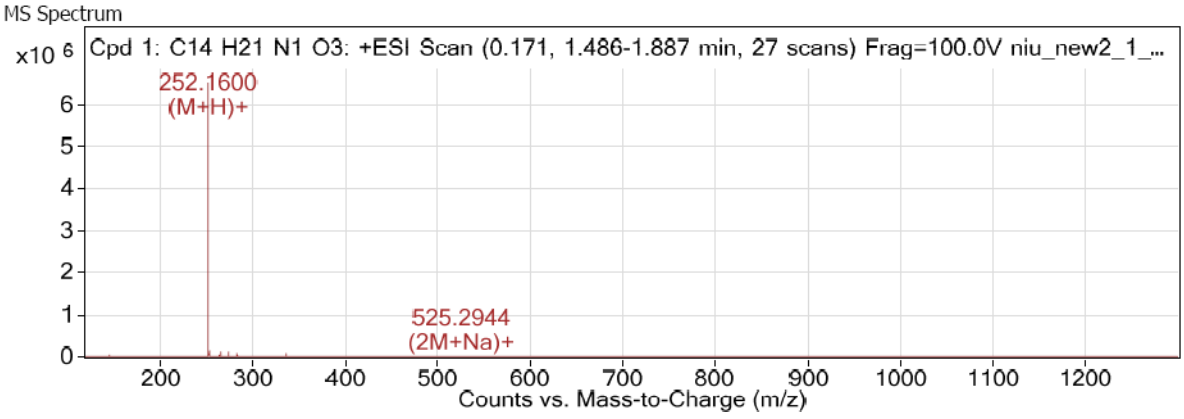

Figure 10-6. ESI-MS spectrum of **1**.

10.5.2 Synthesis of 2

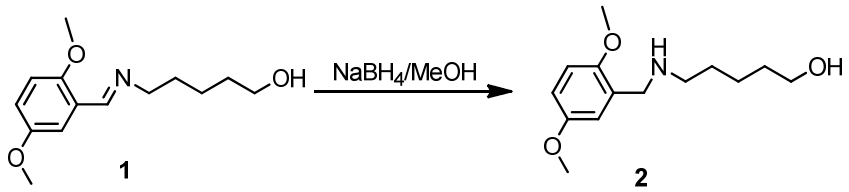

Scheme 10-6. Preparation of **3**.

1 (2.8 g, 11 mmol) was dissolved in MeOH (20 mL). $NaBH_4$ (1.0 g, 28 mmol) was added **slowly** to the solution **in small portion (important!)**. The solution was refluxed for 20 hours. After reaction, the solvent was removed. The product was partitioned between H_2O and DCM, the aqueous phase was washed with DCM. The combined organic phase was washed with H_2O and NaCl (aq. sat.) and dried over Na_2SO_4. After solvent was removed, a yellow oil was obtained (2.64 g, 94%). ^{1}H-NMR ($CDCl_3$, 500MHz, Figure 10-7): δ: 6.80 (d, ^4J = 3 Hz, 1.0 H, H_4), 6.76 (m, 2.1 H, H_2 and H_3), 3.76 (s, 2.9 H, OCH_3), 3.74 (s, 3.1 H, OCH_3), 3.71 (s, 2.0 H, H_1), 3.56 (t, ^3J = 6 Hz, 2.0 H, H_9), 2.57 (t, ^3J = 6 Hz, 2.1 H, H_5), 1.53 (m, 3.8 H, H_6 and H_7), 1.37 (m, 1.8 H, H_8). 4.612 (0.22 H, impurity). ESI-MS (Figure 10-8); calcd for **2**: 253.1693 , fould ***m/z***, 253.1678, error: 5.93 ppm.

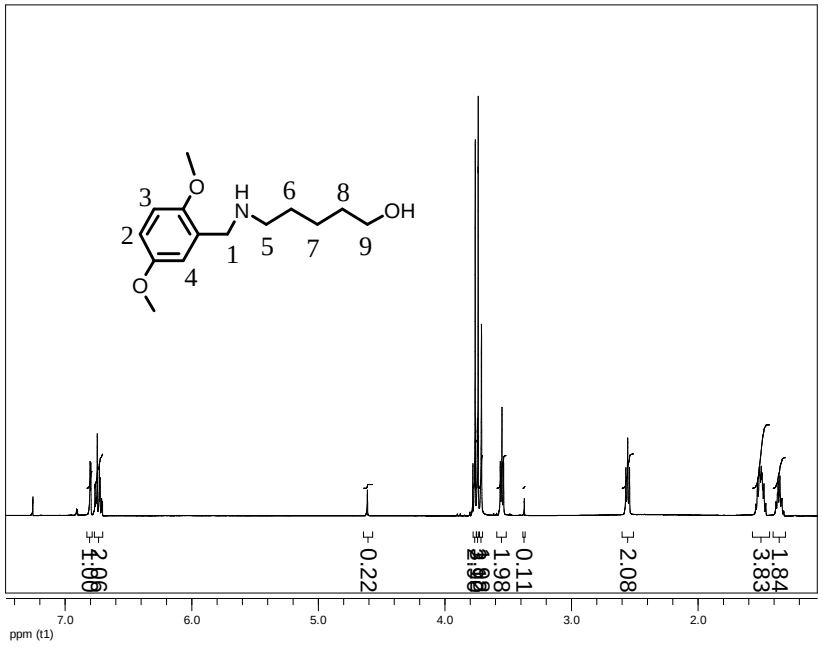

Figure 10-7. 500 MHz ^{1}H-NMR spectrum ($CDCl_3$, room temperature) of **2**.

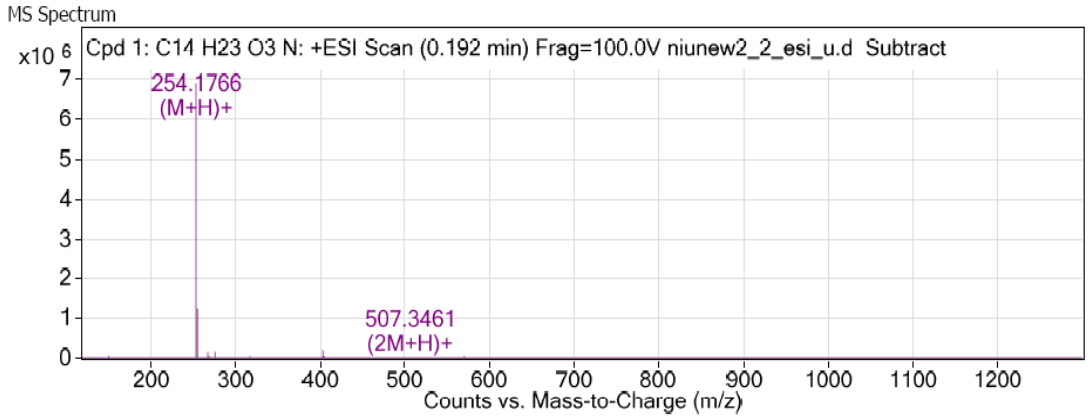

Figure 10-8. ESI-MS spectrum of **2**.

10.5.4 Synthesis 4

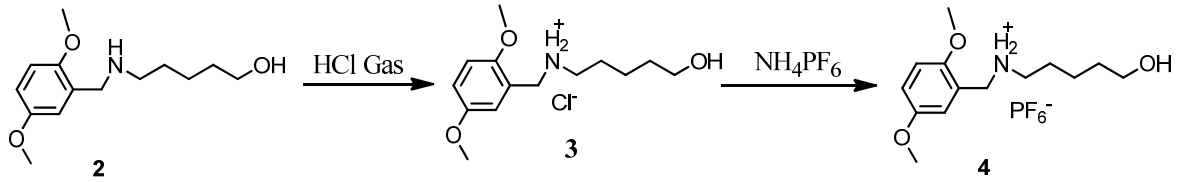

Scheme 10-7. Preparation of **4**

N_2 gas was bubbled through a flask containing HCl (37% aq.) and then bubbled into an ethyl acetate (EA) solution of **2** (5.0 g, 19.7 mmol). A white solid precipitated out immediately. The solid was collected by filtration and washed with EA. Then solid was dissolved in DI H_2O and excessive NH_4PF_6 (9.67 g, 59.2 mmol) were added. The resulting white solid was collected, washed with DI H_2O and dried in a vacuum oven (6.3 g, 81%) of colorless solid, mp 85.0-86.0 °C.). ^{1}H-NMR (acetonitrile-d_3, 500 MHz, Figure 10-9): δ: 7.00 (m, 2.0 H, H_2 and H_3), 6.93 (d, ^4J = 3 Hz, 1.0 H, H_4), 4.12 (s, 2.0 H, H_1), 3.85 (s, 3.0 H, OCH_3), 3.76 (s, 3.0 H, OCH_3), 3.51 (t, ^3J = 6 Hz, 2.0 H, H_9), 3.01 (t, ^3J = 6 Hz, 2.0 H, H_5), 1.71 (m, 2.0 H, H_6), 1.53 (m, 2.0 H, H_8), 1.40 (m, 2.0 H, H_7). ^{13}C-NMR (acetonitrile-d_3, 125 MHz, Figure 10-10): δ: 153.62, 151.94, 119.20, 117.67, 115.72, 111.89, 61.20, 55.64, 55.50, 47.94, 47.72, 31.56, 25.16, 22.48. ESI-MS (Figure 10-11); calcd for **4**: 254.1752 $[M\text{-}PF_6^-]^+$, found: *m/z*, 254.1756 $[M\text{-}PF_6^-]^+$, error: -1.8 ppm.

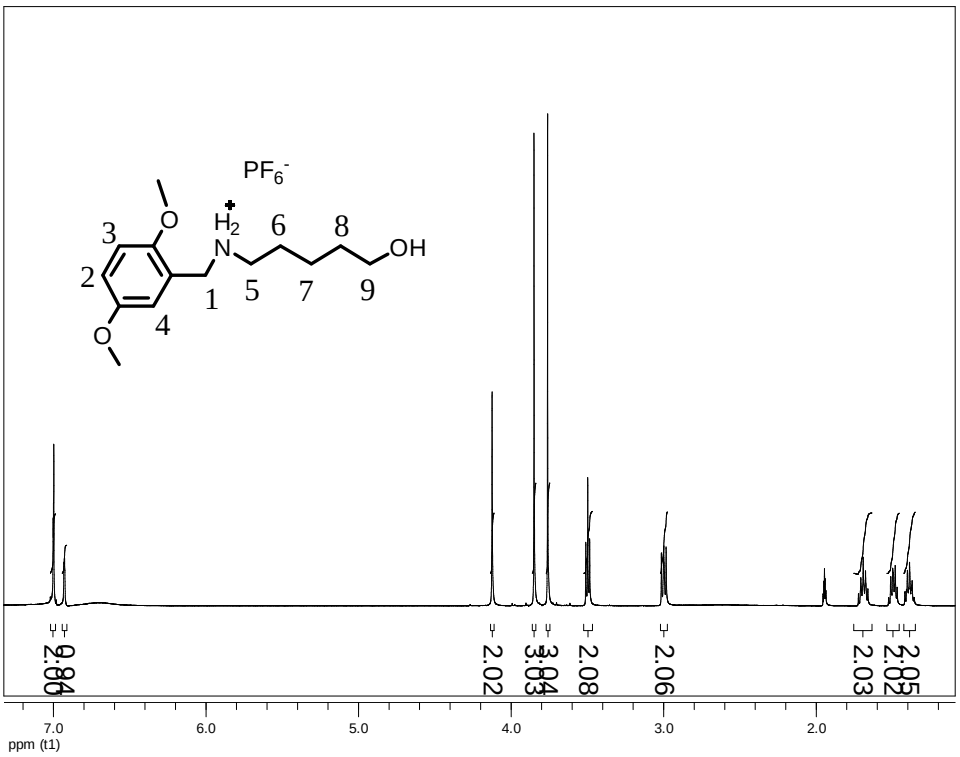

Figure 10-9. 500 MHz ^{1}H-NMR spectrum (acetonitrile-d_3, room temperature) of **4**.

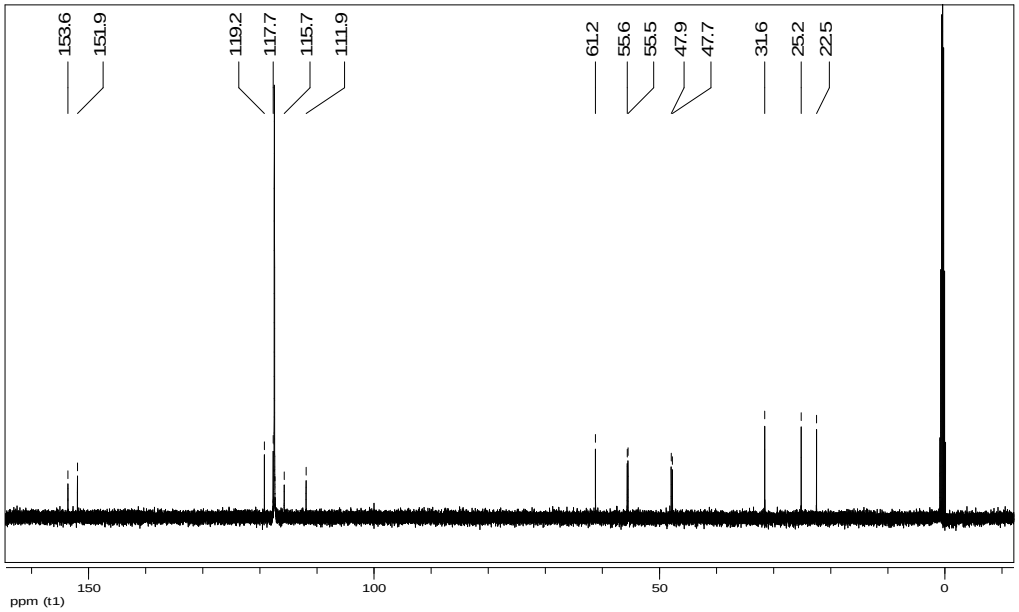

Figure 10-10.125 MHz ^{13}C-NMR spectrum (acetonitrile-d_3, room temperature) of **4**.

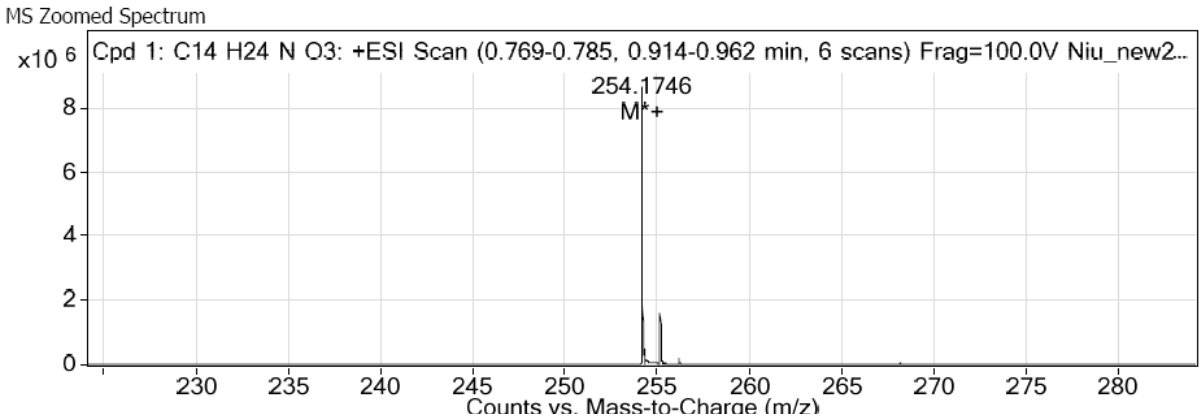

Figure 10-11. ESI-MS spectrum of **4**.

10.5.5 Synthesis of [2]rotaxane

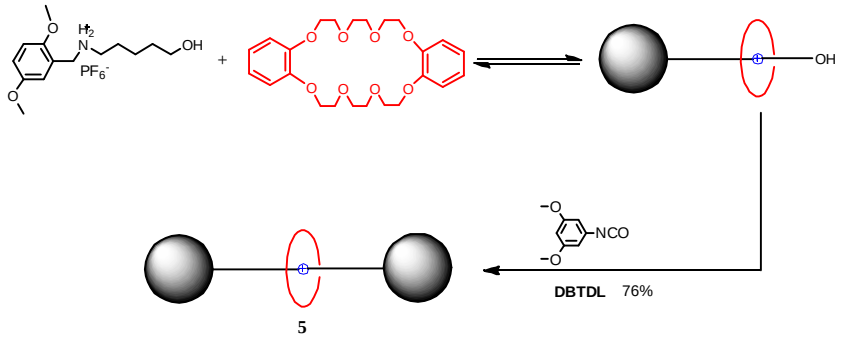

Scheme 10-8. Synthesis of [2]rotaxane based on DB24C8 and **4**.

4 (300 mg, 0.751 mmol) and DB24C8 (352 mg, 0.786 mmol) were dried in drying pistol with P_2O_5 at 65 °C overnight. The solid mixture was dissolved in DCM (20 mL). The solution was stirred under N_2 for 10 hours. 3,5-Dimehoxyphenyl isocyanate (161 mg, 0.899 mmol) and di(n-butyl)tin dilaurate (DBTDL, 51.5 μl) were added into the solution. The solution was stirred at RT for 2 days. Then the mixture was submitted to a silica gel column (HE/EA=1:1 Then DCM:MeOH=97:3) and a wax like solid (585 mg, 76%) was obtained after purification, mp 64.0-65.0 °C. ^{1}H-NMR ($CDCl_3$, 400 MHz, Figure 10-12): δ: 7.13 (br, 2.9 H, -NH_2^+- and –NH-), 6.95 (s, 2.0 H, H_{10}), 6.90 (m, 8.2 H, H_{12} and H_{13}), 6.75 (m, ^4J = 3 Hz, 1.1 H, H_4), 6.70 (m, 2.0 H, H_2 and H_3), 6.15 (d, ^4J = 3 Hz, 1.0 H, H_{11}), 4.53 (s, 1.9 H, H_1), 4.25 (m, 4.0 H, $H_{\alpha'}$), 4.09 (m, 4.0 H, H_α), 3.86 (m, 8.7 H, H_β), 3.76 (s, 6.3 H, OCH_3), 3.67 (m, 12.0 H, H_γ, H_{12} and H_9), 3.46 (m,

4.3 H, $H_{\gamma'}$), 3.31 (m, 2.2 H, H_5), 1.42 (m, 2.0 H, H_6), 1.30 (m, 2.3 H, H_8), 1.08 (m, 2.0 H, H_7). ^{13}C-NMR (125 MHz, $CDCl_3$) (Figure 10-13): δ: 161.05, 153.52, 153.16, 151.55, 147.46, 140.10, 121.62, 121.14, 117.57, 114.83, 112.50, 111.14, 96.54, 95.68, 77.25, 77.00, 76.74, 70.72, 70.18, 68.00, 64.21, 55.57, 55.37, 55.36, 49.13, 48.20, 28.11, 25.84, 22.74. 29.76 (grease). ESI-MS (Figure 10-14): calcd for 881.4436 $[M\text{-}PF_6^-]^+$, found: *m/z*, 881.4417 $[M\text{-}PF_6^-]^+$, error: -2.1 ppm.

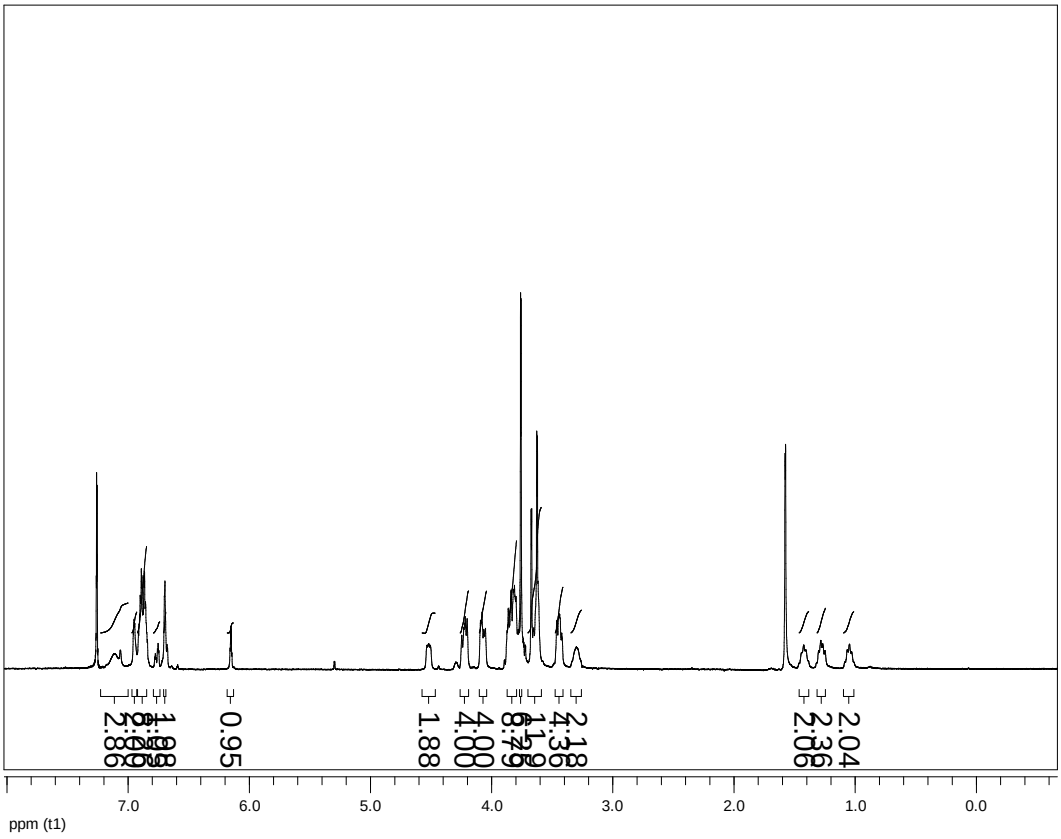

Figure 10-12. 400 MHz ^{1}H-NMR spectrum ($CDCl_3$, room temperature) of [2]rotaxane.

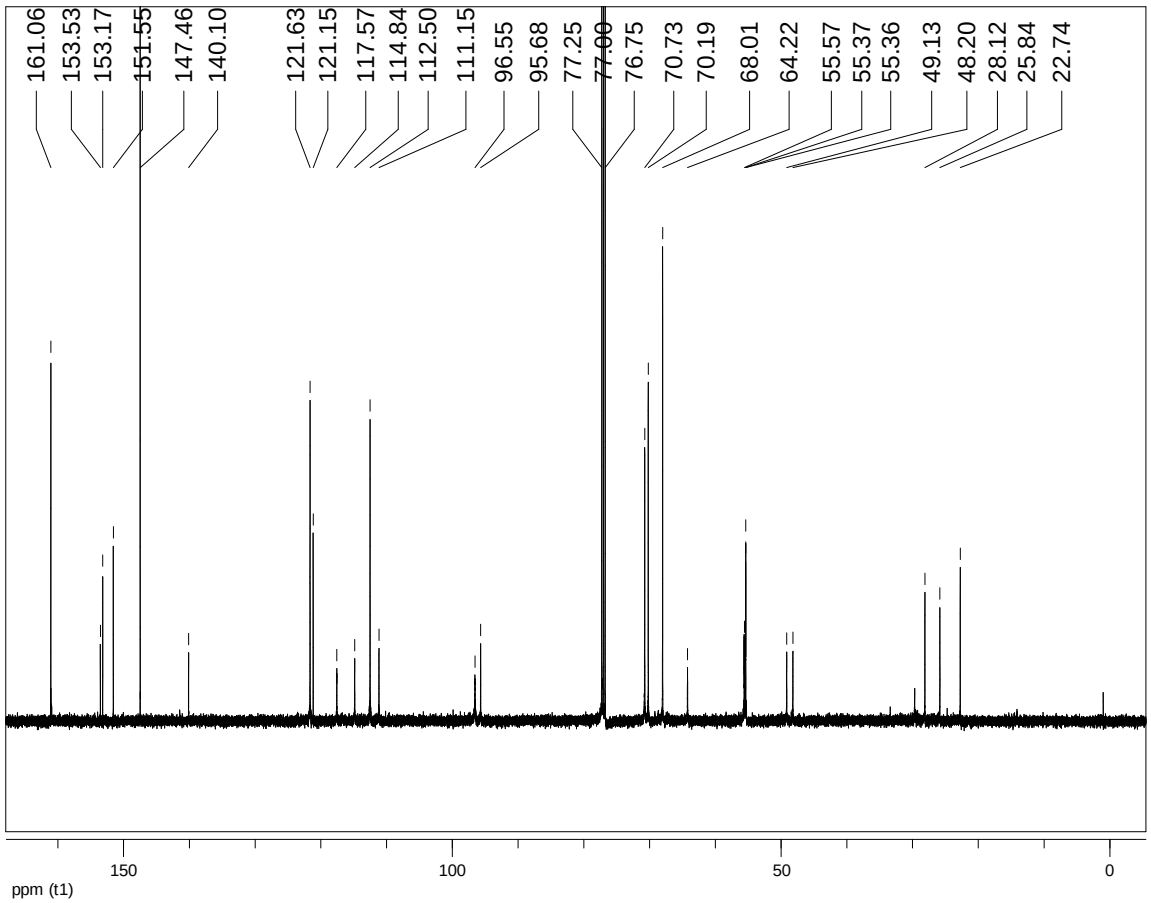

Figure 10-13. 125 MHz ^{13}C-NMR spectrum ($CDCl_3$, room temperature) of [2]rotaxane.

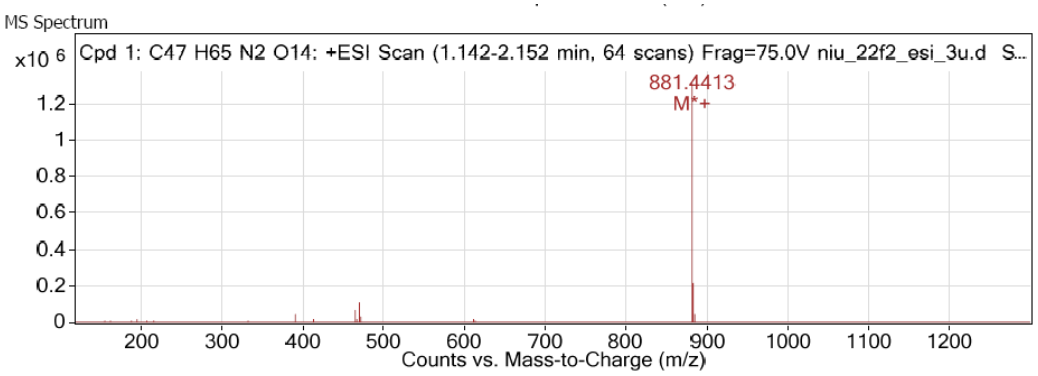

Figure 10-14. ESI-MS spectrum of [2]rotaxane.

10.5.6 ESI-MS of [2]semirotaxane

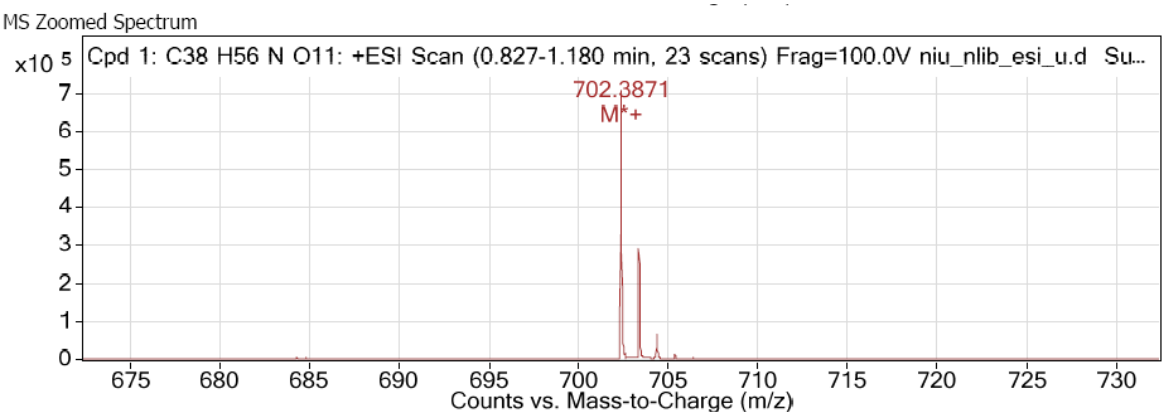

Figure 10-15. ESI-MS spectrum of [2]semirotaxane based on DB24C8 and **4**.

References

(1) (a) Gibson, H. W. In *Large Ring Molecules*; Semlyen, J. A., Ed.; John Wiley & Sons: New York, 1996; Chapter 6, pp 191-262. (b) Raymo, F. M.; Stoddart, J. F. *Chem. Rev.* **1999**, *99*, 1643-1664. (c) Harada, A. *Acc. Chem. Res.* **2001**, *34*, 456-464. (d) Herna′ndez, J. V.; Kay, E. R.; Leigh, D. A. *Science*. **2004**, *306*, 1532–1537. (e) Wenz, G.; Han, B.–H.; Müller, A. *Chem. Rev.* **2006**, *106*, 782-817. (f) Lankshear, M. D.; Beer, P. D. *Acc. Chem. Res.* **2007**, *40*, 657-668. (g) Vickers, M. S.; Beer, P. D. *Chem. Soc. Rev.* **2007**, *36*, 211-225. (h) Colquhoun, H. M.; Zhu, Z.; Cardin, C. J.; White, A. J. P.; Drew, M. G. B.; Gan, Y. *Org. Lett.* **2010**, *12*, 3756-3759. (i) Kim, S. K.; Sessler, J. L. *Chem. Soc. Rev.* **2010**, *39*, 3784-3809. (j) Gasa, T. B.; Valente, C.; Stoddart, J. F. *Chem. Soc. Rev.* **2011**, *40*, 57-78.

(2) Reviews: (a) Ciferri, A. *Supramolecular Polymers*; Marcel-Dekker: New York, 2000. (b) Brunsveld, L.; Folmer, B. J. B.; Meijer, E. W.; Sijbesma, R. P. *Chem. Rev.* **2001**, *101*, 4071-4098. (c) Huang, F.; Gibson, H. W. *Prog. Polym. Sci.* **2005**, *30*, 982-1018. (d) Takata, T.; *Polymer J.* **2006**, *38*, 1-20. (e) De Greef, T. F. A.; Smulders, M. M. J.; Wolffs, M.; Schenning, A. P. H. J.; Sijbesma, R. P.; Meijer, E.

W. *Chem. Rev.* **2009**, *109*, 5687-5754. (f) Harada, A.; Hashidzume, A.; Yamaguchi, H.; Takashima, Y. *Chem. Rev.* **2009**, *109*, 5974-6023. (g) Niu, Z.; Gibson, H. W. *Chem. Rev.* **2009**, *109*, 6024-6046. (h) Faiz, J. A.; Heitz, V.; Sauvage, J.-P. *Chem. Soc. Rev.* **2009**, *38*, 422-442. (i) Fang, L.; Olson, M. A.; Benitez, D.; Tkatchouk, E.; Goddard III, W. A.; Stoddart, J. F. *Chem. Soc. Rev.* **2010**, *39*, 17-29. (j) Thibeault, D.; Morin, J.-F. *Molecules* **2010**, *15*, 3709-3730. (k) Gavina, P.; Tatay, S. *Curr. Org. Syn.* **2010**, *7*, 24-43.

(3) Sobransingh, D.; Kaifer, A. E. *Org. Lett.*, **2006**, Vol. 8, 3247.

(4) (a) Sindelar, V.; Silvi, S.; Kaifer, A. E. *Chem. Commun*. **2006**, 2185-2187. (b) Huang, F. H.; Switek, K. A.; Gibson, H. W. *Chem. Commun*., **2005**, 3655–3657**.**

(5) (a) Qu, D. H.; Wang, Q. C.; Ren, J.; Tian, H. *Org. Lett*. **2004**, 6, 2085-2088. (b) Murakami, H.; Kawabuchi, A.; Kotoo, K.; Kunitake, M.; Nakashima, N. *J. Am. Chem. Soc*.**1997**, 119, 7605-7606.

(6) (a) Aston, P. R.; Fyfe, M. C. T.; Hickingbottom, S. K.; Stoddart, J. F.; White, A. J. P.; Williams, D. J. *J. Chem. Soc. Perkin Trans. 2*, **1998**, 2117-2128. (b) Takata, T.; Kihara, N. *Rev. Heteroat. Chem.* **2000**, *22*, 197-218.

(7) See experimental section.

(8) (a) Yen, M.-L.; Chen, N.-C.; Lai, C.-C.; Liu, Y.-H.; Peng, S.-M.; Chiu, S.-H. *Org. Lett.* **2009**, *11*, 4604-4607. (b) Han, M.; Zhang, H.-Y.; Yang, L.-X.; Jiang, Q.; Liu, Y. *Org. Lett.* **2008**, *10*, 5557-5560

Chapter 11.

[2]- and [3]-Pseudorotaxane based on *cis*(*4,4'*)-Dibenzo-30-crown-10 (DB30C10) Crown Ether/Cryptand and Preparation of Functionalized DB30C10 Cryptands

12.1 Introduction

In supramolecular chemistry, crown ethers have been an important class of hosts that bind metal ions and other cationic species well,[1] leading to the formation of pseudorotaxanes[2] - the fundamental building blocks for more advanced supramolecular species,[3] as talked before. Among them, the *cis*(*4,4'*)-dibenzo-30-crown-10 derivatives, such as: **1a-c** in Scheme 11-1, are superior due to their relatively easy accessibility and high binding strengths with paraquat and diquat derivatives.[4] For crown ethers, *N*,*N'*-dialkyl-4,4'-bipyridinium salts (paraquats), such as: **2** and **3a-b** in Scheme 11-1, are commonly used as guests for crown ether hosts.[5] Cryptands,[6] especially pyridine based cryptands, demonstrated much stronger bind abilities to paraquat derivatives due to incorporation of additional strong binding sites and preorganization.

As we have known, the fundamental properties of polymer not only depend on chemical composition, also depend on architecture aspects. Therefore, researchers are extending the concept of self-assembly non-covalent interaction into polymer science in order to prepare materials with unique properties compared with traditional covalent bonds based polymers. As a result, many novel polymers with interesting structure have been reported.[7-10] However, in order to prepare large non-covalent type polymers, monomers with high association constants are required, as talked in Chapter 1. Obviously, pyridine-based cryptands, which demonstrated good

association constant (K_a) for paraquat salts are good monomer precursors. In order to make bifunctionalized or trifunctionalized monomers, functionalized cryptand precursors must be prepared. In this chapter, [2]- and [3]-pseudorotaxanes were designed and prepared based on *cis*(*4,4'*)-Dibenzo-30-crown-10 (DB30C10) cryptand. In addition, preparation and characterization of functionalized DB30C10 cryptands are discussed.

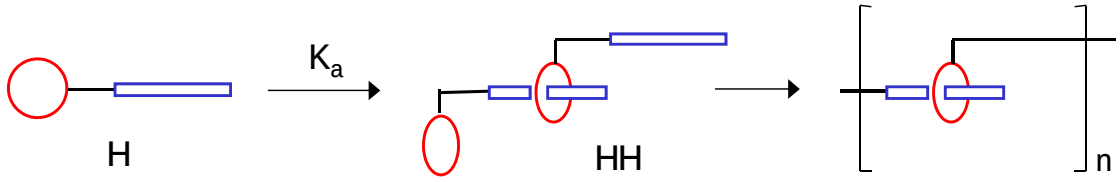

Scheme 11-1. Non-covalent supramolecular polymers based AB type monomers.

11.2 Results and discussion

11.2.1 [2]Pseudorotaxane and [3]pseudorotaxane

Via the highly efficient 6-step synthetic procedure established by our group (Scheme 11-3), *cis*-DB30C10 diester **1a** was prepared in 36% overall yield based on the starting material-3,4-dihydroxybenzoic acid.[4] **1a** was converted into DB30C10 diol **1c** in quantitative yield.[11] DB30C10 based cryptand **2** was prepared in 46% yield via the coupling reaction between **1c** and pyridine-2,6-dicarbonyl dichloride under pseudo-high dilution conditions.[4] The complexation behavior between **1c** and paraquat diethanol **3b** was studied. Although the solutions of **1c** and **3b** were colorless, the mixed solution of **1c** and **3b** was yellow due to the charge transfer between electron-rich aromatic rings of **1c** and electron-poor pyridinium rings of **3b**, good evidence for complexation. Job plot (Figure 11-1) based ^{1}H-NMR data indicated the soichiometry between **1c** and **3b** was 1:1, which was confirmed by an electrospray ionization mass spectrum (ESI-MS): m/z 987.37 [**1c**·**3b**-PF_6]$^+$, 841.40 [**1c**·**3b**-2PF_6-H]$^+$, 421.59 [**1c**·**3b**-2PF_6]$^{2+}$. The association constant (K_a) was determined to be 488 ± 40 mM^{-1}.[12,13]

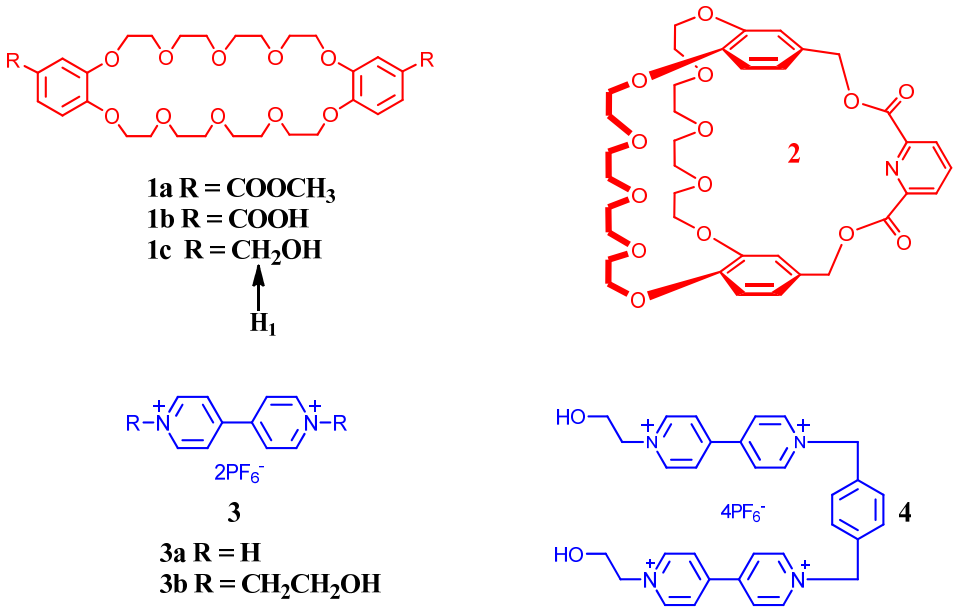

Scheme 11-2. Structures of crown ether derivatives **1a-c** and **2**, dimethyl paraquat **3a-b**, diquat **4** and ferrocene-based *cis*-DB30C10 cryptand **5**.

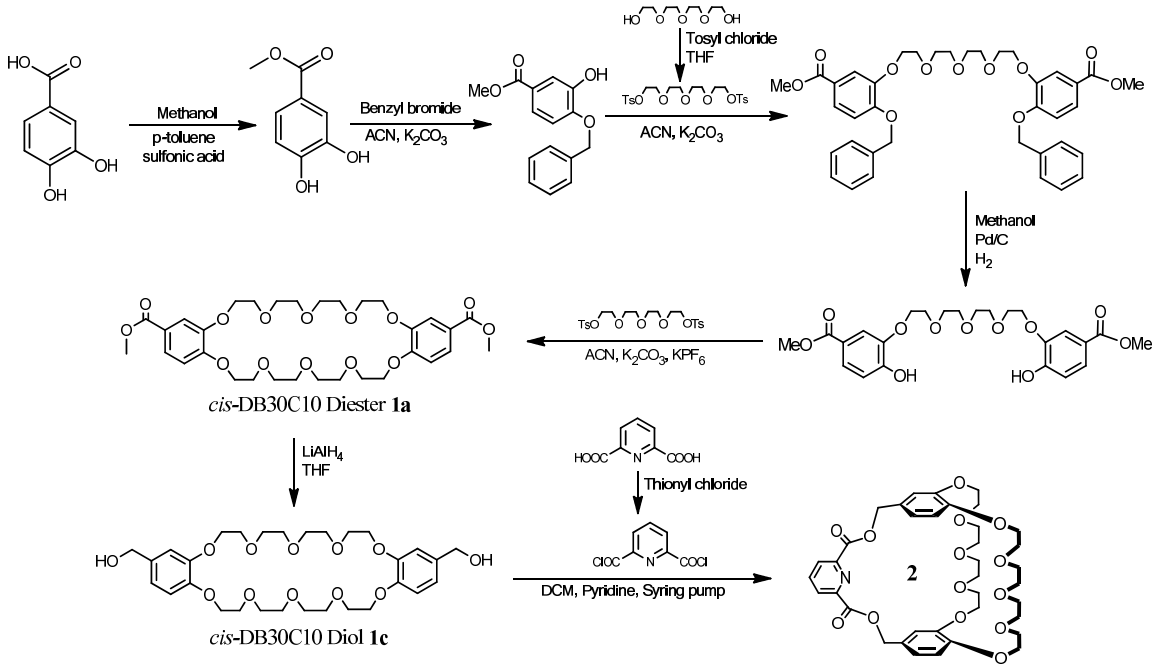

Scheme 11-3. Synthetic procedure for DB32C10 diol (**1c**) and cryptand **2**.

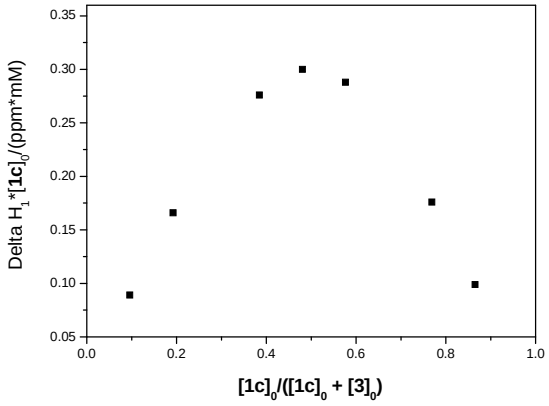

Figure 11-1. Job plot of the complex between **1c** and **3b**. $[\mathbf{1c}]_0 + [\mathbf{3b}]_0 = 10.0$ mM

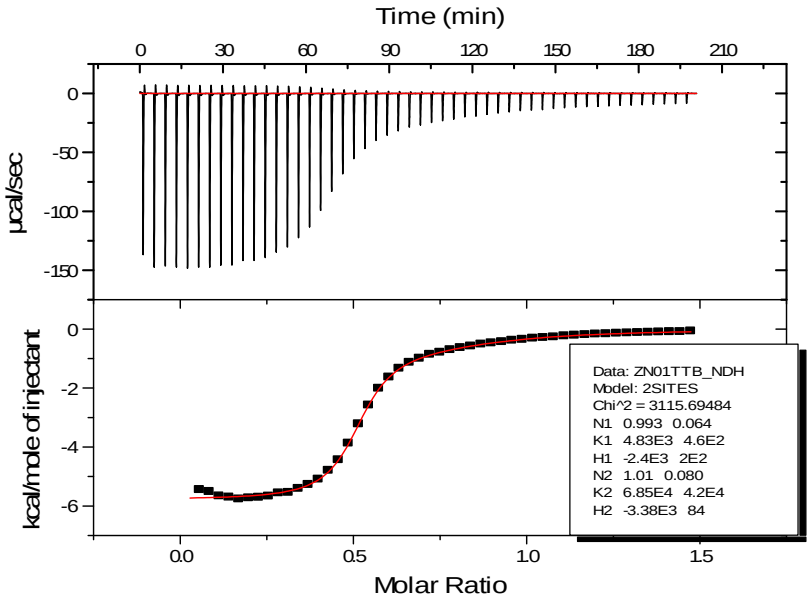

Figure 11-2. ITC curve of **2**·**4** in acetone. The host (**2**) concentration (cell) was 10.0 mM. The guest (**4**) concentration (syringe) was 150 mM. The guest solution was titrated into the host solution (cell) at 25°C.

Based on cryptand **2** and bisparaquat diethanol **4**, a novel [3]pseudorotaxane was designed and prepared. Similar to the complex system between **1b** and **3**, the mixed solution of **2** and **4** was deep yellow, indicating complexation. Based on isothermal titration calorimetry (ITC)

analysis (Figure 11-2), the stichiometry between **2** and **4** was 2:1 and was confirmed by an electrospray ionization mass spectrum (ESI-MS): m/z 1126.31 $[\mathbf{2_2 \cdot 4}\text{-}2PF_6+2H]^{2+}$, 1052.78 $[\mathbf{2_2 \cdot 4}\text{-}3PF_6]^{2+}$, 702.34 $[\mathbf{2_2 \cdot 4}\text{-}3PF_6+H]^{3+}$, 490.55 $[\mathbf{1c \cdot 2}\text{-}4PF_6+H]^{4+}$ [13], as expected. ITC investigation gave $K_1 = 4.8 \pm 0.5 \times 10^3\ M^{-1}$, $K_2 = 6.9 \pm 4 \times 10^4\ M^{-1}$. The ratio $K_2/K_1 = 14.4$ is much higher than the ratio, 0.25, expected for statistical complexation,[14] indicating that the complexation was a cooperative process. The cooperative behavior was ascribed to the existence of inramolecular interactions between the two cryptands, which was reported in another [3]pseudorotaxane system.[ref] In addition, the first threaded cryptand could restrict the rotation freedom of bisparaquat and therefore favor the threading of the second cryptand molecule.

11.2.2 Preparation of functionalized DB30C10 cryptands

As we have known, a high association constant is always required for the preparation of non-covalent supramolecular polymers with high molecular weight. The pyridine-based BMP32C10 cryptand demonstrated the highest association constants with paraquat derivatives.[4] Therefore, during the past 8 years, our group attempted to prepare functionalized DB30C10 cryptands, such **9a** and **9b**. However, all of the attempts have either failed or were very inefficient.[15] Here, the preparation of bromo- and alkyne- functionalized DB30C10 cryptands are discussed.

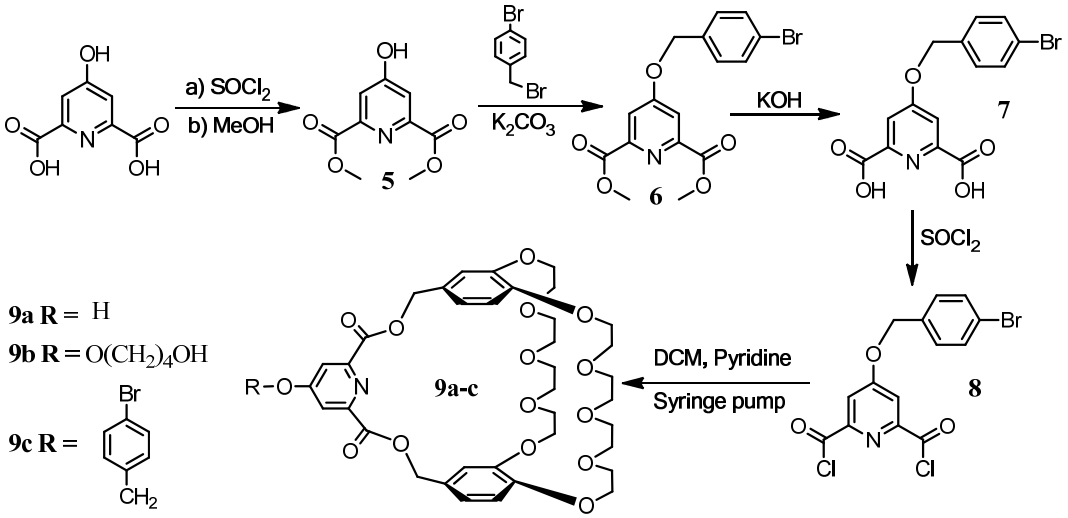

Scheme 11-4. Synthetic strategy I to prepare a halogen functionalized DB30C10 cryptand.

First, a bromo-functionalized DB30C10 cryptand was designed and prepared successfully (Synthetic strategy I in Scheme 11-4). The carboxylic acid groups of chelidamic acid were protected by methyl groups and **5** was obtained in 100% yield.[16] The hydroxyl group of **5** reacted with 4-bromobenzyl bromide and **6** was afforded in 89% yield. Chelidamic acid derivative **7** was obtained in 96% yield after deprotection. **7** was converted into diacid chloride **8** by thionyl chloride and then bromo-functionalized cryptand **9c** was prepared in 36% yield via the coupling reaction between **8** and DB30C10 diol **1b** under pseudo-high dilution conditions. ITC analysis (Figure ?) indicated stichiometry between **9c** and **3a** was 1:1 and was confirmed by an electrospray ionization mass spectrum (ESI-MS): m/z 1244.38 [**9c**·**3a**-PF_6+2H]$^{1+}$ [13]. ITC investigation gave K_a = 5.2 ± 0.3 x 10^4 M^{-1}.

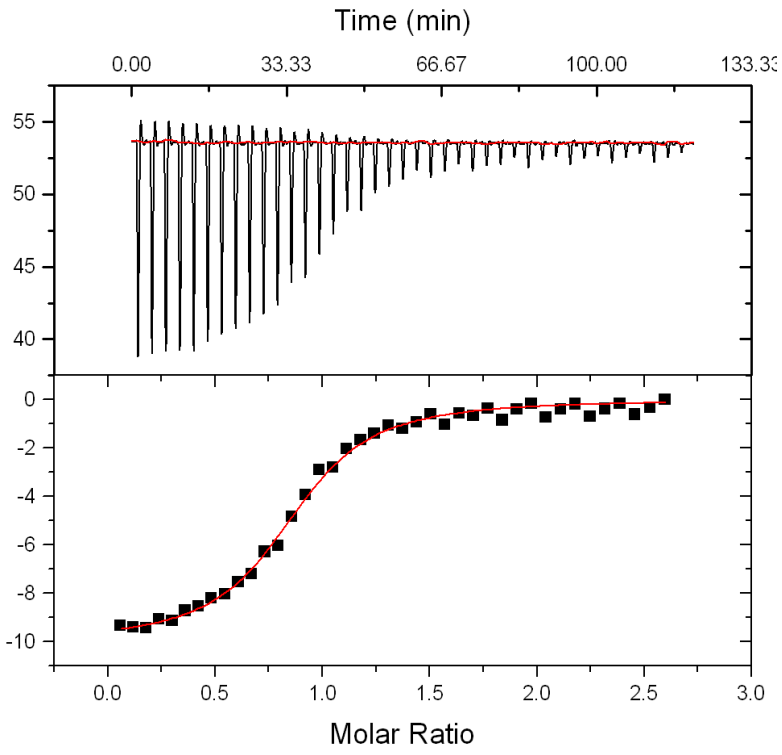

Figure 11-3. ITC curve of **9c**·**3a** in acetonitrile/chloroform =1/1 (v/v). The host (**9c**) concentration (cell) was 0.46 mM. The guest (**3a**) concentration (syringe) was 5.94 mM. The guest solution was titrated into the host solution (cell) at 25°C.

Second, we attempted to prepare an alkyne-functionalized DB30C10 cryptand as shown in Scheme 11-5. First, alkyne-functionalized chelidamate **10** was prepared in 82% yield via the reaction between **5** and propargyl bromide. **10** was hydrolyzed and diacid **11** was prepared in 100% yield. **11** was converted into dichloride **12** and **12** was coupled with DB30C10 diol **1c** , producing alkyne-functionalized cryptand **13**. In the future, based on bromo-functionalized cryptand **9c**, alkyne-functionalized cryptand **13** and paraquat salts, AA and AB type monomers will be prepared. Via the self-assembly between these monomers, non-covalent supramolecular polymers with high molecular weight will be afforded (Scheme 11-6).

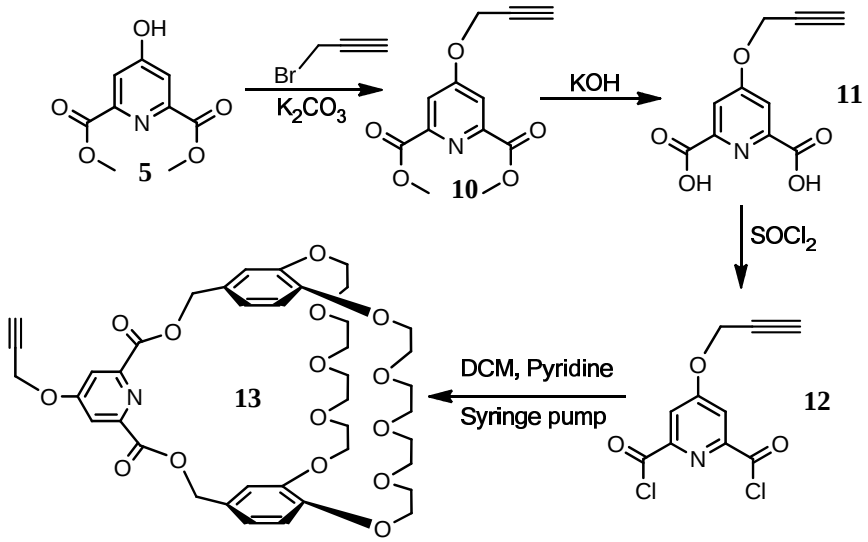

Scheme 11-5. Synthetic strategy II to prepare an alyne functionalized DB30C10 cryptand.

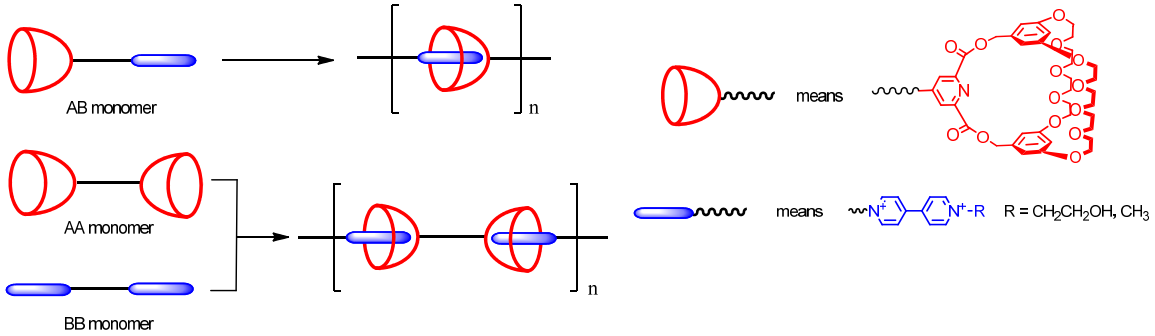

Scheme 11-6. Non-covalent supromoelcular polymers based on functionalized cryptands.

11.3 Conclusions

In summary, DB30C10 derivatives and pyridine-based DB30C10 cryptands were prepared by employing the templating method established by our group. A [2]pseudorotaxane was prepared based on DB30C10 diol and paraquat diol. The [3]pseudorotaxane formed via the self-assembly between DB30C10 cryptand and bisparaquat diol occurred in an cooperative manner. In addition, a bromo-functionalized DB30C10 cryptand was successfully designed and prepared. An alkyne-functionalized DB30C10 cryptand was designed and is under preparation; its precursors have been prepared successfully. In the future, based on these functionalized cryptands and paraquat salts, AA and AB type monomer will be prepared. Via the self-assembly between these monomers, non-covalent supramolecular polymers with high molecular weight will be afforded (Scheme 11-5).

11.4 Acknowledgements

This work was supported by the National Science Foundation (DMR0097126 and DMR0704076) and the Petroleum Research Fund administered by the American Chemical Society (40223-AC7 and 47644-AC7). We also acknowledge the National Science Foundation for funds to purchase the Agilent 6220 Accurate Mass TOF LC/MS Spectrometer (CHE-0722638).

11.5 Experimental section

11.5.1 Materials and methods

All the chemicals used in this chapter were reagent grade and used as received. Solvents were either used as purchased or dried according to literature procedures. ^{1}H-NMR spectra were obtained on a JEOL ECLIPSE-500 spectrometer with internal standard TMS. ^{13}C-NMR spectra were collected on a JEOL ECLIPSE-500 spectrometer at 125 MHz. HR-MS were obtained by employing an Agilent LC-ESI-TOF.

11.5.2 Determination of Δ_0 for 1c·3b

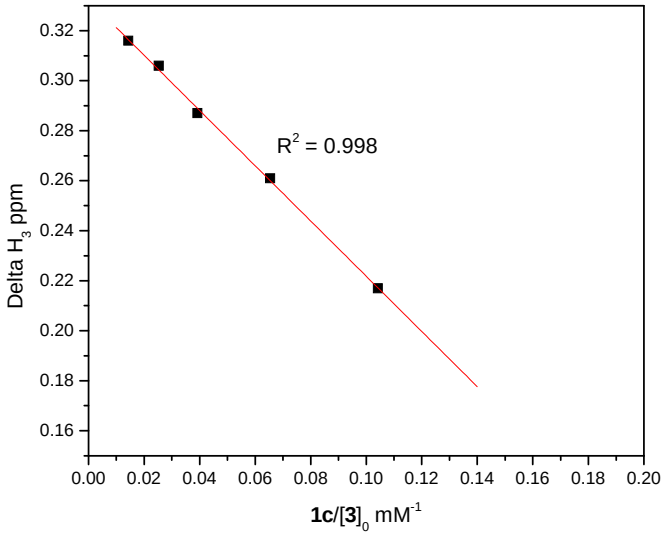

Figure 11-4. Determination of Delta$_0$ of **1c·3b** in acetone-d_6 <v/v>. [**1c**]$_0$ = 8.1 mM.

11.5.3 Synthesis of dimethyl 4-hydroxypyridine-2,6-dicarboxylate (dimethyl chelidamate, 5)

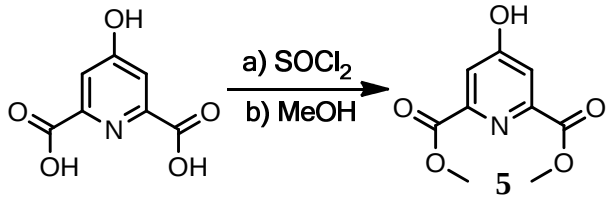

Scheme 11-7. Synthesis of dimethyl 4-hydroxypyridine-2,6-dicarboxylate (**5**)

Thionyl chloride (120 mL) was added dropwise into 400 mL of methanol cooled to 0°C by an ice-water bath and the mixture was stirred at 0°C for 30 mins. Chelidamic acid (25.0 g, 136 mmol) was added and the reaction mixture was allowed to go back to room temperature by removing the ice-water bath. The reaction mixture was stirred at room temperature for 1 day. After reaction, the solvent was removed. A pale-yellow solid was obtained. The solid obtained was redissolved in water. Sodium bicarbonate solution (10%, aq.) was used to neutralize the crude product solution until pH = 7 and a white solid precipitated. The white solid was collected

by filtration, washed with DI water and dried in vacuum oven (28.8 g, 100%), mp 168-169 °C (lit. 165°C[15]). ^{1}H-NMR (DMSO-d_6, 400 MHz) (Figure 11-5): δ: 7.56 (s, 2.0 H), 3.84 (s, 6.0 H).

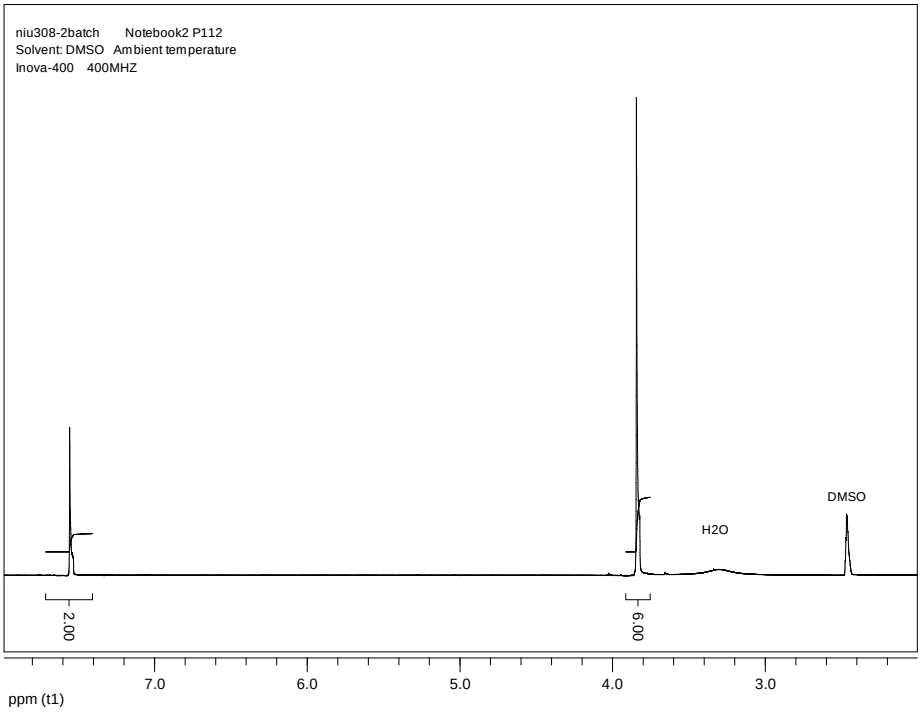

Figure 11-5. 400 MHz ^{1}H-NMR spectrum (DMSO-d_6, room temperature) of **5**.

11.5.4 Synthesis of dimethyl 4-(*p*-bromobenzyloxy)pyridine-2,6-dicarboxylate 6

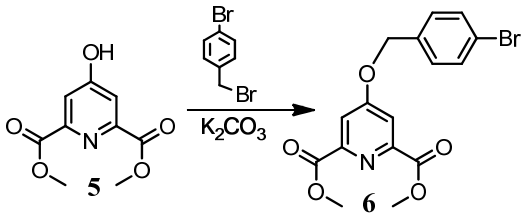

Scheme 11-8. Synthesis of **6**.

Dimethyl chelidamate (14.3 g, 67.9 mmol), 1-bromo-4-(bromomethyl)benzene (16.8 g, 67.9 mmol) and K_2CO_3 (18.6 g) were dissolved in DMF (30 mL). The mixture was exchanged with argon 3 times and the reaction proceeded at 80°C overnight. The mixture was cooled to room temperature. Solvent was removed. The crude product was dissolved in DCM and washed with DI water (3 x) and brine (1 x). The organic phase was dried over Na_2SO_4 and solvent was removed. A white solid (23.1 g, 89 %), mp167.5-168.6 °C, was obtained. ^{1}H-NMR (DMSO-d_6, 400 MHz) (Figure 11-6): δ: 7.87 (s, 1.9 H), 7.56 (d, ^{3}J = 8 Hz, 2.0 H), 7.32 (d, ^{3}J = 8 Hz, 1.8 H),

5.17 (s, 2.1 H), 4.0 (s, 6.0 H). ESI-MS (Figure 11-7): calcd for $[M+Na]^+$: 401.9953, found *m/z*, 401.9935 $[M + Na]^+$, error: -3.06 ppm.

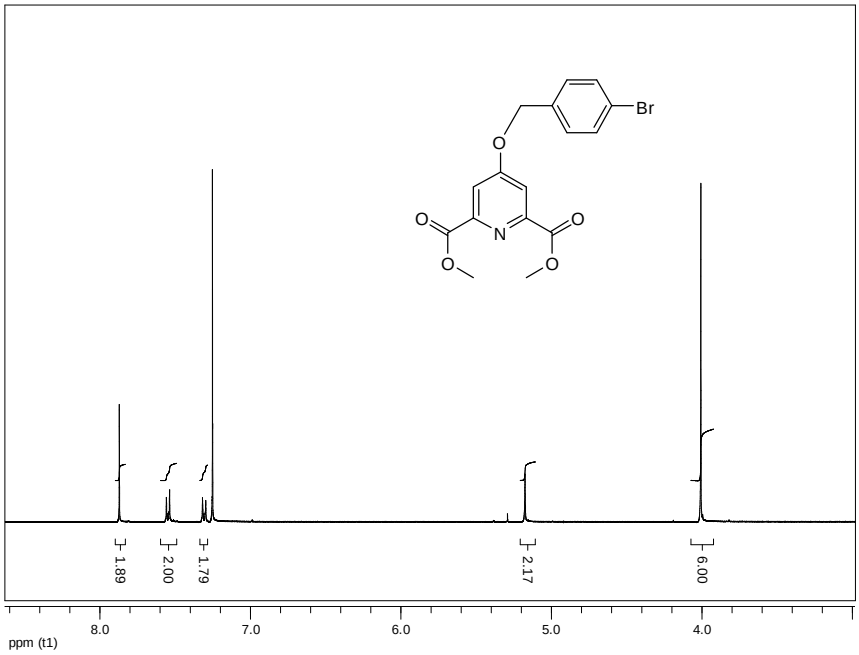

Figure 11-6. 400 MHz ^{1}H-NMR spectrum (DMSO-d_6, room temperature) of **6**.

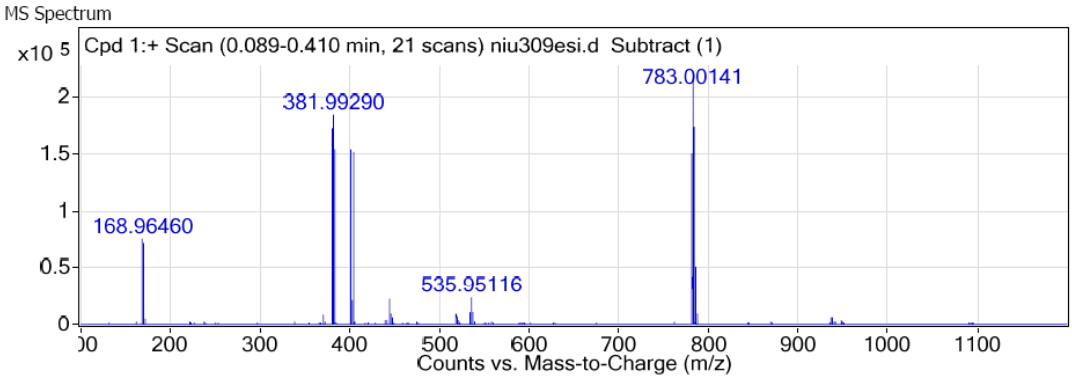

Figure 11-7. ESI-MS of **6**.

11.5.5 Synthesis of 4-(*p*-bromobenzyloxy)pyridine-2,6-dicarboxylic acid 7

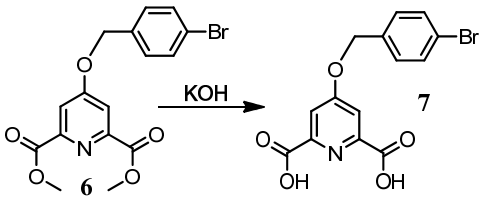

Scheme 11-9. Synthesis of **7**.

6 (21.71 g, 57.2 mmol) was suspended in aqueous KOH (0.5 M, 850 ml). The mixture stirred at reflux for 48 hours and cooled to room temperature. HCl (2M, aq.) was used to neutralize the solution to pH = 4. The white precipitate was collected and dried (19 g, 96%), mp 191-192°C. ^{1}H-NMR (DMSO-d_6, 400 MHz, Figure 11-8): δ: 7.87 (s, 2.0 H), 7.56 (d, ^{3}J = 8 Hz, 2.0 H), 7.32 (d, ^{3}J = 8 Hz, 2.0 H), 5.17 (s, 2.0 H). ^{13}C-NMR (DMSO-d_6, 100 MHz) (Figure 11-9): δ 167.00, 165.87, 150.47, 135.71, 132.16, 130.61, 122.09, 114.54, 69.97. ESI-MS (Figure 11-10): calcd. for $[M+H]^+$: 351.9815, found: *m/z*, 351.9814 $[M + H]^+$, error: -0.45ppm.

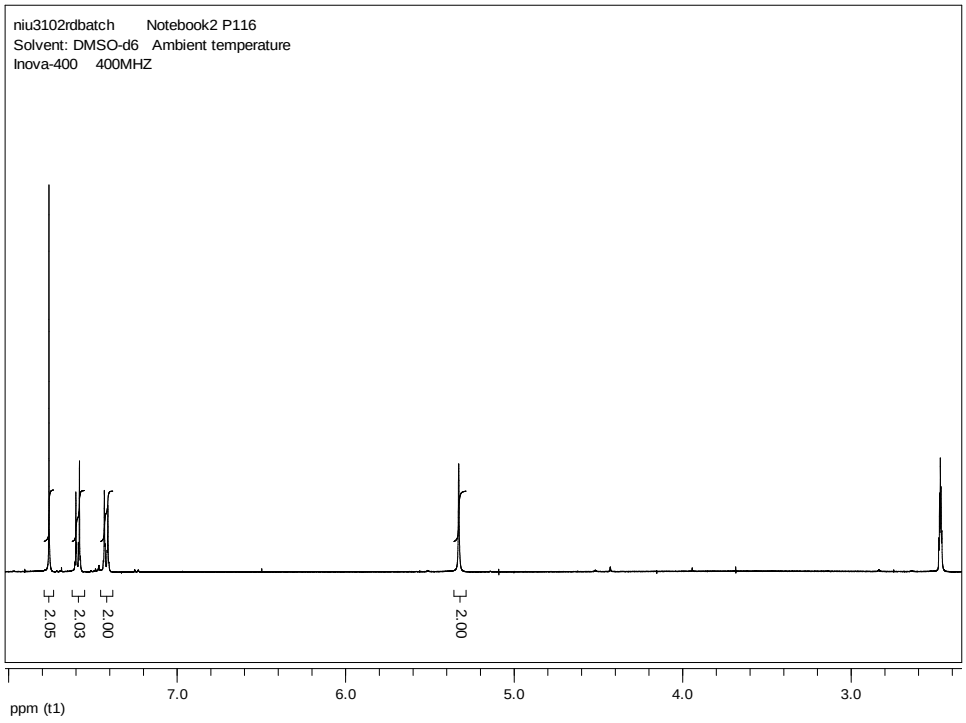

Figure 11-8. 400 MHz ^{1}H-NMR spectrum (DMSO-d_6, room temperature) of **7**.

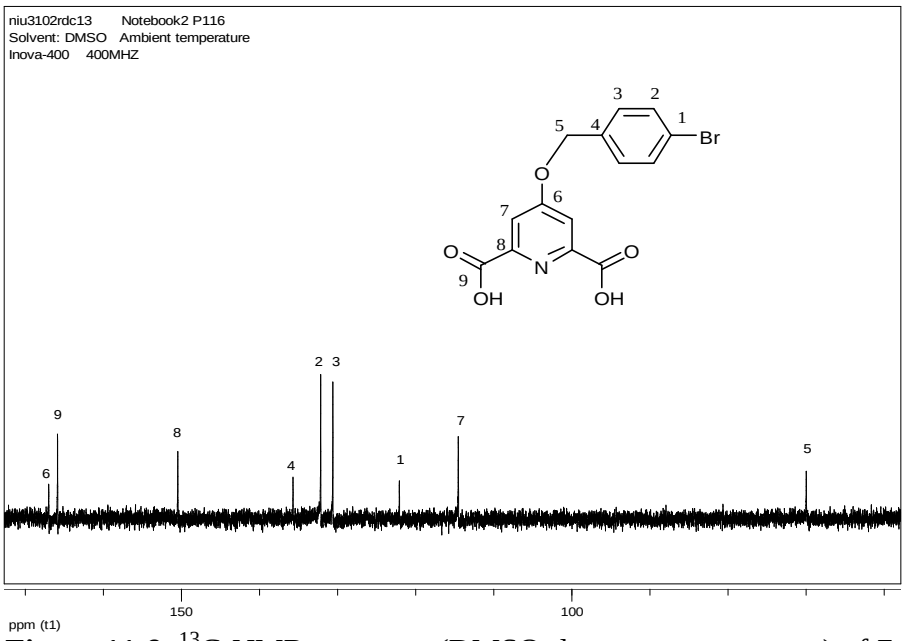

Figure 11-9. ^{13}C-NMR spectrum (DMSO-d_6, room temperature) of **7**.

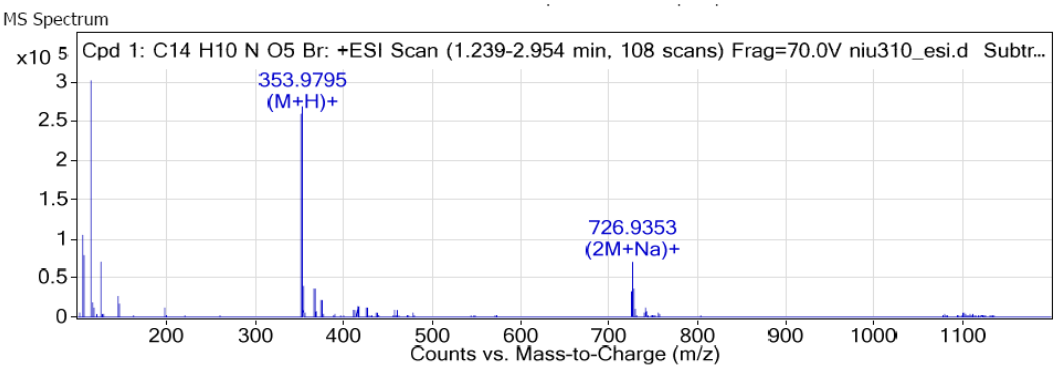

Figure 11-10. ESI-MS spectrum of **7**.

11.5.6 Synthesis of functionalized cryptand 9c

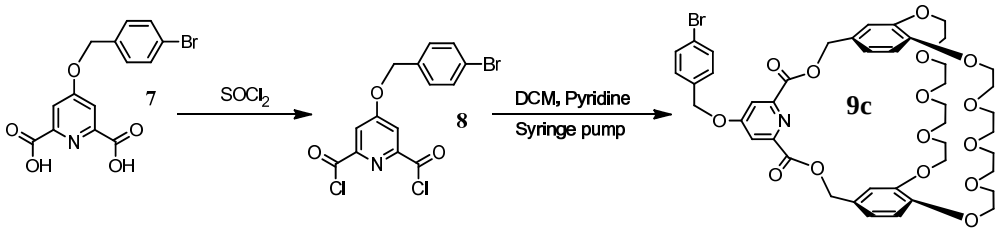

Scheme 11-10. Synthesis of **9c**.

7 (0.21 g, 0.59 mmol) was dissolved in thionyl chloride (15 ml). The mixture was reflux overnight. The suspension became a pink (a little) solution. The thionyl chloride was removed and a white solid was obtained. The solubility of the solid was tested. THF was not a very good solvent, but it dissolved most of the solid. The solid was dissolved THF (anhydrous, 50 mL) and *cis*-DB30C10 diol (0.35 g, 0.59 mmol) was dissolved in DCM (anhydrous, 50 mL). Both solutions were put into 50 ml syringes and added (rate: 0.3 ml/hour) simultaneously to DCM (2000 mL containing pyridine (3 drops). After addition, the mixture was stirred at RT for 3 days. After washing with water, a brown viscous solid was obtained. A neutral alumina column was employed to separate the crude product. A white solid was obtained (0.20 g, 36%), mp 192.3 - 193.6 °C. ^{1}H NMR ($CDCl_3$, 400 MHz, Figure 11-11): δ: 7.88 (s, 2H), 7.58–7.52 (d, J = 8.3 Hz, 2H), 7.35–7.29 (d, J = 8.3 Hz, 2H), 6.94–6.92 (m, 4H), 6.77 (d, J = 8.3 Hz, 2H), 5.32 (s, 4H), 5.21 (s, 2H), 4.18–4.12 (m, 4H), 3.90–3.99 (m, 8H), 3.63–3.82 (m, 22H). ^{13}C-NMR ($CDCl_3$, 100 MHz Figure 11-12): δ 166.31, 164.77, 150.11, 148.98, 148.86, 133.73, 132.03, 129.26, 128.04, 122.76, 121.70, 114.70, 114.19, 113.85, 70.99, 70.75, 70.72, 70.62, 69.93, 69.67, 69.44, 68.96, 68.76, 67.74. ESI-MS (Figure 11-13): calcd. for $[M+2H]^+$: 912.244, found: *m/z*, 912.2437 $[M + H]^+$, error: 0.32 ppm; calcd. for $[M+H_2O]^+$: 931.2702, found: *m/z*, 931.2693 $[M + H]^+$, error: 1.00 ppm.

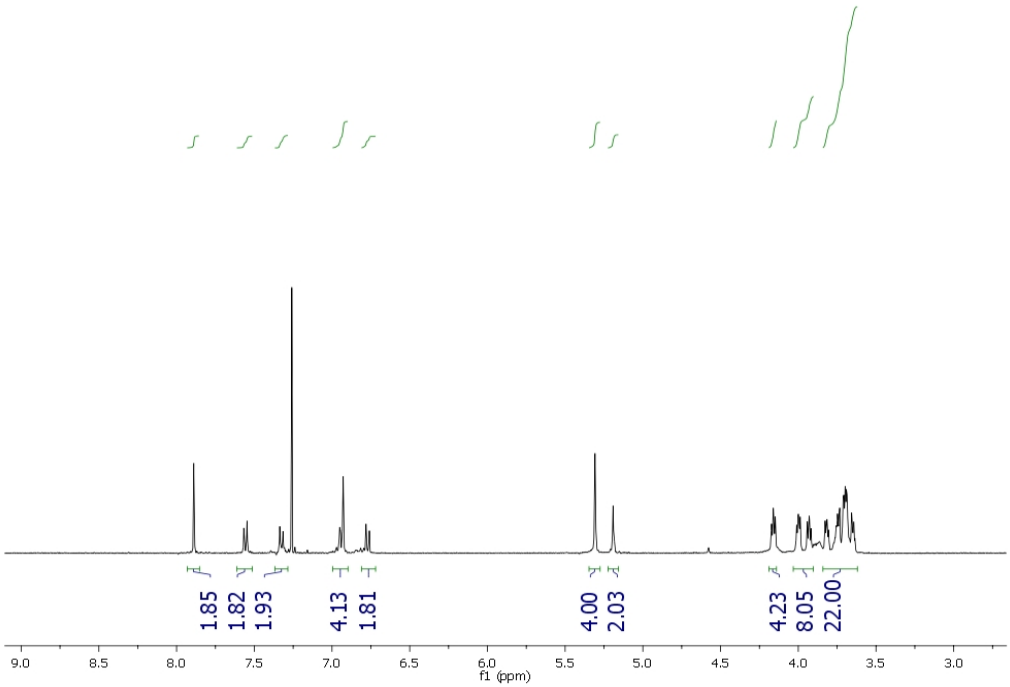

Figure 11-11. 400 MHz ^{1}H-NMR spectrum ($CDCl_3$, room temperature) of **9**.

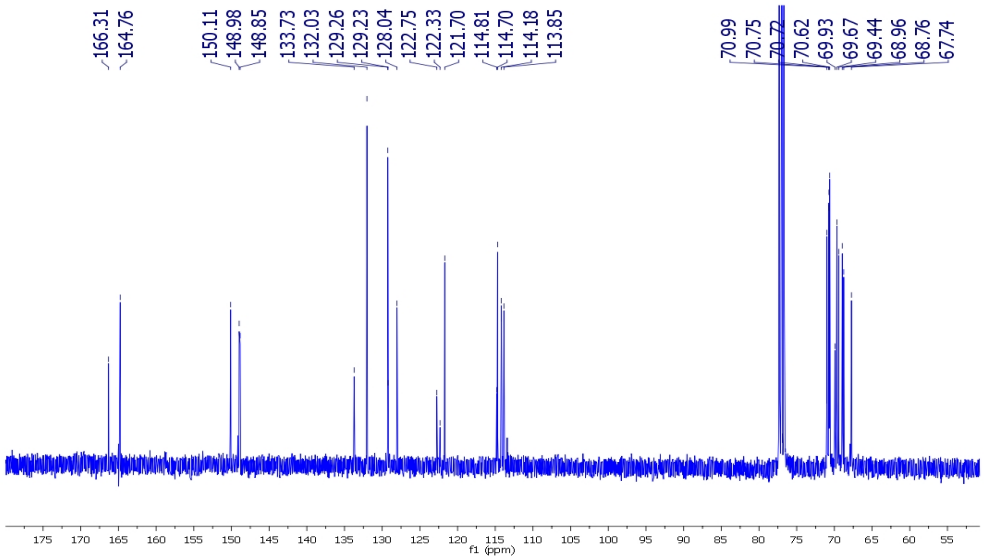

Figure 11-12. 100 MHz ^{13}C-NMR spectrum ($CDCl_3$, room temperature) of **9**.

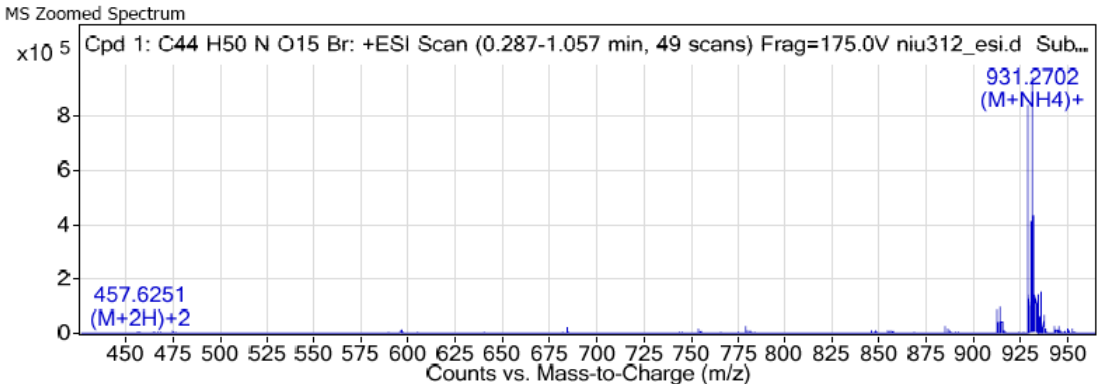

Figure 11-13. ESI-MS spectrum of **9**.

11.5.7 Synthesis of dimethyl 4-(properyloxy)pyridine-2,6-dicarboxylate 10

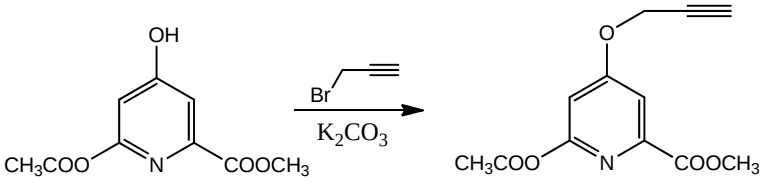

Scheme 11-11. Synthesis of **10**.

5 (5.00 g, 23.6 mmol) and K_2CO_3 were suspended in DMF (100 ml). The suspension was degassed with nitrogen 3 times. Then, propargyl bromide (3.5 g, 24 mmol) was added. The reaction proceeded at 90 °C for 2 days. The mixture was cooled to RT and the K_2CO_3 was filtered. DMF was removed by a rotoevaporator. A brown solid was obtained. The solid was dissolved in DCM and the solution was washed with DI water (6 times) and dried over sodium sulfate. After the solvent was removed, a bright yellow solid was obtained (4.83 g, 82%), mp: 154.1-155.4 °C. TLC showed only one spot. ^{1}H-NMR ($CDCl_3$, 500MHz) (Figure 11-14): δ: 7.89 (d, ^4J = 2 Hz, 2.0 H, aromatic proton), 4.87 (s, 2.3 H, -CH_2), 4.01 (s, 6.5 H, -CH_3), 2.62 (S, 0.91 H, alkyne proton). ^{13}C-NMR ($CDCl_3$) (Figure 11-15): 165.673, 165.085, 149.969, 114.946, 77.703, 76.257, 56.474, 53.403.

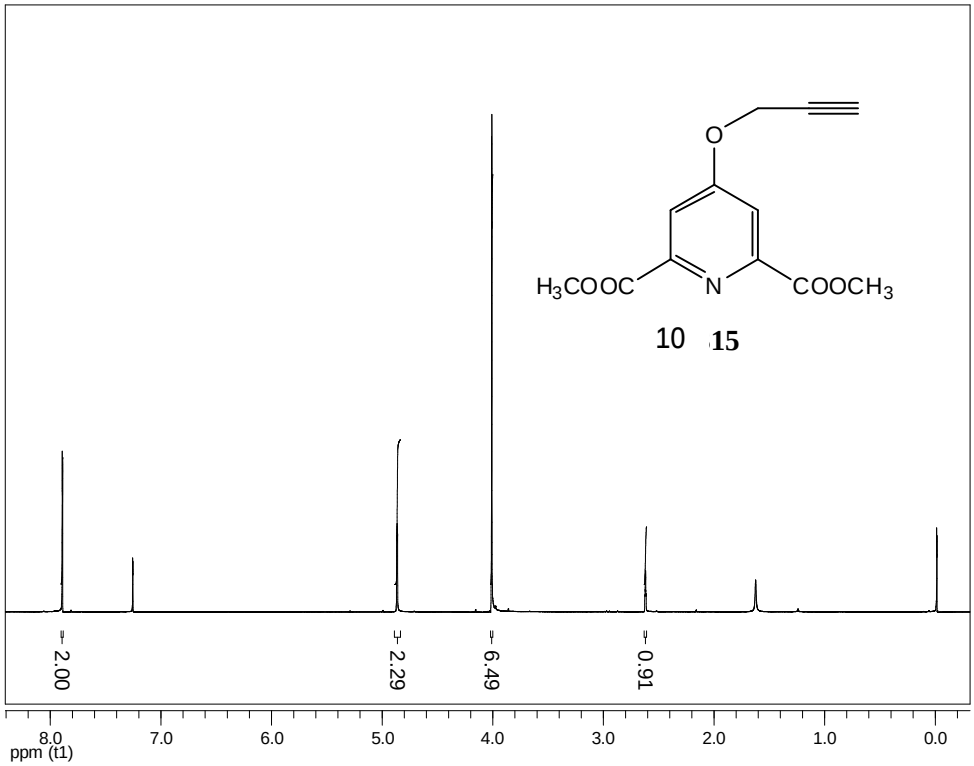

Figure 11-14. 500 MHz ^{1}H-NMR spectrum ($CDCl_3$, room temperature) of **10.**

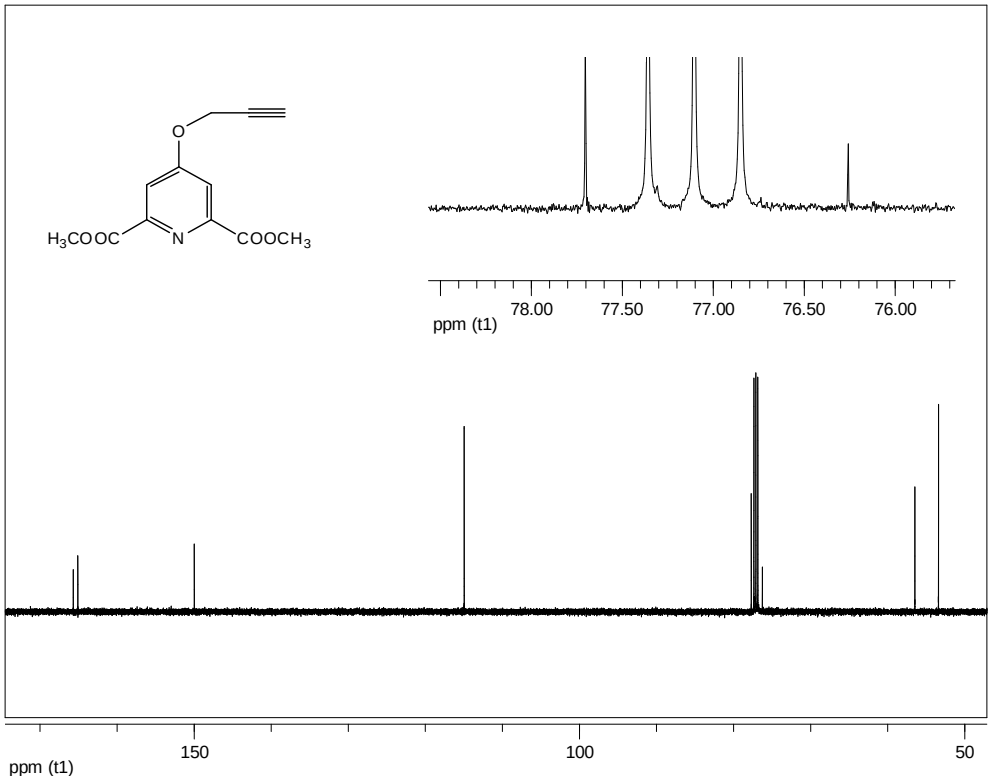

Figure 11-15. 100 MHz ^{13}C-NMR spectrum ($CDCl_3$, room temperature) of **10**.

11.5.8 Synthesis of 4-(proparyloxy)pyridine-2,6-dicarboxylic acid 11

Scheme 11-12. Synthesis of **11**.

10 (2.0 g, 8.0 mmol) was dissolved in hot ethanol (60 mL) with KOH (1.77 g, 31.6 mmol). The suspension was heated for 2 hour in a water bath at 70 ^{o}C, cooled to RT and part of the ethanol was removed. A white solid was obtained and it was dissolved in H_2O. HCl was added until pH= 2-3 and a white precipitate formed. After filtration, a white solid was obtained (1.77 g, 100 %). ^{1}H-NMR (DMSO-d_6, 500MHz, Figure 11-16): δ: 7.66 (s, 2.0 H), 5.10 (s, 2.1 H), 3.74 (s, 0.9 H). ^{13}C-NMR (D_2O, 125MHz, Figure 11-17): 172.49, 163.00, 147.13, 113.62, 79.04, 75.94, 58.57. ESI-MS (Figure 11-18): calcd. for $[M+H]^+$: 222.0397, found: *m/z*, 222.0378 $[M + H]^+$, error: -8.56 ppm. calcd. for $[M+Na]^+$: 244.0216, found: *m/z*, 244.0204 $[M + Na]^+$, error: -5.09 ppm.

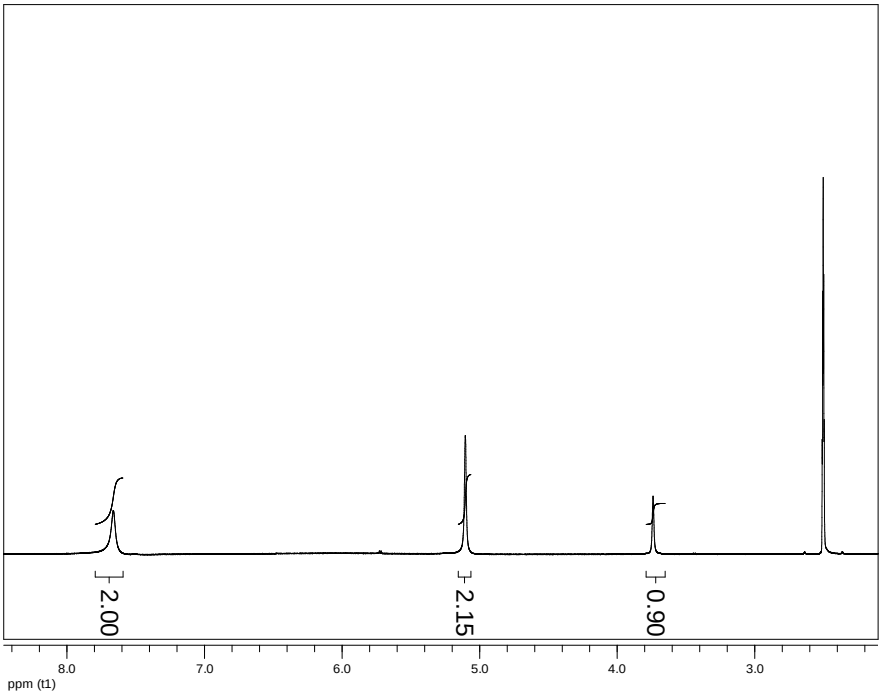

Figure 11-16. 500 MHz ^{1}H-NMR spectrum (DMSO-d_6, room temperature) of **11**.

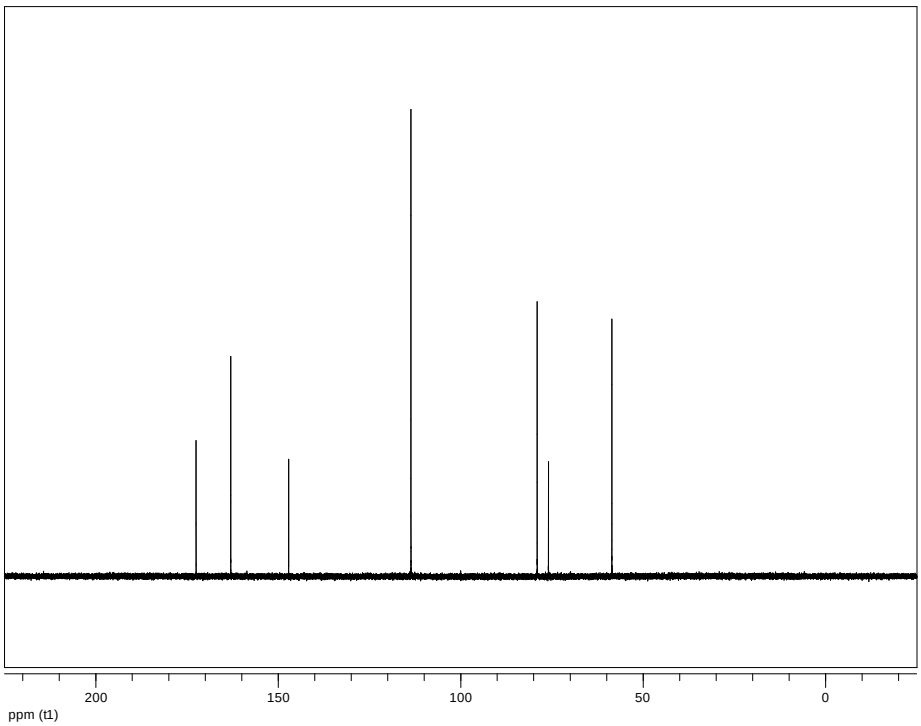

Figure 11-17. 125 MHz ^{13}C-NMR spectrum (D_2O, room temperature) of **11**.

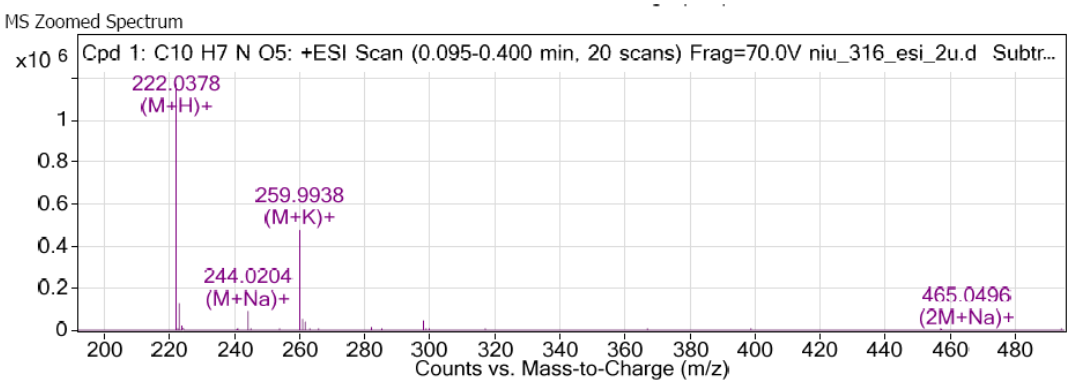

Figure 11-18. ESI-MS of **11**.

11.5.9 Synthesis of alkyne-functionalized DB30C10 cryptand 12

11 (150 mg, 0.67 mmol) was refluxed in thionyl chloride (20 ml) for 24 hours. Excess thionyl chloride was removed by water aspirator and a yellow solid was obtained. It was used directly without purification. DB30C10 diol (400 mg, 0.67 mmol) and the **12** were dissolved in anhydrous DCM (25 ml) respectively. The solutions were added into DCM (1 L) with pyridine (0.02 ml) via a syringe pump at 0.5 ml/h. The reaction mixture was stirred for another 4 days after addition. Part of the DCM was removed and the remaining solution was washed with DI water (3 x) and dried over Na_2SO_4. After the solvent was removed, a brown oil was obtained (solubility in DCM was good). TLC showed three spots (R_f = 0.8, R_f = 0.6 <DB30C10 diol>, R_f = 0). ESI-MS of the crude product (Figure 11-19) showed that desired the product was successfully formed: calcd. for $[M+NH_4]^+$: 799.3289, found: *m/z*, 799.3309 $[M + NH_4]^+$, error: -2.5 ppm.. However, overnight the brown oil became a viscous glue-like liquid (almost insouble in DCM). It was thought that a side reaction happened on the alkyne group in the presence of pyridine. The crude product should be purified immediately after washing.

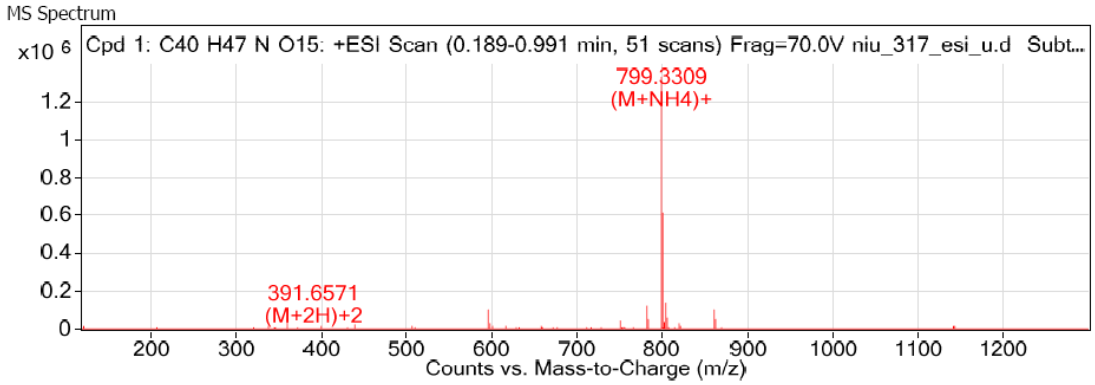

Figure 11-19. 500 MHz ^{1}H-NMR spectrum ($CDCl_3$, room temperature) of crude product of **12** .

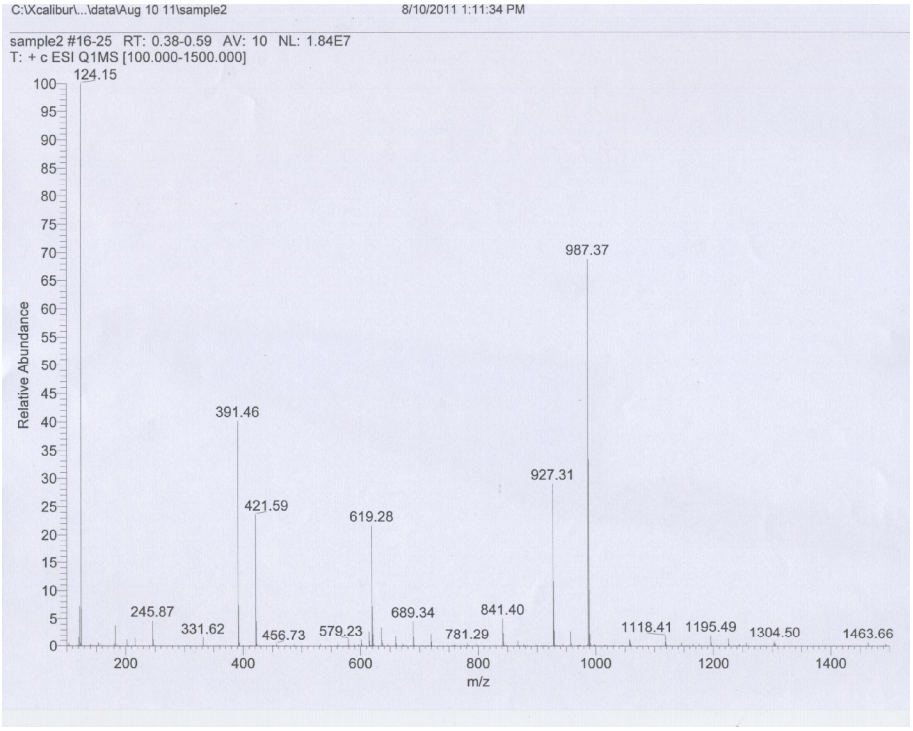

Figure 11-20. ESI-MS of **1c·3b**.

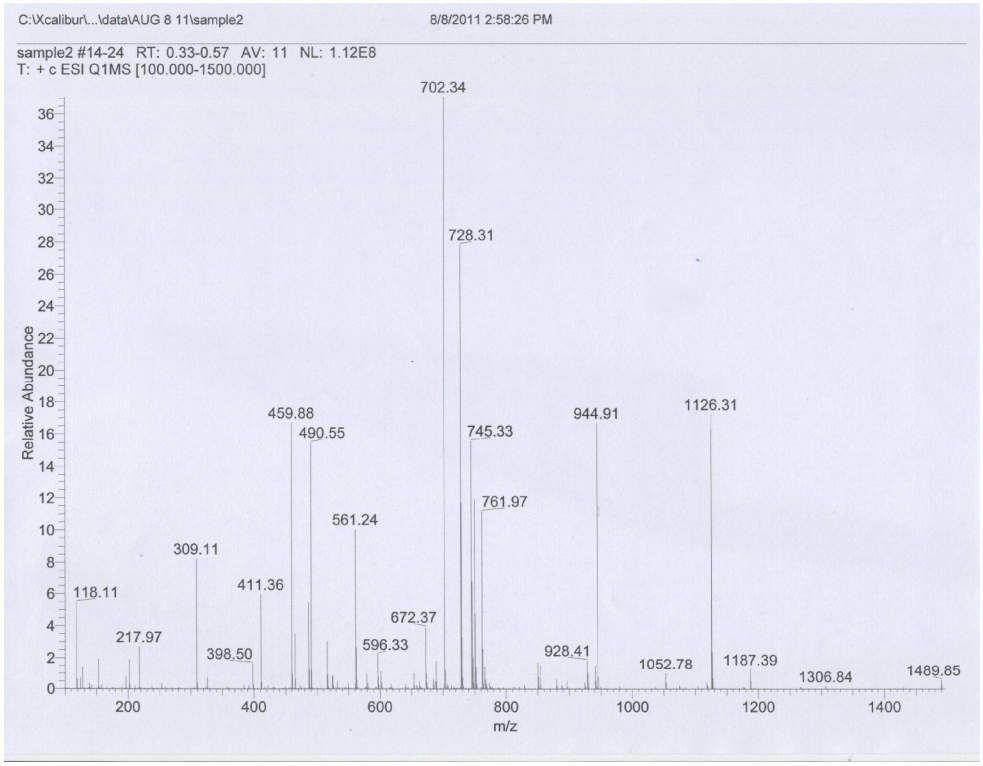

Figure 11-21. ESI-MS of $\mathbf{2_2}$**·4**.

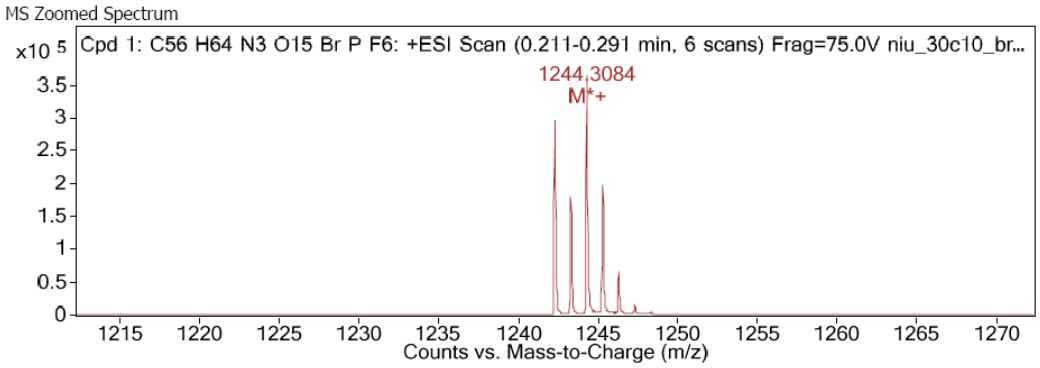

Figure 11-22. ESI-MS of **9c·3a**.

References

(1) (a) Pedersen, C. J. *J. Am. Chem. Soc.* **1967**, *89*, 7017-7036. (c) Pedersen, C. J. *J. Am. Chem. Soc.* **1967**, *89*, 2495-2496. (c) Pedersen, C. J. *J. Org. Chem.* **1971**, *36*, 254-257.

(2) (a) Gibson, H. W. In *Large Ring Molecules*; Semlyen, J. A., Ed.; John Wiley & Sons: New York, 1996; Chapter 6, pp 191-262. (b) Raymo, F. M.; Stoddart, J. F. *Chem. Rev.* **1999**, *99*, 1643-1664. (c) Harada, A. *Acc. Chem. Res.* **2001**, *34*, 456-464. (d) Herna′ndez, J. V.; Kay, E. R.; Leigh, D. A. *Science*. **2004**, *306*, 1532–1537. (e) Wenz, G.; Han, B.–H.; Müller, A. *Chem. Rev.* **2006**, *106*, 782-817. (f) Lankshear, M. D.; Beer, P. D. *Acc. Chem. Res.* **2007**, *40*, 657-668. (g) Vickers, M. S.; Beer, P. D. *Chem. Soc. Rev.* **2007**, *36*, 211-225. (h) Colquhoun, H. M.; Zhu, Z.; Cardin, C. J.; White, A. J. P.; Drew, M. G. B.; Gan, Y. *Org. Lett.* **2010**, *12*, 3756-3759. (i) Kim, S. K.; Sessler, J. L. *Chem. Soc. Rev.* **2010**, *39*, 3784-3809. (j) Gasa, T. B.; Valente, C.; Stoddart, J. F. *Chem. Soc. Rev.* **2011**, *40*, 57-78.

(3) Reviews: (a) Ciferri, A. *Supramolecular Polymers*; Marcel-Dekker: New York, 2000. (b) Brunsveld, L.; Folmer, B. J. B.; Meijer, E. W.; Sijbesma, R. P. *Chem. Rev.* **2001**, *101*, 4071-4098. (c) Huang, F.; Gibson, H. W. *Prog. Polym. Sci.* **2005**, *30*, 982-1018. (d) Takata, T.; *Polymer J.* **2006**, *38*, 1-20. (e) De Greef, T. F. A.; Smulders, M. M. J.;

Wolffs, M.; Schenning, A. P. H. J.; Sijbesma, R. P.; Meijer, E. W. *Chem. Rev.* **2009**, *109*, 5687-5754. (f) Harada, A.; Hashidzume, A.; Yamaguchi, H.; Takashima, Y. *Chem. Rev.* **2009**, *109*, 5974-6023. (g) Niu, Z.; Gibson, H. W. *Chem. Rev.* **2009**, *109*, 6024-6046. (h) Faiz, J. A.; Heitz, V.; Sauvage, J.-P. *Chem. Soc. Rev.* **2009**, *38*, 422-442. (i) Fang, L.; Olson, M. A.; Benitez, D.; Tkatchouk, E.; Goddard III, W. A.; Stoddart, J. F. *Chem. Soc. Rev.* **2010**, *39*, 17-29. (j) Thibeault, D.; Morin, J.-F. *Molecules* **2010**, *15*, 3709-3730. (k) Gavina, P.; Tatay, S. *Curr. Org. Syn.* **2010**, *7*, 24-43.

(4) Pederson, A. M. P.; Ward, E. M.; Schoonover, D. V.; Slebodnick, C.; Gibson, H. W. *J. Org. Chem.* **2008**, *73*, 9094-9101.

(5) Some recent publications: (a) Zhang, M.; Zhu, K.; Huang, F. *Chem. Commun.* **2010**, *46*, 8131-8141. (b) Wang, C.; Olson, M. A.; Fang, L.; Benítez, D.; Tkatchouk, E.; Basu, S.; Basuray, A. N.; Zhang, D.; Zhu, D.; Goddard, W. A.; Stoddart, J. F. *Proc. Nat. Acad. Sci. USA* **2010**, *107*, 13991-13996. (c) Trabolsi, A.; Fahrenbach, A. C.; Dey, S. K.; Share, A. I.; Friedman, D. C.; Basu, S.; Gasa, T. B.; Khashab, N. M.; Saha, S.; Aprahamian, I.; Khatib, H. A.; Flood, A. H.; Stoddart, J. F. *Chem. Commun.* **2010**, *46*, 871-873. (d) Jiang, Y.; Cao, J.; Zhao, J.-M.; Xiang, J.-F.; Chen, C.-F. *J. Org. Chem.* **2010**, *75*, 1767-1770.

(6) (a) Huang, F.; Fronczek, F. R.; Gibson, H. W. *J. Am. Chem. Soc.* **2003**, *125*, 9272-9273. (b) Huang, F.; Gibson, H. W.; Bryant, W. S.; Nagvekar, D. S.; Fronczek, F. R.; *J. Am. Chem. Soc.* **2003**, *125,* 9367-9371. (c) Huang, F.; Zhou, L.; Jones, J. W.; Gibson, H. W.; Ashraf-Khorassani, M. *Chem. Commun.* **2004**, 2670-2671. (d) Huang, F.; Switek, K. A.; Zakharov, L. N.; Fronczek, F. R.; Slebodnick, C.; Lam, M.; Golen, J. A.; Bryant, W. S.; Mason, P. E.; Rheingold, A. L.; Ashraf-Khorassani, M.; Gibson, H. W. *J. Org. Chem.* **2005**, *70*, 3231-3241. (e) Huang, F.; Slebodnick, C.; Switek, K. A.; Gibson, H. W. *Chem. Commun.* **2006**, 1929-1931 (f) Gibson, H. W.; Wang, H.; Slebodnick, C.; Merola, J.; Kassel, S.; Rheingold, A. L. *J. Org. Chem.* **2007**, *72*, 3381-3393. (g) Pederson, A. M.-P.; Vetor, R. C.; Rouser, M. A.; Huang, F.; Slebodnick, C.; Schoonover, D. S.; Gibson, H. W.; *J. Org. Chem.* **2008**, *73*, 5570-5573. (h) Li, S.; Zheng, B.; Huang, F.; Zakharov, L.; Slebodnick, C. Rheingold, A.; Gibson, H. W. *Sci.*

China Chem. **2010**, *53*, 858-862. (i) Zhang, M.; Zhu, K.; Huang, F. *Chem. Commun.* **2010**, *46*, 8131-8141.

(7) (a) Yamaguchi, N.; Gibson, H. W. *Angew. Chem. Int. Ed.* **1999**, *38*, 143-147. (b) Sohgawa, Y.-H.; Fujimori, H.; Shoji, J.; Furusho, Y.; Kihara, N.; Takata, T. *Chem. Lett.* **2001**, 774-775. (c) Oku, T.; Furusho, Y.; Takata, T. *J. Polym. Sci., Part A: Polym. Chem.* **2003**, *41*, 119-123. (d) Gibson, H. W.; Yamaguchi, N.; Jones, J. W. *J. Am. Chem. Soc.* **2003**, *125*, 3522-3533. (e) Huang, F.; Nagvekar, D. S.; Gibson, H. W. *Macromolecules* **2007**, *40,* 3561-3567. (f) Gibson, H. W.; Yamaguchi, N.; Niu, Z.; Jones, J. W.; Rheingold, A. L.; Zakharov, L. N. *J. Polym. Sci., Polym. Chem.* **2010**, *48,* 975-985. (g) Zhou, Q. Z.; Jiang, H. J.; Ding, L.; Wang, F.; Wu, T. *Sci. China: Chem.* **2010**, 53, 1081-1088.

(8) (a) Huang, F.; Gibson, H. W. *J. Am. Chem. Soc.* **2004**, *126*, 14738-14739. (b) Li, S.; Zheng, B.; Chen, J.; Dong, S.; Ma, Z.; Huang, F.; Gibson, H. W. *J. Polym. Sci., Polym. Chem.* **2010**, *48,* 4067-4073.

(9) Huang, F.; Nagvekar, D. S.; Slebodnick, C.; Gibson, H. W. *J. Am. Chem. Soc.* **2004**, *127*, 484-485.

(10) (a) Gibson, H. W.; Yamaguchi, N.; Hamilton, L. M.; Jones, J. W. *J. Am. Chem. Soc.* **2002**, *124*, 4653-4665. (b) Jones, J. W.; Bryant, W. S.; Bosman, A. W.; Janssen, R. A. J.; Meijer, E. W.; Gibson, H. W. *J. Org. Chem.* **2003**, *68*, 2385-2389. (c) Leung, K. C. F.; Mendes, P. M.; Magonov, S. N.; Northrop, B. H.; Kim, S.; Patel, K.; Flood, A. H.; Tseng, H.-R.; Stoddart, J. F. *J. Am. Chem. Soc.* **2006**, *128*, 10707-10715.

(11) Gibson, H. W.; Nagvekar, D. S. *Can. J. Chem.* **1997**, *75*, 1375-1384.

(12) ^{1}H-NMR characterizations were done on solutions with constant [**1c**] and varied [**3**]. Based on these NMR data, Δ_0, the difference in δ values for protons of **1c** in the uncomplexed and fully complexed species, was determined as the y-intercept of a plot of $\Delta = \delta - \delta_u$ *vs.* **11-1c**/[**11-3**]$_0$ in the high initial concentration range of **11-3**: $\Delta_0 = 0.330$ ppm. K_a was calculated from $K_a = (\Delta/\Delta_0)/[(1-\Delta/\Delta_0)([\ \mathbf{11\text{-}3}]_0 - \Delta/\Delta_0\ [\mathbf{11\text{-}1c}]_0)$.

(13) See experimental section.

(14) (a) Marshall, A. G. In *Biophysical Chemistry: Principles, Techniques, and*

Applications, John Wiley & Sons, New York, NY., 1978, pp 70-77. (b) Freifelder, D. M. In *Physical Biochemistry*, W. H. Freeman and Co., New York, 1982, pp 659-660. (c) Connors, K. A. In *Binding Constants*; J. Wiley and Sons, New York, 1987, pp 78-86.

(15) Pederson, A. M.-P. Ph.D. Dissertation, " *Efficient Syntheses of Strong Binding Cryptands and their Derivatives for Supramolecular Polymer Synthesis*". URN. etd-02052009-125852.

(16) Fibel, L. R.; Spoerri, P. E. *J. Am. Chem. Soc.* **1948**, *70*, 3908-3911.

TOC Graphic:

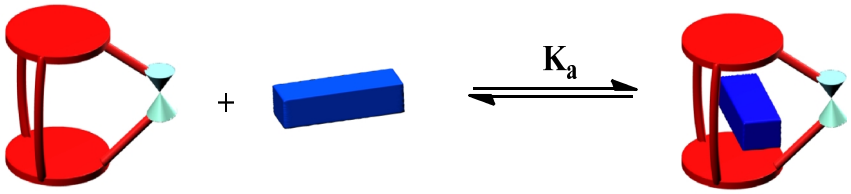

Abstract:

A *cis*(*4,4'*)-Dibenzo-30-crown-10 (*cis*-DB30C10) cryptand bearing an organometallic bridge, ferrocene, was prepared via 1-(3'-dimethylaminopropyl)-3-ethylcarbodiimide hydrochloride (EDCI) coupling of the crown ether diol with ferrocenedicarboxylic acid. The cryptand is dimerized in the solid state via *π*, *π*-stacking and hydrogen bonds. The ferrocene-based cryptand formed novel [2]pseudorotaxanes with paraquat and diquat PF_6 salts with association constants (K_a) of 1.7 ± 0.1 x 10^3 and 4.2 ± 0.3 x 10^4 M^{-1} in acetone-d_6, respectively.

Chapter 12.

Novel [2]Pseudorotaxanes Formed via the Self-Assembly of a Ferrocene-Based *cis*(*4,4′*)-Dibenzo-30-crown-10 Cryptand with Praquat and Diquat

12.1 Introduction

Since Pedersen's first report of crown ether/alkali metal ion complex systems,[1] crown ethers (such as **1a-c** and **2a-c**) have been an important class of hosts that bind metal ions and other cationic species well, leading to the formation of pseudorotaxanes[2] - the fundamental building blocks for more advanced supramolecular species, such, polypseudorotaxanes, polyrotaxanes and polycatenanes.[3] *N,N'*-dialkyl-4,4'-bipyridinium salts and *N,N'*-dialkyl-2,2'-bipyridinium salts, known as paraquat and diquat salts, are commonly used as guests for crown ether hosts.[4] Compared with simple crown ethers which consist of one ethyleneoxy ring, cryptands, multidentate hosts with more than two rings in the molecule, have proved to be much better hosts for paraquat derivatives due to incorporation of additional binding sites and preorganization.[5] Therefore, a series of crown ether-based cryptands have been prepared and their complexation behavior with metal ions and paraquats well studied.[5] Among them, the *cis*(*4,4'*)-dibenzo-30-crown-10 based cryptands are superior due to their relatively easy accessibility via starting materials such as **1a-c** and high binding strengths with paraquat and diquat derivatives.[6] Organometallic materials have gained increased attention as a result of their potential applications: nonlinear optical devices, light emitting diodes, electrochemical sensors, and liquid crystals.[7] The incorporation of an organometallic center in the form of a ferrocene moiety into cryptands provides the possibility to design pseudorotaxane systems with potential

applications in these areas. Moreover, the relatively flexible ferrocene linkage enables the resulting cryptand to change its cavity size to engage guests with different shapes and sizes. Here, we first report the synthesis of a ferrocene-based *cis*-DB30C10 cryptand and novel [2]pseudorotaxanes formed via its self-assembly with paraquat and diquat derivatives.

12.2 Results and discussion

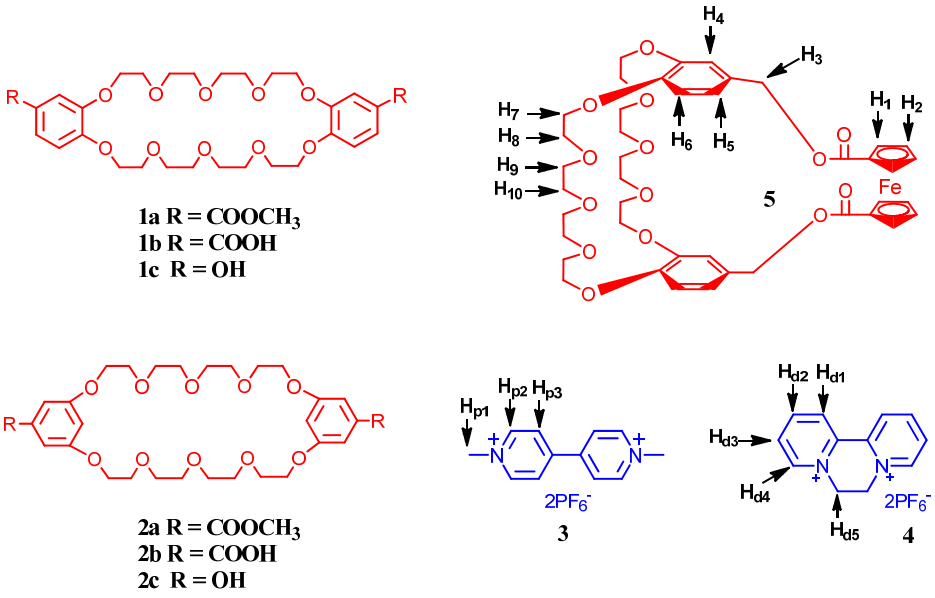

Figure 12-1. Structures of crown ether derivatives **1** and **2**, dimethyl paraquat **3**, diquat **4** and ferrocene-based *cis*-DB30C10 cryptand **5**.

Crown ether **1c** was prepared via the high yielding, regiospecific synthetic method reported by Gibson *et al.*[6] Cryptand **5** was prepared via the EDCI coupling between *cis*-DB30C10 diol (**1c**) and 1,1'-ferrocene dicarboxylic acid in 24% yield under pseudo-high dilution conditions. A single crystal[8] of **5** was grown by vapor-diffusion of pentane into an acetone solution (Figure 12-2). Interestingly, the crystal structure demonstrated that two **5** molecules dimerize in the solid state. Unlike other crown ether-based cryptands[5d,5e,6] in which the two benzo rings are always parallel to each other, cryptand **5** has two perpendicular benzo rings; one

benzo ring participates in the formation of inter-molecular off-set π, π-stacking interactions,[9] which stabilize the cryptand dimer. Moreover, the inter-molecular hydrogen bonds between the oxygen atoms and the ethylene and benzo protons provide additional stabilization of the dimer. This difference between cryptand **5** and other crown ether-based cryptands is ascribed to the relatively flexible ferrocene-containing third bridge, which gives the benzo rings more conformational freedom.

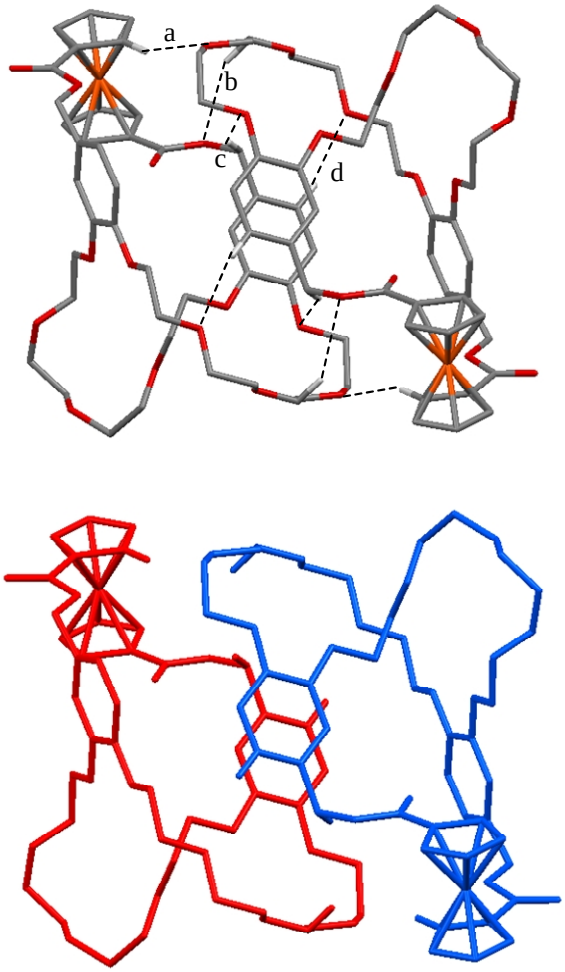

Figure 12-2. The X-ray structure of cryptand **5**. Oxygen atoms are red. Carbon atoms are grey. Iron atoms are brown. Solvent molecules and hydrogen atoms except the ones involved in hydrogen bonds are omitted for

clarity. Upper figure: hydrogen-bond parameters: H···O distances (Å), C···O distances (Å), C-H···O angles (deg): a) 2.248, 3.146, 157; b) 2.686, 3.566, 148; c) 2.709, 3.589, 148; d) 2.762, 3.696, 168; off-set face-to-face π-stacking parameters: centroid-centroid distances (Å): 3.69; ring plane-ring plane inclinations (deg): 0.650. In the bottom figure, one cryptand molecule is red and the other blue in order to guide the reader's eye.

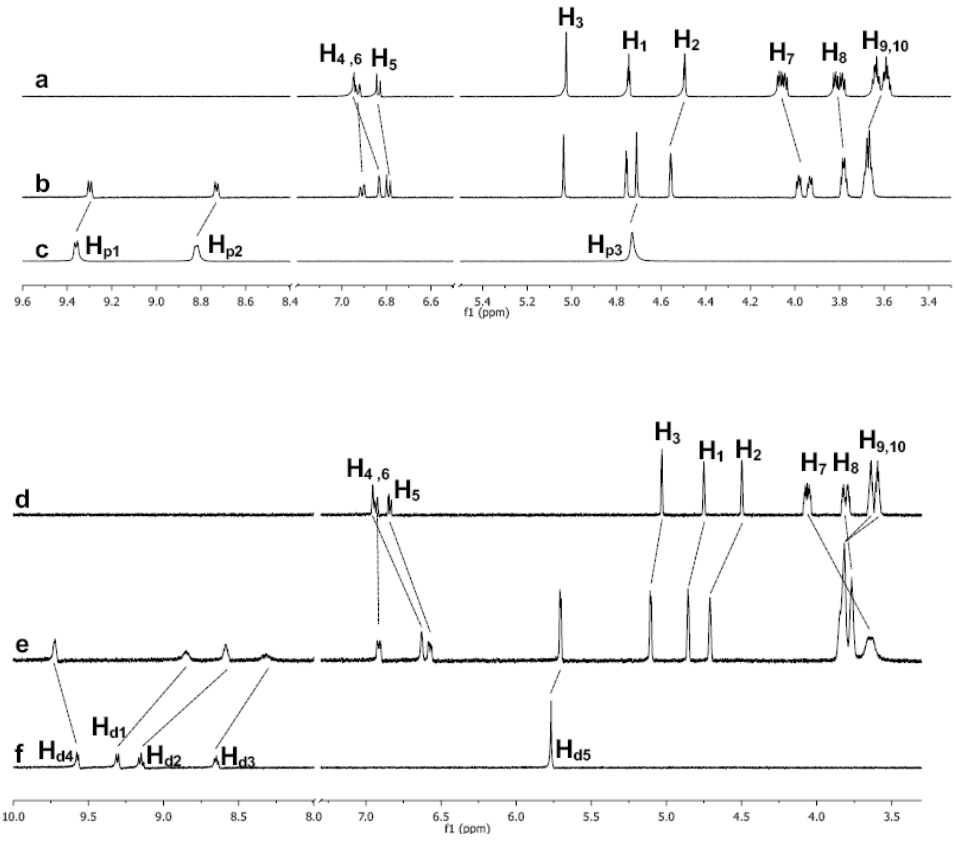

Figure 12-3. Partial ^{1}H-NMR spectra (500 MHz, acetone-d_6, 22°C) of solutions. Upper stacked spectra: (a) cryptand **5**; (b) mixture of **5** and **3** (1/1, mol/mol); (c) guest **3**. Lower stacked spectra: (e) cryptand **5**; (f) mixture of **5** and **4** (1/1, mol/mol); (g) guest **4**.

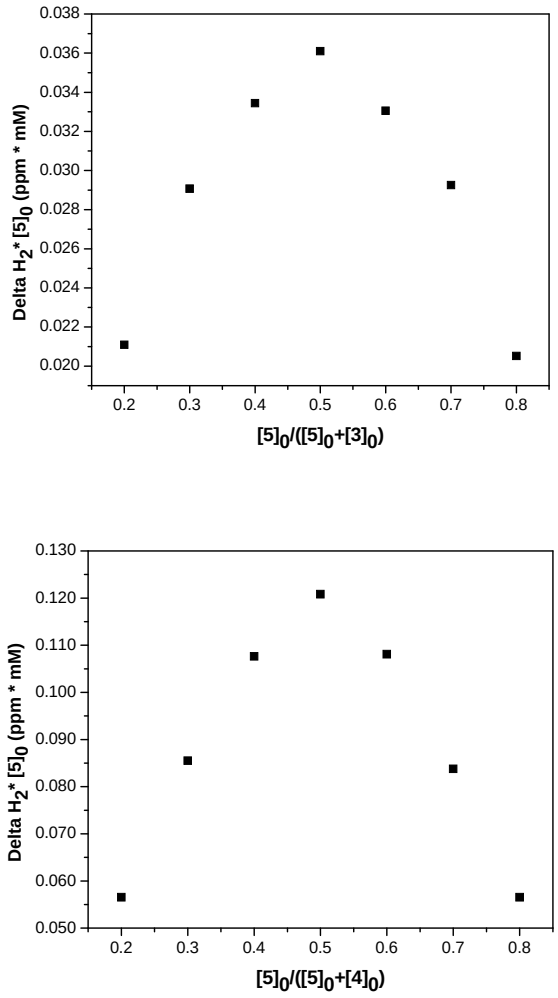

Figure 12-4. Job plots for cryptand **5** with guests **3** (upper plot, $[\mathbf{5}]_0+[\mathbf{4}]_0$ = 0.95 mM) and **4** (lower plot, $[\mathbf{5}]_0+[\mathbf{4}]_0$ = 1.14 mM). The solvent is acetone-d_6.

A solution of cryptand **5** in acetone was pale yellow. After addition of the colorless solution of guest **3**, the mixed solution became much deeper yellow, which is ascribed to charge-transfer interactions between the electron-rich aromatic rings of **5** and the electron-poor pyridinium rings of **3**, good evidence for complexation. ^{1}H-NMR spectra of equimolar solutions of **5** and **3** displayed only one set of peaks, indicating fast exchange complexation (Figure 12-3). In the complex, peaks corresponding to H_4, H_5, H_6, H_7 and H_8 of cryptand **5** and H_{p1} and H_{p2} of

guest **3** moved upfield, while H_2, H_9 and H_{10} of cryptand **5** moved downfield. The peak corresponding to H_7 splits during the complexation, indicating the different chemical environments for the two H_2 atoms in cryptand **5**, possibly due to the asymmetry of the complex. The Job plot[10] (Figure 12-4) showed that the stoichiometry of the complex between cryptand **5** and guest **3** was 1:1 in acetone-d_6. Electrospray ionization mass spectrum (ESI-MS) confirmed the stoichiometry by showing the relevant peak at m/z 1165.34 [**5·3**-PF_6+2H]$^+$. The association constant (K_a) was determined to be 1.7 ± 0.1 x 10^3 M^{-1} in acetone-d_6 based on the proton NMR data.[11]

As for the complex system **5·4**, similarly the color of the mixed solution of cryptand **5** and **4** became much deeper than the color of a solution of **5** due to the charge-transfer interactions between the electron-rich aromatic rings of **5** and the electron-poor pyridinium rings of **4**, providing evidence for complexation. The complexation between cryptand **5** and guest **4** is a fast exchange process according to the ^{1}H-NMR spectra of equimolar solutions of **5** and **4**, which display only one set of peaks (Figure 12-3). Upon complexation, peaks corresponding to H_4, H_5, H_6, H_7 and H_8 of cryptand **5** and H_{d1}, H_{d2}, H_{d3} and H_{d5} of guest **4** moved upfield, while H_1, H_2, H_3, H_9 and H_{10} peaks of cryptand **5** and H_{d4} peak of guest **4** moved downfield. The stoichiometry of the complex between cryptand **5** and guest **4** was determined to be 1:1 in acetone-d_6 by a Job plot (Figure 12-4). ESI-MS confirmed the stoichiometry by revealing the relevant peak at m/z 1163.31 [**5·4**-PF_6+2H]$^+$. The association constant (K_a) was determined to be 4.2 ± 0.3 x 10^4 M^{-1} in acetone-d_6 based on the proton NMR data.[11] Compared with relatively "narrower" paraquat **3**, "broader" diquat **4** molecules can interact with the ethyleneoxy arms of cryptand **5** more tightly, as reported for other systems.[5e, 6] As a result, the K_a between **5** and **4** is ~25 times higher than the K_a between **5** and **3**; that is, the interactions are 1.9 kcal/mol stronger with diquat **4**.

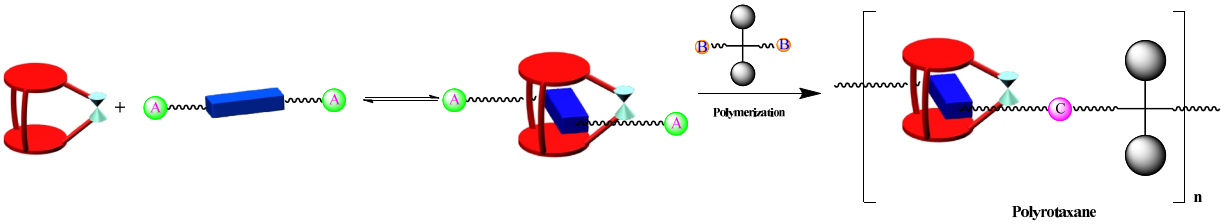

Figure 12-5. Preparation of organometallic polyrotaxanes. Functional group A reacts with functional group B and gives group C.

12.3 Conclusions

In summary, a novel ferrocene-based *cis*-DB30C10 cryptand was prepared. It formed 1:1 [2]pseudorotaxane complexes with paraquat guest **3** and diquat guest **4** as demonstrated by ^{1}H-NMR and ESI-MS. The association constants between cryptand **5** and guests **3** and **4** were determined to be $1.7 \pm 0.1 \times 10^{3}$ and $4.2 \pm 0.3 \times 10^{4}$ M^{-1}, respectively. Due to its relatively good association constants, our current efforts focus on preparation of novel organometallic polyrotaxanes via step-growth polymerization of the [2]pseudorotaxane derived from cryptand **5** and difunctional praquat derivatives with difunctional stoppers (Figure 12-5).

12.4 Acknowledgements

This work was supported by the National Science Foundation (DMR0704076) and the Petroleum Research Fund administered by the American Chemical Society (47644-AC). We also acknowledge the National Science Foundation for funds to purchase the Innova-400 NMR and Agilent 6220 Accurate Mass TOF LC/MS spectrometers (CHE-0131124 & CHE-0722638, respectively).

12.5 Experimental section

12.5.1 Materials and methods

1,1'-Ferrocenedicarboxylic acid, 1-(3'-dimethylaminopropyl)-3-ethylcarbodiimide hydrochloride (EDCI) and 4-dimethylaminopyridine (DMAP) were reagent grade and used as received. *cis*(*4,4'*)-Dibenzo-30-crown-10 diol (**1**),[6] dimethyl paraquat PF_6 (**3**) and diquat PF_6 (**4**)$^{2-}$ [3] were prepared according to literature procedures. Solvents were either used as purchased or dried according to literature procedures. ^{1}H-NMR spectra were obtained on a JEOL ECLIPSE-500 spectrometer with internal standard TMS. ^{13}C-NMR spectra were collected on a JEOL ECLIPSE-500 spectrometer at 125 MHz. HR-MS were obtained by employing an Agilent LC-ESI-TOF.

12.5.2 Synthesis of cryptand 5

EDCI (337 mg, 1.76 mmol) and 4-dimethylaminopyridine (DMAP) (215 mg, 1.76 mmol) were dissolved in 2000 mL of anhydrous DCM. *cis*-DB30C10 diol (**1c**) (260 mg, 0.44 mol) was dissolved in DCM (50 mL) and ferrocene dicarboxylic acid (131 mg, 0.48 mmol) was dissolved in DCM/DMF (13 mL/37 mL). The solutions were put into separate 50 mL syringes and added into the DCM at a rate of 0.2 mL/h using a syringe pump. After addition, the mixture was stirred at RT for another 14 days. Solvent was removed. The brown solid obtained was redissolved in DCM and washed with water. DCM was removed and a brown solid was obtained. A neutral alumina column was employed to purify the crude product. A red solid was obtained and the solid was recrystallized in DCM/pentane. After recrystallization, a dark red solid was obtained (88 mg, 24%), mp: 114-115.6°C. ^{1}H-NMR ($CDCl_3$, 500 MHz, Figure 12-6): δ: 6.91 – 6.86 (dd, *J* = 8, 1 Hz, 2H), 6.86 – 6.83 (d, *J* = 2 Hz, 2H), 6.78 – 6.74 (d, *J* = 8 Hz, 2H), 5.08 (s, 4H), 4.82 – 4.74 (d, *J* = 2, 4H), 4.43 – 4.37 (d, *J* = 2, 4H), 4.13 – 4.02 (m, 8H), 3.89 – 3.80 (m, 8H), 3.73 – 3.61 (m, 16H). ^{13}C-NMR ($CDCl_3$, 101 MHz, Figure 12-7): δ (ppm): 170.47, 149.01, 129.20, 121.76, 114.74, 113.95, 73.11, 72.64, 71.90, 71.01, 70.91, 70.89, 70.77, 69.83, 69.68, 69.07, 69.04, 66.41. HR-ESIMS (Figure 12-8): calcd. For $[M + H]^+$ = 835.2623, found: m/z, 835.2619, error: -0.46 ppm. Calcd. For $[M + H_2O]^+$ = 852.2888, found: m/z, 852.2903, error: 1.74 ppm.

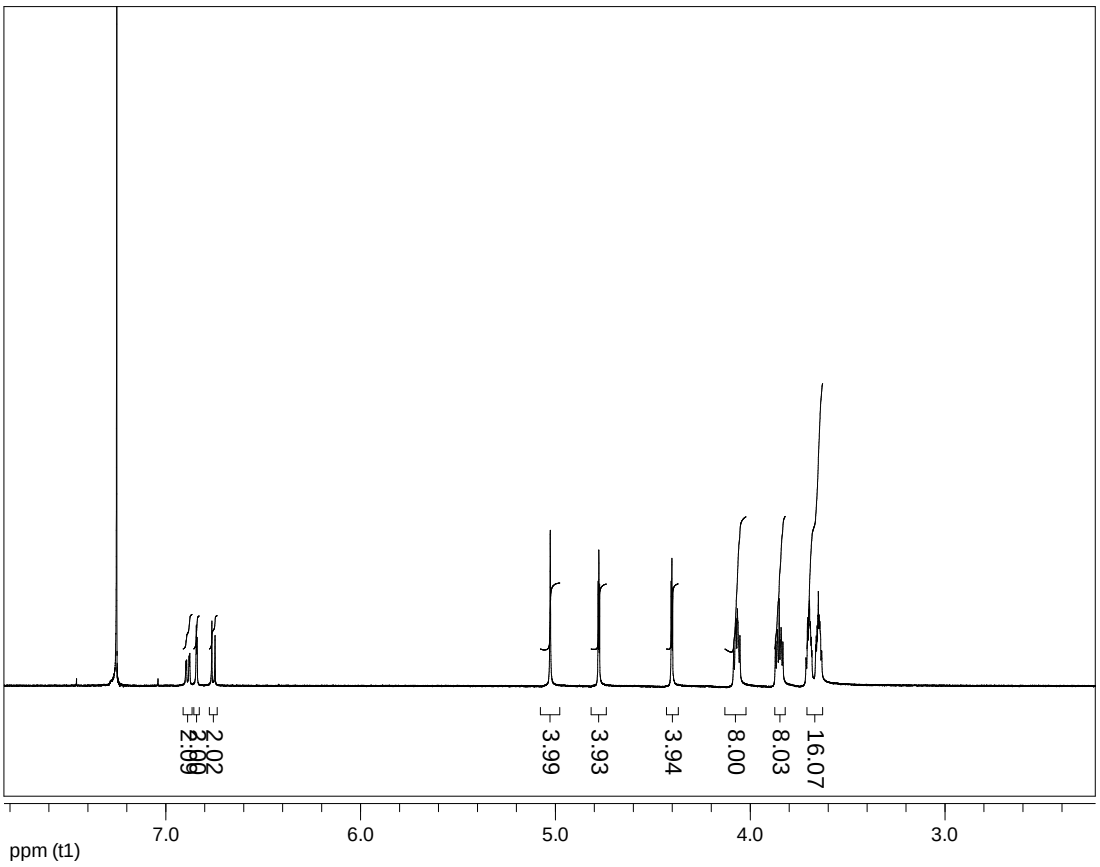

Figure 12-6. ^{1}H-NMR ($CDCl_3$, 500 MHz, room temperature) of cryptand **5**.

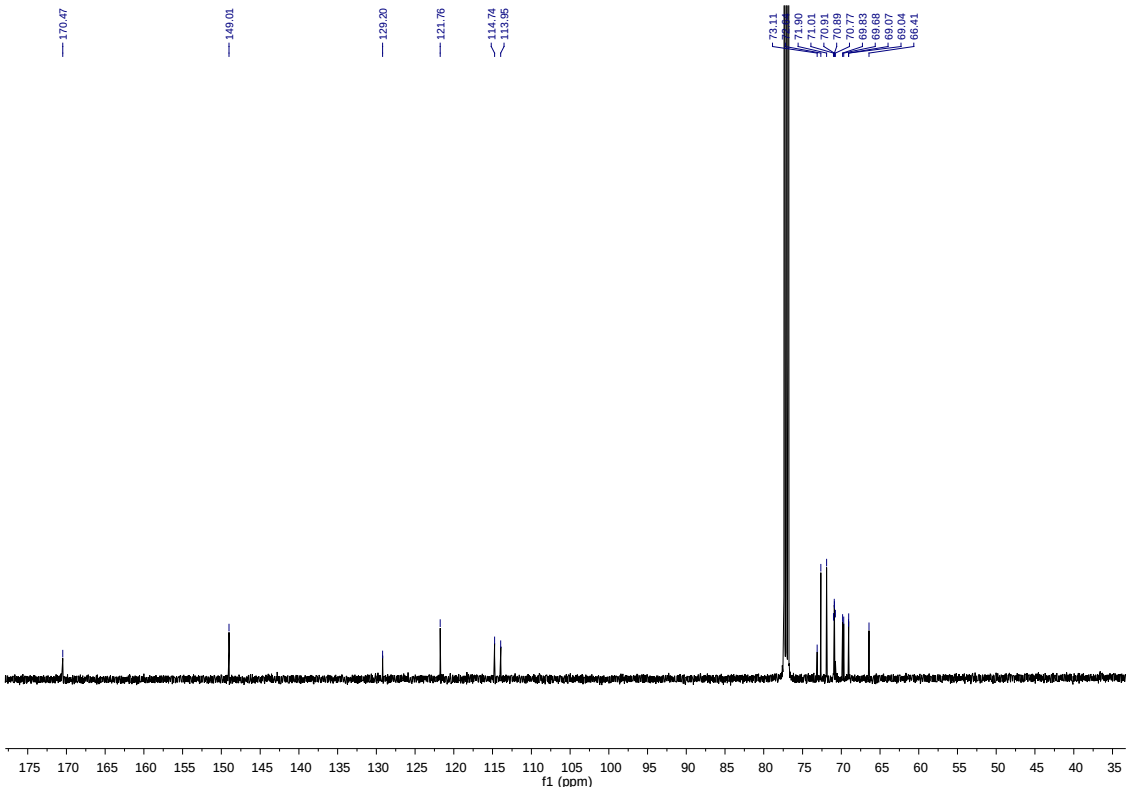

Figure 12-7. ^{13}C-NMR ($CDCl_3$, 125 MHz, room temperature) of cryptand **5**.

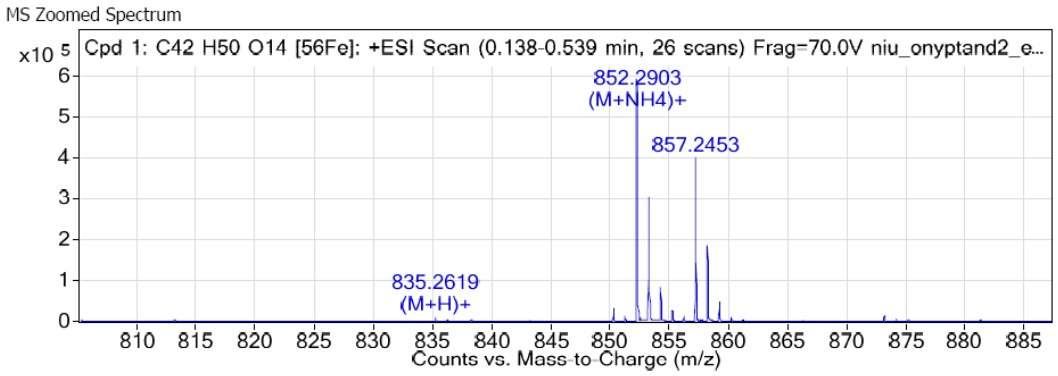

Figure 12-8. Electrospray ionization mass spectrum of cryptand **5**.

12.5.3 Electrospray ionization mass spectrum of 5·3

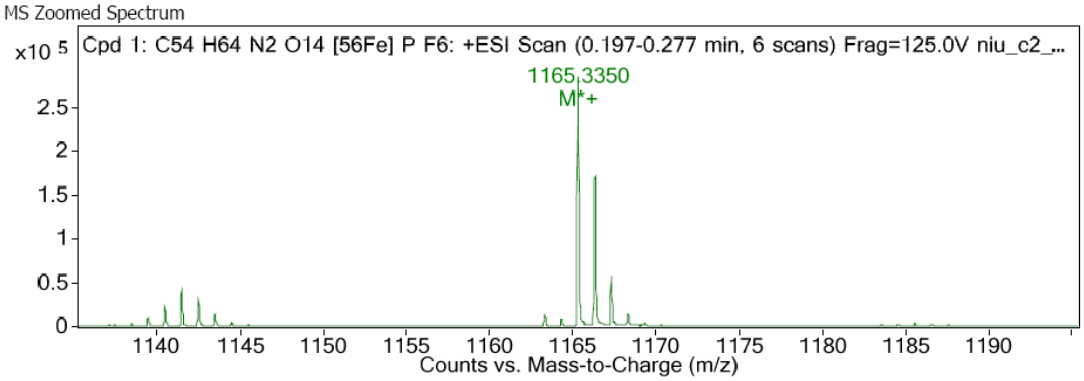

Figure 12-9. Electrospray ionization mass spectrum of **5·3**.

12.5.4 Electrospray ionization mass spectrum of 5·4

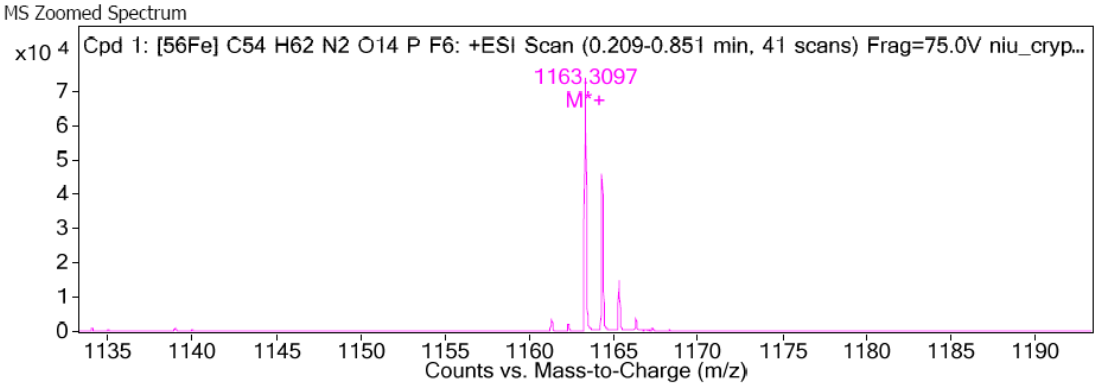

Figure 12-10. Electrospray ionization mass spectrum of **5·4**.

12.5.5 Determination of Δ_0 for 5·3

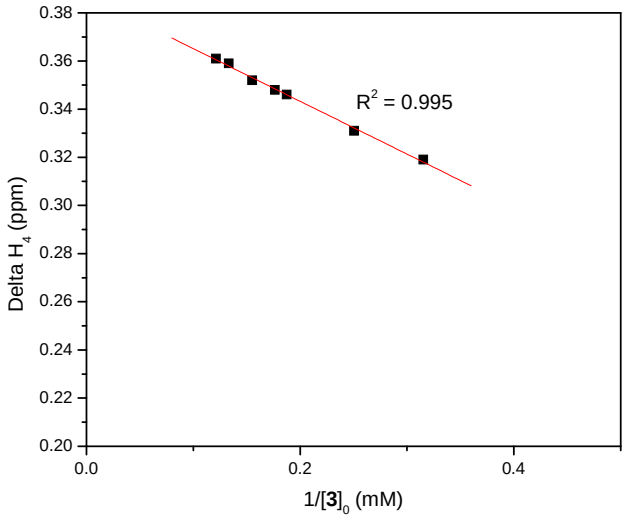

Figure 12-11. Determination of Delta$_0$ for **5·3** in acetone-d$_6$. [**5**]$_0$ = 0.24 mM.

12.5.6 Determination of Δ_0 for 5·4

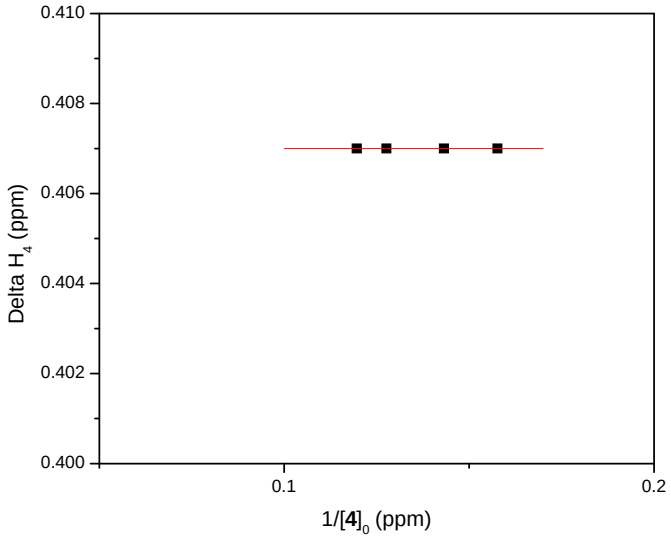

Figure 12-12. Determination of Delta$_0$ for **5·4** in acetone-d$_6$. [**5**]$_0$ = 0.28 mM.

References

(1) (a) Pedersen, C. J. *J. Am. Chem. Soc.* **1967**, *89*, 7017-7036. (c) Pedersen, C. J. *J. Am. Chem. Soc.* **1967**, *89*, 2495-2496. (c) Pedersen, C. J. *J. Org. Chem.* **1971**, *36*, 254-257.

(2) (a) Gibson, H. W. In *Large Ring Molecules*; Semlyen, J. A., Ed.; John Wiley & Sons: New York, 1996; p 191; (b) Raymo, F. M.; Stoddart, J. F. *Chem. Rev.* **1999**, *99*, 1643-1664. (c) Harada, A. *Acc. Chem. Res.* **2001**, 34, 456-464; (d) Hernandez, J. V.; Kay, E. R.; Leigh, D. A.; *Science*. **2004**, 306, 1532–1537.

(3) (a) Huang, F.; Gibson, H. W. *Prog. Polym. Sci.* **2005**, *30*, 982-1018. (b) Lehn, J.-M. *Chem. Soc. Rev.* **2007**, *36*, 151-160. (b) Stoddart, J. F. *Chem. Soc. Rev.* **2009**, *38*, 1802-1820. (c) De Greef, T. F. A.; Smulders, M. M. J.; Wolffs, M.; Schenning, A. P. H. J.; Sijbesma, R. P.; Meijer, E. W. *Chem. Rev.* **2009**, *109*, 5687-5754. (d) Harada, A.; Hashidzume, A.; Yamaguchi, H.; Takashima, Y. *Chem. Rev.* **2009**, *109*, 5974-6023. (e) Niu, Z.; Gibson, H. W. *Chem. Rev.* **2009**, *109*, 6024-6046. (i) Fang, L.; Olson, M. A.; Benitez, D.; Tkatchouk, E.; Goddard III, W. A.; Stoddart, J. F. *Chem. Soc. Rev.* **2010**, *39*, 17-29. (i) Durola, F.; Sauvage, J.-P.; Wenger, O. S. *Coord. Chem. Rev.* **2010**, *254*, 1748-1759. (i) Hanni, K. D.; Leigh, D. A. *Chem. Soc. Rev.* **2010**, *39*, 1240-1251.

(4) Some recent publications: (a) Zhang, M.; Zhu, K.; Huang, F. *Chem. Commun.* **2010**, *46*, 8131-8141. (b) Wang, C.; Olson, M. A.; Fang, L.; Benítez, D.; Tkatchouk, E.; Basu, S.; Basuray, A. N.; Zhang, D.; Zhu, D.; Goddard, W. A.; Stoddart, J. F. *Proc. Nat. Acad. Sci. USA* **2010**, *107*, 13991-13996. (c) Trabolsi, A.; Fahrenbach, A. C.; Dey, S. K.; Share, A. I.; Friedman, D. C.; Basu, S.; Gasa, T. B.; Khashab, N. M.; Saha, S.; Aprahamian, I.; Khatib, H. A.; Flood, A. H.; Stoddart, J. F. *Chem. Commun.* **2010**, *46*, 871-873. (d) Jiang, Y.; Cao, J.; Zhao, J.-M.; Xiang, J.-F.; Chen, C.-F. *J. Org. Chem.* **2010**, *75*, 1767-1770.

(5) (a) Huang, F.; Fronczek, F. R.; Gibson, H. W. *J. Am. Chem. Soc.* **2003**, *125*, 9272-9273. (b) Huang, F.; Gibson, H. W.; Bryant, W. S.; Nagvekar, D. S.; Fronczek, F. R.; *J. Am. Chem. Soc.* **2003**, *125,* 9367-9371. (c) Huang, F.; Zhou, L.; Jones, J. W.; Gibson, H. W.; Ashraf-Khorassani, M. *Chem. Commun.* **2004**, 2670-2671. (d) Huang, F.; Switek, K. A.; Zakharov, L. N.; Fronczek, F. R.; Slebodnick, C.; Lam, M.; Golen, J. A.; Bryant, W. S.; Mason, P. E.; Rheingold, A. L.; Ashraf-Khorassani, M.; Gibson, H. W. *J. Org. Chem.* **2005**, *70*, 3231-3241. (e) Huang, F.; Slebodnick, C.; Switek, K. A.; Gibson, H. W. *Chem. Commun.* **2006**, 1929-1931 (f) Gibson, H. W.; Wang, H.; Slebodnick, C.; Merola, J.; Kassel, S.; Rheingold, A. L. *J. Org. Chem.* **2007**, *72*, 3381-3393. (g) Pederson, A. M.-P.; Vetor, R. C.; Rouser, M. A.; Huang, F.; Slebodnick, C.; Schoonover, D. S.; Gibson, H. W.; *J. Org. Chem.* **2008**, *73*, 5570-5573. (h) Li, S.; Zheng, B.; Huang, F.; Zakharov, L.; Slebodnick, C. Rheingold, A.; Gibson, H. W. *Sci. China Chem.* **2010**, *53*, 858-862. (i) Zhang, M.; Zhu, K.; Huang, F. *Chem. Commun.* **2010**, *46*, 8131-8141.

(6) Pederson, A. M. P.; Ward, E. M.; Schoonover, D. V.; Slebodnick, C.; Gibson, H. W. *J. Org. Chem.* **2008**, *73*, 9094-9101.

(7) (a) Yersin, H. In *Transition Metal and Rare Earth Compounds*; Yersin, H., Ed.; Springer Berlin / Heidelberg: 2004; Vol. 241, p 1-26. (b) Deschenaux, R. In *Ferrocenes*; John Wiley & Sons, Ltd: 2008, p 447-463. (c) Biot, C.; Dive, D. In *Medicinal Organometallic Chemistry*; Jaouen, G., Metzler-Nolte, N., Eds.; Springer Berlin / Heidelberg: 2010; Vol. 32, p 155-193. (d) Di Bella, S.; Dragonetti, C.; Pizzotti, M.; Roberto, D.; Tessore, F.; Ugo, R. In *Molecular Organometallic Materials for Optics*; Bozec, H., Guerchais, V., Eds.; Springer Berlin / Heidelberg: 2010; Vol. 28, p 1-55. (e) Crabtree, R. H. *Organometallics* **2011**, *30*, 17-19. (f) Higgins, S. J.; Nichols, R. J.; Martin, S.; Cea, P.; van der Zant, H. S. J.; Richter, M. M.; Low, P. J. *Organometallics* **2011**, *30*, 7-12.

(8) Crystal data of cryptand **5**: plate, yellow, 0.03 x 0.08 x 0.83 mm^3, $C_{48}H_{62}FeO_{16}$, *FW* = 950.83. Triclinic, space group P1; a = 8.3545(7) Å, b = 17.1254(13) Å, c = 17.2420(11) Å; α = 108.742(6)°, β = 102.820(6)°, 90.587(6)°; *V* = 2268.9(3) $Å^3$; *Z*

= 2, D_c = 1.392 Mg/m^3, T = 100 K, μ = 3.281 mm^{-1}, 40824 measured reflections, 9304 independent reflections (R_{int} = 0.0689), 590 parameters, F(000) = 1008, R_1 = 0.0599, wR_2 = 0.1526 [$I > 2\sigma(I)$], maximum residual density 0.841 e.Å^{-3}, and GoF(F^2) = 1.035. The structure was solved using SHELXS-97[8a] and refined using SHELXL-97[8a] via OLEX2.[8b] CrysAlisPro v171.34.40, Oxford Diffraction: Wroclaw, Poland, 2010. (a) Sheldrick, G. M. *Acta Cryst.* **2008**, *A64*, 112-122. (b) Dolomanov, O.V.; Bourhis, L. J.; Gildea, R. J.; Howard, J. A. K.; Puschmann, H. **J. Appl. Cryst. 2009**, *42*, 339–341.

(9) (a) Hunter, C. A.; Sanders, J. K. M.; *J. Am. Chem. Soc.* **1990**, *112*, 5525-5534. (b) Hohenstein, E. G.; Sherrill, C. D.; *J. Phys. Chem. A* **2009**, *113*, 878-886.

(10) (a) Job, P. *Ann. Chim. Appl.* **1928**, 113-203. (b) Hirose, K.; *J. Incl. Phenom. Macrocyc. Chem.* **2001**, *39*, 193-209.

(11) ^{1}H-NMR characterizations were done on solutions with constant [**5**] and varied [**3**]. Based on these NMR data, Δ_o, the difference in δ values for proton H_4 of **5** in the uncomplexed and fully complexed species, was determined to be 0.387 ppm as the y-intercept of a plot of $\Delta = \delta - \delta_u$ *vs.* $1/[\mathbf{3}]_0$ in the high initial concentration range of **3**. K_a was calculated from $K_a = (\Delta/\Delta_0)/[(1-\Delta/\Delta_0)([\mathbf{2}]_0-\Delta/\Delta_0\ [\mathbf{1c}]_0)$. For the **5**·**4** system, when the ratio of $[\mathbf{4}]_0/[\mathbf{5}]_0$ was higher than 23/1, no further chemical shift change was observed and the cryptand **5** was considered as fully complexed. The Δ_o was determined to be 0.407 ppm.

(12) (a) Asakawa, M.; Ashton, P. R.; Ballardini, R.; Balzani, V.; Bělohradský, M.; Gandolfi, M. T.; Kocian, O.; Prodi, L.; Raymo, F. M.; Stoddart, J. F.; Venturi, M. *J. Am. Chem. Soc.* **1997**, 119, 302-310. (b) Xiao, Y.; Chu, L.; Sanakis, Y.; Liu, P. *J. Am. Chem. Soc.* **2009**, *131*, 9931-9933.

Chapter 13.

Attempts to Prepare Real Linear Polycatenanes and Preparation and Characterization of [2]Pseudorotaxane based on Bis(*meta*-phenylene)-32-crown-10 (BMP32C10) and Bisphenanthroline

13.1 Introduction

Since the first small molecule-based catenane was experimentally realized in 1960,[1,2] many catenanes have been synthesized and studied.[2-9] Although many [2]-, [3]-[10-20] , [5]-, [7]-catenanes[21-24] and poly[2]catenanes[25-32] have been reported, to our knowledge, real polycatenanes (Scheme 13-1), whose backbones are exclusively composed of the macrocyclic components interlocked mechanically with each other, are still unknown. The synthesis of real polycatenanes is a significant challenge, primarily because of the requirements for achieving high molecular weight polymers and those for cyclization. To achieve high molecular weights in step-growth polymerizations high concentrations of monomers are required to minimize cyclization and achieve high conversions per the Carothers equation.[33] On the other hand, formation of cyclic species requires dilute conditions to avoid formation of linear oligomers.[34,35] The mechanically linked polycatenanes are of great interest because of their possible unusual properties as a result of inherent flexibility compared with traditional polymers, so synthesis of real polycatenanes is quite an attractive goal.

In this chapter, a templating method is used. Two synthetic steps will be used to prepare real polycatenanes: polymer formation and ring formation (Scheme 13-1). First, a U-shaped building block **1** is prepared. Rigid U-shaped monomer **2** is afforded via the deprotection reaction of monomer **1**. U-shaped monomers **2** are linked together via a metal ion and high

molecular weight polymer **3** will thus be obtained. The cyclization occurs between the two deprotected reactive groups of repeating unit **3**. The high dilution technique is used to prevent or minimize the inter-macromolecular reaction. Finally, the concave linkage Z of **3**, i. e., the metal ion, is removed and a real polycatenane is obtained in which all of the cyclic components are connected mechanically.

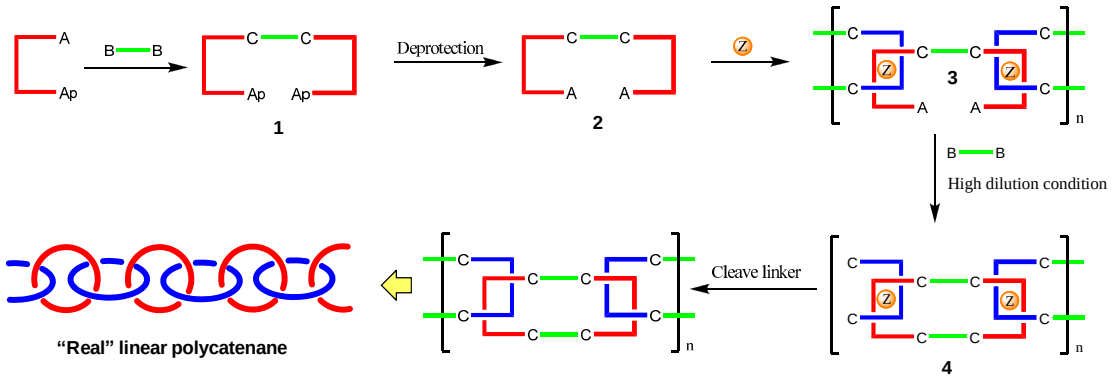

Scheme 13-1. "Universal joint monomer" route to polycatenanes by sequential polymerization /cyclization. A denotes reactive groups. A_p denotes the protected groups. Group A reacts with group B producing group C, z represents metal ions.

Our efforts focused on the use of the 1,10-phenanthroline systems that Sauvage et al.[36] pioneered; these compounds quantitatively form tetrahedral 2:1 complexes with copper(I); This step constitutes formation of the Z tether in general structure **3**. Additionally, the geometric constraints, i. e., rigidity and length, of the complex prevent the arms from rotating by each other.

12.2 Results and discussion

Synthetic strategy I is shown in Scheme 13-2. First, 4-bromobenyaldehyde was reduced by $NaBH_4$ and 4-bromobenzyl alcohol **5** was obtained in 100% yield. The hydroxyl group of 4-bromobenzyl alcohol was protected by dihydropyran and 4-bromobenzyl tetrahydropyranyl ether (**6**) was obtained in 92% yield. **6** was reacted with *n*-butyllithium first; then the reaction mixture was directly reacted with anhydrous 1,10-phenanthroline and then oxidized with manganese dioxide.[37] After purification, compound **8** was obtained in 11.3% yield. The yield is pretty low.

This reaction was repeated several times. However, the yield couldn't be improved. The low yield became a "bottle-neck". So another strategy was employed, as shown in Scheme 13-3.

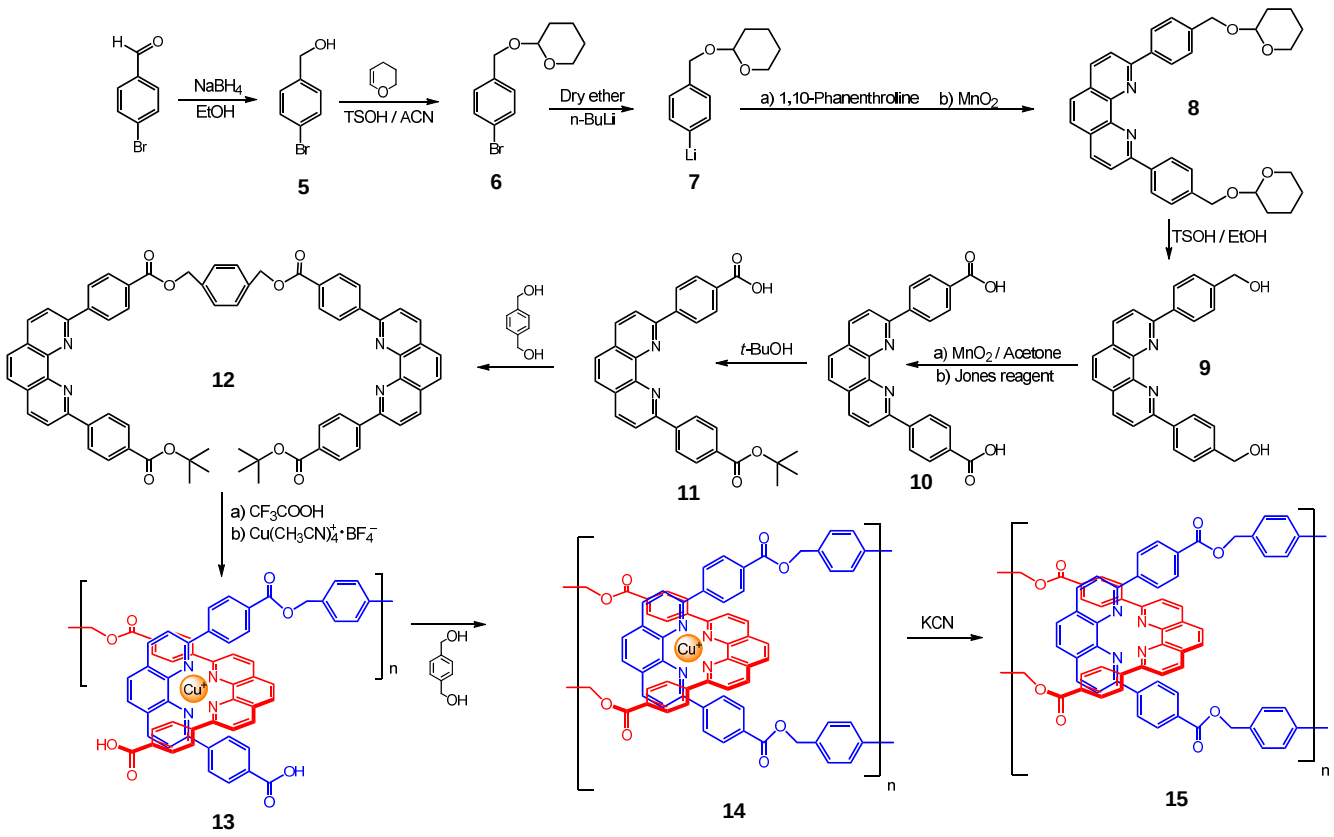

Scheme 13-2. Synthetic strategy I for real polycatenane.

In strategy II first, a literature reported method[38] was employed to prepare phenanthroline derivative **18**. However, the yield was very low. Finally, an optimized method was found and used to prepare **18** in 67% yield and purification was simple (no column was used during purification), compared with the traditional reported method. Then, **18** was converted into **19** in 92% yield via an optimized method. One hydroxyl group of **19** was protected by a benzyl group and **20** was obtained in 46% yield. **20** was reacted with terephthaloyl chloride to afford **21a** as a white solid in 82% after purification. However, the solubility of **21a** was really bad even in strong solvents, such as dimethyl sulfoxide (DMSO). It was thought that the terephthalate favored the close-packing of the molecules and led to the bad solubility. It has been well known that the isophathalate group disfavors the close-packing of molecules. Thus, the isophathalate

group was introduced; **21b** was prepared in 80% yield via the coupling reaction between **20** and isophthalyol dichloride. As expected, the solubility of **21b** was better than that of **21a**. However, it still aggregated after two days storage. Obviously, the low solubility disfavors the preparation of polymers such as **23**. In order to increase the solubility of the "U"-shaped molecule, the 5-*tert*butylisophathalate group was introduced into the "U" shaped molecule. **21c** was prepared in 91% via 1-ethyl-3-(3'-dimethylaminopropyl)carbodiimide (EDCI) coupling between **20** and 5-*tert*butylisophathalic acid.

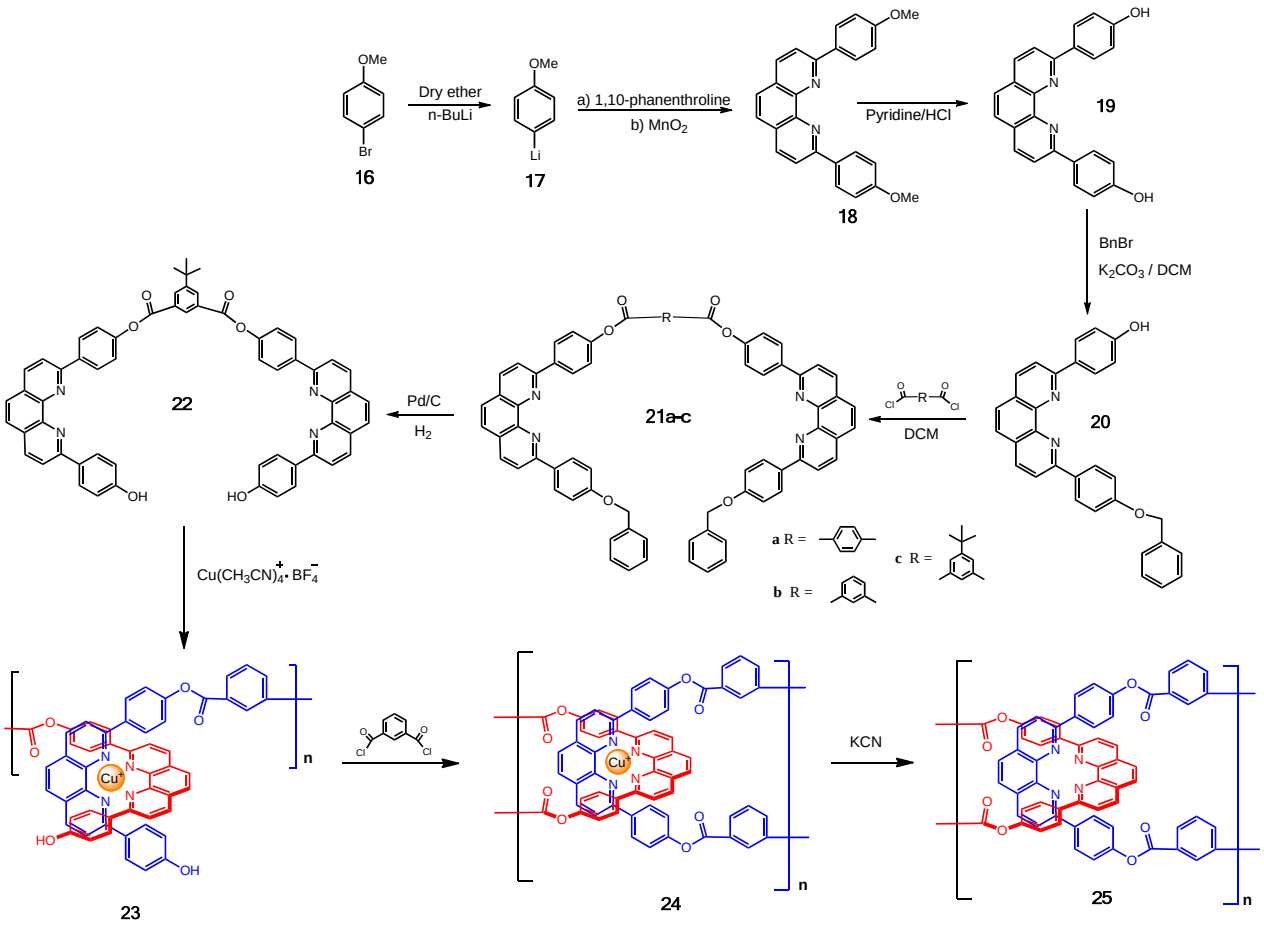

Scheme 13-3. Synthetic strategy II for real polycatenane.

As expected, the solubility of **21c** was pretty good and it could be easily dissolved in dicholormethane and DMSO. In the future, unprotected "U" shaped molecule **22** will be prepared by hydrogenolysis of the benzyl protecting group. Then the "U" shaped monomers **22** will be linked together by Cu(I) ion and polymer **23** will be afforded. Cyclization will be

performed on polymer **23** and polymer **24** should be obtained. After demetallization, real linear polycatenane **25** will be afforded.

It was thought the big aromatic rings of phenanthroline possibly would favor the "taco" shape structures observed in the complexes of bis(*meta*-phenylene)-32-crown-10 (BMP32C10) and paraquats. Therefore, based on hydroxyl-functionalized phenanthroline derivative **20**, BMP32C10 based bisphenanthroline derivative **26** was prepared in 90% yield. ^{1}H-NMR spectra of solutions of **26** and dimethyl paraquat contained only one set of peaks, indicating that the complexation is a fast exchange process. In the complex of **26·DMP**, the peaks corresponding H_1 and H_2 of 2**6** and H_{p1} and H_{p2} of guest **DMP** shifted upfield. In addition, the signals corresponding to H_5, H_6, H_7, H_8, H_9, H_{10}, H_{11}, H_{12} and H_{13} on the phenanthroline arms of 2**6** shifted downfield upon complexation, indicating that the phenanthroline arm participated in the complexation. A Job plot demonstrated that the ratio between **26** and **DMP** was 1:1, which was confirmed by electrospray ionization mass spectrum (ESI-MS): m/z 1828.14 [**26·DMP**-PF_6+H]$^{+}$.[39] The association constant (K_a) was determined to be 430 ± 36 M^{-1} in $CDCl_3$/CD_3CN (1/1, v/v).

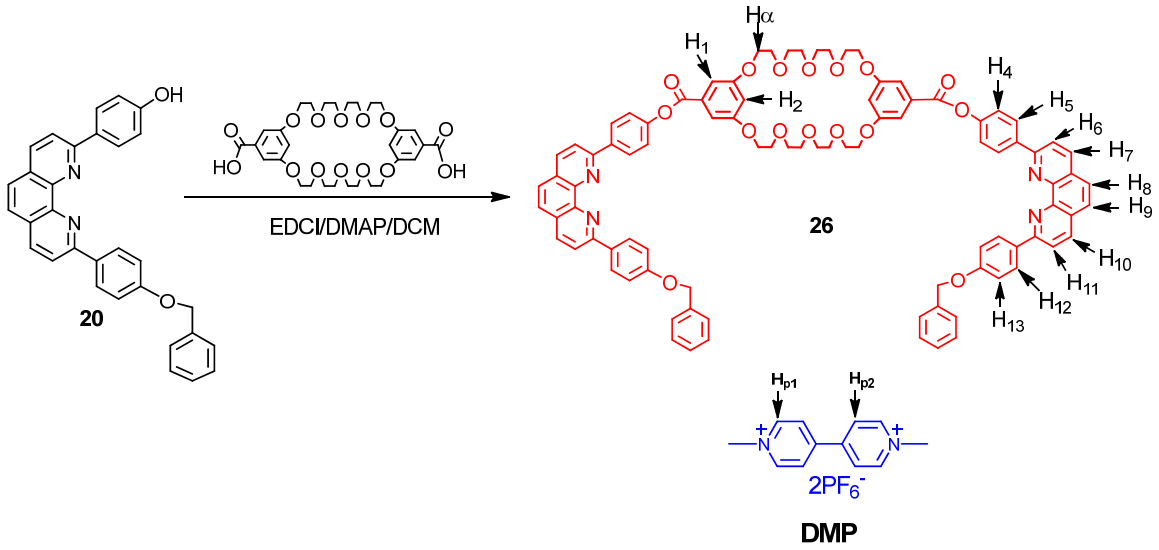

Scheme 13-4. Synthesis of **26**.

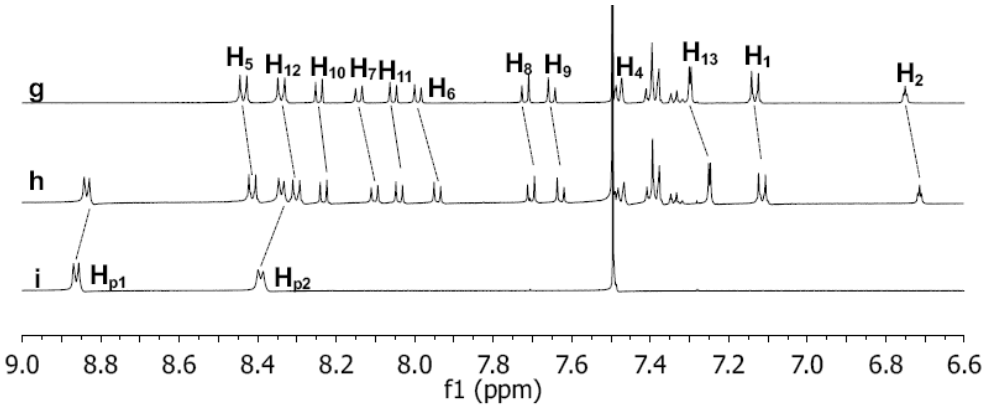

Figure 13-1. Stacked partial proton NMR spectra (500 MHz, $CDCl_3/CD_3CN$ = 1/1 <v/v>, 25°C) of: Upper (a) 2**6**. (b) 2**6** and **DMP** mixture . (c) **DMP**;

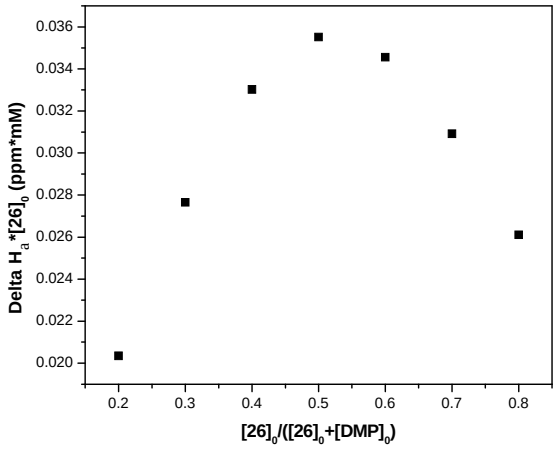

Figure 13-2. Job plot of the complex between **26** and **DMP** in $CDCl_3/CD_3CN$ = 1/1 <v/v>.

13.3 Conclusions

In summary, in order to prepare linear polycatenanes, the preparation of which represent a real synthetic challenge, a series phenanthroline derivatives were designed and prepared. The "U" shaped monomer **22** was successfully prepared in relative high yield. In the future, based on monomer **22**, real linear polycatenanes will be prepared. In addition, a novel diphenanthroline-

based BMP32C10 **26** was prepared in high yield and the complexation behavior between **26** and **DMP** was studied. The stoichiometry between **26** and **DMP** was 1:1 and the association constant (K_a) was determined to be 430 ± 36 M^{-1} in $CDCl_3/CD_3CN$ (1/1, v/v).

13.4 Acknowledgements

This work was supported by the National Science Foundation (DMR0704076) and the Petroleum Research Fund administered by the American Chemical Society (47644-AC). We also acknowledge the National Science Foundation for funds to purchase the Innova-400 NMR and Agilent 6220 Accurate Mass TOF LC/MS spectrometers (CHE-0131124 & CHE-0722638, respectively).

13.5 Experimental Section

13.5.1 Materials and methods

All the chemicals were reagent grade and used as received. Bis(*meta*-phenylene)-32-crown-10 (BMP32C10) diacid [40] and dimethyl paraquat PF_6 (**DMP**)[41] were prepared according to literature procedures. Solvents were either used as purchased or dried according to literature procedures. ^{1}H-NMR spectra were obtained on a JEOL ECLIPSE-500 spectrometer and an INOVA-400 spectrometer with internal standard TMS. ^{13}C-NMR spectra were collected on a JEOL ECLIPSE-500 spectrometer at 125 MHz and an INOVA-400 spectrometer at 101 MHz. HR-MS were obtained by employing an Agilent LC-ESI-TOF and an Applied Biosystems 4800 MALDI TOF/TOF. Isothermal titration calorimetry was performed on a Microcal MCS instrument; raw isotherm data were collected using the Microcal Observer software. Integration and fitting of the isothermal data (K_a and ΔH) were accomplished using Origin software with a one set of sites algorithm.

13.5.2 Synthesis of 4-bromobenzyl alcohol (5)

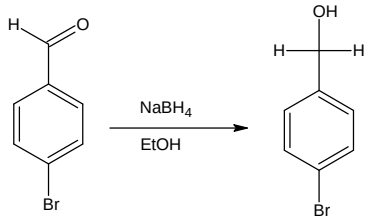

Scheme 13-5. Synthesis of the *p*-bromobenzyl alcohol (**5**).

4-Bromobenyaldehyde (80 g, 0.43 mol) and $NaBH_4$ (20 g, 0.53 mol) were dissolved in EtOH (2000 mL, dried by molecular sieves overnight). The reaction proceeded at room temperature under N_2 for 12 hours. After silica gel column purification, a white crystal-like product (81.4 g, 100%) was obtained,mp 76.0-77.1℃ (lit: 75.0-77.0℃[41]). ^{1}H-NMR ($(CD_3)_2CO$, 400 MHz) (**Figure 13-3**): δ: 7.46 (d, ^3J = 8 Hz, 2.0 H, H_1), 7.30 (d, ^3J = 8 Hz, 2.1 H, H_2), 4.57 (d, ^3J = 6 Hz, 2.1 H, methylene H), 4.28 (t, ^3J = 6 Hz, 0.98 H, OH).

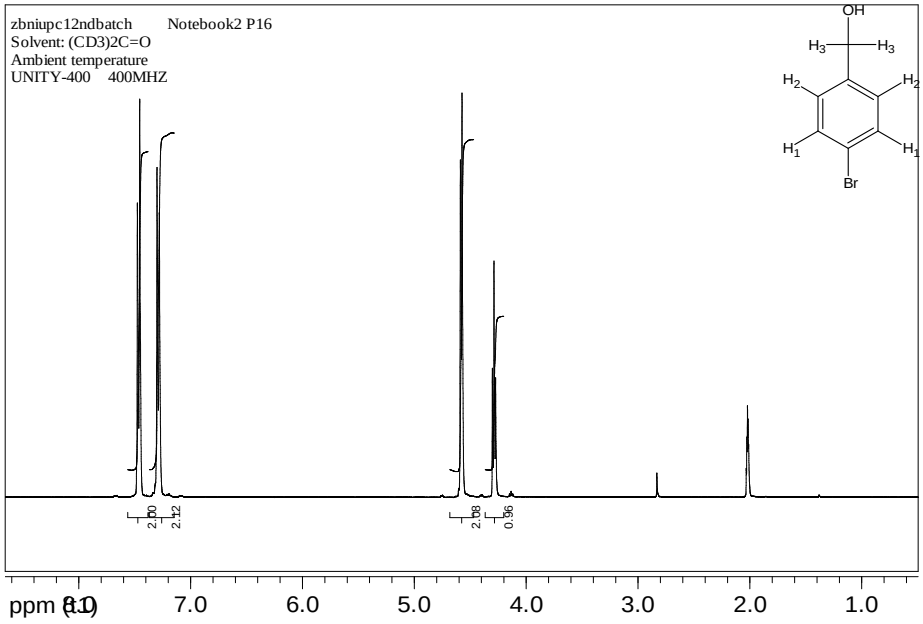

Figure 13-3. 400 MHz ^{1}H-NMR spectrum ($(CD_3)_2CO$, room temperature) of 4-bromobenzyl alcohol (**5**).

13.5.3 Synthesis of p-Bromobenzyl tetrahydropyranyl ether (6)

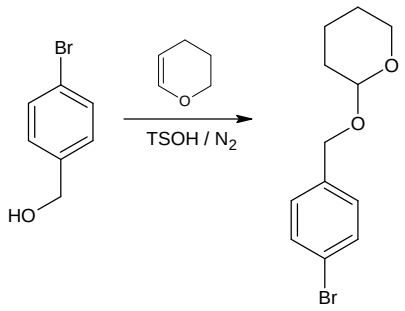

Scheme 13-6. Synthesis of the *p*-bromobenzyl tetrahydropyranyl ether (**6**).

p-Bromobenzyl alcohol (60 g, 0.32 mol) was added to dihydropyran (27.18 g, 0.32 mol) in dry acetonitrile (360 mL, dried by molecular sieves) along with a catalytic amount *p*-toluenesulfonic acid. The reaction proceeded at room temperature for 1 day. Solvent was removed. The dark brown oil-like product was dissolved in water/ether, then the organic phase was washed with Na_2CO_3 (10%, aq.), water and NaCl (aq., sat.). A silica gel column was employed to purify the crude product. After purification, **6** was obtained as a colorless oil (80.0 g, 92% yield. ^{1}H-NMR ($(CD_3)_2CO$, 400 MHz) (**Figure 13-4**): δ: 7.49 (d, ^3J = 8 Hz, 2.0 H, H_1), 7.30 (d, ^3J = 8 Hz, 1.98 H, H_2), 4.68 (m, 2.0 H, methylene H), 4.43 (d, ^3J = 8 Hz, 1.0 H, H_7), 3.80 & 3.47 (1.0 H & 1.0 H, H_6), 1.17 – 1.80 (m, 6.3 H, H_3 & H_4 & H_5).

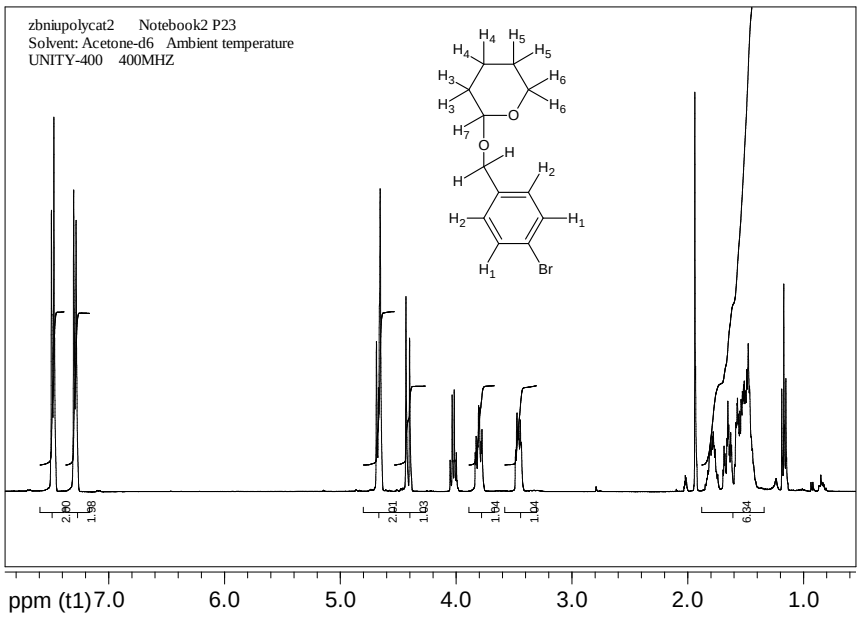

Figure 13-4. 400 MHz ^{1}H-NMR spectrum ($(CD_3)_2CO$, room temperature) of *p*-bromobenzyl tetrahydropyranyl ether (**6**).

13.5.4 Synthesis of 2,9-bis[(*p*-Tetrahydropyranyloxymethyl)phenyl]-1,10-phenanthroline (8)

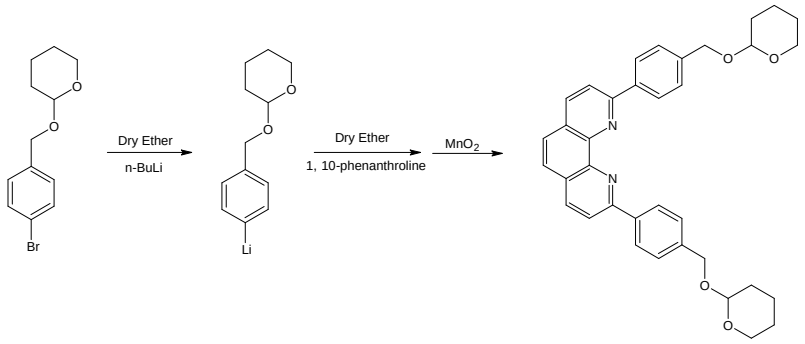

Scheme 13-7. Synthesis of 2,9-bis[*p*-(Tetrahydropyranyloxymethyl)phenyl]-1,10-phenanthroline (**8**).

Before reactions, all the glassware and cannula were heated in the oven and blow with nitrogen. The diethyl ether used as solvent was dried over sodium metal.

p-Bromobenzyl tetrahydropyranyl ether (3.06 g, 11.5 mmol) was dissolved in dry diethyl ether (120 mL). The flask was exchanged with high purity argon under low pressure (3 times;

calcium chloride was used as the desiccant in the gas line). Fresh *n*-butyllithium solution (12 mmol, 7.0 mL / 1.6 M in pentane) was slowly added into the solution by glass syringe at room temperature. Immediately, a light yellow precipitate was formed. The reaction proceeded at room temperature for 4 hours. The light yellow mixture was transferred to a suspension of 1,10-phenanthroline (0.88 g, 4.8 mmol) in dry ether (100 mL) via a cannula under the pressure of argon. Almost at the same time, the color of the mixture became dark red. The reaction proceeded at 0℃ for 4 hours and then at room temperature for 2 days. After addition of water (100 mL), the color of the mixture changed from dark red to orange and a large amount of precipitate was formed. The aqueous layer was washed with methylene dichloride (DCM, 125 mL x 3 times). The collected organic layer was rearomatized by continuous addition of activated MnO_2 (10 g x 5). The reaction was monitored by TLC (silica gel, chloroform : methanol = 98 : 2 was used as developing agent). The MnO_2 powder was removed by filtration. After filtration, a brown oil was obtained. A silica gel column was used to purify the crude product. However, the relative low solubility of the crude product made the column separation difficult. A big silica gel column must be used and the overlapping between different fractions was serious. After purification, **8** was obtained (0.28 g, 11.3%), mp 233-234 ^{o}C (lit. 234-236).[37] ^{1}H-NMR (acetone-d_6, 400 MHz, Figure 13-5): δ: 8.58 (d, ^{3}J = 8 Hz, 3.5 H, H_{10}), 8.43 (d, ^{3}J = 8 Hz, 2.0 H, H_4 & H_7), 8.29 (s, 1.8 H, H_5 & H_6), 7.60 (d, ^{3}J = 8 Hz, 3.6 H, H_{11}), 4.83 (d, ^{4}J = 12 Hz, 1.9 H, H_{12}), 4.73 (t, ^{3}J = 4 Hz,, 1.8 H, H_{13}), 4.54 (d, ^{4}J = 12 Hz, 1.7 H, H_{12}), 3.90 (m, 2.0 H, H_{17}), 3.52 (m, 2.2 H, H_{17}), 1.47 – 1.86 (m, 14 H, $H_{14\text{-}16}$).

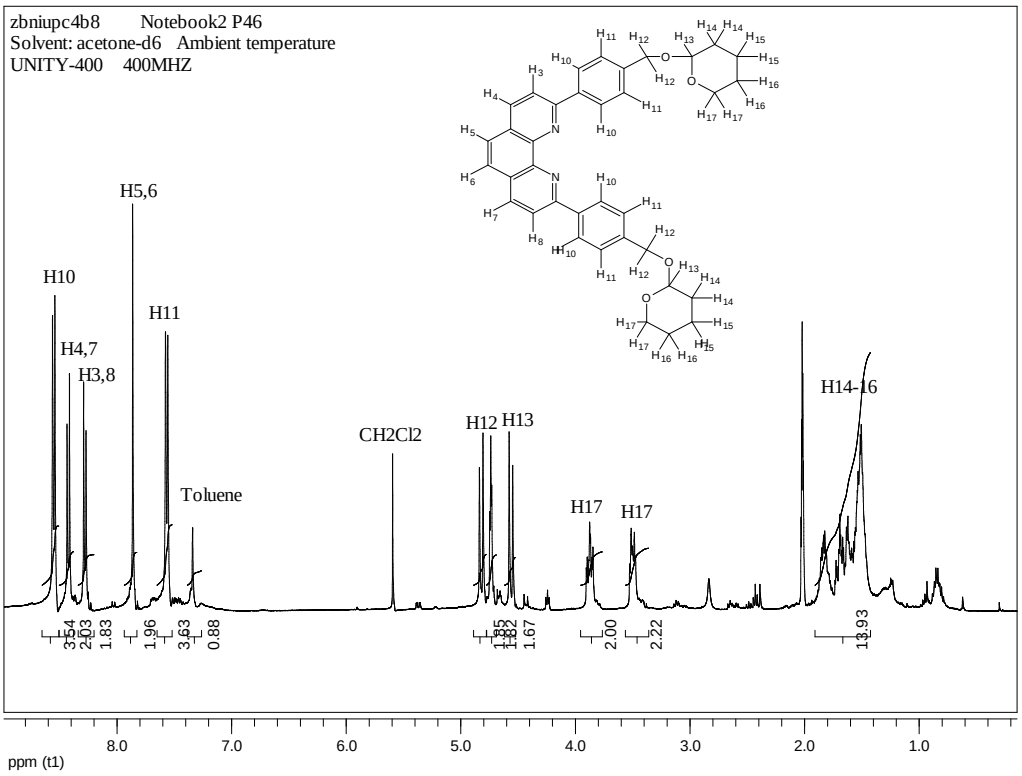

Figure 13-5. 400 MHz ^{1}H-NMR spectrum ($(CD_3)_2CO$, room temperature) of **8**.

13.5.5 Synthesis of 2,9-Bis(*p*-methoxyphenyl)-1,10-phenanthroline (18) via optimized method

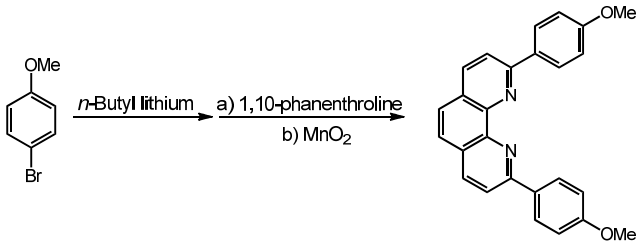

Scheme 13-7. Synthesis of **18**.

Before the reaction, all the glassware was heated in the oven and cooled under blowing N_2. THF was distilled from sodium metal. 1,10-Phenanthroline (Alfa-Ascar, 97%) was recrystallized in toluene and dried in a vacuum oven with P_2O_5.

p-Bromoanisole (5.76 mL, 45 mmol) was dissolved in dry THF (40 mL) and the solution was exchanged with argon 5 times. The solution was cooled in a dry ice/acetone bath to -78 °C. A *n*-butyllithium solution (1.6 M in hexane, 49 mL, 76 mmol) was added slowly into the *p*-bromoanisole solution and the reaction mixture was stirred at this temperature for 2 hours. The dry ice bath was then removed, and the reaction mixture was ***gradually raised to 0 °C (in the air) before it was placed in an ice bath*** **(key step)**. After the temperature stopped increasing, this clear solution was transferred *via* cannula to a THF solution (25 mL) of 1,10-phenanthroline (2.00 g, 11.1 mmol) submerged in an ice bath. The mixture was stirred overnight and then hydrolyzed with water at room temperature for 30 minutes. The THF layer was decanted, and the aqueous layer was washed with dichloromethane (3 times). The combined organic layers were rearomatized with MnO_2 (25 g). After completion of the reaction, the mixture was dried over anhydrous Na_2SO_4 and filtered. The filtrate was concentrated to provide a mixture of yellow solid and yellow oil. The crude product was recrystallized in toluene and fine crystals was obtained (3.0 g, 69%), mp: 178-179 °C (lit[38a] 179 °C).^{1}H-NMR ($CDCl_3$, 500MHz) (Figure 13-6): δ: 8.45 (d, ^3J = 8 Hz, 4.0 H), 8.27 (d, ^3J = 8 Hz, 2.1 H), 8.10 (d, ^3J = 8 Hz, 2.0 H), 7.74 (s, 2.0 H), 7.12 (d, ^3J = 8 Hz, 4.0 H), 3.92 (s, 6.0 H). Solvent peaks: 5.30 (s, DCM), 2.36 (s, toluene), 1.50 (s, H_2O). ^{13}C-NMR ($CDCl_3$) (Figure 13-S5): δ: 160.87, 156.33, 146.01, 136.77, 132.16, 128.97, 127.52, 125.60, 119.30, 114.17, 55.39.

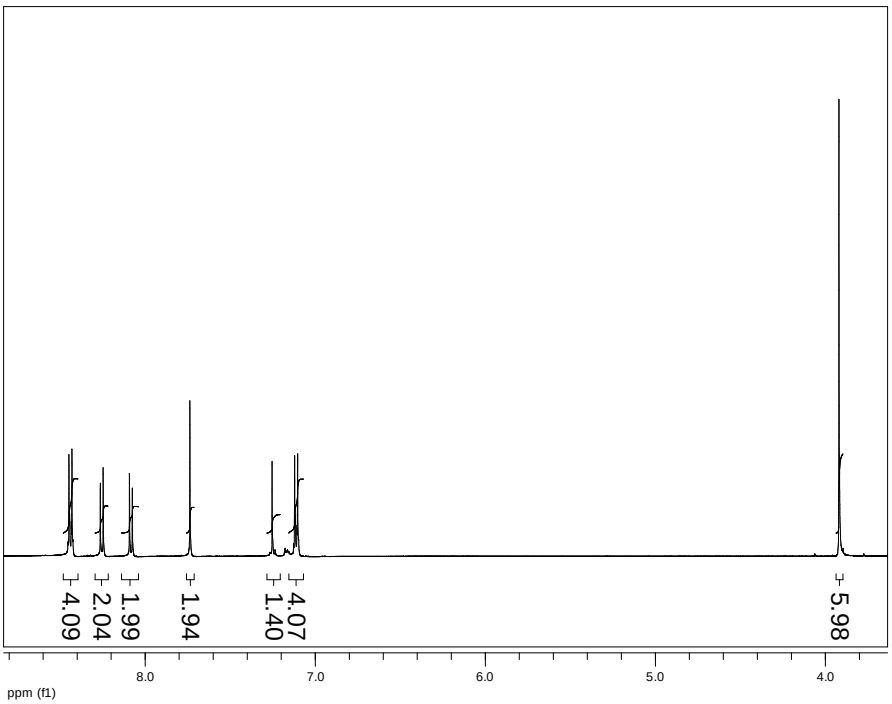

Figure 13-6. 500 MHz ^{1}H-NMR spectrum ($CDCl_3$, room temperature) of **18**.

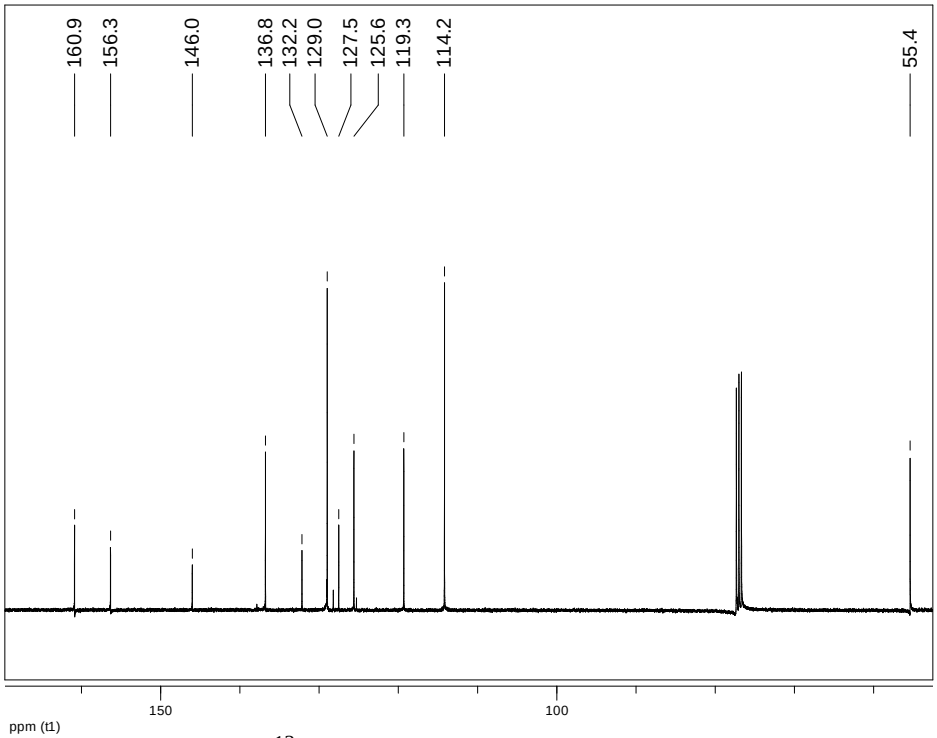

Figure 13-7. 125 MHz ^{13}C-NMR spectrum ($CDCl_3$, room temperature) of **18**.

13.5.6 Synthesis of 2,9-Bis(*p*-hydroxyphenyl)-1,10-phenanthroline (19)

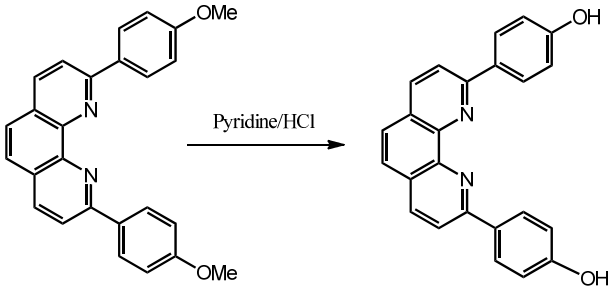

105 **106**

Scheme 13-8. Synthesis of **19**.

HCl (37%, 17.6 mL) was added to pyridine (16 mL) dropwise at room temperature. Then a Dean-Stark trap and a thermometer were equipped and the solution was heated until the internal temperature was up to 210 °C in order to remove water. After the mixture was cooled to 140 °C, 2,9-bis(4-methoxyphenyl)-1,10-phenanthroline (**18**) (6.0 g, 15 mmol) was added as a solid. The yellow mixture was stirred and refluxed at 180 °C for 3 hours. The hot reaction mixture was diluted with boiling water very slowly (carefully!) and the bright yellow suspension was poured into hot water (60 mL). The resulted suspension was cooled down and filtered to give a yellow solid. The solid was added to a mixture of water/ethanol (250 mL/85 mL). While the suspension was being stirred, dilute NaOH solution was added. The pH was monitored with a pH meter. It took two days to neutralize the suspension. Every time, the pH value increased to 7.5-7.8 after addition of dilute NaOH solution. But after 10 to 20 mins stirring, the pH value went back to 5 to 6. Finally, the pH seemed stable. Then the suspension was further diluted with hot water (300 mL) and filtered to afford a yellow solid, whidh was dried in vacuum oven with P_2O_5 overnight and a dark red solid was obtained. ^{1}H-NMR showed it was still a mixture of protonated product and desired product. The solid was dissolved in DMF (500 mL) and $NaHCO_3$ (2 equivalents) was added. The suspension was heated to 80°C for 30 mins. DMF was removed and the solid was dispersed into H_2O. After filtration, a yellow solid was obtained. The solid was dried in a vacuum oven with P_2O_5 and a dark red solid was obtained (5.12 g, 92%) mp > 260°C

(lit. N/A). ^{1}H-NMR (DMSO-d_6, 500MHz) (Figure 13-8): δ: 9.90 (s, 2.0 H), 8.48 (d, ^{3}J = 8 Hz, 2.1 H), 8.38 (d, ^{3}J = 8 Hz, 4.1 H), 8.28 (d, ^{3}J = 8 Hz, 2.0 H), 7.98 (s, 2.1 H), 7.02 (d, ^{3}J = 8 Hz, 4.1 H). ^{13}C-NMR (125 MHz, DMSO-d_6, Figure 13-9): 159.519, 155.753, 145.690, 137.468, 130.314, 129.202, 127.602, 125.970, 119.467, 116.173.

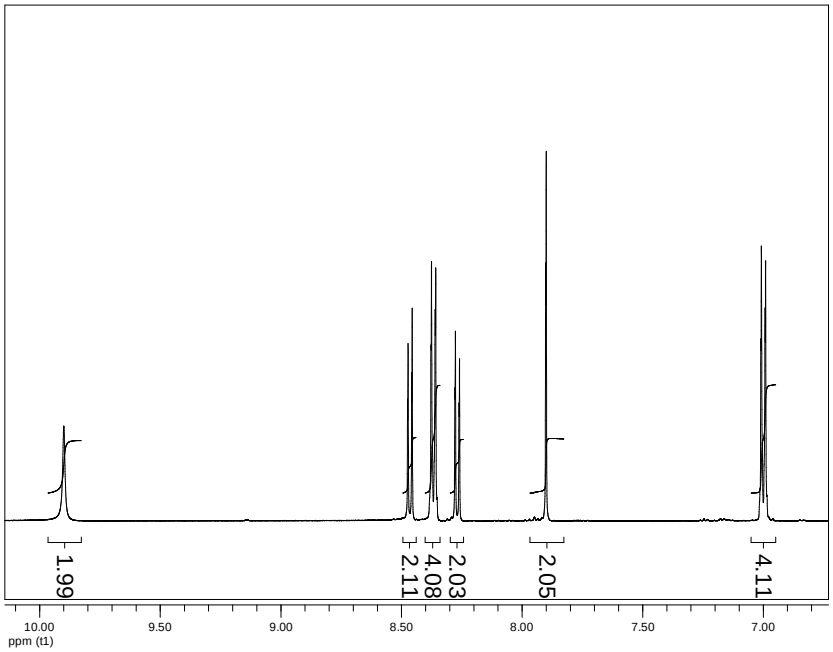

Figure 13-8. 500 MHz ^{1}H-NMR spectrum (DMSO-d_6, room temperature) **19**.

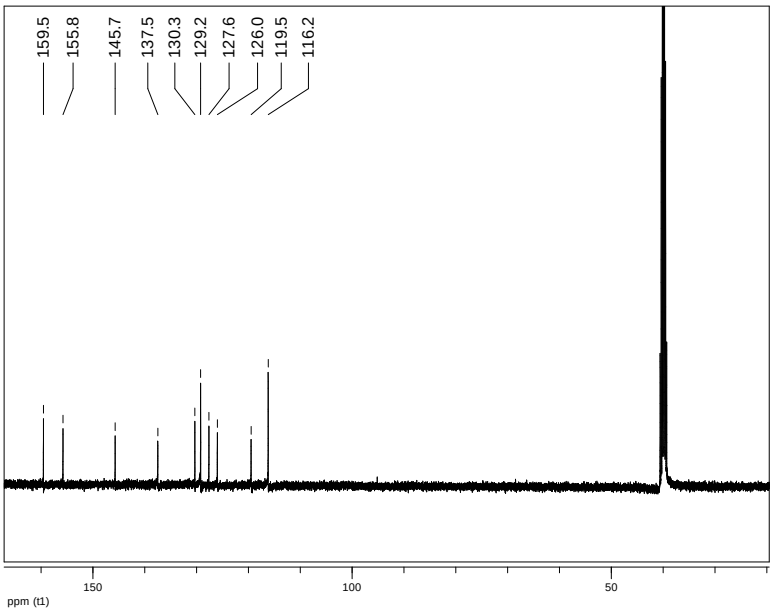

Figure 13-9. 125 MHz ^{13}C-NMR spectrum (DMSO-d_6, room temperature) of **19**.

13.5.7 Synthesis of 2-(*p*-Hydroxyphenyl)-9-(*p*-benzyloxyphenyl)-1,10-phenanthroline (20)

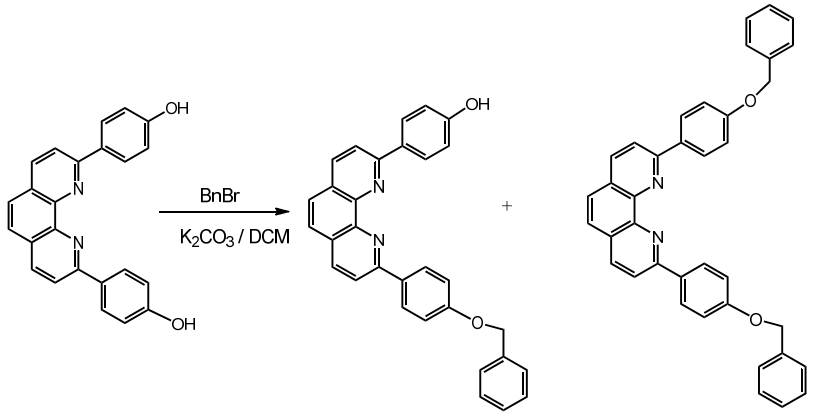

Scheme 13-9. Synthesis of 2-(*p*-Hydroxyphenyl)-9-(*p*-benzyloxyphenyl)-1,10-phenanthroline (**20**).

19 (4.7 g, 13 mmol) was dissolved in DMF (600 mL). K_2CO_3 (3.5 g, 26 mmol) was added into the solution. The mixture was exchanged with argon (3 times) and heated to 60 °C by oil-bath. Benzyl bromide (2.32 g, 13.5 mmol) was dissolved in DMF (50 mL) and added dropwise (over 30 hours). After addition, the mixture was stirred at 80 °C for 2 days, filtered and the DMF was removed under high vacuum. A brown solid was obtained. The solid was redissolved in DCM (the solubility was bad and some amount of solid particle suspended in the solution) and washed with DI water/HCl (aq., 2M) until pH=7-8 (difficult!). A lot of red solid existed in the water phase. The red solid was collected by filtration. According to ^{1}H-NMR, it was the starting material-**19**. The DCM phase was collected and a brown solid was obtained after the solvent was removed. The solid was dried in vacuum oven with P_2O_5 overnight and purified by a huge silica gel column. **20** (2.69 g, 46%) was obtained as an off-white solid, mp > 342 ℃. ^{1}H-NMR ($CDCl_3$, 400 MHz, Figure 13-10): δ: 8.40 (d, ^{3}J = 8 Hz, 2.1 H, H_{o2}), 8.36 (d, ^{3}J = 8 Hz, 2.0 H, H_{o1}), 8.28 (dd, ^{3}J = 8 Hz, ^{4}J = 2 Hz, 2.1 H, H_4 and H_7), 8.07 (m, 2.0 H, H_3 and H_8), 7.75 (s, 2.0 H, H_5 and H_6), 7.50 (d, ^{3}J = 8 Hz, 2.0 H, H_9), 7.34-7.43 (m, 2.9 H, H_{10}), 7.18 (d, ^{3}J = 8 Hz, 2.0 H, H_{m2}), 7.01 (d, ^{3}J = 8 Hz, 1.9 H, H_{m1}), 5.32 (bs, 0.73 H, OH), 5.17 (s, 2.0 H, CH_2). ^{13}C-NMR (101 MHz, DMSO-d_6, Figure 13-11): δ: 160.3, 159.6, 155.9, 155.4, 145.8, 145.8, 137.7, 137.6, 137.5, 132.1, 130.4, 129.3, 129.2, 129.0, 128.4, 128.3, 127.9, 127.7, 126.3, 126.0, 119.8, 119.6, 116.2, 115.7, 69.9. ESI-MS (Figure 13-12); calcd. for **20:** 454.1681 , found: *m/z*, 455.1750 [M + H^+].

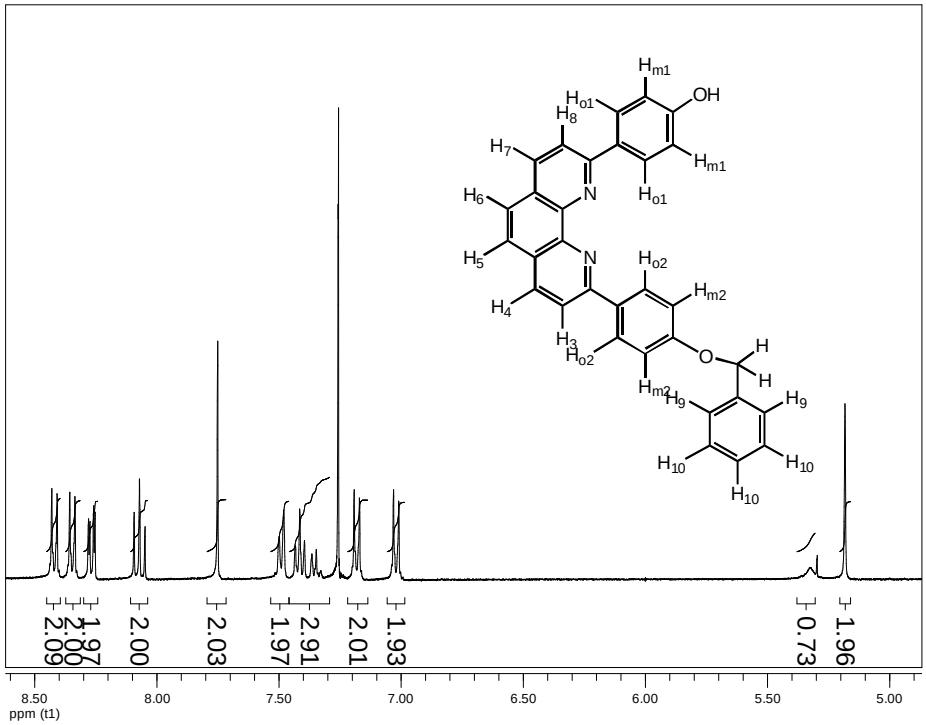

Figure 13-10. 500 MHz ^{1}H-NMR spectrum ($CDCl_3$, room temperature) **20**.

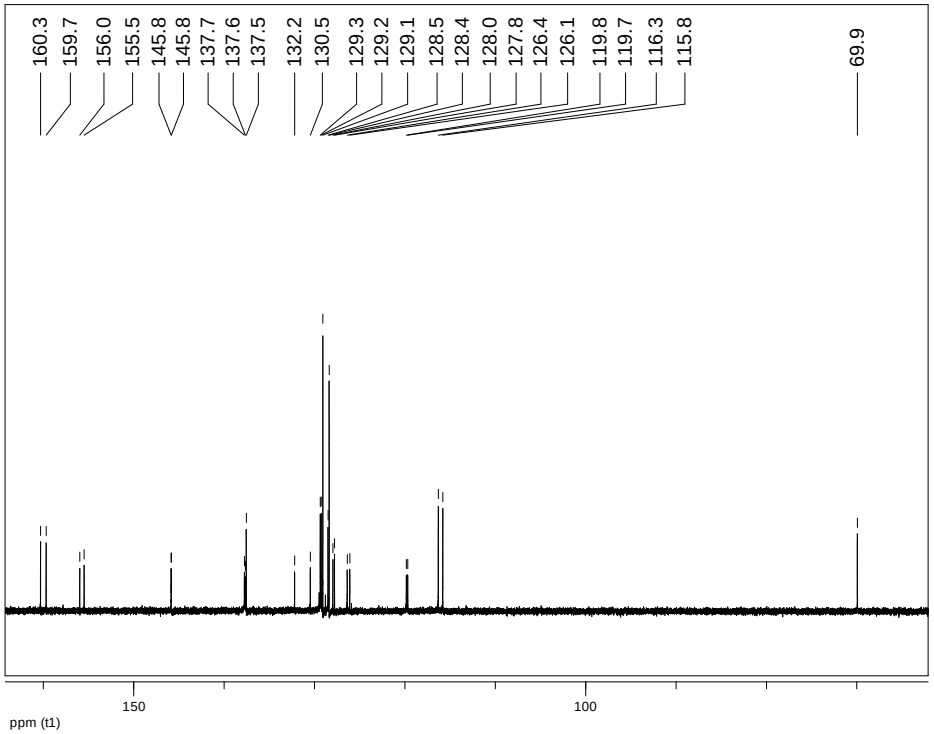

Figure 13-11. 125 MHz ^{13}C-NMR spectrum (DMSO-d_6, Room temperature) of **20**.

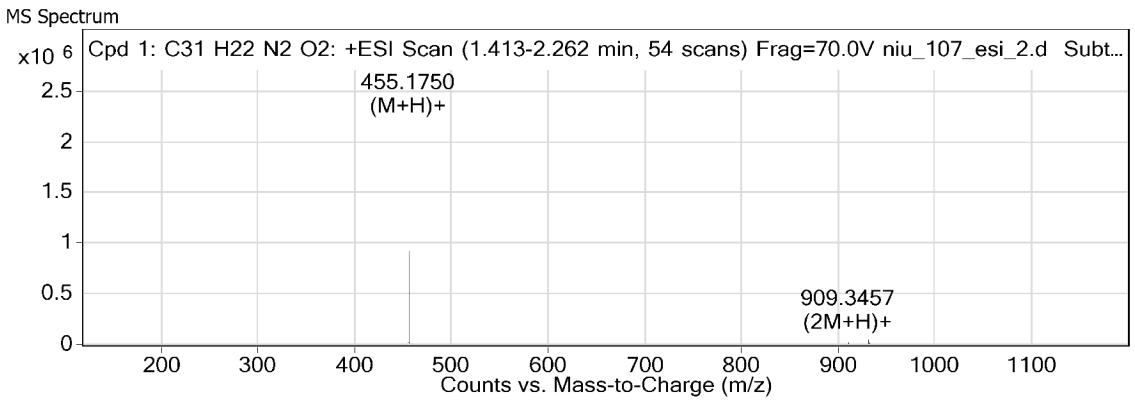

Figure 13-12. ESI-MS spectrum of **20**.

13.5.8 Synthesis of 21a

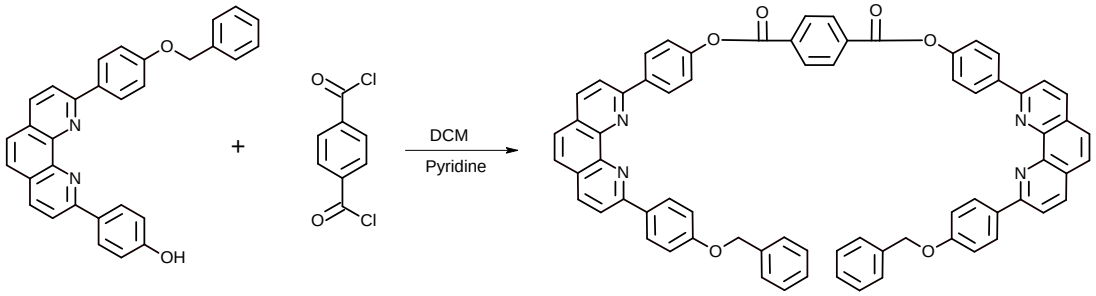

Scheme 13-10. Synthesis of the **21a**.

20 (80 mg, 0.18 mmol) and terephthaloyl chloride (18 mg, 0.09mmol) were mixed together and DCM (10 mL, anhydrous) and pyridine (2 drops) were added. The mixture was heated to reflux. After 14 hours, a lot of fine powder precipitated. A few drops of water were added. The mixture was stirred for another half hour. Solvent was removed. A yellow solid (0.107 g) was obtained. The product was redissolved in DCM (bad solubility, a large amount DCM must be used) washed with $NaHCO_3$ / NaOH (PH =11), DI water and dried in the vacuum oven with P_2O_5. A silica gel column was employed to purify the final product. Gradient elution was performed: DCM:MeOH = 100 : 1 to DCM:MeOH =95 : 5. At the beginning, the first

fraction was a transparent solution in the tube, but white thin films were formed after a short time (about 5 mins), mp > 250 °C. The solvent was removed. The white solid was almost insoluble in common solvents – DCM, chloroform, methanol, ethyl acetate, DMF, DMSO. ^{1}H-NMR ($CDCl_3$, 400MHz) (**Figure 13-13**): the peaks were too weak to be integrated correctly although the sample was scanned about 1000 times, but in the enlarged Figure 13-the spectrum matched that expected for the desired product. The mass spectrum (MALDI-TOF**, Figure 13-14**) proved it was the product we wanted: calcd for **8**: 1038.1377, found *m/z* 1038 [M-H^{+}].

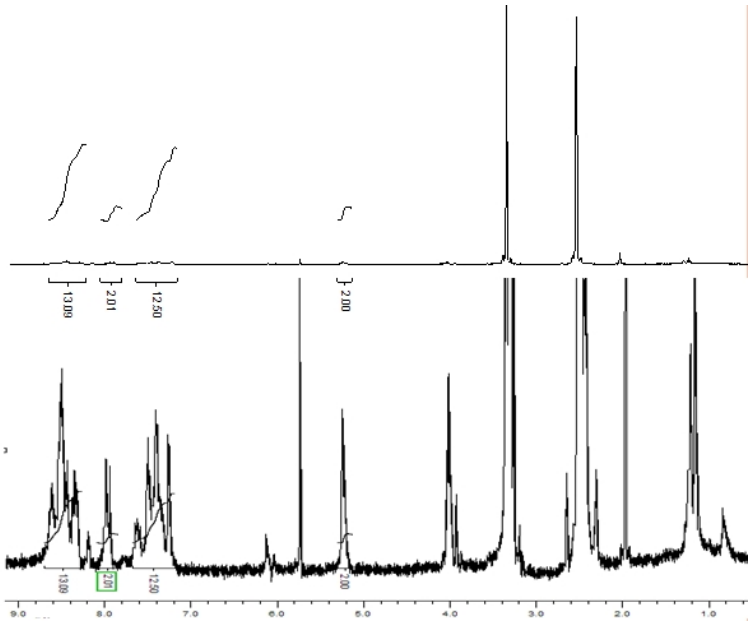

Figure 13-13. 400 MHz ^{1}H-NMR spectrum (DMSO-d_6, room temperature) of **21a**. Top: original spectrum; Low: enlarged spectrum

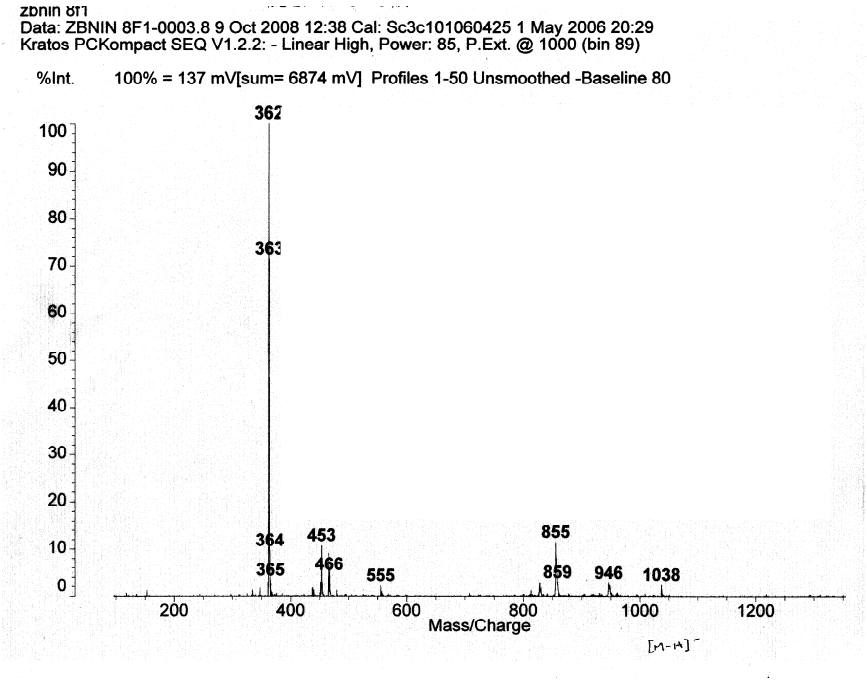

Figure 13-14. MALDI-TOF MS of **21a**.

13.5.9 Synthesis of 21b

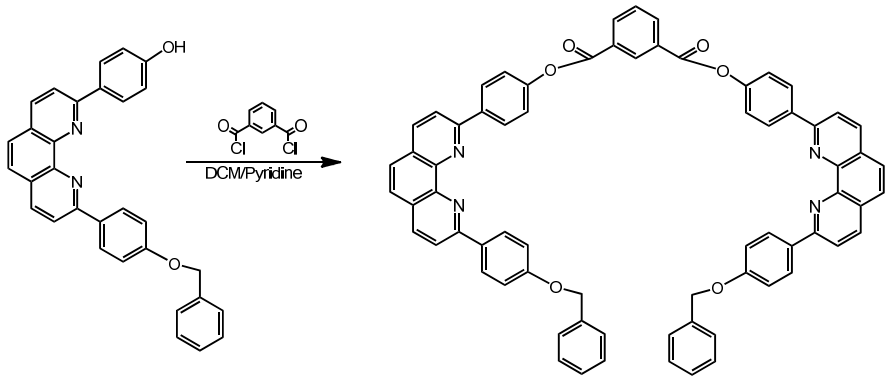

Scheme 13-11. Synthesis of **21b**.

20 (100 mg, 0.22 mmol) and isophthalyol dichloride (98%, 22.3 mg, 0.108 mmol) were dissolved in DCM (anhydrous, 80 mL). Pyridine (dry, 0.02 mL) was added to the solution. The solution was refluxed for 2 days. A yellow solid precipitated during the reaction. The solution was washed with DI water, dilute NaOH solution, DI water again and dried over Na_2SO_4. *The solubility of the crude product in DCM was not good.* TLC showed three spots

(DCM/MeOH=96/4). Two silica gel columns were used to purify the mixture and a yellow solid was obtained (182 mg, 80%), mp 195-196 ^{o}C. ^{1}H-NMR ($CDCl_3$, 400 MHz, Figure 13-15): δ: 9.14 (s, 1.1 H, H_{11}), 8.57 (m, 6.7 H, H_{o1} + H_{13}), 8.44 (d, ^{3}J = 8 Hz, 4.2 H, H_{o2}), 8.34 (d, ^{3}J = 8 Hz, 2.3 H, H_4), 8.30 (d, ^{3}J = 8 Hz, 2.1 H, H_7), 8.16 (d, ^{3}J = 8 Hz, 2.0 H, H_3), 7.79 (s, 4.0 H, H_5 and H_6), 7.53 (m, 5.3 H, H_{12} + H_{m1}), 7.53 (d, ^{3}J = 8 Hz, 4.1 H, H_9), 7.41 (m, 4.1 H, H_{10}), 7.18 (d, ^{3}J = 8 Hz, 3.9 H, H_{m2}), 5.18 (s, 4.0 H, CH_2). ESI-MS (Figure 13-16); calcd. for **21b**: 1038.3417, found: *m/z*, 1039.3493 [M + H^{+}]; After two days, the **21b** in the NMR tube aggregated into cotton-like solid. According to the NMR spectrum, no chemical change occurred.

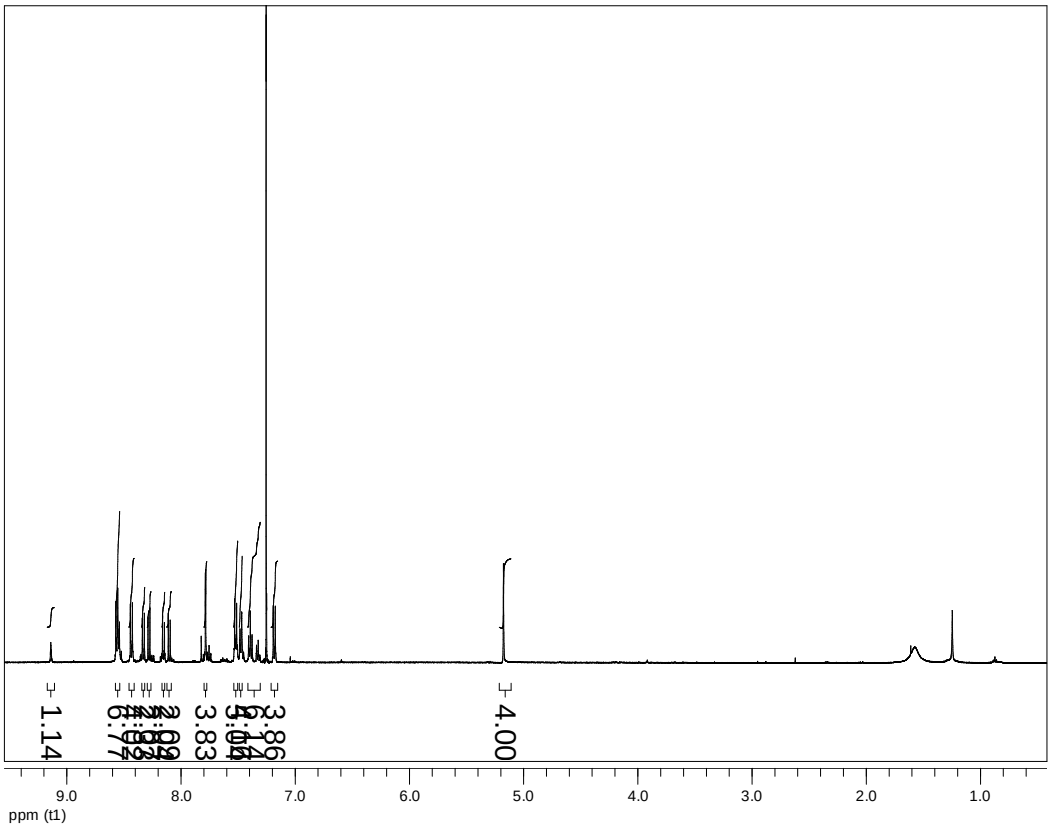

Figure 13-15. 500 MHz ^{1}H-NMR spectrum ($CDCl_3$, room temperature)**21b**.

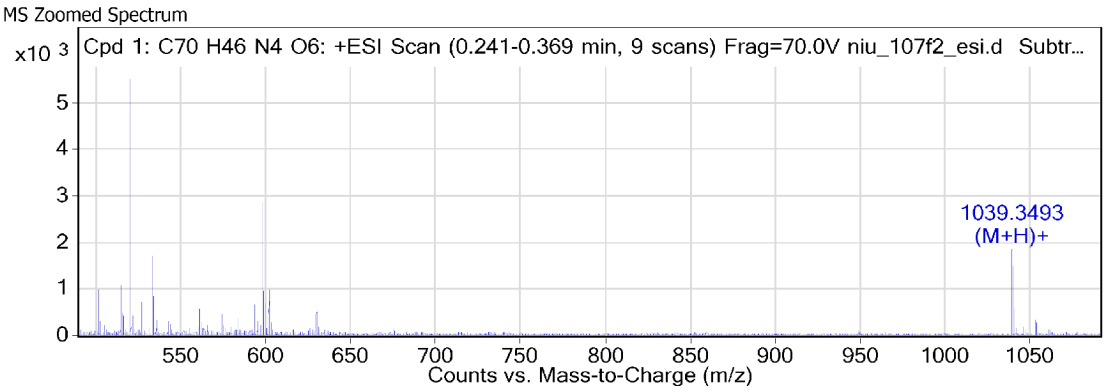

Figure 13-16. ESI-MS spectrum of **21b**.

13.5.10 Synthesis of 21c

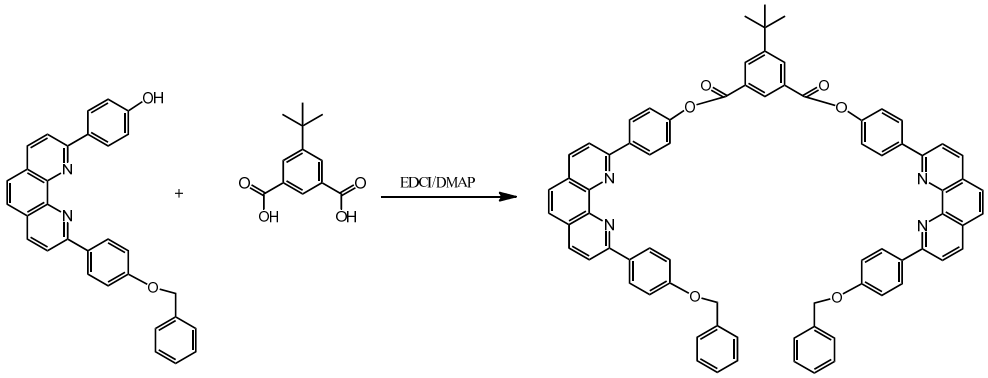

Scheme 13-12. Synthesis of **21c**.

20 (500.0 mg, 1.1 mmol), 5-*tert*butylisophathalic acid (115.0 mg, 0.5 mmol), EDCI (512.0 mg, 3.3 mmol) and DMAP (403.2 mg, 3.3 mmol) were dissolved in DCM (anhydrous, 100 mL) and a clear pale-yellow solution was obtained. The solution was stirred at RT under argon for 6 days. After reaction, the DCM phase was washed with DI water (5 times) and dried over Na_2SO_4. A silica gel column was used to purify the crude product. After purification, a white solid was obtained (1.10 g, 91%), mp > 255 ^oC. ^1H-NMR ($CDCl_3$, 400MHz, Figure 13-17): δ: 8.98–8.96 (m, 1H, H_9), 8.58–8.55 (m, 6H, H_{10}+H_{O1}), 8.46–8.42 (m, 4H, H_{O2}), 8.34 – 8.31 (d, J = 8.4 Hz,

2H, H_4), 8.29 – 8.26 (d, J = 8.4 Hz, 2H, H_7), 8.17 – 8.14 (d, J = 8.4 Hz, 2H, H_3), 8.12 – 8.08 (d, J = 8.4 Hz, 2H, H_8), 7.81 – 7.77 (m, 4H, H_5 + H_6), 7.54 – 7.50 (m, 4H, H_{m1}), 7.50 – 7.45 (m, 4H, H_{12}), 7.43 – 7.36 (m, 4H, H_{13}), 7.35 – 7.29 (m, 2H, H_{14}), 7.20 – 7.16 (m, 4H, H_{m2}), 5.19 – 5.17 (s, 4H, H_{11}), 1.50 – 1.47 (s, 9H, CH_3). ^{13}C-NMR ($CDCl_3$, Figure 13-18): δ: 164.70, 160.26, 156.60, 155.90, 152.95, 152.07, 146.23, 146.18, 137.62, 137.09, 136.95, 136.90, 132.45, 132.33, 130.21, 129.29, 129.12, 129.05, 128.70, 128.08, 128.05, 127.67, 127.62, 126.29, 125.65, 122.14, 119.91, 119.57, 115.27, 70.16, 35.32, 31.35. ESI-MS (Figure 13-19); calcd. for **[21c**+H**]**$^+$: 1094.4038, found: *m/z*, 1094.4068 [M + H^+], error: 2.8 ppm;

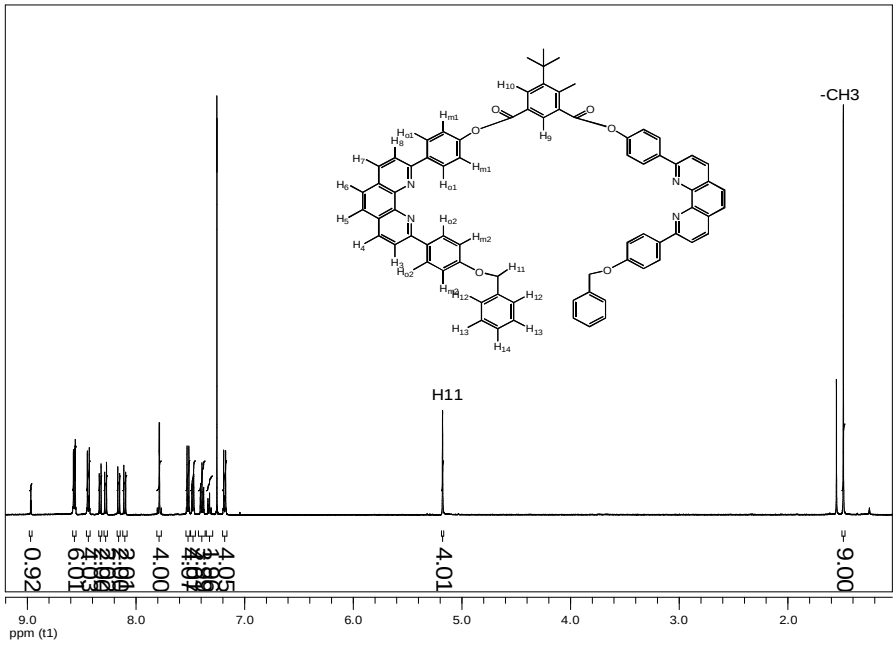

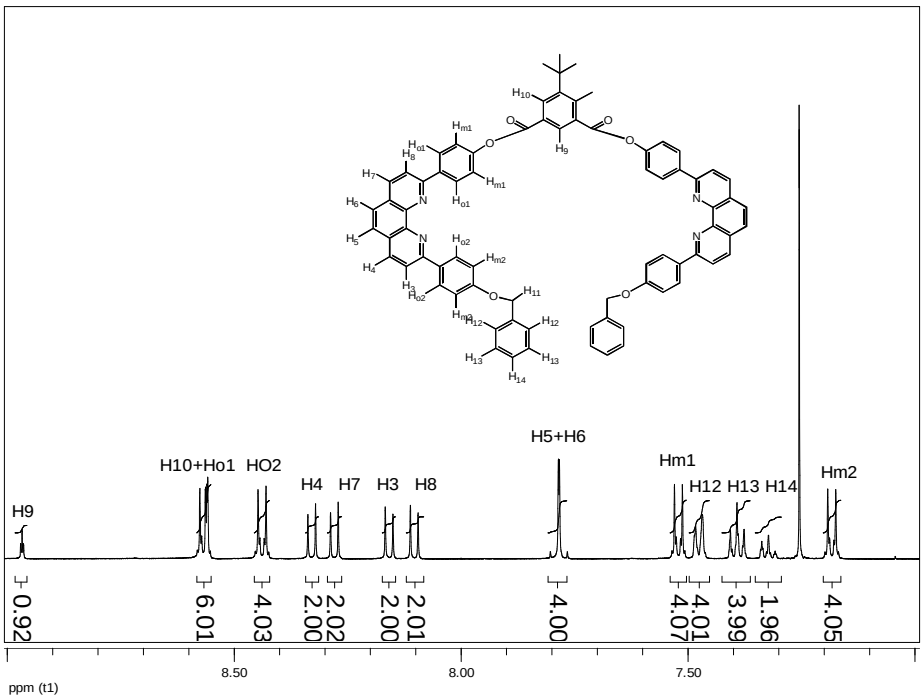

Figure 13-17. 500 MHz ^{1}H-NMR spectrum ($CDCl_3$, room temperature) **21c**. Upper, full spectrum. Bottom: Enlarged spectrum.

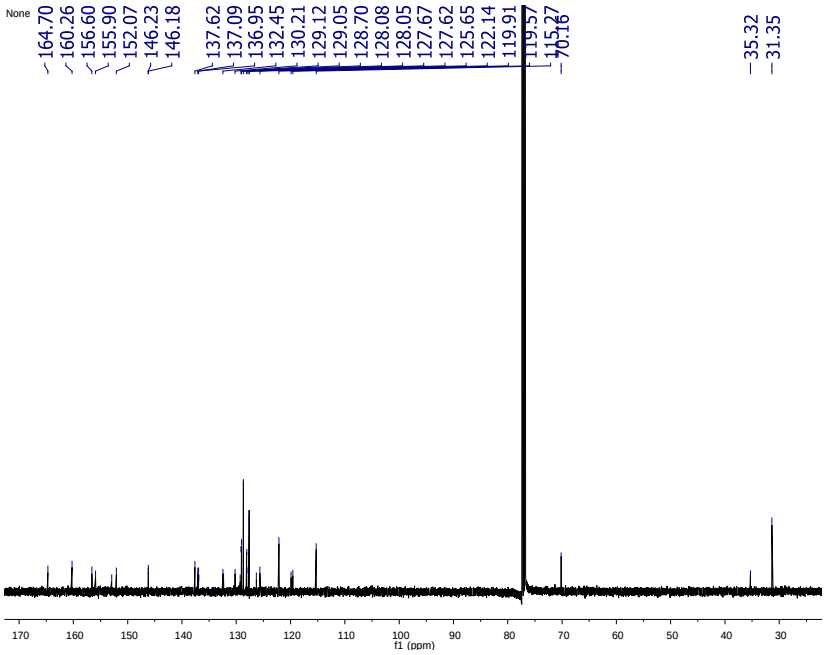

Figure 13-18. 500 MHz ^{13}C-NMR spectrum ($CDCl_3$, room temperature) **21c**.

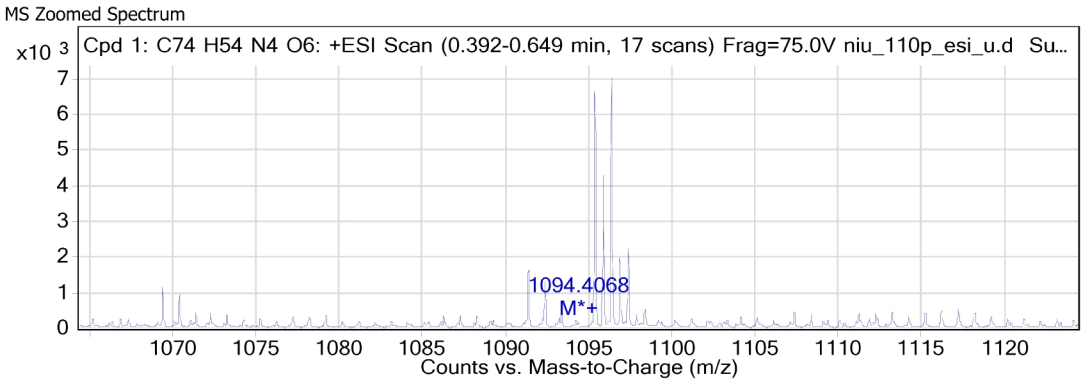

Figure 13-19. ESI-MS spectrum of **21c**.

13.5.11 Synthesis of 26

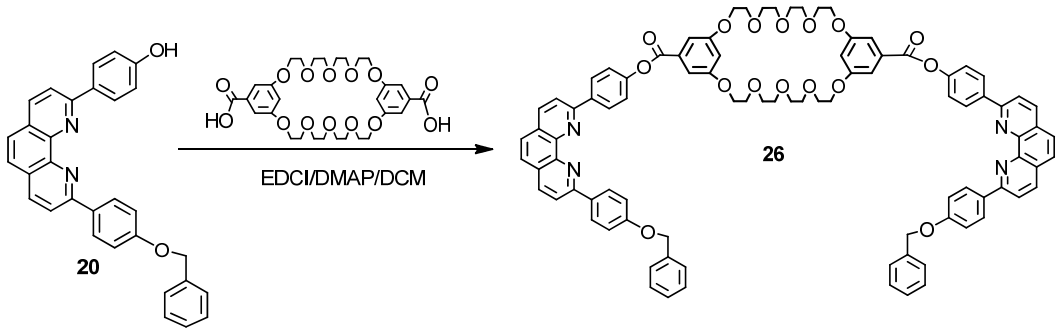

Scheme 13-14. Synthesis of **26**.

BMP32C10 diacid (350 mg, 0.64 mmol), 107 (641 mg, 1.41 mmol), EDCI (1.17 mg, 6.10 mmol) and DMAP (720 mg, 6.10 mmol) were dissolved in 50 mL of DCM. The mixture was stirred for 4 days, washed with DI water (5 times) and dried over sodium sulfate. After solvent removal, a pale yellow liquid was obtained, which was pre-purified by a short silica gel column (DCM:Hexane = 1:1 then DCM:MeOH = 100 : 1). A pale yellow solid was obtained. According to NMR, it was almost pure. Further purification was performed on a regular silica gel column (EA:HE = 1:2 then DCM:MeOH = 98:2). Then a pale yellow solid was obtained (862 mg, 90%), mp 106.1-107.6 °C. ^{1}H-NMR ($CDCl_3$, 500 MHz, Figure 13-20): 8.48 (d, J = 8 Hz, 4.0 H), 8.41 (d, 3J = 8 Hz, 4.0 H), 8.24 (d, 3J = 8 Hz, 2.0 H), 8.17 (d, 3J = 8 Hz, 2.0 H), 8.07 (dd, 3J = 8 Hz, 4.0 H), 7.74 (quart, 3J = 8 Hz, 4.0 H), 7.49 (d, 3J = 7 Hz, 4.0 H), 7.32-7.47 (m, 13 H), 7.18 (d,

3J = 8 Hz, 4.0 H), 6.76 (t, 4J = 2 Hz, 2.0 H), 5.17 (s, 4.0 H), 4.18 (t, 3J = 4 Hz, 8.2 H), 3.92 (t, 3J = 4 Hz, 8.2 H), 3.75 (m, 16.4 H). ^{13}C-NMR ($CDCl_3$, 125, RT, Figure 13-21S19) δ : 164.82, 160.21, 160.04, 156.45, 155.83, 152.13, 146.11, 137.32, 136.97, 136.92, 136.78, 132.40, 131.33, 129.10, 128.94, 128.70, 128.09, 127.91, 127.65, 127.56, 126.12, 125.59, 122.10, 119.80, 119.45, 115.22, 108.64, 107.64, 71.03, 70.14, 69.72, 68.09. HR-ESIMS (Figure 13-22): $[M+2H]^+$ calcd. 1498.5628, found: m/z, 1498.5601, error: -1.86 ppm.

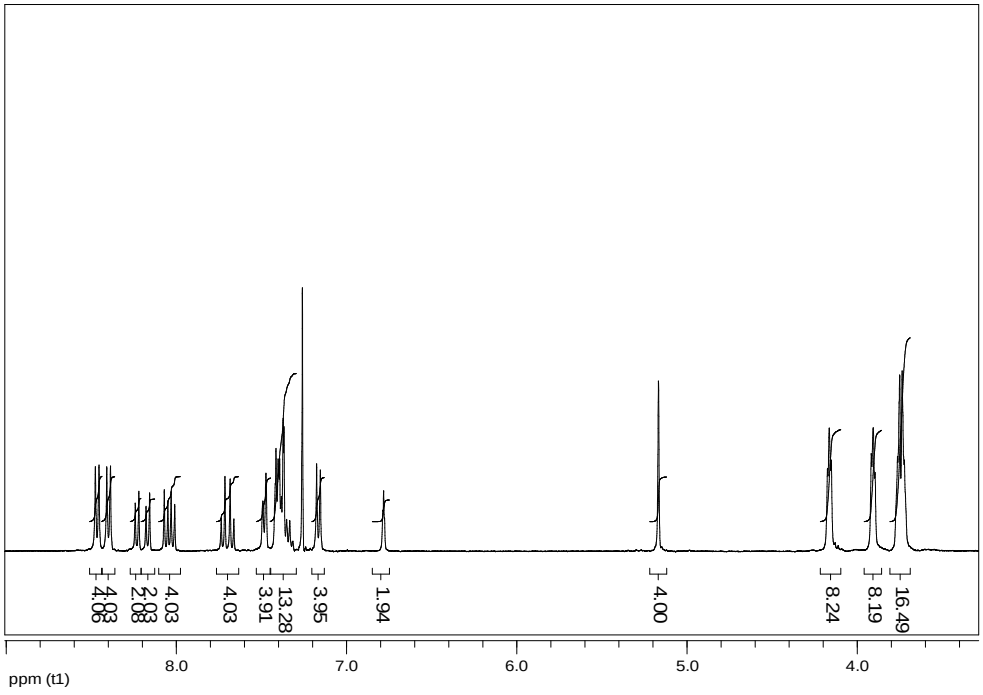

Figure 13-20. 500 MHz ^{1}H-NMR spectrum ($CDCl_3$, room temperature) of **26**.

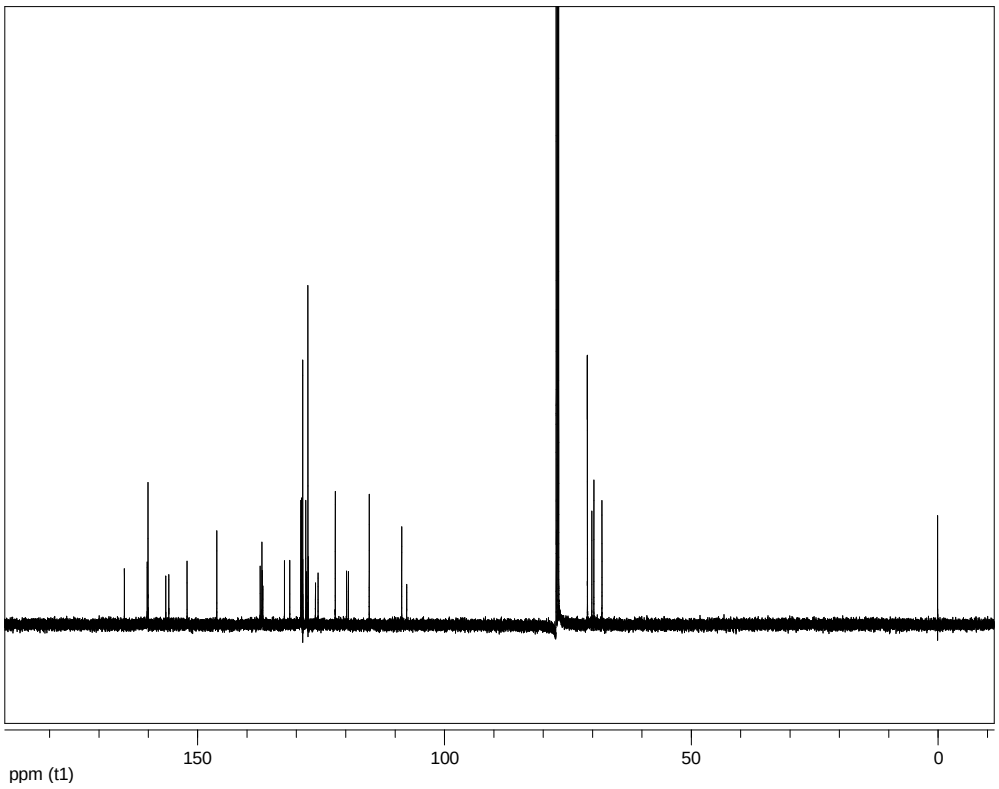

Figure 13-21. 125 MHz ^{13}C-NMR ($CDCl_3$, RT) spectrum of **26**.

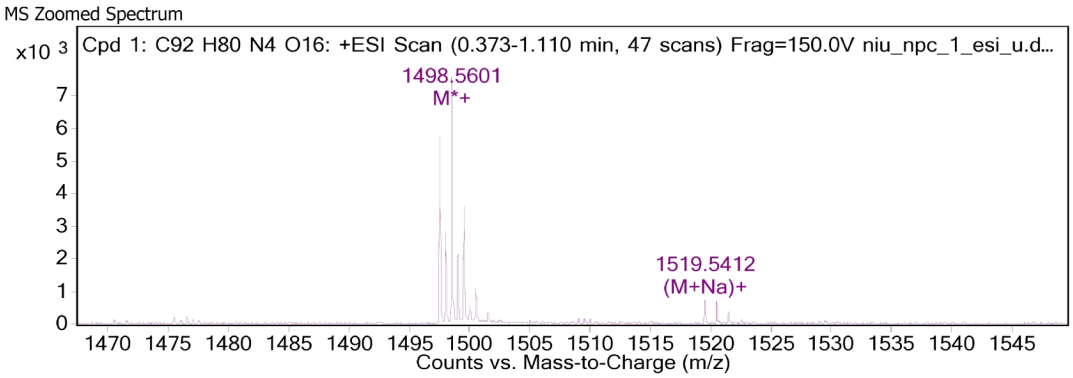

Figure 13-22. ESI-MS spectrum of **26**.

13.5.12 ESI-MS analysis of 26·DMP

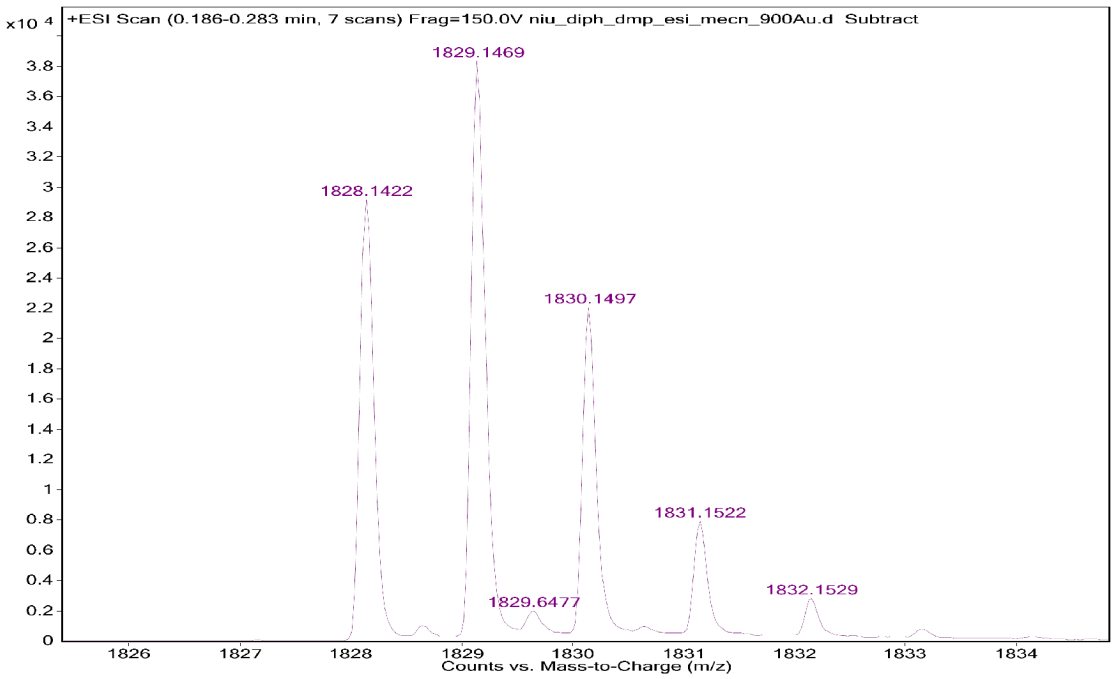

Figure 13-23. Electrospray ionization mass spectrum of **26·DMP**.

References

(1) Schill, G.; Luttringhaus, A. *Angew. Chem.* **1964**, *76*, 567-568.

(2) Wasserman, E. *J. Am. Chem. Soc.* **1960**, *82*, 4433-4434.

(3) Arico, F.; Badjic, J. D.; Cantrill, S. J.; Flood, A. H.; Leung, K. C. F.; Liu, Y.; Stoddart, J. F. *Topics Curr. Chem.* **2005**, 203-259.

(4) Beer, P. D.; Sambrook, M. R.; Curiel, D. *Chem. Comm.* **2006**, 2105-2117.

(5) Blazani, V.; Credi, A.; Ferrer, B.; Silvi, S.; Venturi, M. *Topics Curr. Chem.* **2005**, 1-27.

(6) Bogadan, A.; Rudzevich, Y.; Vysotsky, M. O.; Boehemer, V. *Chem. Comm.* **2006**, 2941-2952.

(7) Credi, A. *J. Phys.: Cond. Matter* **2006**, S1779-S1795.

(8) Flamigni, L.; Heitz, V.; Sauvage, J.-P. *Struct. Bonding* **2006**, 217-261.

(9) Leigh, D. A.; Perez, E. M. *Topics Curr. Chem.* **2006**, 185-208.

(10) Unsal, O.; Godt, A. *Chem. Eur. J.* **1999**, *5*, 1728-1733.

(11) Godt, A.; Unsal, O.; Enkelmann, V. *Chem. Eur. J.* **2000**, *6*, 3522-3530.

(12) Godt, A.; Unsal, O.; Roos, M. *J. Org. Chem* **2000**, *65*, 2837-2842.

(13) Godt, A.; Duda, S.; Unsal, O.; Thiel, J.; Harter, A.; Roos, M.; Tschierske, C.; Diele, S. *Chem. Eur. J.* **2002**, *8*, 5094-5106.

(14) Duda, S.; Godt, A. *Eur. J. Org. Chem.* **2003**, *17*, 3412-3420.

(15) Iwamoto, H.; Itoh, K.; Nagamiya, H.; Fukazawa, Y. *Tetrahedron Lett.* **2003**, *44*, 5773-5776.

(16) Jeschke, G.; Godt, A. *ChemPhysChem* **2003**, *4*, 1328-1334.

(17) Shah, M. R.; Duda, S.; Mueller, B.; Godt, A.; Malik, A. *J. Am. Chem. Soc.* **2003**, *125*, 5408-5414.

(18) Godt, A. *Eur. J. Org. Chem.* **2004**, *8*, 1639-1654.

(19) Hubbard, A. L.; Davision, G. J. E.; Patel, R. H.; Wisner, J. A.; Loeb, S., J. *Chem, Comm.* **2004**, 138-139.

(20) Godt, A.; Jeschke, G. *Magn, Res. Chem.* **2005**, S110-S118.

(21) Ashton, P. R.; Baldoni, V.; Balzani, V.; Classens, C. G.; Credi, A.; Hoffmann, H., D. A.; Raymo, F. M.; Stoddart, J. F.; Venturi, M.; White, A. J. P.; Williams, D. J. *Eur, J. Org. Chem.* **2000**, *7*, 1121.

(22) Amabilino, D. B.; Ashton, P. R.; Baldoni, V.; Boyd, S. E.; Credi, A.; Lee, J. Y.; Menzer, S.; Stoddart, J. F.; Venturi, M.; Williams, D. J. *J. Am. Chem. Soc.* **1998**, *20*, 4295-4307.

(23) Amabilino, D. B.; Ashton, P. R.; Boyd, S. E.; Lee, J. Y.; Menzer, S.; Stoddart, J. F.; Williams, D. J. *Angew. Chem., Int. Ed. Engl.* **1997**, *36*, 2070-2072.

(24) Amabilino, D. B.; Ashton, P. R.; Brown, C. L.; Cordoca, E.; Godinez, L. A.; Goodnow, T. T.; Kaifer, A. E.; Newton, S. P. *J. Am. Chem. Soc.* **1995**, *117*, 1271-1293.

(25) Logemann, E. *J. Mathematical Chem.* **1993**, *13*, 47-51.

(26) Weidmann, J.-L.; Kern, J.-M.; Sauvage, J.-P.; Geerts, Y.; Muscat, D. *Chem. Comm.*

1996, *10*, 1243-1244.

(27) Hamers, C.; Raymo, F. M.; Stoddart, J. F. *Eur. J. Org. Chem.* **1998**, *10*, 2109-2117.

(28) Weidmann, J.-L.; Kern, J.-M.; Sauvage, J.-P.; Muscat, D.; Mullins, S.; Kohler, W.; Rosenauer, C. *Chem. Eur. J.* **1999**, *5*, 1841-1851.

(29) Simone, D. L.; Swager, T. M. *J. Am. Chem. Soc.* **2000**, *122*, 9300-9301.

(30) Raehm, L.; Hamilton, D. G.; Sanders, J. K. *SynLett.* **2002**, 1743-1761.

(31) Fustin, C.-A.; Bailly, C.; Clarkson, G. J.; De Groote, P.; Galow, T. H.; Leigh, D. A.; Robertson, D.; Slawin, A. M. Z.; Wong, J. K. Y. *J. Am. Chem. Soc.* **2003**, *125*, 2200-2207.

(32) Watanabe, N.; Ikari, Y.; Kihara, N.; Takata, T. *Macromolecules* **2004**, *37*, 6663-6666.

(33) Carother, C. H. *Trans. Far. Soc.* **1936**, *32*, 39-53.

(34) Dietrich, B.; Viout, P.; M., L. J. *Macrocyclic Chemistry*; VCH: New York, 1993.

(35) Illuminati, G.; Mandolini, L. *Acc. Chem. Res.* **1981**, *14*, 95-102.

(36) Niu, Z.; Gibson, H. W. *Chem. Rev.* **2009**, *109*, 6024-6046.

(37) Alonso-Vante, N., Nierengarten, J. F., Sauvage, J. P., *J. Chem. Soc. Dalton.Trans.*, **1994**, *11*, 1649-1654.

(38) (a) Dietrich-Buchecker, C.; Sauvage, J. P. *Tetrahedron* **1990**, *46*, 503.; (b) Yang, H., Sleiman, H. F., *Angew. Chem. Int. Ed.* **2008**, 47, 2443 –2446.

(39) See experimental section.

(40) Gibson, H. W.; Nagvekar, D. S. *Can. J. Chem.* **1997**, *75*, 1375-1384.

(41) Elliott, M.; Janes, N. F.; Pearson, B. C. *J. Sci. Food. Agric.* **1967**, *18*, 325-331

Chapter 14.

Conclusions and Future Work

The research presented in this dissertation focused on the design, preparation and characterization of novel crown ether based host/guest complex systems, such as, pseudorotaxanes, semirotaxanes and rotaxanes. Several new crown ether based supramolecular motifs were designed and successfully prepared. By introducing cryptand-based pseudorotaxane systems into polymers, novel pseudorotaxane-type supramolecular polymers were prepared successfully. In addition, attempts to make real linear polycatenanes were made.

First, by the self-assembly of a bis(meta-phenylene)-32-crown-10 bearing two electron-donating groups (carbazoles) with electron-accepting paraquat derivatives, the first [2]pseudorotaxane and the first pseudocryptand-type poly[2]pseudorotaxane based on bis(meta-phenylene)-32-crown-10 were isolated as crystalline solids as shown by X-ray analyses.[1]

Second, the first dual component pseudocryptand-type [2]pseudorotaxanes were designed and prepared via the self-assembly of synthetically easily accessible bis(meta-phenylene)-32-crown-10 pyridyl, quinolyl and naphthyridyl derivatives with paraquat. The formation of the pseudocryptand structures in the complexes remarkably improved the association constant by forming the third pseudo-bridge via H-bonding with the guest and π–stacking of the heterocyclic units.[2]

Third, a pseudocryptand-type [2]pseudorotaxane was formed via the self-assembly of a dipyridyl bis(*meta*-phenylene)-32-crown-10 (BMP32C10) derivative and a paraquat derivative. Due to the basicity of the pyridyl group, which forms the third pseudo-bridge of the pseudocryptand, this pseudorotaxane represents the first system with acid-base adjustable association constants, i. e., finite both in acidic and neutral conditions.

Fourth, the first pseudocryptand-type supramolecular [3]pseudorotaxane was designed and prepared via the self-assembly of a bispicolinate BMP32C10 derivative and a bisparaquat. The complexation behavior was cooperative. In addition, the complex comprised of the

BMP32C10 derivative and a cyclic bisparaquat demonstrated strong binding; interestingly, a poly[2]pseudocatenane structure was formed in the solid state for the first time.[3]

Fifth, two novel bis(*meta*-phenylene)-32-crown-10-based cryptands, bearing covalent and metal complex linkages, were designed and prepared. By employing the self-assembly of these biscryptands, which can be viewed as AA monomers, and a bisparaquat, which can be viewed as a BB monomer, the first AA/BB-type linear supramolecular polymers with relatively high molecular weights were successfully prepared.[4]

Sixth, via the self-assembly of two bis(*meta*-phenylene)-32-crown-10-based cryptands, bearing covalent and metal complex (ferrocene) linkages, with dimethyl paraquat, novel [3]pseudorotaxanes were formed statistically and anticooperatively, respectively.[5]

Seventh, from a hydroxyl-functionalized secondary ammonium salt and DB24C8 a [2]semirotaxane and a [2]rotaxane were prepared successfully. X-ray analysis of a single crystal of the [2]semirotaxane confirmed its semirotaxane nature. In addition, the formation of the [2]semirotaxane was demonstrated to be reversibly controlled by adding KPF_6 and 18C6 sequentially. This system affords a way to prepare novel supramolecular polymers.

Eighth, DB30C10 derivatives and pyridine-based DB30C10 cryptands were prepared by employing the templating method established by our group. A [2]pseudorotaxane was prepared based on DB30C10 diol and paraquat diol. The [3]pseudorotaxane formed via the self-assembly between DB30C10 cryptand and bisparaquat diol occurred in an cooperative manner. In addition, a bromo-functionalized DB30C10 cryptand was successfully designed and prepared. An alkyne-functionalized DB30C10 cryptand was designed and is under preparation; its precursors have been prepared successfully. In the future, based on these functionalized cryptands and paraquat salts, AA and AB type monomers will be prepared. Via the self-assembly between these monomers, non-covalent supramolecular polymers with high molecular weight will be afforded.

Tenth, a novel *cis*(*4,4'*)-dibenzo-30-crown-10 (*cis*-DB30C10) cryptand bearing an organometallic bridge, ferrocene, was prepared via 1-(3'-dimethylaminopropyl)-3-ethylcarbodiimide hydrochloride (EDCI) coupling of the crown ether diol with ferrocene dicarboxylic acid. The cryptand is dimerized in the solid state via π, π-stacking and hydrogen bonds. The ferrocene-based cryptand formed novel [2]pseudorotaxanes with paraquat and diquat

PF_6 salts with association constants (K_a) of $1.7 \pm 0.1 \times 10^3$ and $4.2 \pm 0.3 \times 10^4$ M^{-1} in acetone-d_6, respectively.

Eleventh, In order to prepare linear polycatenanes, the preparation of which represent a real synthetic challenge, a series phenanthroline derivatives were designed and prepared. A "U" shaped monomer was successfully prepared in relative high yield with good solubility. In the future, real linear polycatenanes will be prepared. In addition, a novel diphenanthroline-based BMP32C10 derivative was prepared in high yield and the complexation behavior between it and dimethyl paraquat was studied.

Based on the results from chapter 5, we know that the pseudocryptand structure formation of BMP32C10 derivatives in the complex, which is driven by π,π-stacking and hydrogen bonds, causes the remarkable improvement of the association constant values. However, these BMP32C10 derivatives still need to consume energy to change their conformation in order to bind paraquat. So if they are preorganized during the synthetic steps by making a real cryptand based on similar chemical structures, the association constants could be improved further. In the future, based on methyl 4-hydroxyquinoline-2-carboxylate and BMP32C10 diol, diquinolyl-based BMP32C10 cryptand **2-4** with different third bridge lengths will be synthesized (Figure 14-1) and they are expected to have much better complexation ability with paraquats than even the regular BMP32C10 based cryptands studied previously.

In addition, based on the hydroxyl-functionalized BMP32C10 based cryptand **5**, which demonstrated relatively good complexation ability with paraquat (2.0×10^4 M^{-1}),[6] cryptand-based ATRP initiator **6** can be prepared via the reaction between **5** and 2-bromo-2-methylpropanoyl bromide. By incorporating cryptand-based ATRP initiator **6** into polyurethanes, polyrotaxane-type polyATRP initiator **8** will be afforded. ATRP polymerization can be performed on the branches of **8** and a novel polyrotaxane-type comb polymer will be obtained. To the best of our knowledge, no similar polyrotaxane-type comb polymer has been reported so far.

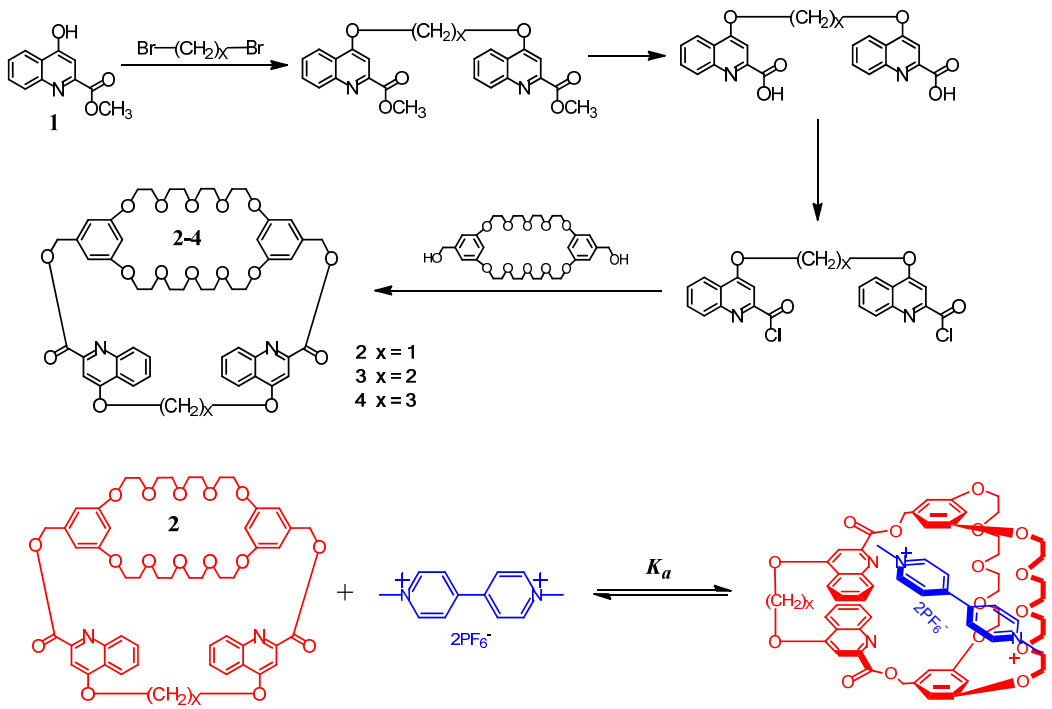

Scheme 14-1. Schematic illustration of formation novel [2]pseudorotaxanes based on diquinolyl-based BMP32C10 cryptands **2**-**4**.

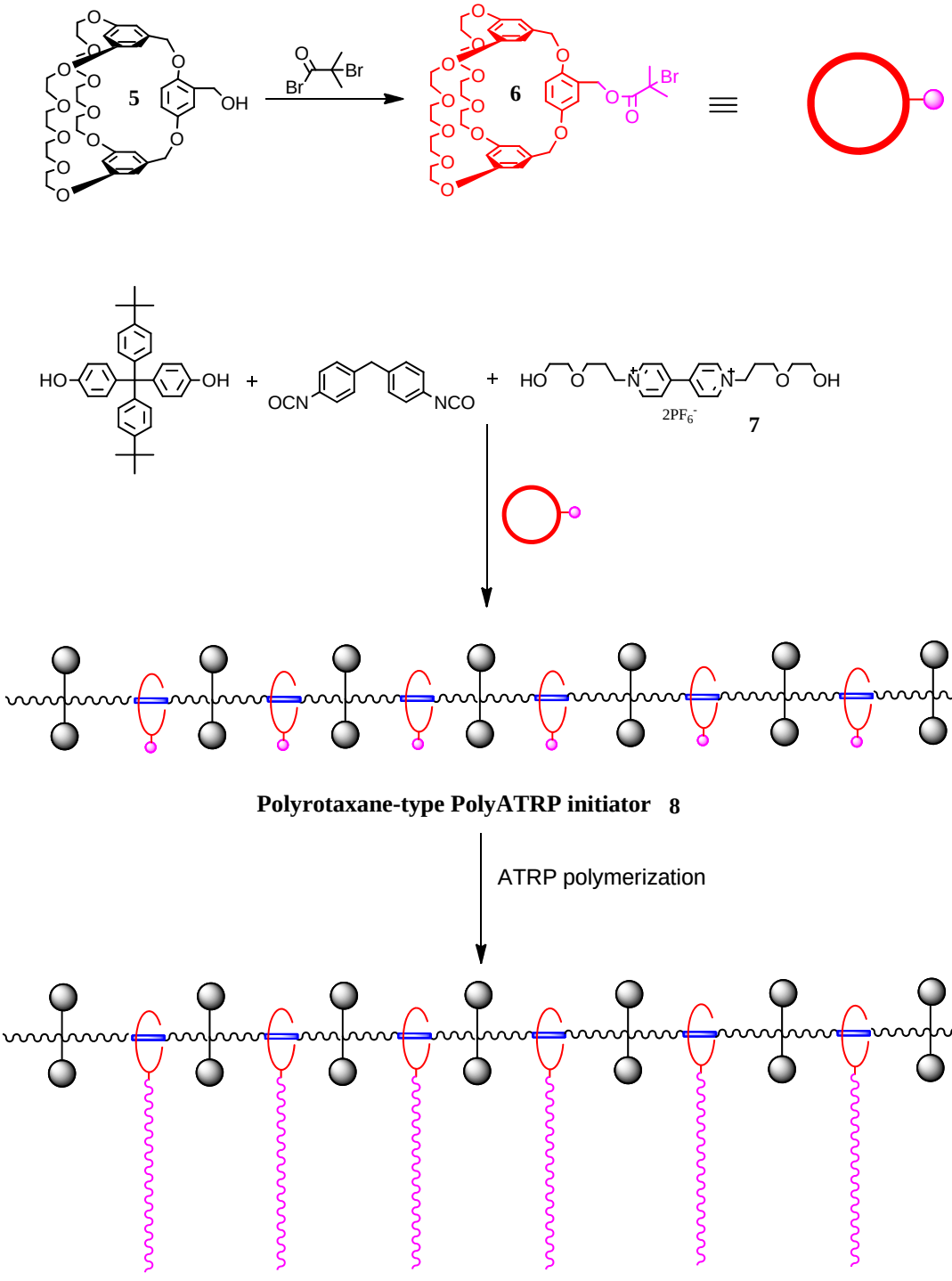

Scheme 14-2. Schematic illustration of preparation of novel polyrotaxane-type polyATRP initiator and polyrotaxane-type comb polymer **9.**

References

(1) Niu, Z.; Slebodnick, C.; Bonrad, K.; Huang, F.; Gibson, H. W. *Org. Let.* **2011**, *13*, 2872–2875.

(2) Niu, Z.; Slebodnick, C.; Schoonover, D.; Azurmendi, H.; Harich, K.; Gibson, H. W. *Org. Lett.* **2011**, *13*, 3992-3995.

(3) Niu, Z.; Slebodnick, C.; Gibson, H. W. *Org. Let.* **2011**, *13* ASAP August 3.

(4) Niu, Z.; Huang, F.; Gibson, H. W. *J. Am. Chem. Soc.* **2011**, *133*, 2836-2839.

(5) Niu, Z.; Slebodnick, C.; Azurmendi, H.; Huang, F.; Gibson, H. W. *Org. Bio. Chem.* DOI: 10.1039/c1ob06299a.

(6) Pederson, A. M.-P.; Vetor, R. C.; Rouser, M. A.; Huang, F.; Slebodnick, C.; Schoonover, D. S.; Gibson, H. W. *J. Org. Chem.* **2008**, *73*, 5570-5573.